JNC TN1410 2000-002

Second Progress Report on Research and Development for the Geological Disposal of HLW in Japan

H12 : Project to Establish the Scientific and Technical Basis for HLW Disposal in Japan

Supporting Report 1
Geological Environment in Japan

April 2000

JNC
Japan Nuclear Cycle Development Institute

本資料の全部または一部を複写・複製・転載する場合は、下記にお問い合わせください。

〒319-1184　茨城県那珂郡東海村村松4番地49
核燃料サイクル開発機構
技術展開部　技術協力課
Inquiries about copyright and reproduction should be addressed to :
Technical Cooperation Sections,
Technology Management Division,
Japan Nuclear Cycle Development Institute
4-49,Muramatsu, Tokai-Mura, Naka-Gun, Ibaraki, 319-1184,
Japan

© 核燃料サイクル開発機構（Japan Nuclear Cycle Development Institute）
2000

Preface

From the beginning, it must be emphasized that the project to establish a technical basis for HLW disposal in Japan (H12) was carried out in the absence of both an implementing body responsible for HLW disposal and legislation to regulate such disposal. Like the First Progress Report (H3), which was published in 1992, it is predominantly a compilation of the results of R&D studies relevant to HLW management.

For the benefit of those unfamiliar with the Japanese waste management program, the English version of the H12 Project Overview Report provides a clear picture of the current status of work in Japan and a perspective on the future following the major reorganization of responsibilities initiated during the year 2000. The report also aims to provide some insight into the political and cultural context of the program and key information on the physical and geological features of Japan for a foreign technical audience.

Although the H12 Project is coordinated by JNC (Japan Nuclear Cycle Development Institute), relevant R&D is carried out by a wide range of organizations in Japan. The three Supporting Reports of the Project are designed to provide a unique snapshot of the diversity and depth of the scientific and technological basis supporting the HLW program in Japan - much of which is not available otherwise in English language publications. Many of the individual studies reported were, however, initiated without central planning. A major integration effort was implemented by the "Coordination Conference" group but, nevertheless, inconsistencies and limited integration and synthesis may be apparent when compared to other national programs managed by a single organization.

A further constraint is the extreme political sensitivity associated with selection of potential sites. The challenge of demonstrating that suitable sites can be found despite Japan's active tectonics has to be balanced against a desire to avoid specification of preferred locations or host rocks. The usual need to focus engineering and performance assessment studies on clearly defined geological databases is in conflict with the wish to remain as generic as possible. This dichotomy results in a more generic approach in which a lot of emphasis is placed on data from particular geoscientific study sites (mainly Tono and Kamaishi). These studies should thus be seen more as an illustration of the application of specific concepts, models and databases rather than as a strict evaluation of potential sites.

The three Supporting Reports cover the general areas of Geology, Engineering and Performance Assessment, respectively. The differences in the boundary conditions for these reports are important to recognize. Supporting Report 1 (Geology) aims to illustrate that areas with suitable geological stability to host a repository exist in Japan and to provide a comprehensive overview of the general characteristics of rock formations and groundwater in Japan, based on information collected in the field of earth sciences and on information from more detailed studies carried out within the HLW management program. Supporting Report 2 (Engineering) aims to summarize all Japanese studies to date on engineered barrier systems and also to illustrate potential repository designs and operational procedures for a wide range of potentially suitable geological formations - focusing, in particular, on the varying mechanical properties of different rocks. Supporting Report 3 (Performance Assessment) summarizes analyses of the long-term safety of various potential repository options. Because of the need to "freeze" performance assessment databases at a relatively early stage, the Reference Case defined is seen to be somewhat optimistic in certain respects and pessimistic in others, when considered in the light of the latest findings reported in Supporting Reports 1 and 2. Nevertheless, a very wide range of parameter variations is analyzed to ensure that all

data uncertainties are examined and that the conclusion derived - namely that the disposal concepts considered can meet international safety standards - is robust.

This Supporting Report consists of three chapters, organized to correspond to the content of the Overview Report and to respond to the issues raised by the AEC Guidelines (see Section 1.3.2). The framework of the studies being carried out by JNC is also considered.

In Chapter I, issues such as the role of the geological environment in HLW disposal, the geological features of Japan and the approach to studies of the geological environment are presented as background. The results of separate studies of the geological environment are then presented in detail in appropriate sections of the subsequent chapters.

Chapters II and III report on the long-term stability and characteristics of the geological environment which are important in considering the disposal concept. These chapters were written with the aim of providing technical support to the relevant sections of the Overview Report and, again, to respond to the individual R&D issues raised in the AEC Guidelines. In Chapter II, the present state of knowledge and latest information on natural phenomena in Japan, such as volcanic activity and fault movement, are discussed, together with descriptions of the methods applied in their study. This was done with the purpose of presenting scientific evidence to show that there are locations in Japan where the geological environment is sufficiently stable to allow safe geological disposal of HLW. In Chapter III, the latest information on rock formation and groundwater characteristics, which are considered important for a multibarrier disposal concept, are summarized. The aim is to provide an understanding of the general characteristics of the deep geological environment of Japan from a disposal viewpoint, based on the results of field surveys and literature studies. In the last section of Chapter III, the results of natural analogue studies at, inter alia, the Tono uranium deposit are also summarized.

In the Appendix, the present status of technology and equipment for studying the geological environment is described. This Appendix lists the most recently available technology and instrumentation developed by JNC.

Efforts were made to ensure that there was transparency both in the presentation of the results and also in the derivation of the necessary concepts. It has proved impractical, however, to include all the details of the research program and thus appropriate references are made as necessary.

Summary

Scope

The geological environment has two main functions in terms of ensuring the safety of geological disposal. One relates to the fundamental long-term stability of the site and the other to the properties of the host rock formations and groundwater which facilitate the emplacement and functioning of the engineered barrier system (EBS) and the natural barrier function. With these functions in mind, the feasibility of selecting a geological environment in Japan, which is appropriate for geological disposal, is discussed, based on findings obtained from case studies and field measurements.

Methodology

Long-term stability of the geological environment

Japan is located in a tectonically active belt that surrounds the Pacific Ocean. Volcanism, earthquakes and crustal movements are features of such active belts and are more significant in Japan than in most other countries. Therefore, important natural phenomena to be examined in Japan include fault movement, volcanic activity, uplift/denudation and climatic/sea-level changes.

The aim was to investigate the occurrence of these natural phenomena and the extent of changes in the geological environment caused by them, with particular reference to their potential effects on the performance of the geological disposal system. Therefore, case studies were carried out in regions where records of the natural phenomena mentioned above could be observed. In addition, a countrywide review was undertaken of relevant knowledge and information accumulated in the various fields of earth science.

Important characteristics of the deep geological environment

In order to provide information relevant to understanding the deep geological environment for geological disposal, field studies and in-situ measurements in the Tono area and the Kamaishi mine, as well as a review of the relevant literature, have been carried out.

The Tono area is located in Gifu Prefecture, central Japan and is known for the existence of one of the biggest sandstone-type uranium ore deposits in Japan. The study at Tono, which started in 1986, has mainly mainly on understanding the geological environment both in Neogene sedimentary rocks and Cretaceous granitic basement, as well as the migration behavior of natural uranium-series nuclides within the uranium deposit in the sedimentary rock.

The Kamaishi in-situ experiment project was carried out from 1988 to 1998, in granitic rocks in Iwate Prefecture, northeast Japan, to characterize fracture domains and their influence on the hydrological and geochemical conditions. Additionally, the influence of drift excavation on the mechanical properties of the rock was also investigated.

Results and discussion

Existence of stable geological environments in Japan

Key findings to date regarding the history of natural phenomena and the extent of their influence on the geological environment are summarized below with a view to determining

the existence of potentially stable geological environments in Japan.

Fault movement

Major fault activity in Japan has occurred repeatedly at existing localized active faults for several hundred thousand years or more, and the crustal stress field can generally be considered to have remained unchanged during this period. Therefore, regional characteristics of fault activity can be estimated for the future, assuming that patterns in the past will continue.

Active faults in Japan often diverge near the surface. To calculate the areas affected by their past displacements and to estimate their effects in the future, it is practicable to treat them as "fault zones", consisting of adjacent faults and folding. The widths of the fault zones range up to several kilometers and show little evidence of changes over the past several hundred thousand years.

The most significant effects of fault movements on the geological environment are dynamic effects such as fracturing, crushing and subsequent displacement of the rock mass. The extent over which rocks are crushed by fault movement (fault crushed zone) varies for each fault. However, the fault crushed zone generally becomes wider as the fault becomes longer and displacement accumulates. A relationship between these parameters has been proposed. According to the results of a literature survey of the characteristics of major active faults in Japan, the width of the fault crushed zone is generally several meters to several hundred meters at most. There are reports, however, to the effect that minor faults are observed in the surrounding rock mass a few kilometers distant from the major fault.

Accordingly, when selecting a site, an appropriate clearance should be ensured between the disposal facility and major active faults. The influences of distant active faults can be assessed with reference to the performance of the EBS and the disposal facility design. In-situ measurements in the Kamaishi mine revealed that the impact of seismic ground motion on deep underground environment will probably be small.

Volcanic activity

The locations where volcanic activity occurs are defined by tectonic plate layout and subduction angle, and there is little possibility that the locations of volcanic activity will change to a significant degree unless there is a major change in the plate tectonic situation. The history of volcanic activity in the Quaternary (i.e. from approximately 1.7 million years ago to the present) suggests that the locations in which volcanic activity occurs are limited to distinct regions and that there is little change in these locations over these timescales.

Therefore, assessments of the future locations of volcanic activity can be based on chronological and spatial changes in volcanic activity during the Quaternary period or the last several hundred thousand years. In addition, the distribution of volcanic material extruded after the Miocene coincides more or less with the distribution of current volcanoes. This suggests that the present locations of volcanic activity can be traced back to these periods.

In volcanic areas and their immediate surroundings, temperature increases caused by magma and hot rock bodies, intrusion of hydrothermal water and volcanic gas released from magma may change the hydraulic and geochemical characteristics of groundwater. According to geothermal gradient maps based on deep borehole data from all over Japan and the results of case studies in some volcanic areas, the range of these effects generally extends several km to

20 km from the volcanic center.

Uplift and denudation

Uplift and subsidence are cumulative phenomena. Formation of mountains and plains in Japan can be considered to be the result of continuous expansive uplift and subsidence over a long period of time. Each area of a crustal stress field, determined mainly by plate movements, has unique uplift and subsidence features. Such trends have continued throughout the Quaternary (or for at least the past several hundred thousand years) and are expected to continue in the same way in areas where the stress field is stable. Therefore, the extent of changes to be assumed for the future can be estimated by extrapolating from past changes. The amount of uplift estimated for the next 100,000 years is less than 100 m in many areas, except in some high mountains and at the tips of peninsulas.

It is thought that the denudation rate in Japan is several meters to 100 m per 100,000 years, except for some high mountains and the tips of peninsulas. These values have been estimated by different methods, employing information about the quantity of sand deposited in dams, the age of hills/terraces and the volume of valleys carved into them and the relative altitudes of bottoms of paleo-rivers. The rate of denudation in the future must be estimated with reference to the local topography and its predicted changes in the future.

Climatic and sea-level changes

The potential effects of climatic and sea-level changes on the geological environment include changes in groundwater flow and groundwater chemistry. In addition, the effects of alpine glaciers and permafrost during glacial epochs should also be taken into consideration.

Global glacial-interglacial cycles of climatic and sea-level changes with 100,000 year periodicity have been confirmed for more than several hundred thousand years in the past. Around Japan, the sea-level was at its lowest point approximately 20,000 years ago, when it was approximately 120 m below the current level. After that, the sea-level rose rapidly to reach 0 - 5 m higher than the current sea-level approximately 6,000 years ago. Pollen analyses and data on glacial topography suggest that the average annual air temperature in Japan ranged between 8°C lower and 2 - 3°C higher than at present. During glacial periods in Japan, the annual amount of precipitation decreased to 50 - 70 percent of the current amount.

The present climatic situation is slightly after the peak of an interglacial period. It is expected that the general trend will be for the climate to become colder and for the sea-level to fall during the next 70,000 - 80,000 years. The effects of this lowering of temperature will be the development of permafrost and freezing cracks, which will be limited to Hokkaido and to some high mountains in Honshu.

Characteristics of the deep geological environment of Japan

This section focuses on those characteristics of the rock and groundwater in deep geological environments which are important for the design and performance assessment (PA) of the geological disposal system.

Characteristics of groundwater flow

The hydraulic gradient and the permeability of the rock are major controls on the movement of deep groundwater and depend mainly on geological structures and geographic conditions.

Measurements near the surface show that hydraulic gradients are generally defined by local

topography. Data from in-situ hydraulic measurements carried out in the Tono area show that the hydraulic gradient at a depth of several hundred meters is lower than the value measured near the surface.

Data from the published literature in Japan, taken mainly from the civil engineering field, were compiled in order to investigate the permeability of different rock types. At the same time, these data were compared with measurements taken at several hundred points in the Tono area and Kamaishi mine. It is concluded that permeabilities obtained from the literature data were more than an order of magnitude higher than the data provided from the Tono area and Kamaishi mine. Excluding crushed or damaged zones around faults, the permeability of deep rock formations in Japan can be considered to range less than 10^{-7}m s^{-1}.

Geochemical characteristics of groundwater

Groundwater chemistry is determined by the origin of the water and its reactions with rocks. In Japan, groundwater originating from seawater may exist near the coast and groundwater from magma may exist in volcanic regions. In both cases, the concentration of dissolved components will be higher than in groundwater originating from atmospheric precipitation. Magmatic groundwater is considered to be unimportant because volcanic regions will be avoided during the site selection process.

Measurements of low mineralized groundwater in the Tono area and Kamaishi mine show that water chemistry becomes reducing deep underground. This phenomenon can be explained by reactions between the groundwater, the major minerals that constitute the rock, clay minerals, microorganisms and organic substances.

It is speculated that the groundwater in the sedimentary rocks in the Tono area originated from precipitation approximately 15,000 years ago, based on measurements of stable isotopes (oxygen and hydrogen) and radioactive isotopes (e.g. tritium and radioactive carbon). The redox potential of the groundwater in sedimentary rocks in the area under investigation is around –300 mV approximately 160 m below ground surface. The water chemistry is Na-Ca-HCO_3 type in the upper part and Na-HCO_3 type at depth. Microscopic observations of minerals along the transport pathway, water-rock interaction experiments, thermodynamic analyses and mass balance calculations allow these changes to be interpreted in terms of silicate mineral dissolution near the surface, ion exchange reactions with clay minerals and the dissolution of carbonate and sulfate minerals. Redox potential is influenced by the HS^--SO_4^{2-} ion couple.

The ratios of oxygen and hydrogen stable isotopes indicate that the groundwater in granite at Tono also originated from atmospheric precipitation. The Eh value is around –300 mV approximately 500 - 1,000 m below the surface. The analytical results show that sulfur chemical species, such as SO_4^{2-} and HS^- are highly likely to contribute to the redox potential. The water chemistry was found to change from Na-Ca-HCO_3 type to Na-HCO_3 type with increasing depth. A similar tendency was observed for groundwater in granite at the Kamaishi mine.

Physical characteristics of rock formations

The physical characteristics of rock formations can be subdivided into the characteristics of the site (e.g. geothermal gradient and stress state) and the properties of the rock itself (e.g. porosity and strength).

According to deep borehole data collected throughout Japan, geothermal gradients are lower than 5°C per 100 m, and approximately 3°C per 100 m on average in most areas excluding volcanic regions.

Based on the results obtained in the Tono area and Kamaishi mine as well as analyses of existing data, a common tendency is for the vertical stress to almost equal the lithostatic load. Additionally, the ratio between vertical stress and horizontal stress typically approaches a value around 1 as depth increases.

In order to evaluate the Excavation Disturbed Zone (EDZ), changes in mechanical, hydraulic and chemical properties before and after tunnel excavation were studied in the Tono and Kamaishi mines. The results of these in-situ investigations show that in both sedimentary and crystalline rocks, the mechanical influence of blasting extends up to approximately 1 m from the tunnel wall. Permeability increases over a similar spatial range. However, it does not always increase in a uniform manner.

Characteristics related to solute transport

The studies in the Tono area and the Kamaishi mine show that the distribution and form of rock matrix pores and fractures, which may provide solute transport pathways, differ depending on rock type and region. The matrix pores and fractures are generally expected to sorb substances on the surfaces of minerals that constitute the rock or fracture infill.

Pore structures observed in numerous mines and tunnels were investigated in order to clarify the mechanisms of underground solute transport. The results of the investigations at the Kamaishi and Tono mines showed that fracture networks developed in crystalline rocks and old sedimentary rocks provide the major transport pathways. On the other hand, matrix pores and microfractures provide the major transport pathways and sorption sites in recent sedimentary rocks. It was also confirmed that clay minerals and ferrous minerals, such as mica and pyrite, display generally higher radionuclide sorption than quartz and feldspar. In addition, natural analogue studies, involving the tracing of natural uranium-series nuclides in fractured granitic rock at the Kamaishi mine confirmed that matrix diffusion actually occurred in deep underground fractures.

Conclusion

The locations, spatial extents, regularity and effects of natural phenomena that may potentially influence the long-term stability of geological environments were investigated over timescales of several hundred thousand years or more. This work was constrained by variability in the quantity and accuracy of information, which depended on the type of phenomena and the regions involved. The locations of localized phenomena, such as volcanic activity and major fault movements, can be well specified. By selecting an appropriate disposal site, it will be possible to reduce to acceptably low level the probability that these phenomena may have significant effects on a repository. On the other hand, gradual phenomena such as uplift/subsidence, denudation and climatic and sea-level changes are more ubiquitous. It is, nevertheless, possible to estimate future trends and their potential effects by extrapolating data obtained on the current rate and the extent of such phenomena. Using this approach, it is possible to select a stable geological environment that will not be significantly altered by such phenomena and/or to implement necessary engineering countermeasures against potential effects.

A great deal of data have been obtained concerning the characteristics of rock formations and groundwaters that are important for the proper functioning of the multibarrier system, particularly from geoscientific studies carried out in the Tono area and the Kamaishi mine. These data led to the conclusion that there are deep geological environments that can maintain the integrity of the EBS for a long period of time and that the rock formations themselves can function as a natural barrier. For example, typically, groundwater deep underground can be considered to be reducing and to migrate only slowly, thereby effectively retarding radionuclides.

It is planned to accumulate further, more reliable data from case studies and field measurements. In this context, JNC is planning to construct deep underground research laboratories in order to demonstrate site investigation technologies for the deep geological environment and the results will support the selection and characterization of a disposal site.

List of Contents

Chapter I Introduction

1.1 The role of the geological environment in deep disposal I- 1
1) The geological disposal concept and mechanisms for ensuring safety I- 1
2) The expected role of the geological environment I- 1
3) The long-term stability of the geological environment I- 2
4) Important characteristics of the geological environment I- 4

1.2 Geological features of Japan I- 4
1) Tectonic setting of Japan I- 4
2) Distribution of geological units I- 5
3) Geographic conditions I- 5

1.3 Studies of the geological environment I- 5

1.3.1 Approaches I- 5
1) Basic concept I- 5
2) Study methods I- 6

1.3.2 Assessments and requirements stipulated by the Government I- 7
1) Government assessment of H3 I- 7
2) Studies subsequent to H3 I- 8
3) The objectives and content of H12 I- 8

References I- 11

Chapter II Long-term Stability of the Geological Environment of Japan

2.1 Research on the long-term stability of the geological environment II- 1

2.1.1 Natural phenomena relevant to the long-term stability of the geological environment II- 1

2.1.2 Predictive evaluation of natural phenomena in the future II- 3

2.2 Tectonics of the Japanese islands II- 4

2.2.1 Plate movements in the Japanese islands and the adjacent sea areas II- 4

2.2.2 Significant change in plate system II- 7

2.2.3 Neotectonics II- 8
1) Chishima Arc II- 8
2) Northeast Japan Arc II- 8
3) Izu-Ogasawara Arc II- 8
4) Southwest Japan Arc II- 9
5) Ryukyu Arc II- 9

2.3 Earthquakes and fault movement II- 10

2.3.1 Fault movement in Japan II- 10
1) History of active fault movement II- 10
2) Regional variations in active faults II- 13

3) Extent of the range of active fault movement II- 23
4) Movement of faults other than active faults II- 26
2.3.2 Effects of fault movement on the geological environment II- 27
1) Effects of fault movement II- 27
2) Influence of seismic activity II- 33
2.3.3 Summary II- 38
2.4 Volcanism II- 40
2.4.1 Characteristics of volcanism in Japan II- 40
1) Quaternary volcanoes and tectonic setting II- 40
2) Subsurface structure beneath the volcanic edifice II- 43
3) Spatial and temporal distribution of Quaternary volcanoes II- 44
4) Regularity of volcanism and its future prediction II- 52
2.4.2 The effect of volcanism on the geological environment II- 54
1) Distribution of Quaternary volcanoes and geothermal gradient II- 54
2) Geothermal structural model II- 58
3) Critical parameters controlling geothermal structure II- 60
4) Hydrothermal systems II- 66
5) Geochemistry of hydrothermal solutions II- 74
6) Thermal effects of intrusive magma II- 83
2.4.3 Summary II- 86
2.5 Uplift, subsidence and denudation II- 91
2.5.1 Characteristics of uplift, subsidence and denudation in Japan II- 91
1) Uplift and subsidence II- 91
2) Prediction of uplift and subsidence II-112
3) Denudation II-117
2.5.2 The effects of uplift, subsidence and denudation on the geological environment II-136
1) Direct effects II-136
2) Indirect effects II-137
2.5.3 Summary II-138
2.6 Climatic and sea-level changes II-141
2.6.1 Characteristics of climatic and sea-level changes II-141
1) Analytical method for climatic and sea-level changes II-141
2) Climatic and sea-level changes during the Quaternary II-144
3) Climatic and sea-level changes after the last glacial stage II-144
4) Mechanism of climatic and sea-level changes II-150
5) Prediction of climatic and sea-level changes II-150
2.6.2 Effects on the geological environment of climatic and sea-level changes II-150
1) Effects of permafrost II-151
2) Effects on denudation II-157
3) Effects on hydraulics and water chemistry II-157
4) Effects of global warming II-158
2.6.3 Summary II-159
References II-162

Chapter III Characteristics of the Geological Environment of Japan

3.1 Studies on the characteristics of the geological environment III- 1

3.1.1 Essential characteristics of a geological disposal environment III- 1
1) Geological structures III- 2
2) Characteristics of groundwater flow III- 3
3) Geochemical characteristics of groundwater III- 4
4) Thermal and mechanical properties of the rock mass III- 4
5) Solute transport in the rock mass III- 5

3.1.2 Data on characteristics of the geological environment III- 5

3.2 Geological structures III- 7

3.2.1 Characteristic features of geological structures in Japan III- 7

3.2.2 Geological structures and transport pathways III- 7
1) Matrix porosity, bedding planes, unconformities, dikes and sills III- 8
2) Fractures and faults III- 10

3.2.3 Fracture parameters III- 11
1) Fracture orientation III- 11
2) Shape defined by lateral limit of fracture surface III- 14
3) Distribution of fracture radius III- 14
4) Distribution of fracture frequencies III- 14
5) Spatial distribution of fractures III- 16
6) Distribution of fracture transmissivity III- 16
7) Distribution of fracture apertures III- 16

3.3 Groundwater flow characteristics III- 19

3.3.1 Groundwater flow properties in the deep underground environment of Japan III- 19
1) Hydraulic gradients deep underground III- 19
2) Hydraulic conductivity of the deep underground rock mass III- 20
3) Freshwater/saline water boundary III- 28

3.3.2 Investigation and analysis of deep groundwater flow III- 30
1) Study of regional groundwater flow in the Tono area III- 31
2) Investigation of the effect of shaft excavation on groundwater flow in the Tono area III- 34
3) Investigation of groundwater flow around tunnels in the Kamaishi mine III- 41

3.3.3 Summary III- 47

3.4 Geochemical characteristics of groundwater III- 48

3.4.1 Geochemical characteristics of groundwater in Japan III- 48
1) Geochemical characteristics of meteoric groundwater III- 48
2) Geochemical characteristics of marine groundwater III- 49

3.4.2 Case studies on the geochemical characteristics of deep groundwater III- 49
1) The Tono area III- 55
2) Kamaishi mine III- 62

3.4.3 Case studies on colloids, organic materials and microbes in deep groundwater III- 66
1) Colloids III- 66
2) Organic materials III- 67

3) Microbes III- 67
3.4.4 Summary III- 69
3.5 Thermal and mechanical properties of the rock mass III- 73
3.5.1 Thermal characteristics of the rock mass at depth III- 73
1) Thermal properties III- 73
2) Geothermal gradients III- 74
3.5.2 Mechanical properties of the rock mass at depth III- 81
1) Statistical examination of physical properties III- 81
2) In situ stresses III- 92
3) Time-dependent behavior of the rock mass III- 95
3.5.3 Excavation disturbance III- 98
1) Studies on excavation disturbance at Tono III- 98
2) Study of excavation disturbance at Kamaishi III-105
3.5.4 Summary III-109
3.6 Solute transport in the rock mass III-114
3.6.1 Case studies in the Tono area III-114
1) Microscopic pore space geometry III-114
2) Chemical retardation (sorption / mineralization) III-117
3) Chemical retardation (coprecipitation) III-119
4) Colloid-facilitated solute transport III-121
3.6.2 Case studies at the Kamaishi mine III-121
1) Microscopic pore space geometry III-121
2) Physical retardation (matrix diffusion) III-122
3) Chemical retardation (sorption) III-125
3.6.3 Summary III-128
3.7 Natural analogue studies III-129
3.7.1 Examples of natural analogue studies III-129
1) Migration and retardation of natural uranium series nuclides III-130
2) Natural analogue studies relevant to matrix diffusion III-133
3.7.2 Summary III-133
References III-135

Appendix Techniques for Investigating the Geological Environment

List of Figures

Figure 1.1-1 Natural phenomena to be considered in geological disposal (A), Reactions and processes in rocks and groundwater (B)

Figure 1.2-1 Schematic illustration of topography and groundwater flow in Japan

Figure 1.3-1 Research and development for geological disposal

Figure 2.1-1 Natural phenomena affecting the long-term stability of the geological environment

Figure 2.2-1 Plates around Japan

Figure 2.2-2 Crustal structure of Plate boundaries around the Japanese Island

Figure 2.3-1 Relationship between the amount of accumulated displacement at major active faults and their age

Figure 2.3-2 Active faults in Japan

Figure 2.3-3 Frequency of active faults in Japan

Figure 2.3-4 Distribution map of horizontal strain rates of the earth's crust caused by the dislocation of active faults

Figure 2.3-5 Distribution map of active faults by type

Figure 2.3-6 Loci of the maximum principal stress

Figure 2.3-7 Fault provinces of Japan

Figure 2.3-8 Geological structure of a reverse fault (Senya fault)

Figure 2.3-9 An example of an 'active fault zone'

Figure 2.3-10 Relationship between cumulative displacement along the fault and the width of shear (crushed) zone for major strike faults from throughout the world

Figure 2.3-11 Geological map along the Active Fault Survey Tunnel, Mozumi-Sukenobu Fault

Figure 2.3-12 Map showing the location and chemical compositions of spring waters and the locations where the water table dropped after the 1995 Hyogoken-Nanbu earthquake in the northern part of Awaji Island

Figure 2.3-13 Ratios of ground accelerations due to earthquakes at the K-6 seismograph and other seismographs in the Kamaishi mine

Figure 2.3-14 Relationship between the theoretical amount of strain and change in water pressure observed in boreholes drilled from gallery at the Kamaishi mine

Figure 2.4-1 Tectonic setting and distribution of Quaternary volcanoes in Japan

Figure 2.4-2 An example (Yotei volcano) of the contents of the Catalog of Quaternary Volcanoes in Japan

Figure 2.4-3a Histogram of volumes of the Quaternary volcanoes in Japan

Figure 2.4-3b Histogram of durations of activity of the Quaternary volcanoes in Japan

Figure 2.4-4a Temporal and spatial distribution of volcanoes during the Quaternary in

northeastern Japan

Figure 2.4-4b Temporal and spatial distribution of volcanoes during the Quaternary in southwestern Japan

Figure 2.4-5 Shift of volcanic front in northeast Japan

Figure 2.4-6 Temporal and spatial distribution of the eruptive centers of Quaternary volcanoes in the Sengan volcanic region

Figure 2.4-7 Distribution of volcanic rocks and plutonic rocks from the late Miocene

Figure 2.4-8 Histogram of distances from volcanoes formed within the last million years to the nearest earlier volcano in the Sengan volcanic area

Figure 2.4-9 Histogram of distances from volcanoes formed within the last hundred thousand years to the nearest earlier volcano in the Higashi-Izu monogenetic volcano group

Figure 2.4-10 Geothermal gradient map of Japan

Figure 2.4-11 Change in geothermal gradient with distance from volcanic centers

Figure 2.4-12aCross-sections showing the thermal structure of Hokkaido

Figure 2.4-12bCross-sections showing the thermal structure of northeast Honshu

Figure 2.4-12cCross-sections showing the thermal structure of Kyushu

Figure 2.4-13 Model of heat source (magma reservoir)

Figure 2.4-14 Temperature change around a magma reservoir

Figure 2.4-15 Geothermal cross-sections in the Hohi, Sengan and Kurikoma areas

Figure 2.4-16 Vertical one-dimensional groundwater flow model

Figure 2.4-17 Distribution of fluid flow velocity in vertical direction in the Sengan volcanic region

Figure 2.4-18 Distribution of fluid flow velocity in vertical direction in the Hohi volcanic region

Figure 2.4-19 Distribution map showing variations in pH in hot spring waters from Tohoku, northeast Japan

Figure 2.4-20 Distribution map showing variations in pH in hot spring waters from Kyushu

Figure 2.4-21 Change in the pH of hot springs from volcanic centers in the Sengan volcanic region

Figure 2.4-22 Relationship between anion index (A.I.) of hot springs and the distances from the centers of volcanoes

Figure 2.4-23 Change in groundwater $^{3}He/^{4}He$ ratio with distance from volcanic centers

Figure 2.4-24 Heat flow and changes in the pH of hot springs with respect to distance from a volcano

Figure 2.4-25 Relationship between average heat flow around volcanoes and spatial range of acid hot springs (pH<4.8)

Figure 2.4-26 Variation of mineral ages as a function of distance from the intrusive contact

Figure 2.4-27 Geological map of the Takahama district and locations of samples

Figure 2.4-28 Ages of each mineral plotted versus distance from the Takahama-Kuroiwa intrusive rock

Figure 2.4-29 Temperature around the Takahama-Kuroiwa intrusive rock estimated from mineral ages

Figure 2.5-1 Distribution of types of deformation in Japan, deduced from geological and geographical structures

Figure 2.5-2 Current elevations of former shorelines formed during the last interglacial maximum

Figure 2.5-3 Uplift rates estimated from height of former shorelines in areas characterized by each deformation type shown Figure 2.5-2

Figure 2.5-4 Height distribution of Stage 9 (about 320 ka) shoreline in the northern part of the Sanriku coast (Type C; unit:m)

Figure 2.5-5 Height distribution of Stage 5e (about 125 ka) shoreline in the Muroto Peninsula (Type D; unit : m)

Figure 2.5-6 Regional distribution of Quaternary basins

Figure 2.5-7a Burial depth and age of sediments in major Quaternary sedimentary basins in Japan

Figure 2.5-7b Accumulated subsidence in the main plains

Figure 2.5-8 Contour map showing base-level of the Quaternary sediments in the Shonai Plain, Japan Sea side of northeast Honshu

Figure 2.5-9 Geological structure of northeast Honshu

Figure 2.5-10 Strain distribution in northeast Honshu

Figure 2.5-11 Stress profile and tectonic data across the northeast of Honshu

Figure 2.5-12 Relationship between amount of uplift and formation age of marine terraces

Figure 2.5-13 Relationship between denudation rate and geology

Figure 2.5-14 Relation between denudation rate and meteoric precipitation

Figure 2.5-15 Distribution of denudation rates

Figure 2.5-16 Relationship between altitude and standard altitude dispersion

Figure 2.5-17 Denudation rate of different mountains calculated from altitude dispersion

Figure 2.5-18 Changes in mean altitude from various initial altitudes at different rates of uplift

Figure 2.5-19 Transition of erosion rate of rocky coast in the Holocene

Figure 2.5-20 Case study areas for denudation rate

Figure 2.5-21 Relationship between average denudation depth and formation age of several river terraces and one pyroclastic flow plateaus

Figure 2.5-22 Relation between uplift and denudation rates of marine terraces formed in the last interglacial stage

Figure 2.5-23 Denudation process of a riverbed (example of Kabura and Sagami rivers)

Figure 2.6-1 Sea-level changes during the past 350,000 years

Figure 2.6-2 Changes in oxygen isotope ratio during the last 300 ka and the definition of glacial and interglacial stages

Figure 2.6-3 Summary of benthic $\delta^{18}O$ records over the last 5 Ma

Figure 2.6-4 Sea level curve during the past 20ka

Figure 2.6-5 Shoreline of the last glacial maximum and mean annual surface air temperature of Japan

Figure 2.6-6 Mean annual air temperature at the surface and amount of precipitation over the last 100ka in Japan

Figure 2.6-7 Thickness of permafrost and mean annual surface air temperature

Figure 2.6-8 Distribution of permafrost and glaciers at 20ka ago

Figure 2.6-9a Growth of permafrost when annual mean surface air temperature decreases from 7 ℃ to -7℃ in 10^4 years

Figure 2.6-9b Subsurface temperature profile of Fig.2.6- 9a

Figure 2.6-10 Continuous $\delta^{18}O$ (‰) record of the GRIP ice core during the last 200,000 years

Figure 3.1-1 Characteristics of the geological environment of importance for a multibarrier system

Figure 3.2-1 Geological structures of significance to waste disposal

Figure 3.2-2 Structural elements relevant as transport pathways

Figure 3.2-3 Fracture patterns observed at the Kamaishi mine

Figure 3.2-4 Major fracture structures identified at the Kamaishi mine

Figure 3.2-5 Fracture geometry observed on the core sample in granite

Figure 3.2-6 Fracture density in different rock types

Figure 3.2-7 Stereographic projection of fracture orientations

Figure 3.2-8 Fracture map for Kikuma underground oil storage site

Figure 3.2-9 Fracture density distribution of granite

Figure 3.2-10 Flow compartments observed at the Kamaishi mine

Figure 3.2-11 Estimated transmissivity distribution based on in situ measurements at the Kamaishi mine

Figure 3.3-1 Conceptual illustration of groundwater flow

Figure 3.3-2 Histogram of near-surface hydraulic gradient for each topographic type

Figure 3.3-3 Histogram of hydraulic gradient calculated in the groundwater flow analyses in the Tono region

Figure 3.3-4 Relationship between topographic and hydraulic gradients

Figure 3.3-5 Histogram of hydraulic conductivity

Figure 3.3-6 Relationship between depth and hydraulic conductivity in granite

Figure 3.3-7 Ghyben-Herzberg's law between freshwater and seawater

Figure 3.3-8 Example of the groundwater flow simulation in the Tono region

Figure 3.3-9 Geological setting of the Tono mine

Figure 3.3-10 Subsurface hydrological investigation system

Figure 3.3-11 Hydrological-geological structure model for analysis of the Tono area

Figure 3.3-12 Piezometric head distribution along the bore holes measuring porewater pressure during sinking of the No.2 shaft

Figure 3.3-13 Comparison of simulated and measured nonsteady transition of inflows

Figure 3.3-14 Relationship between distance from No.2 shaft and decrease of hydraulic head

Figure 3.3-15 Modelling of a 3-dimensional channel network using Don-Chan model

Figure 3.3-16 Concentration of recovered tracer versus time after tracer injection; a comparison of measured values and values simulated by the Don-Chan model

Figure 3.4-1 Hexadiagrams illustrating the variation in groundwater chemistry as a function of depth

Figure 3.4-2 Basic approach for groundwater evolution model

Figure 3.4-3 Schematic view of the Tono research area

Figure 3.4-4 Changes in groundwater chemistry in sedimentary rocks in the Tono area as a function of depth

Figure 3.4-5 Microscopic and SEM observation of granite

Figure 3.4-6 Eh-pH diagrams of iron and sulfur species

Figure 3.4-7 Changes in groundwater chemistry in granite in the Tono area as a function of depth

Figure 3.4-8 Geochemical evolution of deep groundwater

Figure 3.4-9 Schematic view of the Kamaishi mine

Figure 3.4-10 Isotopic composition of the Kamaishi groundwater

Figure 3.4-11 Groundwater variations in the Kamaishi mine

Figure 3.4-12 Phase diagram and saturation index of the Kamaishi groundwater

Figure 3.4-13 Colloids particle sampled from groundwater in the sedimentary rocks at the Tono area

Figure 3.4-14 Bacteria observed in the granite of the Tono area

Figure 3.5-1 Histograms showing thermal conductivity

Figure 3.5-2 Distribution of thermal conductivity

Figure 3.5-3 Probability curve of thermal conductivity

Figure 3.5-4 Histograms showing specific heat

Figure 3.5-5 Distribution of specific heat

Figure 3.5-6 Probability curve of specific heat

Figure 3.5-7 Histograms showing coefficient of linear thermal expansion

Figure 3.5-8 Distribution of coefficient of linear thermal expansion

Figure 3.5-9 Probability curve of coefficient of linear thermal expansion
Figure 3.5-10 Correlation between depth and thermal properties
Figure 3.5-11 Distribution of geothermal gradients in Japan
Figure 3.5-12 Histograms showing effective porosity
Figure 3.5-13 Distribution of effective porosity
Figure 3.5-14 Probability curve of effective porosity
Figure 3.5-15 Histograms showing unconfined compressive strength
Figure 3.5-16 Distribution of unconfined compressive strength
Figure 3.5-17 Probability curve of unconfined compressive strength
Figure 3.5-18 Histograms showing Young's modulus
Figure 3.5-19 Distribution of Young's modulus
Figure 3.5-20 Probability curve of Young's modulus
Figure 3.5-21 Histograms showing Poisson's ratio
Figure 3.5-22 Distribution of Poisson's ratio
Figure 3.5-23 Probability curve of Poisson's ratio
Figure 3.5-24 Histograms showing tensile strength
Figure 3.5-25 Distribution of tensile strength
Figure 3.5-26 Probability curve of tensile strength
Figure 3.5-27 Histograms showing cohesion
Figure 3.5-28 Distribution of cohesion
Figure 3.5-29 Probability curve of cohesion
Figure 3.5-30 Histograms showing internal friction angle
Figure 3.5-31 Distribution of internal friction angle
Figure 3.5-32 Probability curve of internal friction angle
Figure 3.5-33 Relationship between unconfined compressive strength and other properties
Figure 3.5-34 Correlation between depth and rock physical properties
Figure 3.5-35 Distribution of initial stress as a function of depth
Figure 3.5-36 Layout and result of initial stress measurement at the Tono mine
Figure 3.5-37 Layout and result of initial stress measurement at the Kamaishi mine
Figure 3.5-38 Geology and in-situ experimental area at the Tono mine
Figure 3.5-39 Section view of No.2 shaft
Figure 3.5-40 Result of borehole expansion test in section B of No.2 shaft
Figure 3.5-41 Result of hydraulic test in section B of No.2 shaft
Figure 3.5-42 Measured and analysed strain variation due to shaft excavation
Figure 3.5-43 Layout of the excavation disturbance experiment by blasting in the NATM drift

at the Tono mine

Figure 3.5-44 Layout of the excavation disturbance experiment by mechanical excavation in the NATM drift at the Tono mine

Figure 3.5-45 Results of a geophysical survey of the EDZ in the Tono mine

Figure 3.5-46 Porewater pressure and hydraulic conductivity changes due to mechanical excavation in the Tono mine

Figure 3.5-47 Mesh layout and input data for numerical analysis of rock mass displacement

Figure 3.5-48 Rock mass displacements measured by extensometers compared to the numerical analysis using FEM

Figure 3.5-49 Layout of the excavation disturbance experiment in the 550 m level drift in the Kamaishi mine

Figure 3.5-50 Hydraulic conductivity and modulus of deformation changes due to KD-89 drift excavation at the Kamaishi mine

Figure 3.5-51 Layout of the excavation disturbance experiment in the 250m level drift of the Kamaishi mine

Figure 3.5-52 Result of seismic refraction survey (250m level drift of the Kamaishi mine)

Figure 3.5-53 Result of measurement using Pac-ex at the Kamaishi mine

Figure 3.5-54 Result of numerical analysis of rock mass stress (250m level drift of the Kamaishi mine)

Figure 3.5-55 Conceptual illustration of the geological environment surrounding a tunnel

Figure 3.6-1 Geological overview of the Tono mine and location of investigated sections

Figure 3.6-2 Natural uranium concentration in a sedimentary rock from the Tono mine

Figure 3.6-3 Pathways for nuclide migration in sedimentary rocks

Figure 3.6-4 Natural uranium retardation associated with iron-containing minerals in sedimentary rocks from the Tono mine

Figure 3.6-5 Batch Kd values for various sedimentary rocks from the Tono mine and their constituents

Figure 3.6-6 Geochemical processes of ^{238}U-decay series in sedimentary rocks from the Tono mine

Figure 3.6-7 Iron and ^{238}U-decay series profiles from a water-conducting fracture into the Toki granite matrix

Figure 3.6-8 In situ connected porosity behind a water-conducting fracture in a crystalline rock from the Kamaishi mine

Figure 3.6-9 Pathways for nuclide migration in fractured crystalline rocks

Figure 3.6-10 Distribution of *in situ* connected porosity behind a water-conducting fracture in Kurihashi granodiorite at the Kamaishi mine

Figure 3.6-11 Small-scale conceptual model of a water-conducting fracture in Kurihashi granodiorite at the Kamaishi mine

Figure 3.6-12 ^{238}U-decay series profiles from a water-conducting fracture into Kurihashi

granodiorite matrix at the Kamaishi mine

Figure 3.6-13 Retardation of different inactive tracers in a water-conducting fracture in Kurihashi granodiorite at the Kamaishi mine

Figure 3.7-1 Concentration profile of uranium in Tsukiyoshi fault, Tono uranium deposit

List of Tables

Table 2.3-1 Major inland earthquakes and their associated surface fault

Table 2.3-2 Characteristics of fault provinces in Japan

Table 2.5-1 Methods for estimating uplift and subsidence

Table 2.5-2 Examples of uplift rates in "fold and fault" type areas

Table 2.5-3 Examples of uplift rates in "reverse fault block" areas

Table 2.5-4 Examples of uplift rates in "lateral-slip fault block" type areas

Table 2.5-5 Examples of uplift rates in "warping" type areas

Table 2.5-6 Uplift rates estimated from deformed marine terraces

Table 2.5-7 Uplift rates around the Sagami Bay

Table 2.5-8 Examples of amounts of subsidence in major plains and basins in Japan

Table 2.5-9 Processes responsible for denudation

Table 2.5-10 Denudation rates estimated from the volume of sediments in major dams in Japan

Table 2.5-11 Denudation rates estimated from the volumes of alluvium and alluvial fans

Table 2.5-12 Rates of marine erosion in the Holocene

Table 2.5-13 Denudation rates estimated from the volumes of valleys that dissect terraces

Table 2.5-14 Deepening rates of riverbeds

Table 2.5-15 Examples of weathering rates of rocks

Table 2.6-1 Main indicators of Quaternary paleoclimate

Table 3.1-1 Information on characteristics of the geological environment

Table 3.3-1 Hydraulic conductivity of fault and fracture zones

Table 3.3-2 Water balance of the Shoma river area and the Tono mine area

Table 3.4-1 Groundwater chemistry in the Tono area

Table 3.4-2 Chemistry of the Kamaishi groundwater

Table 3.4-3 Redox potential and pH of groundwater in Japan

Table 3.4-4 Chemistry of the Horonobe groundwater

Table 3.4-5 Trace element concentrations and the organic component in the Tono groundwater

Table 3.4-6 Characterization of microbial activities in the groundwater at the Tono area

Table 3.5-1 Statistical table of physical properties of rocks in Japan

Chapter I

Introduction

Chapter I Introduction

1.1 The role of the geological environment in deep disposal

1) The geological disposal concept and mechanisms for ensuring safety

The concept of geological disposal involves isolating high-level radioactive waste (HLW) from the human environment for long periods of time, thereby ensuring that future generations are not adversely affected by the waste. It is proposed to accomplish this by solidifying the HLW into a stable vitrified waste form and then disposing of it deep in a stable geological environment using an appropriate engineered barrier system (EBS). The current assumption is that disposal will take place at a depth of several hundred meters up to 1000 m and that the repository will have an areal extent of several square kilometers. The possibility that HLW disposed of in such a manner might affect the human environment is considered in two main scenarios.

The first of these is associated with physical proximity of the HLW to the human environment and is known as the "isolation failure scenario". This scenario considers the possibilities that waste might be ejected by volcanic eruption or the repository exposed by erosion.

The other scenario considers transport of radionuclides from the waste to the human environment with flowing groundwater and is termed the "groundwater scenario". In this scenario, the most important processes are considered to be the chemical reactions controlling the dissolution of radionuclides from the waste and the flow of groundwater.

To limit the effects on a HLW repository of processes represented in the above scenarios, the following measures are considered necessary. The selected disposal site has to be in a stable geological environment which is not expected to be adversely affected by future tectonic activity over long periods of time. In addition to this, an appropriate multibarrier system has to be developed, providing an optimized combination of an EBS and the geological disposal medium. Currently, it is planned to seal the vitrified waste in a metal overpack and to surround the resulting waste packages, emplaced in suitable underground cavities, with a clay buffer material.

2) The expected role of the geological environment

It is expected that the geological environment will play the following roles in ensuring the safety of HLW disposal:

i. Firstly, it will physically isolate the waste and maintain a sufficient distance between the waste and the human environment for a sufficiently long period of time. In order to achieve this goal, it is important to select both an appropriate location and an adequate depth for the repository. This approach will ensure that natural phenomena do not degrade the repository or the surrounding rock formations significantly.

ii. The second role is to maintain an environment that is favorable for the functioning of the EBS. It is expected that the properties of the groundwater and the rock formations around the EBS will contribute to maintaining the performance of the EBS and that favorable conditions will be maintained for a considerable length of time. It is particularly important to design and construct the EBS appropriately, in accordance with the site-specific conditions of the geological environment.

iii. The third role of the geological environment is to function as a natural barrier to radionuclide migration. Even if radionuclides are released from the EBS to the geosphere, their migration should be limited by the slow movement of groundwater and retarded by interactions with the groundwater and minerals present along the transport pathways in the rock. It should also be noted that a function of a natural barrier is that radionuclides will be dispersed and diluted in rock formations as they migrate in the groundwater.

If a geological environment is to perform these roles, then the physical and chemical characteristics of the rock formations and groundwater therein (hereafter "**characteristics of the geological environment**") should remain suitable for a sufficiently long period of time to allow the multibarrier system to perform adequately. This goal can be achieved by selecting a sufficiently stable location and by taking appropriate engineering measures.

Potentially, these characteristics of the geological environment may be perturbed by both natural phenomena and future human activities. Future human intrusion into the deep underground environment may occur during exploration for, or acquisition of, underground resources. Therefore, when planning a repository, it is necessary to avoid regions that have deep, underground natural resources that may be exploited in the future. The distribution of underground resources in Japan is currently well documented, as described in H3 (PNC, 1992). It can be stated confidently that many areas of Japan have no significant natural resources and that most resources that do occur are small and not presently economically viable. In addition, the absence of underground resources at any future candidate disposal site can be confirmed during field investigations. For these reasons, this report does not discuss underground resources in Japan further.

Rather, from the perspective of HLW disposal in Japan, tectonic processes are the most important influence on the characteristics of the geological environment. Potentially suitable repository host rocks should be located in environments that are sufficiently stable from a tectonic viewpoint. Hereafter, long-term tectonic stability is referred to as the "**long-term stability of the geological environment**". This does not mean that all aspects of the geological environment have to remain completely unchanged over the required periods of time. Instead, it means that the ranges over which the conditions may vary should have an insignificant effect on the performance of the multibarrier system (Figure 1.1-1). The consequences of climatic change will be superimposed upon these tectonic effects.

3) The long-term stability of the geological environment

In order for the geological disposal system to perform its desired function in ensuring safety, the geological environment at a disposal site must maintain favorable environmental conditions and functions for a long period of time. It is important to study the natural phenomena that will potentially have most influence on the long-term stability of the geological environment and to thoroughly understand their characteristics and effects. In particular, as Japan is located in one of the most tectonically active regions in the world, sufficient attention must be paid to tectonic movements and related phenomena, such as volcanism and faulting.

In Japan, it is important to understand the effects and spatial distributions of the following natural phenomena (see Chapter II, Section 2.1.1):

i. fault movement

ii. volcanic activity
iii. uplift and denudation
iv. climatic and sea-level changes.

In subsequent discussions, the term "**natural phenomena**" is understood to mean these four phenomena, which are considered further in Chapter II.

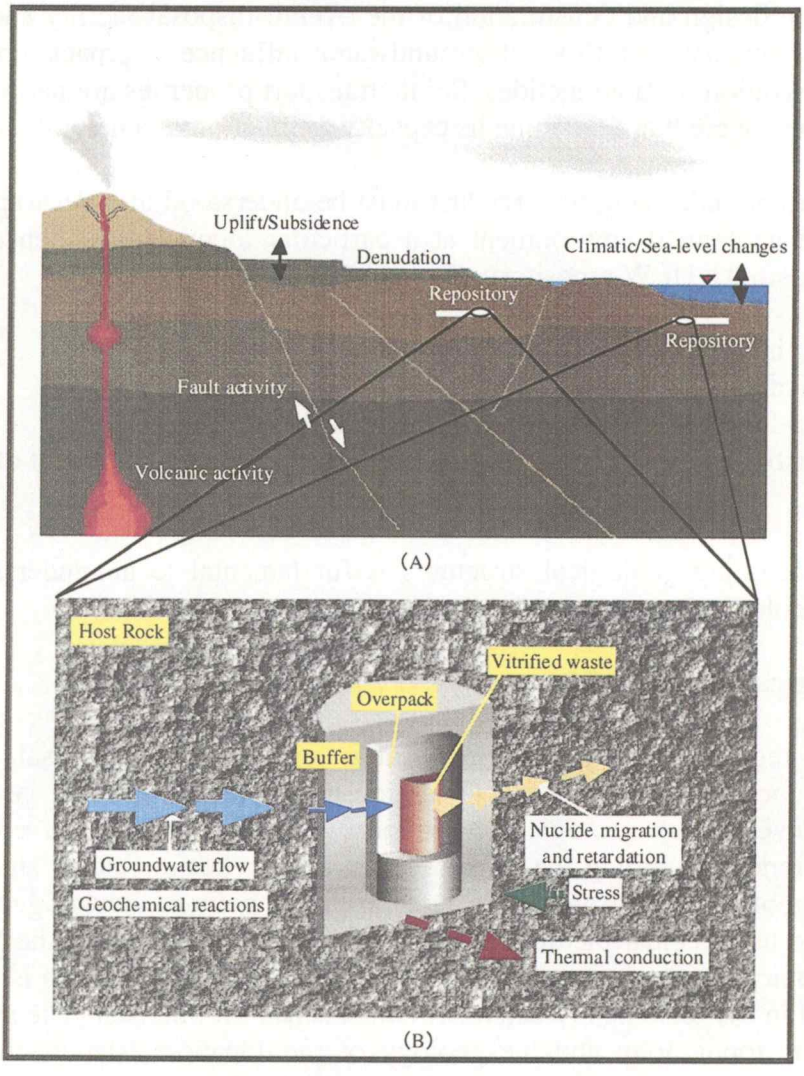


Figure 1.1-1 Natural phenomena to be considered in geological disposal (A) Reactions and processes in rocks and groundwater (B)

The general features of these natural phenomena were summarized in H3, which demonstrated the possibility of evaluating future activities of natural phenomena based on records of past activities. As stated in the AEC Guidelines (AEC, 1997), "sudden natural phenomena", such as abrupt fault movements and volcanic activity, have occurred in the past over relatively limited geographic ranges. Therefore, the effects of these phenomena can be estimated from local records of past activities. Records of past spatial distributions of these phenomena can be used to site a repository in such a way as to reduce to an acceptably low level the probability that their future effects will be significant. On the other hand, the future

effects of "gradual natural phenomena" can be estimated using regional, relatively accurate topographic and geological records. Processes that fall into this second category include uplift/subsidence, denudation, sedimentation, climatic changes and sea-level variations.

4) Important characteristics of the geological environment

The most relevant characteristics of the geological environment are those that potentially affect the construction, installation and performance of the EBS and the functioning of the geosphere as a natural barrier. For example, rock mechanical and thermal properties are important for the design and construction of the overall disposal facility and the engineered barriers. The chemistry and flow of groundwater influence overpack corrosion and the leaching and migration of radionuclides. Solute transport properties are particularly important aspects of the geosphere that determine its capacity to function as a natural barrier.

The most important underlying features that must be understood in order to predict the future behavior of the geological environment at a particular location, and hence to evaluate its suitability for hosting a HLW repository, are:

i. forces driving groundwater flow
ii. geochemical characteristics of the groundwater
iii. thermal and mechanical properties of the rock mass
iv. characteristics of the rock that control mass transport (e.g. movement of solutes and water).

Information concerning geological structures is fundamental to an understanding of these aspects of the geological environment.

1.2 Geological features of Japan

Basic thinking regarding the concept and safety of geological disposal is more or less common to all countries which are implementing R&D programs on the geological disposal of HLW. However, since geological conditions vary from country to country, there are inevitably differences regarding the priorities and approaches of related studies. In order to understand the geological environment of Japan from the point of view of geological disposal, it is necessary to have a clear picture of the geological characteristics of the Japanese islands. While the geological environment of much of Europe and North America is relatively stable, Japan is located in the tectonically active Circum-Pacific Mobile Belt. The nature of this belt is evident in the topography and the geology of the Japanese islands; the topography is mountainous and rugged, there are many volcanoes and volcanic rocks are widely distributed. The geological environment consists of many different rock types and geological structures and the geographic position of the islands plays an important role in controlling the movement of groundwater and other related phenomena.

1) Tectonic setting of Japan

The Japanese islands comprise a narrow island arc extending along the eastern margin of the Asian continent. A narrow trench, up to 8,000 m in depth, runs parallel to the islands on the oceanic (Pacific Ocean) side. On the islands, volcanic belts occur parallel to the trench and uplift and subsidence, seismic activity and faulting are observed. Such natural activities are controlled mainly by the configuration of the tectonic plates and their mode of movement.

The Japanese islands straddle the Eurasian and North American continental plates. On the

Pacific Ocean side, the Pacific Ocean and Philippine Sea plates are subducted under the islands (see also Figures 2.2-1, 2.4-1). The volcanic activity of the Japanese islands is related to the depth of subduction of these oceanic plates; hence, volcanoes do not exist on the Pacific Ocean side of northeast Japan, where the subducted plate is at shallow depth. Crustal movements, such as faulting, uplift and subsidence, are related to the magnitudes and orientations of the stresses generated by the collision and subduction of the plates. This is illustrated by the fact that the arcuate form of the islands and the distribution of the mountainous terrain are normal to the direction of subduction of the oceanic plates beneath the continental plates.

2) Distribution of geological units

The tectonic setting of the Japanese islands is reflected in the distribution of geological formations. The present geology of Japan consists of numerous rocks types with diverse geneses and ages. Japan is also transected by tectonic lines (major structural discontinuities) and thus the geological strata and rock bodies can be fragmented. The distribution of rocks in Japan is documented in various geological maps published by the Geological Survey of Japan (GSJ). These show that, of the rocks exposed at the surface, sedimentary rocks occupy slightly under 60% of the area, igneous rocks somewhat less than 40% and metamorphic rocks about 4%. At the depth targeted for geological disposal, however, the area occupied by sedimentary rocks is believed to be smaller than at the surface.

There are numerous volcanoes and volcanic rocks are widely distributed in volcanic regions. In non-volcanic regions, the geosphere is generally composed of basement rocks, consisting of pre-Neogene sedimentary rocks and crystalline (igneous and metamorphic) rocks and overlying younger sedimentary rocks or unconsolidated sediments. However, the thickness of the sedimentary cover differs from place to place, and the basement rocks directly crop out in some areas.

3) Geographic conditions

Japan has a rugged topography. Hills and mountainous areas, including volcanoes, occupy a large part of the country and, in many areas, mountains are close to the coast. These factors have a significant influence on the behavior and chemistry of the groundwater.

In addition, a relatively temperate climate, abundant rainfall and an island geography are important features. The groundwater level is generally high in Japan and rock formations are saturated nearly to the surface. Freshwater that originates as meteoric precipitation tends to flow from the land towards the coast following topographic gradients. Near the coast, this freshwater will tend to overlie, and mix with, more dense saline water that originates in the ocean. Therefore, near the coast, there is an underground transition between shallower freshwater and deeper saline water (Figure 1.2-1).

1.3 Studies of the geological environment

1.3.1 Approaches

1) Basic concept

Government policy regarding research into geological aspects of deep disposal of HLW has been to consider general issues and not to restrict research to particular locations or geological environments/rock types. The report entitled "Radioactive Waste Processing and Disposal Measures (Interim Report)" (AEC, 1984) stated that "...it is now clear that, with the exception of clearly inferior rocks such as unconsolidated material, a broad range of rocks can be

considered as 'effective geological units' for geological disposal in Japan". This statement indicates that there is the "prospect of securing safety of the geological disposal system through installing appropriate engineered barriers in accordance with the geological conditions, rather than specifying the types of rocks". This approach of investigating a number of geological environments has been maintained to the present day and it is stated in the "Long-Term Program for Research, Development and Utilization of Nuclear Energy" (AEC, 1994) that "In R&D at present, consideration should be given to a broad range of geological environments".

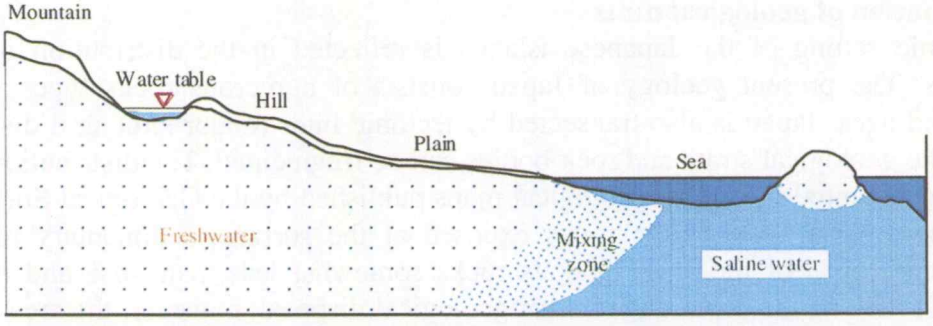


Figure 1.2-1 Schematic illustration of topography and groundwater flow in Japan

However, the nature of the geological environment can vary considerably depending on a number of factors (e.g. rock type, geological structure, topography, climate and depth). As yet, specific disposal sites have not been identified. Therefore, it is important firstly to define what are considered to be potentially suitable geological environments in Japan and then to determine the evolution of these environments and evaluate the implications for the performance of a multibarrier system.

2) Study methods

In order to understand the nature and likely evolution of potentially suitable geological environments in Japan, it is necessary to collect data on geology, hydrogeology and hydrochemistry and to study the effects that relevant natural phenomena could have on a disposal system. Information on the geological environment of Japan has been collected primarily by conducting literature surveys.

Most of the information, however, was not acquired from the point of view of HLW disposal and high quality information on the relevant characteristics of deep geological environments (e.g. the flow and chemistry of deep groundwater and solute transport within rock masses) is therefore limited. To acquire such fundamental data, it is necessary to carry out in situ studies of geological environments. As part of these studies, the temporal and spatial scales of the geological disposal system must be taken into account and systematic data must be acquired on the spatial distribution and temporal changes in rock and groundwater properties. With these objectives in mind, integrated studies have been conducted, including the development and testing of relevant technologies for site investigation and analytical techniques. Such studies were carried out in the Tono area (Tono mine and vicinity) in Gifu Prefecture and the Kamaishi mine in Iwate Prefecture, using existing underground tunnels and new boreholes. These studies are referred to collectively as "**geoscientific studies**". Their objective is to investigate the nature of the deep geological environment and the natural processes and

reactions occurring there. The results of these studies are compared with existing literature data and examined with reference to theoretical analyses and experimental results.

To investigate the effects of natural phenomena on the stability of the geological environment, it is necessary to acquire quantitative data, with sufficient spatial and temporal resolution, on the distributions and magnitudes of these phenomena. This information is then used to evaluate the possibility that these phenomena will occur at any given location. For this purpose, other important aspects of geoscientific studies are case studies of regions for which clear geological records of the histories of natural phenomena exist. The objective of these studies is to investigate the past activity of natural phenomena and their effect on the geological environment. Although the geological evolution of the earth (from its formation 4.6 billion years ago) is not fully understood, information from the most recent geological period, the Quaternary (from 1.7 million years ago to the present), is generally more abundant and data are often more accurate. The activities of natural phenomena and their effects on the geological environment during the Quaternary (particularly the last one hundred thousand to several hundred thousand years) have been examined using topographic and geological records in order to clarify spatial patterns and temporal trends, thereby providing some indication of future potential changes and their possible effects on the geological environment.

Geoscientific studies aim to consolidate and integrate the general understanding of the geological environment of Japan and are, therefore, distinct from a site selection program. The results of geoscientific studies are expected to contribute widely to earth science in general as well as to form the basis of an R&D program for geological disposal (Figure 1.3-1).

1.3.2 Assessments and requirements stipulated by the Government

1) Government assessment of H3

In the report entitled "Research and Development on Geological Disposal of High-Level Radioactive Waste, First Progress Report – 1991" ("H3"; PNC, 1992), information on the geological environment of Japan was presented from the viewpoint of geological disposal and the report submitted to the Government for review.

In its report "On the Progress of Research and Development in Geological Disposal of High-Level Radioactive Waste" (AEC, 1993), the AEC finds, with reference to H3, that "...information concerning the geological environment has been systematically extracted and organized for future use in geological disposal from information and data accumulated in the earth sciences. The development of site investigation techniques for acquiring accurate and precise geological environmental data has also been reviewed. Data on the deep subsurface geological environment are being acquired as necessary information for performance assessment (PA). The availability of measured data is limited and it is therefore clear that further data acquisition is necessary". This report further states, regarding future issues, that "The focus should be on geological environmental conditions important for long-term safety and on the development and improvement of site investigation techniques and instrumentation for determining the characteristics of deep geological environments, including geological structure, distribution of rock formations, rock mechanics and hydrogeological and geochemical characteristics of groundwater. At the same time, the influence of the following natural phenomena - igneous activity, seismic activity, fault movements, uplift and denudation, climatic changes and sea-level changes- on the multibarrier system should be assessed".

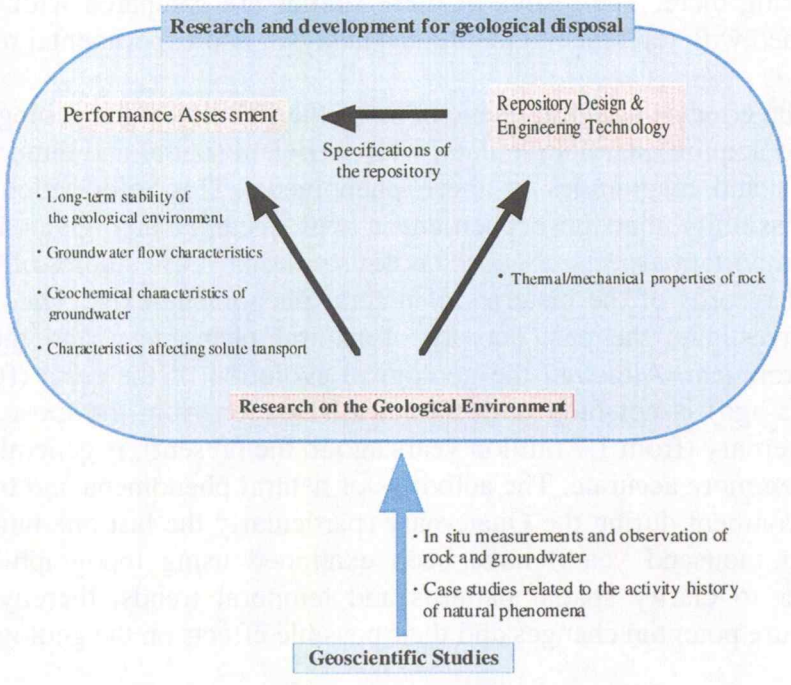


Figure 1.3-1 Research and development for geological disposal

2) Studies subsequent to H3

In order to respond to the recommendations of the Government, the geoscientific studies in the Tono area and Kamaishi mine were expanded. Techniques and instrumentation for accurate measurement of the features of deep geological environments were developed and additional data acquired regarding groundwater flow and chemistry and rock mechanical properties. In situ conditions at depths down to 1000 m have been investigated.

State-of-the-art-reviews have been carried out of important natural phenomena, such as volcanic and fault activity. Field-based case studies have also been performed and information on past records of natural phenomena and their influence on the geological environment has been collected and evaluated.

The results of these studies have been reported to relevant scientific organizations and the overall results have been summarized and reported in the public domain (PNC, 1993, 1994, 1996).

3) The objectives and content of H12

In April 1997, the AEC's Advisory Committee on Nuclear Fuel Cycle Backend Policy issued a report entitled "Guidelines on Research and Development Relating to Geological Disposal of High-Level Radioactive Waste in Japan" (the "AEC Guidelines"; AEC, 1997). The report stated that "demonstrating the technical reliability and safety of the geological disposal concept for HLW" should be the target for H12. In order to accomplish this, it was indicated that there was a need to demonstrate: 1) the presence of geological environments suitable for geological disposal, 2) the technical feasibility of constructing engineered barriers and disposal facilities, and 3) the long-term safety of the geological disposal system. This demonstration had to be based on reliable data.

To meet these objectives, it was necessary to obtain measured data and a thorough

understanding of the properties of deep groundwaters and rock formations. In addition, accurate information on natural phenomena that may possibly affect the geological environment had to be accumulated and processed. The aim was to confirm that there is sufficient evidence to show that areas of Japan exist where these natural phenomena will not affect the safety of a repository to an unacceptable extent.

Following the basic approach to research and development described in the AEC Guidelines, JNC identified the following major research targets for H12:

i. to estimate future activities of natural phenomena that may affect the deep geological environment, by considering the regularity of past activity indicated by geological records;
ii. to demonstrate the possibility that sufficiently stable geological environments for HLW disposal exist in Japan;
iii. to summarize the general characteristics of rock formations and groundwater that are relevant to HLW disposal in Japan, using information collected in the fields of earth science and civil engineering and information from more detailed studies in the Tono area and the Kamaishi mine.

The AEC Guidelines list the following items as technically important issues for accomplishing the above R&D target.

(1) Information on the long-term stability of the geological environment
Acquire and process information concerning the characteristics of the following natural phenomena and their effect on the geological environment:

i. Fault activity: the history and pattern of active fault movements; the range of their effects on the surrounding geological environment; the effects of seismic activity on groundwater flow and chemistry.
ii. Volcanic activity: the scale, regional distribution, temporal changes and mechanisms of activity; the distribution of geothermal systems; thermal effects on the geological environment.
iii. Uplift/subsidence and denudation: the scale and rate of changes; regional distribution; time-dependence and mechanisms.
iv. Climatic and sea-level changes: pattern and scale of changes; effects on denudation and groundwater flow.

(2) Information on the characteristics of the geological environment
Assuming that the target depth of the repository is up to 1000 m, to acquire and process the following data:

i. Geological structure: the nature and distribution/continuity of rock formations; characteristics of fault crushed zones (as basic information on groundwater flow, geochemistry, rock mechanics).
ii. Groundwater flow: groundwater recharge; permeability of rock formations; distribution of hydraulic gradients.
iii. Groundwater geochemistry: chemical composition; redox potential.
iv. Rock mechanics: physical properties; dynamic properties; stress distribution; effect of tunneling on rock masses.
v. Solute transport: flowpaths and mechanisms of solute transport; sorption and retardation

capabilities of rock masses (based on their pore structure and mineralogical characteristics).

(3) Investigation technologies for the deep geological environment

With the assumption that the target depth of the repository is up to 1000 m, to develop, improve and establish site investigation technologies and equipment for acquiring reliable data with minimum disturbance to the geological environment.

i. Development of groundwater investigation equipment: hydrogeological testing equipment such as crosshole hydraulic test systems; hydrochemical testing equipment such as packer-type groundwater samplers.
ii. Improvement of geophysical surveying technology: resistivity and seismic tomography; radar reflection method.
iii. Establishment of a site investigation methodology: examination of investigation methods and applicability of equipment through field testing; confirmation of the quality and accuracy of acquired data; combination of various equipment and methods.

(4) Information from natural analogue studies

The results acquired through research on uranium deposits will be examined to investigate how it can be used most effectively in PA and site characterization programs.

References

AEC (1984) : Radioactive Waste Processing and Disposal Measures (Interim Report), the Advisory Committee on Radioactive Waste Management, the Atomic Energy Commission of Japan (in Japanese).

AEC (1993) : On the Progress of Research and Development in Geological Disposal of High-Level Radioactive Waste, the Advisory Committee on Radioactive Waste Management, the Atomic Energy Commission of Japan (in Japanese).

AEC (1994) : Long-term Program for Research, Development and Utilization of Nuclear Energy, the Atomic Energy Commission of Japan.

AEC (1997) : Guidelines on Research and Development Relating to Geological Disposal of High-level Radioactive Waste in Japan, Advisory Committee on Nuclear Fuel Cycle Backend Policy, Atomic Energy Commission of Japan.

PNC (1992): Research and Development on Geological Disposal of High-level Radioactive Waste, First Progress Report - H3. PNC TN 1410 93-059.

PNC (1993) : Special number for Research and Development on Geological Disposal of High-level Radioactive Waste, PNC Technical Review, No.85, PNC TN1340 93-001 (in Japanese).

PNC (1994) : Present status of Research and Development on Geological Disposal of High-level Radioactive Waste, PNC TN1410 94-094 (in Japanese).

PNC (1996) : Present status of Research and Development on Geological Disposal of High-level Radioactive Waste, PNC TN1410 96-071 (in Japanese).

Chapter II

Long-term Stability of the Geological Environment of Japan

Chapter II Long-term Stability of the Geological Environment of Japan

The first requirement for geological disposal of HLW in Japan is to select a sufficiently stable geological environment and then, to ensure safety, to construct an appropriate engineered barrier system (EBS) in this environment. As yet, as a specific site has not been selected and the aim of current research is to demonstrate that such an environment can be found in Japan. Research related to this subject has to investigate the possible future occurrence and extent of natural phenomena and their potential effects on the geological environment, based on past geological records.

There is a large body of scientific literature which covers relevant natural phenomena. In H3, a review of this literature was presented, which recognized that there is some kind of order (e.g. pattern of spatial distribution, trend of temporal change) to the occurrence of natural phenomena. Based on this, it was concluded that future occurrences of natural phenomena could be predicted. Since publication of H3, in order to demonstrate the existence of sufficiently stable geological environments in Japan, more relevant data based on recent scientific advances and field-based case studies conducted by JNC have been taken into consideration. Based on these data, the possible occurrence, variability and effects of natural phenomena are examined.

This chapter describes the results of this research. The fundamental points to be discussed are listed in Section 2.1. The tectonic evolution of the Japanese islands is examined in Section 2.2, in the light of recent developments in earth science. Section 2.3 and the following sections are devoted to individual natural phenomena, with emphasis on their spatial and temporal distribution and their effects on the geological environment.

2.1 Research on the long-term stability of the geological environment

2.1.1 Natural phenomena relevant to the long-term stability of the geological environment

The IAEA has prepared a comprehensive list of natural phenomena that may affect the long-term stability of geological environments. This list includes all the important factors to be considered when selecting candidate disposal sites and conducting a PA (IAEA, 1985, 1994). However, when defining criteria for assessing repository performance, each country emphasizes natural phenomena that are relevant to its own tectonic setting and natural conditions (e.g. USDOE, 1982; Nagra, 1985; AECL, 1994; SKB, 1994). For example, in northern European countries, it is assumed that glaciers will form 10,000 years or so from now (e.g. SKI, 1995), but volcanic activity is considered unimportant. In contrast, the study performed at Yucca Mountain in the USA emphasized the importance of local volcanic activity (e.g. NRC, 1995).

This chapter focuses on the following "natural phenomena" that are particularly important for Japan (Figure 2.1-1):

i. fault movement
ii. volcanic activity
iii. uplift and denudation
iv. climatic and sea-level changes.

These natural phenomena have been defined taking into account the natural features of the Japanese islands and examples in other countries. The four groups are also regarded as standards in the guidelines issued by the IAEA and other countries. Natural phenomena that do not fall into any of the four groups, but which are cited in some guidelines, include diapirism of rock salt and the impact of large meteorites. However, the former does not exist in Japan and the latter occurs very rarely (Shimizu and Ishimaru, 1993; Goodwin et al., 1994). Additionally, a large meteorite impact would have a massive destructive effect on the human environment that would far outweigh any influence caused by releases from a repository. Therefore, both diapirism and meteorite impacts have been excluded from further consideration here.

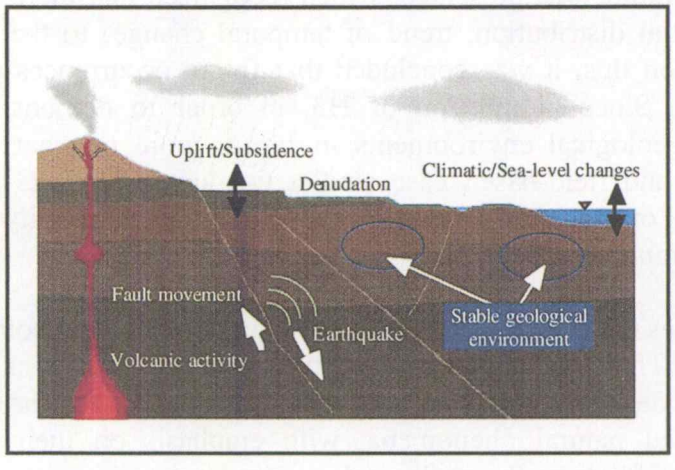


Figure 2.1-1 Natural phenomena affecting the long-term stability of the geological environment

In Japan, both volcanic activity and/or major fault movement could potentially have a catastrophic impact on any underground disposal system placed in the vicinity of faults or volcanoes. However, the most significant effects of volcanoes and major fault movements are geographically restricted and it is therefore possible to site a repository so as to reduce, to an acceptably low level, the probability that these phenomena may have significant effects.

Nevertheless, the effects of some phenomena, such as regional uplift/subsidence and denudation/sedimentation, accumulate over long time periods. It is necessary to understand their spatial extents and to predict their cumulative effects over timescales relevant to PA, to ensure that a repository can be suitably designed and sited.

Since Japan is located at a middle latitude, where the climate is relatively temperate, the land is expected to remain free of extensive glaciers during cold climatic periods that cause ice sheets to develop further north. However, it is expected that, in Japan, such climatic variations will cause changes in temperature and the amount of meteoric precipitation. These changes will in turn affect denudation rates and groundwater flow. In the latter case, the effects will be greater and earlier at shallow depths than at greater depth. It is also anticipated that sea-level changes may alter the distribution of the seawater/freshwater transition zone in coastal areas of Japan.

2.1.2 Predictive evaluation of natural phenomena in the future

The basic approach used to estimate activities of natural phenomena in the future is to make extrapolations from their occurrence in the past. To achieve this in connection with HLW disposal, it is important to understand the activities of relevant natural phenomena on scales of time and space that are relevant to PA and the design of a disposal facility.

The general spatial distributions and effects of natural phenomena in Japan are readily understandable. For example, there is a general consensus of scientific opinion that fault movements have a certain periodicity and volcanic activity occurs in specific regions. Present geological and topographic features record occurrences of these phenomena in the past. This evidence can be used to determine trends or patterns in the various natural phenomena, allowing the likelihood of natural phenomena occurring in the future and the scale of the associated changes to be estimated.

A time cut-off for PA has not yet been established in Japan. However, the AEC Guidelines state that JNC should consider a future time interval of 100,000 years, using geological evidence for the last several hundred thousand years. This timescale is relevant only for the study of the natural phenomena presented here, as defined by the AEC Guidelines, and is distinct from the timescale that would be considered by a PA.

In Japan, natural phenomena are controlled by the configuration and relative movements of the tectonic plates. The tectonic setting of the Japanese islands has not changed at least over the last several hundred thousand years, as described in the next section. Consequently, when estimating future spatial distributions of natural phenomena in Japan for the next hundred thousand years, it is reasonable to consider that the patterns and trends in tectonic activity over the past several hundred thousand years will continue. It is also justifiable to assume that geological phenomena caused by the tectonic setting of Japan will progress with predictable trends for at least the next hundred thousand years. However, confident prediction of these effects requires a detailed understanding of regional tectonic variations and an appreciation of the uncertainties associated with these assessments in each region considered.

2.2 Tectonics of the Japanese islands

2.2.1 Plate movements in the Japanese islands and the adjacent sea areas

The Japanese islands and the adjacent sea areas are located near the margins of the Pacific Ocean, Philippine Sea, Eurasian and North American plates (Figure 2.2-1). The Pacific Ocean plate is subducting beneath Hokkaido and northeast Japan along the Chishima Trench, Japan Trench and Izu-Ogasawara Trench. The Philippine Sea plate is subducting beneath Kanto and southwest Japan along the Sagami Trough and Nankai Trough. Based on a plate movement model (DeMets et al., 1990), Seno (1993) calculated relative velocities between the neighboring plates around the Japanese islands 8.4 to 8.7 cm per year along the Chishima and Japan Trenches between the Pacific Ocean and North American plates and 0.7 to 1.1 cm per year along the eastern margin of the Japan Sea between the North American and Eurasian plates, respectively. They range from 3.1 to 7 cm per year between the Eurasian and Philippine Sea plates and from 2 to 6 cm per year between the Pacific and Philippine Sea plates, respectively.

The Pacific Ocean plate, subducting towards the Chishima, Northeast Japan and Izu-Ogasawara Arcs, started expanding and growing from the Jurassic to Cretaceous. A temporal change in movement of the Pacific Ocean plate is evidenced by the arrangement of volcanic seamount ranges produced by a hot-spot: it continued to move in a definite direction between 15 Ma ago and 5 to 2.5 Ma ago, when it changed counterclockwise movement, giving rise to an increase in the subduction rate towards the Japanese islands (Cox and Engebretson, 1985; Pollitz, 1986). Since the present Pacific Ocean plate is moving westwards, it subducts obliquely towards the Chishima Arc and normally towards the Northeast Japan Arc.

The Philippine Sea plate is divided into the Shikoku and Philippine Basins by the Kyushu-Palau Ridge. These two basins, which are subducting towards the Southwest Japan Arc and the Ryukyu Arc, respectively, are marginal seas that started expanding and growing around 27 to 23 Ma ago (Nishimura and Yuasa, 1991; Okino et al., 1998; Kasuga et al., 1999). While the Philippine Sea plate is thought to have started subducting northwards after the formation of the Shikoku Basin (Seno and Maruyama, 1984; Nishimura and Yuasa, 1991), the subduction was presumably interrupted in the late Miocene (Uto, 1995). Subsequently, the plate resumed a northwestwards subduction around 6 Ma ago, which is supported by the relationship between the length of the subducting slab and the convergence rate of the plate (Kobayashi and Isezaki, 1976; Matsubara, 1980), the deposition age of turbidites on the southern side of the Nankai Trough (Seno and Maruyama, 1984) and the formation age of geological structures of the outer ridge-forearc basin zone of southwest Japan (Sugiyama,1991). The Philippine Sea plate, which is moving towards the northwest at the moment, is subducting obliquely towards the Southwest Japan Arc and normally towards the Ryukyu Arc, respectively.

Tectonic profiles representing the transitional zones from land to sea in the respective island arcs are shown in Figure 2.2-2 (Hino, 1999). The subduction angle of the oceanic crust in the forearc regions in all of the subduction zones ranges from 5 to 10°, which is nearly equal to the average inclination of the sea bottom forming the land-side slope of the respective deep-sea trenches. However, the subduction angles of the oceanic crust estimated from the hypocenter distribution in the subduction zones are significantly larger than the above-mentioned values, indicating an abrupt change in inclination of the oceanic crust after the subduction in trenches. The clearest bending of the oceanic crust on the land side of the trench

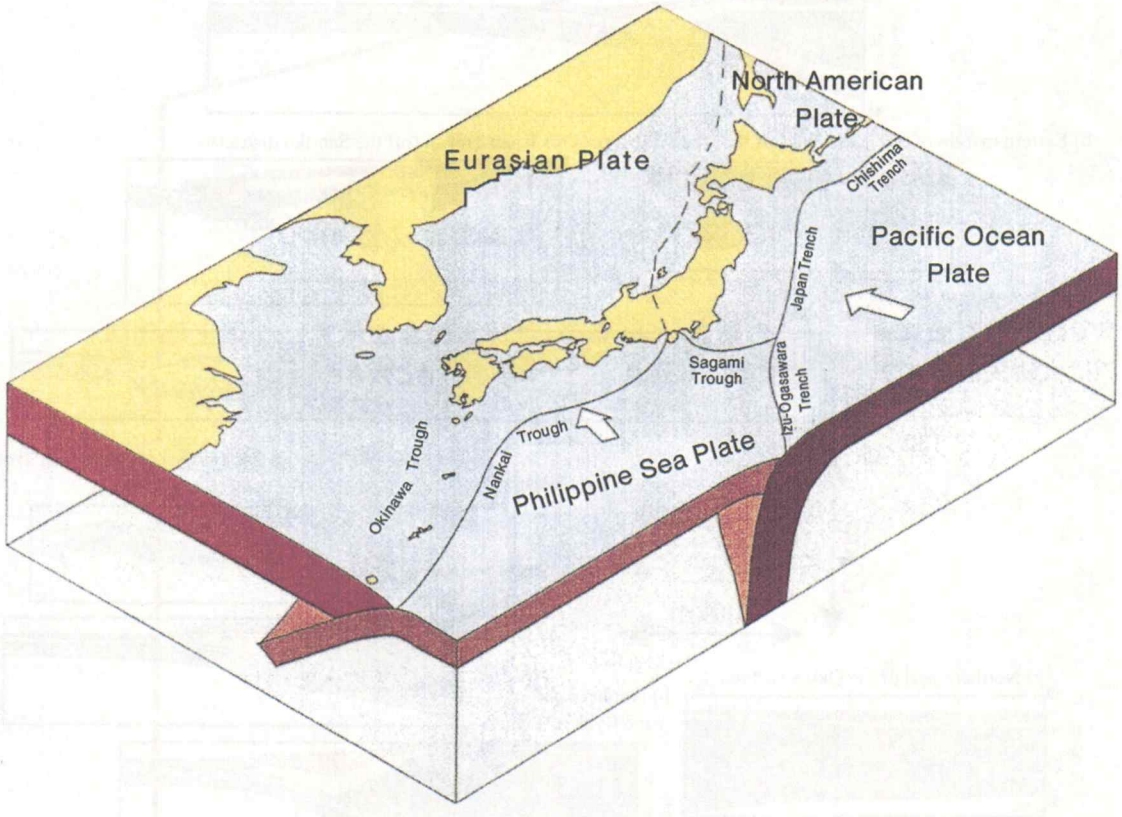


Figure 2.2-1 Plates around Japan (after the Earthquake Research Committee, 1997)

The arrows in the figure indicate the relative movement of each oceanic plate against the continental plate. The dotted line shows a inferred boundary between the North American Plate and the Eurasan Plate.

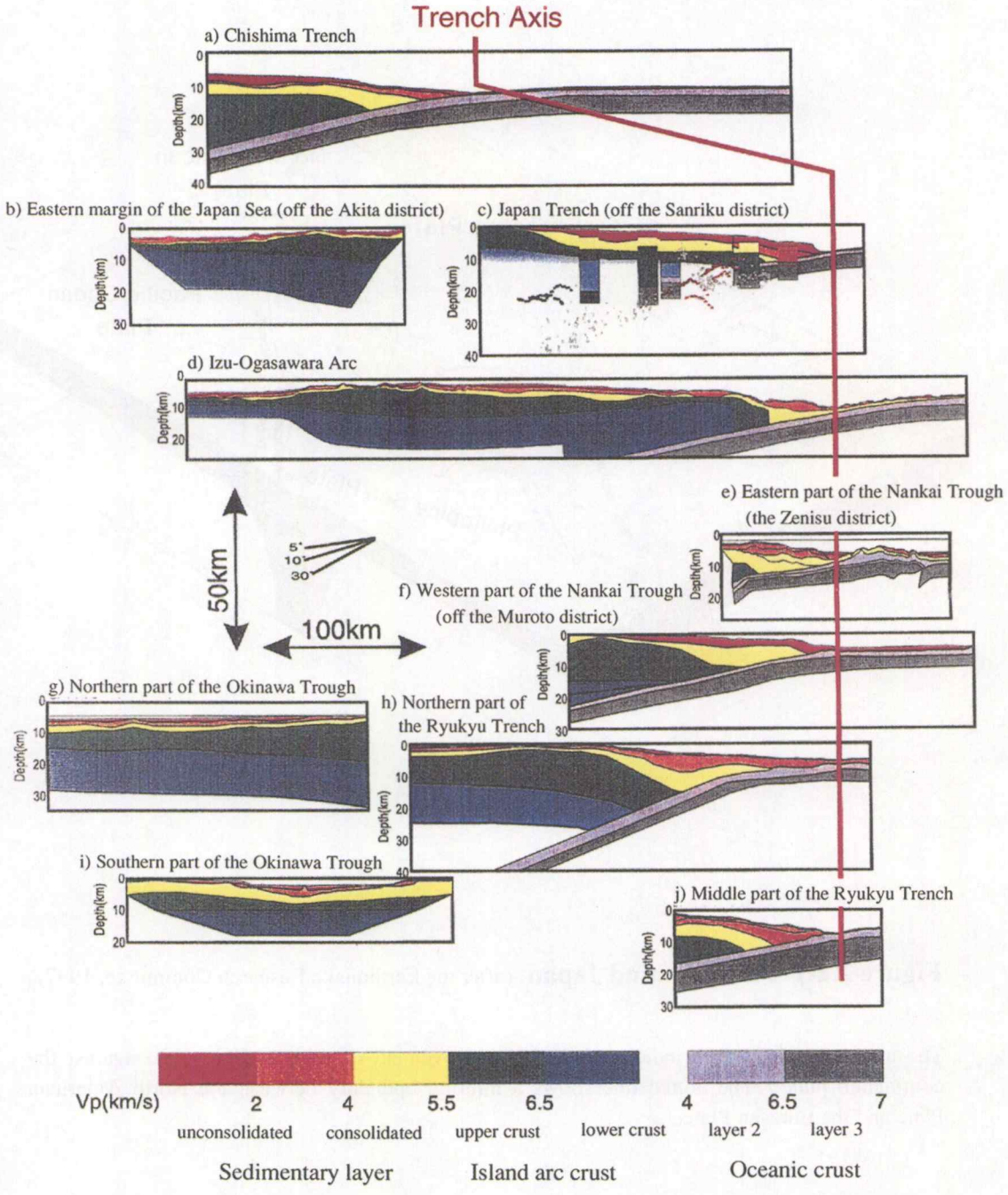


Figure 2.2-2 Crustal structure of plate boundaries around the Japanese Island
(after Hino, 1999)

These figures are based on the data obtained through refraction and wide angle reflection seismic prospecting using submarine seismometer (self-float type) etc.

is seen off the Sanriku district, where the subduction angle abruptly changes about 100 km from the trench axis. Such abrupt changes in subduction angle are also recognized about 50 km or less from the axis of the Nankai Trough and the Ryukyu Trench. The Pacific Ocean plate shows no significant regional difference in thickness of the subducting oceanic crust, whereas the Philippine Sea plate displays a large regional difference. This is probably because the oceanic crust of the Philippine Sea plate differs from place to place, according to the nature of the basins in which the crust formed and the formation ages of these basins.

2.2.2 Significant change in plate system

Plate movement can be expressed as a rotation of lithosphere approximating a solid body, around the Eulerian pole. Accordingly, as long as there is no change in the global plate system, the direction and velocity of plate movement should remain nearly fixed. A significant change in the plate system occurs to adjust old convergence boundaries that come to a standstill because of the formation of a new divergence boundary (rifting) or a continent-continent, continent-microcontinent, or continent-huge seamount collision. A significant change in the plate system is accompanied by a change in regional stress, leading to a new stage of crustal movement. Thus, a change in regional stress field and pattern of crustal movement is considered to be closely related to a significant change in the plate system (Kano and Murata, 1998).

Expansion of back-arc basins and the collision of island arcs occurred, causing significant changees in the plate system around the Japanese islands. For example, the Japan Sea, Chishima Basin and Shikoku Basin formed in the early to middle Miocene, marking an epoch of great change in the plate system. Many back-arc basins expanded in the western Pacific region. Although this is presumably related to the advanced age of the subducted oceanic plates (Molnar and Atwater, 1978), there are several views on the cause. While significant change in a plate system in connection with expansion of back-arc basins could bring about a change in regional stress fields and volcanic fields, the start of the change is thought to depend on the rate of significant change of the plate system. It took a million and more than ten million years respectively for the Southwest Japan Arc and the Northeast Japan Arc to rotate in association with the expansion of the Japan Sea (Jolivet et al., 1994). The expansion of the Chishima and Shikoku Basins also took more than ten million years from beginning to end (Seno and Maruyama, 1984; Kimura and Tamaki, 1986; Yuasa, 1991; Okino et al., 1998;). Thus, it is estimated to take at least a million years for a significant change in a plate system associated with the formation of back-arc basins.

A continental block or a volcanic arc carried by a subducting plate may be accreted as part of an accretion prism and the subduction zone may turn into a collision boundary. In the Japanese islands, collisions occurred between the Chishima Arc and the Northeast Japan Arc and between the Southwest Japan Arc and the Izu-Ogasawara Arc. The oblique subduction of the Pacific Ocean plate into the Chishima Trench has caused a right-lateral slip of the forearc of the Chishima Arc against the back-arc since the late Miocene. The forearc also moved westwards to collide with the Northeast Japan Arc (Kimura, 1981). Further, the collision shifted the plate boundary from the central part of Hokkaido to the eastern margin of the Japan Sea in the middle Pleistocene (Nakamura, 1983; Seno, 1986; Kimura et al., 1986). Thus, the collision of island arcs could have given rise to a migration of the plate boundary, which started in the Pliocene and ended in the middle Pleistocene or later in Hokkaido. This also indicates that it takes at least a million years for a significant change in the plate system.

The Pacific, Philippine Sea and North American plates join off the Boso Peninsula to result in a triple junction of plate boundaries (Seno, 1986; Niitsuma, 1994). Since the triple junction point is shifted to the west by the northwestwards subduction of the Philippine Sea plate, the Japan and Izu-Ogasawara Trenches are also expected to move. However, both trenches move by as little as 4 to 5 cm per year. Therefore, it is unlikely that the trench migration seriously affects the movement of the Pacific Ocean plate (Niitsuma, 1994). While tectonic erosion presumably occurs around the Japanese islands, except for the Nankai Trough (Kimura and Saito, 1998), it is unlikely that this would cause a dramatic shift of the trenches in the coming 100,000 years or so.

2.2.3 Neotectonics

It is thought that the original form of the present Japanese islands was defined 30 to 50 Ma ago due to tensile tectonics unlike the present system. Present tectonics are characterized mainly by a horizontal shortening. Neotectonics are defined as tectonics essentially identical to the present one. The start of neotectonics is controlled by geological processes at various depths and localities (for instance, tectonic balance identified by Kimura and Saito, 1998; flat-ramp structure in the stratified lower crust identified by Sato and Ikeda, 1999; delamination of mantle lid identified by Ikeda, 1999). The following outlines the characteristics of crustal movements and the start of neotectonics in various regions.

1) Chishima Arc

The regional stress field of the Chishima Arc has been characterized by a NW-SE to WNW-ESE compression since the latter half of the middle Miocene (Watanabe, 1986). Most of the N-S to NNW-SSE faults distributed in the northern part of Central Hokkaido have been activated as eastward-thrusting reverse faults since the Pliocene, when an E-W compressive field started to prevail (Yamagishi, 1986; Awata et al., 1997). The southern part of Central Hokkaido, particularly the Hidaka Mountains, attained a maximum uplift rate in the late Miocene, but this has slowed since the Pliocene (Miyasaka, 1987). Reverse faults distributed between the eastern margin of the Kabato Mountains and the eastern margin of the Ishikari Lowland were first activated in the middle Pleistocene or later (Awata et al., 1997).

2) Northeast Japan Arc

The regional stress field of the Northeast Japan Arc changed from intermediate to compressive in the Pliocene to the earliest Pleistocene (Sato, 1994). The Ohu mountain range and the back-arc side including the Dewa Hills started undergoing compressive deformation at clearly different times, i.e. at 1.0 Ma ago and at 3.5 Ma ago, respectively (Awata and Kakimi, 1985; Awata, 1988). Consequently, the beginning of the neotectonics of Northeast Japan can be traced back some 1.0 Ma and 3.5 Ma in the Ohu mountain range and the back-arc side, respectively. Also, once the plate boundary had shifted to the eastern margin of the Japan Sea, the southern part of the Northeast Japan Arc is thought to have been situated in the present tectonic regime since the middle Pleistocene (Takeuchi, 1999).

3) Izu-Ogasawara Arc

The conjunction between the Izu-Ogasawara and Southwest Japan Arcs has experienced a complicated tectonic movement, caused by a multiple collision of the Paleo-Izu Arc since the middle Miocene. This area was dominated by an E-W uplift (E-W uplifting of the Misaka mountain range) under a strong N-S compression untill 4 Ma ago and then by an N-S uplift (uplift of the Akaishi mountain range) under a westwards compression (Ishibashi, 1995). Back-arc rifts, including the Smith Rift, were developed in the northern part of the Izu-

Ogasawara Arc around 2.4 Ma ago (Tokuyama et al., 1999; Taylor, 1991; Nishimura and Yuasa, 1991).

4) Southwest Japan Arc

While the Southwest Japan Arc was under an N-S compression in the Pliocene as a whole, the inner belt turned into an E-W compressive field in the Quaternary. The Southwest Japan Arc has predominantly E-W, NE-SW and N-S trending faults, of which N-S reverse faults and NE-SW strike-slip faults began to be activated in an E-W compressive field and still remain active at present. On the other hand, the E-W trending faults were activated as reverse faults in the N-S compression in the Pliocene but their activity then ended under the subsequent E-W compression (Okamura, 1990). A NNW-SSE compressive stress field (E-W faults and folds) was developed in the southern part of the Japan Sea on the back-arc side of Southwest Japan between 6 Ma and 4 Ma ago. In the Quaternary, the compressive stress field changed direction to E-W (development of an N-S uplift zone) off the San-in district and to NW-SE in the Hokuriku region (off Ishikawa and Toyama) (Ito and Arato, 1999).

5) Ryukyu Arc

The Okinawa Trough, an equivalent to a back-arc basin, occurs to the west of the Ryukyu Arc. The trough was formed around 6 Ma ago and resumed expansion around 1.6 Ma ago, which has lasted to the present (Furukawa, 1991; Kimura et al., 1999). The expansion of the back-arc basin is thought to be caused by the beginning of an oblique subduction of the Philippine Sea plate (Kimura, 1990). It is pointed out that a steady expansion is proceeding at a rate of 10 mm per year in the offshore area to the west of Kyushu, corresponding with the northern part of the Ryukyu Arc (Tada, 1990). The expansion began around 6 Ma ago (Nagaoka, 1999) as a result of the expansion of the back-arc basin running along the Okinawa Trough (Park et al., 1997). The expansion has made the southern part of Kyushu rotate counterclockwise since about 2 Ma ago (Kamata, 1999).

Thus, the present tectonics of the Japanese islands formed mainly in the Pliocene to the Pleistocene despite a minor regional difference in age, and no significant change either in crustal movements (including the localization and amplitude of uplift and subsidence, the rate of crustal movements, the direction and rate of fault movement and the migration of the faulting field) or in volcanic fields has been recognized for the past hundreds of thousands to millions of years. Consequently, as long as there is no significant change in plate system, the present tendency of crustal movements and the present volcanic fields are expected to be maintained in the future. Even if some changes were to occur in the present plate system, current tectonic movements and volcanic activities would probably not undergo any dramatic change for several 100,000 years in the future, because it usually takes more than a million years for any significant change in plate system. As the expansion of back-arc basins and the collision of micro-continents and mega-seamounts are seemingly proceeding in some regions, it is required to estimate the amplitude of their future changes through a detailed study of the characteristics of crustal movements (including temporal change in patterns and rates of crustal movements) on the basis of objective data.

2.3 Earthquakes and fault movement

The potential effects of earthquakes and fault movements on a geological disposal system include:

- dynamic effects, caused by the shearing of fractures and faults that traverse the geological disposal system (i.e. displacement of individual fault surfaces);
- hydraulic and geochemical effects caused by the movement of groundwater, such as the penetration of oxidizing groundwater into the deep subsurface or an abrupt rise of groundwater from depth to the ground surface.

If there is a high possibility that these effects may impair the integrity of the geological disposal system, some measures should be taken in order to protect the system. There is a basic policy that the geological disposal system should be designed taking into account the maximum likely magnitude of any earthquake that may affect it.

In this context, it is important to understand the characteristics of current fault movements and the spatial extent and magnitude of the effects caused by these movements, and to estimate the spatial extent of future fault movements and their effects on the geological environment. This section investigates movements that are expected to occur in the future, taking into account the characteristics of past earthquakes and fault movements in Japan. From the point of view of an initial repository siting exercise, the most important faults are those that have shown significant and repeated movements within a time frame in the order of 10^5 years and that may show such dislocations in the future. These faults are referred to as "**active faults**" (This terminology is in widespread use in Japan when discussing tectonics and is consequently retained here. The large-scale features involved are, in any case, of direct importance for siting. The extent of possible future movement of relevant faults is an important topic of ongoing and future investigation).

2.3.1 Fault movement in Japan

Large earthquakes which have occurred in a shallow inland area of Japan caused deformation and displacement of the topography and geological structures near the ground surface (Table 2.3-1). The cumulative displacement of topographies along major active faults in Japan allows an examination of how active faults appeared and have developed in the last several hundreds of thousands of years. The degree of fault activity in the future and the extent of its effects can be estimated by identifying the regularity and localization of faulting in the past. This section investigates the methods that can be used to estimate the possibility of future fault movement. The basic approach is to identify the history of active fault movement and its regularity, as well as the regional characteristics of movement.

1) History of active fault movement

(1) Accumulation of fault displacement

The relationship between the orientation and amount of fault displacement and the ages of the displaced topographic and geological features suggest that displacements have accumulated along major active faults for the past several hundred thousand years. The older the topography, the greater the accumulated displacement (Sugimura and Matsuda, 1965; Okada, 1973). The average displacement rate of major active faults that can be observed today ranges from 0.01 to 10 m per thousand years. No significant changes in past orientations and the rates of displacement of active faults have been observed (Figure 2.3-1). Thus, active faults in

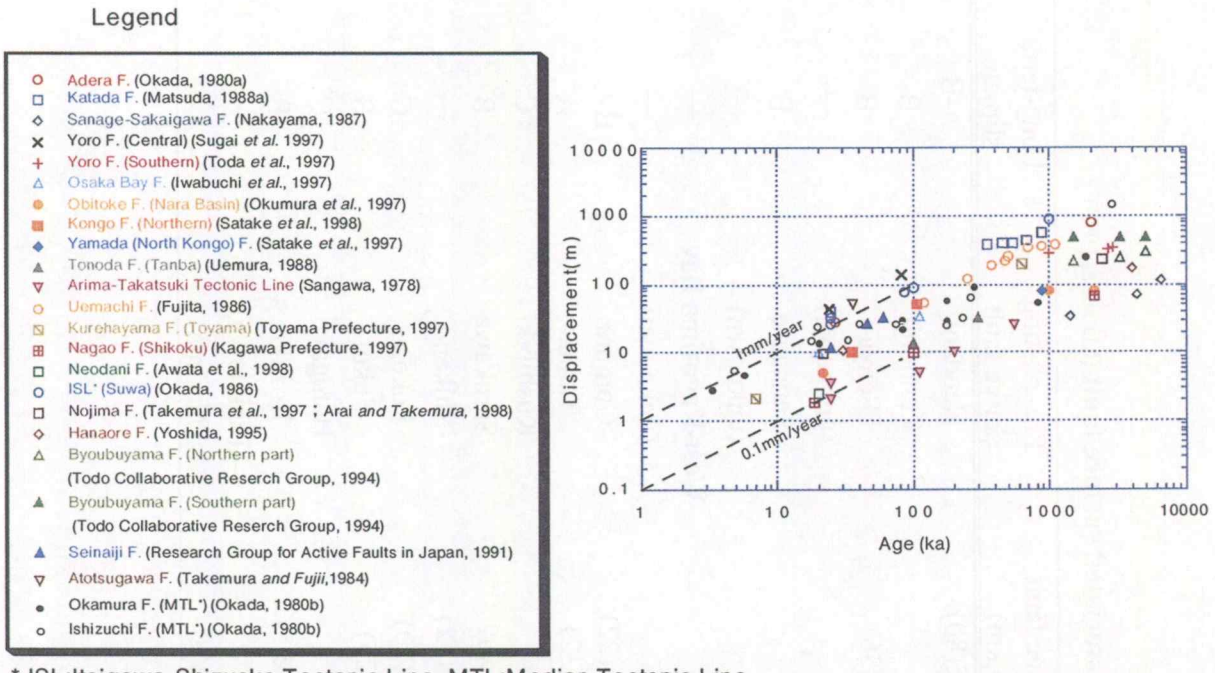
Table 2.3-1 Major inland earthquakes and their associated surface fault (Matsuda, 1998)

	Earthquakes	M (JMA)	Main surface fault (Length,km)	Pre-existing active fault	Long-term sliprate
1891	Nobi	8.0	Neodani(80)	Neodani	A-B
1894	Shonai	7.0	—	Kannonji	B
1896	Riku-u	7.2	Senya(36)	Senya	B
1900	Miyagiken-hokubu	7.0	—	(unknown)	—
1909	Gono	6.8	—	Yanagase	B
1914	Akita-senpoku	7.1	—	(unknown)	—
1914	Sakurajima	7.1	—	West-Kagosima Bay	—
1925	Kitatajima	6.8	Tai?	(unknown)	—
1927	Kita-Tango	7.3	Gomura(22)	Gomura	B-C
1930	Kita-Izu	7.3	Tanna(32)	Tanna	A
1931	Nishi-Saitama	6.9	—	Kushibiki	C
1939	Oga	6.8	Sarukawa?	Sarukawa	B
1943	Tottori	7.2	Shikano(12)	Shikano	—
1945	Mikawa	6.8	Fukozu(20)	Fukozu	C
1948	Fukui	7.1	Fukui(25)	Fukui	B
1961	Kitamino	7.0	—	Hatogayu	C
1974	Izuhanto-oki	6.9	Irozaki(5.5)	Irozaki	B
1984	Naganoken-seibu	6.8	—	(unknown)	—
1995	Hyogoken-nanbu	7.2	Nojima(9)	Nojima	A-B

Major inland earthquake data (1885-1996, $M \geqq 6.8$, $d \leqq 20$km, where M=Magnitude)

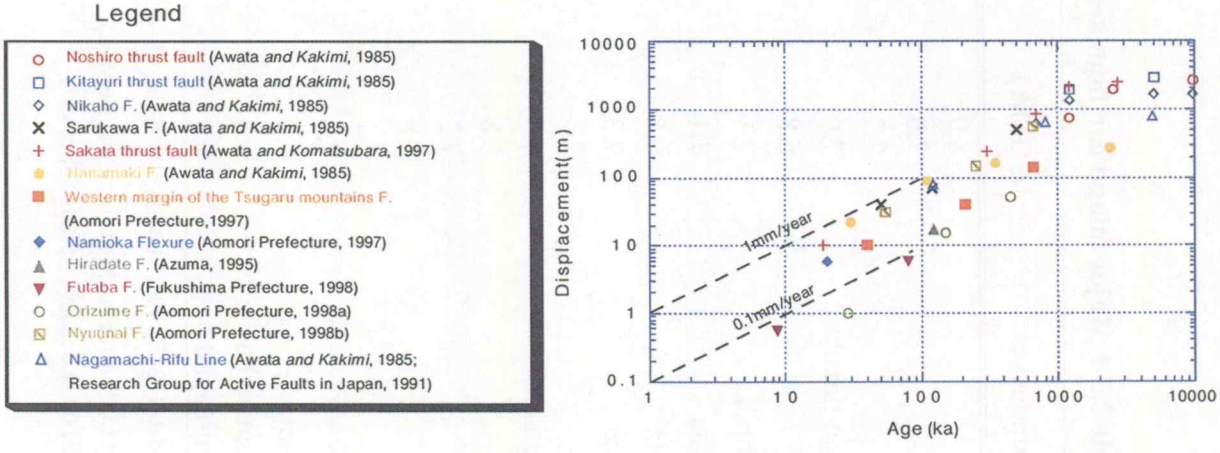
Magnitude data according to JMA (Japan Meteorological Agency)

Sliprate (A: 1-10 m ka^{-1}, B: 0.1-1.0 m ka^{-1}, C: 0.01-0.1 m ka^{-1})



* ISL:Itoigawa-Shizuoka Tectonic Line, MTL:Median Tectonic Line

Major active faults in southwest Japan



Major active faults in northeast Honshu

Figure 2.3-1 Relationship between the amount of accumulated displacement at major active faults and their age

Japan have moved with a consistent orientation and rate for at least the past several hundred thousand years.

(2) Start of fault displacement

As shown in Figure 2.3-1, there are some faults in Japan that have been active for more than one million years. The starting time of active faulting is mentioned below to allow examination of the duration of the present mode of activity.

While the present mode of faulting in some areas of northeast Japan can be traced back to the Pliocene, faults on the Japan Sea side generally became active earlier than those on the Ohu backbone range side (Awata, 1988). In southwest Japan, major reverse faults such as the Yoro and Atera fault systems have been active since the beginning of the Quaternary (Okada , 1986), while some of the lateral slip-faults represented by the Median Tectonic Line extending from Shikoku to Kii Peninsula were activated as a reverse fault at the beginning of the Quaternary. However, the present right-lateral slip of the Median Tectonic Line started in the latter half of the Quaternary (Sangawa, 1986), while the present mode of faulting in southwest Japan presumably appeared around 0.5 Ma ago (Fujita, 1993). The present crustal movements of the Japanese islands are thought to have started 3.5 to 0.5 Ma ago in northeast Japan and at the beginning of the Quaternary to 0.5 Ma ago in southwest Japan.

Thus, presently active faults became active at least hundreds of thousands of years ago and have remained active since then.

2) Regional variations in active faults

The distribution of active faults and their regional variations are presented below.

(1) Distribution maps of active faults

Publications that identify occurrences of both proven and possible active faults include:

i. "Active Faults in Japan" (Research Group for Active Faults of Japan, 1991);
ii. A series of "1:500,000 Neotectonic Maps" published by the Geological Survey of Japan (e.g. Sangawa et al., 1987);
iii. "Quaternary Map of Japan (I. Topographical, geological and active tectonic map (1:1,000,000)" (Japan Association for the Quaternary Research, 1987)

The Working Group for Compilation of 1:2,000,000 Active Fault Map (1999) defined active faults as faults reactivated for the past several hundreds of thousands of years to form clear displaced landforms at the surface. The Working Group compiled a "1:2,000,000 Distribution Map of Active Faults" (Figure 2.3-2) through detailed inspection of aerial photographs. The map classifies active faults into two varieties: actual and inferred. The former have given positive evidence of repeated activity over the last hundreds of thousands years, including standard criteria such as the dislocation of terraces and systematic bending of streams. In contrast, inferred active faults lack solid evidence for recent activity despite having similar topographic features to actual active faults.

The distribution of most of the active faults shown in the 1:2,000,000 Distribution Map of Active Faults is nearly identical to that in "Active Faults in Japan" (Research Group for Active Faults of Japan, 1991). However, because of the difference in their definition of active faults, a careful comparison of both maps indicates that the former excludes faults activated only in the first half of the Quaternary period. The distribution of active faults shown in the

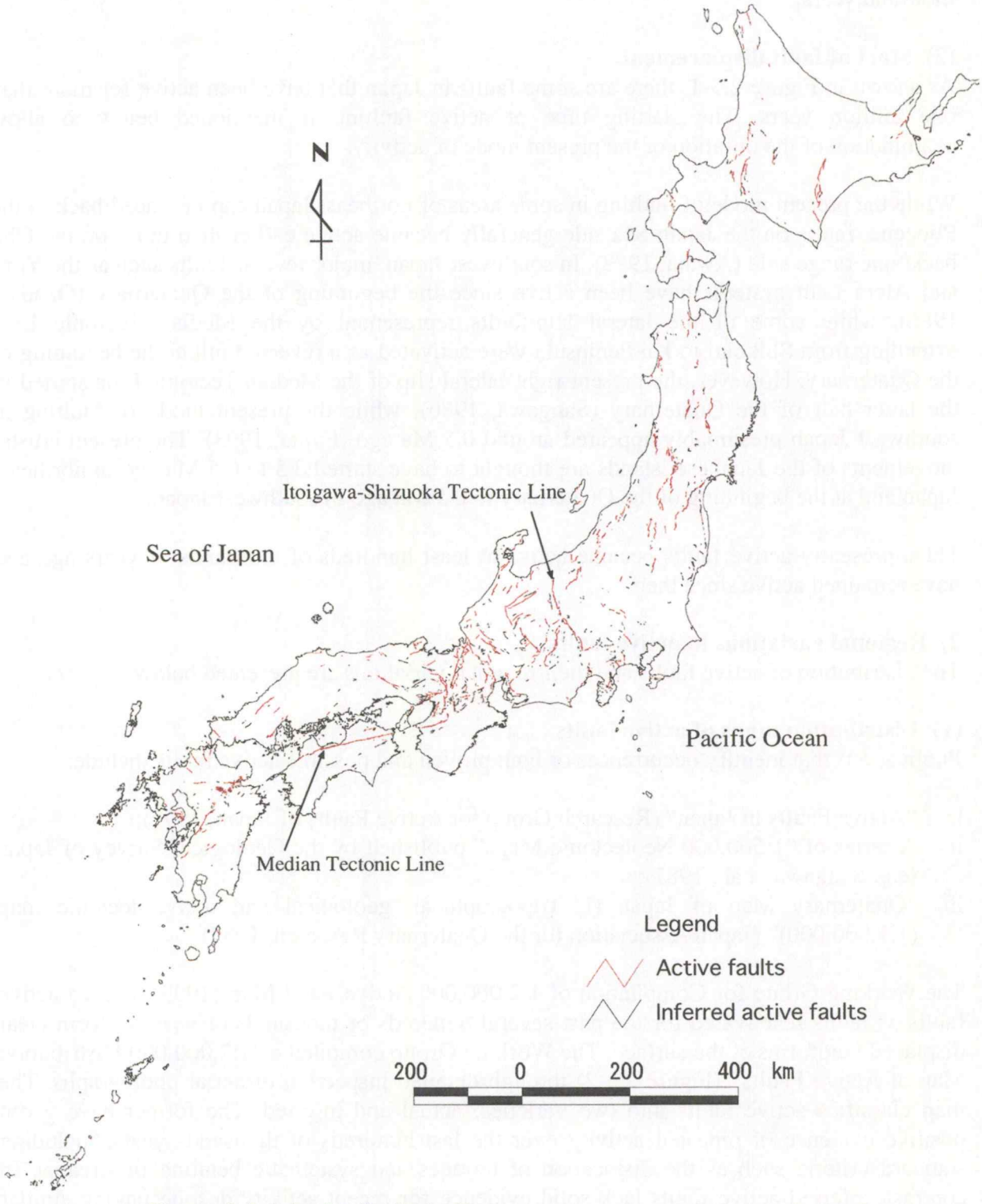


Figure 2.3-2 Active faults in Japan (from Working Group for compilation of 1:2,000,000 Active Fault Map, 1999)

"Active faults" in this map mean that they are identified as cutting the geographical features or geological formations that have been formed during the last several hundred thousand years.

former is closest to that in the "1:500,000 Neotectonic Maps" due to the similarity of the definition of active faults. The recent improvement in techniques for detecting active faults allowed the "1:2,000,000 Distribution Map of Active Faults" to include newly discovered active faults that neither the "Quaternary Map of Japan" nor the "1:500,000 Neotectonic Maps" showed. However, even recent techniques for interpreting aerial photographs can miss active faults which are buried under large plains such as the Niigata and Ishikari Plains or that have a low degree of activity measuring less than 0.01 m per 1,000 years.

(2) Distribution and types of active faults

Using mainly the "1:2,000,000 Distribution Map of Active Faults" (Working Group for Compilation of 1:2,000,000 Active Fault Map, 1999), an attempt is made to estimate fault activities for the next 100,000 years. This is done on the basis of regional differences in distributions and types of active faults formed during the last several hundreds of thousands of years. Active faults in offshore areas are excluded from the present evaluation, because any distribution map of active faults does not carry any offshore information comparable to onland active faults, except for some small areas. Data acquisition to examine active faults in coastal areas is desirable, following the example of an offshore survey shown in "Submarine Active Fault Map off the Tokai District" (Research Group for Active Submarine Faults off Tokai, 1999).

Figure 2.3-3 shows the cumulative length of active faults distributed in each area of Japan. The frequency of active faults is relatively high in the inner zone of northeast Japan (on the western side of the Kitakami-Shirakawa lowland zone); it is also high in the inner zone of southwest Japan (in the northern part of the Median Tectonic Line). On the other hand, the frequency is low in the outer zone of northeast Japan and in the outer zone of southwest Japan. More detailed study shows that there are some regions where no active faults exist over wide areas, even in the inner zone of northeast Japan and in the inner zone of southwest Japan. On the other hand, active faults are concentrated in the region called the "Kinki Triangle", delineated by Tsuruga - the Naruto strait - Ise bay, and the "Hida-Kiso-Mino region" in the western part of the Itoigawa-Shizuoka Tectonic Line. These regions have a high frequency of active faults and have many faults with a high level of activity.

Kaizuka and Imaizumi (1984) proposed a method to estimate the degree of fault activity for individual districts, on the basis of crustal strain rates calculated from the length and displacement rate of active faults. The crustal strain rates calculated by this method show large values in the Kinki Triangle and the Hida-Kiso-Mino districts (Figure 2.3-4).

The next issue to be discussed is the type of displacement shown by active faults. Reverse faults with a south-north strike are concentrated in northeast Honshu and in the Kinki area. In contrast, left-lateral faults with a northeast-southwest strike are concentrated in the west of central Japan. The active faults in central Kyushu are characteristically normal faults that are orientated in an east-west direction. The Izu Peninsula and its northern adjacent district differ from the other districts in trends and types of active faults, characterized by NW-SE right-lateral and reverse faults and NE-SW left-lateral faults (Matusda, 1973; Research Group for Active Faults of Japan (eds.), 1991).

The polarization of distribution of active faults and the localization of their degree of activity and type are also described in the "Active Faults in Japan". Broadly speaking, the localization of active faults that has prevailed for the last several hundreds of thousands of years can be seen throughout the Quaternary period.

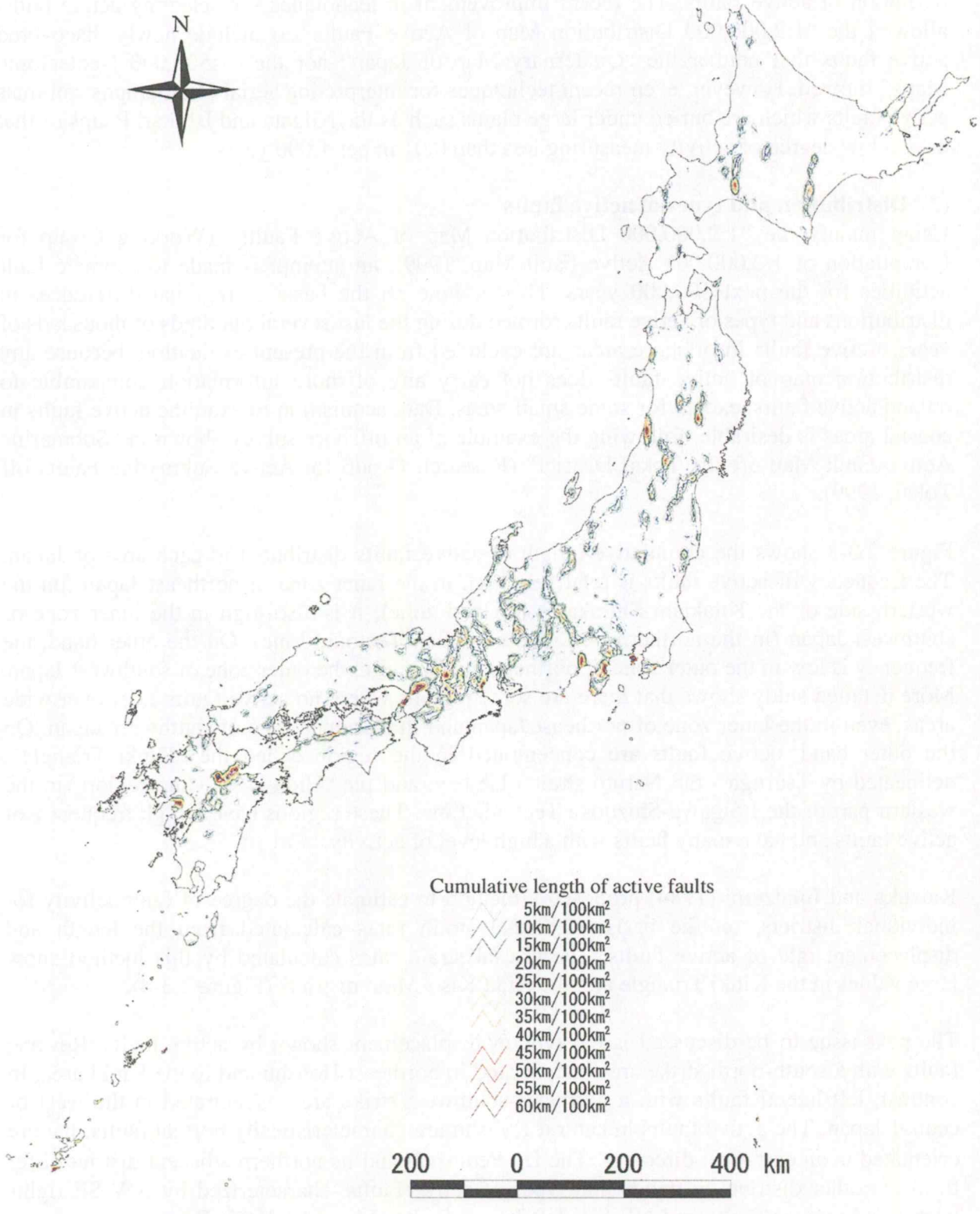


Figure 2.3-3 Frequency of active faults in Japan

Cumulative length of active faults in each of the grid (10km×10km). This map is made by connecting the density values, which are obtained by moving the grid at intervals of 5 km and plotted the density values at the center of each grid, by contour lines. After the data by the Working Group for Compilation of 1:2,000,000 Active Fault Map (1999).

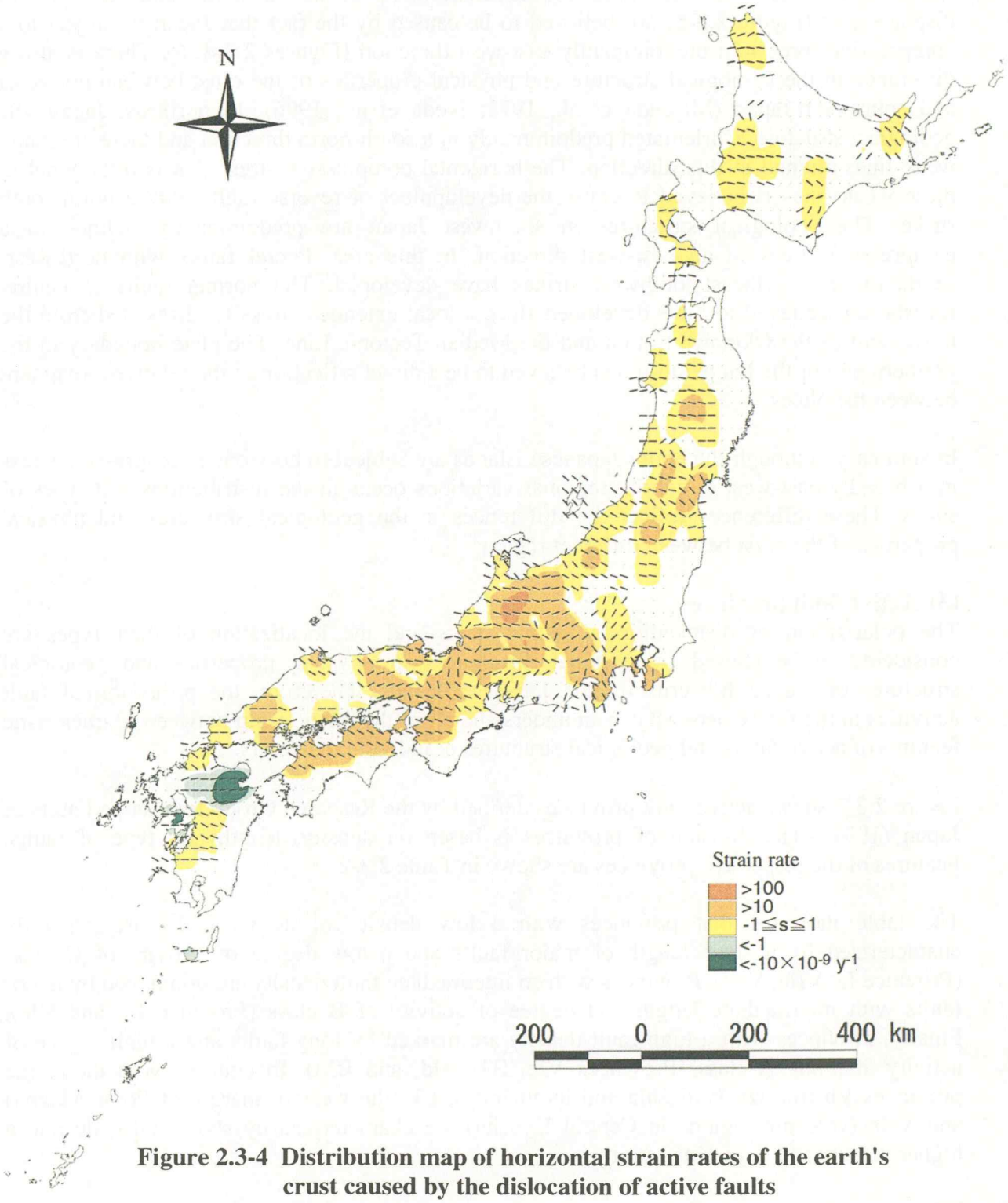


Figure 2.3-4 Distribution map of horizontal strain rates of the earth's crust caused by the dislocation of active faults

This is a comparative distribution map of the rates of horizontal strain caused by the dislocation of active faults, which are obtained from the average dislocation rates and lengths of major inland active faults. This map is made by connecting the strain values, which are obtained by moving a grid with a side 40 km long at intervals of 5 km and plotted at the center of each grid, by colored contour lines. The analysis follows Kaizuka and Imaizumi (1984) and takes account of types of faults. The solid lines show the directions of maximum horizontal stress.

The regional variations observed in the distribution of active faults and the type of displacement (Figure 2.3-5) are believed to be caused by the fact that Japan is subject to a compressive force in a predominantly east-west direction (Figures 2.3-4, 6). There is also a difference in the geological structure and physical properties of the crust between northeast and southwest Japan (Matsuda et al., 1978; Ikeda et al., 1996). In northeast Japan, the geological structure is orientated predominantly in a south-north direction and there are many weak lines aligned in this direction. The horizontal compressive stress that is orthogonal to these weak lines is believed to cause the development of reverse faults with a north-south strike. The geological structures in southwest Japan are predominantly oblique to a compressive stress in an east-west direction. In this area, lateral faults with northwest-southeast and northeast-southwest strikes have developed. The normal faults in central Kyushu are believed to have developed since a local extended stress field resulted from the movement of the Okinawa trough and the Median Tectonic Line. The plate boundary in the northern part of the Izu peninsula is believed to be a direct reflection of the relative movement between the plates.

In summary, although the entire Japanese islands are subject to horizontal compressive stress in a broadly east-west direction, regional variations occur in the distributions and types of stress. These differences reflect the differences in the geological structures and physical properties of the crust between different regions.

(3) Active fault provinces

The polarization of distribution of active faults and the localization of their types are considered to be caused by regional differences in physical properties and geological structures of the earth's crust in the Japanese islands. Therefore, the projection of fault activities in the future necessitates an understanding of the relationship between characteristic features of active faults and geological structures in individual districts.

Figure 2.3-7 shows active fault provinces defined by the Research Group for Active Faults of Japan (1991). The division of provinces is based on density, length and type of faults. Features of the respective provinces are shown in Table 2.3-2.

The table indicates that provinces with a low density of active faults are generally characterized by a short length of major faults and a low degree of activity of C class (Province Ia, VIIa, VIII). Provinces with an intermediate fault density are dominated by major faults with intermediate length and degree of activity of B class (Province IIb and VIe). Finally, provinces with a high fault density are marked by long faults and a high degree of activity attaining A class (Provinces VIc, BT, VId, and BM). In contrast with these, the provinces Vb (the Izu Peninsula and its vicinity), BF (the western margin of Fossa Magna) and VIIb (volcanic regions in Central Kyushu) are characterized by short faults, despite a higher density and degree of activity.

While the Japanese islands are under an E-W compressive stress as a whole, active faults clearly show different distributions and types, which reflect regional differences in geological structures and physical properties of the earth's crust. Regional geological structures and general trends of active faults in the respective provinces have given rise to the localization of their distribution densities and degrees of activity for the last several hundreds of thousands of years, resulting in repetition of faulting with a regularity and continuity peculiar to each of the fault provinces. Further, no dramatic changes in relative plate movements are expected in the future, so that the probability of significant change in regional stress fields is presumed to be



Figure 2.3-5 Distribution map of active faults by type

(Working Group for Compilation of 1:2,000,000 Active Fault Map ,1999)

This map shows the distribution of active faults (including inferred ones) by type (normal, reverse, right-lateral and left-lateral). Faults lacking information on dislocation sense are not shown in this map.

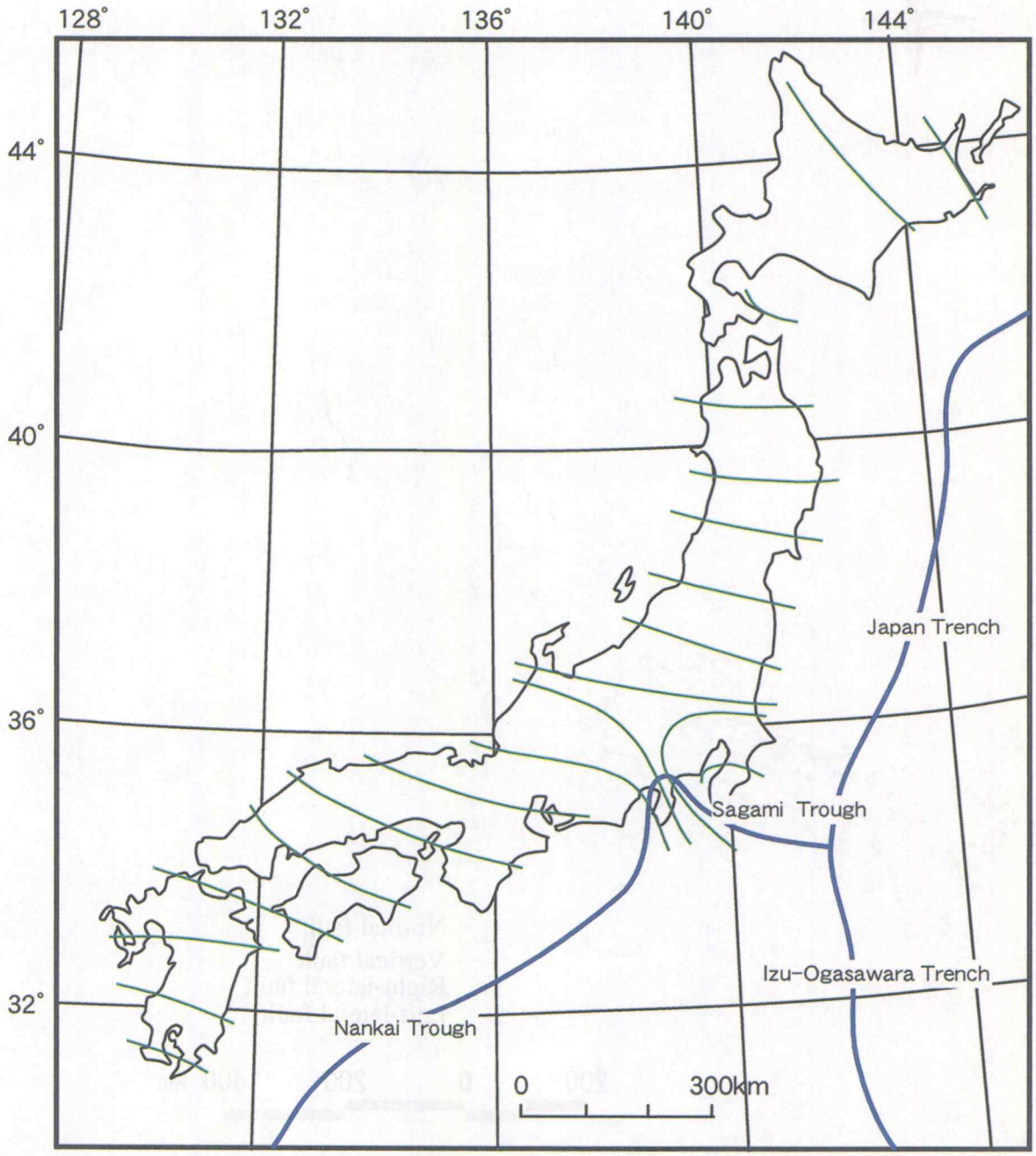


Figure 2.3-6 Loci of the maximum principal stress

(Matsuda et al., 1978)

Loci of the maximum principal stress, based on data on active faults, Quaternary volcanoes (including dikes), earthquakes, and in-situ stress measurements. Japan is subject to a compressive force in a predominantly east-west direction.

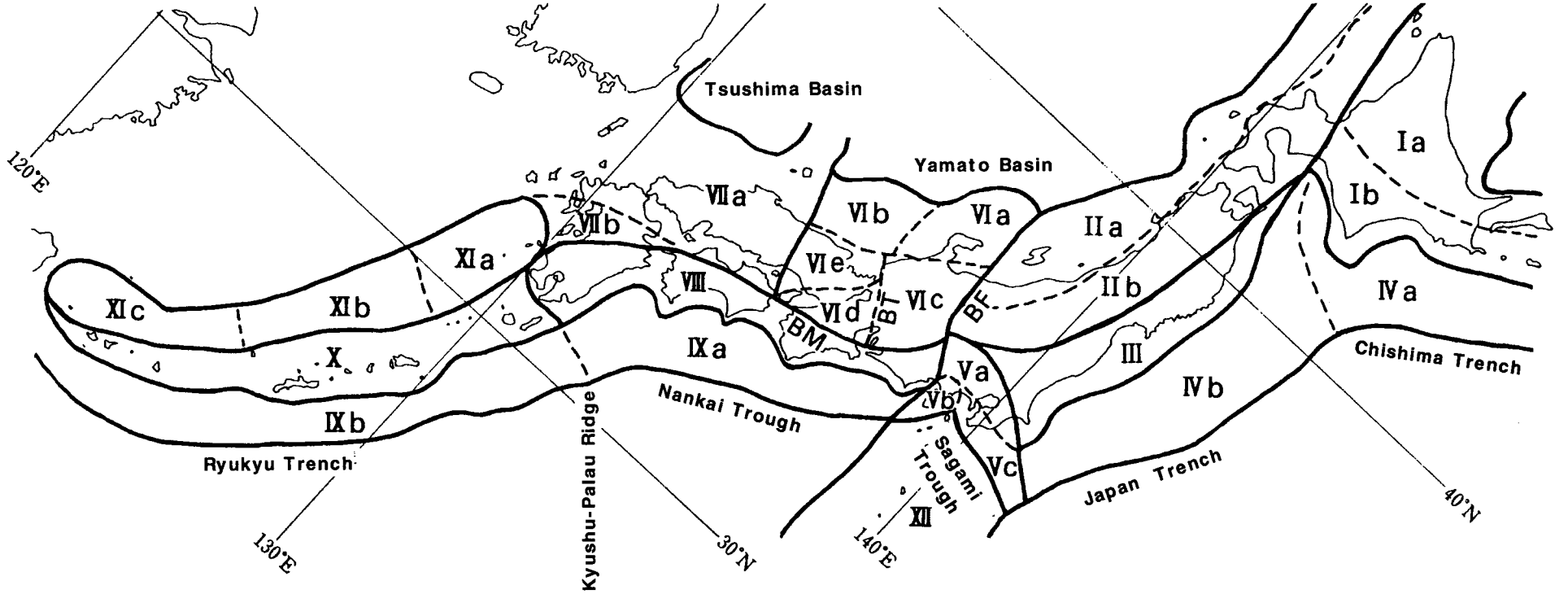


Figure 2.3-7 Fault provinces of Japan (Research Group for Active Faults in Japan, 1991)

Refer to Table 2.3-2 for province names and other information.

Table 2.3-2 Characteristics of fault provinces in Japan (after Research Group for Active Faults of Japan, 1991)

	Division		Subdivision	Density	Length of the main fault*	Activity of the main fault**	Fault type***	Note
I	Hokkaido (Main part)	a	Inner zone	Small	Short	C	Reverse ?	
		b	Outer zone	Small	Medium	B	Reverse	
II	Inner zone of northeast Japan	a	Continental slope	Large	Long	A ?	Reverse	Sea bed
		b	Land	Medium	Medium	B	Reverse	Reverse fault zone, volcanic belt
III	Outer zone of northeast Japan			Very small	Medium	B	Reverse or Lateral	
IV	Pacific Ocean slope of Eastern Japan	a	South coast	Large	Long	A ?	Reverse or Lateral ?	Sea bed
		b	Sanriku, Joban and Kashima open sea	Large	Long	A ?	Reverse	Sea bed
V	Izu-Ogasawara arc tip	a	Around Kanto Mountains	Medium	Short	B	Reverse or Lateral	
		b	Around Izu Peninsula	Large	Short	A・B	Lateral	Volcanic belt
		c	Northern edge of the Sagami trough	Large	Long	A	Reverse or Lateral	Mainly sea bed
BF	Western margin zone of the Fossa Magna			Large	Short	A	Lateral or Reverse	
VI	East of Inner zone of Southwest Japan	a	Around the Noto Peninsula	Small	Short	B・C	Reverse	Land and sea bed
		b	Around the Oki trough	Medium	Medium	B ?	Reverse?	Sea bed
		c	Chubu mountain	Large	Long	A	Lateral or Reverse	
		BT	Tsuruga Bay-Ise Bay line zone	Large	Medium	A・B	Lateral or Reverse	
		d	Trangular region in Kinki area	Large	Medium	B・A	Reverse or Lateral	
		e	Northwest of the Kinki area	Medium	Medium	B	Lateral or Reverse	
VII	West of the Inner zone of Southwest Japan	a	Chugoku, Setouchi and Kitakyushu	Small	Short	B・C	Lateral or Reverse	
		b	Central Kyushu volcanic area	Large	Short	B	Normal	Normal fault zone, volcanic belt
BM	Median Tectonic Line zone			Large	Long	A	Lateral	
VIII	Outer zone of Southwest Japan			Very small	Short	B・C	Reverse or Lateral	
IX	Pacific Ocean slope of Western Japan	a	Nankai Trough landward slope	Large	Long	A	Reverse or Lateral	Sea bed
		b	Ryukyu ocean trench landward slope	Medium ?	Long	A ?	Reverse or Lateral	Sea bed
X	Ryukyu arc			Medium or Large	Medium	B・C	Normal	Sea bed and land
XI	Okinawa trough	a	Northeast of the Okinawa trough	Medium	Long	B ?	Normal	Sea bed
		b	Center of the Okinawa trough	Large	Medium	A ?	Normal	Sea bed
		c	Southwest of the Okinawa trough	Large	Long	A	Normal	Sea bed
XII	North of the Izu-Ogasawara arc							Sea bed and west part are volcanic area.

* Short : L≦20km, Medium : 20<L<50km, Long : L≧50km. L is the length on the attached map. Original material is different on sea bed and land.

** S ($m\ ka^{-1}$) :Average displacement rate in the Quaternary. A:10>S≧1, B:1>S≧0.1, C:0.1>S≧0.01

*** Reverse:Reverse fault, Normal:Normal fault, Lateral:Lateral fault

small (Section 2.2). Consequently, fault activities for the next 100,000 years can be evaluated by extrapolating from the past activities for most regions in Japan.

Fault densities for the active fault provinces shown in Table 2.3-2 indicate the average for the respective provinces, each of which has a local difference in distribution density. Further, characteristics such as length, degree of activity and type of faults in the table represent major faults and are not always consistent with individual faults. Therefore, characteristic features of individual faults should be examined in a survey of site selection program, giving consideration to geological structures, features of neighboring faults and crustal stress.

3) Extent of the range of active fault movement

(1) Width

The possibility that the width of an active fault zone may extend in the future is discussed. An evaluation was made of whether a reverse fault zone, which consists of several reverse faults running nearly parallel to one another, has extended during the past one million years. Geophysical exploration was conducted across a reverse fault zone at the eastern edge of the Yokote basin. This study showed that, during the past several hundred thousand years, the fault zone has propagated over a range of about 2 km near the surface (Figure 2.3-8). It is also estimated that multiple faults, running parallel to one another, converge into a single fault in sedimentary rocks 1 to 2 km from the ground surface (Sato and Hirata, 1998). The width of propagation during the past several hundred thousand years also ranges in the order of 10^0 km in the direction of the basin for other typical reverse fault zones, such as the Inadani fault zone (Yamaguchi, 1988) and Shinjo basin fault zone (Suzuki, 1988). The extent of propagation on the surface is believed to depend on the thickness of the sedimentary cover of a basin (Suzuki, 1988). The above findings indicate that the possible propagation of a reverse fault zone in the future of interest may be less than 10 km and occurs in the direction of the basin. On the other hand, normal fault zones, which are observed in central - southern Kyushu, have been reducing in width toward the centers of grabens over a period of a million years (Kamata and Kodama, 1993). Therefore, there is little possibility that the width of normal fault zones might be extended significantly in the future over the timescales of interest.

(2) Length

It is known that the length of an active fault (L, in km) is proportional to the cumulative displacement (ΣD, in meters), that is $\log\Sigma D = 1.17\log L - 1.03$ (Ranalli, 1977). This relationship results in the equation $\Sigma D = 10^{-1} L$ (Matsuda, 1988b). The relationship between the average displacement rate (S, m ka^{-1}) and the time to be considered (T, ka) can be represented by the equation $S = \Sigma D / T$ (Matsuda, 1975). The future extension of length (ΔL, km) of an active fault can be estimated according to the equation as $\Delta L = (S \times T) \times 10$. When it is assumed that S=(0.1 to 10)m per thousand years and T = 100,000 years, ΔL is calculated to be 0.1 to 10km.

(3) Examples of active fault zones

Matsuda (1990) grouped a series of faults forming a line at intervals less than 5 km and a group of parallel faults less than 5 km from each other to designate them "seismogenic faults" with the potential to independently cause earthquakes. Such a grouping of faults is important for estimating the scale of earthquakes. On the basis of the "1:2,000,000 Distribution Map of Active Faults" made by the Working Group for Compilation of 1:2,000,000 Active Fault Map (1999), the division of active fault zones is exemplified the fields of the future faulting in the following (Figure 2.3-9).

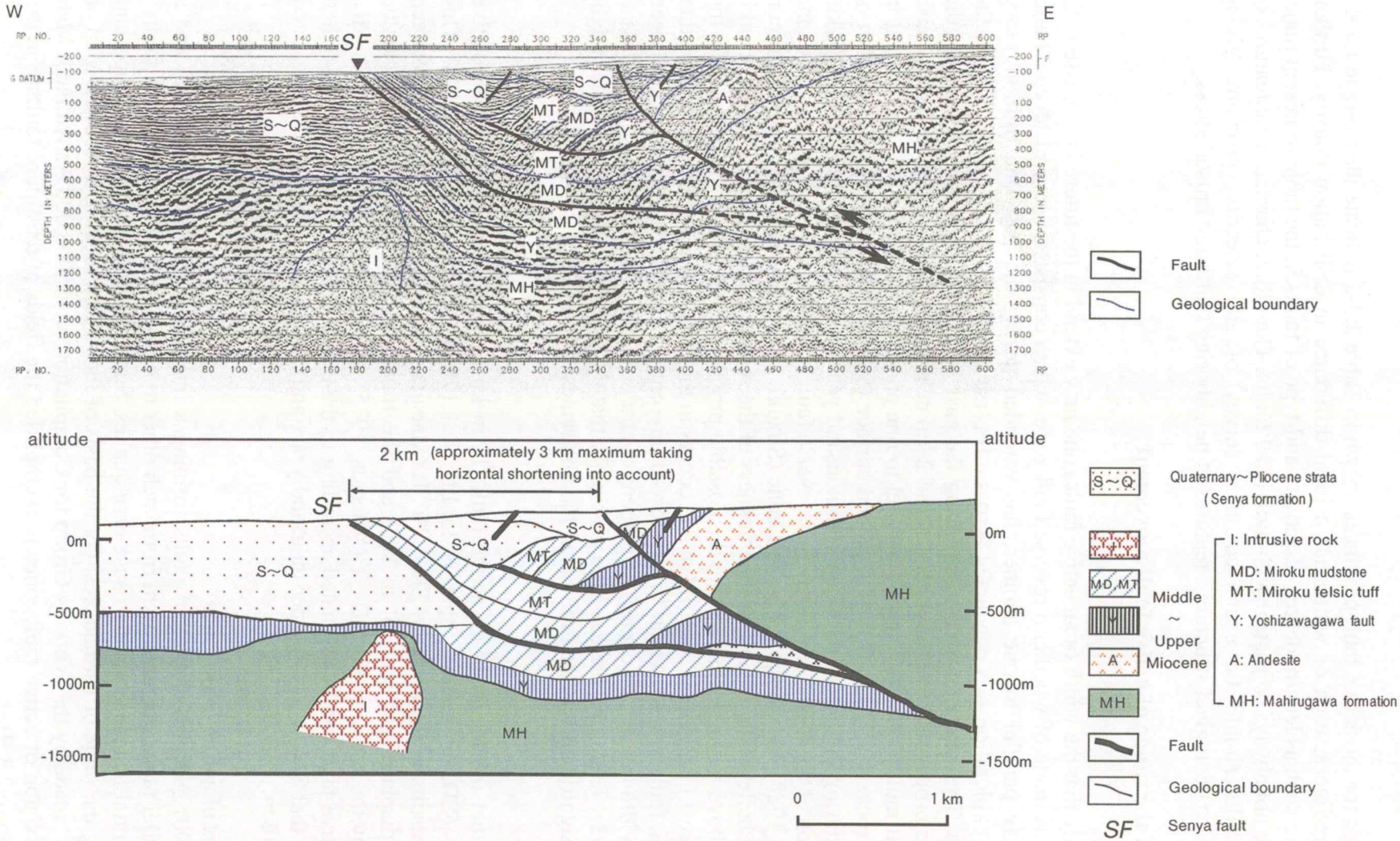


Figure 2.3-8 Geological structure of a reverse fault (Senya fault) (after Sato.et al., 2000)

Upper: seismic profiling across the faults. Lower: postulated geological cross-section.

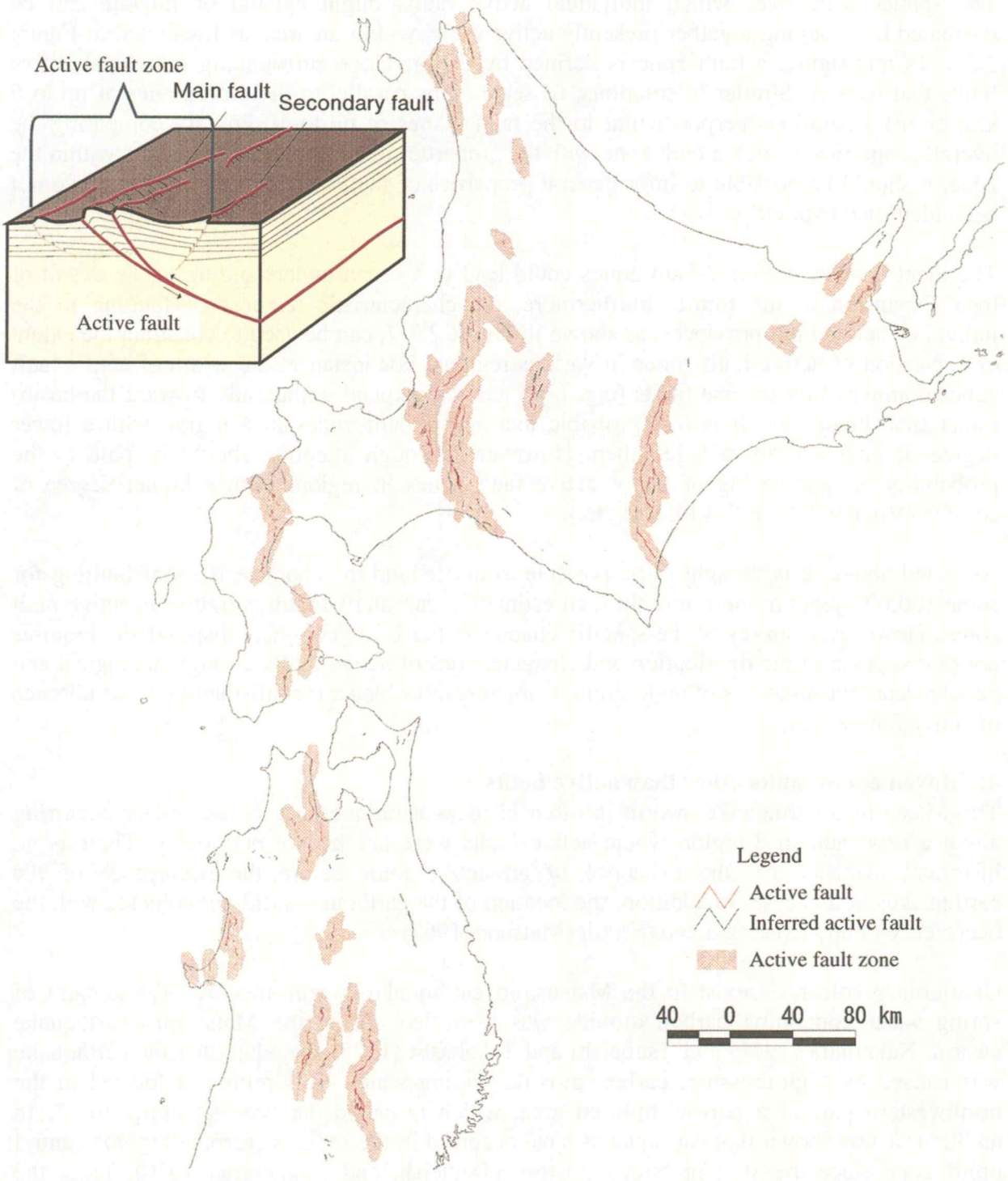


Figure 2.3-9 An example of an 'active fault zone'

An example of an 'active fault zone' based on the data of the '1: 2,000,000 Active Fault Map' (Working Group for Compilation of 1:2,000,000 Active Fault Map, 1999) is shown. Inferred active faults near actual faults are also considered. The block diagram (left above) shows schematically an active fault zone.

The spatial scale over which individual active faults might expand or migrate can be estimated by grouping together presently active faults within an area, as illustrated in Figure 2.3-9. In this figure, a fault zone is defined by the envelope surrounding individual active faults that have: i) Similar orientations; ii) separations parallel to the fault planes of up to 5 km; or iii) separations perpendicular to the fault planes of up to 10 km. By comparing the overall properties of such a fault zone with the properties of individual active faults within the zone, it should be possible to infer general properties of faults within the zone that have not been identified explicitly.

The identification of active fault zones could lead to a broad understanding of the extent of their expansion in the future. Furthermore, the characteristic features of faulting in the individual active fault provinces, as shown in Figure 2.3-7, can be used to constrain the extent of expansion of active fault zones in various regions. For instance, the width of active fault zones dominated by reverse faults (e.g. I, II) tends to expand unilaterally (toward the basin) rather than bilaterally. It is less probable that active fault zones in a region with a lower degree of fault activity will lengthen. However, thorough attention should be paid to the probability of lengthening of major active fault zones in regions with a higher degree of activity (Vb, BF, VIc, BT, VId, BM etc.).

As stated above, it is thought to be possible to understand the characteristics of faulting for some 100,000 years in the future through estimating cumulative fault activities in active fault zones. However, a survey of the specific characteristics of a geological disposal site requires not only a grasp of the distribution and characteristics of active faults through geological and geophysical investigations of underground structures, but also a reconfirmation of the absence of active fault zones.

4) Movement of faults other than active faults

The Matsushiro earthquake swarm is often cited as a unique case of seismicity occurring along a new fault in a region where active faults were not known previously. There is no historical evidence for the existence of an active fault before the occurrence of the earthquakes in this case. In addition, the location of the earthquakes did not coincide with the occurrence of any existing inactive fault (Matsuda, 1967).

Quarternary volcanoes exist in the Matsushiro earthquake swarm area. A large amount of spring water containing carbon dioxide was identified during the Matsushiro earthquake swarm. Nakamura (1971) and Tsuneishi and Takahashi (1975) speculate that the earthquake was caused by high-pressure, carbon dioxide-bearing water. This region is located in the northwestern part of a narrow uplifted area, which is called the "central uplift zone". In addition, it was shown that earthquakes have occurred in the regions surrounding this central uplift zone since the start of human history (Tsuneishi and Nakamura., 1970). Thus, the Matsushiro earthquake swarm is considered as a unique example in which earthquakes occurred owing to the unique hydraulic and geological characteristics of the area and was followed by the appearance of new faults at the ground surface.

The frictional strength of a fault is lower than the stress required to create a new fault. Once a fault is formed, it becomes a weak interface that may potentially be re-activated, even if it is located in a stress field which is not orientated along the plane of weakness (Scholz, 1993). Should a new fault occur, it could initially develop gradually as an assembly of small fractures (e.g. Scholz, 1993). There is little possibility that such a fault will immediately develop into a large-scale fault that causes a large displacement.

The Japanese islands have been subject to a stress field similar to the present for at least the past several hundred thousand years. All the structural weaknesses that are active today (i.e. active faults) have been displaced repeatedly in the past (Research Group for Active Faults of Japan (eds.), 1991). A study of displaced topographies, including dated terraces, indicates that faults that have activated periodically for the last several hundreds of thousands of years are all restricted to active fault zones (Working Group for Compilation of 1:2,000,000 Active Fault Map, 1999). Consequently, it is unlikely that a new active fault will be formed in the next 100,000 years in an active fault-free area in Japan, with the exception of volcanic regions. However, the Kochien fault forming the southern part of the Tokachi Plain's west-margin fault zone (about 100 km long), which is located at the southwest tip of the outer arc of the Chishima Arc, probably became active within the last several hundreds of thousands of years or less (Togo, 1982; Togo and Ono, 1994). This fault was formed by reactivation of the Hiroo fault activated in the Neogene. Thus, around a larger active fault zone, the existence of faults with dip and strike identical to those of the active fault zone should be examined. The possibility of these faults reactivating should be evaluated by considering the movement pattern of active faults in the fault province and the rate of horizontal strain caused by faulting.

There is little possibility that a new fault might occur in the future and have a significant effect on the geological environment in regions where no active fault exists. However, detailed hydraulic investigations should be conducted in regions that have unique hydraulic and geological characteristics, where earthquake swarms have occurred in the past.

2.3.2 Effects of fault movement on the geological environment

Possible effects of fault movement on the geological environment include:

- fracturing and crushing;
- the penetration of oxidizing groundwater into deep geological formations;
- a sudden rise of groundwater to the ground surface.

In order to reduce to an acceptable levels the likelihood that these potential effects will be significant, any geological disposal system must be located at a suitable distance from major active faults.

1) Effects of fault movement

(1) Mechanical effects

Most of the active faults in Japan move intermittently. The displacement per movement of a fault is typically a maximum of a few meters. Geological formations around the faults are crushed and deformed as the displacements have accumulated over the last several hundred thousand years. The spatial range of fracturing and crushing arising from such fault activity is examined here.

Records of rock fracturing and crushing caused by fault movement are remain in the form of "fault rocks", such as fault gouge, fault breccia and cataclasite. Some of these fault rocks were formed in deep geological formations in the remote past and were exposed at the surface as a result of subsequent uplift and denudation. In this study, areas where fault rocks are distributed are treated as crushed zones associated with active faults (hereafter "fault crushed zones").

The major fault crushed zones in Japan are those of the:

- Atera Fault, which is approximately 500 m wide and 60 km long;
- Neodani Fault System (Nukumi Fault), which is approximately 200 m wide and 80 km long;
- Median Tectonic Line (Iyo Fault), which is approximately 200 m wide and 500 km long (Ogata and Honsho, 1981).

In addition, the Rokko-Awajishima Fault Zone (Nojima Fault) measures about 50 m in width (Rin et al., 1998).

Ogata and Honsho (1981) contend that, in a granite in the Chubu region, there is the following relationship between the length, L (m), and the width, W (cm), of a crushed zone:

$$\text{Log } L = 0.68 \pm 0.32 + 0.87 \log W$$

In addition, Otsuki (1978) points out that field and laboratory data on faults, both in Japan and abroad, indicate a relationship between the width of a crushed zone and the cumulative displacement (Figure 2.3-10). This relationship can be used to estimate the widths of fault crushed zones from the scale (length and cumulative displacement) of the associated faults. For example, the crushed zone of a fault with a cumulative displacement of 10 km is estimated to be roughly 200 m in width.

The mechanical effects around a fault crushed zone are now examined. The area where fractures in a rock mass, formed by fault movement, are distributed, is reported to be in the order of 10^{-2} relative to the length of the fault (Vermilye and Scholz, 1998).

The Komyo Fault stretches for about 50 km from south to north, between the southeast part of Iida City (Nagano Prefecture) and the northern part of Hamamatsu City (Shizuoka Prefecture). The distribution frequency of minor faults decreases as the distance from the Komyo Fault increases and approaches zero at a distance of about 2 km (Tsuneishi, 1984).

The isotopic ages of principal minerals (potassium feldspar, biotite and amphibole) in rocks distributed around the Median Tectonic Line in the Kayumi district (Mie Prefecture) vary according to the distance from the Median Tectonic Line, becoming almost uniform at a distance of about 1,800 m from the Median Tectonic Line (Takagi et al, 1989). These spatial ranges may be considered as the zones where minor faults and fractures, formed in the early stage of fault growth, have developed (hereafter the "process zones")(Vermilye and Scholz, 1998). Tsuneishi (1984) indicates that most of the minor faults around major faults would stop moving after the major faults have been formed. However, because the possibility of future movements of minor faults in these zones cannot be ruled out, these zones are currently regarded as areas affected by the crushing and deformation of active faults.

A study was conducted to examine the effects on underground structures of fracturing and crushing due to displacement of an active fault. Two cases can be cited:

- the Kita-Izu Earthquake in 1930: This earthquake had a magnitude of 7.3 on the Richter Scale and was caused by the movement of an active fault crossing the Tanna Tunnel.
- the Izu-Ohshima-Kinkai Earthquake in 1978: This earthquake had a magnitude of 7.0 and affected the Izukyu Inatori Tunnel.

At the time of the first earthquake, a displacement of about 2 m was observed in the fault

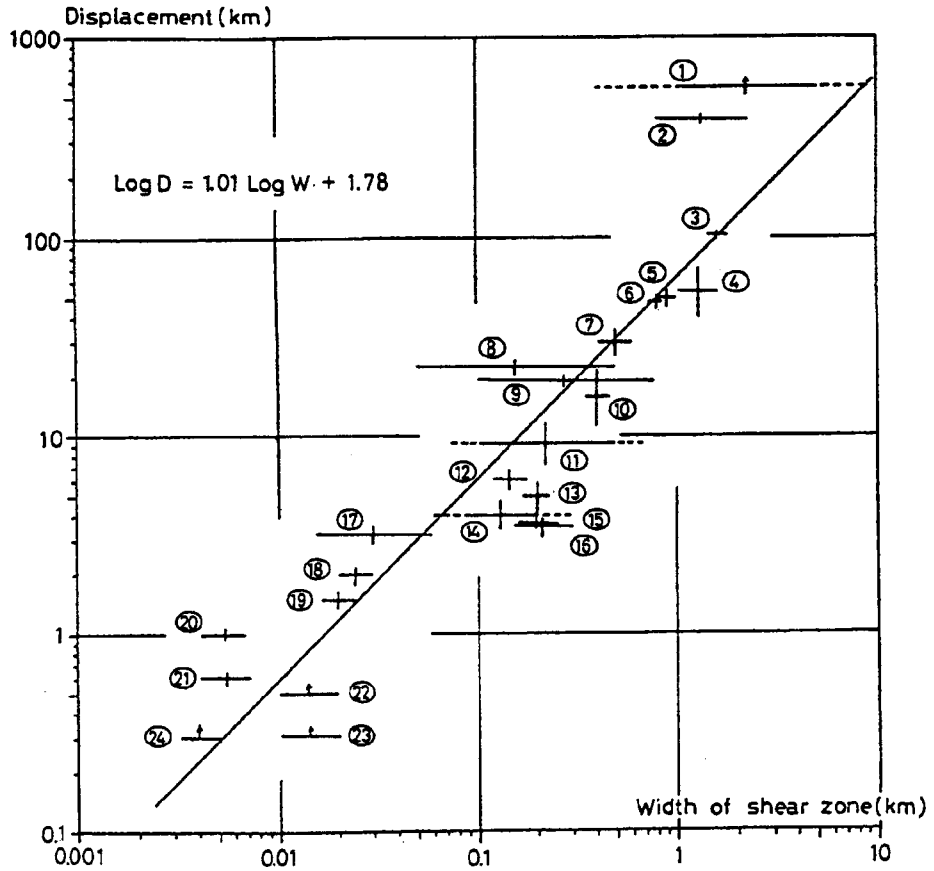


Figure 2.3-10 Relationship between cumulative displacement along the fault and the width of shear (crushed) zone for major strike faults from throughout the world (Otsuki, 1978)

1.San Andreas fault
2.Alpine fault
3.Great Glen fault
4.Garlock fault
5.Bok Bak fault
6.Death Valley-Furnace Creek fault
7.Hizume-Kesenuma fault
8.Akaishi tectonic line
9.Hope fault
10.Agua Blanca fault
11.Atera fault
12.Blue Cut fault
13.Nukumi fault
14.Tsurukawa shear zone
15.Oppara fault
16.Sekigahara-Yanagase fault
17.Atotsugawa fault
18.Hirose-Hase fault
19.NS trending faults which shift the Kannawa fault
20.Tanna fault
21.NS trending faults which shift the Kannawa fault
22.Toyano fault
23.Sahata fault
24.Hanaore fault

crushed zone in the Tanna Fault. Deformation was observed to have occurred in an area extending for about 1.5 km to the west of the fault crushed zone (Hada, 1981).

After the 1978 Izu-Ohshima-Kinkai Earthquake, a displacement of about 50-70 cm was observed to have occurred along the Inatori-Ominesan Fault. Deformation was recognized to have occurred over an area within a radius of 400 m of the crushed zone (Onoda et al., 1978). This deformation is thought to have been caused by strain relief.

The Hyogoken-Nanbu earthquake (M=7.2 on the Richter Scale) on January 17, 1995 caused damage to tunnels mostly due to caving in the crushed zone (Koyama et al., 1996).

Thus, the effects on underground structures of fracturing and crushing caused by fault movements are limited to the immediate vicinity of the fault crushed zones. It follows that fracturing and crushing caused by recent fault movements would affect underground structures only in the close vicinity of fault crushed zones. However, to confidently select a stable host rock for any future HLW repository, it is necessary to take a conservative approach. This involves selecting stable rock formations that are clearly beyond any observed influence of presently active fault. Therefore, it is appropriate to designate both the crushed zones associated with fault movements and the surrounding process zone as the zones potentially affected by active fault zones. The cases cited in this study are relatively large active faults. Therefore, if active faults are smaller, the affected zones may be much narrower. In all cases, the zone of mechanical effects will have to be determined by conducting detailed surveys.

(2) Thermal effects

When fault movement occurs, the deep geological formations surrounding the fault become intensely hot (Fukudome, 1984). Pseudotachylites were found to have formed along the fault plane in a crushed zone (Uda et al., 1995). However, the pseudotachylites discovered measure several millimeters to one centimeter in width, suggesting that the effects of heat from fault movement would extend only locally. A zircon fission-track dating survey was conducted using a drilling core sample taken from the Nojima Fault. This survey revealed that track lengths in the crushed zone (about 30 m wide) at a depth of 340-390 meters are 30 to 50 percent shorter than those found outside the crushed zone. Therefore, the crushed zone may have reached a temperature as high as 200-300°C. However no thermal effects were observed outside this zone (Tagami et al., 1998).

A borehole survey was conducted in the Nojima Fault. This survey found that relatively low-temperature (below 150°C) minerals, including smectites and zeolites, exist abundantly in the 2 m wide central part of the crushed zone. These minerals occur where the thickest gouges are found, at depths of 500 - 1,800 m (Fujimoto et al., 1998). In addition, smectites were observed in the crushed zone of the Mozumi Fault, one of the faults in the Atozugawa Fault System. Here, no traces of recrystallization caused by heating were found (Satake and Murata, 1998).

An evaluation of thermal hysteresis, based on the distribution of pseudotachylites and the fission-track dating method, suggests that, when active faults move, heat might be produced along the fault plane and temperatures of over 200°C might be attained. Nevertheless, there is no evidence that sufficiently high temperatures continue for sufficiently long periods to cause smectites to alter in geological formations surrounding active faults at depths of several hundreds of meters. Therefore, it is concluded that the significant thermal effects of fault movement are only temporary and limited to the crushed zone.

(3) Hydraulic effects

It is commonly supposed that a fault would form a highly permeable zone. However, under some circumstances, a fault may provide a hydraulic barrier (e.g. Chester et al., 1993). Therefore, fault movements may affect underground hydraulics by either enhancing or reducing the permeability of the fault crushed zone. Near to the fault, water levels may change in wells and the chemistry of spring water may change. The extent and range of the hydraulic effects are discussed below.

Firstly, a comparison between the permeability of active and inactive fault crushed zones is made. Two surveys of the permeability of active faults can be cited:

- hydraulic investigations conducted using injection tests and elastic waves two years after the Hyogoken-Nanbu earthquake;
- hydraulic tests carried out on the Mozumi-Sukenobu Fault in the Atozugawa Fault System.

The results of these tests show that the hydraulic conductivities of active fault crushed zones in the Nojima Fault and the Mozumi-Sukenobu Fault (Figure 2.3-11) are around 10^{-6} m s^{-1} (Kitagawa et al., 1997) and between 10^{-6} and 10^{-9} m s^{-1} (Nohara et al., 1999), respectively. In comparison, the hydraulic conductivities of twelve inactive fault crushed zones that have been investigated are in the range 3 x 10^{-5} - 1.6 x 10^{-8} m s^{-1} (Okamoto et al., 1984). Thus, no significant differences in the permeabilities between active and inactive fault crushed zones are observed. The small hydraulic conductivities of the Mozumi-Sukenobu Fault may be caused by a decrease in permeability as fracture apertures are filled with precipitated minerals, with lapse of time after the fault movement (Forster et al., 1998).

In contrast, tests in the Nojima Fault conducted using elastic waves found that highly permeable zones (10 cm - 3 m in width) exist in the fault rocks. Two zones occur in cataclasites and three in fault gouges (Ito et al., 1996). Uda et al. (1998) have suggested that clay rich in Fe_2O_3, occurring in apertures of fractures in cataclasites at a depth of 1,300 meters, indicates the penetration of oxidizing water from near the surface into deep geological formations. The results of laboratory experiments indicate that, as shear displacement occurs between two rocks, the hydraulic conductivities increases by one to two orders of magnitude in granite (Esaki et al., 1991) and decreases in sedimentary rock (Olsson, 1992).

Therefore, the possibility cannot be ruled out that, when active fault movement occurs, a preferential water pathway may be formed in the fault crushed zone. Furthermore, there is a possibility that the pathway may extend to the ground surface. However, with time, the apertures of fractures will be filled with precipitated minerals to such an extent that the permeability of the fault crushed zone will drop to the same level as that of the inactive fault crushed zone.

Only limited data are available on changes in the level of groundwater near the ground surface. Therefore, it is difficult to evaluate directly the hydraulic changes in rock masses around a fault before and after fault movement. Here, these hydraulic changes are evaluated indirectly from the results of surveys of groundwater levels and water chemistry before and after the earthquake at the Nojima Fault.

Immediately after the Hyogoken-Nanbu earthquake, large spring water flows were observed in and around the associated Nojima Fault. A sharp drop in the water level in wells in nearby

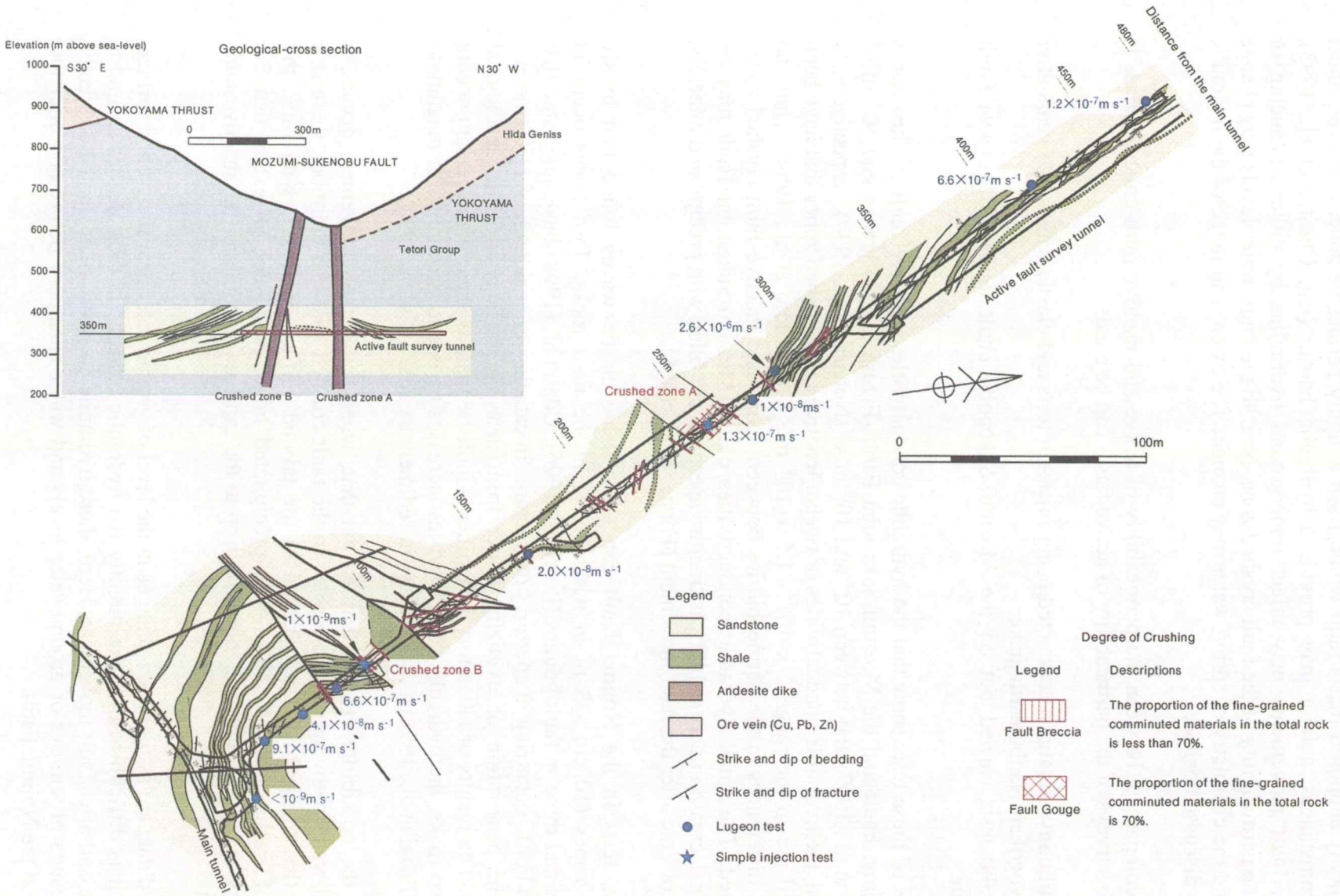


Figure 2.3-11 Geological map along the Active Fault Survey Tunnel, Mozumi-Sukenobu Fault
(after Ito et al., 1998)

The hydraulic conductivity of crushed zones and surrounding rocks is 10^{-6} - 10^{-9} m s^{-1}.

mountain ridges was also detected. Figure 2.3-12 shows the locations of spring water and the decline in groundwater level. The springs were located not only in the vicinity of the fault, but also in lowlands in the northern part of Awaji Island. A drop in the water level took place mainly in mountainous districts over 100 m above sea level (Sato and Takahashi, 1997). Approximately halfway up the mountains, spring water flows increased temporarily after the earthquake, but stopped soon afterwards. Thus, hydraulic changes were observed over a wide of the northern part of Awaji Island. Stable hydrogen and oxygen isotope ratios of spring waters were measured at locations where unusual spring flows were observed after the earthquake. These data indicate that the spring water recharge area was near the mountain ridges. The tritium age of spring water suggested recharge times several years to several decades ago (Sato et al., 1999). Movement of deep water to the surface is not indicated by these data. Hence, it is presumed that the significant effects on groundwater flow resulting from fault movements would extend predominantly over shallow geological formations.

(4) Geochemical effects

The geochemical effects of fault movements are examined, using the results mainly from surveys of the Nojima Fault.

At three springs (Goi no Shimizu, Daishi no Shimizu, and Shoki no Mizu) around the Nojima Fault, the chemistry of spring water was measured before and after fault movement. The pH of spring water from these sources was between 7.2 and 7.7 and EC was between 37.3 and 45.4 mS m^{-1}, which are distributed within the normal range for groundwaters from the granite of Awaji Island. Groundwater surveys in the Mozumi-Sukenobu Fault (Satake and Murata, 1998) showed that the composition of groundwater in the fault crushed zone lies within the compositional range of groundwater originating from typical Japanese meteoric precipitation.

Mineralogical observations in crushed zones and the characteristics of mineral alteration provide evidence of the properties of fluids that have passed through these zones. Traces of hydrothermal solutions, underground gas and oxidizing surface water are found at some points in crushed zones. In the borehole penetrating through the Nojima Fault, altered zones were observed in the fault rocks. These zones were characterized by the dissolution of colored minerals and the argillation of feldspars and extended from the fault for 50 m into the hanging wall (in granite) and 5 cm into the footwall (in sedimentary rock) (Tanaka et al., 1998). Furthermore, the reported distribution of iron oxide in the Nojima Fault is limited to the fault crushed zone (Uda et al., 1998). These altered zones are not observed at a distance from the fault crushed zone (Kobayashi et al., 1998). These observations are consistent with the view that fault movements have had no significant geochemical effects around the Nojima Fault, except in an area of several tens of meters near the fault crushed zone.

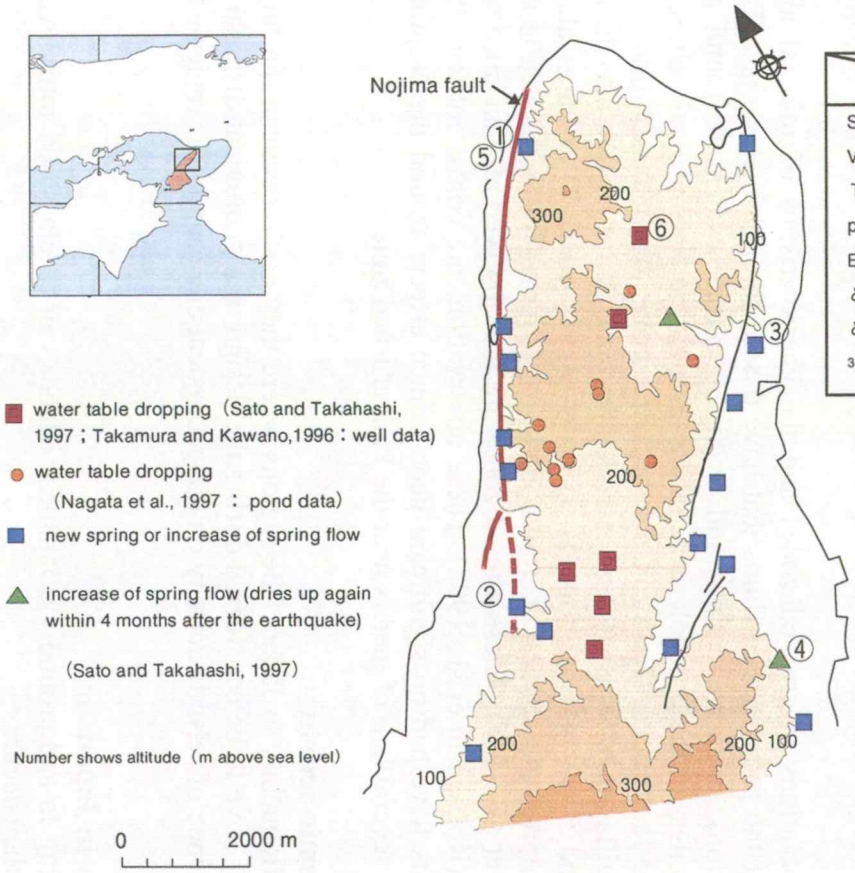
2) Influence of seismic activity

Earthquakes occur frequently in Japan. The regions where they could occur in the future and the scales of activity have to be considered during the design of a geological disposal system for HLW. The influence of seismic activity on the geological environment is reviewed in this section.

(1) Seismic activity in Japan

Earthquakes occurring in and around the Japanese islands can be classified into three types, according to where they occur:

i. inter-plate earthquakes;



springs	① Nojimaezaki		② Ogura	③ Kusumoto Riv.		④ Shoki no Mizu
Sampling date	1995/5	1997/8	1997/8	1995/5	1997/8	1995/1
Volume (ℓ /sec)	0.24	0.03	6.50	2.22	0.29	9.44
T (℃)	16.1	16.6	19.8	n.d.	18.1	15.4
pH	8.0	7.8	7.3	n.d.	7.69	7.2
EC (μS/cm)	403	295	418	n.d.	348	277
δ D (‰)	-47.0	-48.9	-45.7	-46.8	-46.1	-47.4
δ ^{18}O (‰)	-7.7	-7.7	-7.0	-7.4	-7.5	-7.3
^{3}H (TU)	n.d.	6.41.	3.71	n.d.	3.09	n.d.

wells	⑤ Esaki	⑥ Nuruyu	
Sampling date	1997/8	1995/5	1997/8
Volume (ℓ /sec)	-	-	-
T (℃)	13.6	17.0	17.4
pH	8.0	7.6	7.64
EC (μS/cm)	377	382	406
δ D (‰)	-41.9	-47.4	-45.7
δ ^{18}O (‰)	-6.9	-7.6	-7.5
^{3}H (TU)	n.d.	n.d.	3.14

Figure 2.3-12 Map showing the location and chemical compositions of spring waters and the locations where the water table dropped after the 1995 Hyogoken-Nanbu earthquake in the northern part of Awaji Island

ii. deep intraplate earthquakes;
iii. shallow inland earthquakes.

The hypocenters of inter-plate earthquakes, which are relatively large in activity, are located in the offshore area. There is generally a separation of approximately 50 to several hundred kilometers between these hypocenters and the surface of the onshore area. An exception is the region surrounding the Izu Peninsula, where the plate boundary is close to the land. Most shallow inland earthquakes are considered to be associated with fault activity due to the crustal stress caused by relative plate movements. Shallow inland earthquakes are relatively small in scale, but their hypocenters are often at a depth of 20 km or less. The magnitudes of these earthquakes are usually proportional to the sizes of the active faults and/or to the area of plate boundary surfaces. Hence, earthquakes of this type tend to occur repeatedly in the same area with similar magnitude (Hagiwara, 1991; Matsuda, 1975).

Hagiwara (1991) identified seismic regions of the Japanese islands based on the distributions of active faults and historical earthquakes, and estimated the maximum magnitude of earthquakes for each region. Such estimates may be valid for at least 100,000 years in the future, because there is no evidence that large changes in the crustal stress field in Japan have occurred during the past several hundreds thousand years.

(2) Influence of earthquakes on the geological environment

It is important to evaluate the potential effects on the underground environment of ground motion and changes in groundwater chemistry and flow caused by earthquakes. Here, such an evaluation is made using the results of observations obtained at the Kamaishi mine (Ishimaru and Shimizu, 1997; Shimizu, et al., 1996).

344 earthquakes were recorded at the Kamaishi mine from February 1990 to March 1998. The hypocenters of most of these earthquakes were located beneath the Pacific Ocean, off the coast between Aomori and Miyagi Prefectures, at distances of 20 to 250 km from the Kamaishi mine. However, the largest earthquake observed, with a magnitude of M8.1, was the Hokkaido Toho-oki earthquake that occurred on October 4, 1994. This earthquake had a hypocenter at a distance of 675 km from the Kamaishi mine.

During these earthquakes, the maximum acceleration deep underground was approximately 1/2 to 1/4 of the acceleration at the surface. The ratio of the accelerations at any two points more than 150 m below the ground surface rarely changes (Figure 2.3-13). The same trend was also seen at the Hosokura mine in sedimentary rock (Komada et al., 1989). Therefore, there are no apparent differences in the relative responses to earthquakes in different lithologies; similar responses are recognized in both granite and sedimentary rock.

Fukushima and Tanaka (1990) derived the following relationship between the distance from an earthquake hypocenter and the attenuation of the maximum acceleration of the rock mass:

$$\mathrm{Log}A = 0.41M - \log (R + 0.032 \times 10^{0.41M}) - 0.0034R + 1.30$$

(where A is the maximum acceleration (m s^{-2}), R is the distance (m) and M is the magnitude)

The maximum ground acceleration observed at the Kamaishi mine was either equal to, or lower than, the acceleration suggested by this equation.

The maximum acceleration amplitudes observed in horizontal and vertical motions have an

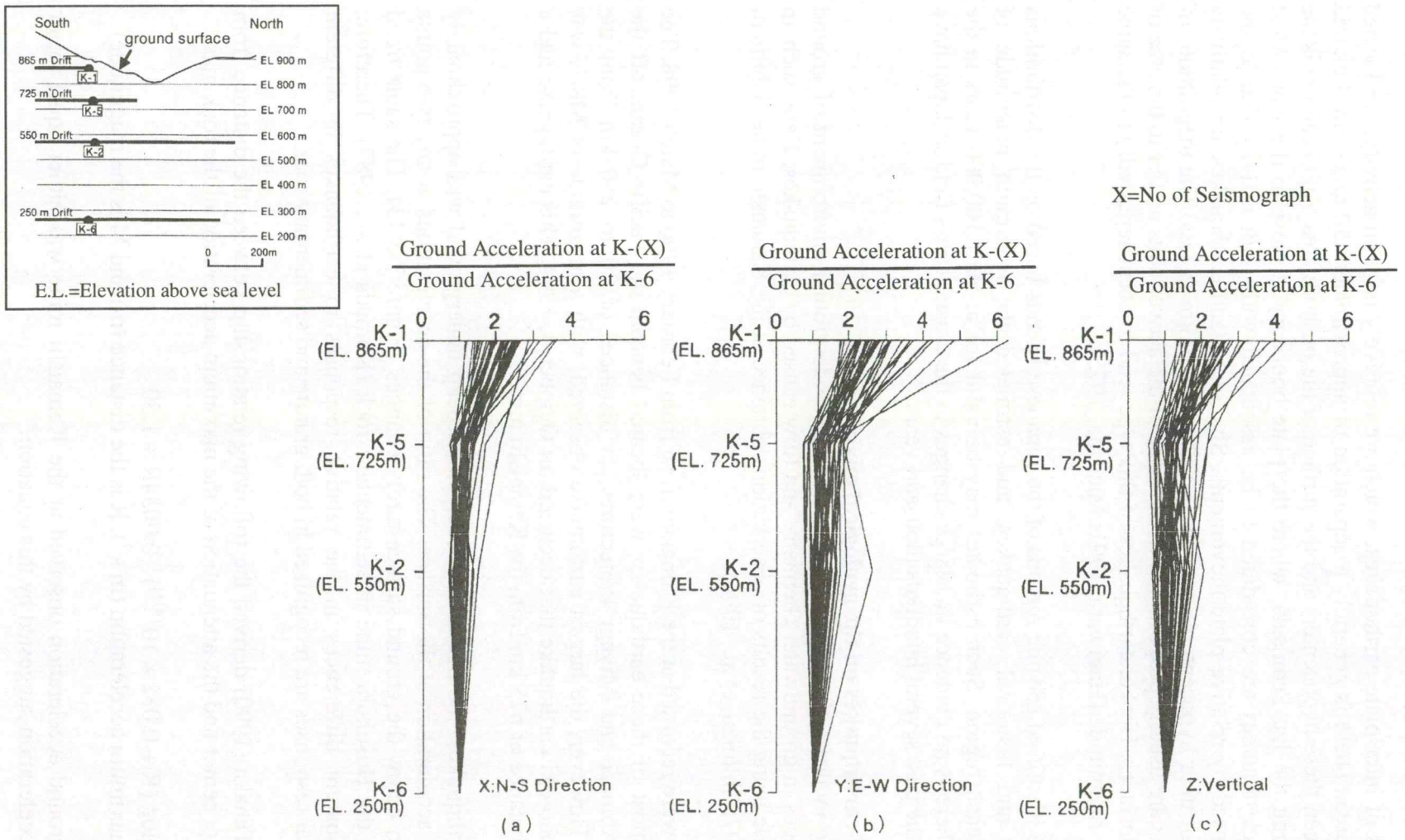


Figure 2.3-13 Ratios of ground accelerations due to earthquakes at the K-6 seismograph and other seismographs in the Kamaishi mine (Shimizu et al., 1996)

(a) N-S direction, (b) E-W direction, (c) vertical direction. This figure includes 41 earthquakes observed during the period from January 1991 to December 1994.

average ratio of 0.7. Most of these ratios are less than 1 at the time when the horizontal motion is at its peak. The velocity response spectrum of observed earthquakes was approximately similar to that calculated according to Fukushima (1994).

These results show that the dynamic influence of earthquake vibrations on the deep underground environment is smaller than their influence on near surface environments. At the same time, the future behavior of rock masses during maximum earthquake vibrations is considered to be predictable, because the observations and the theoretical results agreed well.

Next, the influence of the earthquake vibrations on groundwater flow is evaluated using observations of hydraulic pressure changes in the Kamaishi mine. The hydraulic pressure was monitored from 1990 onwards (Ishimaru and Shimizu, 1997; Shimizu et al., 1996). The observed seasonal changes in hydraulic pressure were approximately 0.1 MPa. Groundwater pressure changes due to earthquake vibrations were found to occur during 27 of the 334 earthquakes monitored. The largest hydraulic pressure change associated with these earthquakes was 0.035 MPa in the KWP-2 hole; the changes in the KWP-1 hole ranged through less than approximately 0.01 MPa. The largest hydraulic pressure changes that would occur anywhere over at the Kamaishi mine during an earthquake have been estimated to be less than seasonal variation of 0.1 MPa (Shimizu et al., 1996).

The results from the investigations at the Kamaishi mine showed that hydraulic pressure perturbations due to an earthquake did not persist for more than several weeks. After this time span, measured hydraulic pressures returned to their normal trend (Aoki et al., 1999).

Similar evidence for a relatively short-term influence of earthquakes has also been reported at other locations. For example, Kawabe (1991) reported changes in the groundwater table during the Nankaido earthquake of 1946. It is known that, at the time of this earthquake, there was a reduction of approximately 14 m in the water levels of the four sources of the Dogo Hot Spring, which were excavated to a depth of up to 303 m. However, these water levels returned to their original positions after three months. Similar phenomena were also observed at the Dogo Hot Spring during Nankaido earthquakes in the Hakuho, Hoei and Ansei periods.

Waters from springs in the tunnels of the Kamaishi mine were analyzed before and after earthquakes, to establish if the earthquakes influenced the groundwater chemistry. However, significant changes in groundwater chemistry were not observed. Only minor changes were observed in SO_4 and HCO_3 in four cases (Aoki et al., 1999).

Accordingly, the results from the investigations at the Kamaishi mine showed that most changes in the groundwater flow and chemistry due to earthquakes were temporary. Furthermore, the changes were small compared with changes due to other factors, including seasonal ones. These results indicate that the influence of earthquakes on the geological environment deep underground is limited.

Shimizu et al. (1996) are reviewing the correlation between the hydraulic pressure change during an earthquake and the rock mass strain. Pressure data for 27 earthquakes at the Kamaishi mine were used. The approaches of Dobrovolsky et al. (1979) and Okada (1995) were applied to calculate the rock mass strain. In these approaches, the strain is calculated from the magnitudes and hypocentral distances.

No detectable hydraulic pressure changes were caused by earthquakes that were calculated to

produce a strain smaller than 10^{-8} (when the approach of Dobrovolsky et al. (1979) was used to calculate strain) or smaller than 10^{-10} (when the approach of Okada (1995) was used). On the other hand, the hydraulic pressure did change during more than 60% of the earthquakes with theoretical strains larger than these values (Figure 2.3-14). Approximately 0.05 μm of residual strain was recorded with a crystal tube extensometer-type rock mass strain gauge at the Kamaishi mine during the Miyagi-ken-oki earthquake on October 11, 1997. Then, a hydraulic pressure change of 2.4 KPa was observed. Thus, the results suggest that the earthquakes that cause hydraulic pressure changes might generate residual strain in the rock mass.

2.3.3 Summary

Major earthquakes and fault movements in the shallow inland area of Japan have occurred repeatedly at existing active fault zones for the past several hundred thousand years. The nature of these movements has been similar throughout this period. It is considered that, during this time, a stable crustal stress field has been maintained. Therefore, it is predicted that the present stress field and associated fault movements will continue for at least 100,000 years in the future.

The mechanical influence of fault activity on the geological environment is limited mainly to fault crushed zones. The extent of this influence is several meters to several hundred meters at most. The range over which associated small faults are distributed in the surrounding rock mass is considered to be within a few kilometers of large active faults.

A detailed investigation of the closest active faults to any future site proposed for HLW disposal should be performed. This investigation should allow an appropriate distance between the disposal facilities and the active faults to be defined. This is necessary because the sizes of regions affected by fault activity depend on the sizes of the active faults. In addition, an in-depth investigation should be performed at the site to identify whether or not there are small active faults that cannot be recognized during regional surveys. This approach will allow detailed siting to avoid the influence of such faults. The effects of earthquakes also should be considered during the design of the geological disposal system. However, the influence of earthquake vibrations several hundred meters underground or deeper is generally regarded to be small.

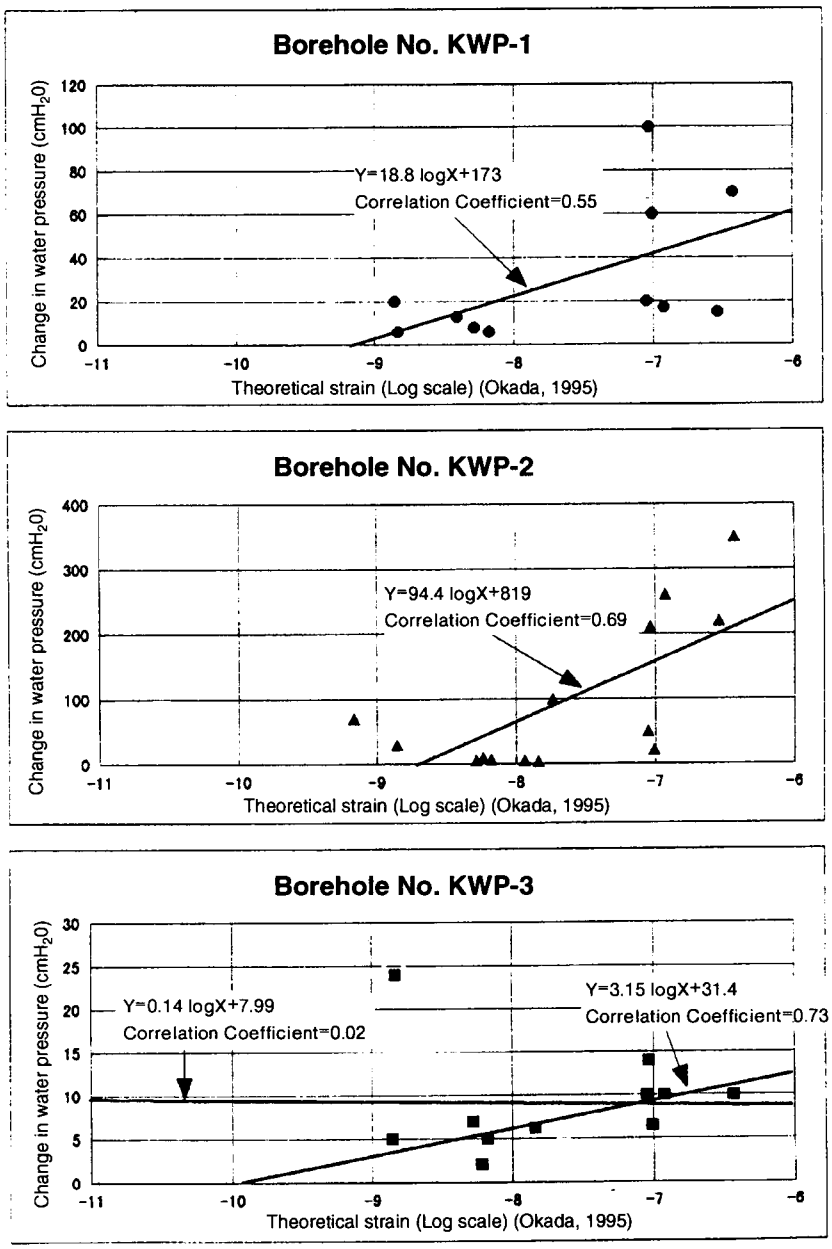


Figure 2.3-14 Relationship between the theoretical amount of strain and change in water pressure observed in boreholes drilled from gallery at the Kamaishi mine

2.4 Volcanism

Volcanic activity (and other igneous activity) is expressed as an eruption at the surface, intrusion into the earth's crust and related processes of magma generation deep in the earth (Aramaki, 1996). The influences of volcanic activity on the geological environment include:

- dynamic destruction and subsidence of basement rocks, caused by the intrusion and eruption of magma;
- an increase in rock temperature due to heat released from the magma;
- creation of hydrothermal convection systems (causing changes in the groundwater flow system) and thermal, hydrogeological and geochemical changes in groundwater owing to mixing between hot water and volcanic gas and water/rock interactions at elevated temperatures.

These processes are important factors affecting the long-term stability of the geological environment. An understanding of the spatial and temporal nature of these processes will assist in the selection of an appropriate disposal site.

2.4.1 Characteristics of volcanism in Japan

Magmatic intrusion, eruption and the formation of calderas due to volcanic and magmatic activity cause significant changes to the geological environment. The probability that these phenomena, particularly the intrusion/eruption of magma, will have significant effects should be reduced to acceptably low levels by selecting an appropriate disposal site. Therefore, it is necessary to understand regional variations and temporal changes in volcanic and magmatic activity in the Japanese islands and to identify the locations where volcanism may occur in the future.

1) Quaternary volcanoes and tectonic setting

Most volcanoes are located at divergent and convergent plate boundaries. Japan and its vicinity are located in the subduction zone of a convergent plate boundary. There are approximately 350 Quaternary volcanoes in Japan (Committee for Catalog of Quaternary Volcanoes in Japan (ed.), 1999). These Quaternary volcanoes are mainly divided between the East Japan Volcanic Belt, running from Kurile Islands, Hokkaido, northeast Honshu and Izu to Mariana Islands, and the West Japan Volcanic Belt, running from San-in and Kyushu to the Seinan Islands (Sugimura, 1960) (Figure 2.4-1).

(1) East Japan Volcanic Belt

The East Japan Volcanic Belt is situated on the North American, Eurasian and Philippine Sea plates; the Pacific Ocean plate subducts beneath these plates. The volcanic front (the line connecting volcanoes closest to the trench) is located sub-parallel to the Kurile, northeast Honshu and Izu-Ogasawara arc-trench systems. Seismicity associated with the subducting plate occurs 100 to 110 km beneath the volcanic front. Volcanoes in the eastern part of Hokkaido are located in the southwest of the Kurile Arc and are arranged in an en echelon pattern trending northeast to southwest, oblique to the elongation of the Kurile Arc. Apart from the Rishiri volcano, all the volcanoes are within 60 km of the volcanic front. The volcanic front, which trends ENE-WSW in the eastern part of Hokkaido, changes its direction to N-S in southwest Hokkaido and runs roughly parallel to the Northeast Honshu Arc. However, where the two arcs meet, there is a region, about 50 km long, without volcanoes (Nakagawa et al., 1995).

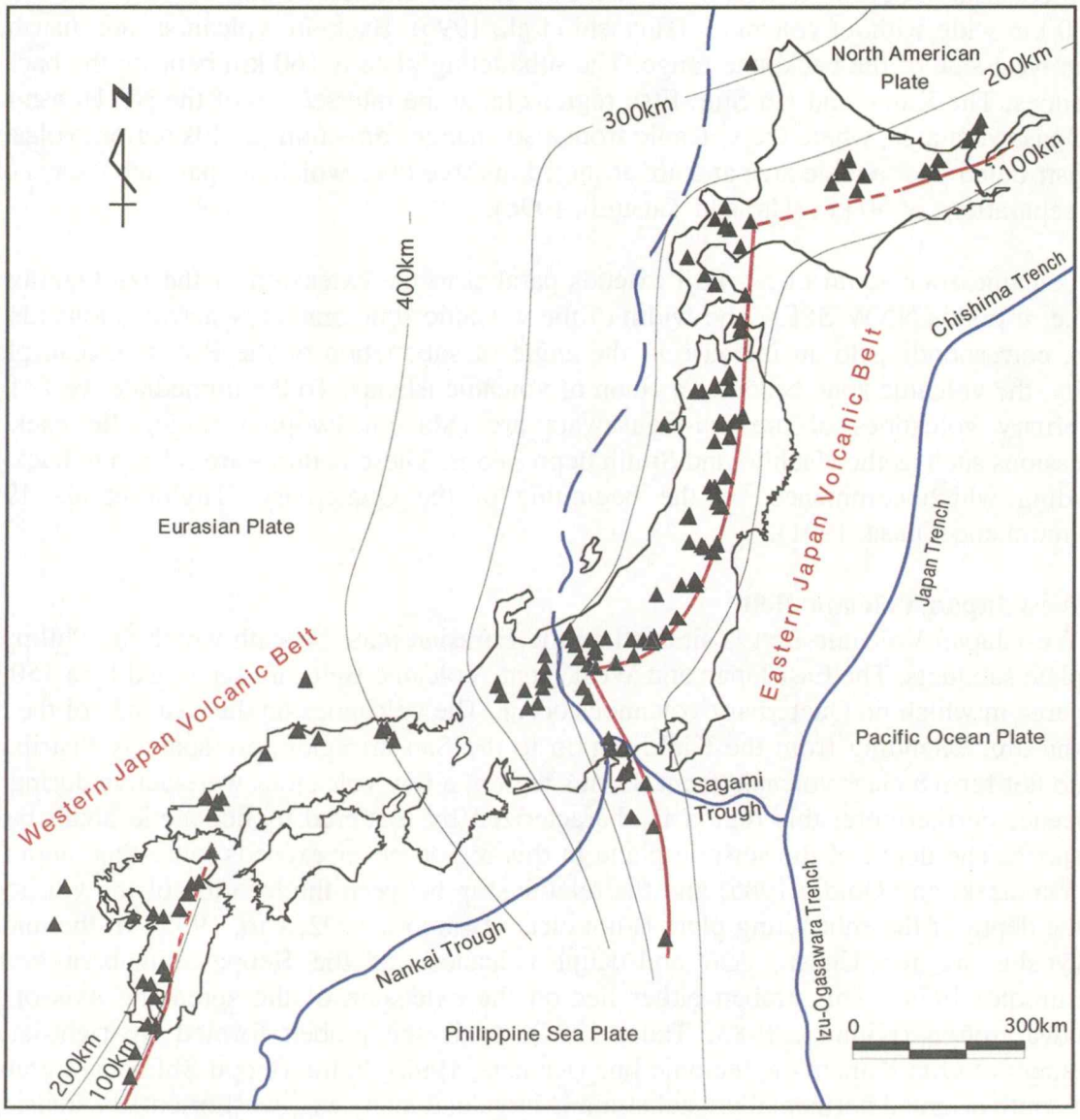


Figure 2.4-1 Tectonic setting and distribution of Quaternary volcanoes in Japan
(after the Committee for Catalog of Quaternary Volcanoes in Japan, 1999)

The Quaternary volcanoes in Japan have a clear spatial relationship to the oceanic plates (i.e. the Pacific Ocean Plate and Philippine Sea Plate), forming a belt which runs almost parallel to the trenches where the oceanic plates are subducting.

Quaternary volcanoes in northeast Honshu are distributed both along the volcanic front and in the back-arc region. Along the volcanic front, they form a central, linear mountain chain, referred to as the "backbone range". Volcanoes in the backbone range form 7 clusters, each of which consists of several to tens of volcanoes. Between one cluster and the next is a zone 50 to 100 km wide without volcanoes (Hayashi et al., 1996). Back-arc volcanoes are distributed on the west side of the backbone range. The subducting plate is 160 km beneath the back-arc volcanoes. The Kanto and Ko-Shin-Etsu regions lie at the intersection of the NE Honshu and Izu-Ogasawara arcs, where the volcanic front also changes direction. In this region, volcanoes are distributed over a wide area and are arranged in three lines which are parallel to each other with separations of 50 km (Uto and Tatsumi, 1996).

The volcanic zone south of Mt Fuji extends parallel to the extension of the Izu-Ogasawara arc (i.e. it trends NNW-SSE). The width of the volcanic zone gradually narrows towards the south, corresponding to an increase in the angle of subduction of the Pacific Ocean plate. Finally, the volcanic zone becomes a chain of volcanic islands. To the immediate west of the Quaternary volcanoes of the Izu-Ogasawara arc (Shichito-Iwojima ridge), lie back-arc depressions such as the Hachijo and Smith depressions. These features are related to back-arc spreading which commenced at the beginning of the Quaternary (Taylor et al., 1991; Nishimura and Yuasa, 1991).

(2) West Japan Volcanic Belt

The West Japan Volcanic Belt is situated on the Eurasian plate beneath which the Philippine Sea plate subducts. The East Japan and West Japan Volcanic Belts are separated by a 150 km wide area in which no Quaternary volcanoes occur. The volcanoes on the east side of the SW Honshu arc, extending from the Kinki region to the San-in region, are sparsely distributed and do not form a clear volcanic front. In this region, a few volcanoes were active during the Holocene. Furthermore, this region is characterized by scattered monogenetic alkali basalt volcanoes. The depth of the seismic plane in this region never exceeds more than about 80 km (Yamazaki and Ooida, 1985) and the relationship between the location of the volcanoes and the depth of the subducting plate is not clear (Iwamori, 1992; Uto, 1995). In the middle of Kyushu are the Unzen, Aso and Kuju volcanoes of the Beppu-Shimabara graben (Matsumoto, 1979). This graben either lies on the extension of the spreading axis of the Okinawa trough (Kimura, 1983; Tada, 1984), or is the graben formed by right-lateral movement of Oita-Kumamoto tectonic line (Kamata, 1992). In the Beppu-Shimabara graben, north-south oriented horizontal crustal strain is large and many east-west oriented extensional faults exist. Between the Kirishima and Aso volcanoes in the southern part of Kyushu, there is a gap of 150 km without any volcanoes; this gap corresponds to the west side of the subducted Kyushu-Palau seamount chain.

The angle of subduction in the middle of Kyushu (near the Aso volcano) is 70°, whereas in the south of Kyushu (near the Kirishima volcano) it is 50°. There is, however, no deep seismic plane directly beneath the Aso volcano (Kamo et al., 1990). The volcanic front of the Ryukyu Arc is clearly defined by the line of volcanoes extending from the Kirishima volcano southwest to Okinawa-Torishima; however, no Quaternary land volcanoes are known to the south of Okinawa-Torishima. Seamounts and knolls with geomagnetic anomalies occur along the extension of the volcanic front in this region and these may be the expression of Quaternary volcanoes (Furukawa, 1991). The deep seismic plane directly beneath the volcanic front in this region is at a depth of about 100 km. The Okinawa trough is on the back-arc side of the volcanic front and this is regarded as evidence of spreading beginning in the early Quaternary (Kimura et al., 1985).

(3) Volcanic belts and plate configuration

The above discussion has shown that the density and pattern of Quaternary volcanoes varies from one region of Japan to another. However, the location of the volcanic belts is closely related to the geometry of the subducting plates. In most cases, the deep seismic plane is at a depth of between 100 and 150 km beneath the volcanic front. Other island arc volcanic belts have seismic zones at similar depths. The widths of the volcanic belts are related to the angle of plate subduction; the steeper the angle the narrower the width of the volcanic belt (Tatsumi, 1995).

The density of volcanoes within a volcanic belt is controlled by the age of the subducting plate and its movement direction (Uto and Tatsumi, 1996). Arcs that have well defined volcanic fronts, such as the NE Japan and Ryukyu Arcs, are underlain by comparatively old plates subducting perpendicular to the volcanic front. However, in SW Japan, the subducting plate is relatively young (the Shikoku Basin) and subducts obliquely. Because the plate in the former case subducts efficiently, it causes well developed convections in the mantle wedge, which result in active volcanism (Uto and Tatsumi, 1996).

In conclusion, the characteristic distribution of the Quaternary volcanoes in Japan is related to the arrangement of the plates, the relative direction and angle of subduction, the age of the subducting plates and the maximum depth of subduction.

2) Subsurface structure beneath the volcanic edifice

Magma generated by melting of the earth's crust or upper mantle may erupt at the surface and form volcanic craters, or it may be held in subsurface magma chambers. Estimating the possibility of an eruption in a particular area requires knowledge of the magmatic plumbing system (Takahashi, 1997) and the factors influencing it.

(1) Magmatic plumbing system

Data on the location of magma chambers within the crust can be obtained directly from the distribution of earthquake hypocenters and the analysis of earthquake focal mechanisms. Also, it is possible to locate magma chambers through the interpretation of S-waves and the analysis of sonic velocity (e.g. Hasegawa and Matsumoto, 1997; Ukawa, 1994) and the electromagnetic structure of the crust (e.g. Kagiyama, 1997). It is possible to estimate the depth of a magma chamber using a two-pyroxene geobarometer (Nimis, 1995) or normative plot of bulk composition (Baker and Eggler, 1983). Also, volcanic necks and radial dykes inside stratovolcanoes correspond to central vents and lateral volcanoes (Nakamura, 1969). This information can be used to understand the spatial structure of the magma supply system.

Takahashi and Takahashi (1995) and Takahashi (1997) considered the spatial and temporal arrangement and structure of the magma supply system through compilation of recent information for several active volcanoes in Japan. They concluded that basaltic polygenetic volcanoes have one magma plumbing system connected to the upper mantle and that magma chambers are developed on several structural levels. On the other hand, andesitic polygenetic volcanoes have plural magma plumbing systems and magma is supplied to the chamber beneath the volcano from deeper magma chambers. The magma chamber that feeds the volcano is at a depth of several to tens of kilometers.

(2) Magmatic plumbing system and tectonics

The factors controlling the spatial structure of the magma supply system include the density structure of the crust, the magma supply rate from the mantle and the crustal stress field. The

density structure of the crust controls the depth and location at which the magma chamber tends to form. The magma supply rate and duration control the size and future growth of the magma chamber. The crustal stress field controls the form of the magma supply system and its stability (Takahashi and Takahashi, 1995). Of these, the orientation of the principal stresses is thought to control the orientation and location of the central vent and radial dikes.

Takahashi (1994a) defined volcanoes whose central vent had moved less than 1.5 km during the last ten thousand years as "stable vent-type polygenetic volcanoes"; volcanoes whose central vent had moved more than 1.5 km were defined as "unstable vent-type polygenetic volcanoes". The factors controlling the stability of these volcanoes are the regional and local stress distribution. In extensional stress fields, open fractures may form and unstable vent-type polygenetic volcanoes tend to develop. In compressional stress fields, open fractures are less likely to occur and stable vent-type polygenetic volcanoes are dominant. However, if local tension exists within a regional compressional stress field, unstable vent-type polygenetic volcanoes could form.

The arrangement of volcanic craters reflects the stress field within the crust. Radial dikes change their orientation away from the central vent and become parallel to σ_{Hmax} (the maximum horizontal compressive stress); craters also align in the direction of σ_{Hmax} (Nakamura, 1969). Takahashi (1994b) classified the Quaternary volcanoes of Japan into P-type (crater alignment parallel to the P axis) and O-type (crater alignment oblique or perpendicular to the P axis), where the P axis is the direction of σ_{Hmax}. O-type volcanoes tend to occur in uplifted topographic heights bounded by one or more fault(s). These are considered to have formed due to gravity sliding in the uplifted blocks.

If a large volume of felsic magma erupts in a short time, the top of the magma chamber subsides and a collapse caldera is formed at the surface. Collapse calderas are classified into Valles-type, funnel shape and Nigorikawa-type (Aramaki, 1983). The largest collapse caldera in Japan is the Aso caldera that measures 25 km from north to south and 18 km from east to west. A collapse caldera is only formed if a large magma chamber existed beneath a volcano. The regional stress field controls the size of the magma chamber. Takahashi (1995) pointed out that, for a large quantity of magma to accumulate, a slow crustal strain rate is required.

In summary, the existence of magma chambers, their depth and size can be estimated from the analysis of sonic velocities and the electromagnetic structure of the crust. The spatial arrangement of the magma supply system can be investigated by studying the tectonics and crustal stress field in the area.

3) Spatial and temporal distribution of Quaternary volcanoes

(1) Catalog of Quaternary volcanoes in Japan

In order to develop a detailed understanding of Quaternary volcanism in the Japanese islands, a detailed database is required, which records information such as the age and size of volcanoes, the cycle of eruptions and temporal and spatial changes in volcanism. Examples of such databases are the Catalog of Active Volcanoes published by IAVCEI, the National Catalog of Active Volcanoes in Japan published by the Japan Meteorological Agency and Volcanoes of Japan (2nd edition) published by the Geological Survey of Japan. However, these sources do not include all the information on volcanoes required to identify the areas where a suitable site for HLW disposal might be located. Therefore, a new database, called the Catalog of Quaternary Volcanoes in Japan (Committee for Catalog of Quaternary

Volcanoes in Japan (ed.), 1999) was prepared. This database includes all the Quaternary volcanoes in the Japanese islands with brief descriptions of their characteristic features.

The principal source for the new catalog is Volcanoes of Japan (2nd edition), published by the Geological Survey of Japan. However, the information has been updated. For each volcano, the catalog lists the following information:

- type of volcano
- classification of the volcanic rocks in the volcano
- dates of eruptions
- chemical composition (SiO_2 weight percent)
- the number of analytical studies
- list of references
- map of the volcano.

An example of the contents of the catalog is shown in Figure 2.4-2.

The number of Quaternary volcanoes (i.e. volcanoes that have erupted within the last 2 million years) listed in the catalog is approximately 350. Figures 2.4-3a and 2.4-3b are histograms showing the total volumes of Quaternary volcanoes and the durations of their activities. The mode of the volume data occurs between 0 and 10 km^3, while that of the duration of activity occurs between 100 and 200 thousand years. The average volume is 41.3 km^3 and the average duration of activity is 382,000 years.

(2) Spatial and temporal distribution of Quaternary volcanoes in Japan

Figures 2.4-4a and 2.4-4b show the distribution of volcanoes that have erupted between the present and 500,000 years (0.5 Ma) ago, from 0.5 to 1 Ma ago, from 1 to 1.5 Ma ago and from 1.5 to 2 Ma ago. This shows that the Quaternary volcanoes occur within the East Japan Volcanic Belt and the West Japan Volcanic Belt and that there have been no Quaternary volcanoes on the trench sides of the volcanic fronts. Figure 2.4-5 shows the temporal change in the volcanic front in NE Japan for four time periods (Umeda et al., 1999c). This shows that the volcanic front since 2 Ma ago lies within the range 20 to 30 km wide along the backbone range.

It can be concluded that there has been no change in location of volcanism on the scale of the island arc (several hundred km) since the beginning of the Quaternary. However, changes have occurred within some volcanic regions (i.e. on the scale of several tens of km), including expansion or shrinkage of active volcanic regions.

(3) Spatial and temporal distribution of volcanic regions

Investigations of the spatial and temporal changes in volcanism require detailed data from individual volcanoes. Two volcanic regions have been studied in sufficient detail to elucidate the pattern of volcanism over time, namely the Sengan region (Umeda et al., 1998; Ohba and Umeda, 1999) and the Hisatsu region (Yokose et al., 1998). Their evolution is outlined below.

In the Sengan region in NE Japan, which covers an area of 50 km from east to west and 30 km from north to south, there are 37 volcanoes. In Figure 2.4-6, the locations of active volcanoes are shown for four time periods:

i. from the present to 0.5 Ma ago

English

レコード番号 42

火山番号 194　火山名 羊蹄

備考 年代測定値欄：Yo-III; 羊蹄第３軽石・スコリア層, Yo-II; 羊蹄第２軽石・スコリア層, Yo-I; 羊蹄第１軽石・スコリア層, En-a; 恵庭a
降下火砕物の体積はHayakawa(1985)のV(総体積)=12.2×T(層厚)×S(等厚線の囲む面積)の式を使用した．[9]

登録年月日 1997.2.19
修正年月日 1998.12.25

著者 児玉浩・宇井忠英・中川光弘

個別火山体名 羊蹄

別名 後方羊蹄，蝦夷富士，マッカリヌプリ

個別火山体の位置

最高点高度 1989 m

基盤高度 250 m

分布面積 38.5 km^2

火山体体積 18.2 km^3

緯度　経度

地形的 N, E

主火道 42°49'30" N, 140°48'42" E

分析値
Hb.-ol.-bg. hyp.-aug. andesite (SiO2=55.3~64.7%) [1] (15個)
Aug.-hyp. andesite (SiO2=54.2~65.0%) [2] (35個)
Ol.-bg. aug.-hyp.andesite (SiO2=54.2~63.8%) [2] (7個)
Hb.-bg. aug.-hyp. dacite (SiO2=64.4%) [2] (1個)
Aug.-hyp. dacite (SiO2=63.0~65.9%) [2] (5個)

岩石名	玄武岩	玄武岩質安山岩	安山岩
	なし	稀	大部分
	デイサイト	流紋岩	その他
	少ない	なし	

層序
羊蹄火山は洞爺火砕流堆積物とその２次堆積物からなる海抜200-250mの台地上に生じた成層火山である．[2]

火山体の分類
成層火山(SC)

噴出物の分類
[先羊蹄]岩屑なだれ堆積物 0.72km3
[旧期]溶岩流(LF)(不明)
[新期]火砕丘(PC)｜0.23km3
　溶岩流(LF)｜
[北山期]溶岩流(LF)｜(不明)
　火砕丘(PC)｜
[側火山]溶岩円頂丘(LD)スコリア丘
　(PC)0.32km3
降下火砕物
Yo-a 不明
Yo-I 2.0km3
Yo-II 0.5km3
Yo-III 1.1 km3
Yo-ks (不明)
他の８枚 (不明)
(早川由紀夫の12.2TSを使用)
[2,7,8]

年代測定値
Yo-IIIの下部のSpfa-1, Spfl; 4200±1800y.B.P., 14C法[3]
羊蹄山東麓のYo-IIの直下と思われる層準;
25270±1080y.B.P.,27280±1910y.B.P.,14C法[4]
Yo-I上位のEn-aの２次堆積による内陸古砂丘中 ;13100±1200y.B.P.,14C法[5]
Yo-I直下の層準を示すと思われる野幌丘陵の河岸段丘堆積物中の木片;
15000±400y.B.P.,14C法[6]
Yo-a; 5930±2180y.B.P.,14C法[8]
西麓の岩屑なだれ堆積物中の岩片，0.02±0.05Ma K-Ar法 [10]

引用文献

[1]
[2] 藤田豪平(1992)西南北海道，羊蹄火山西部の地質と岩石 -先羊蹄火山・羊蹄火山の活動と噴出物の化学組成変化-.北大卒業論文
[3] 柳田誠(1994)支笏降下軽石1 (Spfa-1)の年代試料．第四紀研究33, 205-207.
[4] 大貫康行・井島行夫・春日井昭・佐藤博明(1977) "N, Us-c"降下軽石層の14C年代-羊蹄火山のテフラとその層位関係について-一日本の第四紀層の14C年代 (115) 一．地球科学, 31, 87-89.
[5] 藤山広武・田沼譲(1972)十勝平野に分布する内陸古砂丘の14C年代一日本の第四紀層の14C年代 (72) 一．地球科学, 26, 136-137.
[6] 柏原信(1970)野幌丘陵南部における低位段丘堆積物の14C年代一日本の第四紀層の14C年代 (58) 一．地球科学, 24, 149-150.
[7] 早住 (宇野) リベカ(1996)第四紀露頭集-日本のテフラ-,日本第四紀学会４０周年特別企画, 128-128p.
[8] 佐々木竜男・片山雅弘・富岡悦郎・佐々木清一・矢沢正士・山田忍・矢野義治・北川芳男(1971)北海道における露食質火山灰の編年に関する研究, 第四紀研究, 10, 117-123.
[9]
[10] 中川光弘他 (未公表)

Nakagawa, M. (1992) Spatial variation in chemical composition of Pliocene and Quaternary volcanic rocks in southern Hokkaido, northeastern Japan arc. J.Fac.Sci., Hokkaido Univ., IV, 23, 175-197
Yanagida, M. (1994) Age of the Shikotsu Pumice Fall-1 Deposit. Quaternary Research, 33, 205-207, in Japanese with English abstract.
Ohnuki, Y., Iijima, Y., Kasugai, A. and Sato, H. (1977) Chikyu Kagaku (Earth Science), 31, 87-89. in Japanese.
Fujiyama, H. and Tanuma, Y. (1972) Chikyu Kagaku (Earth Science), 26, 136-137. in Japanese.
Kashiwabara, M. (1970) Chikyu Kagaku (Earth Science), 24, 149-150. in Japanese.
Uno-Hoshizumi, R. (1972) Inventry of Quaternary Outcrops -Tephras in Japan-, Japan association for Quaternary Research 40th Anniversary special publication, 128-128p. in Japanese.
Sasaki, T., Katayama, M., Tomioka, E., Sasaki, S., Yazawa, M., Yamada, S., Yano, Y and Kitagawa, Y. (1971) Studies on Chronology of Humified Tephras in Hokkaido. Quaternary Res., 10, 117-123. in Japanese with English abstract.
Hayakawa, Y. (1985) Pyroclastic Geology of Towada Volcano.Bull. Earthq. Res.Inst., Univ. Tokyo, 60, 507-592
Nakagawa, M. et al. (unpublished)

Figure 2.4-2 An example (Yotei volcano) of the contents of the Catalog of Quaternary Volcanoes in Japan (Committee for Catalog of Quaternary Volcanoes in Japan, 1999)

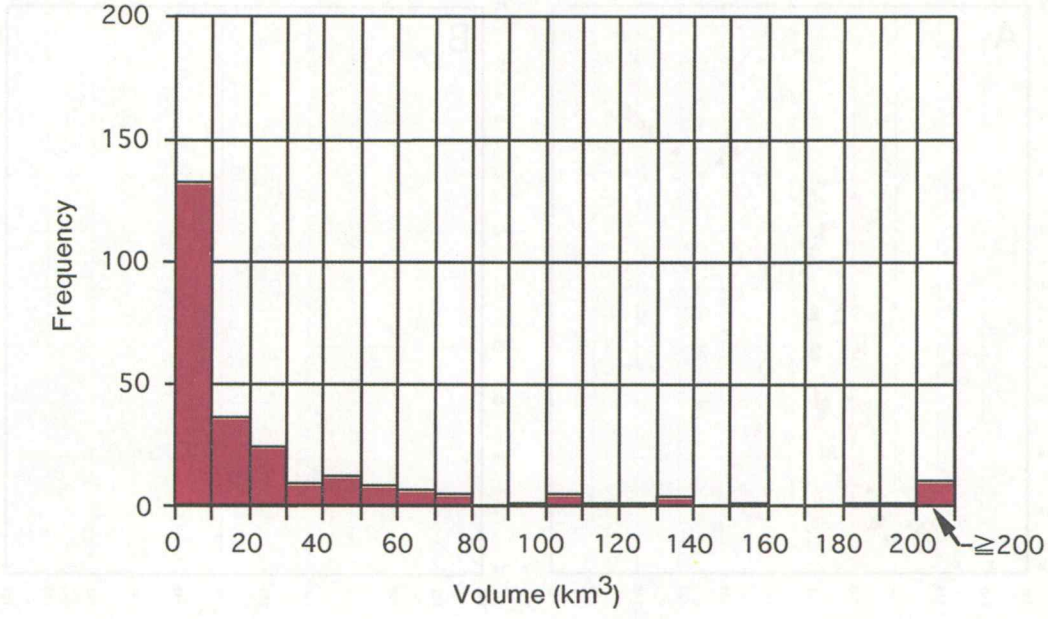


Figure 2.4-3a Histogram of volumes of the Quaternary volcanoes in Japan

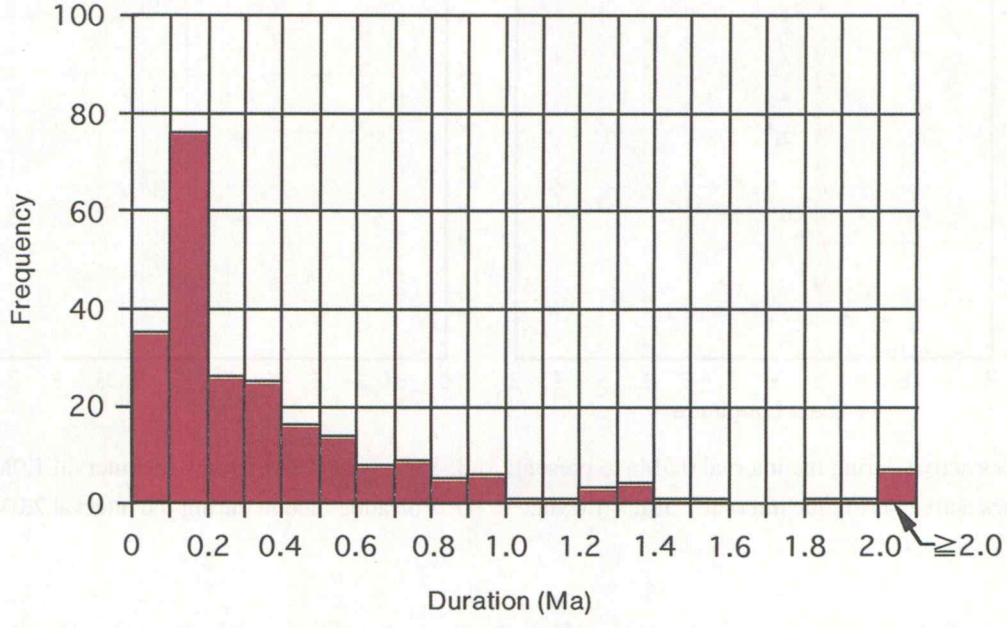
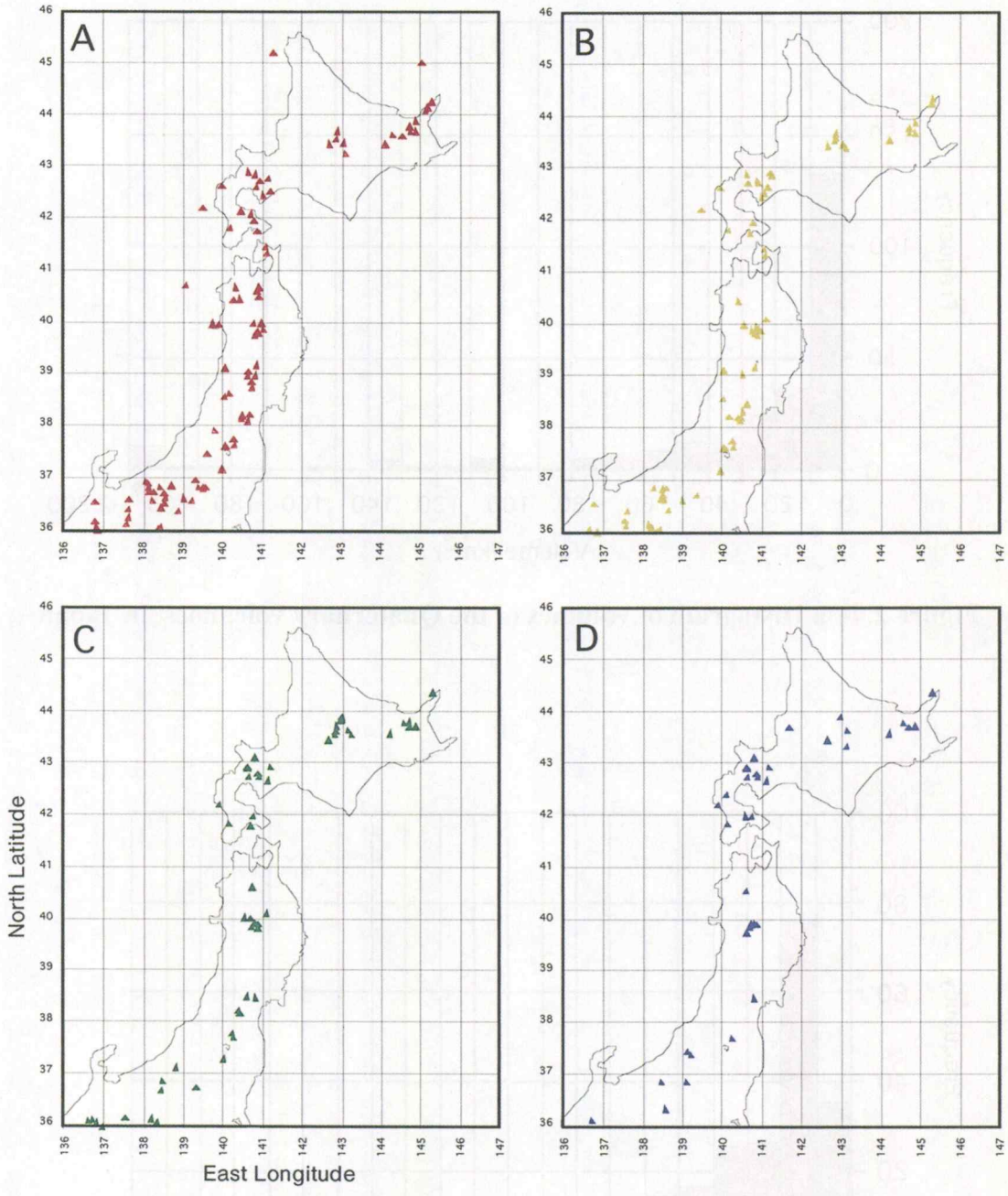


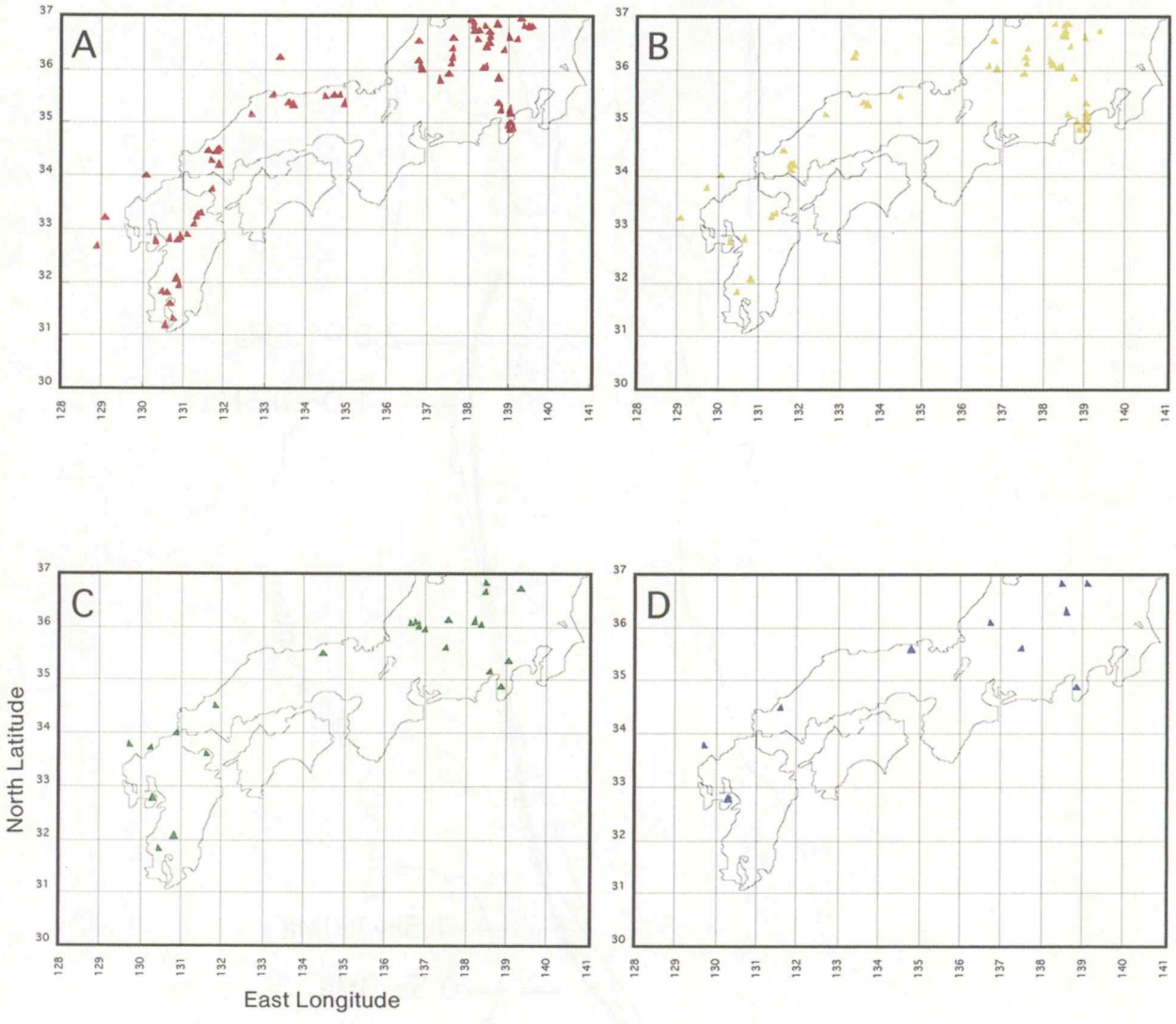
Figure 2.4-3b Histogram of durations of activity of the Quaternary volcanoes in Japan



A: Volcanoes active during the interval 0.5Ma to present; B: Volcanoes active during the interval 1.0Ma - 0.5Ma;
C: Volcanoes active during the interval 1.5Ma - 1.0Ma; D: Volcanoes active during the interval 2.0Ma - 1.5Ma.

Figure 2.4-4a Temporal and spatial distribution of volcanoes during the Quaternary in northeastern Japan (after the Committee for Catalog of Quaternary Volcanoes in Japan, 1999)

Volcanic activity, including the eruption of existing volcanoes and formation of new ones, has occurred repeatedly within restricted areas over the last 2 million years.



A: Volcanoes active during the interval 0.5Ma to present; B: Volcanoes active during the interval 1.0Ma - 0.5Ma;
C: Volcanoes active during the interval 1.5Ma - 1.0Ma; D: Volcanoes active during the interval 2.0Ma - 1.5Ma.

Figure 2.4-4b Temporal and spatial distribution of volcanoes during the Quaternary in southwestern Japan (after the Committee for Catalog of Quaternary Volcanoes in Japan, 1999)

Volcanic activity, including the eruption of existing volcanoes and formation of new ones, has occurred repeatedly within restricted areas over the last 2 million years.

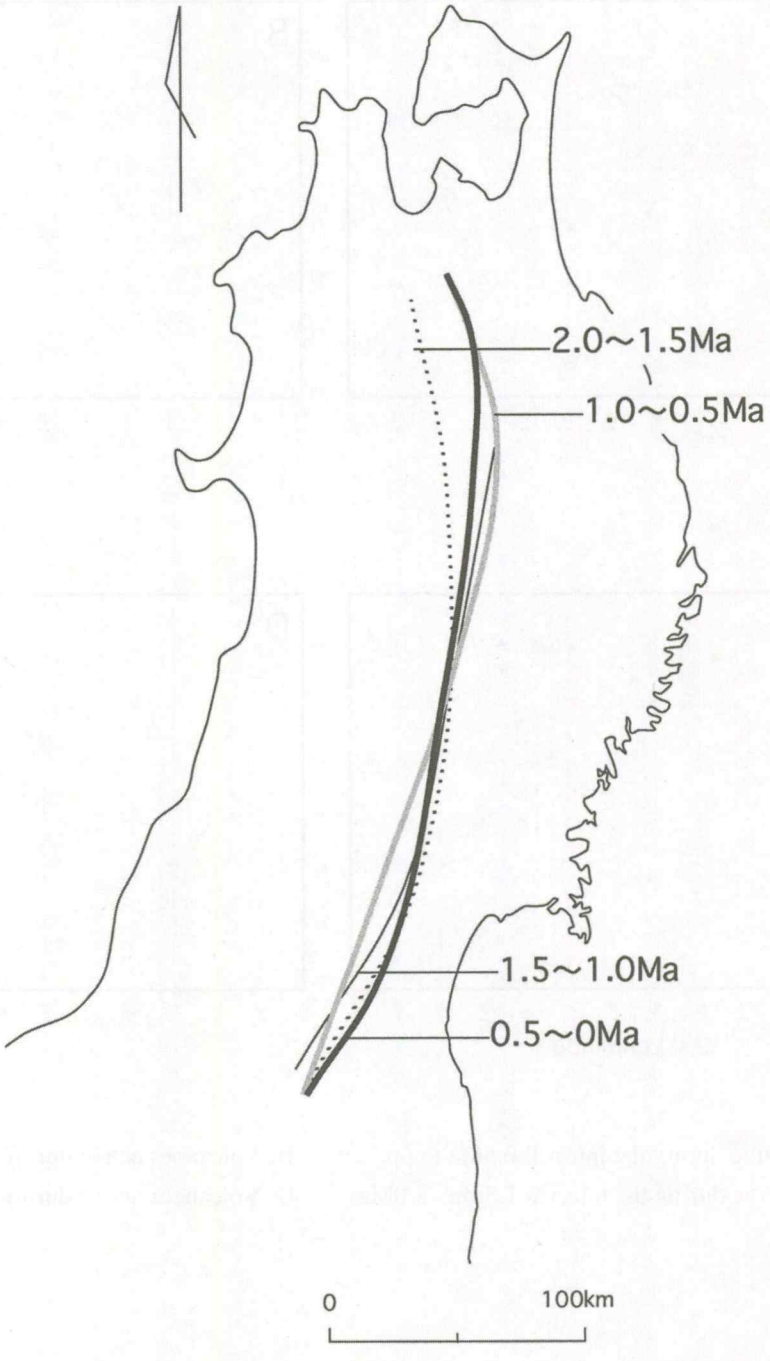


Figure 2.4-5 Shift of volcanic front in northeast Japan
(modified from Umeda et al. ,1999c)

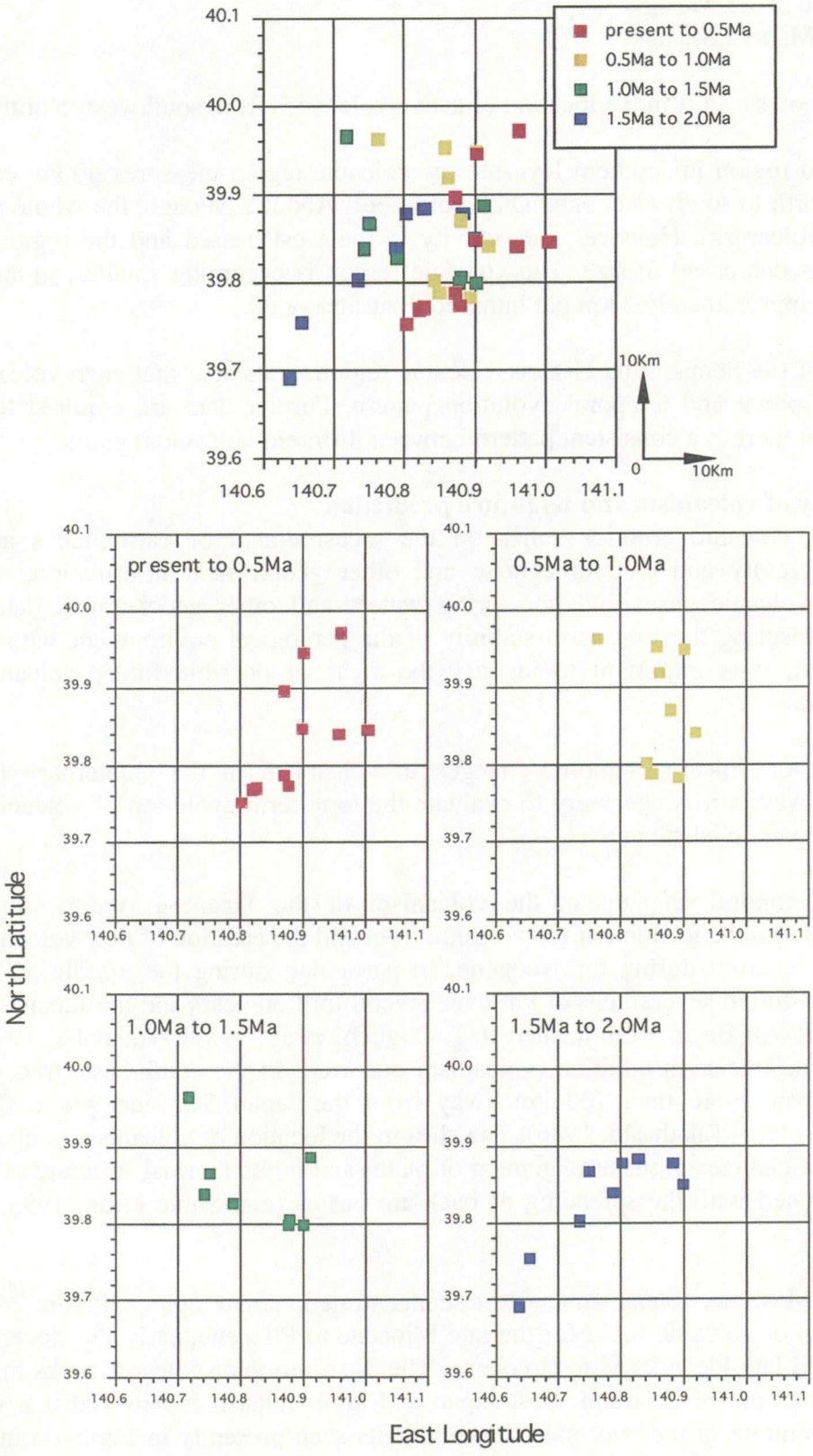


Figure 2.4-6 Temporal and spatial distribution of the eruptive centers of Quaternary volcanoes in the Sengan volcanic region (Umeda et al., 1998)

ii. from 0.5 Ma to 1 Ma ago
iii. from 1 Ma to 1.5 Ma ago
iv. from 1.5 Ma to 2 Ma ago

This figure shows a shift in the location of active volcanoes from southwest to northeast.

In the Hisatsu region in southern Kyushu, the volcanic region measures 60 km east to west and 30 km north to south and contains 20 volcanoes. About 2 Ma ago, the whole region was covered by volcanism. However, the activity in the west ceased and the region of active volcanism has decreased in size. The volcanic region is becoming smaller, in an east-west direction, by approximately 3 km per hundred thousand years.

The studies of the Sengan and Hisatsu volcanic regions indicated that each volcanic region has its own spatial and temporal evolution pattern. Further data are required to establish whether or not there is a consistent pattern between different volcanic regions.

4) Regularity of volcanism and its future prediction

Prediction of volcanic eruption relies on the measurement of earthquakes and crustal movements, gravity and electromagnetic and other geophysical information, as well as sampling of volcanic gases and hot spring waters and other geochemical data. For the purposes of ensuring the long-term stability of the geological environment with respect to HLW disposal, it is important to identify the areas of possible future volcanism using geological data.

On the scale of volcanic regions, changes in volcanism in the Quaternary have been identified. However, it is necessary to evaluate the long-term evolution of volcanism on the scale of the Japanese island arc.

Spatial and temporal changes in the volcanism of the Japanese islands, for example prominent shifts in the location of the volcanic front and the creation of new volcanic regions, have mainly occurred during the Neogene. In particular, during the middle Miocene, the volcanic front shifted several tens of km over several million years and the Japan Sea, Kurile Basin and Shikoku Basin were formed (e.g. Ohguchi et al., 1989; Watanabe, 1994; Hirose and Nakagawa, 1999). In addition, volcanism occurred on the south-east (trench) side of Southwest Japan, more than 100 km away from the Japan Sea side where Quaternary volcanoes exist (e.g. Takahashi, 1986). The shift in the location of volcanism is interpreted to be the result of changes in the arrangement of plates and in the thermal structure of the upper mantle, associated with the spreading of back-arc basins (e.g. Shuto et al., 1993; Sato and Yoshida, 1993).

After the late Miocene, volcanism tended to concentrate in small regions. Figure 2.4-7 shows the distribution of volcanic rocks for the late Miocene to Pliocene, early Pleistocene, middle Pleistocene and late Pleistocene to Holocene. The distribution of volcanic rocks matches the present locations of the East and West Japan Volcanic Belts. It is believed that volcanism began to concentrate in the two main volcanic belts seen presently in Japan during the late Miocene. The movement of the volcanic fronts after the late Miocene is much less than the movement during the middle Miocene. In Northeast Japan, the displacement was about 10 to 15 km towards the west between 8 and 5 Ma ago (Oguchi et al., 1989). In southern Kyushu, the displacement was 6 to 9 mm per year towards the east (Watanabe et al., 1997). Kondo et al. (1998) have also concluded that, in Northeast Japan, volcanism after 14 Ma ago became

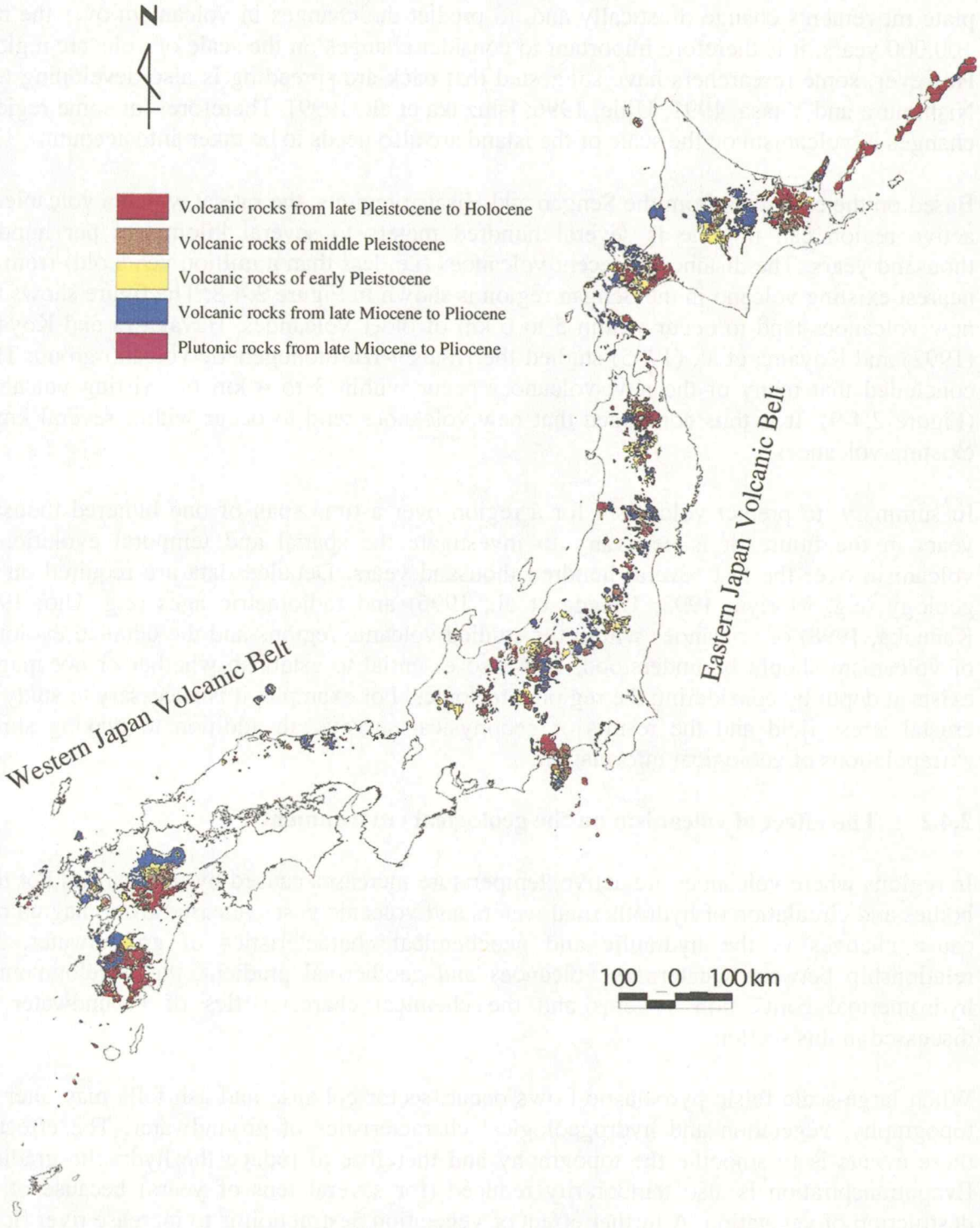


Figure 2.4-7 Distribution of volcanic rocks and plutonic rocks from the late Miocene
(after Geological Survey of Japan, 1992)

Late Miocene-Recent volcanic rocks and plutonic rocks are distributed in the Eastern Japan Volcanic Belt and the Western Japan Volcanic Belt.

concentrated in the volcanic belts.

It is unlikely that there would be changes in volcanism on the scale of the island arc unless plate movements change drastically and, to predict the changes in volcanism over the next 100,000 years, it is therefore important to consider changes on the scale of volcanic regions. However, some researchers have suggested that back-arc spreading is also developing (e.g. Nishimura and Yuasa, 1991; Ujiie, 1996; Ishizuka et al., 1999). Therefore, for some regions, changes in volcanism on the scale of the island arc also needs to be taken into account.

Based on the examples from the Sengan and Hisatsu regions, the rate at which a volcanically active region can migrate is several hundred meters to several kilometers per hundred thousand years. The distance of recent volcanoes (i.e. less than a million years old) from the nearest existing volcano in the Sengan region is shown in Figure 2.4-8. The figure shows that new volcanoes tend to occur within 5 to 6 km of older volcanoes. Hayakawa and Koyama (1992) and Koyama et al. (1995) studied the Higashi-Izu monogenetic volcano group. They concluded that many of the new volcanoes occur within 3 to 4 km of existing volcanoes (Figure 2.4-9). It is thus concluded that new volcanoes tend to occur within several km of existing volcanoes.

In summary, to predict volcanism for a region over a time span of one hundred thousand years in the future, it is necessary to investigate the spatial and temporal evolution of volcanism over the last several hundred thousand years. Detailed data are required on the geology (e.g. Moriya, 1993; Umeda et al., 1996) and radiometric ages (e.g. Uto, 1995; Kaneoka, 1998) of volcanoes within the studied volcanic regions and the detailed evolution of volcanism should be understood. It is also essential to establish whether or not magma exists at depth by considering the regional tectonics. For example, it is necessary to study the crustal stress field and the results of geophysical surveys, in addition to making simple extrapolations of geological information.

2.4.2 The effect of volcanism on the geological environment

In regions where volcanoes are active, temperature increases caused by magma and hot rock bodies and circulation of hydrothermal waters and volcanic gases released from magma may cause changes in the hydraulic and geochemical characteristics of groundwater. The relationship between Quaternary volcanoes and geothermal gradient, the development of hydrothermal convection systems and the chemical characteristics of groundwater are discussed in this section.

When large-scale felsic pyroclastic flows occur, sector collapse and ash falls may alter the topography, vegetation and hydrogeological characteristics of groundwater. The effect of these events is to smoothe the topography and therefore to reduce the hydraulic gradient. Evapotranspiration is also temporarily reduced (for several tens of years) because of the destruction of vegetation. A further effect of vegetation destruction is to increase river flows. Recharge to basement rocks, however, does not seem to change significantly. Therefore, deep hydrogeological effects related to changes in topography and vegetation due to volcanism need not be considered further.

1) Distribution of Quaternary volcanoes and geothermal gradient

To understand quantitatively the relationship between volcanoes and the thermal structure of the surrounding area, as well as the relationship between magma chambers and hot dry rock

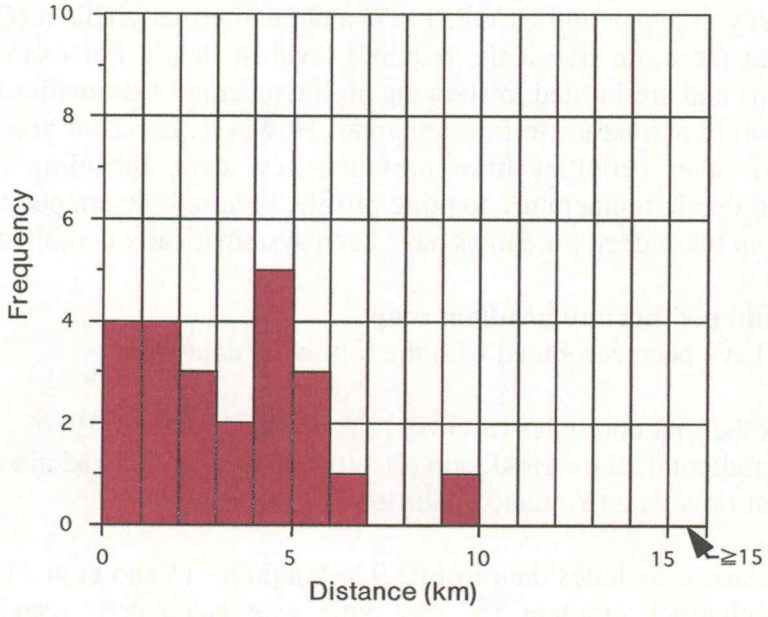


Figure 2.4-8 Histogram of distances from volcanoes formed within the last million years to the nearest earlier volcano in the Sengan volcanic area

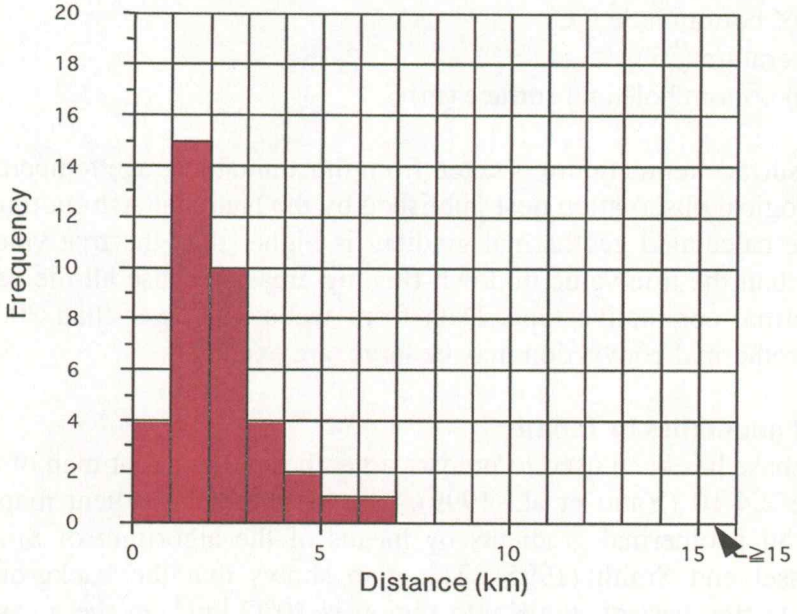


Figure 2.4-9 Histogram of distances from volcanoes formed within the last hundred thousand years to the nearest earlier volcano in the Higashi-Izu monogenetic volcano group

and geothermal effects, it is necessary to study the geothermal structure of the Japanese islands. Data have been published on terrestrial heat flow (Matsubayashi et al., 1992; Geological Survey of Japan and CCOP, 1997) and geothermal gradient (Okubo, 1993; Yano et al., 1994), but these are not at the required level of detail. For example, the data have spatial limitations and are limited to showing high temperature anomalies in volcanic regions and low temperature anomalies in fore-arc areas. However, in recent years, deep drilling for hot springs and other activities have provided new data, including latitude, longitude, elevation, drilled depth, temperature logging profile, bottom hole temperature, standing time, etc. The data from these deep boreholes have been systematically compiled.

(1) Database and geothermal gradient map

The above data have been combined with the following databases:

- data from geothermal boreholes (SIGMA) (Yano and Muraoka, 1986)
- geothermal gradient data for Hokkaido (Geological Survey of Hokkaido, 1995)
- terrestrial heat flow data (Yamano et al., 1997)

The resultant database includes data from 1,936 boreholes (Yano et al., 1999; Tanaka et al., 1999). The geothermal gradient (°C per km) was calculated from the difference in temperature between the bottom of a borehole and the surface. If the temperature logging profile is a straight line, it is referred to as a "thermal conductive type" profile. In such cases, the movement of fluid in the rocks is not prominent. In areas with high temperature anomalies, the temperature logging profile tends to be convex.

$$\Delta T = (T_z - T_0) \times 10^3 / z \quad \text{..... 1)}$$

ΔT : geothermal gradient (°C km^{-1})
T_z : temperature of bottom hole (°C)
T_0 : surface temperature (°C)
z : depth between bottom hole and surface (m)

The estimate of surface temperature is taken from the annual average temperature data at the nearest meteorological observation post published by the National Astronomical Observatory (ed.) (1997). The calculated geothermal gradient is higher than the true value in upwelling areas and lower than the true value in down-flowing areas, because all the data are assumed to be of the thermal conductive type. Data from wells shallower than 300 m, where the influence of hydrothermal convection may be large, are excluded.

(2) Geothermal anomalies in Japan

The derived database has been used to prepare a geothermal gradient map of Japan, which is shown in Figure 2.4-10 (Yano et al., 1999). The geothermal gradient map represents the interpolation of all geothermal gradients by means of the algorithm of Smith and Wessel (1990) and Wessel and Smith (1995). The map shows that the background geothermal gradient in, and to the west of, the Kanto region is 20°C km^{-1}; in the areas of Chubu, the north of Hokuriku, Tohoku and Hokkaido, it is 30 to 50°C km^{-1}. High anomaly areas include east Hokkaido (Shiretoko and Akan regions), central Hokkaido (Taisetsu and Tokachi regions), southwest Hokkaido (Jozankei, Niseko, Shikotsu, Toya, and Oshima Peninsula regions), the Tohoku backbone range (Shimokita, Hakkoda, Sengan, Kurikoma, Zao, Azuma, Aizu, Hijiori, Nasu, Shiobara, and Kusatsu-Shirane regions), the Hida Mountains and the surrounding region, the east Izu Peninsula region, the south Kii Peninsula region, the central San-in region, central Kyushu (Beppu and Shimabara regions) and south Kyushu (Kirishima

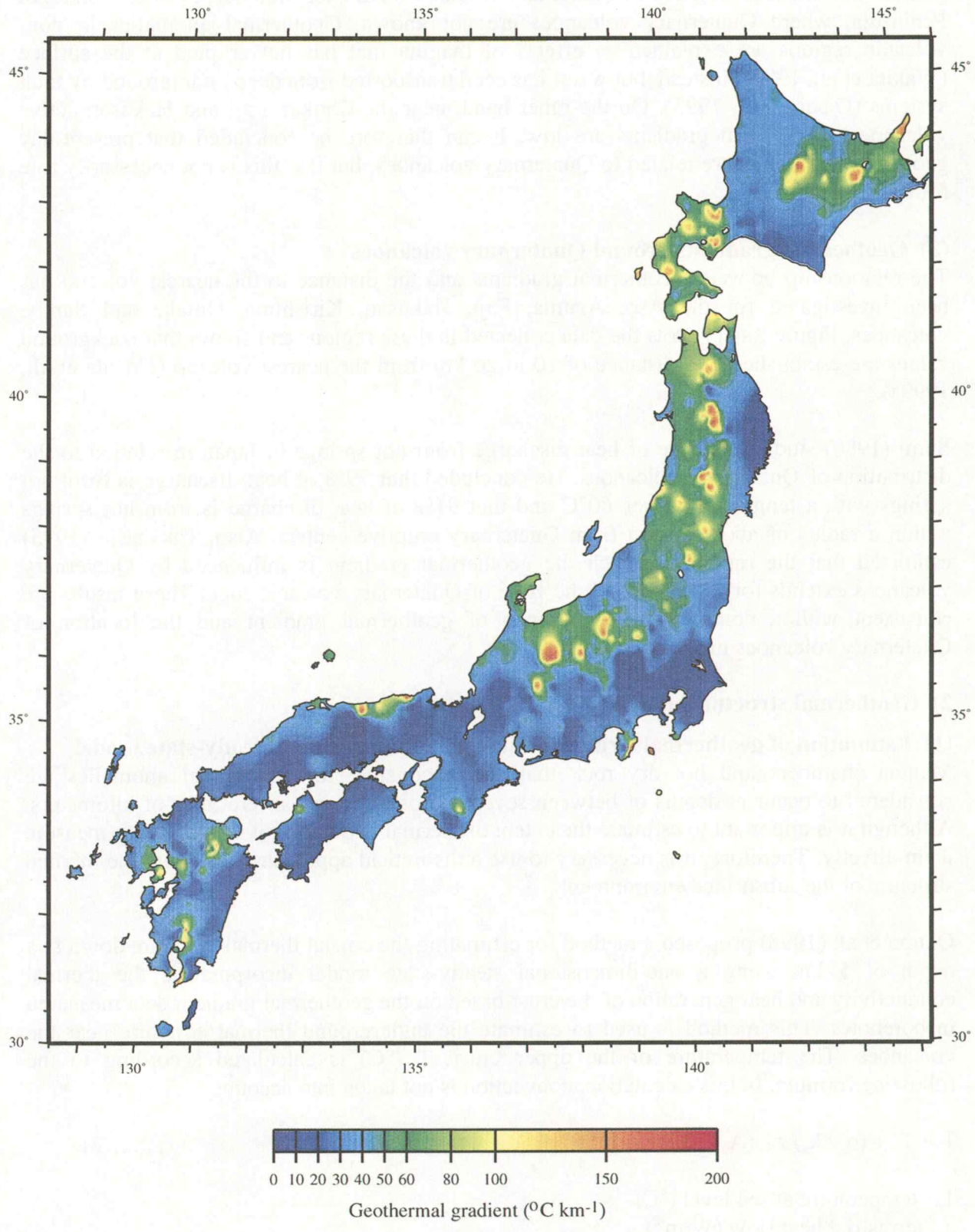


Figure 2.4-10 Geothermal gradient map of Japan (Yano et al., 1999)

and Ibusuki regions). The locations of regions with anomalously high geothermal gradients generally coincide with those of Quaternary volcanoes. An exception occurs in the south Kii Peninsula, where Quaternary volcanoes are not known. Geothermal anomalies in non-volcanic regions are explained as effects of magma that has not erupted at the surface (Wakita et al., 1987). Instead, hot water has been transported from deep underground by fault systems (Oishi et al., 1995). On the other hand, near the Chokai, Fuji and Hakusan active volcanoes, geothermal gradients are low. It can therefore be concluded that present-day geothermal gradients are related to Quaternary volcanoes, but that this is not necessarily true for each volcano.

(3) Geothermal gradients around Quaternary volcanoes

The relationship between geothermal gradients and the distance to the nearest volcano has been investigated for the Aso, Azuma, Fuji, Hakusan, Kirishima, Ontake and Sambe volcanoes. Figure 2.4-11 plots the data collected in these regions and shows that background values are established at a distance of 10 to 20 km from the nearest volcano (Umeda et al., 1999a).

Sumi (1980) studied the rate of heat discharge from hot springs in Japan in relation to the distribution of Quaternary volcanoes. He concluded that 79% of heat discharge is from hot springs with a temperature over 60°C and that 91% of heat discharge is from hot springs within a radius of about 20 km from Quaternary eruptive centers. Also, Takahashi (1995) estimated that the region in which the geothermal gradient is influenced by Quaternary volcanoes extends for 5 km beyond the zone of Quaternary volcanic rock. These results are consistent with a comparison of the map of geothermal gradient and the location of Quaternary volcanoes in Japan.

2) Geothermal structural model

(1) Estimation of geothermal structure using a one-dimensional steady-state model

Magma chambers and hot dry rock that are responsible for geothermal anomalies are considered to occur at depths of between several kilometers and several tens of kilometers. Although it is important to estimate the extent of thermal anomalies, it is not easy to measure them directly. Therefore, it is necessary to use a theoretical approach to estimate the thermal structure of the subsurface environment.

Okubo et al. (1998) proposed a method for estimating the crustal thermal structure down to a depth of 5 km using a one-dimensional steady-state model incorporating the thermal conductivity and heat generation of the crust based on the geothermal gradient data measured in boreholes. This method is used to estimate the underground thermal structure near the volcanoes. The temperature of the upper crust, T (°C) is calculated according to the following formula. In this calculation, convection is not taken into account.

$$T = T_0 + (q_s / k_u)\, z - (A_u / 2k_u)\, z^2 \qquad \text{..... 2)}$$

T_0: temperature at sea level (°C)
q_s: terrestrial heat flow (W m^{-2})
k_u: thermal conductivity (W m^{-1} $°C^{-1}$) of the upper crust
A_u: heat generation of the upper crust (W m^{-3})
z : depth (m)

The selected parameter values for thermal conductivity and heat generation in Japan are 2.26

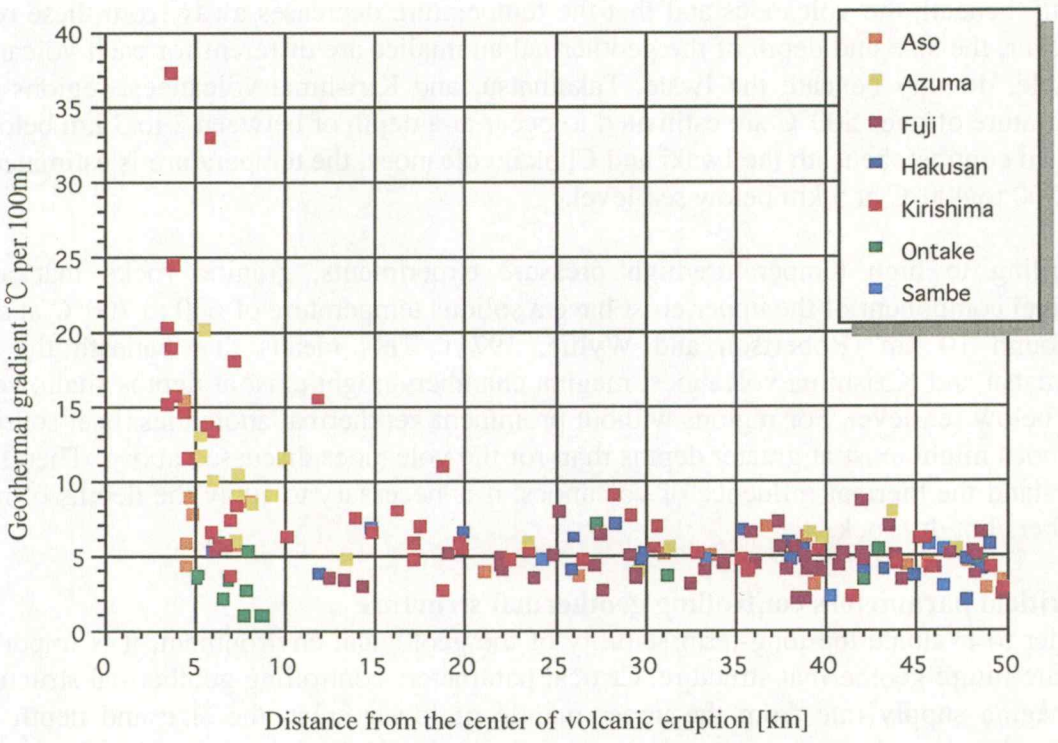


Figure 2.4-11 Change in geothermal gradient with distance from volcanic centers (after Umeda et al., 1999)

The geothermal gradient decreases with distance from the volcano.

$W\ m^{-1}\ °C^{-1}$ (Yano et al., 1994) and 1.5 $\mu W\ m^{-3}$ (Okubo et al., 1998), respectively.

The 2D temperature distributions estimated from data for the Akan, Daisetsu, Niseko-Kuttara volcanoes in Hokkaido, Iwate, Chokai-Kurikoma, Azuma volcanoes in northeast Honshu, and Kuju, Unzen-Aso, Kirishima volcanoes in Kyushu, are shown in Figures 2.4-12a, b, c. These figures illustrate that high temperature regions, thought to be heat sources, exist directly beneath the volcanoes and that the temperature decreases away from these regions. However, the size and depth of the geothermal anomalies are different for each volcano. For example, directly beneath the Iwate, Takamatsu, and Kirishima volcanoes, regions with a temperature of over 500°C are estimated to occur at a depth of between 2 to 3 km below sea-level. In contrast, beneath the Iwaki and Chokai volcanoes, the temperature is estimated to be only 300 to 400°C at 5 km below sea-level.

According to high temperature/high pressure experiments, granitic rocks that are the principal component of the upper crust have a solidus temperature of 600 to 700°C at a depth of around 10 km (Robertson and Wyllie, 1971). This means that beneath the Iwate, Takamatsu and Kirishima volcanoes, magma chambers might exist at depths shallower than 5 km below sea-level. For regions without prominent geothermal anomalies, heat sources for volcanoes might exist at greater depths than for the volcanoes discussed above. Therefore, to understand the thermal influence of volcanoes, it is necessary to study the depths of magma chambers/hot dry rock.

3) Critical parameters controlling geothermal structure

In order to evaluate the long-term stability of the geological environment, it is important to estimate future geothermal structure. Critical parameters controlling geothermal structure are the magma supply rate from the upper mantle or lower crust, the size and depth of the magma chamber, the regional geothermal gradient, the thermal conductivity of surrounding rock, etc. This section presents the results of a sensitivity analysis which evaluates the importance of the magma supply rate and the size and depth of the magma chamber.

The temperature profile of a magma chamber will evolve with time and this will impact on the thermal structure of the surrounding rock. These changes have been modeled using a non-steady-state thermal conduction model of the magma chamber and the volume of magma supplied to it.

(1) Model of the magma chamber

A two-dimensional axially symmetric model (Tomiya, 1995), in which the supply of magma is modeled explicitly, represents the magma chamber (heat source). This model consists of a cylindrical magma chamber and a vent that provides both a source and a sink (Figure 2.4-13). The temperature within the magma chamber is assumed to be uniform and the flow of magma into the chamber is constant. After reaching thermal equilibrium, the magma is assumed to erupt at a different rate at which magma is supplied to the magma chamber. Magma firstly (t=0) intrudes into the magma chamber and is then transported to the vent in short pulses, during which heat is lost to the surrounding rock. Using these assumptions, the evolution of the crustal thermal structure was calculated by changing the supply or discharge rate of the magma. The temperature, T, is given by the thermal conduction formula shown below.

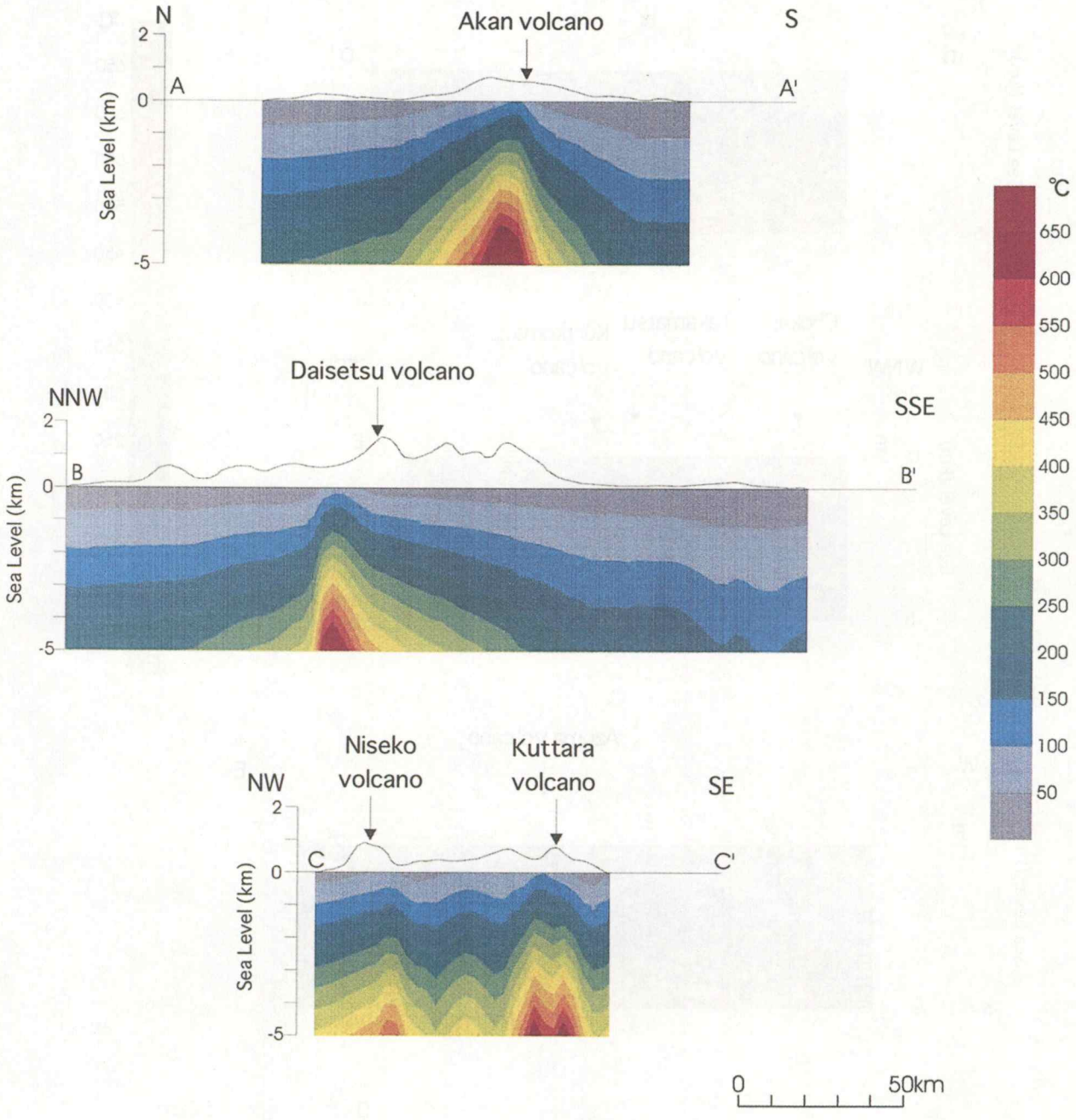


Figure 2.4-12a Cross-sections showing the thermal structure of Hokkaido (A-A': Akan, B-B': Daisetsu, C-C': Niseko-Kuttara) (Umeda et al., 1999a)

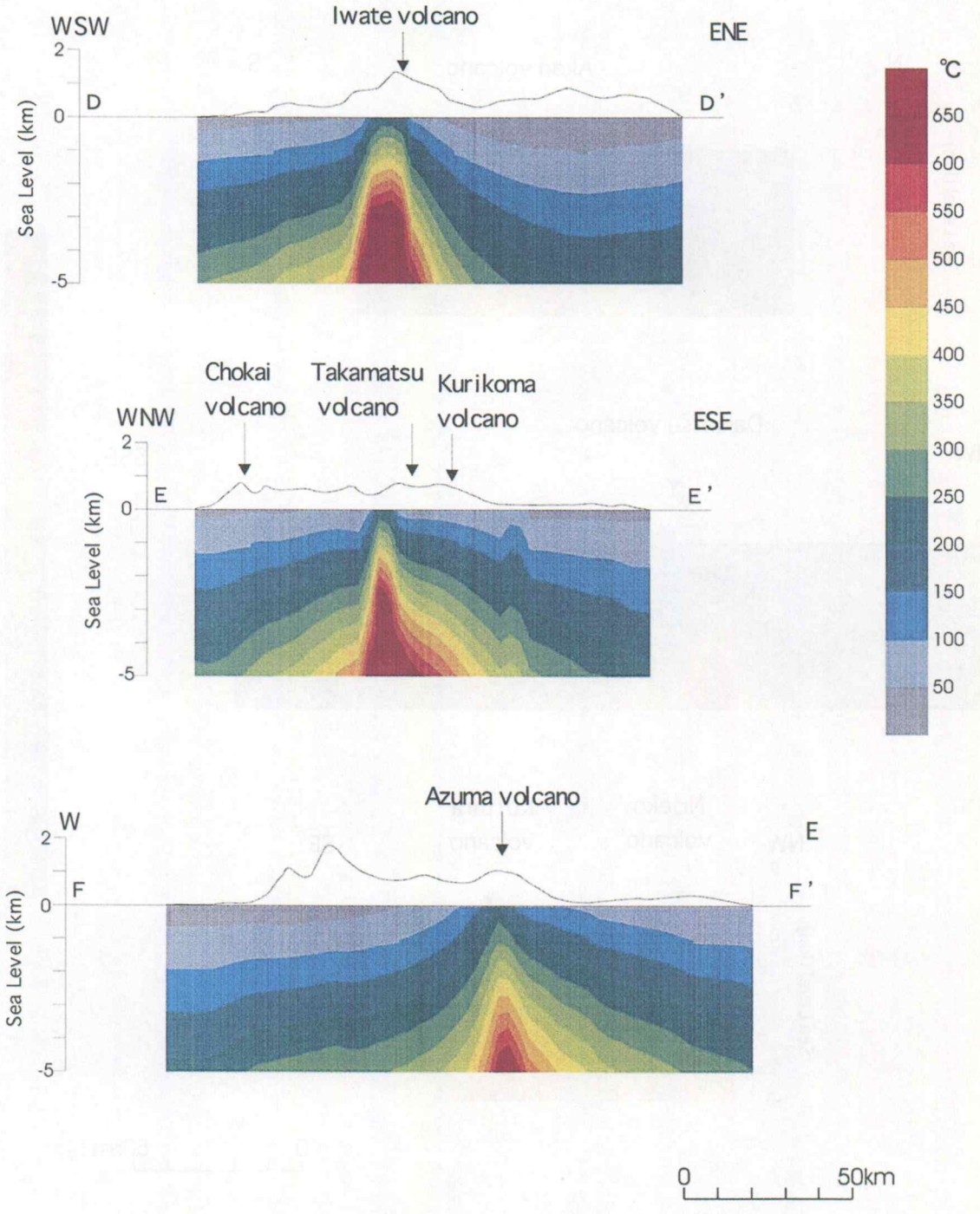


Figure 2.4-12b Cross-sections showing the thermal structure of northeast Honshu (D-D': Iwate, E-E': Chokai-Kurikoma, F-F': Azuma) (Umeda et al., 1999a)

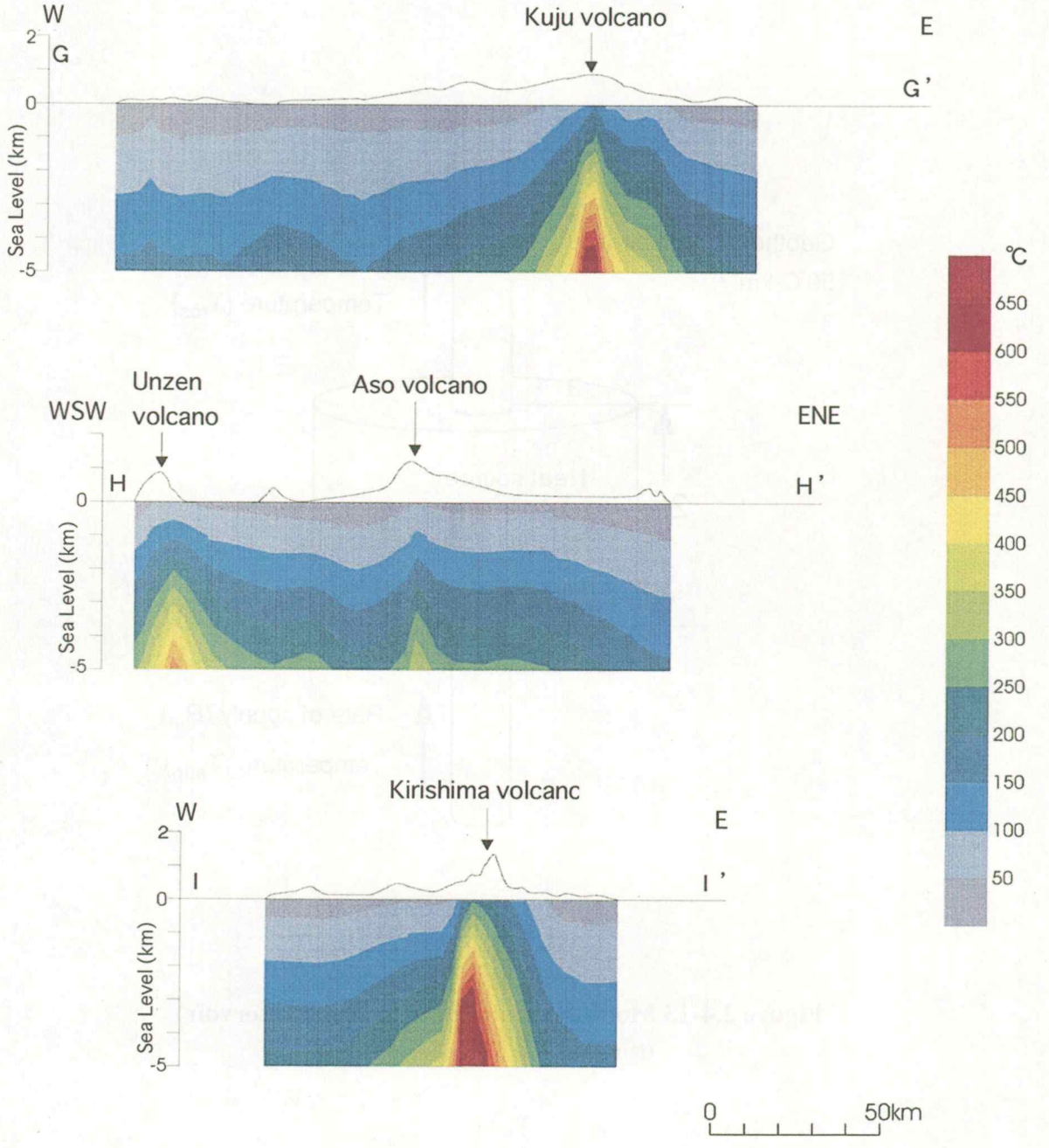


Figure 2.4-12c Cross-sections showing the thermal structure of Kyushu (G-G': Kuju, H-H': Unzen-Aso, I-I': Kirishima) (Umeda et al., 1999a)

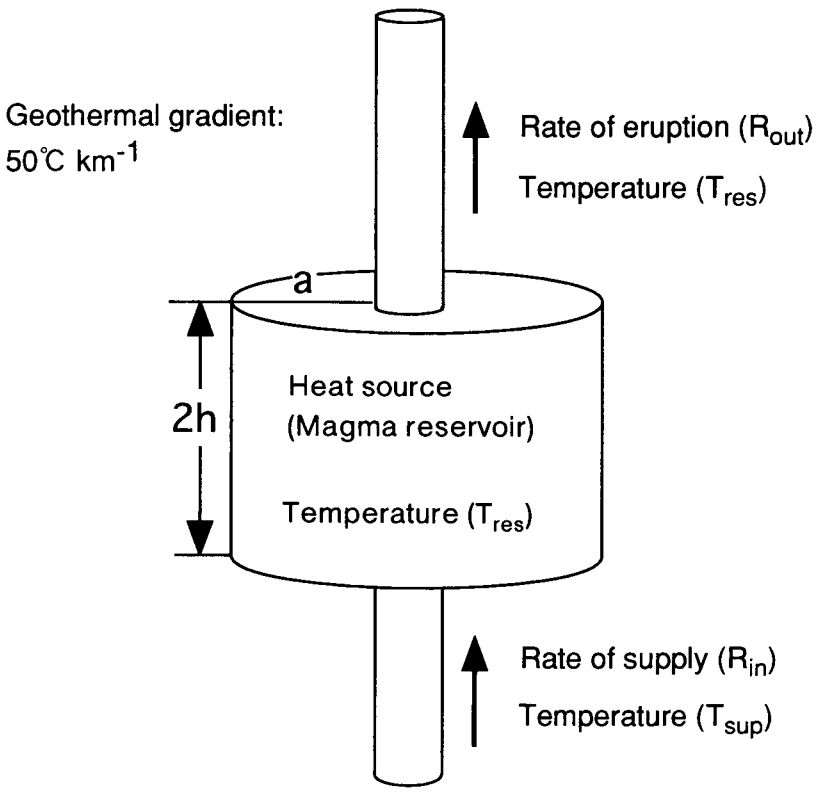


Figure 2.4-13 Model of heat source (magma reservoir)
(modified from Tomiya ,1995)

$$\frac{\partial T}{\partial t} = \kappa \left[\frac{1}{r} \times \frac{\partial}{\partial r} \left(r \frac{\partial T}{\partial r} \right) + \frac{\partial^2 T}{\partial z^2} \right] \quad \text{..... 3-1)}$$

This is solved using the finite difference method. In the above,
t : time (s)
κ: thermal diffusion coefficient of the country rock ($m^2\ s^{-1}$)
r : horizontal distance (m)
z : vertical distance (m)

For the magma chamber temperature, T_{res}, the formula for energy conservation,

$$\rho_1 c_1^* \frac{\partial (T_{res} V)}{\partial t} = -\rho_2 c_2 \kappa \int_s \mathrm{grad}T \times dS + R_{in} \rho_1 c_1 T_{sup} - R_{out} \rho_1 c_1 T_{res} \quad \text{..... 3-2)}$$

$$\rho_1 c_1^* \frac{\partial (T_{res} V)}{\partial t} = -\rho_1 c_1^* (d\, T_{res} V + d\, V\, d\, T_{res}) / dt \quad \text{..... 3-3)}$$

is solved, where
$d\, V\, d / dt = R_{in} - R_{out}$
ρ_1 : density of the magma ($kg\ m^{-3}$)
ρ_2 : density of the country rock ($kg\ m^{-3}$)
c_1 : specific heat of the magma ($J\ kg^{-1}\ ^\circ C^{-1}$)
c_2 : specific heat of the country rock ($J\ kg^{-1}\ ^\circ C^{-1}$)

V : volume of magma chamber (m^3)
T_{sup} : temperature of supplied magma (°C)
R_{in} : rate of magma supply from deep underground ($m^3\ s^{-1}$)
R_{out} : rate of magma discharge from magma chamber ($m^3\ s^{-1}$)

S means surface of magma chamber. c_1^* is the specific heat of magma, including the effect of latent heat of crystallization and is given by,

$$c_1^* = c_1 \left[1 + \frac{L}{c_1 (T_L - T_S)} \right] \quad \text{..... 3-4)}$$

Where,
L : latent heat of crystallization ($J\ kg^{-1}$)
T_L : liquidus temperature (°C)
T_S : solidus temperature (°C)

Constant temperature boundary conditions are set for the top, bottom and sides of the model. Geothermal gradients are defined as 50°C km^{-1}. Other parameters are the same as those used by Tomiya (1995). Also, when the reservoir temperature falls below that of the solidus, the vent is closed and supply of magma is stopped.

(2) Life of the magma chamber and geothermal structure

Four cases were simulated, each one considering a unique combination of depth and size of the heat source and magmatic supply and discharge rate. The effect on the duration of the magma chamber and the geothermal structure was examined (Umeda et al., 1999a).

In the first case, a magma chamber of 1 km radius and 2 km height occurs at a depth of 5 km. Figure 2.4-14a shows the geothermal structure around the magma chamber after 50,000, 100,000 and 300,000 years, when the supply and discharge of the magma occurred at a rate of 1 km^3 per thousand years (1 km^3 ka^{-1}). The temperature of the magma chamber also exceeds the solidus temperature and the life of the magma chamber is not exhausted, as long as the supply rate from deeper underground does not decrease. The temperature of the surrounding rock gradually increases over a greater distance from the vicinity of the chamber and the geothermal structure reaches a steady state after about 300,000 years. After the magma chamber is formed, the geothermal profile from 1-2 km depth is constant, even after 100,000 years.

In Case 2, a magma chamber of 4 km radius and 4 km height occurs at a depth of 5 km. Figure 2.4-14b shows the geothermal structure around the magma after 50,000, 100,000 and 300,000 years, when the supply and discharge of the magma occurred at a rate of 1 km^3 ka^{-1}. After 100,000 years, the temperature of the magma chamber does not exceed 700°C and thus remains lower than the solidus temperature. Therefore, the magma has already solidified. The thermal perturbation expands after the magma reservoir disappears. According to these models, the larger the magma chamber, the greater the loss of heat from the surface. This may be balanced by an increase in the supply rate of magma. For example, if the magma supply rate is in the order of 0.1-1 km^3 ka^{-1}, a constant temperature can be maintained by a magma chamber with a diameter of a few kilometers. If the magma supply rate is 1 km^3 ka^{-1} and the volume of the chamber is a few km^3, a time in the order of 100,000 years is required for the magma chamber to heat the surrounding rocks significantly. In regions such as Iwate, the west of Kurikoma and the east of Kirishima, geothermal anomalies are observed; it is possible that magma chambers several km^3 in volume exist below these regions.

In Case 3, a magma chamber of 4 km radius and 4 km height is located at a depth of 10 km. Figure 2.4-14c shows the geothermal structure around the magma after 50,000, 100,000 and 300,000 years, when the supply and discharge of the magma were set at a rate of 1 km^3 ka^{-1}. The rocks are also at temperatures above the solidus temperature. If the depth increases, a magma chamber with a volume of several hundred km^3 can maintain the thermal structure over several 100,000 years. However, the heating effect exerted by the magma does not reach to within 1 to 2 km of the surface. A significant geothermal anomaly due to the magma chamber occurs only below a depth of about 5 km underground.

In Case 4, a magma chamber with a radius of 4 km and a height of 4 km is located at 10 km depth. Figure 2.4-14d shows the geothermal structure around the magma after 50,000, 100,000 and 300,000 years, when the supply of the magma was set at a rate of 2 km^3 ka^{-1} and discharge of the magma at a rate of 1 km^3 ka^{-1}. The temperature of the magma chamber after 100,000 years is lower than the solidus temperature. The size of the magma chamber increases in proportion to the magma supply rate and can be thermally maintained over several 100,000 years.

4) Hydrothermal systems

Heating of groundwater in regions of high heat flow causes a reduction in water density and

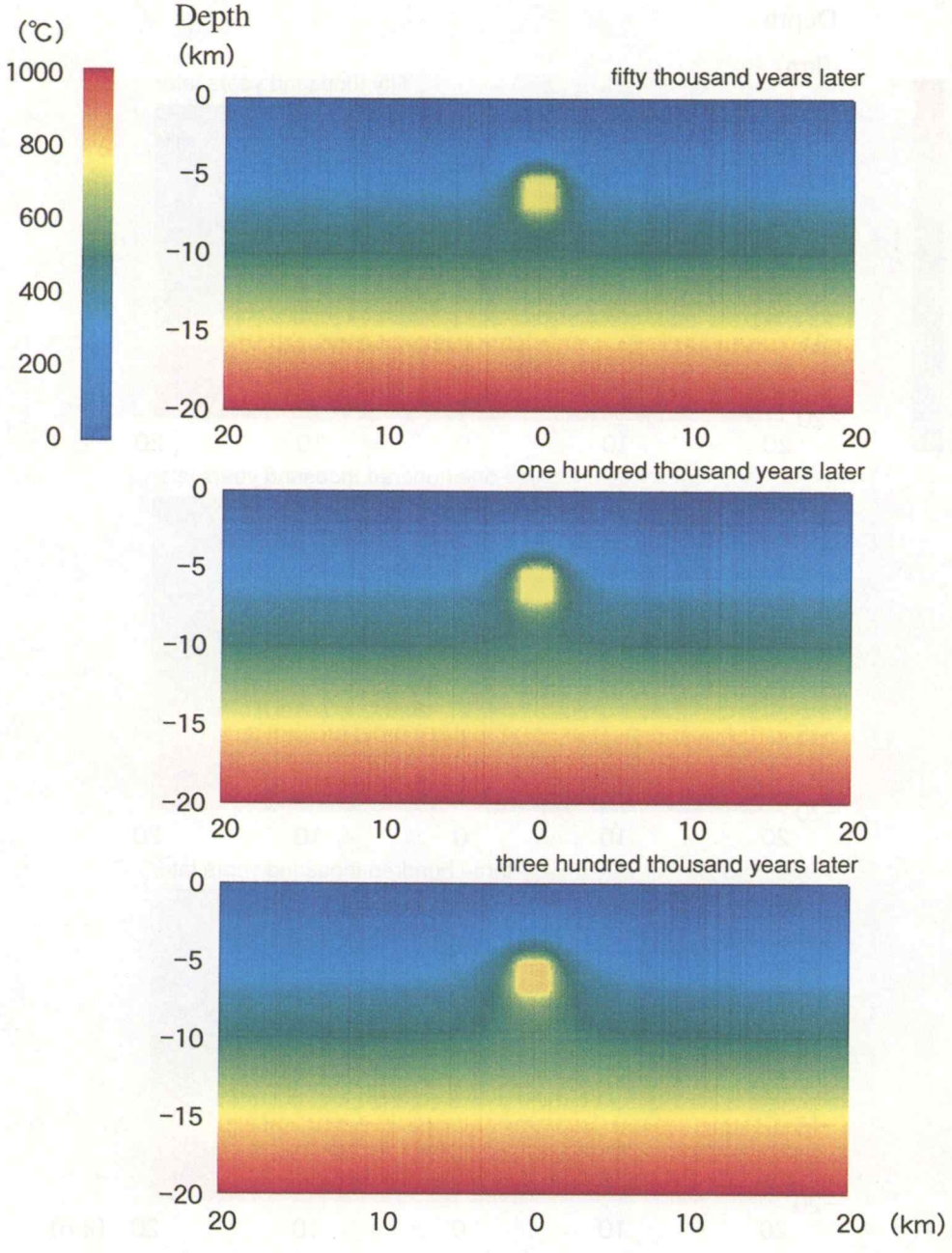


Figure 2.4-14a Temperature change around a magma reservoir

(<Case1> Size of magma reservoir : radius=1 km, height=2 km,
Depth of magma reservoir : 5 km)

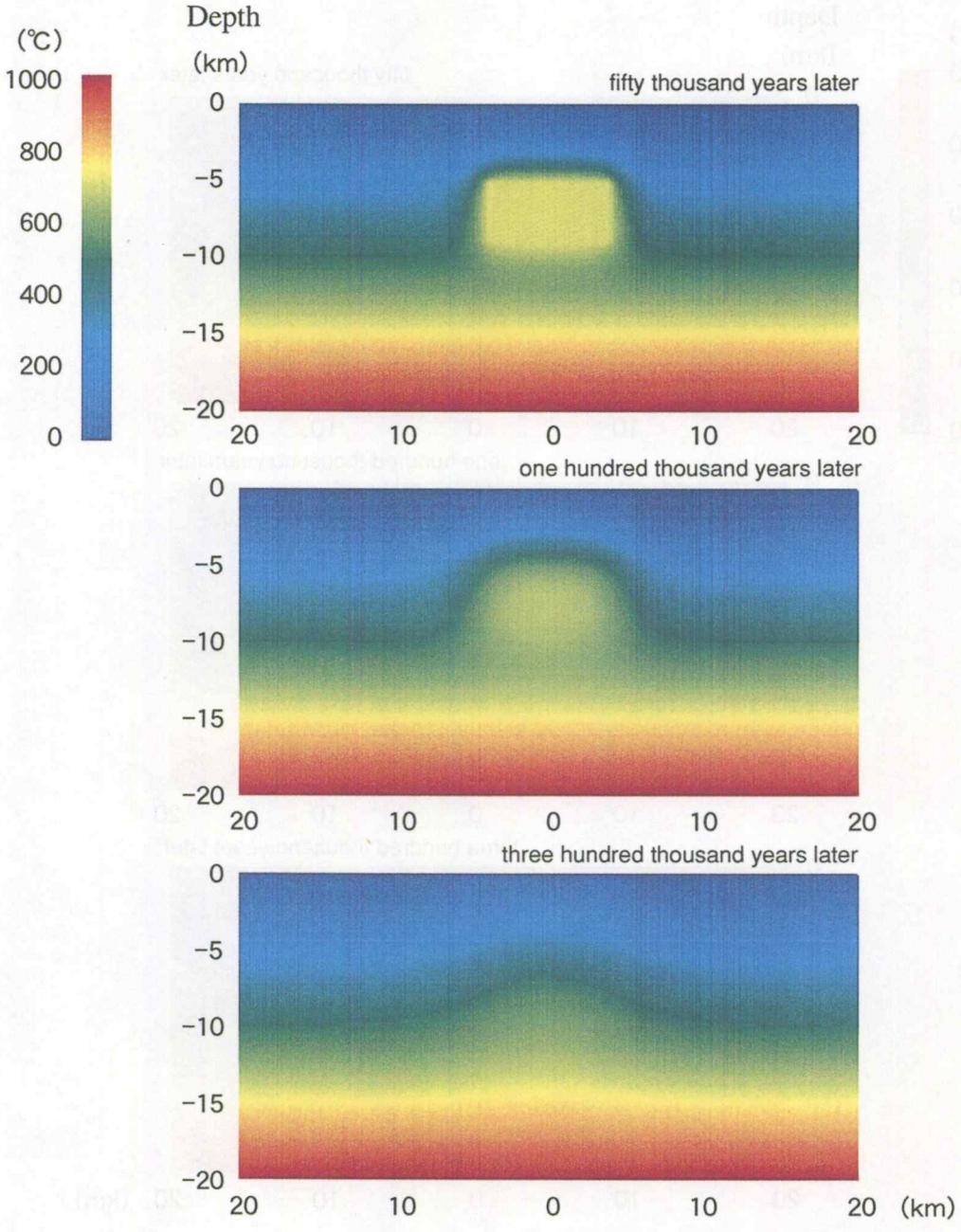


Figure 2.4-14b Temperature change around a magma reservoir

(<Case2> Size of magma reservoir : radius=4 km, height=4 km,
depth of magma reservoir : 5 km)

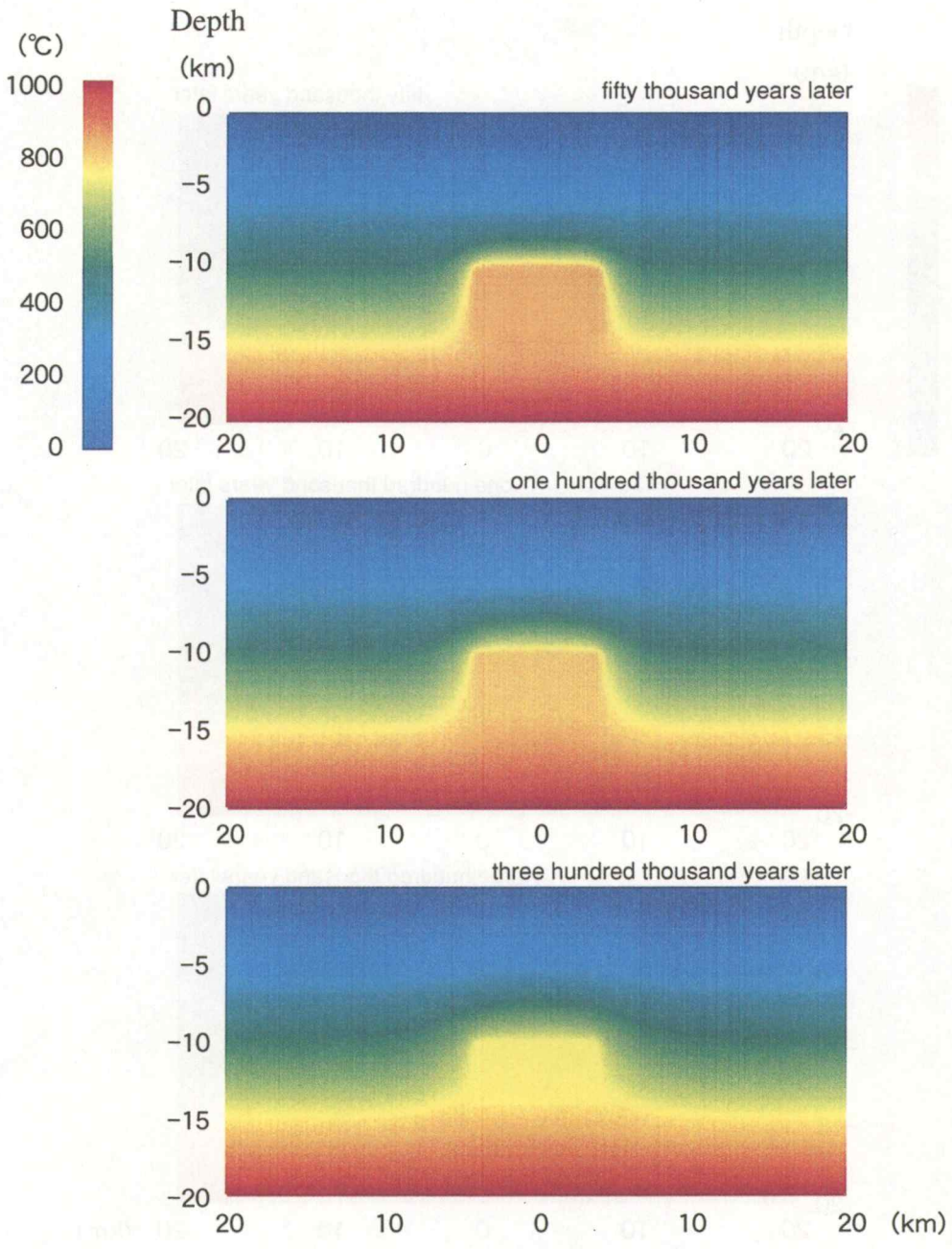


Figure 2.4-14c Temperature change around a magma reservoir

(<Case3> Size of magma reservoir : radius=4 km, height=4 km,
Depth of magma reservoir : 10 km)

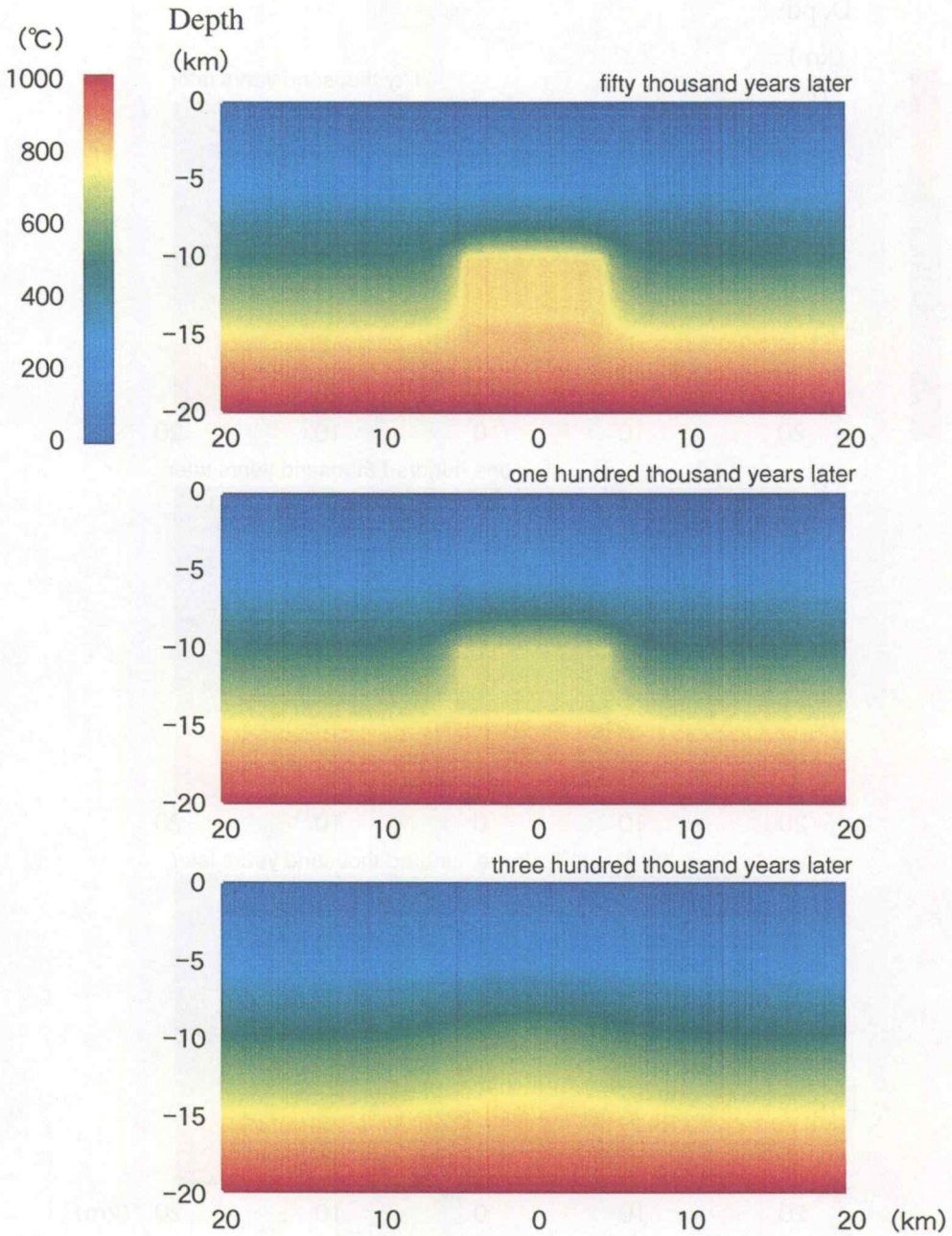


Figure 2.4-14d Temperature change around a magma reservoir

(<Case4> Rate of magma supply is two times greater than in Case 3)

the formation of hydrothermal convection currents. Theoretical considerations have led some authors to suggest that these currents are created when the geothermal gradient reaches a certain threshold value (Horton and Rogers, 1945). The size of a hydrothermal convection system depends partly on the hydraulic gradient. However, if the rate of the fluid flow immediately above the heat source is below 10^{-10} m s^{-1}, hydrothermal convection currents are not created (Kato et al., 1996).

The size and depth of hydrothermal convection systems can be determined by temperature logging. For example, Tamanyu (1994) estimated the size and depth of the hydrothermal convection system in Hohi in Kyushu and in the Sengan and Kurikoma regions of NE Honshu from temperature logging profiles and interpretations of the geological structure. According to this approach, the width of the hydrothermal convection system is greater than 10 km at a depth of 2 to 3 km in all regions (Figure 2.4-15). The size and depth of these hydrothermal convection systems is closely related to geological structure. Convection systems are well developed in permeable Quaternary and Neogene strata, but do not occur in Paleogene rocks. In any case, hydrothermal convection systems are limited to regions of high geothermal gradient which surround volcanoes.

(1) Estimation of fluid velocity using a one-dimensional heat and fluid flow model

The general equation for simultaneous non-steady heat and fluid flow through isotropic, homogeneous and fully saturated porous media is:

$$k \frac{d^2T}{dz^2} = -\rho c v \frac{dT}{dz} \quad \text{..... 4-1)}$$

where:
k : thermal conductivity of solid-fluid system (W m^{-1} $°C^{-1}$)
T : temperature (°C)
ρ : density of fluid (kg m^{-3})
c : specific heat of solid-fluid system (kJ kg^{-1} $°C^{-1}$)
v : fluid velocity in the z direction (m s^{-1})

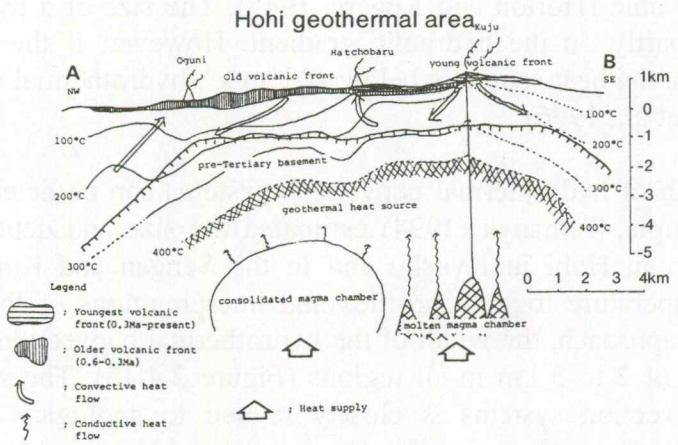
The approach of Bredehoeft and Papadopulos (1965) was followed. They considered vertical steady anisothermal groundwater flow through the semi-confining layer of an aquifer system (Figure 2.4-16), in which the temperature along a vertical section through the semi-confining layer was measured at three or more points. These temperature measurements should satisfy the solution to the following boundary value problem describing both heat and groundwater flow in the semi-confining layer.

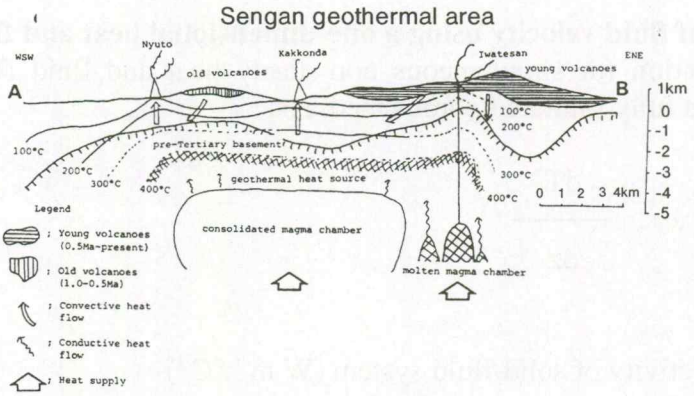
Applying boundary conditions $T_z = T_0$ at Z = 0, and $T_z = T_L$ at Z = L, the solution is,

$$T_z = T_0 + (T_L - T_0) \frac{\exp(\beta z / L - 1)}{\exp(\beta) - 1} \quad \text{..... 4-2)}$$

$$\beta = -\rho cvL / K \quad \text{..... 4-3)}$$

where:
T_z : temperature at depth z (°C)





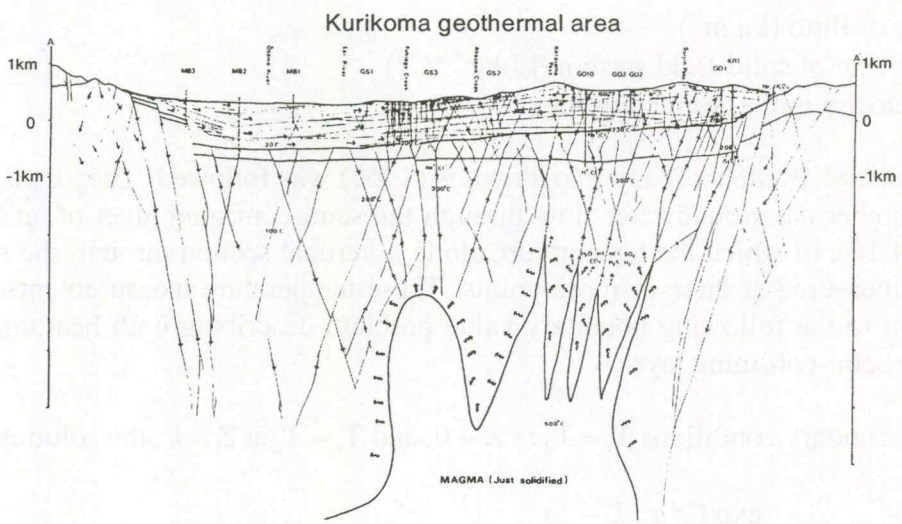


Figure 2.4-15 Geothermal cross-sections in the Hohi, Sengan and Kurikoma areas (Tamanyu, 1994)

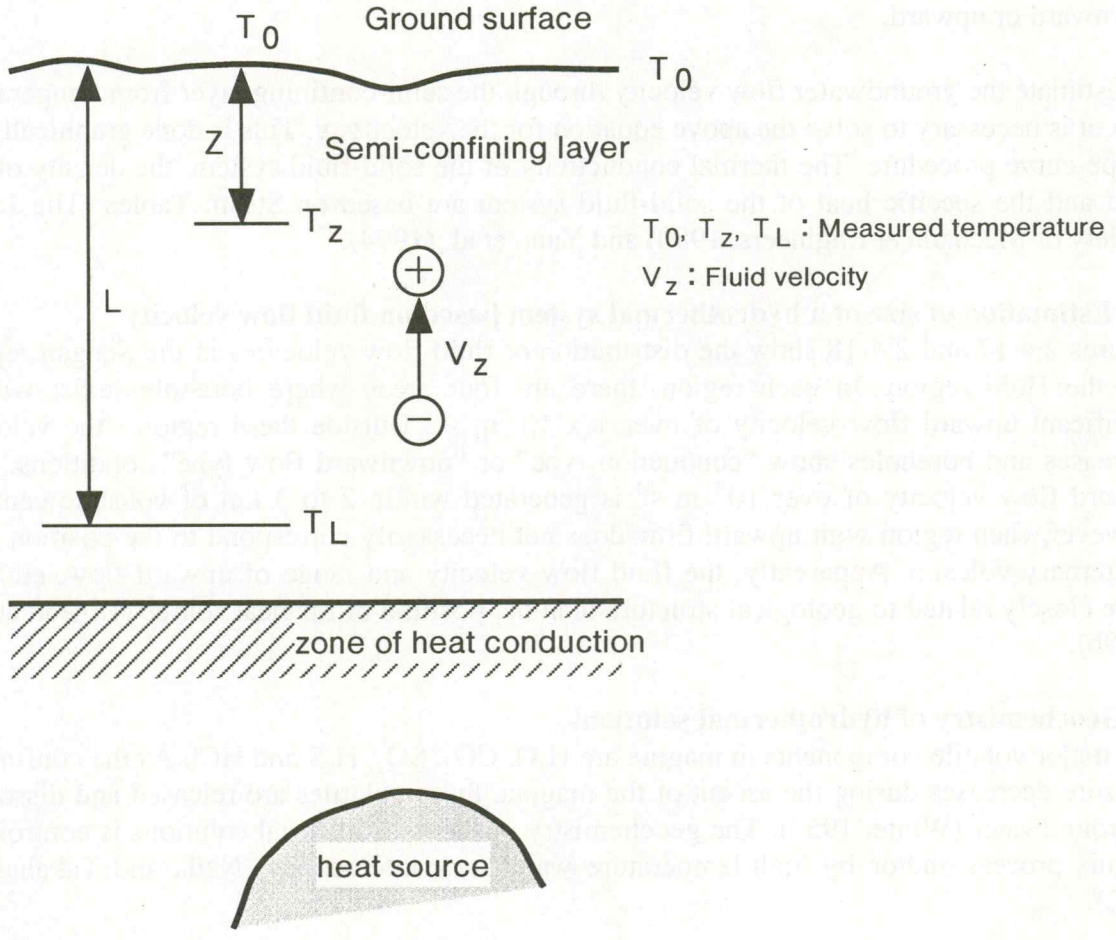


Figure 2.4-16 Vertical one-dimensional groundwater flow model
(modified from Bredehoeft and Papadopulos, 1965)

T_0: uppermost temperature (°C)
T_L: lowermost temperature (°C)
L : length of vertical section over which temperature measurements extend (vertical distance between T_0 and T_L) (m)

and β is a dimensionless parameter that is positive or negative depending on whether v is downward or upward.

To estimate the groundwater flow velocity through the semi-confining layer from temperature data, it is necessary to solve the above equation for the velocity, v. This is done graphically by a type-curve procedure. The thermal conductivity of the solid-fluid system, the density of the fluid and the specific heat of the solid-fluid system are based on Steam Tables (The Japan Society of Mechanical Engineers, 1980) and Yano et al. (1994).

(2) Estimation of size of a hydrothermal system based on fluid flow velocity

Figures 2.4-17 and 2.4-18 show the distribution of fluid flow velocities in the Sengan region and the Hohi region. In each region, there are four areas where boreholes exist with a significant upward flow velocity of over 1 x 10^{-9} m s^{-1}. Outside these regions, the velocity decreases and boreholes show "conduction type" or "downward flow type" conditions. The upward flow velocity of over 10^{-9} m s^{-1} is generated within 2 to 3 km of volcanic centers. However, each region with upward flow does not necessarily correspond to the position of a Quaternary volcano. Apparently, the fluid flow velocity and range of upward flow, etc. are more closely related to geological structure than the position of the heat source (Umeda et al., 1999b).

5) Geochemistry of hydrothermal solutions

The major volatile components in magma are H_2O, CO_2, SO_2, H_2S and HCl. As the confining pressure decreases during the ascent of the magma, these volatiles are released and dissolve in groundwater (White, 1957). The geochemistry of the hydrothermal solutions is controlled by this process and/or by high-temperature water-rock interactions (Noda and Takahashi, 1992).

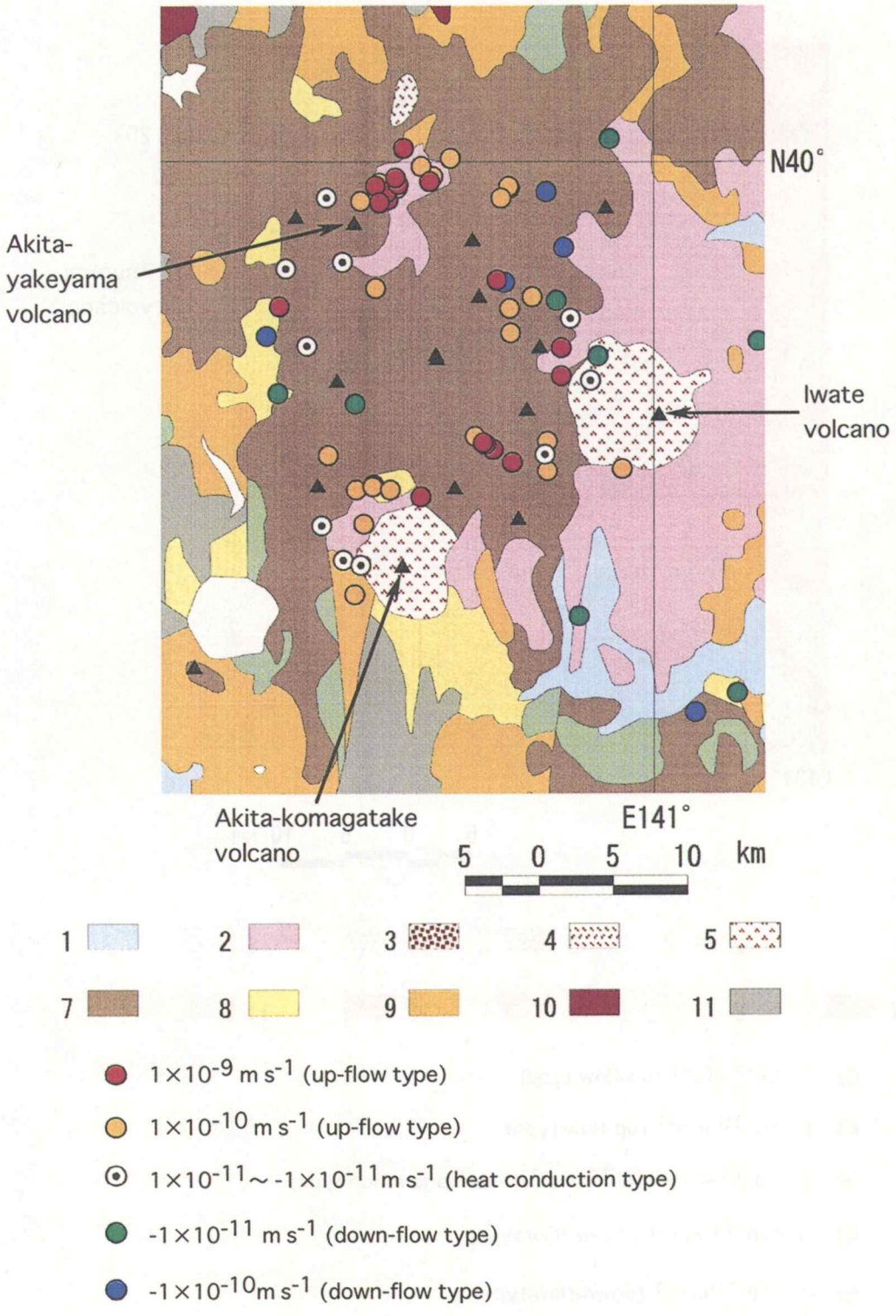
(1) Chemical composition of hot springs around volcanoes

When volatile magma components are dissolved in groundwater, acidic solutions with significant concentrations of Cl^- and SO_4^{2-} are produced. Figures 2.4-19 and 2.4-20 show the pH of hot spring water for the Northeast Japan and Kyushu regions respectively (Komatsu and Umeda, 1999). Acidic hot springs with a pH lower than 4.8 occur around Quaternary volcanoes (HCO_3 can only exist in significant amounts in water with pH greater than around 4.8 and groundwater with a pH below 4.8 therefore corresponds to the natural acidic groundwater field of Noda and Takahashi (1992)). The relationship between the pH of hot spring water and the distance to the nearest eruptive center in the Sengan region is shown in Figure 2.4-21. Hot springs with a pH below 4.8 tend to occur within 10 km of the volcanoes.

Noda (1987) proposed an anion index (A.I.) as an indicator for estimating the proximity of a water to a center of geothermal activity. The A.I. is calculated from the major anion composition of a hot spring water according to the following:

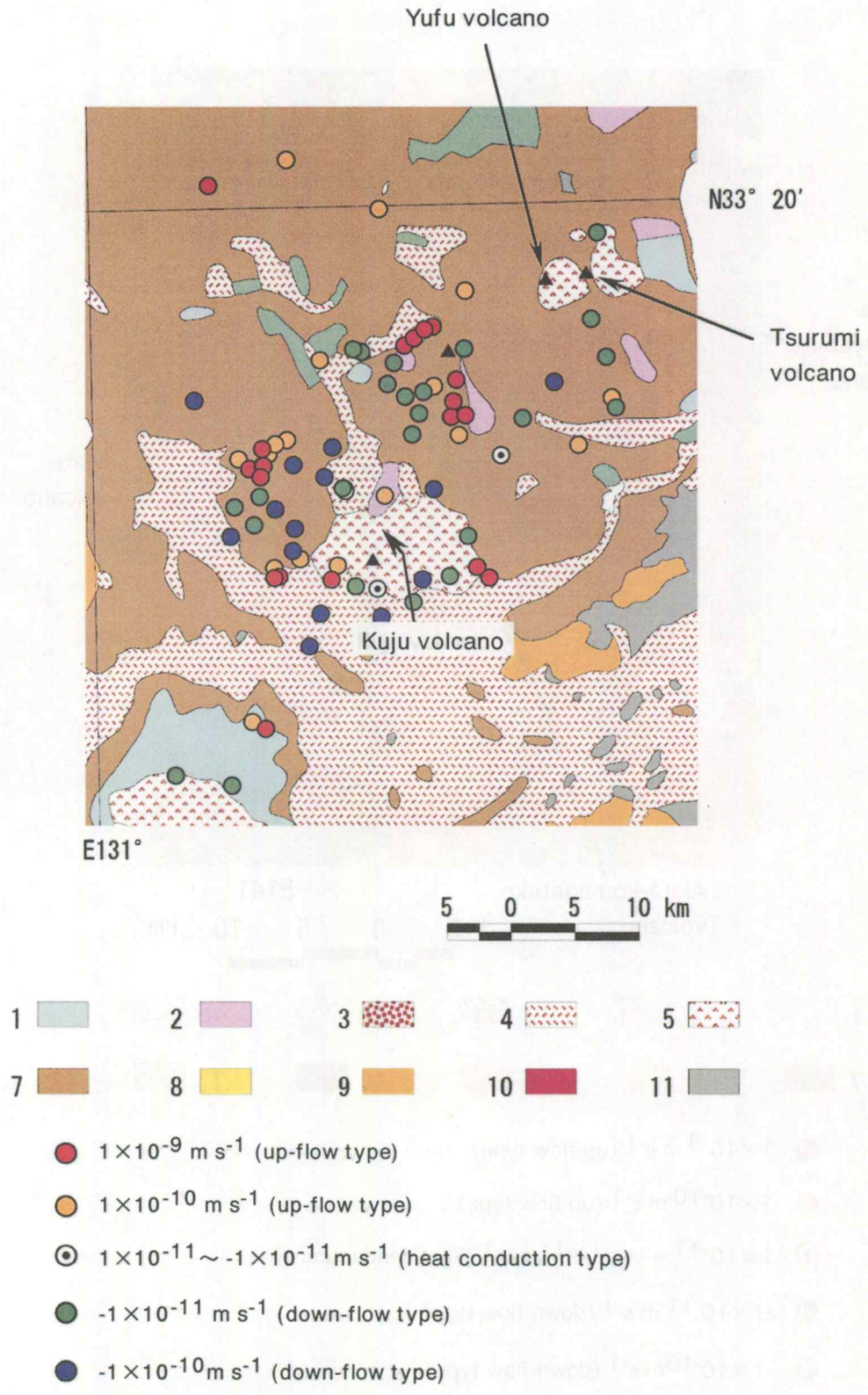
$$A.I. = 0.5 \times (SO_4 / (Cl + SO_4) + (Cl + SO_4) / (Cl + SO_4 + HCO_3)) \quad \text{..... 5-1)}$$

Here, the unit of concentration is the equivalent.



1: Holocene and late Pleistocene series, 2: Debris, 3: Holocene and late Pleistocene felsic volcanic rocks,
4: Holocene and late Pleistocene pyroclastics, 5: Holocene and late Pleistocene mafic volcanic rocks,
6: Middle Pleistocene to Pliocene series, 7: Middle Pleistocene to Pliocene volcanic rocks, 8: Miocene series,
9: Miocene volcanic rocks, 10: Neogene plutonic rocks, 11: Pre-Neogene system

Figure 2.4-17 Distribution of fluid flow velocity in vertical direction in the Sengan volcanic region (Umeda et al., 1999b)



1: Holocene and late Pleistocene series, 2: Debris, 3: Holocene and late Pleistocene felsic volcanic rocks,
4: Holocene and late Pleistocene pyroclastics, 5: Holocene and late Pleistocene mafic volcanic rocks,
6: Middle Pleistocene to Pliocene series, 7: Middle Pleistocene to Pliocene volcanic rocks, 8: Miocene series,
9: Miocene volcanic rocks, 10: Neogene plutonic rocks, 11: Pre-Neogene system

Figure 2.4-18 Distribution of fluid flow velocity in vertical direction in the Hohi volcanic region (Umeda et al., 1999b)

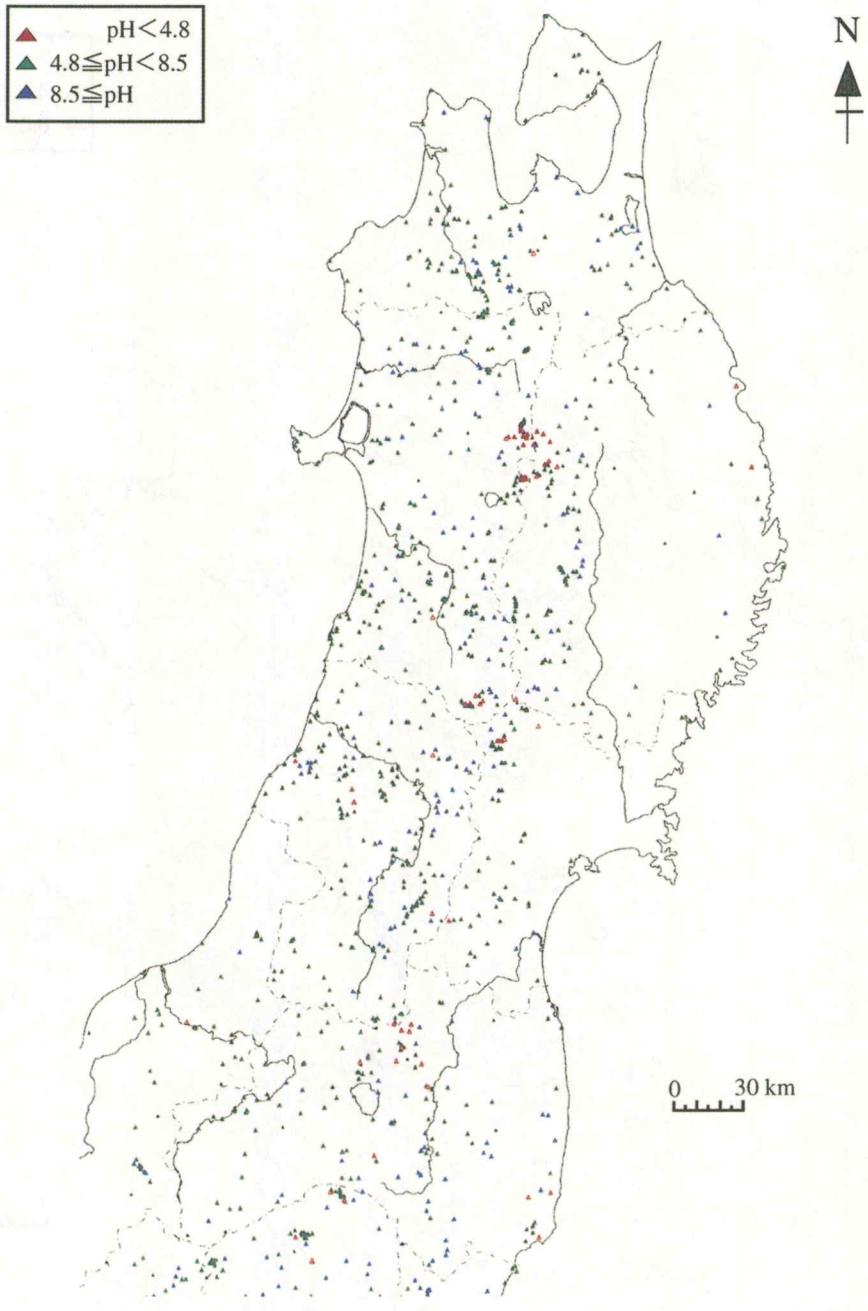


Figure 2.4-19 Distribution map showing variations in pH in hot spring waters from Tohoku, northeast Japan (Komatsu and Umeda, 1999)

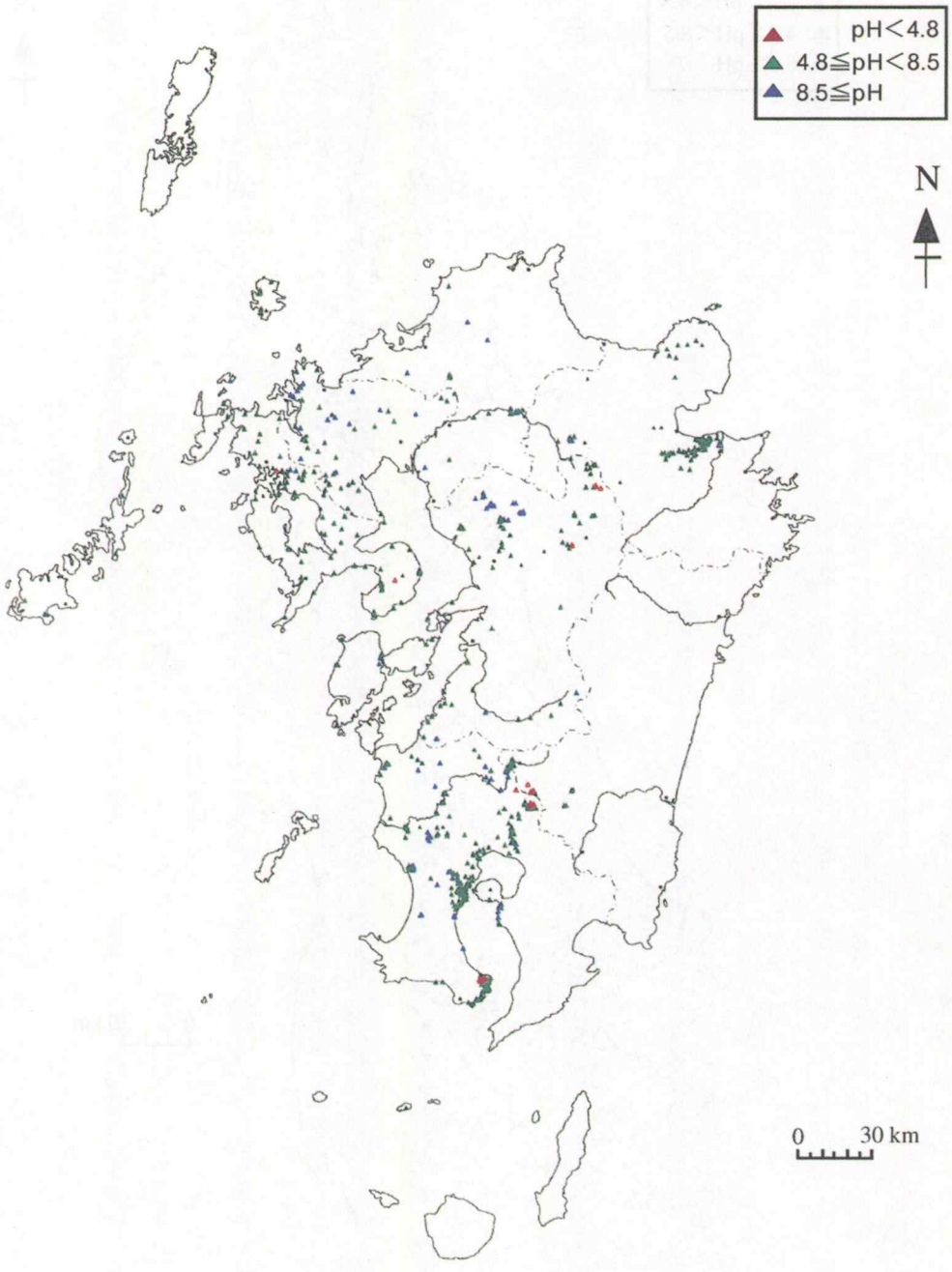


Figure 2.4-20 Distribution map showing variations in pH in hot spring waters from Kyushu (Komatsu and Umeda, 1999)

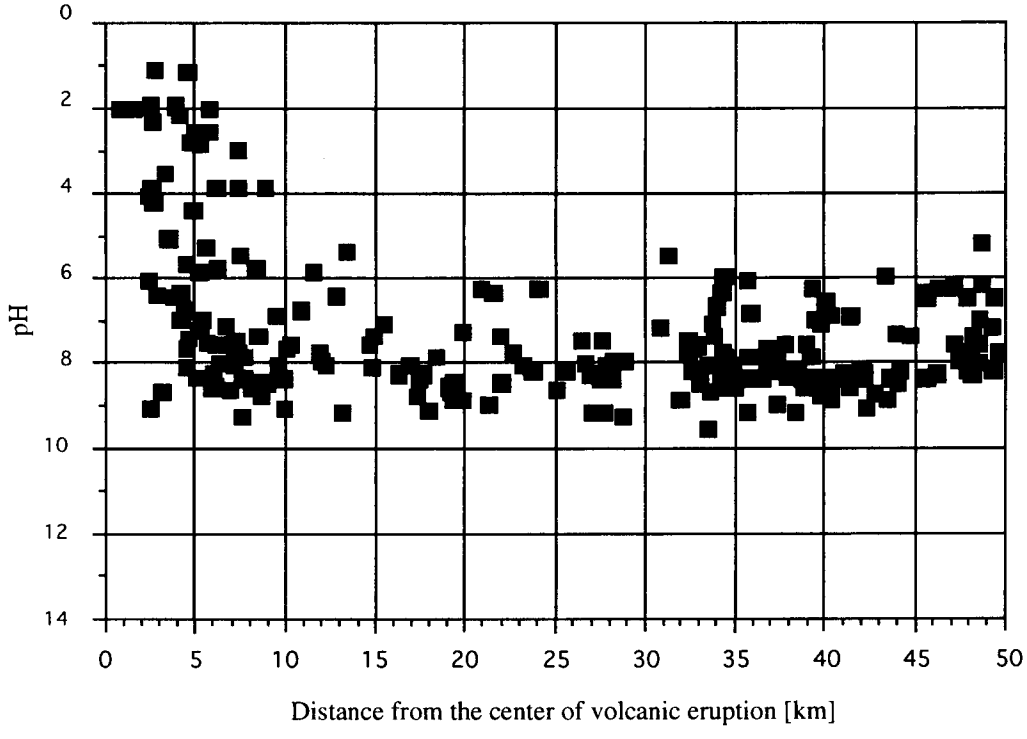


Figure 2.4-21 Change in the pH of hot springs from volcanic centers in the Sengan volcanic region (after Komatsu and Umeda, 1999)

The pH decreases with distance from the volcano. In Japan, a hot spring is defined as one where groundwater temperature is greater than 25 ℃.

The A.I. is around unity in areas where geothermal activity is highest, because only SO_4 is dissolved significantly in the hot spring water. The A.I. gradually decreases with increasing distance from a center of activity, with the appearance of Cl-type thermal water and with mixing of HCO_3-type water.

A.I.s which approach unity indicate waters that occur closer to the main fumarole. In the Bandai-Adatara volcanic region, there are springs with an A.I. close to one at the top of the Bandai, Adatara, Tomuraushi and Azuma volcanoes (NEDO, 1991). The A.I.s decrease from the top to the flank of the volcanoes and the contours for the A.I. values tend to make a concentric pattern. Figure 2.4-22 shows the relationship between A.I. and distance from the Tomuraushi, Adatara, Bandai, and Akita-Komagatake volcanoes. The A.I. decreases away from the center of each volcano, but the rate of decrease is different for each volcano. Also, it should be noted that hot springs in regions without a high temperature anomaly (i.e. those in non-volcanic regions) have an A.I. close to 0, suggesting that there is no contribution from magmatic volatiles for these hot springs.

CO_2, SO_2, H_2S and HCl contained in volcanic gas are chemically very reactive and, once released from the magma, are difficult to trace. On the other hand, the trace amount of He contained in the volatile gas is inert and does not react with other elements. ^3He is one of the primordial components of the earth. It originates in the mantle and is brought to the surface of the earth by the convection of magma. On the other hand, ^4He is generated from the radioactive decay of U and Th in the rock. The maximum $^3He/^4He$ isotopic ratio in a subduction zone is around 1×10^{-5}. In contrast, in the atmosphere the ratio is 1.4×10^{-6} and in the crust it is 1×10^{-7} to 1×10^{-8}. Therefore, the $^3He/^4He$ ratio can be used to investigate the existence of magma. Sakamoto et al. (1992) studied the relationship between the distance from the centers of volcanoes and the ratios of the He isotopes (Figure 2.4-23). According to this study, the He isotopic ratio becomes smaller with distance from the center of a volcano (Sano, 1988).

(2) Relationship between heat flow and geochemical effect

To understand the relationship between heat flow and the geochemical effect of volcanism, heat flow around a Quaternary volcano was estimated (Umeda, 1999; Umeda et al., 1999b). It is important to consider the effect of convecting hot water in the calculation of shallow crustal temperatures, for areas where such convective heat transfer dominates. Shallow crustal temperatures are estimated from a one-dimensional steady-state energy equation for heat transfer using combined conduction and advection in a homogeneous, porous medium, 4-1). At the surface, the boundary condition is:

$$Q = K \left. \frac{dT}{dz} \right|_{z=0} + \rho c v (T_0 - T_{air}) \qquad \text{..... 5-2)}$$

where T_0 is the temperature of the discharging hot water at the surface, T_{air} is the air temperature and Q is the total heat flow ($W\ m^{-2}$). Equation 5-2) is solved using 4-2) and 4-3) as follows:

$$Q = \rho cv \left[\frac{T_L - T_0}{\exp(\beta) - 1} + (T_0 - T_{air}) \right] \qquad \text{..... 5-3)}$$

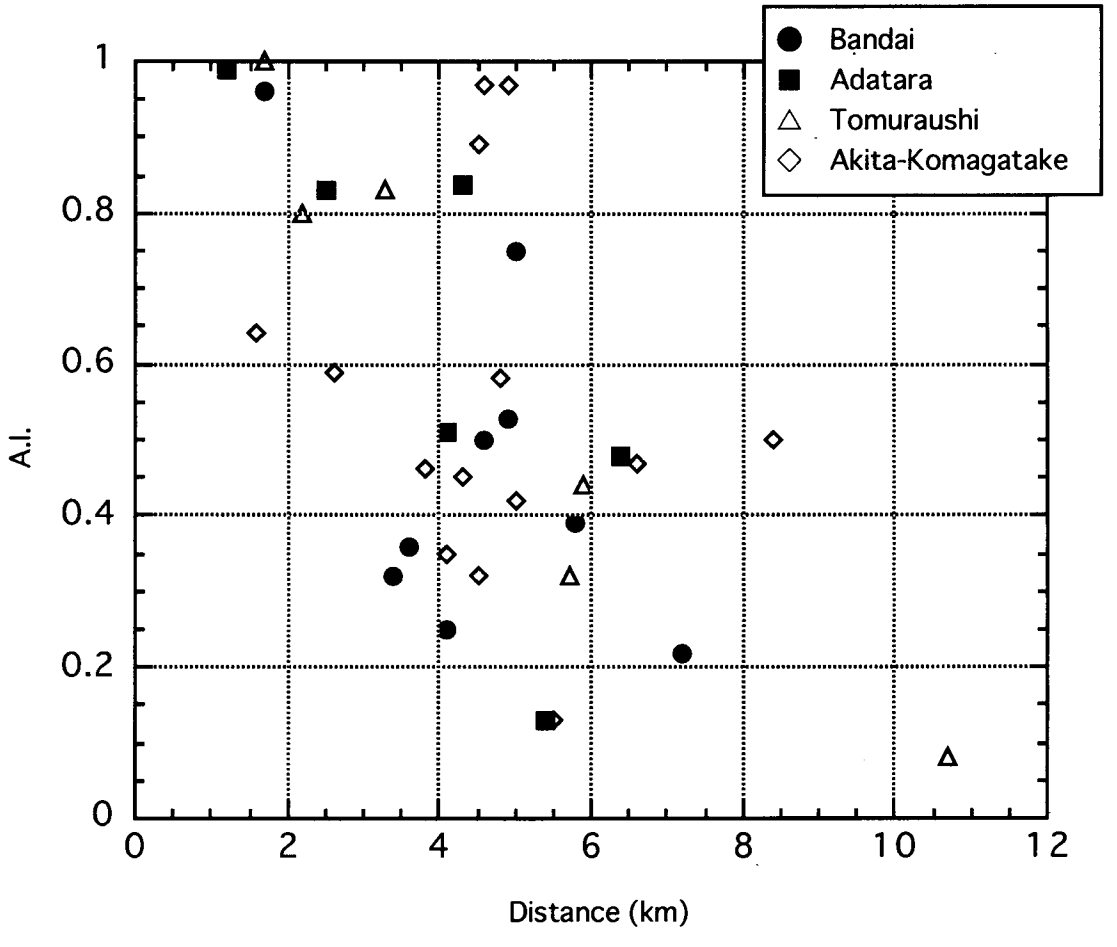


Figure 2.4-22 Relationship between anion index (A.I.) of hot springs and the distances from the centers of volcanoes (Komatsu and Umeda, 1999)

$$A.I. = 0.5 \times \left(SO_4 / (Cl + SO_4) + (Cl + SO_4) / (Cl + SO_4 + HCO_3) \right)$$

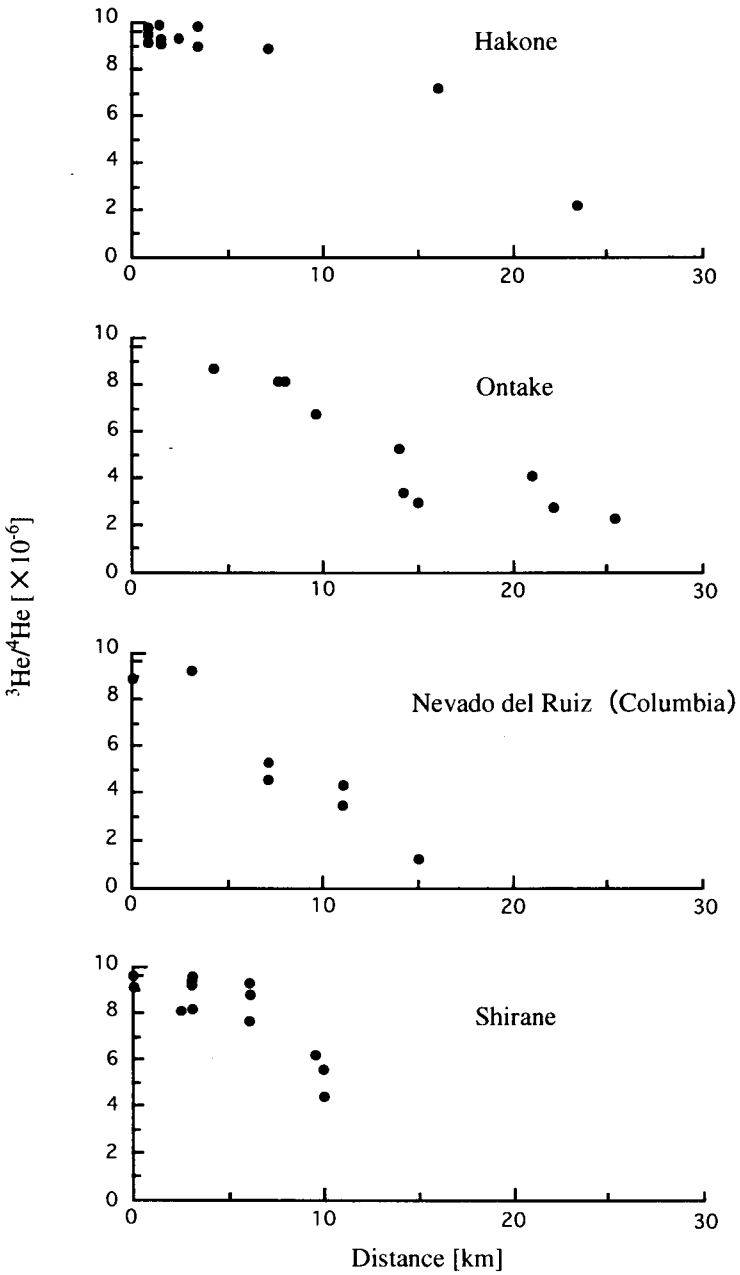


Figure 2.4-23 Change in groundwater $^3He/^4He$ ratio with distance from volcanic centers (after Sakamoto et al., 1992)

$^3He/^4He$ ratios in groundwater decrease with distance from the center of volcano.

Using the above method, the heat flow in each borehole within a radius of 10 km of each volcano is estimated. The average heat flow around a volcano is defined as the mean value of heat flow calculated in all boreholes within a 10 km radius. The average heat flow of the Akan, Niseco, Zao, Kuju and Kirishima volcanoes is 0.22 W m^{-2}, 0.15 W m^{-2}, 0.20 W m^{-2}, 0.36 W m^{-2} and 0.40 W m^{-2} respectively.

The Cl^-, SO_4^{2-} and HCO_3^- contents of hot spring waters around a volcano are higher than the mean values (Cl^- : 20.6 mg l^{-1}, SO_4^{2-} : 9.0 mg l^{-1}, HCO_3^- : 145.3 mg l^{-1}) of groundwater in Japan (Seo and Shimizu, 1992). The highest values for Cl^-, SO_4^{2-} and HCO_3^- contents in hot spring waters within a radius of 10 km of volcanoes are 500 to 4,500 mg l^{-1}, 1,500 to 4,000 mg l^{-1} and 500 to 3,000 mg l^{-1} respectively. However, the concentrations of some dissolved components are lower within the volcanic center. The largest distances for which acidic (pH < 4.8) hot spring water occurs from the Kirishima, Kuju, Zao, Niseko and Akan volcanoes are 6.8 km, 4.3 km, 4.8 km, 10.3 km and 8.2 km respectively (Figure 2.4-24). There is a clear correlation between these distances and the average heat flow around the volcanoes (Figure 2.4-25). Thus, the average heat flow around the volcano is an important indicator that may be used to judge the effect of volcanism on the groundwater chemistry.

6) Thermal effects of intrusive magma

Over long timescales, the thermal structure of the subsurface environment is controlled by heat sources at depths of several kilometers. However, if magma rises from the magma chamber to shallow depths, the temperature at shallow depths would be elevated. It is therefore necessary to estimate the rise in temperature due to volcanism or emplacement of magma at shallow depths and the time required for cooling and solidification of the magma. The thermal history of a region surrounding a Neogene intrusive dike is discussed below.

Ages measured using K-Ar, Rb-Sr and fission track (FT) methods on various rocks and minerals indicate the time at which the rock mass cooled below a specific temperature (referred to as the closure temperature). The closure temperature is different for each method and for each mineral dated. Thus, using different methods and different minerals from within the same rock, it is possible to deduce the thermal history of the rock. Using K-Ar and Rb-Sr methods, Hart (1964) measured the ages of feldspar, biotite and amphibole in the Eldora stock (diameter about 5 km, age about 54 Ma), which intruded pre-Cambrian rocks of the Front Range (Colorado). The results indicated that, within about 1 km from the contact of the intrusion, the mineral ages had been affected by heating (Figure 2.4-26).

Tagami and Shimada (1996) dated zircon in the Takatsukiyama Granite (diameter about 10 km, age about 15 Ma) and the country rocks in the Shimanto Belt by the FT method. It is ascertained that the zircons within about 4 km from the granitic intrusive body are rejuvenated and their FT age within 3 km from the contact is identical to that of the granitic body.

Komatsu et al. (1997) measured the thermoluminescence (TL) of quartz in the Okumaruzawa granite (Paleogene). This is the country rock of the Suiendani vent (diameter about 500 m), which was a feeder to the Okuhida pyroclastic flow deposit. According to their results, the ages within 200 m of the vent were similar to the age derived for the vent itself. This means that, within 200 m of the vent, the temperature measured using this method reached above 300°C, which is the electron trap release temperature.

In order to study the thermal effects of the Takahama-Kuroiwa intrusive body (diameter about 500 m) emplaced in the Neogene period on the country rocks composed of the Ryoke

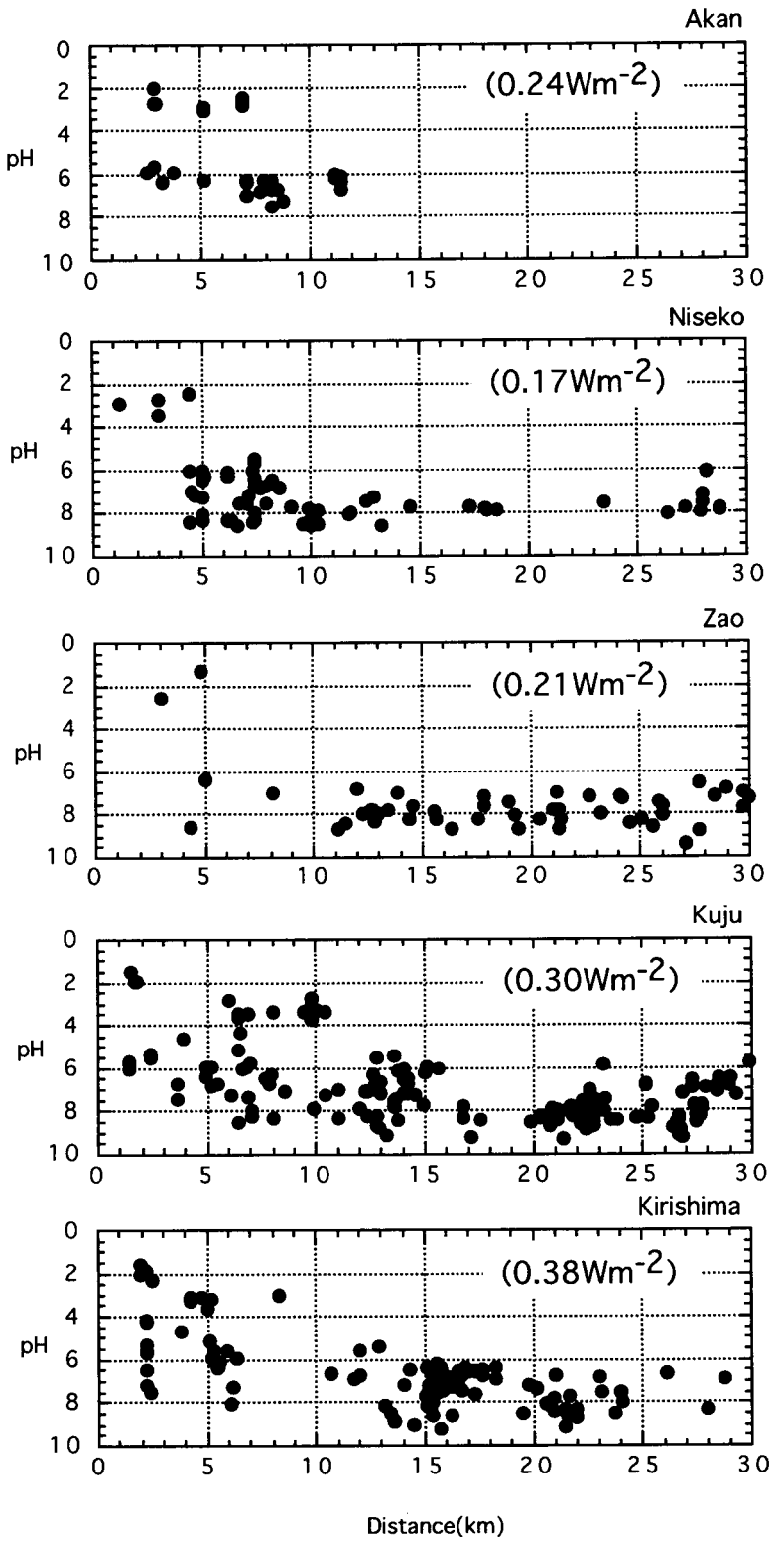


Figure 2.4-24 Heat flow and changes in the pH of hot springs with respect to distance from a volcano

Heat flow (Wm^{-2}) was calculated from the data obtained from boreholes within 10 km of each volcanic center.

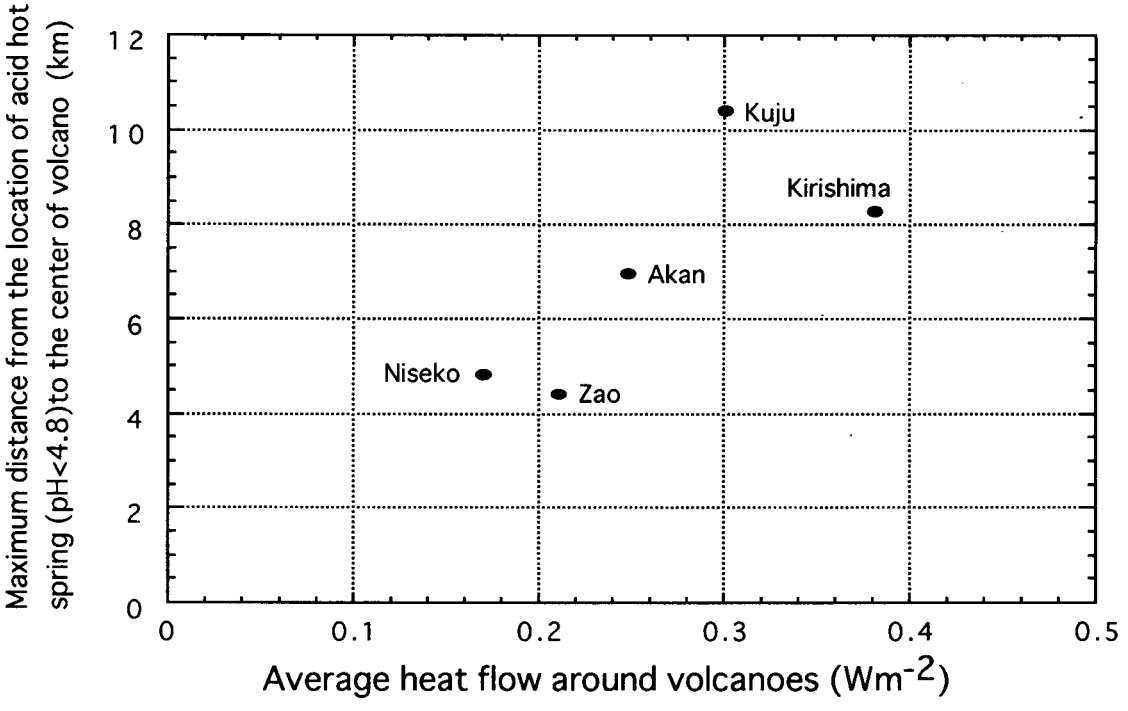


Figure 2.4-25 Relationship between average heat flow around volcanoes and spatial range of acid hot springs (pH<4.8)

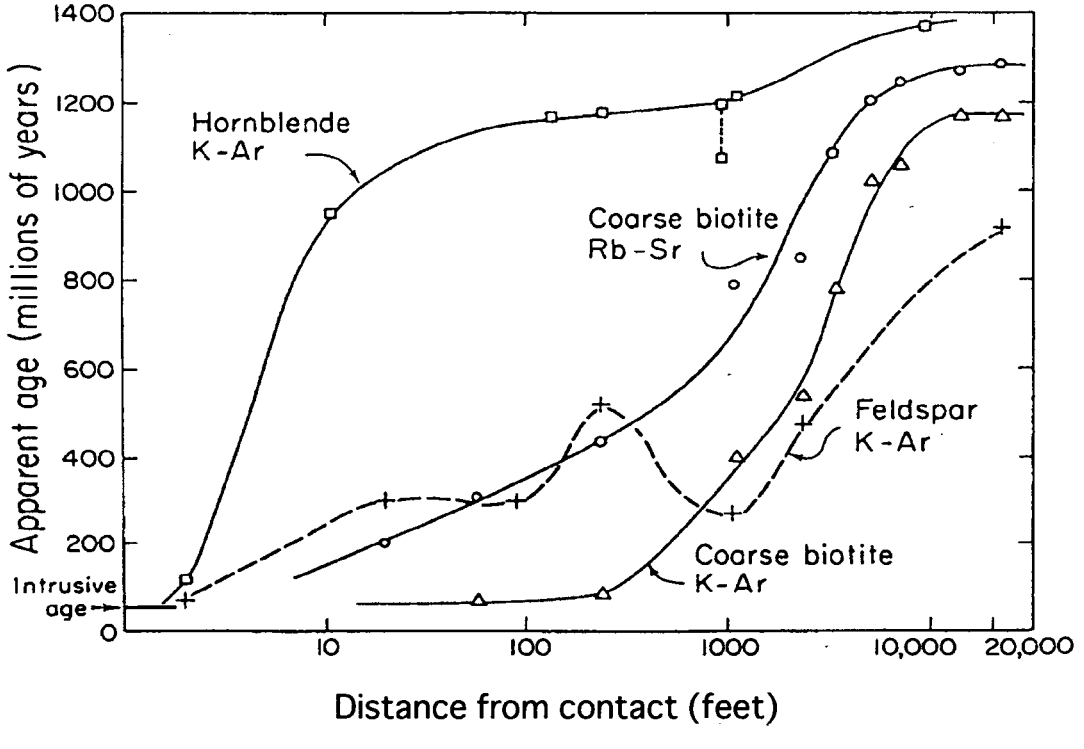


Figure 2.4-26 Variation of mineral ages as a function of distance from the intrusive contact (Hart, 1964)

Granites, various dating methods were applied (Komatsu et al., 1998; Umeda et al., 1999d), namely, K-Ar dating of hornblende and biotite, FT dating of zircon and apatite, and track-length measurement of zircon to five specimens collected at a distance of 0.1 m (GW-0.1), 1 m (GE-1), 8.5 m (GE-8.5), 51 m (GE-51), and 90 m (GE-90) from the margin of the intrusive body, respectively (Figure 2.4-27). The K-Ar age of biotite in the specimen GW-0.1 is perturbed by about 10 %, as compared with the age of biotite in the other specimens. The K-Ar ages of hornblende in all the specimens and biotite in the specimens collected at a distance exceeding 8.5 m from the intrusive body are not reset by annealing. The FT ages of zircon have been perturbed for the specimens GW-0.1, GE-1 and GE-8.5, and particularly the FT age of zircon in the specimen GW-0.1 is nearly coincident with the formation age of the intrusive body. Thus, zircon in the specimen GW-0.1 has probably exceeded the partial annealing zone (PAZ) to be completely reset by the heat from the intrusive body. Further, zircon grains collected within 8.5 m from the intrusive body are presumed to have lost part of the fission tracks because of a high temperature in the PAZ. According to the FT dating of apatite, the ages of the specimens GW-0.1, GE-1 and GE-8.5 are almost identical to the formation age of the intrusive rock, and the age of the specimen GE-51 is more or less rejuvenated. Thus, it is presumed that not only apatite grains within 8.5 m from the intrusive body have exceeded the PAZ to be reset, but the temperature at a distance of 51 m from the intrusive body also rose to the PAZ (Figure 2.4-28).

Since the shortening of fission tracks depends on the temperature and duration of annealing, it is not enough to simply estimate the temperature range of the PAZ. Thus, the duration of annealing by the formation of the intrusive rock was estimated using a one-dimensional thermal diffusion model. As a result, it has been ascertained that the temperature reached a maximum in a few to tens of years and then gradually decreased to drop to below 100°C in 300 to 400 years at any sampling point. Consequently, the duration of annealing is estimated at several hundreds of years at most. Assuming that it ranges from 100 to 1,000 years, data from the experimental annealing of zircon (Yamada et al., 1995) allow the maximum temperatures of the specimens to be estimated. Sample GW-0.1, with complete resetting of fission tracks (shortening rate 0), yielded an estimated maximum of more than 560°C, specimen GE-1 with a shortening rate of 0.85 an estimated maximum of 330 to 370°C, and the specimen GE-8.5 with a shortening rate of 0.95, an estimated maximum of 270 to 300°C. Besides, the data on experimental annealing of apatite (Laslett et al., 1987) suggest that the annealing temperature exceeded 180°C for all the specimens within 8.5 m and 60 to 90°C for the specimen GE-51. Thus, the temperature of the country rocks around the Takahama-Kuroiwa intrusive body probably rose to more than 560°C, 330 to 370°C, 270 to 300°C, and 60 to 90°C at distances of 0.1 m, 1 m, 8.5 m and 51 m from the contact, respectively (Figure 2.4-29). However, no thermal effect is recognized at a distance exceeding 51 m from the contact.

To summarize, the temperature around an intrusive body is temporarily raised by the heat from the intrusive magma, but the extent of thermal effects to reset the age of minerals is estimated to be a few times smaller than the diameter of the intrusive body.

2.4.3 Summary

Post-Miocene volcanism in the Japanese islands is concentrated in certain regions. Present-day activity occurs within the East Japan and West Japan Volcanic Belts. Since the Quaternary, the volcanic front has been stable and, during this period, volcanism has become more concentrated within existing volcanic regions. Therefore, predictions of volcanic

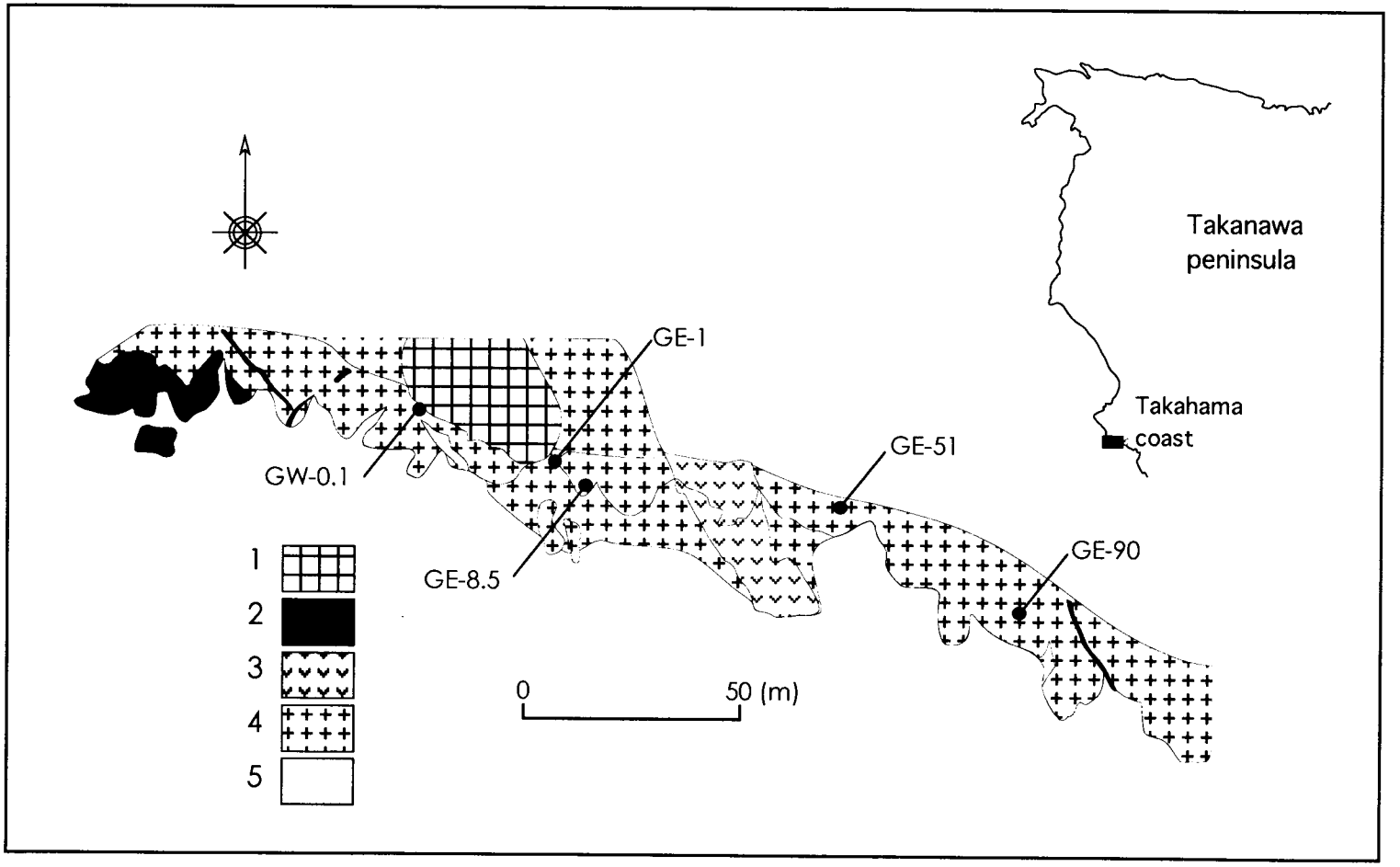


Figure 2.4-27 Geological map of the Takahama district and locations of samples
(Umeda et al., 1999d)

1: Takahama-Kuroiwa intrusive rock (andesite), 2: Andesite dikes,
3: Granite porphyry, 4: Granodiorite, 5: Aplite

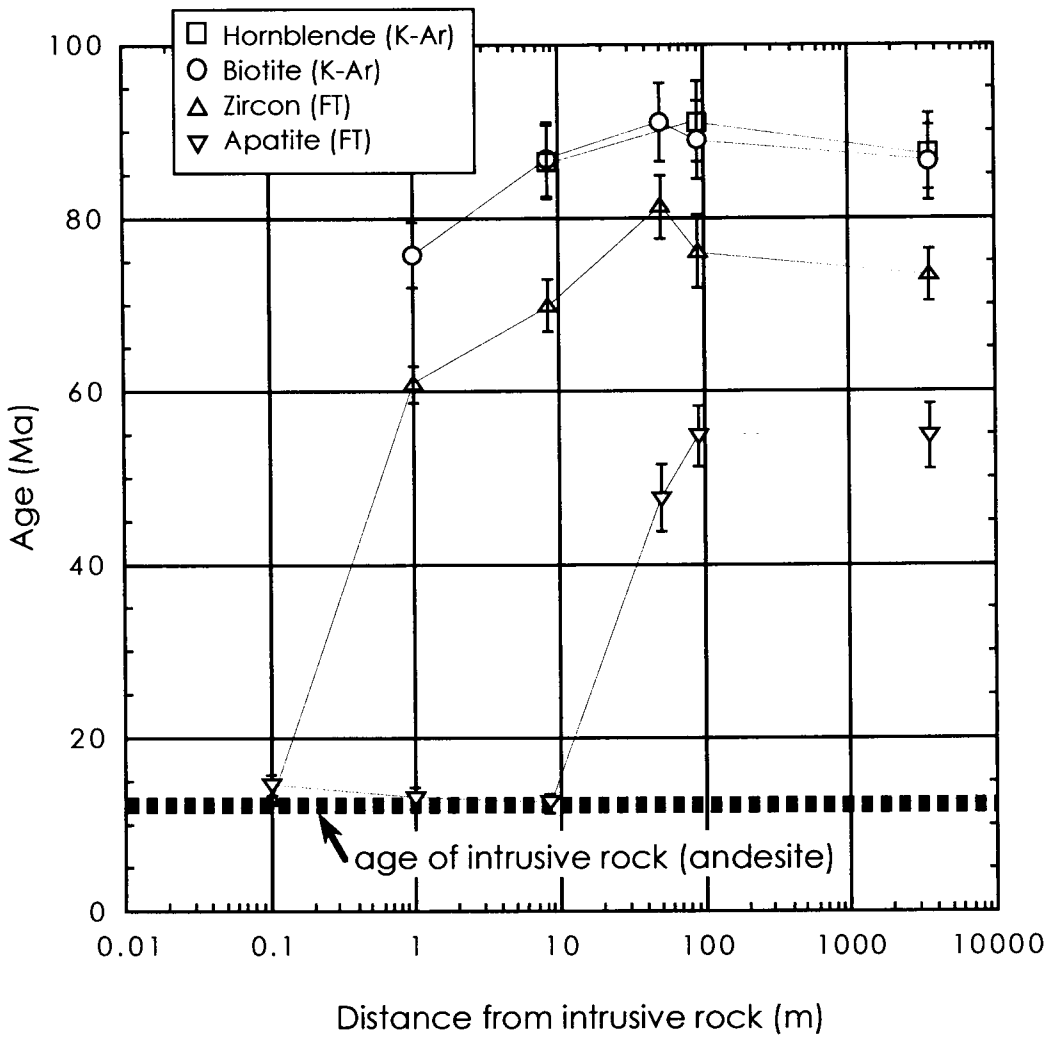


Figure 2.4-28 Ages of each mineral plotted versus distance from the Takahama-Kuroiwa intrusive rock
(Umeda et al., 1999d)

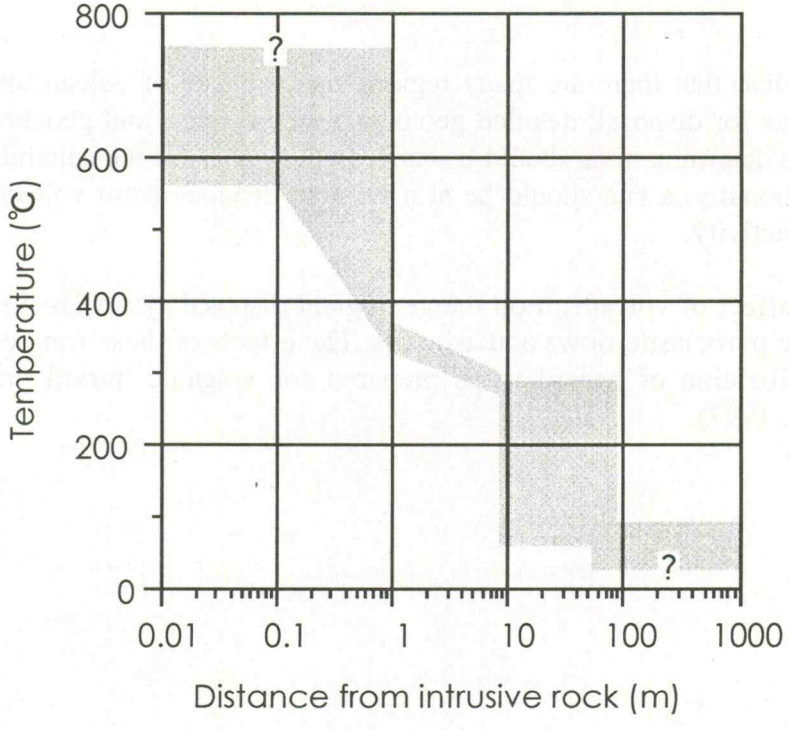


Figure 2.4-29 Temperature around the Takahama-Kuroiwa intrusive rock estimated from mineral ages
(Umeda et al., 1999d)

activity during the next one hundred thousand years can be based on the spatial and temporal evolution of volcanism over the last few hundred thousand years. These predictions must be based not only on extrapolations of existing data but also on research on tectonics, including crustal stresses and the distribution of subsurface magma chambers.

Volcanoes affect the thermal, hydrogeological and geochemical environment of the surrounding regions by providing a magma chamber and causing the development of hot dry rock. The influence of volcanoes tends to decrease away from the location of an eruption center, but the rates at which influences change with increasing distance differ from volcano to volcano.

In any case, it is clear that there are many regions that are free of volcanism in Japan. To select a suitable area for disposal, detailed geological, geophysical and geochemical surveys and radioactive age determinations should be carried out to confirm the suitability of the area for disposal. Additionally, a site should be at a suitable distance from volcanoes and other centers of igneous activity.

Another potential affect of volcanism on the geological disposal system is the development of large-scale felsic pyroclastic flows and ash falls. The effects of these can be minimized or avoided by the utilization of hazard maps prepared for volcanic hazard prevention (e.g. Aramaki, 1993; Ui, 1997).

2.5 Uplift, subsidence and denudation

Uplift and subsidence occurring in the geological past deformed and displaced both the surface and deeper rock formation and the effects of these processes are now recognizable as tectonic landforms and geological structures. Denudation lowers the land surface towards a base-level of denudation. Evidence of the process is recognized in landforms produced by denudation and in deposits carried from various dissected and eroded areas.

Uplift, subsidence and denudation produce changes in topographic gradients and affect the thickness of the overburden. These changes may cause variations in hydraulic gradients driving groundwater flow and in groundwater levels. In areas of uplift, the occurrence of large-scale denudation is possible. This process may cause rock formation that are initially buried deeply to come close to ground surface. Additionally, such uplift may be accompanied by flushing of deep underground water by meteoric water. Uplift in coastal areas may exert a particularly significant effect because sea-level is the base-level of denudation. Thus, uplift of a coast, especially when it occurs during a sea-level drop corresponding to a period of glaciation, will have a particularly marked effect on the denudation rate and groundwater conditions.

In order to assess the long-term stability of geological environments, it is important to predict future changes in the topographic gradient and the thickness of the overburden. In the following, spatial and temporal variations in uplift, subsidence and denudation are described. The processes that must be understood to make predictions of future trends are also discussed. Additionally, case studies of changes in topographic gradients and other features caused by uplift, subsidence and denudation are described.

2.5.1 Characteristics of uplift, subsidence and denudation in Japan

1) Uplift and subsidence

An increase in the elevation of an area above the base-level of denudation, due to uplift, may increase its topographic gradient and result in the potential for denudation rates to increase. Conversely, subsidence and associated sedimentation will increase the thickness of the overburden covering an area.

The effects of uplift and subsidence have tended to accumulate at relatively uniform rates and/or with characteristic trends in any given area that is relevant to the present study throughout the last several hundred thousand years. Therefore, predictions of future uplift and subsidence, based on evidence of these processes in the past, are considered feasible. To make such predictions confidently, it is necessary to understand the relationships between uplift and subsidence and crustal movements reflected in earthquakes, fault activities and other natural phenomena. In this section, the methods available to investigate uplift and subsidence in the Japanese islands are discussed.

(1) Analytical methods for uplift and subsidence

There are three basic methods for investigating the rate and distribution of uplift and subsidence (i.e. movement patterns), according to the period being investigated, as shown in Table 2.5-1. It is important to make complementary use of these methods because each method has its advantages and disadvantages.

The geodesic method uses land surveying data, acquired by methods such as leveling, and

tidal data. This method is suitable for making accurate estimates of the rates and distributions of crustal movements throughout Japan. Nationwide variations in movement rates have been researched by Danhara (1971), Aubrey and Emery (1986) and Kato and Tsumura (1979). The literature indicates that the Japanese islands move vertically at a rate of one to several millimeters per year; in a very few areas, the rate is more than 10 mm per year.

Recently developed Global Positioning Systems (GPS), based upon satellite ranging, are capable of observing nationwide crustal movements (particularly horizontal movements) more accurately and quickly than land surveying (e.g. Tada et al., 1997). However, the geodesic method has been applied for only a short period of time of about 100 years in Japan. This interval is shorter than the repeat interval of large earthquakes in most areas and cumulative uplift or subsidence patterns associated with earth movements that cause earthquakes cannot therefore be resolved by this method. The movement patterns obtained by this method are also likely to differ from the average trends in long-term crustal movements obtained by topographic or geological methods. For example, the distribution of marine terrace indicates that the coast of Sanriku has uplifted over a long period of time, but the tidal data indicate a tendency for subsidence.

The topographic method uses deformed topography such as marine and river terraces as an index of crustal movements. This method is effective in an area like Japan, where terraces are locally well-developed, due to local relatively rapid uplift. Nationwide maps are available that show the distribution of marine terraces formed approximately 125,000 years ago and 6,000 years ago (Ota et al., 1987, 1992). Additional investigations of the distribution and ages of marine terraces are being carried out throughout Japan, to provide improved information on the distribution of crustal movements over the past several hundred thousand years (Koike and Machida , eds., 1999).

There are few indicators of the spatial scales and rates of uplift in upland areas. However, Yoshiyama and Yanagida (1995) presented a method to estimate these scales and rates over the last hundred thousand years. Their method was based on measurements of the heights and ages of river terraces. This approach has been improved by Takagi et al. (1999 a) so as to apply it to the uplift that has occurred over the past several hundred thousand years.

Around the tops of mountains, there is a widely distributed denudational low-relief surface, believed to have been formed near sea-level at the end of the Tertiary. The altitude distribution of this surface roughly indicates the distribution of uplift since the beginning of the Quaternary (Research Group for Quaternary Tectonic Map, 1968). The second method involves the simulation of changes in surface altitude over a period of around a million years, using a model for the equilibrium states of denudation and uplift rates (Ohmori, 1987, 1990).

The geological method is used to estimate crustal movement patterns that occurred during and after the sedimentation of strata and is based on information concerning the geometry of a sedimentary surface at the time the sediment was deposited and the thicknesses of overlying strata. The ages of the sedimentary surface and the overlying strata are also required as input.

Although this method has lower spatial and temporal resolutions than the other two, it is capable of estimating the history of crustal movements over a longer period of time. It is particularly relevant when estimating the scale of subsidence of basins and plains during and after the Neogene (Naruse, 1988, 1989, 1990; Koike and Machida, eds., 1999).

In order to improve the resolution of this approach, Fujiwara et al. (1996) have attempted to apply sedimentary facies analysis to coastal sediments in a 20 km x 30 km area in the Boso Peninsula. They estimated the scale of uplift (on a meter scale) and tilting (in ‰ order) over the past 120,000 years. Furthermore, there has been an attempt to estimate the periods when seismic uplift occurred in coastal areas and the associated amounts of uplift. This was carried out by detecting evidence of earthquakes, such as sediment deposited by tsunami (Fujiwara et al., 1997, 1999 a, b, c; Masuda, 1998).

(2) Movement patterns in mountains

Kaizuka et al. (1995) classified the patterns of movement shown by mountains and basins into four types, based on the processes controlling the movements deduced from geological structures and topographic features (Figure 2.5-1). These types are:

i. Fold and fault type;
ii. Reverse fault block type;
iii. Lateral-slip fault block type;
iv. Warping type.

In some areas, patterns of intermediate type occur. The features of the movements are described briefly below.

i. Fold and fault type

The present mountain ranges typical of the Northeast Japan arc consist largely of mountains and basins formed by folds and reverse-faults, characterized by a zonal arrangement of topography and tectonic structures parallel to the island-arc axis (Kitamura, ed., 1986). The zonal arrangement (from easte to west; the Kitakamigawa-Abukumagawa lowland area, the Ohu mountain range, the inland basins, the Dewa hills, and the coastal lowland area along the Japan Sea) has been formed by crustal folding and reverse faulting since the end of the Pliocene. At this time, the east-west horizontal compressive stress strengthened (Sato, 1994; Otsuki, 1995) and produced uplift and subsidence structure marked by a wavelength of about 50 km. North-south trending active faults are developed along the boundaries between mountains and the adjacent plains (basins) (Research Group for Active Faults of Japan, 1991). The plains underlain by a thick sequence of sedimentary formations formed since the Neogene are characterized by the development of active folds causing terrace deformation (Japan Assoc. Quaternary Research, 1987). The uplif rate estimated by the height of coastal terraces is as much as 0.5 mm per year on the back-arc side, which is generally larger than that on the Pacific Ocean side of northeast Japan (Yagi and Yoshikawa, 1988; Miyauchi, 1990). The cumulative uplift throughout the Quaternary period amounts to 1,000 m in the central part of the present type of mountain ranges (Table 2.5-2).

The Akaishi mountain range and the Tanzawa mountains are in a region that has undergone one of the largest degrees of Quaternary uplift anywhere in the Japanese islands. This uplift was caused by the collision between the Honshu arc and the Izu arc (Kaizuka, 1987). The Quaternary uplift of the main ridge of the Akaishi range amounts to as much as 2,500 m (Moriyama, 1990).

ii. Reverse fault block type

This type is characterized by tilted mountain blocks bordered by reverse faults, represented by the mountains in the Kinki Triangle and the Kiso mountain range. The Kinki Triangle is a triangular region that has the Wakasa Bay at the apex, the Hira-Rokko mountains as the

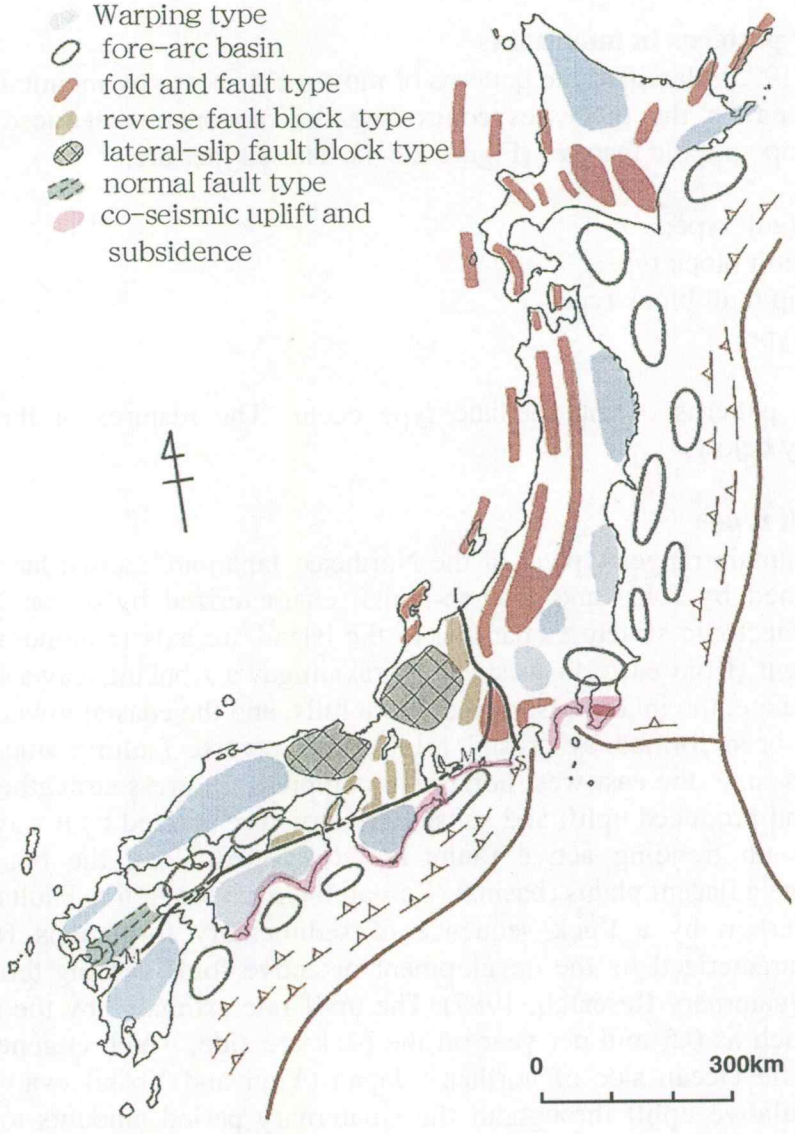


Figure 2.5-1 Distribution of types of deformation in Japan, deduced from geological and geographical structures (modified from Kaizuka et al., 1995)

Table 2.5-1 Methods for estimating uplift and subsidence

	Land survey	Topographic method	Geological method
data	leveling	1) accumulated displacement of land surface (i.e. terrace) 2) equilibrium model of denudation rate and uplift rate	accumulated movement of sediment surface
period	few months ~ 100 years	1) 10^3 ~ 10^5 years (terrace); 2×10^6 years (erosional low-relief surface) 2) 10^7 years	10^6 years scale
time resolution	daily ~ annual	1) 10^3 ~ 10^5 years 2) 10^5 ~ 10^6 years	10^5 ~ 10^6 years (10^3 years)
spatial resolution	cm scale	1 m~10m scale	10m~100m scale

Table 2.5-2 Examples of uplift rates in "fold and fault" type areas

Uplift rates in m per 10,000 years. Values in parentheses show when uplift begun in the specified areas.

Area	Uplift rates estimated from geological structures and heights of erosional low-relief surface	Uplift rates estimated from the heights of terraces	Note
Yubari Mts.	4~5 [2Ma] [2]	2.8~3.2 [0.15Ma] [1]	
Hidaka Range	4~5 [2Ma] [2]	western part 4.0 ~ 5.2 [0.15Ma] [1]	
Ou Range	4~5 [2Ma] [2]	3.3~7.5 [0.12Ma] [3]	4.1mm a^{-1} (by surveying)[4] E-W shortening since 3.5Ma[11]
Dewa Hills	2.5~5 [2Ma] [2] 0.4 [2.5Ma] [5]	2.5~5.4 [0.12Ma] [3]	3.7mm a^{-1} (by surveying)[4] E-W shortening since 3.5Ma [11]
Echigo Hills	2.5~4 [2Ma] [2] 13~17 [0.6Ma] [5]	tilting in the order of 10^{-7}~ 10^{-6} a^{-1} (Max. 2×10^{-6} a^{-1})[4] during the late Pleistocene to Holocene.	tilting in the order of 10^{-7}~10^{-6} a^{-1} (by surveying), uplift rate of anticlines is 0.2~3.3mm a^{-1} [4]
Tanzawa Mts.	30~40 [2.5Ma] [7] 11~36 [3Ma] [14]	2.8 [0.15Ma] [1] 25 [0.08Ma] [13] 30~40 [0.01Ma] [13]	10~15 [1Ma] [6]
Akaishi Range	>12.5 [2Ma] [8], [9]	5.2 [0.15Ma] [1]	70 [1Ma] [6] 8.8mm a^{-1}(by surveying)[10] actively uplifted since 1 Ma[12]

1) Yoshiyama and Yanagida (1995), 2) The research group for Quaternary tectonic map (1968), 3) Tanaka et al. (1997), 4) Mizoue et al. (1980), Iikawa (1983, 1991), Iikawa and Horikawa (1985), Ojiya crustal movement research group (1989), 5) Naruse (1989), 6) Ohmori (1987), 7) Kaizuka (1987), 8) Moriyama (1990), 9) Moriyama and Mitsuno (1989), 10) Iikawa (1991), 11) Sato (1994), 12) Takeuchi (1996), 13) Kaizuka et al. (1995), 14) Soh et al. (1998).

western margin, the Yoro mountains as the eastern margin, and the Median Tectonic Line as the base. The region embraces Biwa Lake, Osaka Bay and Ise Bay (Fujita and Oike, 1981). A lot of fault blocks (mountains and basins) are bounded by north-south trending active faults between the neighborhood of Osaka Bay and the western margin of the Nobi plains. The maximum uplift for the Quaternary period reaches 1,500 m or more in the Chubu mountain region including Hida and Kiso mountains (Table 2.5-3), where tilted blocks represented by mountains and intermountain basins have been formed by faulting since the latest part of the Tertiary period (Takahama et al., 1988; Moriyama,1990).

According to an equilibrium model between uplift rate and denudation rate, the average uplift rate of the Chubu mountain region is estimated at several mm per year (up to 7 mm per year) for the past one million years (Ohmori, 1987). The result is conformable with the fact that this region, with a denudation rate estimated at several mm per year, has maintained an elevation exceeding 2000 m. Geodetic data also support the fact that most of the Chubu mountain region is currently uplifting at the largest rate in Japan (Iikawa, 1991).

This region is characterized by a high concentration of faults with a high degree of activity (Research Group for Active Faults of Japan, 1991), the largest rate of WNW-ESE shortening in Honshu (Kaizuka and Imaizumi, 1984), and strong compressive deformations of the late Cenozoic formations distributed in the foreland. These facts indicate that the extraordinarily high rate of uplift in this region presumably results from strong compressive forces in the earth's crust.

iii. Lateral-slip fault block type

The areas where this type occurs are characterized by crustal shortening that is mainly compensated for by slip faults, and is represented by the northwestern part of the Chubu region (Hida Plateau and Mino Heights) and the western part of the Kinki region (Tanba Plateau). In these areas, the lateral-slip fault blocks are thought to have resulted from uplift and subsequent faulting of peneplains (Moriyama, 1990). The uplift rates of representative mountains are shown in Table 2.5-4. Topographical changes that the Mino Heights have undergone since the late Neogene are clarified by studying the composition and size distribution of pebbles in the Toki sand gravel bed and paleo-currents (Moriyama, 1987, 1990), indicating block movements by faults since the middle Pleistocene epoch.

iv. Warping type

This type of crustal movement occurs in areas with moderately tilting mountain masses. Typical areas are the Kitakami and the Abukuma highlands in northeast Japan as well as the highlands in Chugoku, Shikoku, Kyushu and the Kii Peninsula located in Southwest Japan. In the Kitakami and the Abukuma highlands, the frequency of active faults is low and there is relatively little topographic relief. In these areas, the uplift during the Quaternary was approximately 500 m to 700 m (Table 2.5-5). In the highlands in Shikoku, Kyushu and Kii, uplift during the Quaternary was relatively large and reached 1,000 m at the center of the highlands (Research Group for Quaternary Tectonic Map, 1968). In addition, according to analyses using the equilibrium model of denudation and uplift rate, the average uplift rate over the past one million years was 2.5 mm per year at the center of the Shikoku mountains (Ohmori, 1990). The analysis of geodesic and landform data suggested that the uplift of the Shikoku mountains resulted from the combination of subsidence during large earthquakes and moderate uplift during intervals between earthquakes (e.g. Ohmori, 1990). In the Chugoku region, uplift started in the middle Miocene (Obata, 1991) and uplift during the Quaternary was considered to be 400 m at most (Table 2.5-5).

Table 2.5-3 Examples of uplift rates in "reverse fault block" areas

Uplift rates in m per 10,000 years. Values in parentheses show when uplift began in the specified areas.

Area	Uplift rates estimated from geological structure and heights of erosional low-relief surfaces	Uplift rates estimated from the heights of terraces	Note
Hida Mts.	>7.5 [2Ma] [2]	12.4 ~ 24.4 [0.15Ma] [1]	5~7 [1Ma] [3] mainly uplifted from 3 to 1.4Ma[4),5)] possibly uplifted due to isostatic rebound[8)]
Kiso Mts.	5~7.5 [2Ma] [2]		5 [1Ma] [3] actively uplifted since 1~0.5Ma[5),6),7)]
Rokko Mts.	5 [1Ma] [10]		vertical displacement rate relative to Osaka basin: 10 [1Ma] [10] Reverse fault blocks in the Kinki Triangle have rapidly uplifted since 0.5Ma[9),10)]
Yoro Mts.	6~8 [1Ma] [11]		vertical displacement rate relative to the Nobi plain by the Yoro fault: 20 [1Ma] [11]
Asan Mts.	1.7 ~ 3.9 [2.1 ~ 1.2Ma] [12]		

1) Yoshiyama and Yanagida (1995), 2), Research Group for Quaternary _ectonic Map (1968),
3) Ohmori (1987), 4) Takeuchi (1988), 5) Takeuchi (1996), 6) Moriyama and Mitsuno (1989),
7) Moriyama (1990), 8) Ikeda (1990, 1996), 9) Fujita (1995), 10) Kaizuka et al. (1995),
11) Sugai and Sugiyama (1988), 12) Ueki and Mitsushio (1998).

Table 2.5-4 Examples of uplift rates in "lateral-slip fault block" type areas

Uplift rates in m per 10,000 years. Values in parentheses show when uplift began in the specified areas.

Area	Uplift rates estimated from geological structure and height of erosional low-relief surface	Uplift rates estimated from the heights of terraces	Note
Hida plateau	2.5~7.5 [2Ma] [1),2)]		
Mino plateau			Uplift started in early Pleistocene[3)]. Fault blocks have been formed since middle Pleistocene.[3)]
Tamba plateau	2.5 [2Ma] [1]		

1) The Research Group for Quaternary Tectonic Map (1968), 2) Nogami et al. eds. (1994), 3) Moriyama (1990).

(3) Movement patterns of the coast

In the Japanese islands, several steps of marine terraces formed in the late Quaternary period are widely distributed over a distance of 10 to 20 km landward from the coastline. They are excellent indicators for uplift rates and patterns of crustal movements. In particular, the Shimosueyoshi surface, a marine terrace formed by a widespread transgression some 12.5 ka ago, is distributed at different altitudes ranging from 10 m or less to about 200 m in many parts of the country (Figure 2.5-2). Patterns of coastal movement in the Japanese islands are classified into four types from A to D (mobile districts) on the basis of the height distribution of the marine terraces (Figure 2.5-2). The minimum areas covered by the respective movement types are generally represented by individual hills or lowlands. An assembly of hills or lowlands characterized by a common type of movement forms a mobile district as a whole.

Terraces older than the Shimosueyoshi surface in the respective mobile districts show patterns of movement similar to that of the Shimosueyoshi surface, but have larger relative heights above sea-level. A similar relationship is found between the Shimosueyoshi surface and the lower Holocene terraces. Thus, each of the mobile districts has undergone a cumulative uplift following a definite pattern of movement since the late Quaternary period.

In many regions, the uplift rate before the formation of the Holocene terraces tends to be smaller than that after their completion. This tendency is particularly remarkable in the D type mobile district, where the uplift rate of Holocene terraces is twice to one order of magnitude larger than that of Pleistocene ones.

i. Type A (short wavelength warping)

Neogene strata are distributed in thick layers in the lowland zone along the Japan Sea coast, stretching from the southern part of Hokkaido to the northeast of Honshu. Active folds with a wavelength of 20 to 30 km occurring parallel to the shoreline predominate in this zone. This wavy deformation conforms to the present topography. The anticlines correspond to the positive relief of a piedmont or a peninsula and the synclines correspond to plains (e.g. Japan Assoc. Quaternary Research, 1987).

Figure 2.5-3 shows the formation age of terraces on the abscissa and the uplift rate on the ordinate. The uplift rates were obtained by dividing the uplift of terraces by their formation age. The uplift was obtained by subtracting the sea-level when the terraces formed relative to the present sea-level and the thickness of the strata deposited after terraces became emergent from the present altitude of the terraces (hereafter calculation procedures are the same as this). In any period, the uplift rate was several meters per 10,000 years. Estimated uplift rates vary, even in the same area, because of the tilt caused by folding. Active folds on the Japan Sea side move at relatively high rates. It is presumed that in an anticline, uplift still continued at the rate of approximately 10 m per 10,000 years after the Pleistocene (e.g. Miyauchi, 1988; Yashima and Miyauchi, 1990).

ii. Type B (tilting of small blocks)

Type B areas are those where there is tilting of small blocks (10-30 km long) that are segmented by faults. Typical areas are the Noto Peninsula, the Sado Island and the Wakasa Bay area (Figure 2.5-2). The Noto Peninsula is segmented into small blocks tilting towards the south (i.e. the entire peninsula tilts southwards). The Sado Island consists of three tilted blocks (Ota and Yoshikawa, 1978). The crustal movement pattern in the Hokuriku region, in which hills and mountains were uplifted and plains subsided, is considered to have been

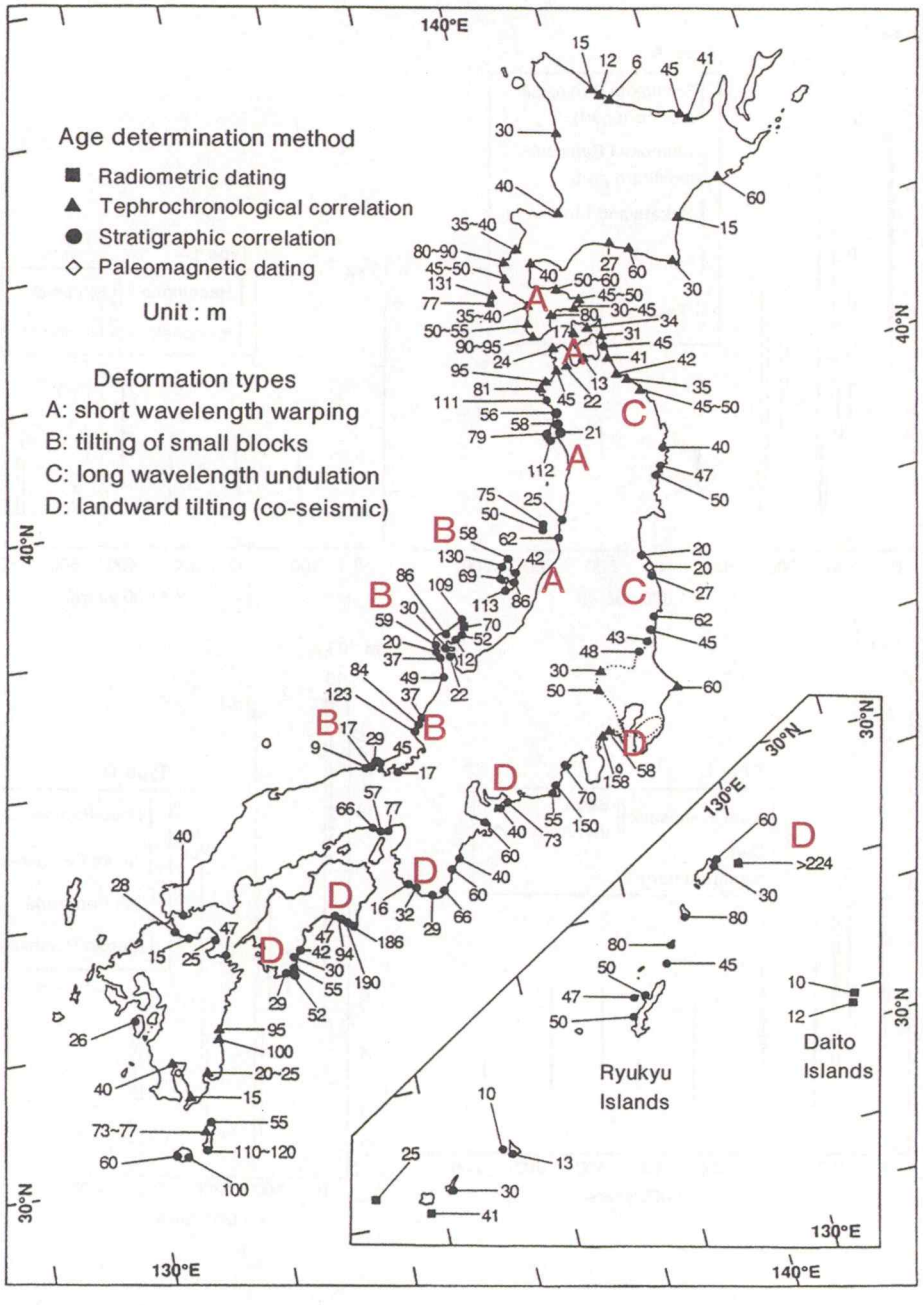


Figure 2.5-2 Current elevations of former shorelines formed during the last interglacial maximum (after Ota, 1996)

Current elevations of former shorelines formed at the peak stage of the last interglacial period (125,000 years ago). What is left after deducting the sea-level of the epoch (i.e. +5m above present sea-level) from the figure shown here represents the amount of uplift in each area during the last 125,000 years.

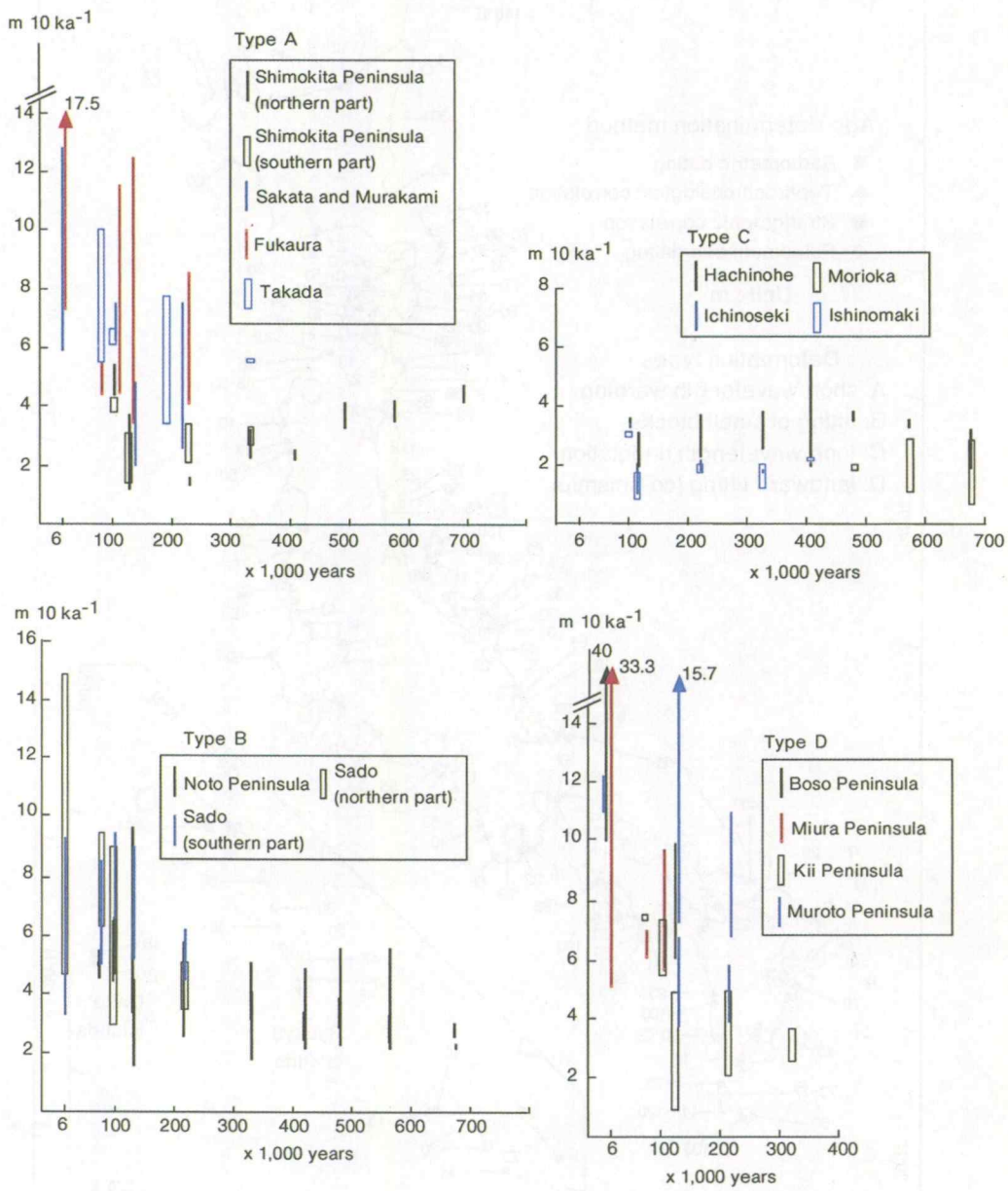


Figure 2.5-3 Uplift rates estimated from height of former shorelines in areas characterized by each deformation type shown in Figure 2.5-2
(data from Koike and Machida, eds., 1999)

Deformation types are the same as in Figure 2.5-2. Vertical bars represent ranges of uplift rates. Type D shows the largest rates.

formed approximately 500,000 years ago (Kaseno et al., 1988). The uplift rate of terraces older than the Holocene, estimated from the altitude distribution of terraces, is 2 to 8 m per 10,000 years. That of the Holocene terraces is most likely to be 5 m or more per 10,000 years and sometimes exceeds 10 m per 10,000 years (Figure 2.5-3). The estimated uplift rate varies in the same area because of the tilting of blocks.

iii. Type C (long wavelength undulation)

Type C coasts undulate very gently (i.e. at a wavelength longer than 100 km) and do not tilt towards the inland side. Typical areas are the Kitakami highlands and the Abukuma highlands. Estimated from the altitude of terraces, uplift rates over the past several hundred thousand years are several meters or less per 10,000 years (Figure 2.5-3). These rates are smaller than for other types. Figure 2.5-4 shows the altitude of marine terraces located in the northern part of the Sanriku Coast that were formed approximately 320,000 years ago (i.e. oxygen isotope stage 9). The former shoreline reaches 131 m in the northern Sannohe cho. All the terraces tilt very gently towards the sea (i.e. average tilting angle several ‰). Analysis of the oxygen isotope ratios in the deep-sea sediment suggests that the sea-level at that time was 5 m higher than at present. The uplift in each location can be calculated by subtracting this sea-level from the elevation of the terrace. The average uplift rate over the past 300,000 years is 3 to 4 m per 10,000 years.

iv. Type D (landward tilting)

The main characteristic of type D is notable landward tilting of coastal zones 30-50 km wide. Type D deformation is distributed on the Pacific ocean coast, which faces the plate boundary located west of the Kanto region (Figures 2.5-1, 2.5-2). Judging from the distribution of crustal deformations that were observed during earthquakes, this movement pattern resulted from the accumulation of seismic uplift that occurred at intervals of 100 to 1000 years (e.g. Shimazaki and Nakata, 1980; Miyashita, 1989; Ohmori, 1990). Here, "seismic uplift" means the uplift caused by strong earthquakes that occurred at the margins of the plates. Uplift caused by one such earthquake is a maximum of several meters to several tens of meters (e.g. Usami, 1987; Maemoku and Tsubono, 1990; Kayane and Yoshikawa, 1986).

The uplift rate estimated from marine terraces is faster than that of other types. The rate is the largest at the point of a peninsula, due to the landward tilting mentioned above. Here, the rate is likely to exceed 15 m per 10,000 years (Figure 2.5-3). In the type D coastal areas, the uplift rate of the Holocene terraces tends to be larger than that of older terraces. In addition, the uplift rate of the Holocene terraces reaches 40 to 50 m per 10,000 years in South Kanto and the southern part of Shikoku. Figure 2.5-5 shows the altitude distribution of the former shoreline of the Shimosueyoshi terrace located around the Muroto Peninsula. The figure indicates the conspicuous inland tilt from the point of the Muroto peninsula. The uplift over the past 120,000 years can be calculated by subtracting the sea-level at the time the terraces formed (approximately 5 m above the present sea-level) from the isoline.

v. Other coasts

There are some coasts that are not classified or that have an intermediate movement pattern. Table 2.5-6 shows the uplift rates estimated from terraces in such areas. Deformation is notable in the vicinity of the Izu Peninsula, which consists of blocks that are delimited by active faults (Table 2.5-7).

(4) Subsidence during the Quaternary

Major plains and basins in Japan are not simple lowlands. In fact, thick strata of Neogene or

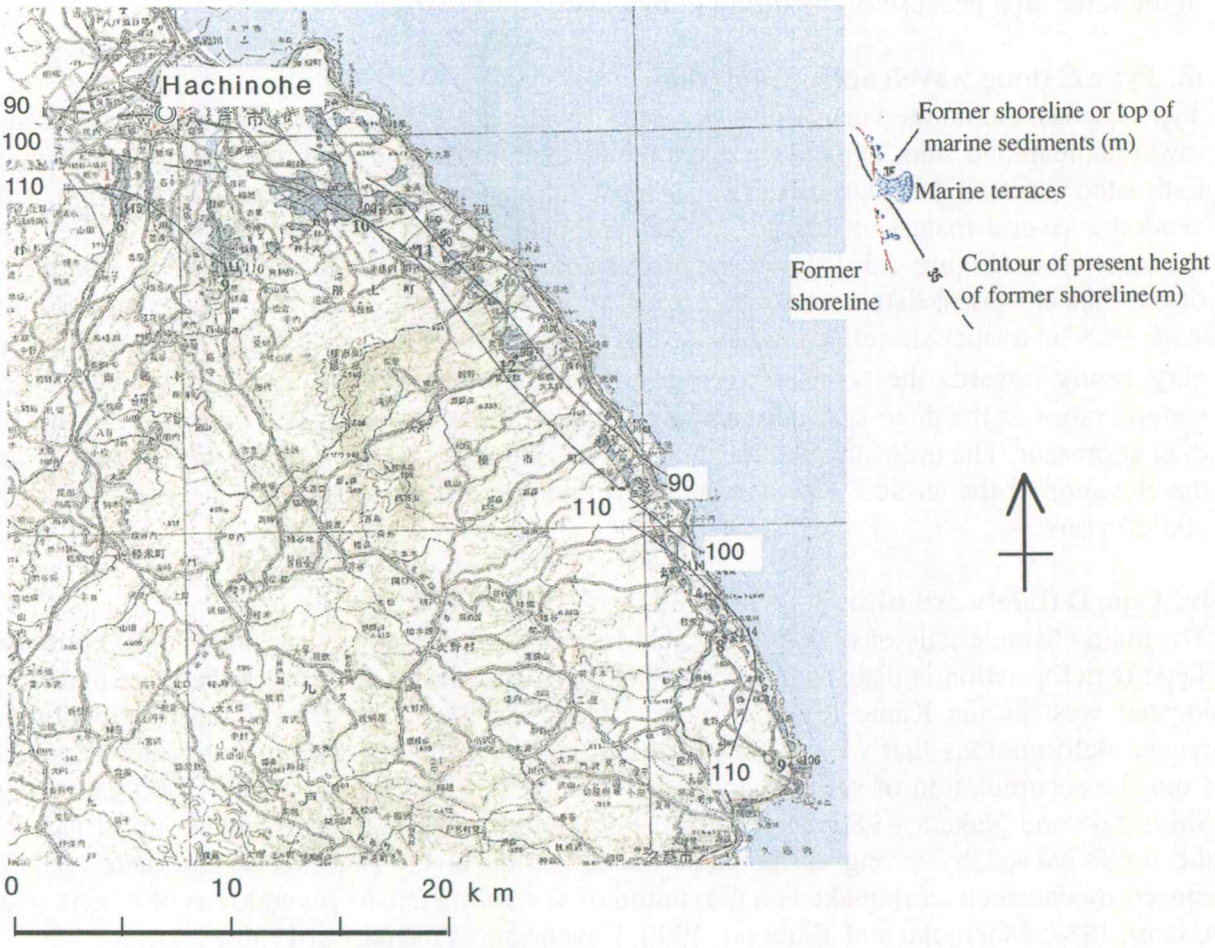


Figure 2.5-4 Height distribution of Stage 9 (about 320 ka) shoreline in the northern part of the Sanriku coast (Type C; unit:m) (data from Koike and Machida, eds., 1999)

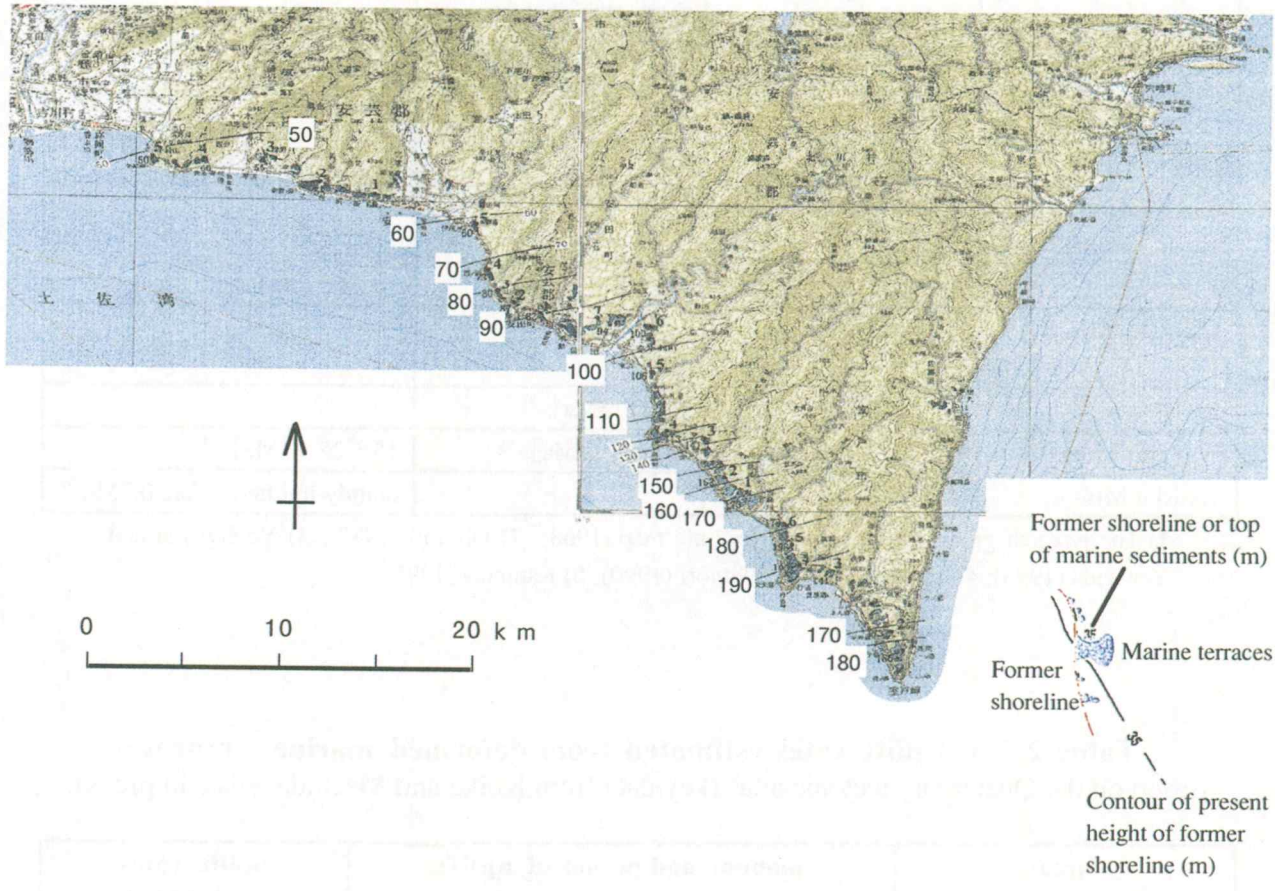


Figure 2.5-5 Height distribution of Stage 5e (about 125 ka) shoreline in the Muroto Peninsula (Type D; unit : m) (data from Koike and Machida, eds., 1999)

Table 2.5-5 Examples of uplift rates in "warping" type areas

Uplift rates in m per 10,000 years. Values in parentheses show when uplift began in the specified areas.

Area	Uplift rates estimated from geological structures and heights of erosional low-relief surfaces	Uplift rates estimated from the heights of terraces	Note
Kitami Mts.	2.5 [2Ma] [1]		
Kitakami and Abukuma Mts.	2.5～3.5 [2Ma] [1]		
Kanto Mts.	4～5 [2Ma] [1]	4.4～8 [0.15Ma] [3]	50～60 [1Ma] [2]
Chugoku Mts.	2～3.5 [2Ma] [1], [4]		
Kii Mts.	4～5 [2Ma] [1]	2 [0.15Ma] [3]	
Shikoku Mts.	4～7.5 [2Ma] [1]	3.2 [0.15Ma] [3]	15～25 [1Ma] [5]
Kyushu Mts.	4～7.5 [2Ma] [1]		mainly uplifted before 0.7Ma.[6]

1) The research group for Quaternary tectonic map (1968), 2) Ohmori (1987), 3) Yoshiyama and Yanagida (1995), 4) Obata (1991), 5) Ohmori (1990), 6) Kanmera (1995).

Table 2.5-6 Uplift rates estimated from deformed marine terraces

Based on the Quaternary tectonic atlas (key data from Koike and Machida, eds., in press).

area	amount and period of uplift	uplift rates (m per 10,000 years)
Urakawa	(33～45m) / 122 ka	2.7～3.7
Erimo	2～10m / 122 ky	0.2～0.8
Tomakomai (hills)	(22～41m) / 122 ka	1.8～3.4
Kitakami lowland		
Yakeishidake	(48.5～111m) / 114 ka	4.3～6.4
Mizusawa	(33.5～76m) / 114 ka	2.9～4.3
Sinmachi	34m / 114 ka	3.0
Marginal area of Kanto Plain (changed to uplift from subsidence around 1 Ma) [1]	3～39m / 122 ka (The active folding with axis of NW-SE developed in the western part of the plain) [2]	0.2～3.2 0.1～0.4 mm a^{-1} (northern part, Late Quaternary) [3]
Kinki		3.0 – 5.7
Kobe, Suma	(36.5～69.5m) / 122 ka	
Hojou, Takasago, Akashi	(31.6～62.6m) / (122～328 ka)	2.6～5.1
Yatsushiro	(19～29m) / 122 ka	1.6～2.4
Kagoshima	68m / 122 ka	5.6

1) e.g. Kaizuka, et al., 1987 2) Japan Assoc. Quaternary Research , 1987
3) Suzuki, 1989; Masuda and Nakazato, 1988.

younger age lie beneath them. They are areas of subsidence (i.e. structural basins) and most of them are still subsiding. In the Japanese islands, a large transgression occurred around 17-15 Ma ago and marine sediments of Miocene age were deposited widely throughout Japan. Then, during the Pliocene (i.e. approximately 5 Ma ago), the Miocene sedimentary basins became smaller and separated. Most of the Quaternary basins were superimposed on these Pliocene basins that contracted and shallowed further (Naruse, 1988, 1990).

Figure 2.5-6 shows the major Quaternary basins. Most of them are oval-shaped and each has a major axis of 50 to 100 km and a minor axis of 30 to 50 km. Inland basins are small and their major axes are less than 50 km. The central parts of the coastal plains are most likely to have subsided during the Quaternary. However, in most areas along the margins of plains, judging from the distribution of strata and terraces, the tendency towards subsidence seems to have changed to uplift during the late Quaternary (Japan Assoc.Quaternary Research, 1987).

Borehole data and results of geophysical exploration using the seismic reflection method have been obtained for geological formations that were deposited on Japan's major plains and basins after 1 Ma ago. Based on this information, the age and depth of burial of strata have been compiled (Figure 2.5-7a). It is possible to approximate the burial depth with the subsidence after sedimentation, because these sediments are mainly shallow marine deposits (Naruse, 1988, 1989). The figure indicates that the subsidence rate is approximately 1 m or less per 1,000 years in many areas. Table 2.5-8 shows the distribution of subsidence (and its rate) in major plains of Japan.

Figure 2.5-7b shows cumulative changes in the thickness of strata formed after 15 Ma ago in the subsiding centers of major plains. The figure is based on data obtained from deep boreholes. If the water depth at the time of sedimentation is ignored, cumulative changes in the thickness of strata are good approximations of cumulative subsidence. Subsidence rate, shown by the slope of the curve, varies according to age and area. The subsidence rate of the plains on the Japan Sea side was large before 15 Ma ago, then decreased and increased again from several Ma ago to the present.

A graben in the central part of Kyushu extends from Beppu in the east to Shimabara in the west. It is an area where the ground was segmented into blocks by normal faults due to a tensile stress field (Kaizuka et al. eds, 1995). The area is regarded as normal fault type. The Beppu-Shimabara graben is an extension of the Okinawa Trough and currently trends in a N-S direction (e.g. Tada, 1985); this is considered to be the cause of the subsidence.

A map showing the subsidence of plains of Japan has been created using the distribution of the base-level depth of the Quaternary strata to approximate the depth of Quaternary subsidence (Koike and Machida, eds., 1999). An example of subsidence of the Shonai Plain is shown in Figure 2.5-8.

Analysis of geodetic and tidal data accumulated for the past 70 years clearly indicates that the Pacific ocean side of northeast Japan has been subsiding and that the subsidence decreases westwards to the Japan Sea side (Danbara, 1971; El-Fiky et al., 1996). The subsidence on the Pacific ocean side implied by the geodetic and tidal data is contrary to long-term uplift indicated by the coastal terraces, although the cause of the contradictory tendencies is unknown.

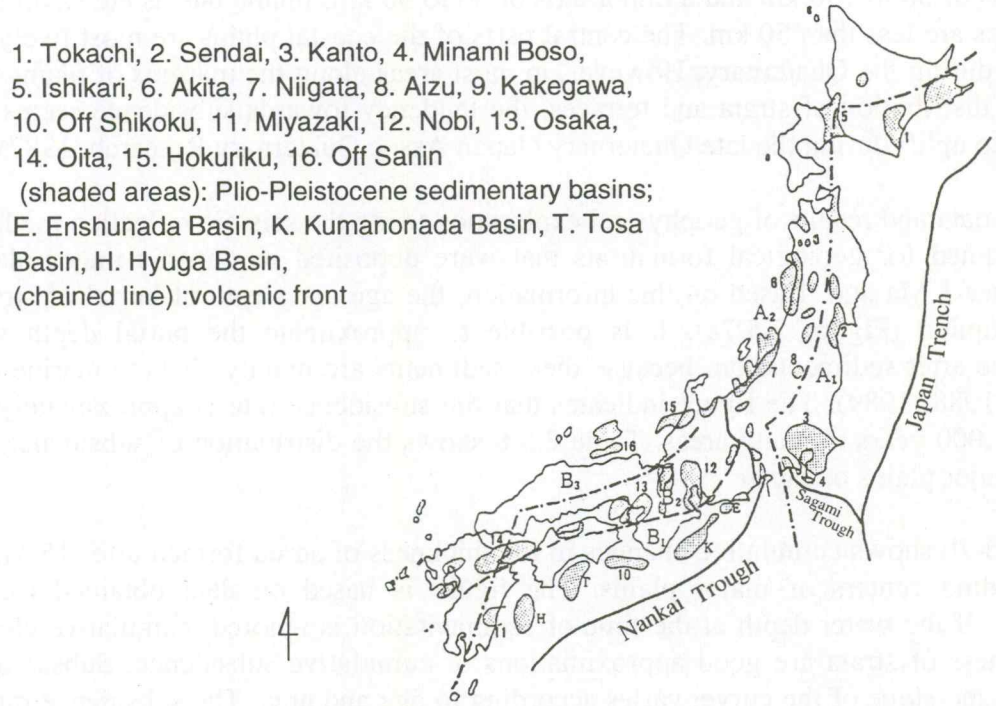
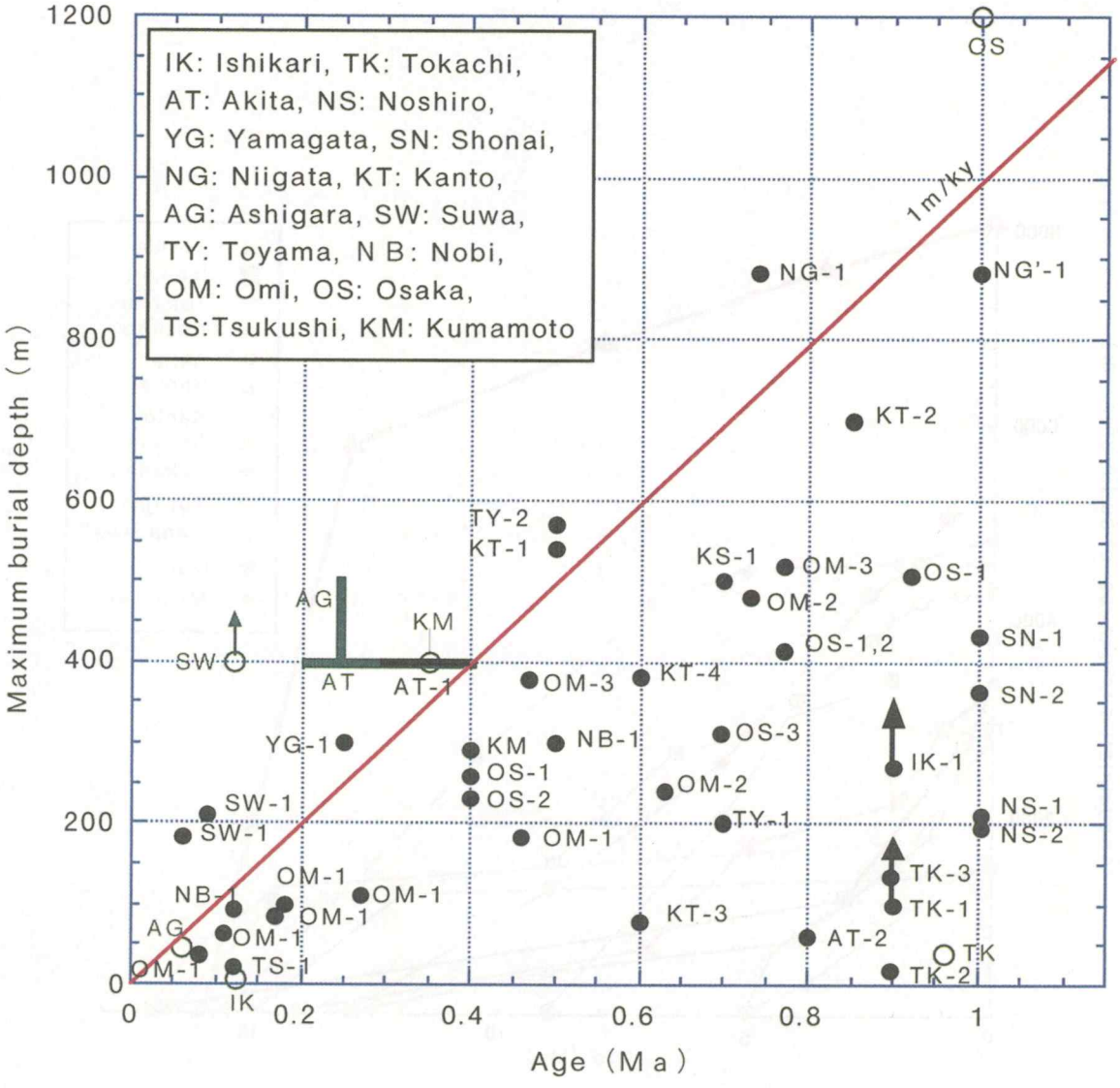


Figure 2.5-6 Regional distribution of Quaternary basins

(Naruse, 1990)



● Drilling data: Fujioka et al. (1977) ; Ikebe et al. (1979) ; Development Committee of the Mining Industry in Hokkaido (1979); Matsuzawa et al. (1981); Osawa et al. (1984); Osawa et al.(1985); Naruse (1988, 1989); Committee of Engineering Geological Map of Kanto District (1996)

○ Burial depths at basin center presumed from geological and seismic reflection profiles: after Table 2.5-8.

Figure 2.5-7a Burial depth and age of sediments in major Quaternary sedimentary basins in Japan

The vertical axis shows the present depth of the layer and the horizontal axis its age. A correction for water depth at sedimentation was done only for the Kanto plain. The burial depths of sediments are roughly converted to the amount of subsidence (Naruse,1988,1989). The amount of subsidence is obtained from depth and age. The amount of subsidence since 1 Ma ago is less than 1,000 m in most plains, and the subsidence rate is less than 1 m per 1,000 years. Basins which have a larger rate are limited to the Uetsu-Fossa Magna-South Kanto zone (Akita, Yamagata, Niigata, Toyama, Suwa, Kanto and Ashigara) and Osaka.

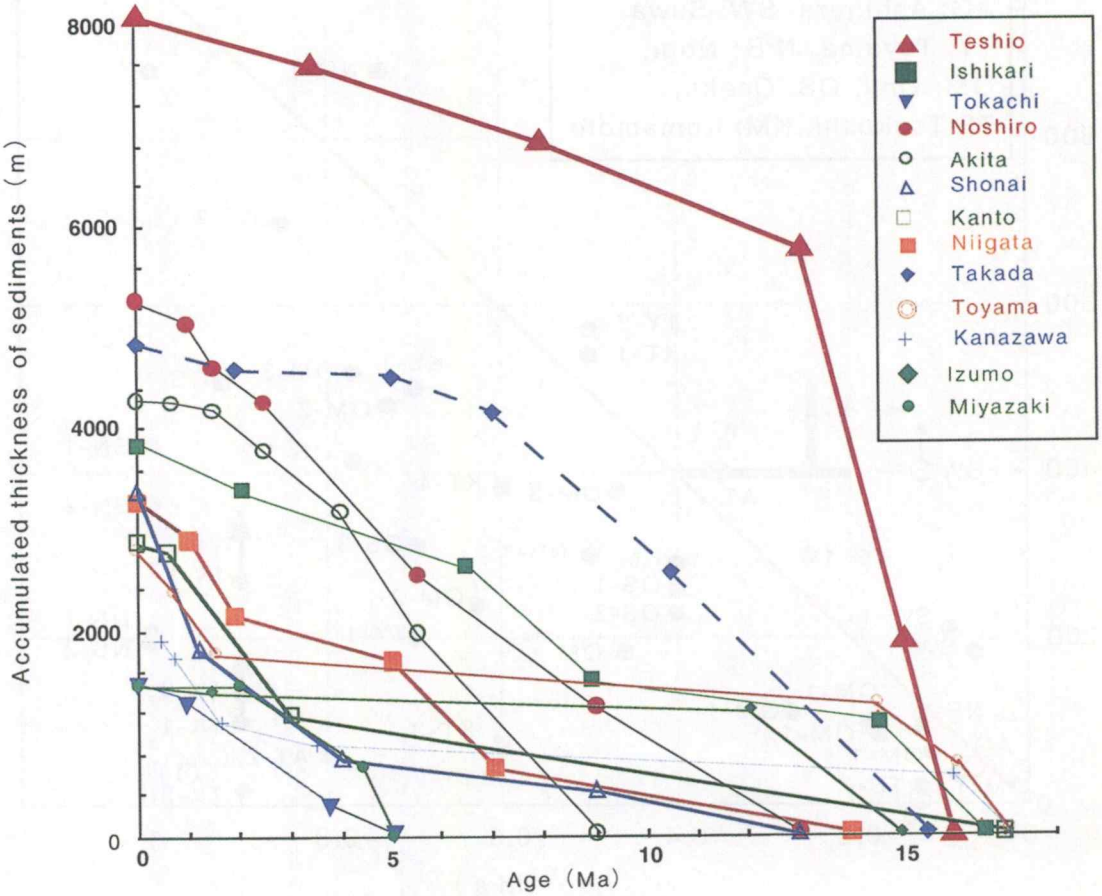


Figure 2.5-7b Accumulated subsidence in the main plains

The vertical axis shows the thickness of sediments under the main plains determined by drilling. The thickness of sediments can be roughly converted to accumulated subsidence (Naruse, 1988, 1989). Drilling data : Fujioka et al. (1977); Ikebe et al. (1979); Development Committee of the Mining Industry in Hokkaido (1979); Matsuzawa et al.1981); Osawa et al. (1984, 1985); Endo and Suzuki (1986); Committee of Engineering Geological Map of Hokuriku District (1991); Committee of Engineering Geological Map of Kanto District (1996).

Table 2.5-7 Uplift rates around the Sagami Bay

Major uplift area	Uplift in Quaternary	Present uplift
Izu Peninsula	· Subsidence has occurred at northern margin of the peninsula since several tens of thousand years ago. · Southern part of the peninsula was uplifted at 1 ~3 mm a^{-1}. (Ishibashi et al., 1982 ; Ota et al., 1983)	Eastern part of the peninsula: uplifting (>1~2 mm a^{-1}) Western part of the peninsula: subsiding (-1.0 ~ -6.5 mm a^{-1}) (Ishii, 1989, 1991; Kato, 1984; Otake and Asada, 1983)
Ashigara Plain	changed to uplift (5 m ka^{-1}) from subsidence (5 m ka^{-1}) around 0.5 Ma (Kaizuka, 1987).	

Table 2.5-8 Examples of amounts of subsidence in major plains and basins in Japan (1)

Subsidence area	Subsidence in Quaternary	Subsidence in post-glacial age
Ishikari Plain	600 m since 1.7 Ma (north of Tomakomai) [1] Max. 1500m since 1.7 Ma (around Sapporo) [1] 5 m since 125 ka (around Tomakomai) [2]	no subsidence after 6ka BP [3] 4mm a^{-1} [4]
Tokachi Plain	Max. 700m since 1.9 Ma [5] 450~500m since 1.7 Ma [1] 40m since 0.96 Ma [5], [6]	5mm a^{-1} in southern part [7] 4~6mm a^{-1} [4]
Teshio Plain	more than 800 m [8] Max. 1500m since 1.7 Ma [1]	0mm a^{-1} [7]
Kushiro Plain	460m since 1.7 Ma [1]	4~6mm a^{-1} [4] 5~10mm a^{-1} [9]
Tsugaru Plain	more than 400m [10]	no subsidence [9]
Shonai Plain	more than 1900m since 3Ma [11] 895m since 1.8 Ma[11]	0~2mm a^{-1} [4]
Yamagata Basin	300m: 1.2m ka^{-1} since 250 ka [12]	4mm a^{-1} [4]
Akita Plain	400m since 400~200 ka [13] 500m since 2.5 Ma[14] 150m since 1.5 Ma[15]	0mm a^{-1} [4]
Noshiro Plain	more than 1000m since 2.5 Ma [14] 163m since 1.5 Ma[16]	0mm a^{-1} [4]

1) Oka (1997), 2) Yoshiyama (1990), 3) Miyoshi et al. (1985), 4) Danhra (1971), 5) Matsuzawa et al. (1981), 6) Oka (1986) 7) Koaze (1994), 8) Fukuzawa (1987), 9) Kato and Tsumura (1979), 10) Osawa and Hirayama (1970) 11) Ikebe et al. (1979), 12) Matsuoka et al. (1984), 13) Naruse (1989), 14) Awata et al. (1986), 15) Fijioka et al. (1977), 16) Osawa et al. (1985), 17) Nagai et al. (1988), 18) Kumai (1997), 19) Naruse (1988), 20) Nirei (1988), 21) Kakimi et al. (1973), 22) Tanaka and Gomi (1988), 23) Saito et al. (1988), 24) Yamazaki (1985), 25) Fujii (1992), 26) Kaseno (1992), 27) Ichihara (1993), 28) Yoshikawa and Yamazaki (1998), 29) Tokai branch of Architecture Institute of Japan, Chubu branch of Japanese Society of Soil Mechanics and Foundation Engineering, and Research Group for Foundation of Nagoya (1969), 30) Kuwahara and Makinouchi (1989), 31) Masuda (1993), 32) Committee of Ground Research, Kansai Ground Data Conference (1998), 33) Takemura et al. (1993), 34) Hase and Iwauchi (1993), 35) Tada (1993), 36) Sugitani (1983), 37) Kido (1993)

Table 2.5-8 Examples of amounts of subsidence in major plains and basins in Japan (2)

Subsidence area	Subsidence in Quaternary	Subsidence in post-glacial age
Suwa Basin	3m/ky : since Late Pleistocene (by fault movement) [17] more than 400 m since 120 ka [18]	2.5m ka^{-1} [17]
Niigata Plain	881～1860m : 0.88～1.56m ka^{-1} since 0.74～1.6 Ma [19]	2mm a^{-1} [4]
Kanto Plain	more than 2500m since 3 Ma [20] 540～1300m : 0.82～1.08m ka^{-1} since 0.5～0.85 Ma [9] 1400m since 1.7-1.9Ma [21]	1～2mm a^{-1} [4], [22] 3～20mm a^{-1} [23] (southern part of Ibaraki Prefecture)
Ashigara Plain	400～500m : 1.6～2m ka^{-1} since 250 ka [24] 45.3m since 0.6Ma [24]	0～2mm a^{-1} [4] 0.6mm/y since 6.3ka [24]
Toyama Plain	200～570m : 0.3～1.14m ka^{-1} since 0.5～0.7Ma [19] about 600 since 0.5Ma (around Kurobe River) [25]	0～2mm a^{-1} [4]
Kaga Plain	more than 500m since 1.2Ma [26]	0～2mm a^{-1} [4]
Omi Basin (Lake Biwa)	subsidence by fault movements through the Quaternary [27] 37～518m : 0.38～0.81m ka^{-1} since 80～800ka [19] Max.1100m since 1.8 Ma [28] (in Lake Biwa)	2～4mm a^{-1} [4]
Nobi Plain	350m since Middle Pleistocene [29] tilting in the order of 10^{-8} a^{-1} [30] 93～300m : 0.6～0.77m ka^{-1} since 120～500ka [19]	2～4 mm a^{-1} [4]
Osaka Plain (Osaka Bay)	subsidence by fault movements through the Quaternary [27] max. 2500m since 3.5Ma (central part of the Bay) [32] more than 1200m since 1 Ma (central part of the Bay) [32] 230～413m : 0.54～0.65m ka^{-1} since 0.4～0.8 Ma [19] 700m/1.25Ma [31]	2～4 mm a^{-1} [4]
Ooita Plain (Beppu Bay)	more than 1.2m/ky since 3Ma in Beppu Bay [33] 1.1m ka^{-1} since 1.2Ma in the upstream of Oita River [34] more than 2000m since 3 Ma [37]	N-S Opening rate of Beppu-Shimabara Graben is 14mm a^{-1} Subsidence rate of the graben is 2.5mm a^{-1} [35]
around Ariake Bay	22m since 120 ka [36] 400m since 350 ka in the Kumamoto Plain [34]	2～4mm a^{-1} [4]

1) Oka (1997), 2) Yoshiyama (1990), 3) Miyoshi et al. (1985), 4) Danhra (1971), 5) Matsuzawa et al. (1981), 6) Oka (1986) 7) Koaze (1994), 8) Fukuzawa (1987), 9) Kato and Tsumura (1979), 10) Osawa and Hirayama (1970) 11) Ikebe et al. (1979), 12) Matsuoka et al. (1984), 13) Naruse (1989), 14) Awata et al. (1986), 15) Fijioka et al. (1977), 16) Osawa et al. (1985), 17) Nagai et al. (1988), 18) Kumai (1997), 19) Naruse (1988), 20) Nirei (1988), 21) Kakimi et al. (1973), 22) Tanaka and Gomi (1988), 23) Saito et al. (1988), 24) Yamazaki (1985), 25) Fujii (1992), 26) Kaseno (1992), 27) Ichihara (1993), 28) Yoshikawa and Yamazaki (1998), 29) Tokai Branch of Architecture Institute of Japan, Chubu Branch of Japanese Society of Soil Mechanics and Foundation Engineering and Research Group for Foundation of Nagoya (1969), 30) Kuwahara and Makinouchi (1989), 31) Masuda (1993), 32) Committee of Ground Research, Kansai Ground Data Conference (1998), 33) Takemura et al. (1993), 34) Hase and Iwauchi (1993), 35) Tada (1993), 36) Sugitani (1983), 37) Kido (1993)

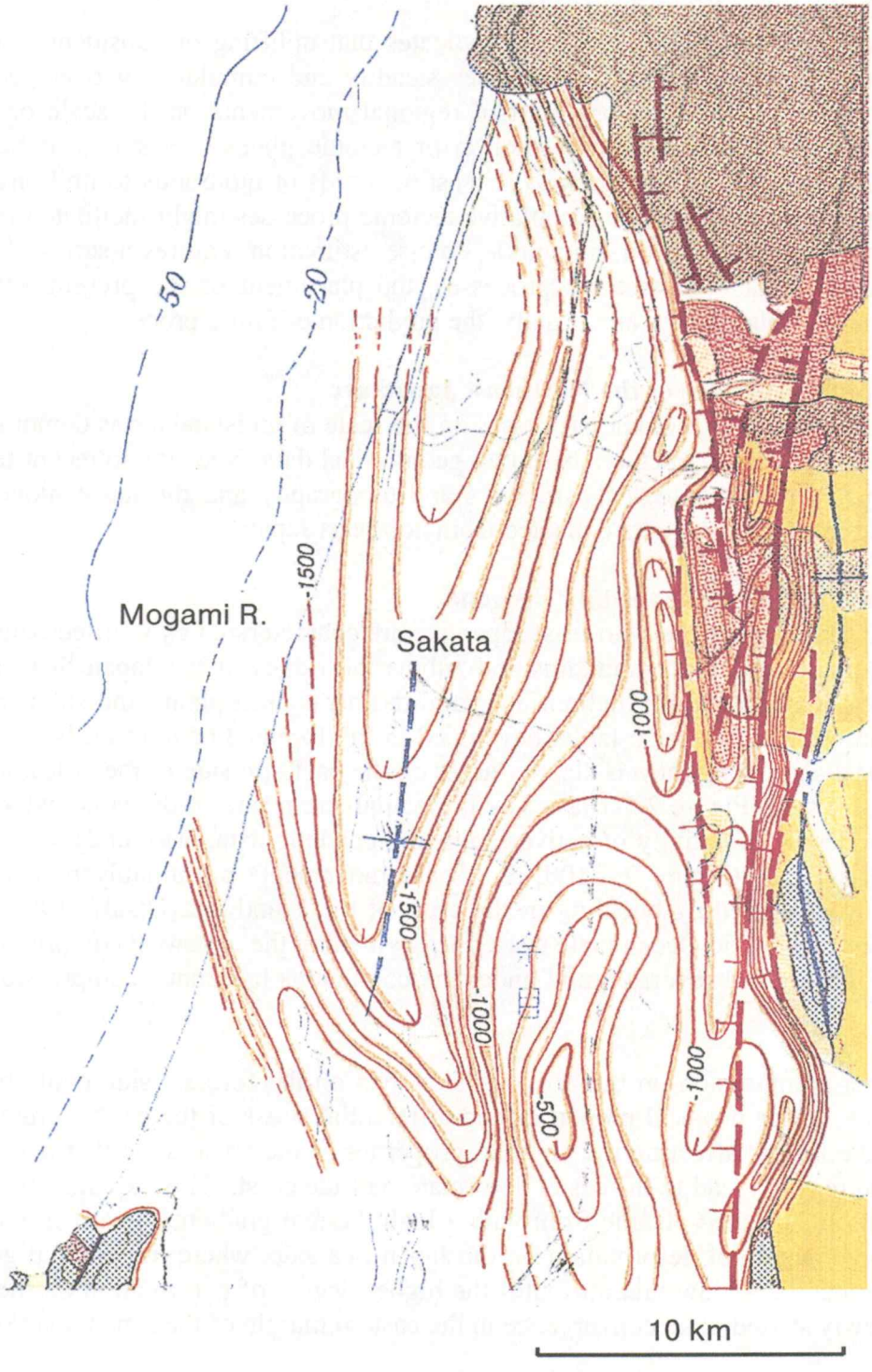


Figure 2.5-8 Contour map showing base-level of the Quaternary sediments in the Shonai Plain, Japan Sea side of northeast Honshu (after Koike and Machida, eds.,1999)

This map indicates approximately the amount of subsidence during the Quaternary. Contours shows depth in meters.

2) Prediction of uplift and subsidence

Geological and topographic evidence indicates that uplifting or subsidence on the scale of mountains and basins (plains) progresses steadily and cumulatively over geological time. These tectonic movements form part of regional movements on the scale of an island arc, which are caused by the relative motion of tectonic plates. As stated in Section 2.2, the cumulative movements date back to at least hundreds of thousands to millions of years ago. Thus, an understanding of the cumulative tectonic processes might facilitate the estimation of future movements (and their amounts). Precise estimation requires a series of investigations aimed at understanding tectonic processes, the placement of the present uplift/subsidence phase in the whole process and, finally, the prediction of future process.

(1) Tectonic processes of the Northeast Japan arc

A method to examine tectonic processes on the scale of an island arc is demonstrated here by a synthesis of crustal structures based on geophysical data, Neogene to recent tectonic history reconstructed from geological structures and topography and the latest movement patterns estimated from geodetic data collected from northeast Japan.

i. Tectonic history since the late Neogene

Tectonic structures of the Northeast Japan arc are characterized by uplifted belts composed of north-south anticlinoria (mountains and submarine ridges in the Japan Sea), subsided belts consisting of north-south synclinoria (inland basins, coastal plains and submarine troughs in the Japan Sea), and reverse faults developed in the foreland of uplifted belts (Figure 2.5-9). The crustal shortening ratio is clearly larger on the back-arc side of the volcanic front than on the fore-arc side (Figure 2.5-10a). The horizontal strain rate of the crust, which is estimated from the degree of activity of active faults and geodetic data, also tends to increase towards the back-arc side (Figure 2.5-10b, c). These movements presumably represent the crustal shortening generated by buckling of the crust of the island arc (Otsuki, 1995) since 3.5 Ma ago, when the Pacific Ocean plate started strengthening the east-west compression, and by the growth of folds and reverse faults under the continuous horizontal compression (Sato, 1989, 1994).

The larger compression on the back-arc side than on the fore-arc side could be attributed to differences in the physical properties and differential stress of the earth's crust (Sato, 1989). One of the factors affecting the physical properties of the crust is the thermal regime. Higher temperature could lead to the easier deformation of the crust. This explains the high degree of deformation near the volcanic front with a high thermal gradient, but it is not an explanation of the high degree of deformation on the Japan Sea side, where the thermal gradient is low. Besides, there is a view that attributes the higher degree of deformation on the back-arc side to the newly started plate convergence in the eastern margin of the Japan Sea (Seno, 1996).

ii. Relationship with crustal structures

Nishikawa et al. (1999) compiled a crustal strength-stress profile to 40 km deep below the surface (uppermost mantle) along an east-west trending line extending for some 180 km between Kamaishi on the Pacific ocean side and Honjo on the Japan Sea side. The most typical crustal movements are expressed, taking account of the thermal dependence of viscosity of the island arc crust and upper mantle (Figure 2.5-11 E, F). This figure shows the amounts of force needed to deform various parts of the crust and the uppermost mantle with a constant horizontal strain rate (4×10^{-15} s^{-1}). Since the fore-arc, volcanic front and back-arc actually differ from each other in horizontal strain rate, this figure does not faithfully reflect reality. However, a constant strain rate had to be employed because detailed data on

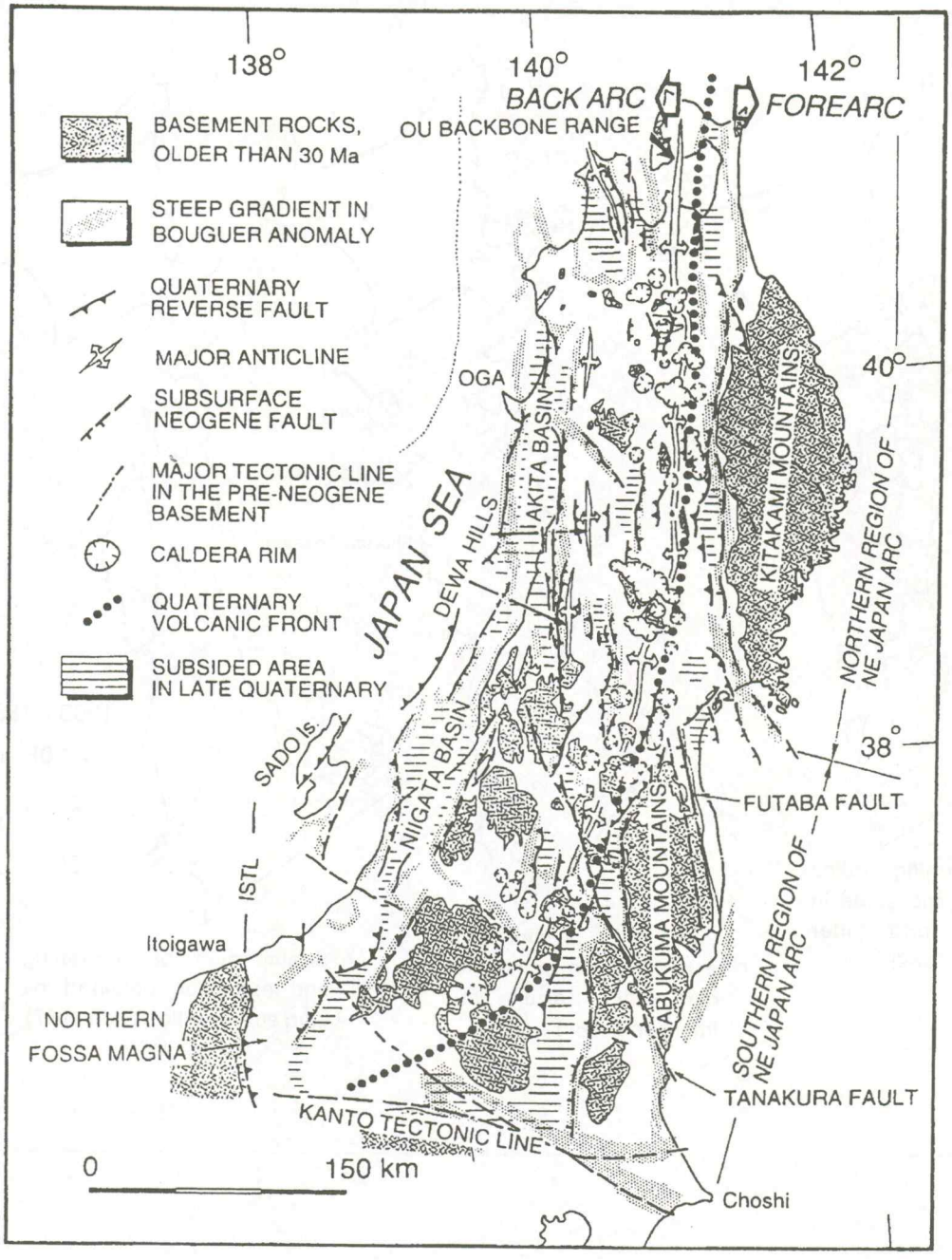


Figure 2.5-9 Geological structure of northeast Honshu (after Sato, 1994)

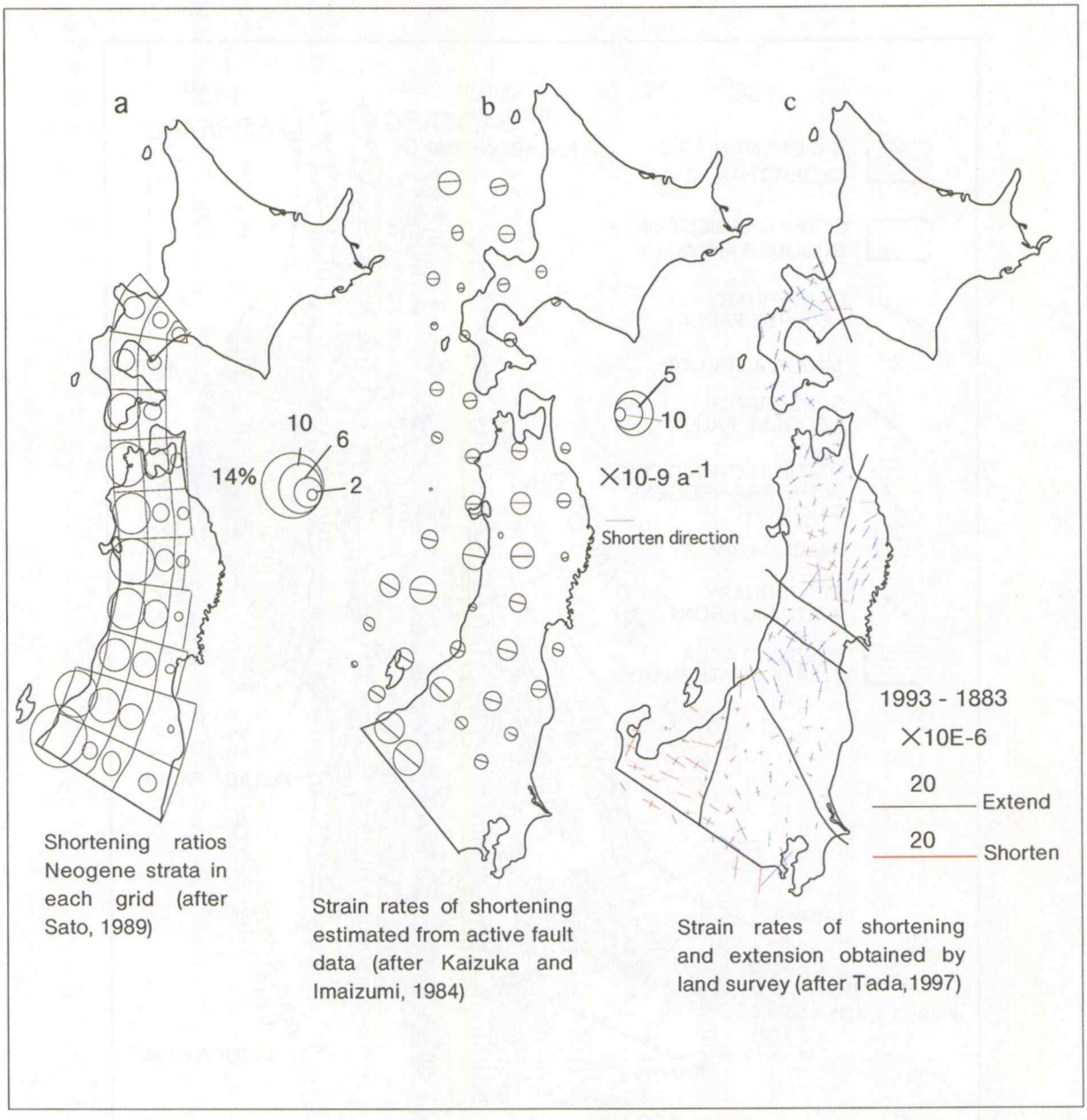


Figure 2.5-10 Strain distribution in northeast Honshu

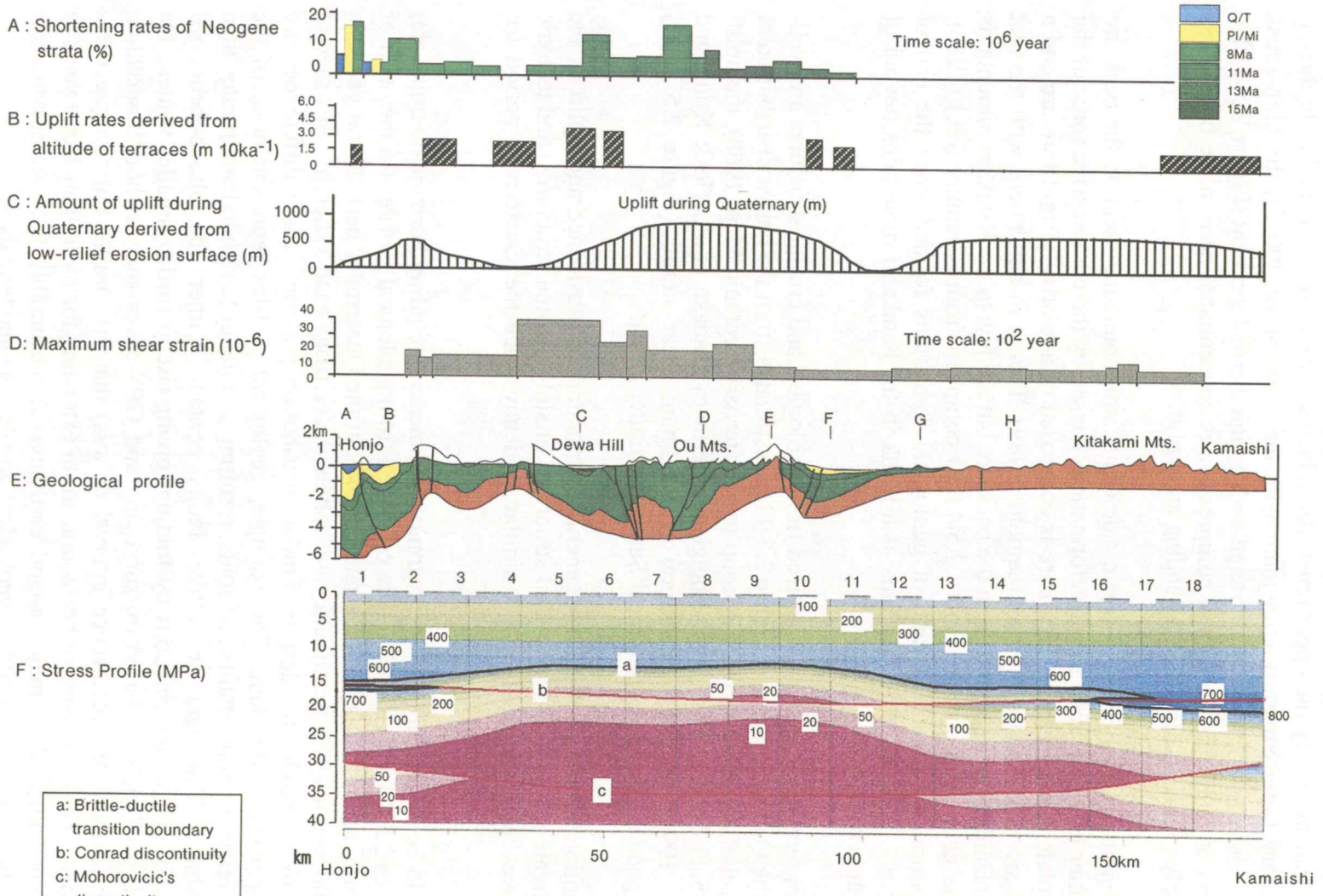


Figure 2.5-11 Stress profile and tectonic data across the northeast of Honshu

E-W section along 39N line (right end: Kamaishi, left end: Honjo) . Similar patterns are shown by geological, geographical and surveying data, although they were collected by different methods and represent different timescales. This fact suggests that tectonic movement has continued at a relatively uniform rate. The deformation pattern of the northeast of the Honshu arc is mainly controlled by the physical properties of the crust.

horizontal strain rate in different areas were lacking.

The stress in the upper crust is more than one order of magnitude larger than that of the lower crust and the uppermost mantle, indicating that the compressive force from the Pacific Ocean plate is mostly transmitted by the upper crust. As indicated by the shape of the brittle-ductile transition boundary (approximately coincident with the isotherm of 400℃), the high-stress layer is thinnest under the Ohu mountain range with a high thermal gradient (Figure 2.5-11 F), so that the stress of a uniform horizontal compression is concentrated here in the high-stress layer, presumably giving rise to upward bending and uplift.

The crustal strength is larger on the fore-arc side (Kitakami mountains) than on the back-arc side, and the latter has undergone larger deformations caused by the compressive force of the Pacific Ocean plate. The Northeast Japan arc is composed of a relatively rigid fore-arc and a less rigid back-arc as pointed out by Shimamoto (1989). This is in agreement with the fact that active faults and folds are abundant in the back-arc but are few in the Kitakami mountains, as shown in the geological profile (Figure 2.5-11 E) compiled from Kitamura (ed.) (1986), and the distribution of shortening ratio of geological formations formed since the end of Neogene (Figure 2.5-11 A), which remains as a blank in the Kitakami mountains devoid of Neogene or younger sediments.

Such patterns of tectonic movements inferred from geological and crustal structures are well-matched with the Quaternary uplift (Figure 2.5-11 C) estimated from the height distribution of erosional low-relief surfaces (Research Group for Quaternary Tectonic Map, 1968), the uplift rate (Figure 2.5-11 B) based on relative heights of terraces (Tanaka et al., 1997; Koike and Machida (ed.), 1999), and the distribution of maximum shear strains (Figure 2.5-11 D) obtained from geodetic data (Geographical Survey Institute, 1997).

The above-mentioned indicates that the general distribution of subsidence and uplift in the Northeast Japan arc is controlled by crustal structures (mainly thermal structures) and tectonic movements have been persisting with a similar tendency since the Quaternary period (or earlier).

Attention should be paid to the rates of tectonic movements (including horizontal strain rate) shown in Figures 2.5-10 and 2.5-11 that are estimated from geological profiles (in the order of millions of years), active faults (average rate throughout the Quaternary period) and geodetic data (about 100 years). The maximum rate values differ from each other by an order of magnitude or more maximum, despite similar distribution patterns. Such differences are caused by properties of the data. For example, geological profiles represent none of the displacements made by minor faults and folds, resulting in smaller horizontal strain rates than the actual values. The data on active faults contain neither the above-mentioned displacements nor plastic deformations by folding, giving rise to further smaller values. On the other hand, geodetic data based on surveying and GPS cover such a short observation period (e.g. an earthquake's recurrence interval or less) that they might fail to represent a long-term change. Thus, the rates of horizontal strain extending for more than 1,000 years (a general recurrence interval of major inland earthquakes) presumably take an intermediate value between the estimations based on geological profiles and geodetic data.

iii. Modeling of crustal movement and geological prediction

The N-S arrangement of uplift zones (mountains) and subsidence zones (basins and lowlands) is interpreted as the buckling of the upper crust under the compressive stress caused by the

Pacific Ocean plate (Otsuki, 1991, 1995). The above-mentioned data on crustal structures (Figures 2.5-11 E, F) also support this interpretation. The shortening of the island arc is compensated largely by reverse faults and adjacent steeply inclined zones (Kitamura (ed.), 1986; Sato, 1992; Sato and Hirata, 1998). Thus, as long as no dramatic change occurs in the movement of the Pacific Ocean plate, the present distribution of uplift and subsidence controlled by crustal buckling would undergo no significant change, persistently giving rise to uplift of mountains and subsidence of basins by reverse faults and folds.

(2) Coastal uplift with a constant rate

While the uplift rate estimated from the altitude of coastal terraces differs from place to place, a constant rate persists for each of the different areas for hundreds of thousands of years. These movements show a definite tendency for the individual mountains and plains, classified into four types from A to D. Movements of type A and B succeed to the structures of the Neogene basement, while the type D is presumed to have started in the middle Pleistocene epoch or later (Ota and Yoshikawa, 1978; Ota, 1996). Figure 2.5-12 shows types A, C and D as examples of uniform uplift. The Shimokita Peninsula illustrates Type A, the northern part of the Coast of Sanriku illustrates type C and the nearby area of the Muroto Peninsula illustrates type D. Uplift, shown on the ordinate in the figure, was calculated by subtracting the sea-level at the time of formation of the terraces relative to present sea-level from the former shoreline altitude measured at each location in the surveying area. There is a strong correlation between formation age and height for all types. This indicates that uplift continues at constant rate in each area. In addition, on the southern coast of Shikoku, there are differences in altitudes of terraces formed during the same age in the same area; this is because of landward tilting. On the northern coast of Sanriku, individual terraces become moderately lower in altitude towards the sea (Figure 2.5-4). However, it is not clear whether this is due to tilting or whether it is caused by the dip of the sea bottom at the time when the terraces formed.

The tendency for uplift rate to be almost constant over the past several hundred thousand years can be found in many other areas (Koike and Machida, eds., 1999). Accordingly, crustal movements over the next hundred thousand years may be estimated by assuming that this tendency will continue. However, on Type D coasts, movement rates after the Holocene tend to be larger, by up to an order of magnitude, than during the Pleistocene. Therefore, in these areas, it is necessary to collect more data on the crustal movement process in order to predict future crustal movements.

3) Denudation

Denudation affects geological environments in several ways, for example by causing changes in the hydraulic field by reducing the overburden or altering topography. Denudation rates depend largely on the specific characteristics of an area and denudation is strongly related to other natural phenomena. The extent of denudation changes according to the increase in relative height from the base-level of denudation due to uplift, the increase and decrease of atmospheric precipitation during glacial and interglacial stages and vertical movements of sea-level.

In this section, the characteristics of denudation in the Japanese islands are outlined. The method used to predict future denudation, based on knowledge of denudation processes and case studies, is discussed. Furthermore, the effects on the geological environment of denudation and uplift and subsidence will also be considered.

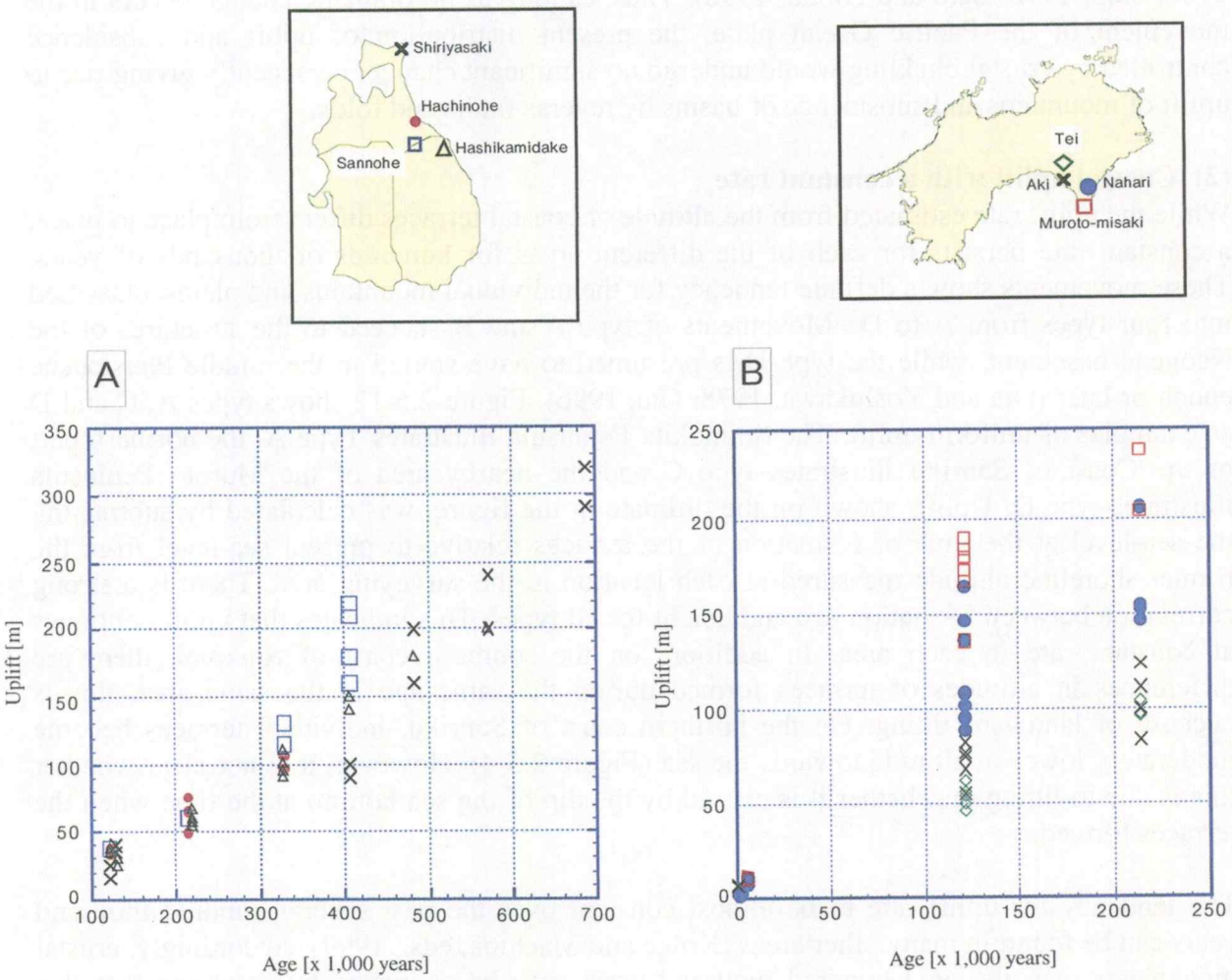


Figure 2.5-12 Relationship between amount of uplift and formation age of marine terraces (after Koike and Machida, 1999)

A: Pacific side of Northeast Japan. B: Southern coast of Shikoku island. The amount of uplift was obtained by subtracting the relative sea-level in each age from the present heights of terraces. Almost constant uplift rates are calculated for each area over the past several hundred thousand years. Such a tendency is also observed in many other areas. B shows landward tilting (from "Muroto-misaki" to "Tei") that is caused by uplift associated with fault movement.

(1) Distribution of denudation rate

Denudation can be classified into five main categories, according to the controlling forces and their effects (Table 2.5-9):

- rain wash;
- fluvial erosion;
- glacial erosion;
- wind erosion;
- marine erosion.

Alternatively, denudation can also be classified into regional denudation and linear denudation (deepening). Regional denudation is the average amount of denudation over a wide area. The denudation rate of a watershed can be estimated from the amount of debris carried by rivers. In contrast, an example of linear denudation is the case of a river creating a deep canyon as it flows. The rate of linear denudation is larger than that of regional denudation.

The temperate, pluvial, undulating Japanese islands have one of the world's largest mean denudation rates (Ohmori, 1983). Here, the denudation rate was estimated from the amount of debris removed by rivers. The largest contributor to denudation in the Japanese islands is considered to be fluvial denudation, including watershed landslides (e.g. Tanaka, 1982; Inoue et al., 1992). Marine abrasion is also prominent since Japan is an island country (e.g. Sunamura, 1992). However, denudation by mountain glaciers during glacial periods is excluded, because it has been shown that this type of denudation is limited to the center of high mountains located in the central part of Honshu or further north,

i. Regional denudation rates

The denudation rate of a watershed can be estimated from the amount of debris removed by rivers. Most of this material is sand deposited at dams, which can be used to estimate the denudation rate. The denudation rate can be expressed by the following equation (e.g. Yoshikawa, 1974; Ohmori, 1978):

$$\text{Denudation rate} = \text{amount of deposited sand} \div \text{number of years elapsed} \div \text{catchment area} \times \text{void rate correction}$$

However, the amount of sedimentation at a dam does not exactly equal the denudation rate, because suspended substances flow out from a dam and there is some removal of sediment. Additionally, there are errors due to measurement and the possibility that some sedimentation has already occurred higher upstream from the dam at which measurements are made. Debris that flows into a reservoir is captured there as deposited sediment. The average capture rate is approximately 60% in the 354 dams in Japan. In addition, the average amount of clay contained in the water in 218 major rivers in Japan is approximately 10% (Kira, 1982). The clay content is a measure of the amount of suspended substances. At a dam that is sufficiently large and unaffected by any other dam upstream, the error is small and the amount of sand deposited at the dam is considered to approximate the average amount of sediment removed by denudation across the entire watershed (Yoshikawa, 1974; Ohmori, 1978; Miyazaki and Ohnishi, 1994). The denudation rate obtained for the watershed at the dam is several tens of centimeters per 1,000 years (Table 2.5-10). In general, this value is used as an average denudation rate in mountainous areas.

Table 2.5-9 Processes responsible for denudation

(revised from Association for the Geological Collaboration in Japan (ed.), 1996)

Variation	energy	process	
		chemical	physical
rain wash	rain fall	corrosion	e.g. wash out by small scale water flow
fluvial erosion	river flow	corrosion	erosion and wash out by water flow
glacial erosion	glaciers, ice sheet		erosion by glacier
wind erosion	wind		sand blasting
marine erosion	waves, etc.	corrosion	e.g. erosion by wave

Table 2.5-10 Denudation rates estimated from the volume of sediments in major dams in Japan

Reference	No. of dams	measuring period (years)	denudation rates (mm ka^{-1})
Yoshikawa (1974)	40	< 15 years	10 ~ 10,000
Ohmori (1978, 1983)	30	< 15 years	330 (average of mountains in Japan)
Tanaka (1982)	428	< 15 years	426 (average of mountains in Japan)
Miyazaki and Onishi (1994)	118	1964 ~ 1991	40 ~ 6,500
Kira (1982)	354	~ 1971	525 (average of mountains in Japan)
Fujiwara et al. (1999c)	82	average 30 years	810 (average of mountains in Japan)

Fujiwara et al. (1999 d) obtained the denudation rate of the watershed using the same method as Ohmori (1978) (Table 2.5-10). They considered that the capacity of any reservoir evaluated should be more than two million m^3 (the capture rate is regarded empirically as approximately 100%) and that the rate of sand deposition should be less than 25% (Ashida and Okumura, 1974; Ashida et al., 1983). Among these dams, they chose ones which are older than 10 years, that are not influenced by dam building and have almost constant changes in their annual flow rates (Ashida and Okumura, 1974; Kira, 1982). Consequently, 82 dams were chosen. To ensure accuracy, denudation rates were obtained only for the period when the cumulative curve of deposited sand increased in a simple fashion (the period measured was an average of approximately 30 years).

- Relationship with topography

In a sufficiently large area, the average denudation rate has a strong correlation with the altitude of the topographic relief, which can be expressed using the equation below (Ohmori, 1978).

$$E = b D \wedge a \qquad \cdots\cdots\cdots (1)$$

Here, E is the average denudation rate in the area (mm a^{-1}); D is the standard deviation of the frequency distribution of altitude in a 1 km square area; a and b are empirical constants; D was calculated using the Digital map 50 m mesh (elevation) Japan I, II and III and Digital National Information (250 m mesh) issued by the Geographical Survey Institute. The data obtained by Fujiwara et al. (1999 d) were also utilized. As a result, the following solution was obtained for equation (1).

$$a = 2.2,\ b = 0.000044\ (R=0.94)$$

- Relationship with geology and precipitation

It is generally recognized that geology affects denudation rate. However, according to the data of Fujiwara et al. (1999 d), a clear correlation was not found between the average denudation rate and the geology that dominates more than 70% of the watershed (Figure 2.5-13). In general, precipitation intensity affects the short-term denudation rate (Miyazaki and Ohnishi, 1994). However, a clear correlation was not found between denudation rate, annual atmospheric precipitation and precipitation intensity (i.e. average value during several tens of years) in the vicinity of the dam (Figure 2.5-14).

From the above analysis, the average denudation rate (regional denudation) in a sufficiently large area, such as the watershed of a dam, is considered to be dominated by the standard dispersion of altitude rather than by precipitation or geology.

- Distribution of denudation rate in Japan

Fujiwara et al. (1999 d) prepared a map which shows the regional distribution of denudation rate based on equation (1) (Figure 2.5-15) by referring to the Digital Map 50 m mesh (elevation) Japan I, II and III. The denudation rate is largest in the Chubu mountains. The rate exceeded more than 1 mm per year in many areas and exceeded several millimeters per year in the central part of the mountains. In areas besides the Chubu Mountains, large denudation rates are also found in the Hidaka, Mikuni, Kanto, Ryohaku, Kii, Shikoku and Kyushu mountains. The rates exceeded 1 mm per year in the central parts of these highlands. In most of the Kitami, Teshio, Kitakami, Abukuma and Chugoku mountains, denudation rates are less than 0.5 mm per year. These rates are similar to those obtained from the surveys of sediments

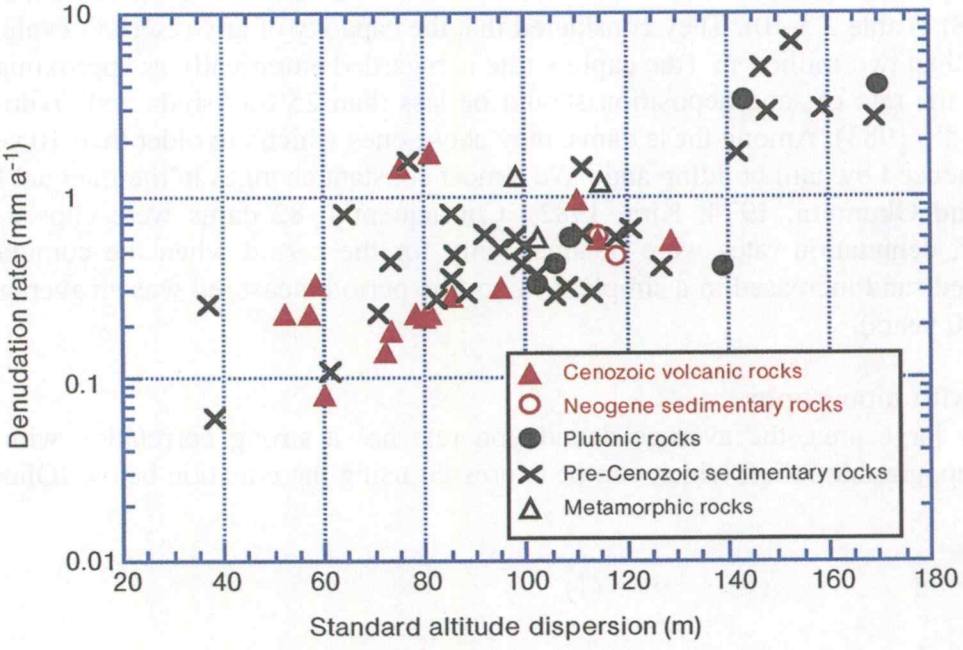


Figure 2.5-13 Relationship between denudation rate and geology

(Fujiwara et al., 1999c)

Standard altitude dispersion is defined as the standard deviation of the frequency distribution of altitude in a 1 km square area.

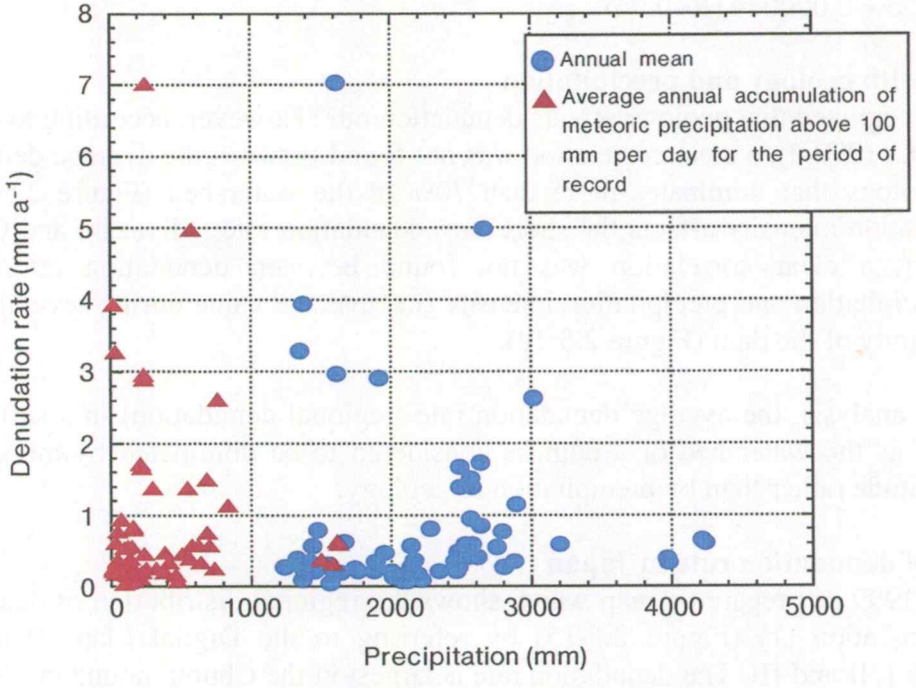


Figure 2.5-14 Relation between denudation rate and meteoric precipitation (Fujiwara et al., 1999c)

The precipitation is a mean for the period over which accumulation measurements were accumulated in each of the dam. Average annual accumulation of meteoric precipitation above 100mm per day for the period of record is the index of precipitation intensity. It is calculated from the accumulation of the value of the day of 100mm or more in precipitation and the mean at the measurement period. There is no correlation between the precipitation condition and the denudation rate.

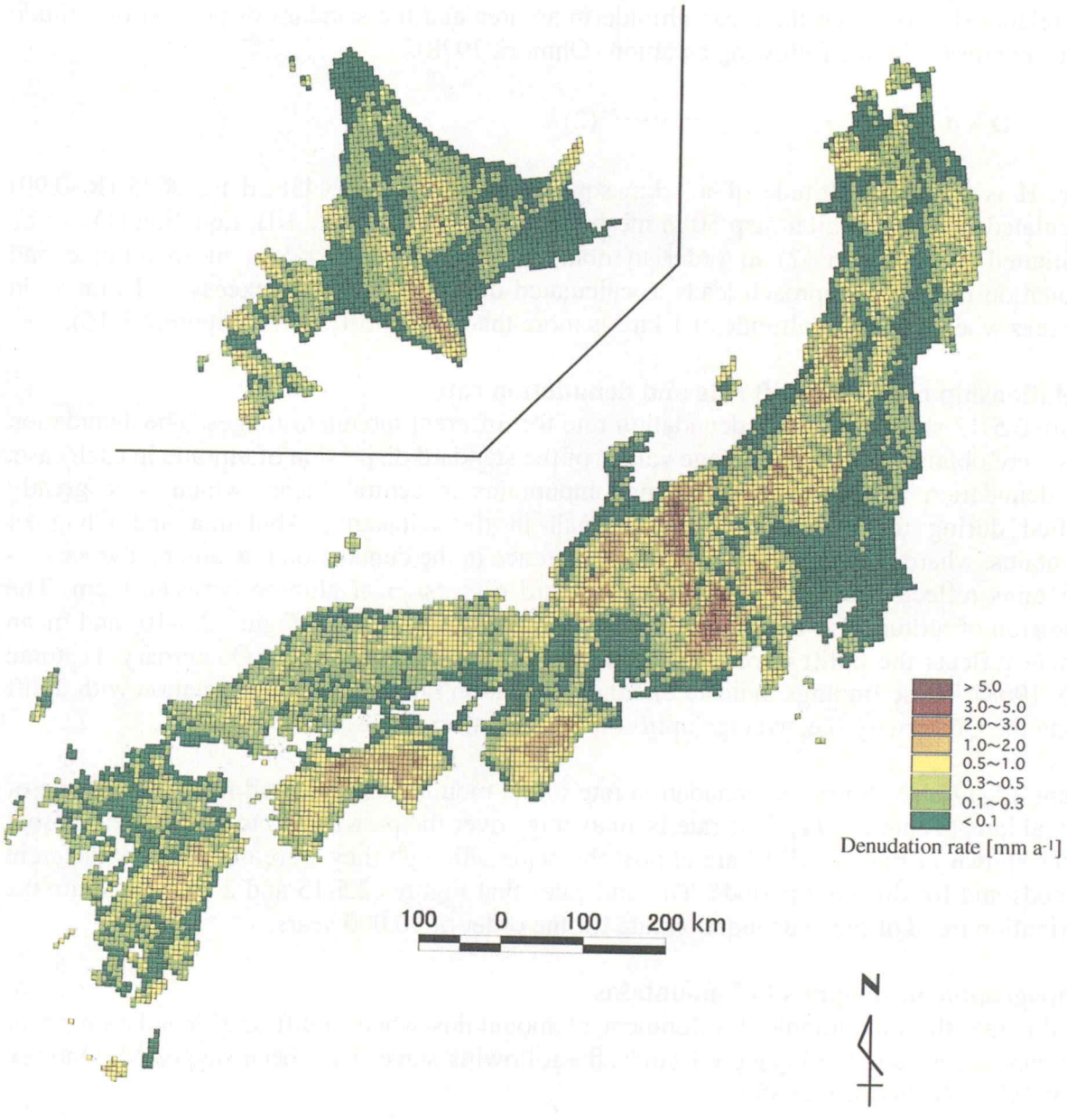


Figure 2.5-15 Distribution of denudation rates (after Fujiwara et al.,1999)

The denudation rates were calculated for 6km square areas based on topographic relief according to a relationship estimated from the results of a survey at 82 dams throughout Japan.

collected at 428 dams in Japan (Tanaka, 1982).

- Relationship with altitude

The relationship between the mean altitude in an area and the standard dispersion of altitude can be expressed by the following equation (Ohmori, 1978):

$$D = d\,H^{c} \qquad \cdots\cdots\cdots (2)$$

Here, H is the mean altitude of a 1 km square area (m), c : 0.4458, d : 3.9645 (R=0.99) (calculated from the Digital map 50 m mesh (elevation) Japan II and III). Equation (1) can be substituted by equation (2) in order to obtain a relationship between mean altitude and denudation rate. This approach leads to calculated denudation rates in excess of 1 mm a^{-1} in the areas where the mean altitude of 1 km^2 is more than 1,200 to 1,300 m (Figure 2.5-16).

- Relationship between uplift rate and denudation rate

Figure 2.5-17 shows the mean denudation rate for different mountain ranges. The denudation rates were obtained from the average values of the standard dispersion of altitude in each case. The denudation rate is large in the high mountains in central Japan, which were greatly uplifted during the Quaternary, but is small in the Kitakami, Abukuma and Chugoku mountains, where there is little uplift. The difference in the denudation rate among the various mountains reflects the difference in the standard dispersion of altitude between them. The dispersion of altitude has a high correlation with the mean altitude (Figure 2.5-16) and mean altitude reflects the uplift during the Quaternary (Research Group for Quaternary Tectonic Map, 1968). These findings indicate that the denudation rate has a high correlation with uplift during the Quaternary (i.e. average uplift rate), as Ohmori (1978) also indicated.

Figure 2.5-17 also shows the denudation rate in the mountains, estimated from the volume of alluvial fans (Table 2.5-11). The rate is an average over the past 10,000 to 25,000 years. Both values shown in Figure 2.5-17 are almost the same although they were obtained by different methods and for different periods. This indicates that Figures 2.5-15 and 2.5-17 illustrate the distribution trend of mean denudation rate for the order of 10,000 years.

- Topographic development of mountains

To illustrate the topographic development of mountains where uplift and denudation occur simultaneously, as in the Japanese islands, the following stages have been suggested (Ohmori, 1978; 1993; Yoshikawa, 1985):

Stage 1: The altitude dispersion and the denudation rate increase with the increase in mean altitude due to uplift.

Stage 2: The denudation rate approaches the uplift rate and both reach an equilibrium state. The mean altitude reaches a maximum value that is then maintained. Mountains reach an equilibrium more rapidly and at a higher altitude as the uplift rate becomes greater. The central part of the Chubu mountains, where uplift progresses at the greatest rate, is considered to be reaching equilibrium condition. In the mountains that have reached equilibrium, the ground uplifted subsequently is denuded.

Stage 3: As the uplift rate decreases, the mean altitude, the standard altitude dispersion and the denudation rate also decrease and a peneplain appears in approximately ten million years.

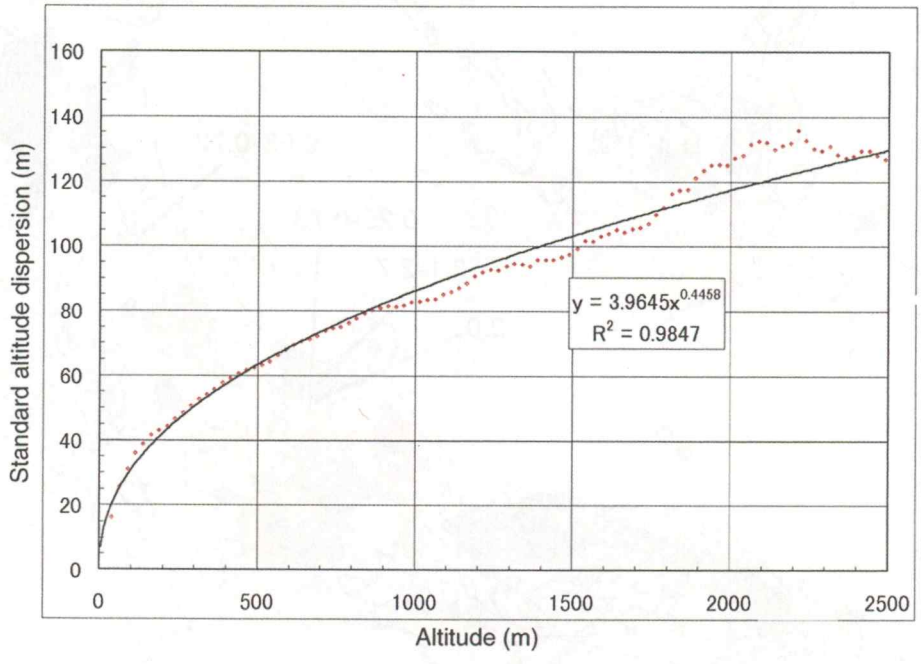


Figure 2.5-16 Relationship between altitude and standard altitude dispersion (after Fujiwara et al., 1999c)

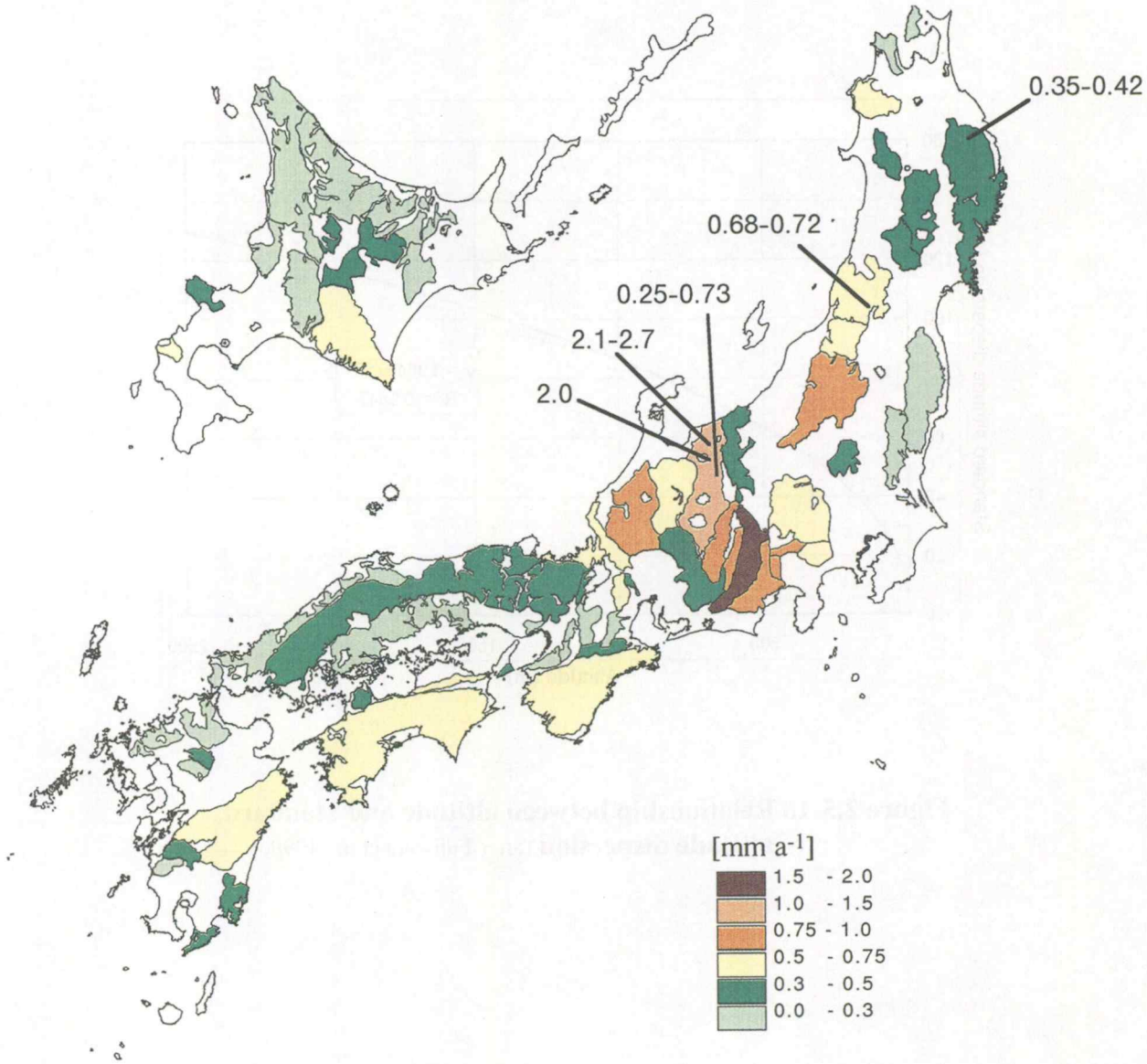


Figure 2.5-17 Denudation rate of different mountains calculated from altitude dispersion
(after Fujiwara et al., 1999c)

The value indicated at the end of each line shows the average denudation rate during 10,000 years calculated from the volume of talus, uplift of terraces, etc. These value coincide with the denudation rate calculated from standard altitude dispersion, although the period and measurement technique are different.

Table 2.5-11 Denudation rates estimated from the volumes of alluvium and alluvial fans

Area	Period (years)	Data	Denudation rates (mm ka^{-1})	Reference
Japan	10,000	volume of alluvium	200 ~1,000	Yoshikawa et al., 1973
Kitakami Mts.	6,000	volume of talus	350~240	Yoshinaga et. al, 1989
Ou Mts.	25,000	volume of alluvial fan	680~720	Akojima, 1983
Drainage basin of alluvial fan	8,500	volume of alluvial fan	5.7*	Oya, 1993
western Hida Mts.	50,000	volume of alluvial cone	78	Iso et al., 1980
Northern Kyushu	8,000 90,000	volume of alluvium volume of alluvium	125 23	Sugitani, 1983
western margin of Matsumoto Basin	13,000	volume of alluvial fan	250~730	Oguchi, 1991
central Hida Mts.	0.4-1 Ma	eroded volume of lava plateau	800~2,000	this report
central Hida Mts.	17,000	volume of Kurobe alluvial fan	1,800	this report
western Miyazaki Plain	17,000	volume of alluvium	84	this report
Osaka Plain and vicinity	17,000	volume of alluvium	240~810	this report
Tama Hills and vicinity	17,000	volume of alluvium	75~1,200	this report
Drainage basin of Arakawa river	17,000	volume of alluvium	80	this report
Shimoosa Plateau	17,000	volume of alluvium	290~520	this report
northern Boso Hills	17,000	volume of alluvium	54~280	this report
Nobi Plain and vicinity	17,000	volume of alluvium	100	this report

* revised using 20% fine grain ratio (Oguchi, 1991).

Transferred volume to marine area of Kurobe alluvial fan is revised using data for sediment transfer in floods.

The amount of denudation in uplifting mountains can be expressed as the difference between the elevation variation curve (Figure 2.5-18) and the elevation increase curve. The elevation variation curve assumes the occurrence of denudation and the elevation increase curve assumes no denudation.

ii. Marine erosion

Flat rocky bottoms on the coast, which extend to as deep as tens of meters, are regarded as wave-cut terraces or abrasion platforms formed by the marine erosion associated with the rising sea-level since the latest glacial epoch (Sunamura, 1972; Kaizuka, 1998). The average abrasion rate in the Holocene epoch was estimated by dividing the widths of wave-cut benches and abrasion platforms devoid of significant uplift by the formation period (about 8,500 to 10,000 years) (Table 2.5-12). Also shown in the table are the ongoing abrasion rates per 1,000 years estimated by comparing old and new versions of maps and aerial photographs (Sunamura, 1992) for comparison with the Holocene rate. The abrasion rate throughout the Holocene epoch tends to be a little larger than that in the last tens of years.

Figure 2.5-19 shows the abrasion rates estimated from the widths of wave-cut terraces at intervals of 10 m depth. The abrasion rate in the period before 7,000 years ago, which is marked by a fast rise in sea-level (Figure 2.5-4), is significantly larger than that in the period of relatively static sea-level prevailing for the past 7,000 years (Takagi et al., 1999b). It is because the Holocene epoch contains such a fast abrasion period that the average abrasion rate throughout the Holocene epoch is larger than that at the present time. This is related to the process of abrasion. Alternating dry and wet conditions and weathering in tidal zones facilitate the destruction and washing-away of rocks at a particular level, giving rise to flat wave-cut benches (Mii, 1962). The above-mentioned process successively proceeds inland in a period of rising sea-level, presumably resulting in the acceleration of coastal erosion. The relationship with geology indicates that the Plio-Pleistocene rocks with a uniaxial strength below tens of kgf cm^{-2} show large abrasion rates (Takagi et al., 1999b). Abrasion rates are also large at capes and peninsulas protruding into the open sea (Takagi et al., 1999b).

(2) Denudation processes

i. Regional denudation

Nine areas were chosen to estimate the amount of denudation (Figure 2.5-20; Table 2.5-13). In these areas, river terraces, marine terraces, pyroclastic flow deposits and lava flows are distributed. The age of each feature and the surrounding landform at the time of formation can be estimated relatively accurately. The denudation of these landforms over the past several hundred thousand years was estimated. The geographic range investigated was 200 to 400 km^2 in each area. Miyawaki and Fujiwara (1997) presumed that these landforms were originally flat plateaus. They considered that the volume of valleys that incise into these plateaus corresponds to the amount of denudation after the formation of the landforms. The average denudation of the entire terrace surfaces (i.e. thickness of denuded layers) can be obtained by dividing the volume of valleys by the area of the terrace surfaces (Table 2.5-13). The denudation of old landforms is greater than that of newer ones. However, the extent of denudation does not increase linearly, but becomes less as time passes. The denudation rate reached approximately 10 m per 100,000 years after denudation started (Figure 2.5-21). In addition, it was recognized that the denudation rate of pyroclastic flow plateaus was likely to be larger than that of the adjacent terraces that are covered by gravel layers.

Figure 2.5-22 shows the relationship between the uplift rate and the denudation rate of marine terraces. This figure compares the current altitude and the average denudation of marine

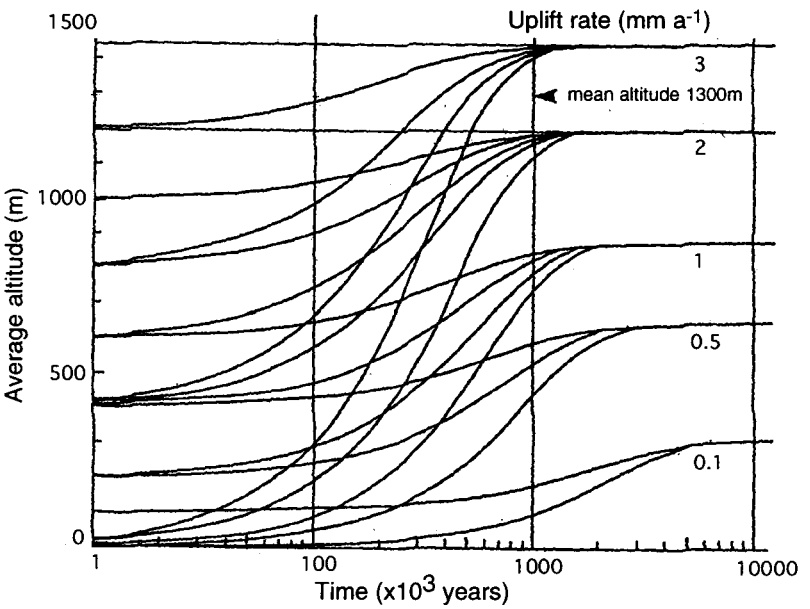


Figure 2.5-18 Changes in mean altitude from various initial altitudes at different rates of uplift (Ohmori, 1990)

Lines show that each mountain will attain a certain constant altitude (the upper limit of altitude) according to the rate of its uplift (elevation variation curve).

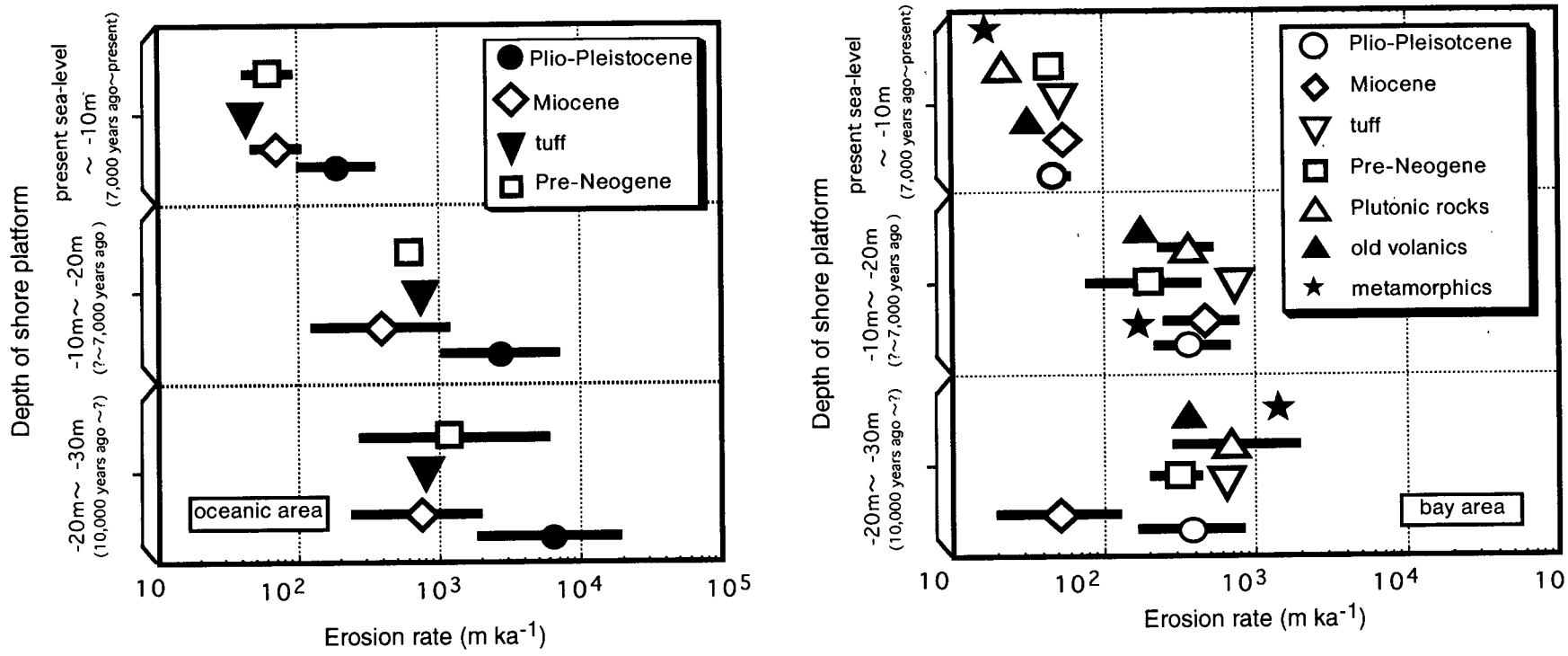


Figure 2.5-19 Transition of erosion rate of rocky coast in the Holocene (Takagi et al. ,1999b)

The vertical axis shows the period required for a sea-level change to a level -30 m to -20m, -20m to -10m, and -10m compare to present sea-level. The horizontal axis shows the erosion rate (coastal retreat rate) calculated from the relation between width of shore platform and formation period.

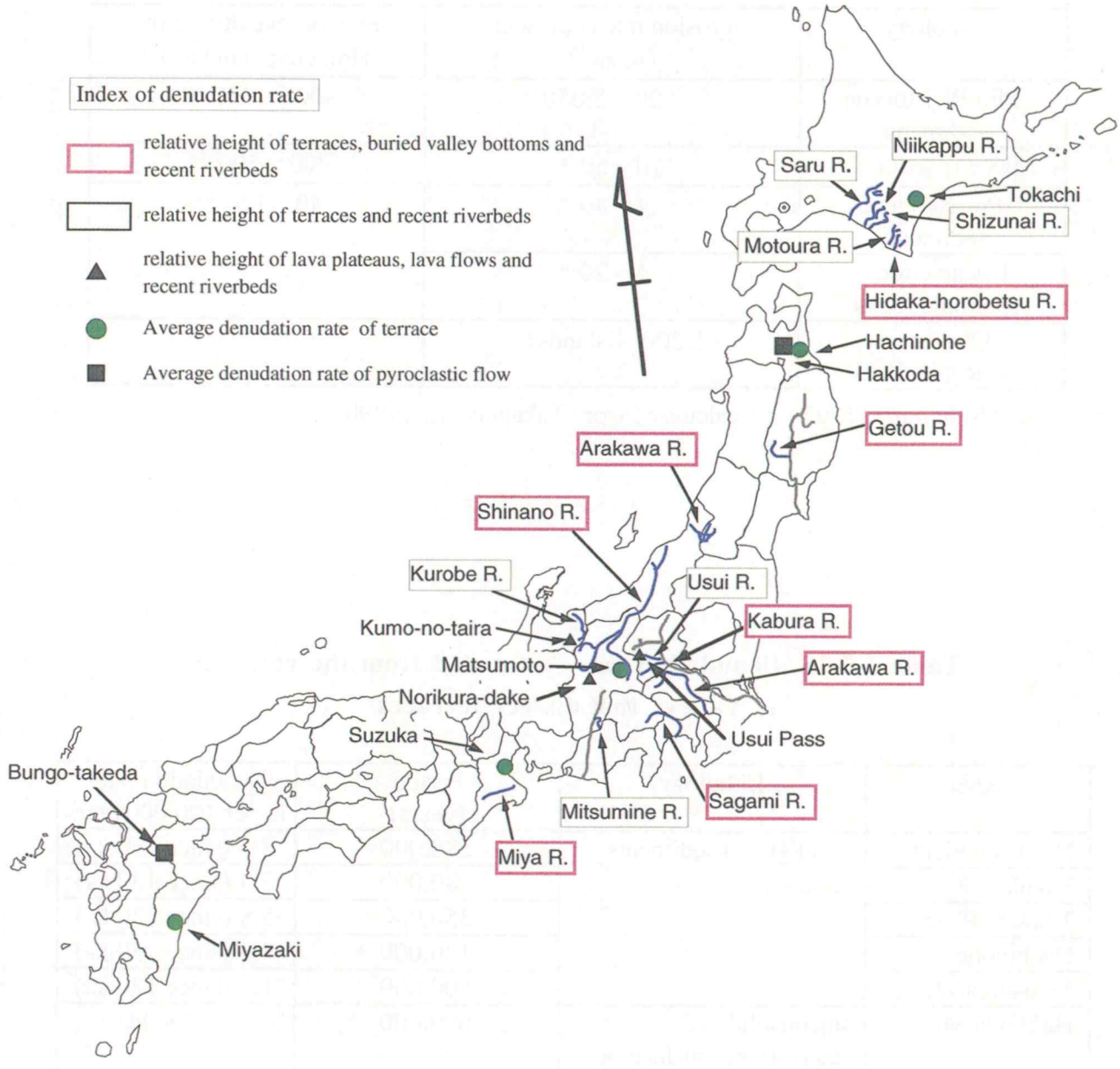


Figure 2.5-20 Case study areas for denudation rate

Table 2.5-12 Rates of marine erosion in the Holocene

lithology	erosion rate at present ($m\ ka^{-1}$)	erosion rate during the Holocene ($m\ ka^{-1}$)
Plio-Pleistocene sediments	20～2,050 *	800～1300 **
Miocene sediments	10～50 *	300～500 **
Pre-Neogene sediments	4～40 *	40～120 **
volcanic rocks plutonic rocks	4～20 *	
Quaternary volcanic rocks	<1,200 (islands) *	

* Sunamura, 1992 ** calculated from Takagi et al., 1999b

Table 2.5-13 Denudation rates estimated from the volumes of valleys that dissect terraces

Area	Lithology	Period (years)	Denudation rates m per 100,000years
Miyazaki Plain	sand gravel sediments terraces	580,000	8.5 (since 130 ka)
Suzuka Mt		180,000	3.3 (since 130 ka)
Tokachi Plain		350,000	5.8 (since 130 ka)
Hachinohe		120,000	2.2 (since 130 ka)
Matsumoto Basin		500,000	1.7 (since 130 ka)
Hakkoda Mt.	unconsolidated depositional surface of pyroclastic flow	600,000	3.7～24
Bungotakeda		90,000	66
Norikura	solid lava flow	60,000～250,000	8.4～27.5
Usui pass		1000,000～1200,000	9.5～11.5

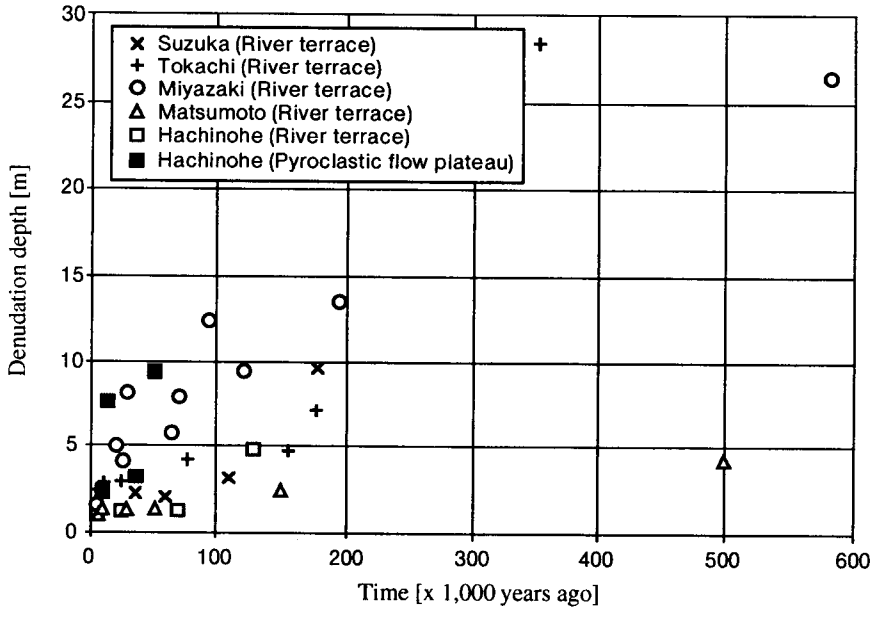


Figure 2.5-21 Relationship between average denudation depth and formation age of several river terraces and one pyroclastic flow plateaus (after Miyawaki and Fujiwara, 1997)

The average denudation rate of terrace and plateau is a few meters to ten meters per 100,000 years.

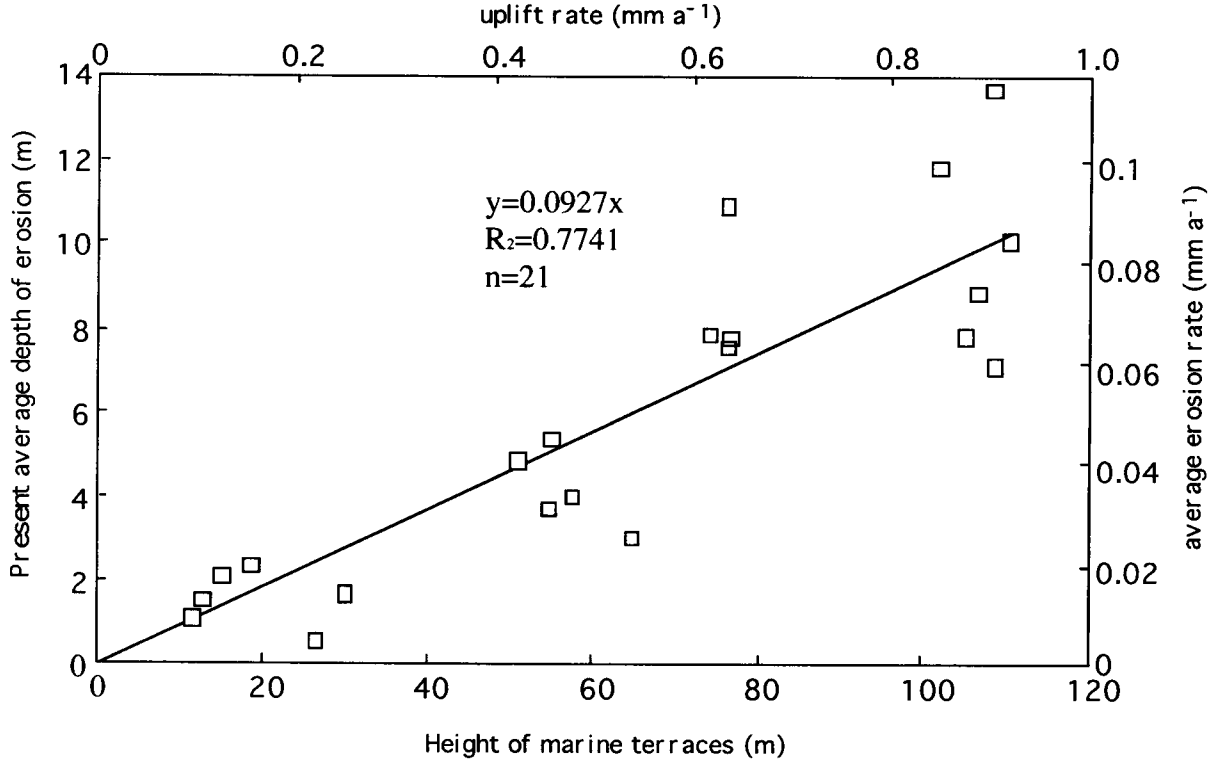


Figure 2.5-22 Relation between uplift and denudation rates of marine terraces formed in the last interglacial stage

The studied areas are emergent shore platforms formed of Neogene sedimentary rocks.

terraces. Data from the Neogene sedimentary rocks that are distributed in northeast Japan show that the marine terraces were formed during the last interglacial epoch (i.e. approximately 120,000 years ago). In addition, the current altitude corresponds more or less to the uplift after the formation of the terraces. The average denudation of the entire terrace surfaces was calculated from the volume of valleys dissecting the terrace surfaces. Uplift and denudation show a good correlation. This indicates that, as the height from the base-level of denudation (i.e. sea-level in this case) increases, the denudation rate also increases. Furthermore, the regional denudation over the last 120,000 years is approximately 10 percent of the volume of the uplift.

ii. Linear denudation (deepening)

In rivers, denudation (i.e. deepening) and sedimentation on the riverbed correspond alternately to climatic and sea-level changes. In an interglacial epoch, the riverbed is deepened and in a glacial epoch, it is aggraded and fill-top terraces and buried valley floors are formed. If the altitudes and formation ages of a series of buried valley floors and fill top terraces are known, it is possible to clarify the history of lowering of riverbeds.

Kaizuka (1969) and many other researchers account for the foregoing cyclic changes in altitudes of riverbeds as follows:

In the middle reach of rivers, the production of detritus increases during a glacial epoch. Sedimentation progresses because detritus accumulates on the riverbed due to the decrease in intensity and frequency of floods. As a result, fill-top terraces are formed. In contrast, production of detritus decreases and the intensity and frequency of floods increase during the interglacial stage, causing deepening to continue. In addition, deepening progresses along coastal areas due to a drop in sea-level during the glacial stage. Alluvium is formed during an interglacial stage as the result of the sedimentation of detritus carried from upstream. Figure 2.5-20 shows 15 rivers investigated. Figure 2.5-23 illustrates the cases of the Kabura river in northern Kanto and the Sagami river in southern Kanto. The figures indicate the repeated occurrence of the deepening and aggradation periods. Deepening periods lasted 20,000 to 30,000 years during the interglacial stage and the aggradation period lasted approximately 70,000 years during the glacial stage (Takagi et al., 1999a). In the case of the Sagami River, the amount of riverbed rise during the aggradation period was 35 to 50 m and the amount of riverbed drop during the deepening period was 70 to 80 m.

The relationships between ages and altitudes of terrace surfaces and buried valley bottoms are shown by two straight lines almost parallel to one another on a graph (Figure 2.5-23). This indicates that the downward denudation of riverbeds in every deepening period catches up with the uplift in the corresponding periods. The uplift rate is almost equal to the long-term deepening rate in the rivers fulfilling this condition (Takagi et al., 1999a). It measures 25 to 35 m per 100,000 years at the Sagami and Kabura rivers. This value presumably represents an average deepening rate throughout the glacial and interglacial epochs. While rapid deepening could take place in an interglacial epoch, the deepening rate is decreased to be equal to the uplift rate of the drainage basins because aggradation periods are contained in a long period covering glacial and interglacial epochs.

The parallel relationship of the two lines in Figure 2.5-23 indicates that it is possible to estimate the long-term deepening rate from data on either terrace surfaces or buried valley bottoms. Eight of the 15 rivers shown in Figure 2.5-20 show a repetition of deepening and aggradation. For the other rivers only data on terraces are available. In these cases, the

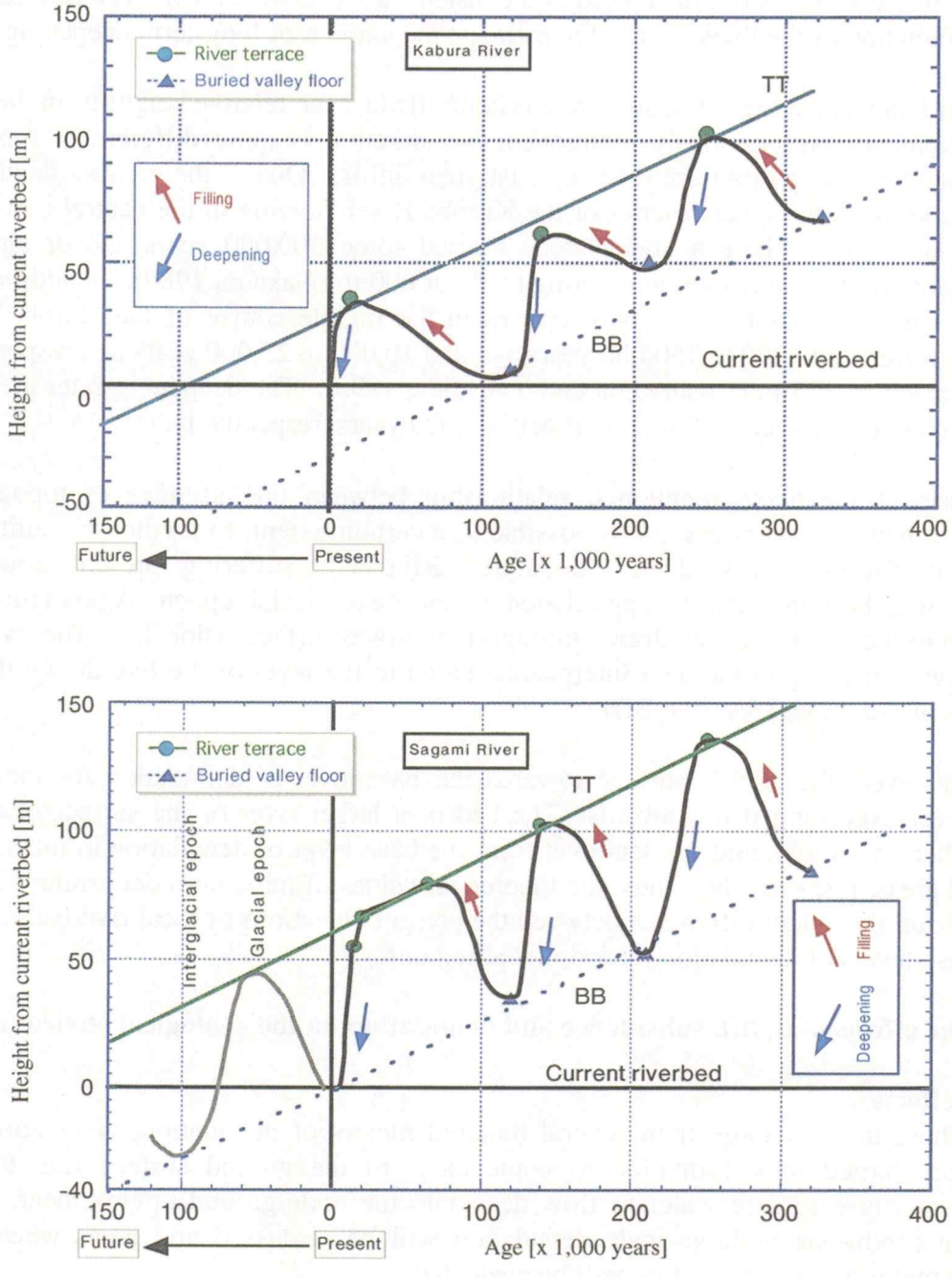


Figure 2.5-23 Denudation process of a riverbed (example of Kabura and Sagami rivers) (Modified from Takagi et al., 1999a)

River valleys were filled with clastic sediments during glacial periods and lowered by deepening during the interglacial periods. A linear relationship is found when the heights of river terraces or buried floors are plotted against their ages. TT represents the trend of uplift and BB can be interpreted as long-term average deepening rate throughout glacial and interglacial periods. The fact that TT and BB are parallel to each other means that long-term average deepening rate depends on the uplift rate of the area (around 25 m per 100,000 years).

altitude of terrace surfaces has decreased at a constant rate (Table 2.5-14). The rates derived from the inclination of the lines are used to estimate the amount of long-term deepening.

On the other hand, since the denudation rate is controlled by the relative height from the base-level of denudation as previously mentioned, the situation is quite different in mountain regions characterized by rapid uplift (or by past great uplift). One of the greatest denudation rates can be seen in the upper reaches of the Kurobe River flowing in the central part of the Hida mountain range, where a lava plateau formed some 300,000 years ago or later has undergone downward denudation amounting to about 600 m (Nakano, 1989). In addition, the maximum relative height between two terraces in the middle course of the Kurobe River, which were formed 140,000 to 150,000 years ago and 10,000 to 25,000 years ago respectively, reaches as much as 305 m (Yoshiyama and Yanagida, 1995). The deepening rates are about 200m per 100,000 years and 210 to 270 m per 100,000 years, respectively.

On the basis of the above-mentioned relationship between the altitudes of topographic surfaces and their formation ages, it is possible to a certain extent, to predict the altitude of terraces and riverbeds formed in the future. Riverbeds suffering present downward denudation will be converted to aggradation in the next glacial epoch. Aggradation will progress up to the level of a line drawn through the terrace surfaces (line TT). The riverbeds undergo new deepening in the next interglacial epoch to the level of the line drawn through the bottoms of buried valleys (line BB).

Denudation lowers the earth's surface towards the base-level of denudation for individual regions, never exceeding it downwards. The bed of a larger river or the surface of a lake, which smaller rivers join, and the sea-level form the base-level of denudation in inland areas and coastal areas, respectively. Thus, the theoretical values of maximum deepening could be calculated from the height difference between the present elevations of local riverbeds and the regional base-levels of denudation for individual regions.

2.5.2 The effects of uplift, subsidence and denudation on the geological environment

1) Direct effects

In areas where there is more than several hundred meters of denudation, denudation may cause deeply buried rock formation to come close to the ground surface (i.e. to form exposures) or cause surface water to flow deep into the underground environment. In this section, the conditions of large-scale denudation will be discussed and areas where such denudation might occur in the future will be evaluated.

Deepening of rivers is most important because this progresses relatively rapidly. The deepening of inland rivers is considered to be almost equal to the amount of uplift, as mentioned above, when considered over a time-span of approximately 100,000 years. Therefore, in areas where the altitude above the base-level of denudation remains high and large denudation rates continue for a long time, the deepening reaches several hundred meters over a period of approximately 100,000 years. These areas are mountains that are uplifting rapidly or have a high altitude above the base-level, due to large uplift that occurred in the past. These types of area are limited in extent, a typical one being the central part of the Chubu Mountains (Central Japan). In other mountains, the uplift rate seldom exceeds 1 m per 1,000 years, even though the amount of uplift is conservatively estimated to be equal to the amount of deepening; the amount of deepening over 100,000 years is approximately 100 m.

In coastal areas, deepening progresses towards sea-level (the base-level of denudation). Therefore, a sea-level drop of about 100 m, which is expected during a glacial epoch, must be taken into account in addition to relative uplift of the land. There are a few cases where the seaward point of a peninsula was greatly uplifted by more than 100 m per 100,000 years. In these areas, if deepening progresses down to sea-level during the next glacial stage, it could possibly reach more than 200 m.

Earthquakes and heavy rains in highlands cause large-scale landslides. Landslides are an important part of the denudation process and directly affect the geological environment. Slope collapses involving more than 10^7 m^3 of material cause characteristic landforms. Collapses of this kind are called large-scale landslides (Machida, 1984). Judging from the topography, there have been large-scale landslides in 333 locations throughout Japan. Most of them are located in Hokkaido, Tohoku and the Chubu region, but only a few are found in western Japan (Machida et al., 1987). These large-scale landslides are closely related to geology and uplift, and more than 50% are in areas where there are volcanic rocks that were formed during and after the Pliocene. Such landslides also occurred in the mountains that uplifted rapidly during the Quaternary (Machida et al., 1987). The depth of the slip surface sometimes reaches several hundred meters (Chigira, 1995). This type of large-scale landslide rapidly changes landforms and ground pressure and may cause the recharge of surface water into the underground environment. One of the causes of large-scale landslides is considered to be the creep of rock formations. The creep area can be estimated to some extent from the distribution of linear hollows (Chigira, 1995).

2) Indirect effects

(1) Hydraulic effects

Changes in the topographic gradient, due to uplift and denudation, are important parameters that must be quantified to estimate the future spatial and temporal variations in the hydraulic gradient. An increase in the topographic gradient is caused by uplift and the maximum tilting rate is 1 to 2 x 10^{-6} a^{-1} where there is active folding with a wavelength of 1 to 10 km (Kaizuka, 1968; Ojiya Crustal Movement Research Group, 1989). If the tilting continues for 100,000 years, the dip increases by 10 to 20 percent.

The rate of increase in the topographic gradient due to denudation (G) can be considered as follows:

G = (increase in the relative height difference between the main stream of a river and a major mountain ridge) ÷ (distance between the valley and the major mountain ridge)

If the increase in the relative height here is taken to be the deepening of the main stream of a river, the foregoing discussion on deepening implies that this value rarely exceeds 100 m per 100,000 years (excluding the Chubu mountains). Actually, since mountain ridges is denuded, it is considered that the increase in the relative height between a valley and mountain ridge is normally much smaller. In addition, the distance between the main stream of a river and a mountain ridge is generally more than several kilometers. The discussion concludes that the increase in the topographic gradient is as follows and that its effect on the hydraulic gradient is limited.

(100 m ÷ several kilometers) × 100 = several percent

The actual development of topography is more complicated. Therefore, for a more accurate discussion, further research is necessary to develop a model that considers landforms (slopes) that have been created due to uplift and denudation.

(2) Geochemical effects

The weathering of rocks is related to the physical and chemical properties of the rocks and groundwater. In the Japanese islands, the average thickness of the weathering layer in granite (i.e. weathering crust) is 50 to 100 m (Kimiya, 1992). Horizontal fractures are concentrated in the lower 5 to 10 m of the weathering layer. This zone has a higher permeability compared with other parts of the rock. Therefore, the boundary between the weathering layer and unweathered rock is likely to become a pathway for atmospheric precipitation seepage (Kojima, 1992).

The weathering crust is produced as a result of chemical weathering of rocks and is one of the factors that indicates the evolution of groundwater chemistry. Throughout Japan, only a kaolinite- montmorillonite type (K-M type) weathering crust can be seen (Utada, 1979). It was formed by the leaching of components other than Si and Al under cool humid climatic conditions. This is often seen in granite, typically where there is decomposed granite and conglomerate. The data indicate that similar chemical weathering occurred during the Quaternary. It is considered that the water/rock interactions that cause groundwater chemistry to evolve have not changed significantly.

Table 2.5-15 shows the weathering rates of rocks from all over the world, compiled by Matsukura (1994, 1997). The maximum increase in thickness of the weathering layer per 1,000 years is ten and several mm for plutonic and igneous rocks, several tens of centimeters for sandstone and tuff and more than one hundred centimeters for limestone. In addition, it is reported that weathering of granite required 80,000 to 280,000 years in Japan (Kimiya, 1975). Furthermore, it is estimated, that under conditions like those occurring in Japan, several million years are required to weather a granite body (Kimiya, 1981). Weathering of mudstone reaches a depth of up to several tens of meters (Chigira, 1988).

The weathered zone of the crust can be considered to be a zone in which the chemical buffering action of rocks is diminished. It is necessary to consider that the sum of denudation and weathering will be a decrease in overburden thickness.

2.5.3 Summary

The approximate spatial variation of uplift and subsidence rates in Japan has been deduced using geological, topographic and geodesic methods. The results indicate that uplift and subsidence are likely to continue at a constant rate and with a predictable trend over several hundred thousand years. A large uplift rate of more than 100 m per 100,000 years was found in fold and fault type and reverse fault block type mountains and along co-seismic uplifting coastlines. There are a few areas where the maximum uplift rate may possibly reach several hundred meters per 100,000 years. On the other hand, the uplift and subsidence rate in many areas is 50 m or less per 100,000 years.

These regional crustal movements are considered to reflect the tectonics of each area and it is presumed that a similar tendency towards uplift or subsidence will continue in each area for as long as the tectonic regime there remains stable. It is predicted that similar tectonic processes to those occurring at present will continue at similar rates to the present for at least

Table 2.5-14 Deepening rates of riverbeds

River	Area	Period(ka)	Deepening rate (m per 100,000 years)
Saru	Hokkaido	50～150	30～150
Hidaka-horobetsu *		250	25～60
Niikappu		250	15～40
Shizunai		250	25～40
Motoura		250	20～25
Arakawa (Niigata) *	Northeast Honshu	320	10～40
Getou *		250	5～15
Saagami	Kanto	320 [3)]	25 [3)]
Arakawa (Chichibu) [3)]		500 [3)]	40 [3)]
Kabura		320 [3)]	25～35 [3)]
Usui		320	15～25
Shinano	Central Japan	320 [3)]	60 [3)]
Mitsumine		210	20～40
Kurobe (middle and lower stream) Kurobe (middle stream) [1)]		250 (65) 140～150	35～80 (210～270) 210～270 [1)]
Kumonotaira [2)] (upper Kurobe R.)		<300 [2)]	>200
Miya *		250	15～20

* 2 cycles of deepening and precipitation

1) Yoshiyama and Yanagida,1995 2) Nakano, 1989: deepening of lava flow by river 3) Takagi et al., 1999a

Table 2.5-15 Examples of weathering rates of rocks
after Matsukura (1994, 1997)

Rock type	Rate (mm per 1,000 years)
Granite	3～15
Andesite	6～9
Tuff (the Oya Stone)	33～250
Sandstone	11～110
Limestone	2.5～1300

the next hundred thousand years. Therefore, patterns of uplift and subsidence are also likely to continue in a similar fashion to the present over this timescale.

The variation in denudation rate for each area has been estimated from the characteristics of regional denudation and linear denudation (deepening). The regional denudation rate has a strong positive correlation with topographic relief. Taking advantage of this feature, a nation-wide distribution map has been created digitally. In addition, the process of deepening has been studied by taking examples from major rivers in Japan. The results indicate that the amount of deepening is approximately the same as the amount of uplift over a time period of the order of 100,000 years. These results also imply that the occurrence of large-scale denudation, which reaches several hundred meters per 100,000 years, is limited to the central part of rapidly uplifting mountains or co-seismic uplifting coasts. Excluding such areas, the depth of denudation over 100,000 years is estimated to be several tens to a hundred meters. The maximum deepening in coastal areas is considered to be less than 200 m per 100,000 years in many cases. However, the amount of uplift and the drop in sea-level during a glacial stage should be added to this figure.

The most important geological environmental considerations are the possibility that uplift and denudation may cause an underground facility to come close to the ground surface or may change groundwater flow patterns and rates. Continuous large-scale uplift and denudation would greatly reduce the thickness of rock covering any repository. In addition, the increase in the topographic gradient due to uplift, subsidence and denudation may also increase the hydraulic gradient.

Predictions of the effects of crustal movements are based largely on theoretical simulations and the results depend on the input and boundary conditions. To simulate the effects more accurately, it is necessary to obtain accurate data on topographic gradients, locations of valleys and ridges, geological structures and the overburden.

The prediction of terraces and riverbeds formed in the future requires data on geology, topography and formation ages and clarification of the process of crustal movements in the respective areas. For areas poor in topographic and chronological data to be used as an indicator of crustal movements (mainly inland areas), additional research is needed. Techniques need to be developed to determine the rates and patterns of crustal movements, such as the development of new age-dating methods and new indicators of tectonic movements on the basis of sedimentary structures. Modeling of topographic changes due to denudation coupled with uplift, climatic and sea-level changes and geology in the respective areas is a problem awaiting solution in the future.

2.6 Climatic and sea-level changes

Global changes in climate and sea-level have been repeated cyclically, taking the form of expansion and reduction of ice-sheets throughout the Quaternary period. Climatic and sea-level changes affect geological environments in various ways, such as a change in rock properties exemplified by the formation of permafrost caused by low temperatures in glacial epochs. Water recharge will be changed by fluctuations in temperature and precipitation. Denudation processes are also affected by varying temperature, precipitation and vegetation. In addition, the migration of coastlines is expected to bring about a shift of the saltwater-freshwater interface.

It is important to predict the extent to which these climate-related effects may affect the stability of the deep geological environment in the future. This section summarizes the past rate and magnitude of climatic and sea-level changes around the Japanese islands. At the same time it evaluates the periodicity of these changes to provide a basis for predicting future changes. In addition, some specific cases of geological environmental changes due to climatic and sea-level fluctuations are discussed.

2.6.1 Characteristics of climatic and sea-level changes

The last 700,000 years of the Quaternary period were marked by a repetition of rapid warming and moderate cooling cycles. The sea-level changed periodically by more than 100 m during these cycles (Figure 2.6-1). During the cooling periods, accompanying the development of ice-sheets, water that evaporated from the sea was locked in ice on the land. Consequently, during such periods, there was a reduction in sea-level. Periods of low sea-level and large volumes of continental ice are called glacial periods. Conversely, periods of relatively high sea-level between the glacial periods are called interglacial periods. The earth's climate is thought to have just passed the peak of the latest interglacial period (Figure 2.6-2). In the Japanese islands, which are located in a mid-latitude monsoon zone, environmental changes due to these factors are expected to occur.

Since climatic and sea-level changes are known to have a notable periodicity, it is possible to predict future changes and their effects on geological environments by quantitatively evaluating past changes that occurred up to the present.

1) Analytical method for climatic and sea-level changes

The periodicity and magnitude of climatic and sea-level changes during the Quaternary can be estimated from geological and geographical features and evidence remaining in the ice-sheets, as shown in Table 2.6-1. Sea-level changes during the last several hundred thousand years have been evaluated around the world, based on altitude distribution of marine terraces and isotopic data from the cores of sediments in the deep sea floor and cores from ice-sheets. Temperature changes have also been determined in many places based on isotopic data and fossil pollen data. However, more data are required for the area around Japan to estimate climatic changes quantitatively.

Analyses of pollen fossils, glacial landforms, sedimentation rates and grain size distributions allow only relative increases and decreases in rainfall in Japan to be estimated. Recently, however, some progress has been made in this area, such as the establishment of a Loess crystallinity index (Fukusawa, 1995; Fukusawa, et al., 1997).

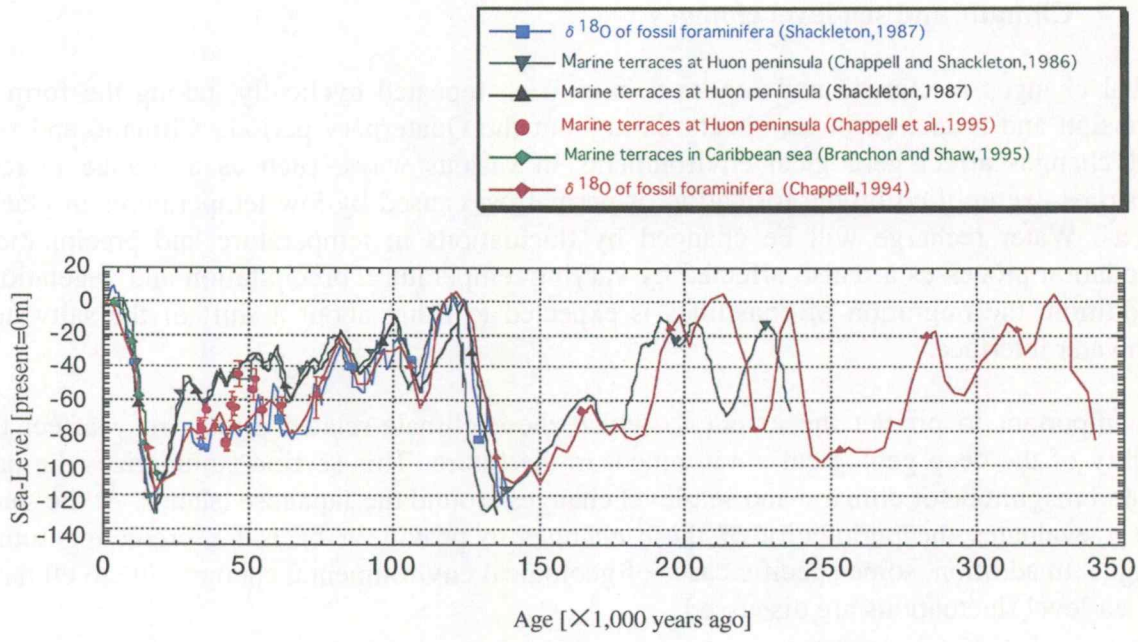


Figure 2.6-1 Sea-level changes during the past 350,000 years

A 100,000 year cycle with rapid sea-level rise followed by gradual fall is dominant. The effect of uplift of marine terraces themselves have been corrected.

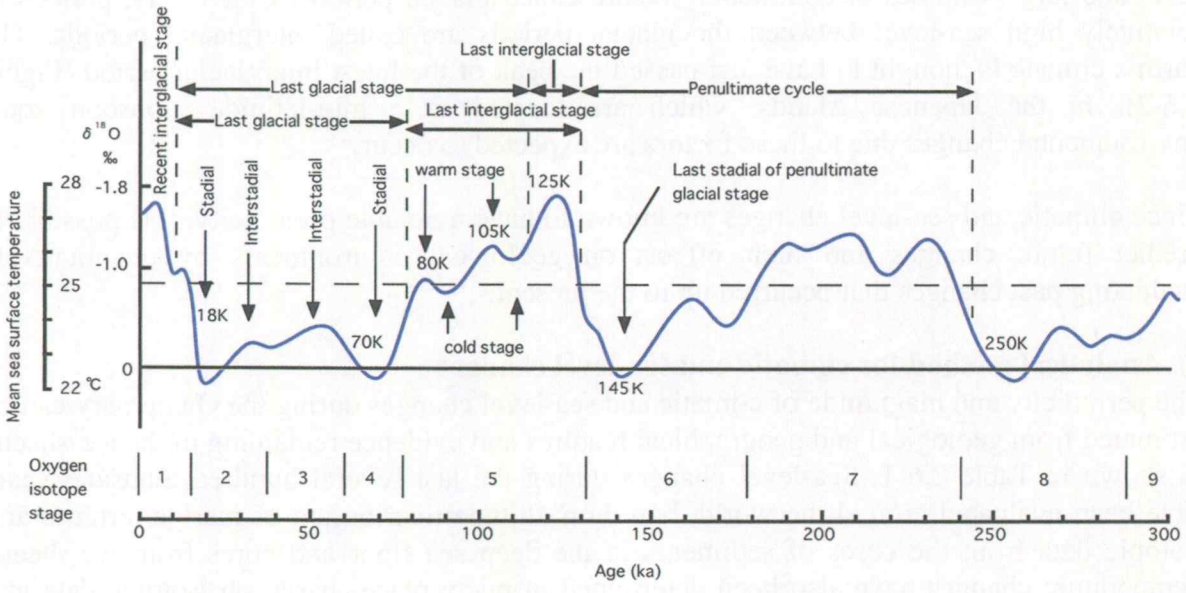


Figure 2.6-2 Changes in oxygen isotope ratio during the last 300 ka and the definition of glacial and interglacial stages (modified from Kobayashi and Sakaguchi, 1977)

The present is just after the peak of an interglacial stages which occur in 10^5 year cycles.

Table 2.6-1 Main indicators of Quaternary paleoclimate

(revised from Masuda and Abe, 1996)

Analyzed material	Indicator	Period	Time resolution	References
marine sediments and topography	aridity index (mean sea surface temperature)	$10^{5\text{-}6}$ year	$10^{2\text{-}3}$ year	CLIMAP, 1981
	$\delta\ ^{18}O$ value (volume of ice sheet)			Broeker and Denton, 1989
	amount and grain size of sediment terrigenous deposits (eolian dust) (aridity index and wind direction)			Rea, 1994
	$\delta\ ^{18}O$ value of coral (seawater temp. and salinity)	$10^{3\text{-}5}$ year	$10^{0\text{-}3}$ year	Dunbar and Coke, 1993
	marine terraces (sea-levels)	10^{5} year	10^{4} year	Kasahara and Sugimura. 1978; Chappell, 1994
non-marine sediments	magnetic susceptibility of loess (temperature and aridity index)	$10^{3\text{-}5}$ year	$10^{2\text{-}4}$ year	Heller and Evans, 1995
	$\delta\ ^{18}O$ value of speleological sediments (temperature)	10^{5} year	10^{3} year	Winogarad et al., 1992
	annual tree rings (temp. and aridity index)	10^{3} year	10^{0} year	Bradley, 1985
lake deposits and their topography	amount of eolian dust, crystallinity of clay mineral (aridity index and wind direction)	$10^{3\text{-}4}$ year	$10^{0\text{-}2}$ year	Fukuzawa, 1995
	pollen and aridity index (temperature and aridity index)	$10^{3\text{-}5}$ year	$10^{0\text{-}3}$ year	Bradley, 1985
	lake terraces and distribution of lake deposits (water balance)	10^{5} year	$10^{3\text{-}4}$ year	Kadomura, 1995
ice sheet core	isotopic ratios of oxygen and hydrogen (temp. and snowfall amount) CO_2, CH_4 density (gas density of air, temp.)	$10^{4\text{-}5}$ year	$10^{0\text{-}3}$ year	Oeschger and Langway, 1989

2) Climatic and sea-level changes during the Quaternary

In the Cainozoic era there was a trend towards general atmospheric cooling. During this era, ice-sheets began to form in the northern hemisphere around 5 Ma ago and became large in scale at around 2.8 Ma ago (Masuda, 1996). The Quaternary has been characterized by a periodic repetition of distinct glacial and interglacial periods, in which the ice-sheets expanded and contracted (Figure 2.6-3). This fluctuation is attributed mainly to a change in the amounts of water vapor being transferred from east to west and vice versa near to the equator and is possibly also due partly to the formation of the Panama land bridge around 3 Ma ago (Brocker and Denton, 1989). In the Late Pliocene and Quaternary, the Asian monsoon pattern began. This was due to a change in the transport route for water vapor across sea and land surrounding the Indian Ocean. This change was in turn triggered by a significant increase in the elevation of the Himalayas and the Rockies at this time (Yasunari, 1987; Ruddiman and Kutzbach, 1989; Nishi and Sakai, 1997).

The sea-level fluctuation curve shown in Figure 2.6.1 was estimated from the oxygen isotope ratio ($\delta^{18}O$) and the altitudes of marine terraces and coral reefs. The curves show similarities even though they were acquired using different methods in different areas. As this figure shows, it is generally accepted that the sea-level has changed in the range +5 m to -120 m compared to the current level.

3) Climatic and sea-level changes after the last glacial stage

During the last glaciation, North America, Greenland, Northern Europe and Northern Asia were covered by ice-sheets and the sea-level was lowered as a result. The ice-sheets largely melted after reaching a peak in size approximately 20,000 years ago and most of them had disappeared from the northern hemisphere by about 6,000 years ago. The overall change in sea-level during the last 20,000 years has been estimated from coral reef data. As Figure 2.6-4 shows, the sea-level has risen by approximately 100 to 120 m from its minimum level. It is estimated from data on ice volumes, that ice melting caused the global sea-level to rise by approximately 110 m at an almost constant rate of 15 m per 1,000 years during the period between 14,000 and 6,000 years ago (Nakada and Lambeck, 1988, 1989).

Figure 2.6-5 shows the distribution of the annual average surface temperature around the Japanese islands around 20,000 years ago, estimated mainly from fossil pollen data. This figure also illustrates the coast around the same time, when the sea-level was assumed to be 100 m lower than today. Temperature and rainfall fluctuations during and after the last glaciation, based on pollen analyses, are shown in Figures 2.6-6a and 2.6-6b. Abundant data for the Japan Sea coast and Central Japan indicate that, 20,000 years ago, the annual average surface temperature was 8°C lower than today. However, the mean annual surface temperature rose dramatically between 20,000 years ago and around 6,000 years ago, when it reached +2 to +3°C higher than the current temperature. During the last glaciation, the decrease in temperature was greater as the latitude became higher. In Hokkaido, the annual average temperature decreased by 10°C to 14 °C.

Around 20,000 years ago, at the peak of the last glacial stage, it is known that the annual rainfall in Japan dropped to between 50 and 70% of the current rainfall. It then rose gradually to the current level about 6,000 years ago (Figure 2.6-6b). The postulated causes of this change are:

- a decrease in typhoon frequencies in the glacial age (Kaizuka, 1962, Sugai, 1992);
- a decrease in water vapor supply by winter monsoons due to the decrease in the area of

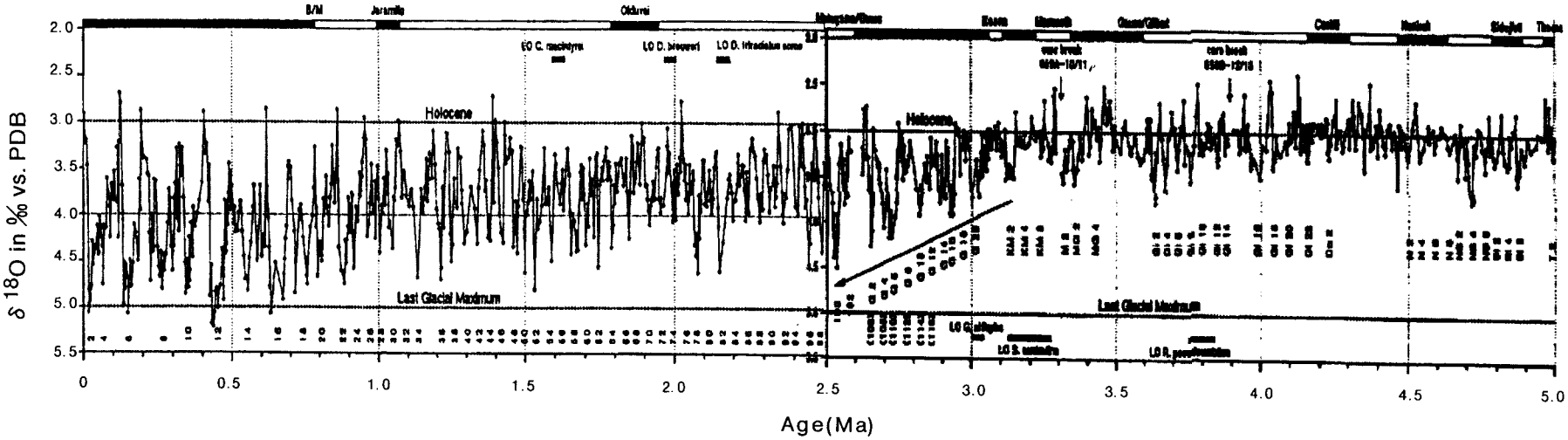


Figure 2.6-3 Summary of benthic δ ^{18}O records over the last 5 Ma (Tiedeman et al., 1994)

During a glacial epoch, ^{16}O accumulates in the continental ice-sheet and the δ ^{18}O value of seawater is increased. This latter value is a good indicator of seawater temperature and the volume of ice-sheets accumulated from atmospheric precipitation. Low values of δ ^{18}O indicate relatively warm seawater temperatures. The amplitude of δ ^{18}O variations has increased during the last 3.0 to 2.0 Ma and climatic changes related to glacial and interglacial epochs have been pronounced since then. A 10^5 year climatic cycle has been obvious since around 700 ka ago.

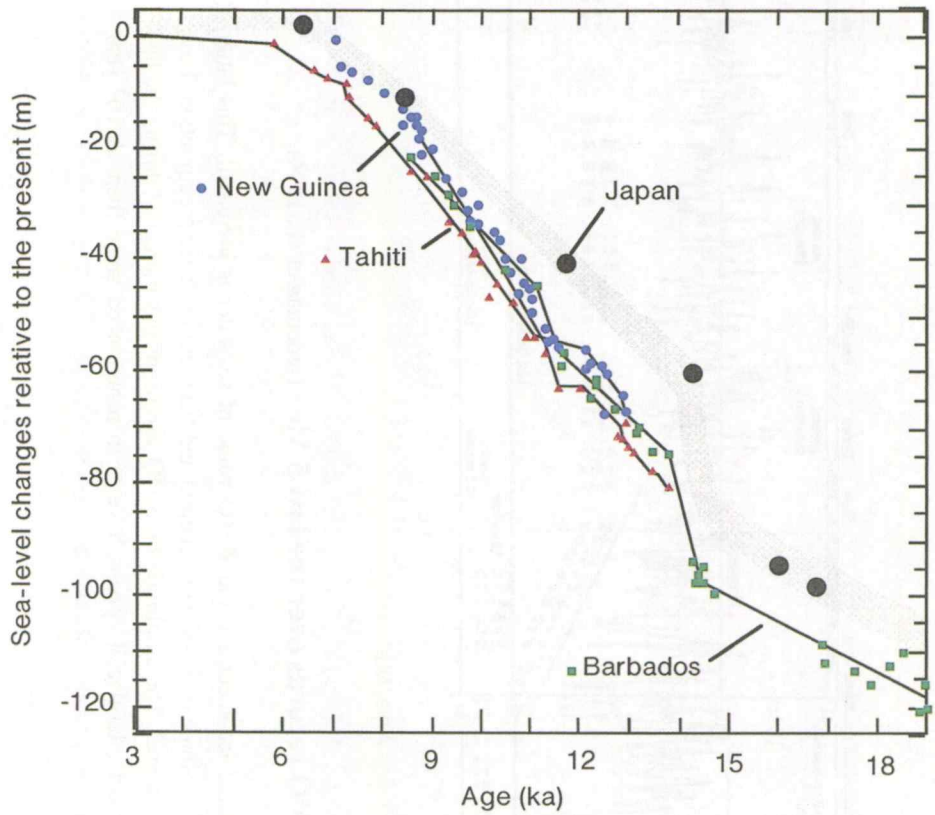


Figure 2.6-4 Sea level curve during the past 20 ka (Saito, 1997)

Ordinate axis is relative sea level change, which includes eustasy and crustal movement.

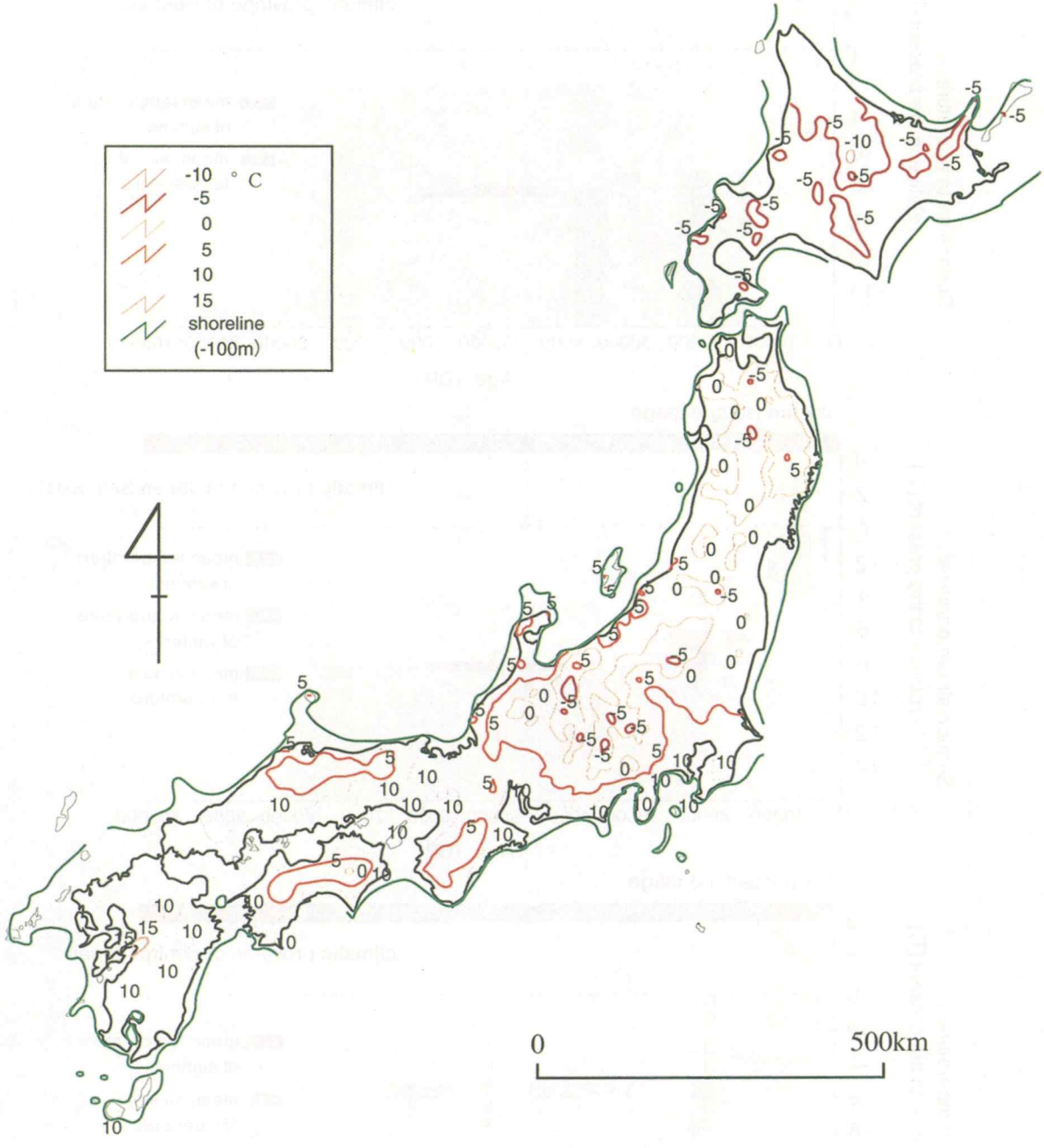


Figure 2.6-5 Shoreline of the last glacial maximum and mean annual surface air temperature of Japan (Matsusue et al., 1999)

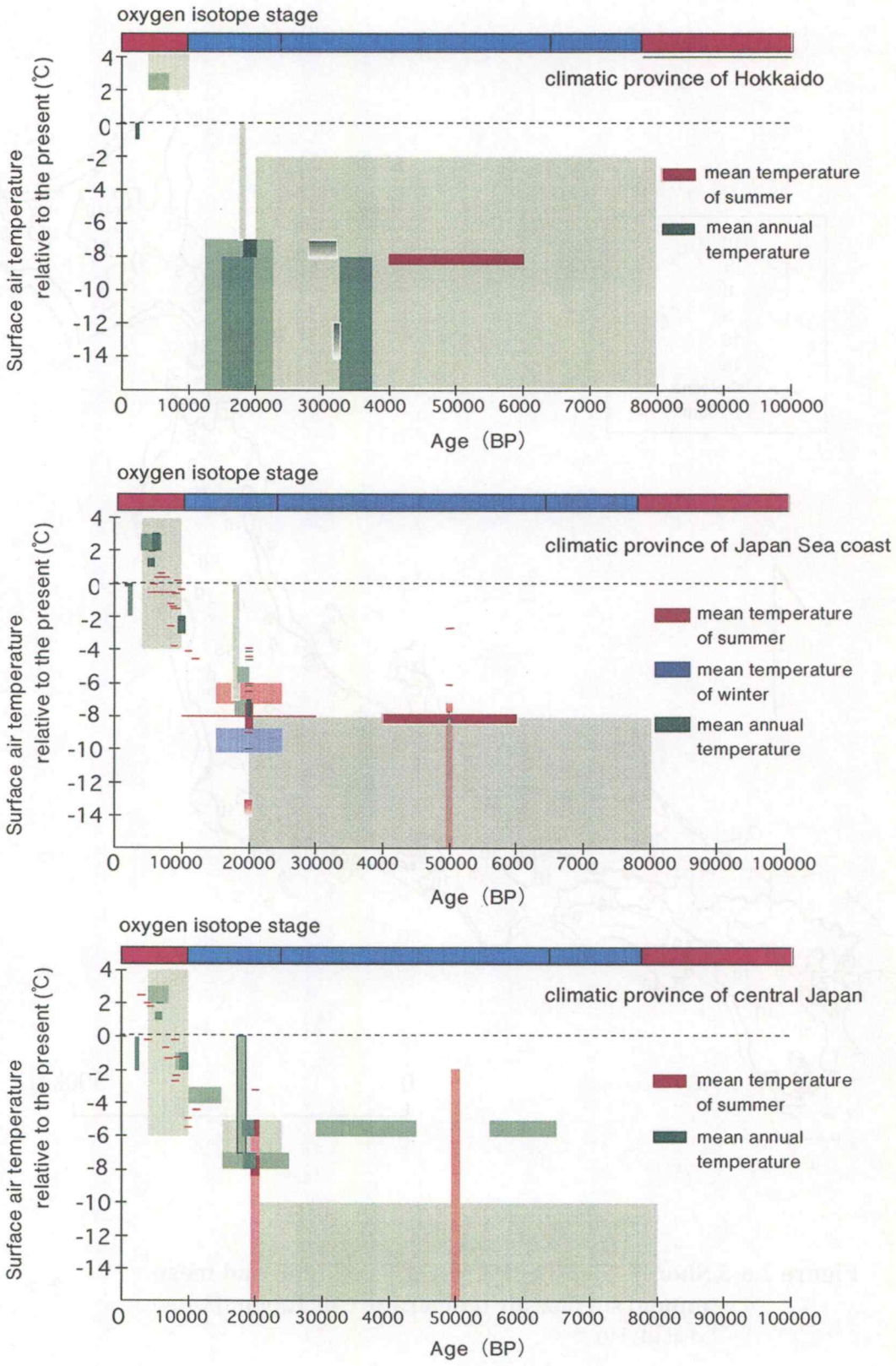


Figure 2.6-6a Mean annual air temperature at the surface and amount of precipitation over the last 100ka in Japan

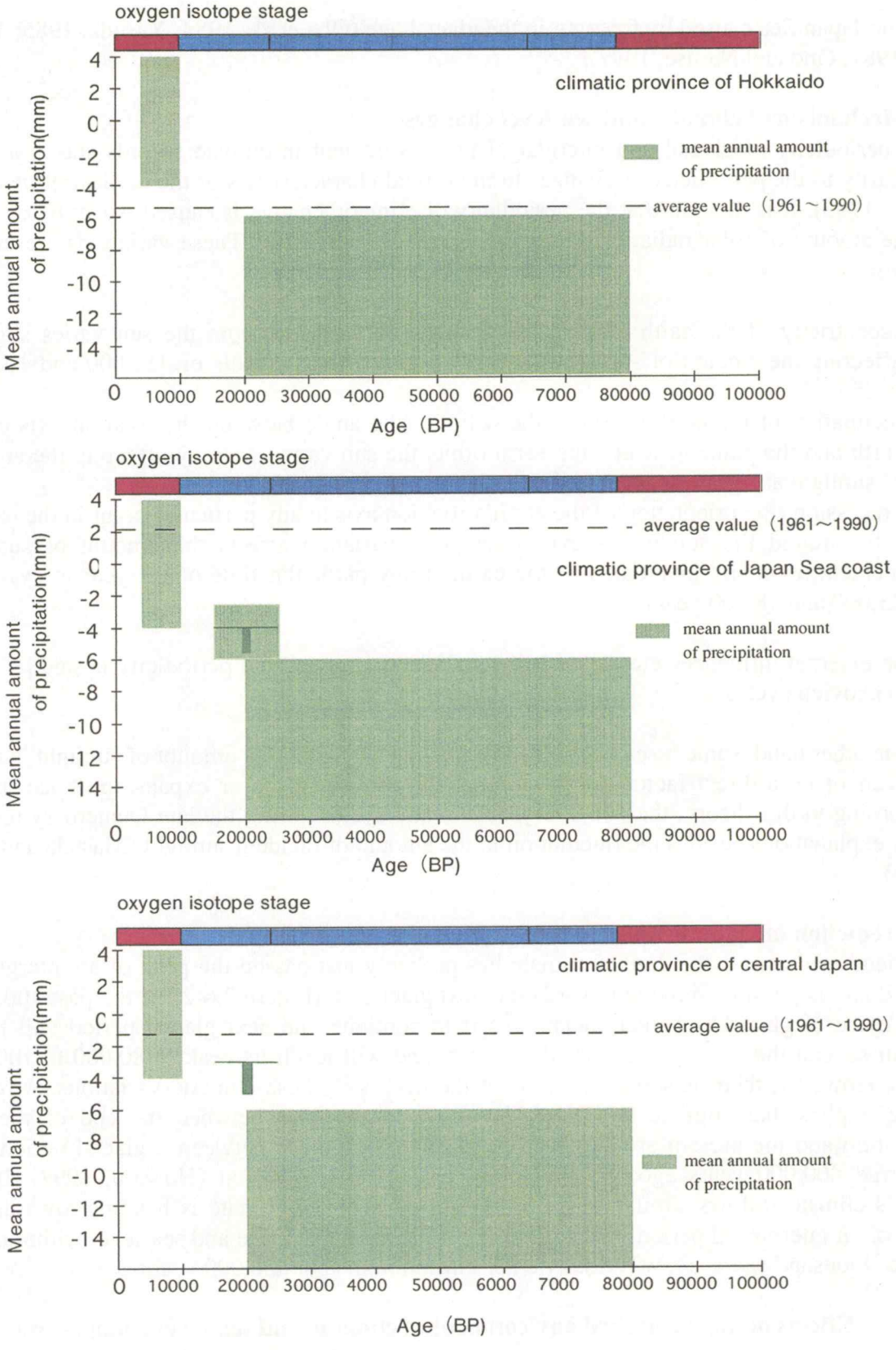


Figure 2.6-6b Mean annual air temperature at the surface and amount of precipitation over the last 100ka in Japan

the Japan Sea caused by freezing in the glacial age (Oba et al., 1984; Yasuda, 1985; Yano, 1987; Ono and Naruse, 1997).

4) Mechanism of climatic and sea-level changes

The periodicity of glacial and interglacial periods evident in climate records shows a close similarity to the periodicity of changes in the orbital characteristics of the earth (Imbrie et al., 1992, 1993). It is thought that the periodicity of climatic change is caused partly by changes in the amount of solar radiation heating the earth's atmosphere. These variations are in turn due to:

- eccentricity of the earth's orbit (the distance of the earth from the sun varies slightly, affecting the amount of sunlight incident on the earth in a cycle of 413,000 and 100,000 years);
- inclination of the earth's axis to the ecliptic (the angle between the rotation axis of the earth and the plane in which the earth orbits the sun varies, thereby affecting the amount of sunlight at certain seasons and latitudes in a cycle of 41,000 years);
- precession (the orientation of the earth's rotation axis at any particular point in the earth's orbit around the sun varies over time. This variation affects the amount of sunlight incident upon any given area of the earth at any particular time of the year in cycles of 23,000 and 18,000 years).

These external influences are called Milankovich forcing and the periodicity is said to show "Milankovich cycles".

On the other hand, some researchers believe that the change in the amount of sunlight is small and cannot be a direct factor in determining the disappearance or expansion of ice-sheets. According to this theory, the 100,000-year climatic cycles during the late Quaternary require other explanations besides the fluctuation in the amount of incident sunlight (Masuda and Abe, 1996).

5) Prediction of climatic and sea-level changes

As mentioned above, the earth's climate has probably just passed the peak of an interglacial period and is possibly moving towards the next glaciation (Figure 2.6-2). If the past 100,000-year cycle of glacial and interglacial ages is to continue, the next glacial period will begin within several thousand years from the present and will reach its peak in 80,000 to 100,000 years. However, there is some doubt about the details of these climatic variations. A recent study implies that climatic variations that have taken place between the end of the last glaciation and the present are similar to those that took place between a glacial period that occurred 400,000 years ago and the following interglacial period (Howard, 1997). If the earth's climate follows similar trends in the future then the climate is heading towards the peak of an interglacial period, will experience a rise in temperature and sea-level within a few tens of thousand years and will finally enter glaciation in about 50,000 years.

2.6.2 Effects on the geological environment of climatic and sea-level changes

From the above discussion, it is apparent that predictions of glaciation effects are important in any predictions of future environments within the next hundred thousand years. Evidence for past glaciations implies that, around the Japanese islands, sea-level will decrease by about 100 m. The average annual surface temperature will decrease by around 10°C and average annual rainfall may be reduced to about half of the current level in some regions. Under these

conditions, permafrost may be formed in some regions. Groundwater flow may be affected, depending largely on the extent to which recharge is changed by the variations in rainfall, formation of permafrost and the associated changes in vegetation. In mountainous areas, freezing of the rock mass and/or the development of mountain glaciers is expected. These processes might possibly cause physical weathering to occur. In coastal areas, riverbeds may deepen, due to a decreased base level of denudation. Furthermore, the orientations of river channels may change, which may also influence groundwater flow.

1) Effects of permafrost

Permafrost is so impermeable that groundwater is prevented from infiltrating downwards or welling up through it. Permafrost causes a great change in groundwater flow in the surface layer (SKI, 1995). When it thaws, a lot of water, due to melting of permafrost and water that has been stored under it, discharges, possibly causing flooding. Once flooding starts, the frozen ground prevents the floodwater from sinking down, resulting in an increase in water level and current velocity which can cause large-scale denudation.

(1) Distribution of permafrost in the last glacial epoch

Permafrost refers to the frozen soil or rock that remains at 0°C or less for a period spanning at least two winters. In Japan, permafrost is considered to exist on high mountains where the annual average surface air temperature is -2°C or less (Yanagimachi, 1992). At present, permafrost in Japan has been confirmed to occur on the upper slopes of Mt. Taisetsu in Hokkaido and around the top of Mt. Fuji (The Association for Geological Collaboration (ed.), 1996). During the last glacial maximum, permafrost extended over the whole area of Hokkaido and the high mountains of Honshu (e.g. Ono and Naruse, 1997). However, the permafrost did not form continuously to depths of hundreds of meters as in Siberia at present. Even in Hokkaido, the permafrost was discontinuous (Ono, 1990,1993; Miura and Hirakawa, 1995) and, even in mountainous areas where it was distributed widely, it probably had a thickness of about 150 m at most (Nakayama, 1995).

The thickness of permafrost is closely related to the annual average surface air temperature (Figure 2.6-7). This relationship was applied to the temperatures shown in Figure 2.6-5 to deduce the past distribution and thickness of permafrost, as shown in Figure 2.6-8.

(2) Depth of permafrost

A thermal conductivity model was used to simulate the growth of permafrost downwards from the ground surface during a glacial epoch in Hokkaido. In the simulation, values for the following parameters, which affect the thermal conductivity, were specified as boundary conditions:

- spatial range and rate of decrease in air temperature at the ground surface;
- subsurface heat flow;
- thickness of fallen snow;
- underground structure;
- soil moisture content.

About 300 cases were simulated in which the boundary conditions were changed. As an example of the output from a simulation, a case in which there was a reduction of the annual average surface air temperature from 7°C to -7°C over a period of 10,000 years is shown in Figure 2.6-9a. This reduction in air temperature is the largest value estimated from fossil pollen data to have occurred in Hokkaido during the last glacial epoch. The simulation shows

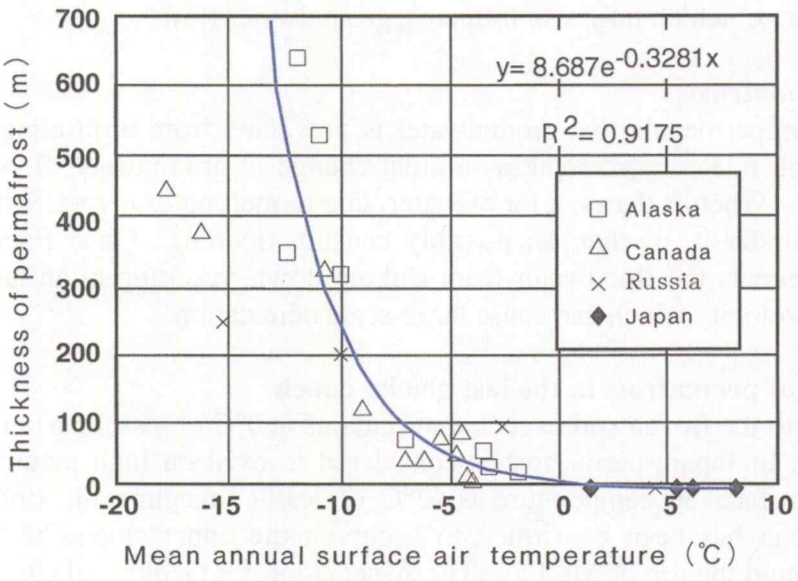


Figure 2.6-7 Thickness of permafrost and mean annual surface air temperature (Matsusue et al, 1999)

Thickness of permafrost is highly correlated with mean annual surface air temperature. Data used to carry out the regression did not include those from Canada. Data are modified from the Editorial Committee of Cyclopedia of Geomorphology (1989), Fukuda et al. (1997), Matsumoto et al. (1994) and Kondo et al. (1978).

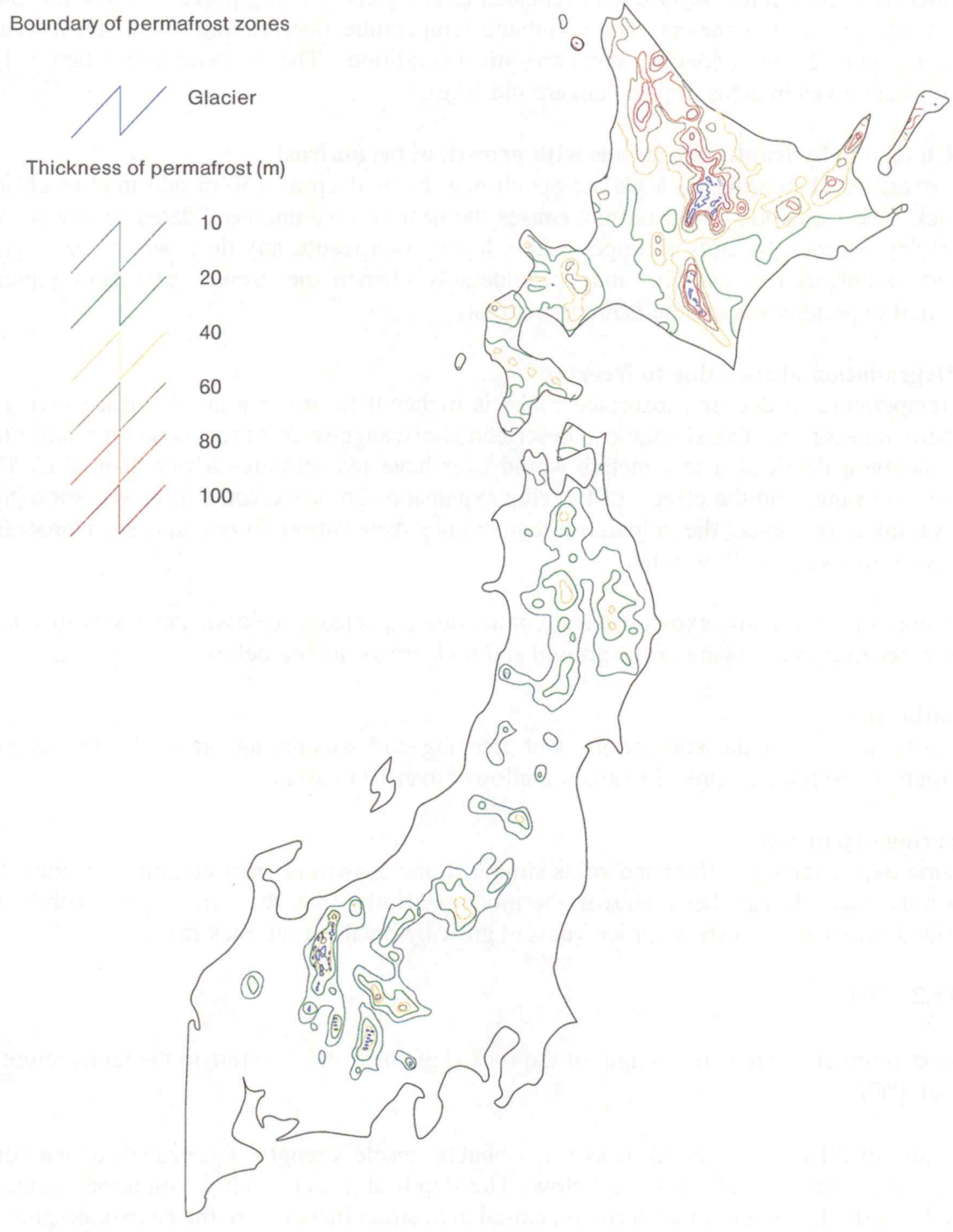


Figure 2.6-8 Distribution of permafrost and glaciers at 20 ka ago
(Matsusue et al., 1999)

that the maximum depth of the frozen soil and rocks was about 150 m (in the case where the snow covering is 100 cm thick and soil moisture content is 20%). The "active layer (melting depth)" shown in the figure refers to a layer melted in summer but frozen in winter. Weathering occurs in this layer due to repeated freezing and melting processes. The thickness of this layer is several meters. The simulated temperature distribution of the subsurface is given in Figure 2.6-9b, under the same analytical conditions. The temperature gradient is low and constant, even in areas deeper than around 10 m.

(3) Change in hydraulic conditions with growth of permafrost

Permafrost developed during a glacial epoch may be as deep as 150 m and may reach into bedrock. The formation of permafrost causes the near surface unconsolidated sediments and underlying bedrock to form an impermeable layer. As a result, any deep water discharge is limited to unfrozen areas. This may considerably change the groundwater flow patterns compared to periods when there is no permafrost.

(4) Degradation of rock due to freezing

The temperature in deeper subsurface rocks is higher than at the ground surface owing to geothermal heat flow. The simulations described above suggest that there is no possibility that rocks below a depth of a few meters would ever have temperatures lower than -7°C. This temperature range and the effects of freezing expansion can be expected in porous rock (tuff, for example). However, the calculated temperature distribution shows that such processes only occur in a very shallow zone.

The nature of weathering, expansion and contraction expected to be associated with this near-surface freezing and thawing of the ground and rock are examined below:

- Weathering

It is concluded from the simulations that freezing and weathering under the temperature conditions considered is limited to areas shallower than 10 to 20 m.

- Freezing expansion

Freezing expansion (growth of ice veins similar to the growth of frost columns) might occur in porous rock. It has been shown thermodynamically that the temperature conditions described below are necessary for ice veins to grow by breaking the rock mass:

$$\sigma_t < 11.2 \times |\theta|$$

where σ_t refers to the tensile strength of the rock (kgf cm^{-2}) and θ refers to the temperature of the rock (°C).

If a value of 50 kgf cm^{-2} is taken as a reasonable tensile strength, the growth of ice veins requires a temperature of –5°C or below. The depth at which such a condition occurs is limited to a shallow region. Furthermore, cumulative stress increases in the deep underground, diminishing the potential for freezing expansion to occur. For these reasons, freezing and expansion processes associated with variations in atmospheric temperature are unlikely to occur in the deeper subsurface under conditions similar to those simulated.

(5) Degradation of rock due to thermal shrinkage

- Thermal stress

The effects of temperature decreases on the rock mass are mainly attributable to the thermal

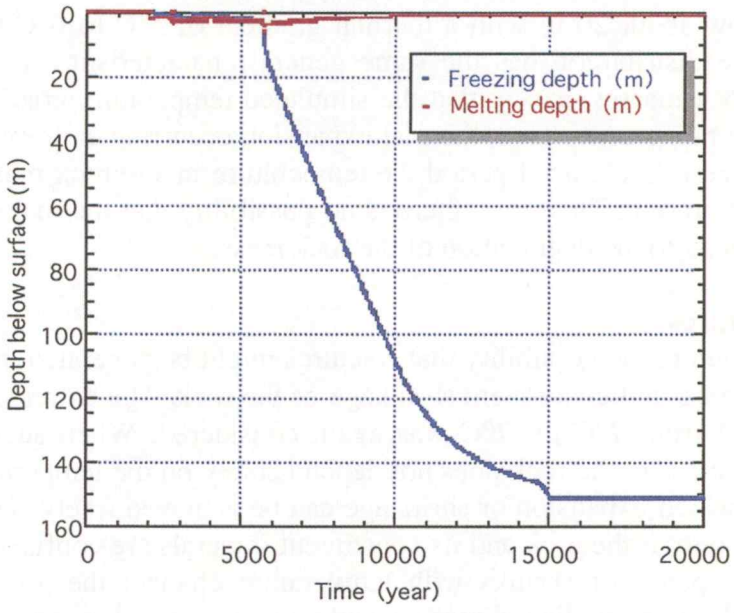


Figure 2.6-9a Growth of permafrost when annual mean surface air temperature decreases from 7 ℃ to -7℃ in 10^4 years

(Matsusue et al., 1999)

Blue line shows depth of permafrost. Snow depth is 100 cm, volume of water in ground is 20% of rock porosity. Red line shows thickness of melting layer in summer. Weathering of rock occurs in this layer by alternation of freezing and melting.

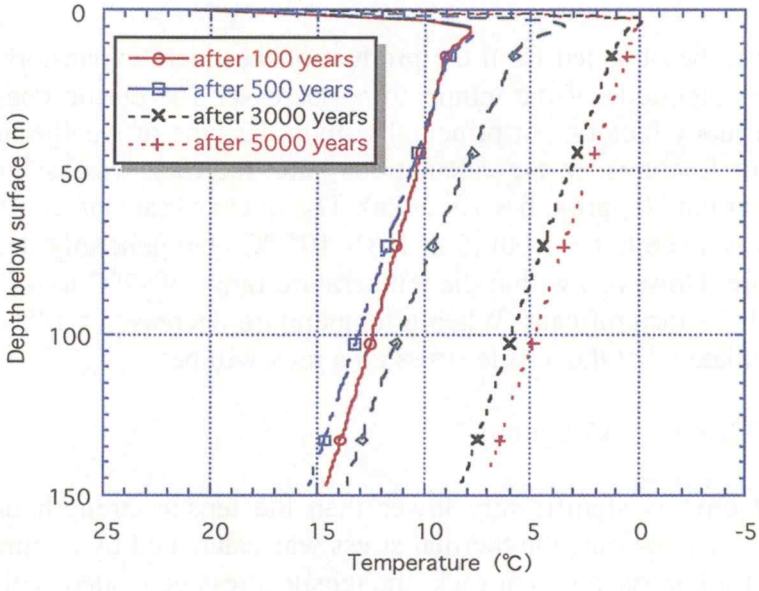


Figure 2.6-9b Subsurface temperature profile of Fig.2.6- 9a

(Matsusue et al., 1999)

Thermal stress in the rock is small except near the ground surface because the geothermal gradient is constant.

expansion characteristics of the rock (which is, in turn, mineral dependent). Each simulation undertaken in the present study shows that temperature increases almost linearly with increasing depth below about 20 m with a thermal gradient of 5°C to 6°C per 100 m. This simulated temperature distribution has the same general characteristics as those measured currently in typical rock masses, except that the simulated temperature gradient is somewhat larger. Over the depth range considered, thermal expansion occurring at present is insufficient to degrade the rock mass. In a glacial period the temperature in any rock mass will generally be even lower than at present. Therefore, there is no possibility that thermal stress within the rock mass itself may lead to the degradation of the rock mass.

- Generation of fractures

Consideration was given to the possibility that fractures might be generated in rock mass, due to a temperature decrease and consequent shrinkage of the rock. The extreme case where the temperature decreased from 7°C to -7°C was again considered. When such a temperature reduction occurs, the stress in the rock does not depend solely on the temperature change, but also on the extent to which expansion or shrinkage can be achieved freely (i.e. an increase in rock stress will occur only if the rock and its constituent minerals are confined). For example, even if the ground expands or shrinks with temperature change, the ground surface can deform relatively freely in the vertical direction, and thus the vertical component of stress due to thermal shrinkage and expansion does not generate significant fractures. On the other hand, rock may not expand or shrink as freely in a horizontal direction. The limiting possibility that horizontal deformation would not occur at all was simulated and the stress caused by cooling and shrinkage was calculated. In this one-dimensional case, the stress, σ_t, which is generated by temperature changes in a rock mass that has both ends fixed, can be obtained by the following equation:

$$\sigma_t = E \times \varepsilon_t$$

where E is the elastic coefficient of the rock mass (MPa) and ε_t is the thermal strain developed during the temperature change.

The thermal strain ε_t can be obtained from the product of the linear expansion coefficient of the rock mass and the magnitude of the temperature decrease. The elastic coefficient of the rock mass depends on many factors, but principally upon the type of weathering of the rock and the development of fractures. In the calculations here, the rock was assigned an elastic coefficient of 6×10^4 kgf cm^{-2} (approx. 6×10^3 MPa). The linear expansion coefficient of rock at room temperature was taken to be about (5 to 10) $\times 10^{-6}$ °C^{-1} but generally decreases with a reduction in temperature. However, within the temperature range of -7°C to +7°C considered here, this variation will be insignificant. When a temperature decrease of 14°C occurs, from +7°C to -7°C, it is calculated that the tensile stress on a rock will be:

$$\sigma_t = (6 \times 10^4) \times (5 \times 10^{-6}) \times 14 = 4.2 \text{ kgf cm}^{-2}$$

This value of 4.2 kgf cm^{-2} is significantly lower than the tensile strength of most rocks. Moreover, in the above calculations, the thermal stress was calculated by assuming that there are no fractures in the rock mass, any real rock, the tensile stress generated will be dissipated in the fractures. When this effect is taken into account, it is found that a rock mass is highly unlikely to degrade due to thermal stress. This will be the case even if a temperature change significantly greater than 14 °C occurs, or if the elastic coefficient and the linear expansion coefficient of the rock mass are greater than the values used in the calculation described here.

The calculated temperature decrease becomes less with increasing depth. Thus, the thermal stress obtained by the above equation is smaller than the value at the ground surface. In addition, compressive stress increases with increasing depth and exceeds the thermal stress at a depth of 15 to 20 m or more. Therefore, tensile stress may not be generated at such depths. Accordingly, the rock mass is unlikely to degrade due to the thermal stress at depths greater than 15 to 20 m.

2) Effects on denudation

As described in Section 2.5.1, climatic and sea-level changes play an important role in the deepening of rivers. Above the upper altitude limit of forests (the tree line), where vegetation does not exist or is scarce, denudation occurs due to freezing and fracture propagation or to periglacial action (e.g. Yanagimachi, 1992).

The tree line becomes lower at higher latitudes. The line is currently around 1500 m in Hokkaido and around 2500 m in the Chubu region of Japan. However, the line descended by about 1700 m during the last glacial epoch (Kaizuka, et al., 1995). Therefore, regions affected significantly by periglacial processes expanded and there was increased denudation and production of sediment in mountainous areas.

Glacial erosion is expected to be one effect of mountain glaciers. However, there has been no development of large-scale glaciers or ice-sheets anywhere in the Japanese islands during the Quaternary. Only small-scale moutain glaciers were formed locally during the glacial epochs (e.g. Ono, 1990 and 1993). Therefore, it can be concluded that no significant effects relevant for HLW disposal will be caused by glacial erosion. In mountain regions, however, slopes may become unstable as a consequence of water flow originating in the melting of surface ice or the melting of permafrost. When the air temperature rises and the permafrost melts, large-scale landslides may occur.

3) Effects on hydraulics and water chemistry

(1) Effects on hydraulic gradients

In order to predict hydraulic gradients in the future, it is important to predict the extent to which topographic gradients may change. Such changes, due to variations in climate and sea-level, may cause changes in the hydraulic gradients that drive groundwater flow. The relationships between deepening and climatic and sea-level change were discussed in Section 2.5.2. Changes in the amount of recharge are important controls on fluctuations in groundwater levels. The data on rainfall and air temperatures necessary to calculate recharge are shown above.

In addition, during cycles of glaciation, rises and falls in sea-level, over a range of around 100 m, change the stress applied to the sea-floor. This process may in turn result in the uplift and subsidence of the sea-floor and the land. This effect is called hydroisostasy and is considered to have caused relative sea-level changes of several meters in the coastal areas of the Japanese islands (Nakada et al., 1991; Nakada et al., 1994).

(2) Movement of the boundary between ocean and continent

The movement of a coastline, due to fluctuations in sea-level, occurs with repeated coastal erosion and coastal sediment deposition. The movement of the coastline, which represents the hydraulic boundary between the ocean and the land, must be incorporated into models of the movement of the seawater/fresh groundwater interface that occurs in the subsurface of coastal areas.

The range of movement of the coastline during the next glacial epoch was reviewed. The sea-level will decrease by about 100 m during the next glacial epoch and approximately the region shown in Figure 2.6-5 will become land.

(3) Change in drainage system

As the sea-level decreased by about 100 m during the last glacial epoch, most of the shallow bays that presently occur in Japan, such as Tokyo Bay and Osaka Bay, became land. The surface drainage system was significantly different from the present. Cores from boreholes and the interpretation of seabed topography have revealed channels during the last glacial age that were buried under Holocene deposits. These data have allowed paleo-drainage systems to be reconstructed (Japan Association for Quaternary Research (ed.), 1987). According to these reconstructions, most rivers currently flowing into Tokyo Bay were joined and composed a river called the "Paleo-Tokyo River" This river flowed through the Uraga Strait into the Pacific Ocean. In Southwest Japan, the Seto Inland Sea became land during this period. It developed two main water systems, both of which flowed into the Pacific Ocean, one from the Kii Strait and the other from the Bungo Strait.

The groundwater levels would have decreased at the same time, but direct estimates of the amounts by which the water tables were depressed are not available.

Present water depth data indicate that these bays and the Inland Sea will probably become land once more during the next glacial epoch. The topographic characteristics of the sea-floor in these areas suggest that development of the drainage systems will be similar to the last glacial epoch.

4) Effects of global warming

It has been postulated that present global warming, attributed to the anthropogenic release of greenhouse gases, may affect the future natural environment. To evaluate the importance of these effects in Japan, it is important to establish how they will influence characteristics of the Japanese climate, including seasonal winds (monsoon), rainy seasons and typhoons (Maejima, 1980). Currently available information does not enable these issues to be addressed definitively (Nakagawa et al., 1997). However, several climatic models have been constructed. There is some variability in the output from these models. However, it is predicted that the concentration of atmospheric carbon dioxide could double during the next 70 to 80 years. It is expected that such a change could cause the annual average air temperature in Japan to rise by 1°C to 2.5°C. It is also predicted that the annual average rainfall will fluctuate between -5% to +10% relative to the current values around Japan (Nakagawa et al., 1997).

To evaluate the significance of these results for HLW disposal, it is important to compare them with natural climatic variations from the start of the last glaciation, about 80,000 years ago to the current interglacial (post-glacial) epoch. During this time, rapid, significant fluctuations occurred that were as great as, or greater than, those predicted to occur from present global warming.

The global rise in average air temperature which can be attributed to human activities since the Industrial Revolution is considered to be about 0.5 °C per 100 years (e.g. Matsuno, 1989; Mann et al., 1998). This rate is much greater than the rate of temperature rise after the coldest period in the last glacial epoch (10°C per 10,000 years = 0.1°C per 100 years).

Anthropogenic warming is predicted to cause a mean global air temperature rise of 2°C from

1990 to 2100. The corresponding rise in global sea-level is expected to be 49 cm (IPCC, 1995). Thus, it is predicted that the sea-level will rise at a rate of 5 mm per year. This rate is more rapid than the rate (1 to 2.5 mm per year) in the last 100 years (IPCC, 1995), and slower than that around the Japanese islands during the post-glacial age (about 9 mm per year), estimated from Figure 2.6-4. In addition, the rise in air temperature of 2°C is close to the value around Japan about 6,000 years ago in the middle of the Jomon transgression.

Furthermore, oxygen isotopic data from ice-sheet cores collected in Greenland and other regions (Figure 2.6-10) indicate that rapid fluctuations in annual average air temperature occurred over periods of a few years to tens of years during the last glacial epoch. These fluctuations occur in cycles of hundreds to thousands of years and are called Dansgaard-Oeschger cycles (Dansgaard et al., 1993). They are thought to be caused by self-induced-perturbations due to repeated partial breakup of continental ice-sheets (e.g. MacAyeal, 1993a, b).

Fluctuations in air temperature generally tend to be larger in higher-latitude regions than in low-latitude areas. Japan is located at middle latitude. Therefore, compared to temperature variations in northern Europe or in higher latitude continents, those in Japan appear to be relatively small. However, the rate at which air temperature increases during a Dansgaard-Oeschger cycle is an order of magnitude greater than that associated with global warming. Conservative prediction of the effects on the geological environment of global warming may be realized by research on the environmental changes due to the Dansgaard-Oeschger cycle. Evidence for such cycles has been detected recently around the Japanese islands (e.g. Tada, 1997, 1998; Fukusawa et al., 1997). Future studies will aid quantitative examination of their effects on air temperatures and sea-levels around Japan.

2.6.3 Summary

Characteristics of climatic and sea-level fluctuations during the Quaternary period have been summarized using data from ice-sheet cores, deep-sea sediments and coastal terraces. Cycles of glacial and interglacial epochs with durations of 100,000 years have occurred for approximately the past 700,000 years. These cycles are thought to have resulted largely from changes in the annual quantity of solar radiation incident upon the earth. These changes were due to secular variation in the earth's orbit.

Relative to its present level, the sea-level around Japan has changed within the range of +several meters to -120 m during the past several hundred thousand years. During the last glacial epoch, the mean annual temperature in Japan is thought to have been up to 8 to 10°C lower than at present. Conversely, during interglacial periods, the mean annual temperature is estimated to have been up to several degrees centigrade higher than the current temperature.

In spite of the limited data on past fluctuations in atmospheric precipitation, it has been estimated that, during a glacial epoch, annual atmospheric precipitation in the Japanese islands was reduced to between 70% and 50% of the current annual amount.

The depth of permafrost formation is highly correlated with the mean annual surface air temperature. It has been shown that permafrost developed to a maximum depth of approximately 150 m in Hokkaido during past glacial periods. However, in Honshu, permafrost developed only on high mountains. It has been calculated that rock mass degradation due to freezing and thawing occurred over a shallow depth of only about 20 m

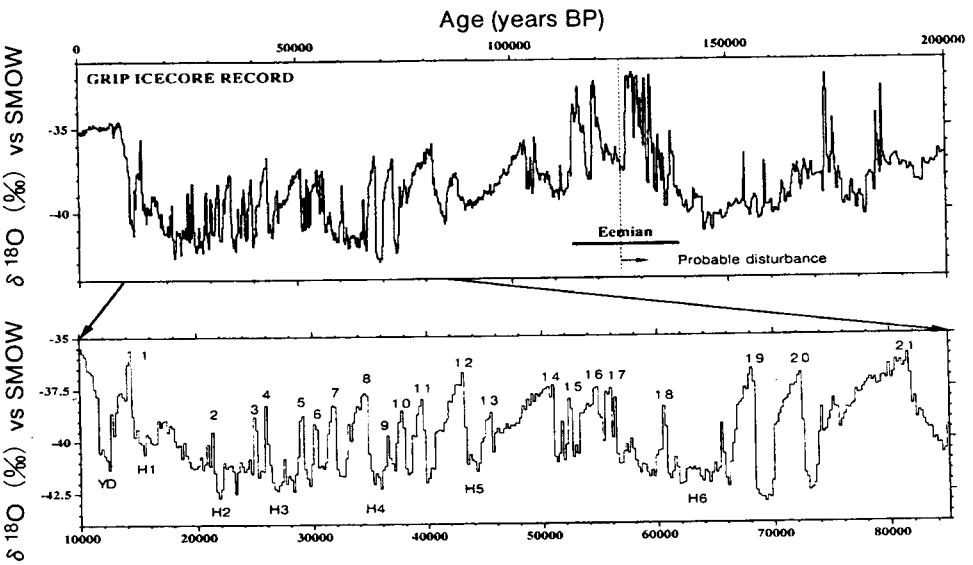


Figure 2.6-10 Continuous $\delta^{18}O$ (‰) record of the GRIP ice core during the last 200,000 years (Tada, 1998; based on Dansgaard et al., 1993)

Millennial-scale oscillations of $\delta^{18}O$ (‰) are called Dansgaard-Oeschger cycles. 1～21: warm period. Yo, H1～H6: major cold period.

from the surface.

In addition to climatic fluctuations over periods of 100,000 years, namely during glacial and interglacial epochs, there will also be rapid climatic fluctuations occurring over shorter intervals of several hundred to several thousand years (i.e. Dansgaard-Oeschger cycles). The start and end of each cycle are abrupt. These cycles have larger spatial scales and are more rapid than climatic fluctuations due to any present anthropogenic global warming.

Potentially, changes in the groundwater flow system due to such climatic fluctuations are important influences on the geological environment. The hydraulics and chemistry of groundwater are expected to change in the next glacial epoch because the sea-level will fall and the topographic gradients driving groundwater flow will generally become larger. Associated fluctuations in atmospheric precipitation will change not only the amount of recharge and groundwater levels, but also the rate and scale of denudation. Permafrost would form impermeable layers, but it may also lead to local channeling of water and, during melting, may itself discharge a lot of water. These effects may also influence denudation.

The prediction of these fluctuations and their influence in the future is largely based on theoretical simulations. The results of these simulations are dependent on the boundary conditions that are input. Therefore, it is important to define accurate boundary conditions in order to ensure that the simulations are realistic. Accordingly, further methods for quantifying past environmental fluctuations require to be developed. These methods will use similar types of data to those acquired already, such as changes in the rates of sedimentation in lakes and the characteristics of fossils and minerals contained therein.

References

(2.1 Research into the long-term stability of the geological environment)

AECL (1994): Environmental Impact Statement on the Concept for Disposal of Canada's Nuclear Fuel Waste, AECL-10711, COG-93-1.

Goodwin, B.W., McConnell, D.B., Anres, T.H., Hajas, W.C., LeNeveu, D.M., Melynk, T.W., Sherman, G.R., Stephens, M.E., Szekely, J.G., Bera, P.C., Cosgrove, C.M., Dougan, K.D., Keeling, S.B ., Kitson, C.I., Lummen, B.C., Oliver, S.E., Witzke, K., Wojoiechowski, L. and Wikjord, A.G. (1994): The Disposal of Canada's Nuclear Fuel Waste: Postclosure Assessment of a Reference System, Appendix F, AECL-10717, COG-93-7.

IAEA (1985): Safety series No.68 : Procedures and Data, Performance Assessment for Underground Radioactive Waste Disposal Systems.

IAEA (1994): Safety series No.111-G-4.1 : Siting of geological disposal Facilities, A Safety Guide, A Publication within the RADWASS Programme.

Nagra (1985): Project Gewähr 1985, NGB 85-01/09, Nagra, Wettingen, Switzerland.

NRC (1995): Technical Bases for Yucca Mountain Standards, National Research Council, National Academy Press, Washington, D.C..

SKI (1995): The central scenario for SITE-94: A climate change scenario. SKI Report 95: 42.

SKB (1994): RD&D-Programme92 Supplement, Treatment and final disposal of nuclear waste, Supplement to the 1992 programme in response to the government decision of December 16, 1993.

Shimizu, K. and Ishimaru, K. (1993): Study on long-term Stability of Geological environment, PNC technical Review., No.85; Radioactive Water management project, PNC TN1340 93-001., pp.166-172 (in Japanese).

USDOE (1982): 10CFR Part 960; Nuclear Waste Policy Act of 1982; General Guidelines for the Recommendation of Sites for the Nuclear Waste Repositories, U.S.Department of Energy.

(2.2 Tectonics of Japanese islands)

Awata, Y. (1988): The Crystal shortning and movement of Pacific Plate of inner part of central Tohoku Japan, Earth Monthly, 10, pp.586-591 (in Japanese).

Awata, Y. and Kakimi, T. (1985): Quaternary tectonics and damaging earthquakes in Northeast Honshu, Japan, Earthq. Predict. Res., 3, pp.231-235.

Awata, Y., Okamura, Y. and Shimokawa, K. (1997): Neotectonic and platetectonic setting in and around the Hokkaido and the inner arc of Northeast Honshu, Japan, Programme and Abstracts Seismol. Soc. Japan, No2, A29 (in Japanese).

Cox, A. and Engebretson, D. (1985): Change in Motion of the Pacific Plate at 5 Myr BP, Nature, 313, pp.472-474.

DeMets, C.R., Gordon, R.G., Argus, D. and Stein, S. (1990): Current plate motion, Geophys. Jour. Inter., 101, pp.425-478.

Earthquake Research Committee (1997): Earthquake activities in Japan, Association for the Development of Earthquake Prediction, Headquarters for earthquake research promotion, Earthquake research committee, pp.7-29 (in Japanese).

Furukawa, M.(1991): Formation Age of the Ryukyu Arc-Okinawa Trough System, Journal of Geography,100,4, pp.552-564 (in Japanese with English abstract).

Hino, R. (1999): Crustal structure of plate boundary zones around Japan. Chishitsu News, 541, p.11-16 (in Japanese).

Ikeda, A. (1999): The tectonics of Hida Plateau and Kinki Triangle Zone since the Pliocene can be explained by delamination of mantle lid?, Chikyu Monthly, 21, pp.137-144 (in Japanese).

Ishibashi, K. (1995): The 1995 Kobe, Japan, earthquake (M7.2) in the "Amurian Plate Eastern Margin Mobil Belt" and its implication to the regional seismic activity (Preliminary), Chishitsu News, 490,14-21 (in Japanese).

Ito, T. and Arato, H. (1999): Tectonic stress around the southern part of Japan Sea since the Pliocene: Western Kyushu, San'in and Hokuriku offshore areas. Chishitsu News, 541, pp.25-31 (in Japanese).

Jolivet, L., Tamaki, K. and Fournier, M. (1994): Japan Sea, opening history and mechanism :A synthesis, Jour. Geophy. Res., 99, pp.22237-22259.

Kamata, H. (1999): Conversion of regional tectonics around 6Ma and 2Ma at boundary zone between Southwest Japan Arc and Ryukyu Arc, Chikyu Monthly, 21, pp.630-636 (in Japanese).

Kano. K. and Murata, A.(1998): Stractural Geology, Asakurashoten, p.298 (in Japanese).

Kasuga, S., Obara, Y. and Okino, K. (1999): New point of view for propagation of back-arc basin, Chikyu Monthly, special issue no.23, pp.123-132 (in Japanese).

Kimura, G. (1981): Tectonics and tectonic stress field around southwest part of Kuril Arc, Jour. Geol. Soc. Japan, 87, pp.757-768 (in Japanese).

Kimura, G. and Tamaki, K. (1986): Collision, rotation and back arc spreading: the case of the Okhotsk and Japan Seas, Tectonics, 5, pp.389-401.

Kimura,G., Kikawa,E. and Tamaki,K. (1986): Amuru-plate and Japanese Island -A prospect after 500,000 years in East Asia-, Earth Monthly, 8, pp.716-724 (in Japanese).

Kimura, G. and Saito, S. (1998): Japan Arc and subduction zone around the world –tectonic balance between erosion and growth-, science journal KAGAKU, 68, pp.42-49 (in Japanese).

Kimura, M. (1990): Genesis and formation of the Okinawa Trogh, Japan. Mem. Geol. Soc. Japan, no.34, pp.77-88.

Kimura, M., Wang, Y. and Yagi, H. (1999): Submarine geostructure and tectonics in the Ryukyu Arc, Chishitsu News, in press (in Japanese).

Kobayashi,K. and Isezaki,N. (1976): Magnetic anomalies in the Sea of Japan and Shikoku Basin: possible tectonic implications. In The Geophysics of the Pacific Ocean Basin and its Margin, Geophys. Monogr. Amer. Geophys. Union, 19, pp.235-252.

Matsubara, Y. (1980): Izu Peninsula and the Phillippin Sea Plate, Earth Monthly, 2, pp.157-163 (in Japanese).

Miyasaka, S. (1987): Mountain growth in collision zone – Uplifting history of the Hidaka Mountains-, Commen. Vol. Prof. M.Matsui, pp195-202 (in Japanese).

Molnar, P. and Atwater, T. (1978): Interarc spreading and Cordilleran tectonics as alternates related to the age of subducted oceanic lithosphere, Earth Planet. Sci. Lett., 41, pp.330-340.

Nagaoka, S. (1999): Mountain growth and tectonics at Kyusyu region, Chikyu Monthly, 21, pp.637-643 (in Japanese).

Nakamura, K. (1983): Possible Nascent Trench along the Eastern Japan Sea as the Convergent Boundary between Eurasian and North American Plates, Bull. Earthq. Res. Inst., 58, pp.711-722 (in Japanese).

Niitsuma, N. (1994): The Tectonic Evolution of Central Japan, In Relation to the Trench-Trench-Trench Type Triple Junction, Abstracts The 101th Annual Meeting Geol. Soc. Japan, pp.169 (in Japanese).

Nishimura, A. and Yuasa, M. (1991): Sumisu Backarc rift in the Izu-Bonin Intra-oceanic arc of the western Pacific, Earth Sci., 45(5), pp.333-344 (in Japanese with English abstract).

Okamura, Y. (1990): Geologic structure of the upper continental slope off Quaternary tectonic movement of the outer zone of southwest Japan, Jour. Geol. Soc. Japan, 96(3), P.223-237 (in Japanese with English abstract).
Okino, K., Kasuga, S. and Ohara, Y. (1998): Evolution of the Parece Vela Basin. Abstract 1998 Japan earth and planetary science joint meeting, pp.35 (in Japanese).
Park, J., Tokuyama, H. and Taira, A. (1997): Backarc rifting of the southern Okinawa Trough from multi-channel seismic reflection data, Abstracts 1997 Japan Earth Planet Sci. Joint Meeting, p.695.
Pollitz, F.F. (1986): Pliocene change in Pacific-plate motion, Nature, 320, pp.738-741.
Sato, H. (1994): The relationship between late Cenozoic tectonic events and stress field and basin development in northeast Japan, jour. Geophys. Res., 99, pp.22261-22274.
Sato, H. and Ikeda, Y. (1999) : Model of Major Faults at the northeast of Japan, Chikyu Monthly, 21, pp.569-575 (in Japanese).
Seno, T.and Maruyama, S. (1984): Paleogeographic reconstruction and origin of the Philippine Sea, Tectonophys., 102, pp.53-84.
Seno, T. (1986): Middle Pleistocene of Japanese Island, Earth Monthly, 8 (12), pp.708-715. (in Japanese).
Seno, T.(1993): Plate motion and earthquake around Japan, science journal KAGAKU, 63, pp.711-719 (in Japanese).
Sugiyama, Y. (1991): Right-lateral strike-slip type of subsidence basin in the Second Setouchi Inland Sea –evolution model of subsidence basin with change of major strike-slip fault activity-, Structural Geology, no36, pp.99-108 (in Japanese).
Tada, T. (1990): Continental rifting in Kyushu, Japan, EOS Trans, AGU, 71(28), pp.917-927.
Takeuchi, A. (1999): Evolution of stress field and tectonics at Hokushin'etsu area since the Pliocene, Chikyu Monthly, 21, pp.583-588 (in Japanese).
Taylor,B., Klaus,A., Glenn,R.B., Moore,G.F., Okumura,Y. and Murakami,F.(1991): Structural Development of Sumisu Rift, Izu-Bonin Arc, Jour. Geophys. Res. 96, pp.16113-16129.
Tokutama, H., Morita, S., Soh, W., Ashi, J. and Kuramoto, S. (1999): Structural development of Izu collision zone and north part of Izu-Bonin Arc, Chishitsu News, in press (in Japanese).
Yuasa, M. (1991): The Reason for the Differences in Geologic Phenomena between Northern and Southern Parts of the Izu-Ogasawara Arc, Journal of Geography, 100(3), pp.458-463 (in Japanese with English abstract).
Uto, K. (1995): The current state and the future of K-Ar and $^{40}Ar/^{39}Ar$ dating of volcanic rocks, Bull. Volcanol. Soc. Japan, 40, Special Issue pp.S27-S46 (in Japanese).
Watanabe, Y. (1986): Neogene regional stress field inferred from the pattern of ore veins in Hokkaido, Japan, Mining Geology, 36(3), pp.209-218 (in Japanese with English abstract).
Yamagishi, H. (1986): Some outcrops of active fault at Hokkaido region, Active Fault Research, 1, pp.19-28 (in Japanese).

(2.3 Earthquakes and fault movement)

Aomori Prefecture (1997): Study of the fault system along the western margin of the Tsugaru mountains and Noheji fault system, Aomori Prefecture Northeastern Japan, Abstract 1997 Results report of investigation of active faults funded by grantinaid in 1995, 1996 fiscal year, pp.11-29 (in Japanese).
Aomori Prefecture (1998a): Study of Orizume fault, Aomori Prefecture Northeastern Japan, Abstract 1997 Main results report of active fault research, Science and Technology

Agency, pp.51-57 (in Japanese).
Aomori Prefecture (1998b): Study of Nyunai fault, Aomori Prefecture Northeastern Japan, Abstract 1997 Main results report of active fault research, Science and Technology Agency, 185-199 (in Japanese).
Aoki, K., Kawamura, M., Ishimaru, T. and Abe, H. (1999): Survey and research of earth quake at Kamaishi mine, Abstract of 1998 Annual Meeting of the Atomic Energy Society of Japan, p.788 (in Japanese).
Arai, R. and Takemura, K (1998): Fission-track ages of the volcanic ash layers in the Osaka Group, northwest part of Awaji island, Japan, Ann.Mtg. Geol. Soc. Japan. p.311 (in Japanese).
Awata, Y. (1988): The Crustal shortning and movement of Pacific Plate of inner part of central Tohoku Japan, Earth Monthly, 10, pp.586-591 (in Japanese).
Awata,Y. and Kakimi,T. (1985): Quaternary Tectonics and Damaging Earthquakes in Northeast Honshu, Japan, Earthq. Predict Res., 3, pp.231-251.
Awata, Y. and Komatsubara, T. (1997): Upper Quaternary system of the eastern Shonai sedimentary basin and the history of crustal movement, The Geological Survey of Japan monthly report, 48, pp.537-565 (in Japanese with English abstract).
Awata, Y., Kariya, Y., Nikaidou, M. and Takase, S. (1998): Recurence interval and displacement per event of the Neodani fault, whichi ruptured in 1891, central Japan, Abstract 1998 Japan earth and planetary science joint meeting, p.317 (in Japanese).
Azuma, T. (1995): Late Quaternary Terraces and Their Deformations on Tsugaru Peninsula, Northeastern Japan, Quaternary Research, 34, 2, pp.75-89 (in Japanese with English abstract).
Chester, F.M., Evans, J.P. and Biegel, R.L. (1993): Internal structure and weakening mechanisms of the San Andreas Fault, J. Geophys. Res., 98, pp.771-786.
Dobrovolsky, I.P., Zubkov. S.I. and Miachkin, V.I. (1979): Estimation of the size of earthquake preparation zones., Pageoph, 117, pp.1025-1044.
Esaki, T., Kimura, T. and Kameda, N. (1991): Shear flow coupling test on rock joints, Proc.7th Int.Cong.Rock Mech., ed. W.Wittke, pp.389-392.
Forster, C.B., Caine, J.S. and Yamazaki, S. (1998): Structure of Fault zone and fluid flow pattern in active fault, Earth Monthly., 20, pp.165-171 (in Japanese).
Fujimoto, K., Otani, T., Tanaka, H., Higuchi, T., Tomita, N., Ito, H., and Susan, M.A. (1998): Feature of fault fracture zone just after earthquake, Earth Monthly "The scientific drilling program of Nojima fault", No.21 special issue, pp.140-153 (in Japanese).
Fujita, K. (1986): The mid-Pleistocene fault block movements and sealevel change, Earth Monthly, 3, pp.725-728 (in Japanese).
Fujita, K. (1993): Neotechtonics around Kinki triangle, Southwest Japan, Hundred years of geology in Japan, centennial volume of the Geological Society of Japan, pp.237-244 (in Japanese).
Fukudome, T. (1984): Viscous heat production during active faulting, Akita Univ. rep., 49, pp.33-40 (in Japanese).
Fukushima, Y. and Tanaka, T. (1990): A new attenuation relation for peak horizontal acceleration of strong earthquake ground motion in Japan., Bull. Seism. Soci. Am., 81, pp.553-575.
Fukushima, Y. (1994): Experiential prediction of earthquake movement based on the theory of generation and transmission of seismic wave, ORI report, pp.93-107 (in Japanese).
Fukushima Prefecture (1998): Study of Futaba fault, Fukushima Prefecture Northeastern Japan, Abstract 1997 Main results report of active fault research, Science and Technology Agency, pp.211-220 (in Japanese).
Hagiwara, T. (1991): Earthquake of Japanese island –Seismotechnology and

seismotechtonics-, Kashima press (in Japanese).
Hada, S. (1981): Engineering problem of active faults, Eng. Geol., 22, pp.17-31.
Ikeda, Y., Shimazaki, K. and Yamazaki, H. (1996): What is active faults, Tokyo Univ. press, pp.64-74 (in Japanese).
Ishimaru, K. and Shimizu, I. (1997): Groundwater pressure changes associated with earthquakes at the Kamaishi Mine, Japan -A study for stability of geological environment in Japan, Proc. of 30th Int'l Geol. Congr., vol.24, pp.31-41.
Ito, H., Kuwahara, Y., Miyazaki, T., Nishizawa, O., Kiguchi, T., Fujimoto, K., Otani, T., Tanaka, H., Higuchi, T., Susan, A., Alan, B. and Yamamoto, H. (1996): Structure and physical properties of the Nojima fault by the active fault drilling, Butsuri-Tansa, 49, 6, pp.522-535 (in Japanese with English abstract).
Ito, T., Takeuchi, A., Tanaka, H., Nishikawa, Y., Sakogaichi, K. and Okada, Y. (1998) : Underground observation field for active fault survey: Survey tunnel of Mozumi-Sukenobu fault (news letter), Monthly Earth, 20, 3, pp.182-198 (in Japanese).
Iwabuchi, Y., Nishikawa, H., Kasuga, S., Miyano, M. and Iimura, T. (1997): The Osaka Bay fault and Basement Structure of the Osaka Bay, Abstract 1997, Japan earth and planetary science joint meeting, p.48 (in Japanese).
Japan Association for the Quaternary Research (1987): Quaternary map of Japan 1 Topograpic, geological and active tectonic map (1/1,000,000), Tokyo Univ. press, 119p. (in Japanese).
Kagawa Prefecture (1997): Faulting history of the Chichio fault, the Median Tectonic Line Active Fault system, Kagawa Prefecture Southwest Japan, Abstract 1997 Results report of survey of active faults funded by subsidy in 1995, 1996 fiscal year, pp.167-172 (in Japanese).
Kaizuka, S. and Imaizumi, T.(1984): Horizontal strain rates of the Japanese islands estimated from Quaternary fault data, Geogra. Rep. TOKYO Metro. Univ., 19, pp.43-65.
Kamata, H. and Kodama, K. (1993): The Hohi volcanic zone as a volcano-tectonic depression and its formation tectonics –Three tectonic events caused by subduction of the Philippine Sea plate under the junction of the Southwest Japan Arc and the Ryukyu Arc-, Mem. Geol. Soc. Japan, 41, pp.129-148 (in Japanese with English abstract).
Kawabe, I. (1991): Hydro-geochemical anomalies associated with earthquakes, Jour. Seis. Soc. Japan, 44, pp.341-364.
Kitagawa, Y., Koizumi, N., Notsu, K. and Igarashi, G. (1997): Water injection and groundwater level changes at Nojima Fault in Awaji Island, Program and Abstracts The seismological society of Japan, 2, p.99 (in Japanese with English abstract).
Kobayashi, K., Ikeda, R., Tanaka, H., Hirano, M. and Matsuda T. (1998): Evaluation of fault fracture zone based on observation of core samples from 1,140m at depth, Scientific drilling program of the Nojima fault Symposium, pp.65-66 (in Japanese).
Komada, H., Sawada, Y. and Aoyama, S. (1989): Earthquake behavior at deep underground observed by three-dimensional alley -Seismic observation at Hosokura mine-, Civil Engineering Laboratory Rep., U88074, pp.1-66 (in Japanese with English abstract).
Koyama, Y., Asakura, T. and Sato, Y (1996), Damages of mountain tunnels suffered from the Grate Earthquake of Hyogo South and restoration, Tunnels and Underground, 27, pp.235-245 (in Japanese with English abstract).
Lin, A., Shigetomi, M., Shimamoto, T., Miyata, T., Takemura, K., Tanaka, H., Uda, S. and Murata, A (1998): Neotectonic History and Activity of Nojima Fault looked at from fault rock, Earth Monthly "The scientific drilling programof Nojima fault", No.21 special issue, pp.208-212 (in Japanese).
Matsuda, T. (1967): Geological characteristics of Matsushiro earthquake fault., Bull. Earthq. Res. Inst. Univ. Tokyo., 45, pp.537-550 (in Japanese with English abstract).

Matsuda, T. (1973): The Median Tectonic Line as an active fault, Median Tectonic Line, Tokyo Univ. press, pp.239-251 (in Japanese).
Matsuda, T. (1975): Magnitude and reccurrence interval of earthquakes from a fault, Jour. Seis. Soc. Japan, 28, pp.269-283 (in Japanese with English abstract).
Matsuda, T. (1988a): Tertiary/Quarternary looked at from crustal movement. -The same outlook on The Quaternary crustal movement-, Earth Monthly, 10, 10, pp.599-603 (in Japanese).
Matsuda, T. (1988b): Mathematical nature of an active fault, Mathematics seismology III, The mathematics study result report of fractal and earthquake phenomenon, Mathematics society for the study of fractal and earthquake phenomenon, Institute of Statistical Mathematics, pp.174-184 (in Japanese).
Matsuda, T. (1990): Seismic zoning map of Japananese islands, with maximum magnitudes derived from active fault data, Bull. Earthq. Res. Inst. Univ. Tokyo., 65, pp.289-319. (in Japanese with English abstract).
Matsuda, T. (1998): Present State of Long-term Prediction of Earthquakes based on Active Fault Data in Japan -An Example for the Itoigawa-Shizuoka Tectonic Line Active Fault System-, Jour. Seismological soc. japan, 50, pp.23-33 (in Japanese with English abstract).
Matsuda, T., Nakamura, K. and Sugimura, A. (1978): Active fault and Neotectonic "Changing Earth I" Chapter 3, Iwanamikoza Earth science 10, Iwanami bookstore press, pp.89-157 (in Japanese).
Nagata, M., Tokunaga, T., Ishibashi, H. and Kashiwagi, T. (1997): Groundwater fluctuations in the northern part of Awaji Island after Hyogoken-Nanbu earthquake, '97 Ann. Mtg., Engineering Geol. Soc. Japan, p.237 (in Japanese with English abstract).
Nakamura, K. (1971): Study from Matsushiro earthquake, Kagakuasahi, 10, pp.127-133 (in Japanese).
Nakayama, K. (1987): The Seto Group and the Sanage-Chita uplift zone in the Vicinty of Mt. Sanage, Aichi Prefecture, Central Japan, Earth Science, 41, 2, pp.114-130 (in Japanese with English abstract).
Nohara, T., Watanabe, K., Tanaka, H., Takebe, A., Yamashita, M. and He, P. (1999): Fracture and permeability of crush zone and rock mass in the penetrating the Mozumi-Sukenobu fault, (in preparation) (in Japanese).
Ogata S. and Honsho, S. (1981): Fault activity evaluation in the case of electric power plants, Jour. Japan Soc. of Engineering Geology, 22,1, pp.67-87 (in Japanese with English abstract).
Okamoto, R., Ogata, M. and Kojima. K. (1984): New outline of civil engineering 14, Geotechtonics, Japan Soc. Civil Engineering ed., 71p. (in Japanese).
Okada, A. (1973): About fault activity of The Median Tectonic Line of Quaternary, Sugimura R., Median Tectonic Line, Tokyo Univ. press, pp.49-86. (in Japanese).
Okada, A. (1980a): Quaternary tectonism in the Pacific side of central Japan. -Change of tectonic process and migration of tectonic province-, Quaternary Research, 19 (3) pp.263-276 (in Japanese with English abstract).
Okada, A. (1980b): Characteristics and forming process the Median Tectonic Line Active Fault System, Earth Monthly, 2, 7, pp.510-517 (in Japanese).
Okada, A. (1986): Active faults and Subduction Zones in central Japan, Earth Monthly, 8, 12, pp.756-762 (in Japanese).
Okada, A. (1995): Simulated emprical law of coseismic crustal deformation., J. Phys. Earth., 43, pp.697-713.
Okumura, K., Sangawa, A., Sugai, T., Takada, M. and Soma, H. (1997): Integrated geological investigation of the Nara-Tenri fault zone, Main results of active fault research in 1996 fiscal year, pp.51-62 (in Japanese).

Olsson, W.A. (1992): The effect of slip on the flow of fluid through a fracture, Geoph. Research Lett. 19, 6, pp.541-543.
Onoda K., Kusuyama, T. and Yoshikawa, K. (1978): Damages of Izuoshima Kinkai earthquake 1 : an example from the railrode tunne, Tunnels and Underground, 9, pp.375-380 (in Japanese).
Otsuki, K. (1978): On the relationship between the width of shear zone and the diplacement along fault, Jour. Geol. Soc. Japan, 84, pp.601-619.
Ranalli, G. (1977): Correlation between length and offset in strike-slip faults, Tectonophysics, 37, pp.T1-T7.
Research Group for Active Faults of Japan (1991): Active Faults in Japan –Sheet maps and Inventories- (Revised Edition), University of Tokyo Press, 443p. (in Japanese).
Research Group for Active Submarine Faults off Tokai (1999): Active Submarine Fault off Tokai, Univ. of Tokyo Press, 151p.
Sangawa, A. (1978): Deformational topography and activity of the central and easten part of the Arima-Takatsuki Tectonic Line in Southwest Japan, Geographiical Review of Japan, 51, 10, pp.760-775 (in Japanese with English abstract).
Sangawa A. (1986): The new crustal movement of the central Kinki area, The monthly earth, 8, pp.752-755.
Sangawa, A., Mizuno, K. and Yamaguchi, S. (1987): Neotectonic Maps of Japan (1:500,000 scale), Geol. Survey of Japan (in Japanese).
Satake, H. and Murata, M. (1998): Groundwater fractuation near the fault , Earth Monthly, "Structure and movement of active fault", 3, pp.160-164 (in Japanese).
Satake, K., Sangawa, A. and Sugai, T. (1998): Trenching study of the Kongo fault system (supplementary research), Geol. Surv. Japan Interim Rep. no. EQ/98/1, pp.151-159 (in Japanese).
Satake, K., Sangawa, A. and Sugai, T. (1997): Integrated geological investigation of the Kongo fault system, Main results of active fault research in 1996 fiscal year., pp.63-72 (in Japanese).
Sato, H. and Hirata, N. (1998): Geostructure of active fault and formation of Japan arc, Science, 68, 1, pp.63-71 (in Japanese).
Sato,H., Ikeda, Y., Imaizumi, T. and Ikawa, T. (2000): Evolution of the Active Senya Thrust Faults, Northern Honshu, japan,Geoph. Res. Lett. (in press)
Sato, T. and Takahashi, M. (1997): Geochemical changes in anomalously discharged groundwater in Awaji Island -after the 1995 Kobe earthquake-, Geochemistry, 31, pp.89-98 (in Japanese with English abstract).
Sato, T., Sakai, R,. Ohsawa, H., Furuya, K., Kodama, T., (1999): Oxygen and hydrogen isotope ratio of the groundwater in which the after earthquake abnormally gushed in Awaji Island out, The Japan hydrology science bulletin, 29, 1, pp.13-24.
Shimizu, I., Osawa, H., Seo, T., Yasuike, S. and Sasaki, S. (1996): Earthquake-related ground motion and groundwater pressur change at the Kamaishi Mine. Eng.Geol., 43, pp.107-118.
Scholz, C.H. (1993): The Mechanics of Earthquakes and Faulting., Kokonshoin, 506p. (in Japanese).
Sugai, T., Sugiyama, Y., Matsumoto, N. and Tsukuda, E. (1997): Late Quaternary activity of the Yoro fault based on the analysis of a 451m core obtained by drilling at the foot of the Yoro Mountains, Geol. Surv. Japan Interim Rep. no. EQ/98/1, pp.67-74 (in Japanese with English abstract).
Sugimura, A. and Matsuda, T. (1965): Atera fault and its displacement vectors., Geol. Soc. Amer. Bull., 76, pp.509-522.
Suzuki, Y. (1988): Active tectonics and evolutional processes of the Shinjo and Yamagata

basins, northeast Japan, Geographical Review of Japan, 61, pp.332-349 (in Japanese with English abstract).

Tagami, T., Hasebe, N., Gamahara, H. and Takemura, K., (1998): Temrperature anomalies around the Nojima fault based on fission track thermochronology for 500m core samples, Earth Monthly, 21 special issue, pp.175-179 (in Japanese).

Takagi, H., Shibata, K., Sugiyama, Y., Utsumi, S. and Matsumoto, T. (1989): Isotopic ages of rocks along the Median Tectonic Line in the Kayumi area, Mie Prefecture., Jour.Min.Petrol.Econ.Geol., 84, pp.75-88 (in Japanese with English abstract).

Takamura, H. and Kawano, T. (1996): Trend of spring water and groundwater in the Awaji island After the 1995 Hyogo-ken -Nanbu earthquake., Hydrological Society, 4, pp.331-338 (in Japanese with English abstract).

Takemura, T. and Fujii, S. (1984): Active faults along the northern margin of the Hida mountains, Central Japan, Quaternary Research, 22, 4, pp.297-312. (in Japanese with English abstract).

Takemura, K., Murata, A., Miyata, T., Lin, A. and Hokada, C. (1997): Adescription of drilling core in "The scientific drilling program of Nojimafault" (stratigraphy and structure, age), Symposium of the scientificdrilling program of Nojima fault, p.155 (in Japanese).

Tanaka H., Higuchi, T., Hinoki,S ., Kosaka, K., Lin, A., Takemura, K., Murata, A. and Miyata, T. (1998): Deformation and alteration of fault rocks along the Ogura 500m core penetrating the Nojima Fault, Awaji Island, Southwest Japan, Earth Monthly "The scientific drilling program of Nojima fault", No.21 special issue, pp.160-164 (in Japanese).

Toda, S., Kawasaki, S., Mitamura, M., Nakagawa, K., Kagawa, T., Yokota, H., Kobayashi, Y. and Okada, A. (1997): Subsurface Stracture and Activities of the Yoro Fault.-Seismic Reflection Survey in Tado Town, Mie Prefecture, Central Japan-, Jour. Seismological soc. japan, 2, 49, pp.429-440. (in Japanese with English abstract).

Todo Collaborative Research Group (1994): Basin block movements of the Upper Cenozoic Second Setouchi Supergroup: an example from the Ena sedimentary basin, Earth Science, 48, 1, pp.17-29 (in Japanese with English abstract).

Togo, M., (1982): On the KochIen fault, "Various cross section of environmental science (The professor Mitsui sixtieth birthday festschrift)", Civil engineering Co., pp.146-152

Togo, M. and Ono, Y. (1994) : On the Tokachi active fault system and the activity characteristics, The Hosei Univ. Tama laboratory report, 9, pp.1-14.

Toyama Prefecture , Research Committee of the Active Fault (1997): Integrated geological survey of the Kurehayama fault in western Toyama Plain, central Japan, Ann. Mtg. Geol. Soc. Japan. p.303 (in Japanese).

Tsuneishi, Y. and Nakamura, K. (1970): Faulting associated with the Matsushiro Swarm Earthquakes, Bull. Earthq. Res. Inst., 48, pp.29-51 (in Japanese with English abstract)

Tsuneishi, Y. and Takahashi, H. (1975): Study on the earthquake generation in Matsushiro, Ann. Mtg. Geol. Soc. Japan. p.72 (in Japanese).

Tsuneishi, Y. (1984): Science of Geological Structure, eddited by Kimura T., Asakurashoten, pp.67-120 (in Japanese).

Uemura, Y. (1988): Deformational topography of the Mitoke fault system, southwestern part of Tanba high land, in Japan, Geographiical Review of Japan, 61 (Ser.A)-6, pp.453-468 (in Japanese with English abstract).

Uda, S., Hiyoshi, N., Miyagawa, J. and Rin, A. (1995): Hyogoken-Nanbu earthquake - geology, disaster-, Japan Soc.of Engineering Geology, Hanshin-Awaji earthquake committee 4.2 Northern part of Awaji island, pp.60-108 (in Japanese).

Uda, S., Rin, A. and Takemura K. (1998): The groudwater flow in the Nojima fractured fault

zone based on the observation of boring core samples, Earth Monthly, 21, pp.171-174 (in Japanese).
Vermilye, J.M. and Scholz, C.H. (1998): The process zone: A microstructural view of fault growth. J. Geophys. Res., Vol. 103, No. B6, pp.12223-12237.
Working Group for Compilation of 1:2,000,000 Active Fault Map (1999): Active Fault Map, The Active Fault Research, Vol.19 (in press) (in Japanese).
Yamaguchi,M. (1988):Formation process of active faults at eastern side of Kiso mountains, Abstract association of Japanese Geographers, pp.108-109 (in Japanese).
Yoshida,S. (1995): Hanaore Fault north of Kyoto and its activity, Chishitsu News, 489, pp.6-16 (in Japanese).

(2.4 Volcanism)

Aramaki, S. (1983): Outline: caldera. Monthly Earth, 5, pp.64-72 (in Japanese).
Aramaki, S. (rep. of the research group) (1993): Scale and characteristics of volcanic hazard. Chap.6. Volcanic hazard map, Results of research on "Prediction of natural disaster and social disturbance prevention", pp.251-326 (in Japanese).
Aramaki, S. (1996): Volcanic phenomenon, Cyclopedia of Earth Sciences, Heibonsha, 230p. (in Japanese).
Baker, D.R. and Eggler, D.H. (1983): Fractionation paths of Atka (Aleutians) high-alumina basalts: Constraints from phase relations, Jour. Volcanol. Geotherm. Res., 18, pp.387-404.
Bredehoeft, J.D. and Papadopulos, I.S. (1965): Rates of vertical groundwater movement estimated from the earth's thermal profile, Water Resources Research, 1, pp.325-328.
Committee for Catalog of Quaternary Volcanoes in Japan (Ui, T., Aramaki, S., Umeda, K., Kawachi, S., Kobayashi, T., Koyama, M., Sato, H., Takahashi, M., Chiba, T., Tsukui, M., Hayashi, S. and Yusa, Y.) ed. (1999): Catalogue of Quaternary Volcanoes in Japan (CD-ROM version) (in Japanese).
Furukawa, M. (1991): Tectonics of Ryukyu arc and earthquake swarm in Iriomote island, Monthly Earth, 13, pp.656-663 (in Japanese).
Geological Survey of Hokkaido (1995): Geothermal gradient map of Hokkaido (1:600,000) (in Japanese with English abstract).
Geological Survey of Japan (1992): Geological Map of Japan 3rd edition (1: 1,000,000) (in Japanese with English abstract).
Geological Survey of Japan and Coordinating Committee for Coastal and Offshore Geoscience Programs in East and Southeast Asia (CCOP) (1997): Heat flow map of East and Southeast Asia, 1:5,000,000 Miscellaneous Map Series 36, Geological Survey of Japan.
Hart, S.R. (1964): The petrology and isotopic-mineral age relations of a contact zone in the Front Range, Colorado. J. Geol., 72, pp.493-525.
Hasegawa, A. and Matsumoto, S. (1997): Deep Structure of Nikko-Shirane Volcano Group in the Northeastern Japan Arc Estimated from Seismic Observations, Bulletin of the Volcanological Society of Japan, 42, pp.S147-155 (in Japanese with English abstract).
Hayakawa, Y. and Koyama, M. (1992): Eruptive History of the Higashi Izu Monogenetic Volcano Field 1: 0-32 ka., Bulletin of the Volcanological Society of Japan, 37, pp.167-181 (in Japanese with English abstract).
Hayashi, S., Umeda, K., Ban, M., Sasaki, M., Yamamoto, M., Ohba, T., Akaishi, K. and Ohguchi, T. (1996): Temporal and spatial distribution of Quaternary volcanoes, northeastern Japan (1) -Spreading of volcanic area toward back-arc side-, Volcano Society Abstract of the 1996 Meeting of Japan., 2, p.88 (in Japanese).
Hirose, W. and Nakagawa, M. (1999): Neogene volcanism in Central-Eastern Hokkaido: Beginning and evolution of arc volcanism inffered from volcanological parameters and

geochemistry, Jour. Geol.Soc. Japan, 105, pp.247-265 (in Japanese with English abstract).
Horton, C.W. and Rogers, F.T. (1945): Convection currents in a porous medium, Jour. Appl. Phys., 16, pp.367-370.
Ishizuka, O., Uto, K., Yuasa, M. and Hochstaedter, A. (1999): Magmatism in the back arc region of Izu-Ogasawara arc -Change of magmatism caused by rifting-, Earth Monthly (Special Issue), 23, pp.89-98 (in Japanese).
Iwamori, H. (1992): Degree of melting and source composition of Cenozoic basalts in Southwest Japan; evidence for mantle upwelling by flux melting, Jour. Geophys. Res., B97, pp.10983-1099.
Kagiyama, T. (1997): Experiment on Volcanic Structure and Magma Supply System for Prediction of Volcanic Eruption, Bulletin of the Volcanological Society of Japan, 42, pp.115-118 (in Japanese).
Kamata, H. (1992): Right-lateral movement of the Oita-Kumamoto Tectonic Line as a western extension of the Median Tectonic Line, originated from rightward, oblique subduction of the Philippine Sea plate, Mem. Geol. Soc. Japan, 40, pp.53-63 (in Japanese with English abstract).
Kamo, K., Nishi, K., Iguchi, M., Furuzawa, T., Teraishi, M., Kagiyama, T., Yamaguchi, M., Takagi, A., Kakuta, T., Ono, H., Sudo, Y., Matsuo, N. and Shimizu, H. (1990): A Joint Study of Earthquakes in the Kyushu Region Using Data from the Universities' Seismic Networks, Journal of the Seismological Society of Japan, 43, pp.543-545 (in Japanese).
Kaneoka, I. (1998): Numerical Dating -From a Decade to 46 Hundred Million Years Ago-, University of Tokyo Press, pp.1-315 (in Japanese).
Kato, M., Kawakami, Y., Hanano, M. and Tominaga, Y. (1996): Velocities of convective ascending flow in several geothermal fields -Analyses based on static temperature logging data-, Abstracts with Programs of 1996 Annual Meeting of Geothermal Research society of Japan, p.A33 (in Japanese).
Kimura, M. (1983): Formation of Okinawa Trough grabens, Mem. Geol. Soc. Japan, 22, pp.141-157 (in Japanese with English abstract).
Kimura, M., Isezaki, N., Furukawa, M. and Ishihara, T. (1985): Geomagnetic Anomalies in the Middle Okinawa Trough, Journal of Geography, 94, pp.156-169. (in Japanese with English abstract).
Komatsu, R., Umeda, K., Saito, H., Tanase, A. and Nagao, T. (1997): Influence of eruption on geological environment (Part2) -Thermal history of rock mass around source vent-, Programme and Abstracts of the Volcanological Society of Japan, p.98 (in Japanese).
Komatsu, R., Umeda, K., Tanase, A. and Danhara, T. (1998): Thermal history of the Takanawa tonalite, Ryoke belt, after magma intrusion, Program and Abstracts of the Volcanological Society of Japan, p.100 (in Japanese).
Komatsu, R.and Umeda, K. (1999): Hot springs and hydrothermal alteration zones in Japan, JNC Technical Review, 4, pp.121-128 (in Japanese with English abstract).
Kondo, H., Kaneko, K. and Tanaka, K. (1998): Characterization of spatial and temporal distribution of volcanoes since 14 Ma in the Northeast Japan arc, Bull. Volcano. Soc. Japan, 43, pp.173-180.
Koyama, M., Hayakawa, Y. and Arai, F. (1995): Eruptive History of the Higashi-Izu Monogenetic Voldano Field 2: Mainly on Volcanoes Older than 32,000 Years Ago, Bull. of the Volcanological Society of Japan, 40, pp.191-209 (in Japanese with English abstract).
Laslett, G.E., Green, P.F., Duddy, I.R. and Gleadow, A.J. (1987): Thermal annealing of fission tracks in apatite, 2, A quantitative analysis, Chem. Geol., 65, pp.1-13.
Matsubayashi, O., Okubo, Y., Yamazaki, T., Joshima, M. and Miyazaki, T. (1992): Heat flow and Curie point depth map of Japan and adjoining areas, scale 1:5,000,000, Geological

Atlas of Japan (Second Edition), Geological Survey of Japan (in Japanese with English abstract).
Matsumoto, Y. (1979): Problems on the volcanic activity and collapse structure in Kyusyu district, Mem. Geol. Soc. Japan, 16, pp.127-139 (in Japanese with English abstract).
Moriya, I. (1993): Long-term prediction of the beginning, scale, type and process of eruption estimated from the past volcanic activity, Scale and characteristics of volcanic hazard, Results of research on "Prediction of natural disaster and social disturbance prevention", pp.5-14 (in Japanese).
Nakagawa, M., Maruyama, H. and Funayama, A. (1995): Distribution and Spatial Variation in Major Elememt Chemistry of Quaternary Volcanoes in Hokkaido, Japan, Bulletin of the Volcanological Society of Japan, 40, pp.13-31 (in Japanese with English abstract).
Nakamura, K. (1969): Arrangement of parasitic cones as a possible key to regional stress field, Bulletin of the Volcanological Society of Japan, 14, pp.8-20 (in Japanese with English abstract).
National Astronomical Observatory (ed.) (1997): Chronological Scientific Tables. Maruzen, 1043p. (in Japanese).
NEDO (New Energy and Industrial Technology Development Organization) (1991): Fluid geochemistry survey report, Bandai area, geothermal resources synthetic exploration in Japan (3rd period), 226p. (in Japanese).
Nimis, P. (1995): A clinopyroxene geobarometer for basaltic systems based on crystal structure modeling, Contrib. Mineral. Petrol., 121, pp.115-125.
Nishimura, A. and Yuasa, M. (1991): Sumisu Backarc Rift in the Izu-Bonin Intra-oceanic Arc of the Western Pacific, Earth Science, 45, pp.333-344 (in Japanese with English abstract).
Nishimura,S. and Mogi,T. (1986) The Interpretation of Discordant Ages of Some Granitic Bodies. Jour. Geotherm. Res. Soc. Jap., 8, pp.145-164.
Noda, T. (1987): Anion Index as an Indicator of Geothermal Activity, Journal of the Geothermal Research Society of Japan, 9, pp.133-141 (in Japanese with English abstract).
Noda, T. and Takahashi, M. (1992): Geochemical classification of source waters relating to geothermal system, Chikyukagaku (Geochemistry), 26, pp.63-82 (in Japanese with English abstract).
Ohba, T. and Umeda, K. (1999): Geology of Hachimantai volcanic field and temporal-spatial variation of the magma compositions, J. min. Petr. Econ. Geol., 94, pp.187-202 (in Japanese with English abstract).
Ohguchi, T., Yoshida, T. and Okami, K. (1989): Historical change of the Neogene and Quaternary volcanic field in the Northeast Honshu Arc, Japan, Mem. Geol. Soc. Japan, 32, pp.431-455 (in Japanese with English abstract).
Oishi, A., Muramatsu, Y., Yoshida, Y. and Hashizume, R. (1995): Hydrothermal Activity in Hongu Area, Wakayama Pref., Based on the Fluid Inclusion Geothermometry, Hot Spring Science, 45, pp.63-75 (in Japanese with English abstract).
Okubo, Y. (1993): Temperature Gradient Map of the Japanese Islands, Journal of the Geothermal Research Society of Japan, 15, pp.1-21 (in Japanese with English abstract).
Okubo, Y., Akita, F. and Tanaka, A. (1998): Thermal Gradient Map and Thermal Structure Model -A Case Study of Hokkaido-, Journal of the Geothermal Research Society of Japan, 20, pp.15-29 (in Japanese with English abstract).
Pollitz, F.F. (1986): Pliocene change in Pacific plate motion, Nature, 320, pp.738-741.
Robertson, J.K. and Wyllie, P.J. (1971): Rock-water system, with special reference to the water-deficient region, Am. Jour. Sci., 271, pp.252-277.
Sakamoto, M., Sano, Y. and Wakita, H. (1992): $^{3}He/^{4}He$ ratio distribution in and around the Hakone volcano, Geochemical Journal, 26, pp.189-195.
Sano, Y. (1988): Helium isotope ratios and techtonics, Chikyukagaku (Geochemistry), 22,

pp.1-11 (in Japanese with English abstract).
Sato, H. and Yoshida, T. (1993): Formation of large collapse calderas and tectonics. Earth Monthly, 15, pp.721-724 (in Japanese).
Seo, T. and Shimizu, K. (1992): Literature survey and analysis of groundwater geochemistry in Japan, PNC Technical Report, PNC-TN7410, 92-017 (in Japanese).
Shuto, K., Ohki, J., Yamamoto, K. and Watanabe, N. (1993): Evolving the continental arc volcanism into the island arc one -Temporal variation of the Tertiary volcanism in the Northeast Japan arc-, Chishitsu News, 464, pp.6-18 (in Japanese).
Smith, W.H.F. and Wessel, P. (1990): Gridding with continuous curvature splines in tension, Geophysics, 55, pp.293-305.
Sugimura, A. (1960): Zonal arrangement of some geophysical and petrological features in Japan and its environs. Jour. Fac. Sci. Univ. Tokyo, Sec. 2, 12, pp.133-153.
Sumi, K. (1980): Relationship between the distributions of the Quaternary volcanoes and the rate of heat discharge by hot water in Japan, Bull. Geol. Surv. Japan, 31, pp.255-266 (in Japanese with English abstract).
Tada, T. (1984): Spreading of the Okinawa Trough and its Relation to the Crustal Deformation in Kyusyu, Journal of the Seismological Society of Japan, 37, pp.407-415 (in Japanese with English abstract).
Tagami, T. and Shimada, C. (1996): Natural long-term annealing of the zircon fission track system around a granitic pluton, Jour. Geophys. Res., 101, B4, pp.8245-8255.
Takahashi, E. and Takahashi, M. (1995): What decides the deep structure of arc volcanoes? Iwanami Kagaku (Science), 65, pp.638-647 (in Japanese).
Takahashi, M. (1995): Classification of Deep-seated Hydrothermal Systems with Their Heat Sources and Geochemical Characteristics, Jour. Japanese Association Hydrol. Sci., 27, pp.95-103 (in Japanese with English abstract).
Takahashi, M. (1986): Island arc magmatism around the time of spreading of Japan Sea, Iwanami Kagaku (Science), 56, pp.103-111 (in Japanese).
Takahashi, M. (1994a): Structure of Polygenetic Volcano and Its Relation to Crustal Stress Field –1, Stable and Unstable Vent Types, Bulletin of the Volcanological Society of Japan, 39, pp.191-206 (in Japanese with English abstract).
Takahashi, M. (1994b): Structure of Polygenetic Volcano and Its Relation to Crustal Stress Field -2. P-type, O-type Volcano, Bulletin of the Volcanological Society of Japan, 39, pp.207-218 (in Japanese with English abstract).
Takahashi, M. (1995): Large-volume Felsic Volcanism and Crustal Strain Rate, Bulletin of the Volcanological Society of Japan, 40, pp.33-42 (in Japanese with English abstract).
Takahashi, M. (1997): The Structure of High Level Crustal Magmatic Plumbing Systems Beneath the Quaternary Arc Volcanoes in Japanese Islands, Bulletin of the Volcanological Society of Japan, 42, pp.S175-187 (in Japanese with English abstract).
Tamanyu, S. (1994): Magma reservoirs from the viewpoint of geothermal modling -Examples from the Hohi, Sengan and Kurikoma geothermal areas in Japan, Mem. Geol. Soc. Japan, No.43, pp.141-155 (in Japanese with English abstract).
Tanaka, A., Yano, Y., Sasada, M., Okubo, Y., Umeda, K., Nakatsuka, N. and Akita, F. (1999): Thermal gradients up to borehole depths in Japan, Bull. Geol. Surv. Japan (in Japanese with English abstract).
Tatsumi, Y. (1995): Subduction Zone Magmatism -A Contribution to Whole Mantle Dynamics-, University of Tokyo Press, pp.1-186 (in Japanese).
Taylor, B., Klaus, A., Glenn, R.B., Moore, G.F., Okumura, Y. and Murakami, F. (1991): Structural Development of Sumisu Rift, Izu-Bonin Arc, Jour. Geophys. Res., 96, pp.16113-16129.
The Japan Society of Mechanical Engineers (1980): JSME Steam Tables, pp.1-124 (in

Japanese).
Tomiya, A. (1995): Thermal effect on the distribution of inland earthquakes caused by magma supply system -application to the Nikko-Shirane volcano-, Earth Monthly, 17, pp.107-112 (in Japanese).
Ui, T. (ed.) (1997): Volcanic Hazards, University of Tokyo Press, pp.1-219 (in Japanese).
Ujiie, H. (1996): Tectonic of Ryukyu arc and environment around coral reef -geological history of Ryukyu islands-, Nature in Japan 8, South-western islands (Nakamura et al. eds.), pp.112-126 (in Japanese).
Ukawa, M. (1994): Ascending of magma estimated from seismic observations below Fuji volcano, Iwanami Kagaku (Science), 64, pp.570-581 (in Japanese).
Umeda, K., Kusanagi, M., Furusawa, A. and Ui, T. (1996): Holocene Eruptive Activity of Yufu-Tsurumi Volcano Group Found from Piston Cores in Beppu Bay, Central Kyushu, Bulletin of the Volcanological Society of Japan, 41, pp.61-71 (in Japanese with English abstract).
Umeda, K., Nakatsuka, N. and Yusa, Y. (1998): Long-term stability of geological environment -a viewpoint of the study on volcanic activity-, 1998 Fall Meeting of the Atomic Energy Society of Japan, Vol.III, p.829 (in Japanese).
Umeda, K. (1999): Heat discharge and geochemical data of hot springs in volcanic areas, Abstracts 1999 Japan Earth and Planetary Science Joint Meeting Sc-005 (in Japanese).
Umeda, K., Komatsu, R and Nakatsuka,N. (1999a): Geothermal Structure Based on Temperature Logging Data of Boreholes in Japan, JNC Technical Review, 2, pp.29-36 (in Japanese with English abstract).
Umeda, K. Komatsu, R. and Ehara, S. (1999b): Velocity of hydrothermal fluid and heat flow in geothermal fields based on borehole temperature data, Journal of the Japan Geothermal Energy Association, 36, pp.219-237 (in Japanese with English abstract).
Umeda, K., Hayashi, S., Ban, M., Sasaki, M., Ohba, T. and Akaishi, K. (1999c): Sequence of the Volcanism and Tectonics during the Last 2.0 Million Years along the Volcanic Front in Tohoku District, NE Japan. Bulletin of the Volcanological Society of Japan, 44, 233-249. (in Japanese with English abstract)
Umeda, K., Komatsu, R. and Yusa, Y. (1999d): Cooling history of the Matsuyama granodiorite and thermal effect of Neogene intrusive rocks in the Ryoke belt, Southwest Japan Arc, Jour. Min, Petrol. Econ. Geol. (in press) (in Japanese with English abstract)
Uto, K. (1995): Volcanoes and Age Determination -Now and Future of K-Ar and $^{40}Ar/^{39}Ar$ Dating-, Bulletin of the Volcanological Society of Japan, 40, pp.S27-46 (in Japanese with English abstract).
Uto, K. and Tatsumi, Y. (1996): Quaternary volcanism of the Japanese Islands, The Island Arc, 5, pp.250-261.
Wakita, H., Sano, Y. and Mizoue, M. (1987): High 3He emanation and seismic swarms observed in a nonvolcanic forearc region, J. Geophys. Res., 92, pp.12539-12546.
Watanabe, K., Izawa, E., Hashimoto, S. and Kagami, H. (1997): Magmatism and tectonics in southern Kyushu, Japan, Abstracts 1997 Japan Earth and Planetary Science Joint Meeting, p.679 (in Japanese).
Watanabe, Y. (1994): Miocene volcanism and tectonics in northeast Hokkaido -Why did the volcanism shift southward?-, Chishitsu News, 483, pp.6-14 (in Japanese).
Wessel, P. and Smith, W.H.F. (1995): New version of the Generic Mapping Tools released, Eos Trans. AGU, 76(33), p.329.
White, D.E. (1957): Thermal waters of volcanic origin, Bull. Geol. Soc. Am., 68, pp.1637-1658.
Yamada, R., Tagami, T., Nishimura, S. and Ito, H. (1995): Annealing kinetics of fission tracks in zircon: an experimental study, Chem. Geol., 122, pp.249-258.

Yamano, M., Kinoshita, M. and Yamagata, T. (1997): Heat flow distribution around the Japanese Islands, Chishitsu News, 517, pp.12-19 (in Japanese).
Yamazaki, F. and Ooida, T. (1985): Configuration of Subducted Philippine Sea Plate beneath the Chubu District, Central Japan, Journal of the Seismological Society of Japan, 38, pp.193-201 (in Japanese with English abstract).
Yano, Y. and Muraoka, H. (1986): Well databese system, Rept. Geol. Surv. Japan, No.265, pp.69-190 (in Japanese with English abstract).
Yano, Y., Okubo, Y. and Shibuya, A. (1994): Temperature Gradient Map of the Japanese Islands Based on Borehole Logging Data. Proceedings of the 91st SEGJ Conference, pp.153-156 (in Japanese).
Yano, Y., Tanaka, A., Takahashi, M., Okubo, Y., Sasada, M., Umeda, K. andNakatsuka, N. (1999): Geothermal gradient map of Japan, Geological Survey of Japan (in Japanese with English abstract).
Yokose, H., Kikuchi, W., Nagao, K. and Kodama, K. (1998): K-Ar ages for the Yahazudake volcanic rocks from southwest Kyushu, Japan, Jour. Min, Petrol. Econ. Geol., 93, pp.151-161 (in Japanese with English abstract).

(2.5 Uplift, subsidence and denudation)

Akojima, I. (1983): Comparison between the past and the present denudation rate of Mountainsaround the Yamagata Basin, Northeast Japan, Trans. Japanese, Geomorp. Union, 4, pp.97-106 (in Japanese with English abstract).
Ashida, K. and Okumura, T. (1974): Study on sedimentation in dams, Ann. Rep. Disaster Prevention Research Institute Kyoto Univ., 17-B. pp.1-16 (in Japanese).
Ashida, K., Takahashi, T. and Dojo, M. (1983): Debris flow disaster of rivers and their counterplans, Morikita Press, 260p. (in Japanese) .
Association for the Geological Collaboration in Japan (ed.) (1996): Chigaku jiten, Heibonsha, 1443p. (in Japanese).
Awata, Y., Osawa, A. and Katahira, S. (1986): Geological sections of Japan, Sea coast, Akita Prefecture, Northeast Japan, In Kitamura, N. ed. Geological data of Cenozoic Northeast Japan, 2 (in Japanese).
Aubrey, D.G. and Emery, K.O. (1986): Relative sea levels of Japan from tide-gauge records, Geological Soc. America Bull., 97, pp.194-205.
Chigira, M. (1988):Chemical weathering of mud rocks-a example of Pleistocene Haizume formation, Niigata Prefecture-, Jour. Geol. Soc. Japan, 96, pp.419-431 (in Japanese with English abstract).
Chigira, M. (1995): Weathering and Degradation, Kinmiraisha , 204p. (in Japanese).
Committee of Engineering Geological Map of Hokuriku District (1991): Geological map and Explanatory Manual of Engineering Geological Map of Hokuriku District, 799p. (in Japanese).
Committee of Engineering Geological Map of Kanto District (1996): Geological map and Explanatory Manual of Engineering Geological Map of Kanto District, 768p. (in Japanese).
Committee of ground research, Kansai ground data conference(1998): Ground Map of Kansai district (New Ed.), 270p. (in Japanese).
Danhara, T.(1971): Synthetic vertical movements in Japan during the recent 70 years, Jour. Geodetic Soc. Japan, vol.17,pp.100-108 (in Japanese with English abstract).
Development committee of the mining industry in Hokkaido (1979): Oil and natural gas resources in Hokkaido, Mining Group of natural Gas 205p. (in Japanese).
El-Fiky, G.S., Kato, T. and Fujii, Y. (1996): Vertical crustal movement in the Tohoku District,

Japan, deduced from dynamic adjustment of leveling and tidal data, Bull. Earthquake Res. Inst., Univ. Tokyo, 71. pp.47-71.
Endo, H. and Suzuki, Y. (1986): Geology of the Tsuma and Takanabe districts, Quadrangle Series. Scale 1:50,000, Geol. Surv. Japan, 105p. (in Japanese with English abstract).
Fujii, S.(1992): The Toyama Plain, Urban Kubota, vol.31, pp.38-47 (in Japanese).
Fujita, K.(1995): In Oba, T., Chinzei, K. and Fujita, K. eds., Nature in Japan 5, Kinki, Iwanami Shoten, pp.5-7 (in Japanese).
Fujita,K. and Oike,K.(1981):Neotectonics and Seismicity of Honshu Arc., Iwanami Kagaku (Science), 51, pp.704-711 (in Japanese).
Fujioka, K., Osawa, A., Takayasu, T. and Ikebe, Y. (1977) Geology of the Akita district, Quadrangle Series, Scale 1:50,000, Geol. Surv. Japan, 75p. (in Japanese with English abstract).
Fujiwara, O., Masuda, F., Sakai, T., Okazaki, H., Saito, A. and Suzuki, T.(1996): Uplifting examined by the late Pleistocene beach deposits in the northern area of the Boso Peninsula, central Japan, Jour. Geol. Soc. Japan, 43, pp.39-46 (in Japanese with English abstract).
Fujiwara, O., Masuda, F., Sakai, T. Fuse, K. and Saito, A. (1997): Tsunami deposits in Holocene bay-floor mud and uplift history of the Boso and Miura Peninsulas, Quat. Res., 36, pp.73-86 (in Japanese with English abstract).
Fujiwara, O., Masuda, F., Sakai, T., Irizuki, T. and Fuse, K. (1999a): Holocene Tsunami deposits detected by drilling in drowned valleys of the Boso and Miura Peninsulas, The Quat. Res., 38, pp.41-58 (in Japanese with English abstract).
Fujiwara, O., Masuda, F., Sakai, T., Irizuki, T. and Fuse, K. (1999b): Bay-floor deposits formed by great earthquakes during the past 10,000 yrs, near the Sagami Trough, Japan, The Quat. Res., 38, pp.489-501 (in Japanese with English abstract).
Fujiwara, O., Masuda, F., Sakai, T., Irizuki, T. and Fuse, K. (1999c): Tsunami deposits in Holocene bay mud in southern Kanto region, Pacific coast of central Japan, Sedimentary Geology (in press).
Fujiwara, O., Sanga, T. and Ohmori, H. (1999d): Regional distribution of erosion rates over the Japanese islands, JNC Technical Review, 5, pp.85-93 (in Japanese with English abstract).
Fukuzawa, H. (1987): The site of sedimentation of Late Neogene bedded siliceous rocks in northern Hokkaido, Japan, Jour. Geological Soc. Japan, 93, pp.37-55 (in Japanese with English abstract).
Geographical Survey Institute (1997): Horizontal Strain of Japan II, 1994-1983.
Hase, Y. and Iwauchi, A. (1993): Displacement of the depressed areas in the graben, estimated by the altitude of the inland sediments in central Kyushu, Japan, Mem. Geol. Soc. Japan, 41, pp.53-72 (in Japanese with English abstract).
Ichihara, M.(1993): The Osaka Group, Sogensha, 340p. (in Japanese).
Iikawa, K.(1983): Recent crustal deformation in relation to the topography in the Uonuma region, Niigata Prefecture, central Japan, Monograph of the Assoc. Geol. Collaboration, Japan, no. 26, pp.151-158 (in Japanese with English abstract).
Iikawa, K(1991): Geodetic survey of central Honshu, Japan. Monograph ,Assoc. Geol. Collab. Japan, 39, pp.1-72 (in Japanese with English abstract).
Iikawa, K. and Horikawa, H. (1985): On the deformation of the alluvial terrace plain in Ojiya, central Japan, Earth Science, 39, pp.296-298 (in Japanese with English abstract).
Ikebe, Y., Ozawa. A. and Inoue, H. (1979): Geology of the Sakata district, Quadrangle Series. Scale 1:50,000, Geol. Surv. Japan, 42p. (in Japanese with English abstract).
Ikeda,Y.(1990):Uplift of mountains by faults. In Yonekura, N., Okada, A. and Moriyama, A. eds., Tectonic Landforms, Kokonshoin, pp.45-59 (in Japanese).

Ikeda, Y. (1996): Observed geographical facts of Hida Mountains, Chikyu Monthly, 18, pp.72-76 (in Japanese).

Inoue, D., Kakuda, T., Kawamura, K. and Tomori, M. (1992): An examination of slope failure characteristics and their relationships with geology and reservoir sedimentation in Japan, Part 1: relationships between slope failure characteristics and geology, Journal of the Japan society of engineering geology, 33, pp.123-132 (in Japanese with English abstract).

Ishibashi, K., Ota, Y. and Matsuda, T. (1982): Holocene marine terraces and vertical crustal movement of Hatsushima Island in Sagami Bay, Jour. Seismo. Soc. Japan, Second Ser., 35, pp.195-212 (in Japanese with English abstract).

Ishii, H. (1989): Recent abnormal uplift on the Izu Peninsula (1980-1988), Bull. Earthq. Res. Inst. Univ. Tokyo, vol.64, pp.313-324 (in Japanese with English abstract).

Ishii, H. (1991): Comments on Abnormal subsidence in the Izu Peninsula appeared in the paper by Kuwayama and Fujii, Jour. Seismo. Soc. Japan, Second Ser., 44, pp.49-52 (in Japanese with English abstract).

Iso, N., Yamakawa, K., Yonezawa, H. and Matsubara, T. (1980): Accumulation rates of alluvial cones, constructed by debris-flow deposits, in the drainage basin of the Takahama river, Gifu Prefecture, central Japan, Geographical Review of Japan, 53, p.699-720 (in Japanese with English abstract).

Japan Assoc. Quaternary Research (1987): Explanatory text for Quaternary Maps of Japan, University of Tokyo Press, 119p. (in Japanese).

Kaizuka, S. (1968): Distribution of Quaternary fold, especially rate and axis direction in Japan, Geogr. Rept. Tokyo Metropol. Univ., 3, pp.1-9.

Kaizuka, S. (1969): Landform development by tectonics and climate change, Iwanami Kagaku (Science) , 39, pp.11-19 (in Japanese).

Kaizuka, S. (1987): Quaternary crustal movements in Kanto, Jour. Geogr., 96, pp.51-68 (in Japanese with English abstract).

Kaizuka, S. (1998): Historical geography, University of Tokyo press, 286p. (in Japanese)

Kaizuka, S. and Imaizumi, T. (1984): Horizontal strain rate of the Japanese islands estimated from Quaternary fault data, Geogr. Rep. Tokyo Metropol. Univ., 19, pp.43-65.

Kaizuka, S., Chinzei, K., Koaze, T., Iozawa, T. Matsuda, T. and Huzita, K. (1995): Nature in Japan 2, -Japanese mountains-, Iwanami Shoten, 277p. (in Japanese).

Kakimi, T., Kinugasa, Y. and Kimura, M. (1973): Neotectonic Map of Tokyo, Scale 1:500,000. Geol. Surv. Japan (in Japanese with English abstract).

Kanmera, K. (1995): When the Kyushu mountains uplifted ? In Uchijima, Z., Kan'mera, K., Tagawa, H. and Kobayashi, S.(eds.): Nature in Japan, Areal version, no.7, Kyushu district", Iwanami Shoten , pp. 60-63 (in Japanese).

Kaseno, Y. (1992): The Kaga plain, Urban Kubota, 31, pp.48-55 (in Japanese).

Kaseno, Y., Miura, S. and Fujii, S. (eds.)(1988): Geology of Japan 5, Chubu district 1, Kyoritushuppan, pp.144-146 (in Japanese).

Kato, T. (1984): Vertical crustal movements in the Tokai district, central Japan, The Quat. Res., 23, pp.111-116 (in Japanese with English abstract).

Kato, T. and Tsumura, K. (1979): Vertical land movement in Japan as deduced from tidal record, (1951-1978), Bull. Eathq. Res. Inst., 54, pp.559-628 (in Japanese with English abstract).

Kayane, T. and Yoshikawa, T. (1986): Comparative study between present and emergent erosional landforms on the southeast coast of Boso Peninsula, Central Japan, Geogr. Rev. Japan, 59A, pp.18-36 (in Japanese with English abstract).

Kido, M. (1993): Tectonic history of the north-western area of "Kuju-Beppu Graben", Mem. Geol. Soc. Japan, 41, pp.107-127 (in Japanese with English abstract).

Kimiya, K. (1975): Rate of weathering of gravels of Granitic rocks in Mikawa and Tomikusa areas, Jour. Geol. Soc. Japan, 81, pp.683-696 (in Japanese with English abstract).
Kimiya, K. (1981): Distribution of weathering crust and their formative period in the Mikawa Highland, Central Japan, Jour. Geol. Soc. Japan, 87, pp.91-102 (in Japanese with English abstract).
Kimiya, K. (1992): Estimation of weathering and alternation for construction work, no.3. Soil and foundations, 40, pp.67-74 (in Japanese).
Kira, H. (1982): Sand Sedimentation on Dam and its counterplans, Morikita Press, 392pp. (in Japanese).
Kitamura, N. (ed.)(1986): Geological database of the Cenozoic in the Northeast Japan Arc, Houbundo (in Japanese).
Koaze, T. (1994): Japan and its nature, Areal Ed. no.1, Hokkaido, Fukuda,M., Isijo,K., Sakai,A., Sakuma,T. and Kikuchi,K. (eds.), Iwanami Shoten, pp.1-26 (in Japanese).
Koike, K. and Machida, H. (eds.) (1999): Quaternary marine terrace atlas, University of Tokyo Press. (in press) (in Japanese).
Kojima, K.(1992): Estimation of weathering and alternation for construction work, no3. Soil and foundations no.2, Recognition of weathering and alternations, Soil and foundations. vol.40, pp.65-70 (in Japanese).
Kumai, H. (1997): History of Lake Suwa, Urban Kubota, 36, pp.2-11 (in Japanese).
Kuwahara, T. and Makinouchi, T. (1989): Characteristics of tilted basins - A case in the Nobi tilting basin, central Japan, Earth Science, 43, pp.354-365 (in Japanese with English abstract).
Machida, H. (1984): Large-scale rockslide, avalances and related phenomena: A short review, Trans. Japanese geomorph. Union, 5, pp.155-178 (in Japanese with English abstract).
Machida, H., Furuya, T., Nakamura, S. and Moriya, I. (1987): Large-scale landslide of Japan, In Shindo, S. (Chief sccientist) Study on natural disasters (1) , Report for grant-in-aid for scientific research, pp.165-182 (in Japanese).
Maemoku, H. and Tsubono, K. (1990): Holocene crustal movement in southern part of Kii Peninsula, Outer zone of Southwest Japan, Jour. Geogr., 99, pp.349-369 (in Japanese with English abstract).
Masuda, F. (1993): Osaka Group and relative sea-level changes -rhythmic alternation of marine and non-marine sedimentation, Chikyu Monthly, Extravol. 8, pp.86-94 (in Japanese).
Masuda, F. (1998):Dynamic stratigraphy based on highly dense data of ^{14}C ages in the Holocene, Jour. Geogr. 107, pp.713-727 (in Japanese with English abstract).
Masuda, F. and Nakazato, H.(1988): Uplift activities of Kashima-Boso Uplift Zone deduced from sedimentary facies, Chikyu Monthly, 10, pp.616-623 (in Japanese).
Matsuda, T. (1984): Northward-convex structure in South Fossa Magna and Collision of Izu Block, Quat. Res., 23, pp.151-154 (in Japanese with English abstract).
Matsukura, Y. (1994): A Review of the Studies on Rock Control in Weathering Processes, Trans. Japanese Geomorph. Union, 15, pp.203-222 (in Japanese with English abstract).
Matsukura, Y. (1997): Weathering Rates of Bedrocks in Artificial and Natural Slopes, Jour. Japan Soc. Engineering Geology, 38, pp.224-231 (in Japanese with English abstract).
Matsuoka, I, Akutsu, J., Manabe, K. and Takeuchi, S. (1984): Quaternary deposits of Yamagata basin- Time-stratigraphy classification and sedimentary environment of the deposits, Jour. Geol. Soc. Japan, 90, pp. 531-549 (in Japanese with English abstract).
Matsuzawa, I., Matsui, M., Kondo, Y., Segawa, S., Tanaka, M. and Kokubo, K. (1981): Geology of the Obihiro district, Quadrangle Series, Scale 1:50,000, Geol. Surv. Japan, 82p. (in Japanese with English abstract).
Mii, H. (1962): Coastal geology of Tanabe Bay, Sci. Rep. Tohoku Univ.(geology), 34(1),

pp.1-93.
Miyashita, K. (1989): Vertical surface displacements in Southwest Japan, estimated from leveling data. Jour. Seismological Soc. Japan, Ser.2, 42, pp.189-197 (in Japanese with English abstract).
Miyauchi, T, (1988): Correlation and chronology of the Late Pleistocene marine terraces in northern Northeast Japan, Geographical Review of Japan, 61(Ser A), pp.404-422 (in Japanese with English abstract).
Miyauchi, T (1990): Late Quaternary folding deduced from marine terrace deformation in the northern Northeast Japan arc, Geogr. Rep. Tokyo Metropl. Univ., 25, pp.99-108.
Miyawaki, M. and Fujiwara, O.(1997): Erosion rates of Quaternary terraces and lava plateaus estimated from the degree of dissection, Abstract 1997 Japan Earth and Planetary Science Joint Meeting., p.600 (in Japanese).
Miyazaki, Y. and Onishi, S. (1994): The yearly changes in reservoir sedimentation and specific sedimentation, Jour. Japan Soc. Civil Eng., 497, pp.81-90 (in Japanese with English abstract).
Miyoshi, M., Ota, Y., Sawa, H., Imaizumi, T. and Kashima, K. (1985): Holocene marine terraces of Okushiri Island, off the western Hokkaido, Japan, Geographical Review of Japan, 58(Ser A), pp.596-608 (in Japanese with English abstract).
Mizoue, M., Nakamura, K. and Izutsuya, S.(1980): Mode of crustal movements as deduced from the precise relevelings in the Ojiya Active Folding Area, Niigata Prefecture, Northeast Japan, Bull. Earth Res., 55, pp.199-224 (in Japanese with English abstract).
Moriyama, A. (1987): Geomorphology and crustal movements in the drainage basins of the Kiso and Yahagi rivers, Central Japan, Geomorphological Review of Japan, vol.60, pp.67-92 (in Japanese with English abstract).
Moriyama, A. (1990): Uplift ages of mountains in Central Japan, In Yonekura, N., Okada, A. and Moriyama, A. ed., Tectonic Landforms, Kokonshoin, pp.87-109 (in Japanese).
Moriyama, A. and Mitsuno, K. (1989): The Uplifting of the Kiso and Akaishi Mountain Ranges Deduced from the Sedimentary Deposits and the Ryuto Surface in the Southern Ina Valley, Central Japan, Geographical Review of Japan, Ser.A, vol.62, pp.691-707 (in Japanese with English abstract).
Nagai, N., Niwa, S., Suzuki, K. and Nemoto, M. (1988): Crustal structure of Fossa Magna and its neighbor: A study on active seismic structure of Central Japan, Report for 1985-1987 research, Part 1, pp.62-77 (in Japanese).
Nakano, S. (1989): Geology of Washiba-Kumonotaira Volcano, Japan Alps, Central Japan, Bull. Volcanological Soc. Japan, Sec. Ser., 34, pp.197-212 (in Japanese with English abstract).
Naruse, H. (1988): After 1 Ma BP subsidence of the Quaternary basins in Japan, Bull. Osaka Univ. Economics., 6, pp.44-65 (in Japanese).
Naruse, H. (1989): Quaternary basining of Japan, Bull. Osaka Univ. Economics, 7, pp.127-149 (in Japanese).
Naruse, H.(1990): Formation and history of Quaternary basins of Japan, Bull. Osaka Univ. Economics, 8, pp.70-85 (in Japanese).
Nirei, H.(1988): Kanto forarc basins -formation history of underground water basins in Kanto-, Urban Kubota, 27, pp.36-45 (in Japanese).
Nishikawa, O., Otsuki, K., Fujiwara, O. and Fuse, K. (1999): Rheology profile crossing the Northeast Honshu arc and its point at issue, Chikyu monthly (extra edition), vol. 27, pp. 130-134 (In Japanese).
Nogami, M., Moriya, I., Hirakawa, K., Koizumi, T., Umitsu, M. and Kato, K. (1994): Nature in Japan, Areal version, no.4, Chubu district, Iwanami Shoten, 182p. (in Japanese).
Obata, H.(1991): Landforms of Chugoku district, Kokonshoin, 262p. (in Japanese).

Oguchi,T. (1991): Quantitative study of sediment transport in mountain drainage basins since the Last Glacial, Trans. Japanese Geomorp. Union, 12, pp.25-39 (in Japanese with English abstract).
Ohmori, H. (1978): Relief structure of the Japanese mountains and their stages in geomorphic development, Bull. Dep. Geogr., Univ. Tokyo, 10, pp.31-85.
Ohmori, H. (1983) Erosion rates and their relation to vegetation from the viewpoint of world-wide distribution, Bull. Dep. Geogr., Univ. Tokyo, 15, pp.77- 91.
Ohmori, H. (1987): Mean Quaternary uplift rates in the central Japanese mountains estimated by means of geomorphological analysis, Bull. Dept. Geogr., Univ. Tokyo, 19, pp. 29-36.
Ohmori, H. (1990): Quaternary uplift rate and its relation to land forms of Mts. Shikoku, Japan, In Yonekura, N. Okada, A. and Moriyama, A. eds., Tectonic landforms, Kokonshoin, pp.60-86.(in Japanese)
Ohmori, H. (1993): Changes in the hypsometric curve through mountain building resulting from concurrent tectonics and denudation, Geomorphology, 8, pp.263-277.
Ojiya Crustal Movement Research Group.(1989): Correlation and deformation of the latest Pleistocene terrace in Ojiya, Niigata Prefecture, Central Japan, Geochemistry., 43, pp.168-171 (in Japanese with English abstract).
Oka, T. (1986): Geology of the Nakashibetsu district, Scale 1:50,000, Geol. Surv. Hokkaido, 75p. (in Japanese with English abstract).
Oka,T. (1997): Study on the neotectonics of Hokkaido and its neighboring seas, with notes on existence of active faults and occurrence of earthquakes in Sapporo and its vicinity, Commem. Vol. Prof. M. Kato, pp.427-449. (in Japanese with English abstract)
Osawa, A. and Hirayama, J. (1970): Geology of the Goshogawara district, Quadrangle Series, Scale 1:50,000, Geol. Surv. Japan, 25p. (in Japanese with English abstract) .
Osawa, A., Ikebe, Y., Hirayama, J., Awata, Y. and Takayasu, T. (1984): Geology of the Noshiro district, Quadrangle Series, Scale 1:50,000, Geol. Surv. Japan, 57p. (in Japanese with English abstract).
Osawa, A., Kujiraoka, A., and Awata, Y. (1985): Geology of the Ugohamada district, Quadrangle Series, Scale 1:50,000, Geol. Surv. Japan, 91p. (in Japanese with English abstract).
Ota, Y.(1996): Last interglacial shorelines in the Japanese Islands, In Koike, k. and Ota, Y. eds. Deforming coasts of Japan, Kokonshoin., pp.69-99 (in Japanese).
Ota, Y., Ishibashi, K. and Moriwaki, H. (1983): Late Holocene uplift of Shikine island on the northern tip of the Philippine sea plate, Jour. Seismo. Soc. Japan, Sec. Ser., 36, pp.587-595 (in Japanese with English abstract).
Ota, Y and Yoshikawa, T. (1978): Regional characteristics and their geodynamic implications of late Quaternary tectonic movement deduced from deformed former shorelines in Japan, Jour. Phys. Earth, 26, Suppl., pp.S379-389.
Ota, Y., Koike, K., Yonekura, N. Miyauchi, T. and Yagi, K. eds. (1987): Middle Holocene shreline map of Japan, Jour. Japan. Cartographers Assoc., 26, Appendix.
Ota, Y., Koike, K., Omura, A. and Miyauchi, T. eds. (1992): Last Interglacial shoreline map of Japan.
Otake, M. and Asada, T. (1983): Recent crustal movement in the Tokai area, Japan as inferred from the seasonal effect corrected levelling data, Jour. Seismo. Soc. Japan, (2nd Ser), 36, pp.597-608 (in Japanese with English abstract).
Otsuki, K. (1991): Crustal buckling under a high thermal gradient condition - An example of Northeast Honshu Arc. Jour. Japan Geothermal Energy Assoc., 28, pp.216-221 (in Japanese with English abstract).
Otsuki, K. (1995): Why is the crustal shortening of northeast Honshu arc larger in the backarc than around the volcanic front?, Jour. Geol. Soc. Japan, 101, pp.179-182 (in Japanese

with English abstract).
Oya, M. (1993): Geomorphology of rivers, Kokonshoin, 253p. (in Japanese).
Research Group for Active Faults of Japan (1991): Active fault in Japan -Sheet maps and Inventories- (Revised Edition), University of Tokyo Press, 473 p. (in Japanese).
Research Group for Quaternary Tectonic Map (1968): Quaternary Tectonic Map of Japan, The Quaternary Research, 7, pp. 182-187 (in Japanese with English abstract).
Saito, E., Watanabe, K. Miyazaki, J., Yasuda, A., Ikeda, K., Hashimoto, T., Hasaka, T., Katsurajima, S. and Isiyama, I. (1988): Recent crustal movement around southwestern part of Ibaragi Prefecture detected by precise leveling survey, Bull. Geol. Surv. Japan, 39, pp. 635-641 (in Japanese).
Sato, H.(1989): Degree of deformation of late Cenozoic strata in the Northeast Honshu Arc, Mem. Geol. Soc. Japan, 32, pp.257-268 (in Japanese with English abstract).
Sato, H. (1992): Late Cenozoic tectonic evolution of the central part of Northern Honshu, Japan, Bull. Geol. Surv. Japan, 43, pp.119-139 (in Japanese with English abstract).
Sato, H. (1994): The relationship between late Cenozoic tectonic events and basin development in northeast Japan, Jour. Geophys. Res., 99, pp.22261-22274.
Sato, H and Hirata, N. (1998): Deep structure of active faults and formation of Japanese Islands, Science Jour. Kagaku , 68, pp.63-71 (in Japanese).
Seno, T.(1996): Fundamentals of plate tectonics, Asakura Shoten, 190p. (in Japanese).
Shimamoto, T. (1989): Rheology of rock mass and plate tectonics -from rigid plate to ductile plate-, Sci. Jour. Kagaku, 59, pp.170-181 (in Japanese).
Shimazaki, K. and Nakata, T. (1980): Time-predictable recurrence model for large earthquakes, Geophysical Research Letters, 7, pp.279-282.
Soh, W., Nakayama, K and Kimura, T. (1998): Arc-arc collision in the Izu collision zone, central Japan, deduced from the Ashigara Basin and adjacent Tanzawa mountains, The Island Arc, 7, pp. 330-341.
Sugai, T. and Sugiyama, Y. (1998): Deep seismic reflection survey of concealed active structures in the Nobi Plain, central Japan, Geol. Surv. Japan Interim report on active fault and paleo-earthquake researches in the 1997 fiscal year., pp.55-66 (in Japanese).
Sugitani, T.(1983): Geomorphological development of the north Ariake Bay Lowland, Kyushu, since the last Interglacial Epoch: A quantitative study, Geomorph. Rev. Japan, 56, pp.403-419 (in Japanese with English abstract).
Sunamura, T.(1972): A study on the formation of continental shelves, Geogr. Rev. Japan, 45, pp.813-828 (in Japanese with English abstract).
Sunamura, T.(1992): Geomorphology of Rocky Coasts, John Wiley & Sons, 302p.
Suzuki, T.(1989): Late Quaternary crustal movements deduced from marine terraces and active faults, Joban coastal region, northeast Japan, Geogr. Rep Tokyo Metrop. Univ., 24, pp. 31-42.
Tada, T. (1985): Spreading of the Okinawa trough and its relation to the crustal deformation in the Kyushu (2), Jour. Seismo. Soc. Japan, 2nd Ser., 38, pp.1-12 (in Japanese with English abstract).
Tada, T.(1993): Crustal deformation in central Kyushu, Japan and its tectonic implication - Rifting and spreading of the Beppu-Shimabara Graben-, Mem. Geol. Soc. Japan, 41, pp.1-12 (in Japanese with English abstract).
Tada, T. (1997): Horizontal strain tectonics of Japanese Islands, Chikyu Monthly, 210, pp.807-811 (in Japanese).
Tada, T., Sagitani, T. and Miyazaki, S. (1997): Tectonics of Japan deduced from GPS observation, Science Jour.(Kagaku), 67, pp.917-927 (in Japanese).
Takagi, T., Yanagida, M., Fujiwara, O. and Ozawa, A. (1999a): River deepening and aggradation estimated from relative heights of river terraces, Jour. Geography (in press)

(in Japanese with English abstract).
Takagi, T., Fujiwara, O. and Sasaki, T. (1999b): A study on rocky coast erosion during the Holocene, Jour. Japan. Soc. Engineer. Geol. (in press)(in Japanese with English abstract).
Takahama, N., Akahane,S. and Kumai,H. (1988): Island Arc disturbance. In Uemura and Yamada eds., Geology of Japan, Chubu district I, Kyoritu Shuppan pp.271-273, (in Japanese).
Takemura, K., Yusa, Y. and Kitaoka, K. (1993): Oita plain and Beppu Bay: Subsurface structure and geological development around Beppu Bay, Mem. Geol. Soc. Japan, 41, pp.35-42. (in Japanese with English abstract)
Tanaka, M. (1982): A map of regional denudation rate in Japanese mountains, Trans. Japan Geomorph. Union, 3, pp.159-167.
Tanaka, Y. and Gomi, T. (1988): Tectonics of peninsulas, Bull. Geograph. Survey Institute, 68, pp.41-55 (in Japanese).
Tanaka, K., Endo, S., Ueda, K. and Chigira, M. (1997): Long-term time change of geological environment of Japan (part 2) - A method for evaluating uplift and subsidence -, Central Res. Inst. Electric Power Industry Report, U96028, pp.1-25 (in Japanese).
Takeuchi, A. (1988): New stress field of Inner zone in Central Japan, Chikyu Monthly, 10, pp.574-580 (in Japanese).
Takeuchi, A. (1996): Change of stress field and volcanism, Chikyu Monthly, 18, pp.92-96. (in Japanese).
Tokai Branch of Architecture Institute of Japan, Chubu Branch of Japanese society of soil mechanics and foundation engineering, and Research Group for foundation of Nagoya (1969): Ground Map of Nagoya, Corona Co., 279p. (in Japanese).
Ueki, T. and Mitsusio, T. (1998): Uplift history of the Asan Mountains, Shikoku, southeast Japan: based on stratigraphy and lithofacies of the Plio-Pleistocene Mitoyo Group, Jour. Geol. Soc. Japan, 104, pp.247-267 (in Japanese with English abstract).
Usami, T. (1987): Materials for comprehensive list of destructive earthquakes in Japan (New Ed.), University of Tokyo press, 434p. (in Japanese).
Utada, M (1979): Weathering and its products, Earth Science 5, Materials and Environments on the surface of Earth, Iwanami Course, Iwanami, pp.10-22.
Yagi, H. and Yoshikawa, K.(1988): Holocene marine terraces and tectonic movements on the Nishi-Tsugaru coast, Northeast Japan. Ann. Tohoku Geogr. Assoc., 40, pp.247-257.
Yashima, K. and Miyauchi, T. (1990): The Tsugaru Land Bridge problem related to Quaternary coastal tectonics, northeast Japan, The Quat. Res., 29, pp.267-275 (in Japanese with English abstract).
Yamazaki, H. (1985): Geology and crustal movements of Ashigara Plain, Chikyu Monthly, 7, pp.466-472 (in Japanese).
Yoshikawa, S. and Yamazaki, H.(1998): History and formation of paleo- and recent Lake Biwa, Urban Kubota,, vol.37, pp.2-11 (in Japanese).
Yoshikawa, T. (1974): Denudation and tectonic movement in contemporary Japan, Bull. Dept. Geogr. Univ. Tokyo, 6, pp.1-14.
Yoshikawa, T.(1985): Geomorphology of humid tectonic zone, University of Tokyo Press, 132p. (in Japanese).
Yoshikawa, T., Sugimura, A., Kaizuka, S., Ota, Y. and Sakaguchi, Y. (1973): On Geomorphology of Japanese Islands, New Ed., University of Tokyo Press, 415p. (in Japanese).
Yoshinaga, S., Saijo, K. and Koiwa, N. (1989): Denudation Process of Mountain Slope During Holocene Based on the Analysis of Talus Cone Aggradation Process, Trans. Japanese Geomorphological Union, 10, pp.179-193 (in Japanese with English abstract).
Yoshiyama, A. (1990): Late Quaternary crustal movement around the Hidaka Mountains,

Hokkaido, Japan, The Quat. Res., 28, pp.369-387 (in Japanese with English abstract).
Yoshiyama, A., and Yanagida, M.(1995): Uplift Rates estimated form Relative Heights of Fluvial Terrace Surfaces and Valley Bottoms, Journal of Geography., 104, pp.809-206 (in Japanese with English abstract).

(2.6 Climatic and sea-level changes)

Bradley, R.S. (1985): Quaternary Paleoclimatology: Methods of paleoclimatic reconstruction, Allen and Unwin, 472p.
Blanchon, P. and Shaw, J. (1995): Reef drowning during the last deglaciation: Evidence for catastrophic sea-level rise and ice-sheet collapse, Geology, 23, pp.4-8.
Brocker, W.S. and Denton, G.H. (1989): The role of ocean-atmosphere reorganization in glacial cycles, Geochem. Cosmoshim. Acta, 53, pp.2465-2501.
Chappell. J. (1994): Upper Quaternary sea levels, coral terraces, oxygen isotopes and deep-sea temperatures, Jour. Geogr. 103(7), pp.828-840.
Chappell, J. and Shackleton, N.J. (1986): Oxygen isotopes and sea level, Nature, 324, pp.137-140.
Chappell, J. ,Omura, A., Esat, T., McCulloch, M., Pandolfi, J., Ota, Y., and Pillans,B. (1995): Reconciliation of Late Quaternary Sea Levels Derived from Coal terraces at Huon Peninsula with Deep Sea Oxygen Records, Journal Geography., 104, pp.777-784 (in Japanese with English abstract).
CLIMAP Project Members (1981): Seasonal reconstruction of the earth's surface at the last glacial maximum, Geol. Soc. America, Map and Chart Ser. MC-36.
Dansgaard, W., Johnsen, S.J., Clausen, H.B., Dahl-Jensen, D., Gundestrup, N.S., Hanlmer, C.U., Hividberg, C.S., Steffensen, J.P., Svehnbjomsdottir, A.E., Jouze, I.J. and Bond, G. (1993): Evidence for general instability of past climate from 250-kyr ice core record, Nature, 364, pp.218-220.
Dunbar, R.B. and Coke, J. (ed.) (1993): Coral records of ocean-atmosphere variability, NOAA climate and global change program Special Rept. No.10, 38p.
Editorial committee of cyclopedia of geomorphology (1981) : Cyclopedia of geomorphology, Ninomiya shoten, 767p. (in Japanese).
Fukuda, M., Kouchi, A. and Takahashi, S. (1997): Science of the polar regions. 179p. University of Hokkaido Press (in Japanese).
Fukusawa, H. (1995): Non-glacial varved lake sediment as a natural timekeeper and detector on environmental changes, The Quat. Res., 34, pp.135-149 (in Japanese with English abstract).
Fukusawa, H., Fujiwara, O., Oi, K., Yamada, K., Kato, M., Ono, Y., Ise, A. and Yoneta, S. (1997): High-resolution reconstruction of Asia monsoon fluctuation estimated from lacustrine, bay and loess sediments, Chikyu Monthly, 19, pp.463-468 (in Japanese).
Heller, F. and Evans, M.E. (1995): Loess magnetism, Rev. Geophys., 33, pp.211-240.
Howard, W.R. (1997): A warm future in the past, Nature, 388, pp.418-419.
Imbrie, J., Boyle, E.A., Clemens, S.C., Duffy, A., Howard, W.R., Kukla, G., Kutzbach, J., Martinson, D.G., McIntyre, A., Mix, A.C., Molfino, B., Morley, J.J., Peterson, L.C., Pisias, N.G., Prell, W.L., Raymo, M.E, Shackleton, N.J. and Toggweiler, J.R.(1992): On the structure and origin of major glaciation cycles, 1. Linear responses to Milankovitch forcing. Paleoceanography, 7, pp.701-738.
Imbrie, J., Berger, A., Boyle, E.A., Clemens, S.C., Duffy, A., Howard, W.R., Kukla, G., Kutzbach, J., Martinson, D.G., McIntyre, A., Mix, A.C., Molfino, B., Morley, J.J., Peterson L.C., Pisias, N.G., Prell, W.L., Raymo, M.E, Shackleton, N.J. and Toggweiler, J.R.(1993): On the structure and origin of major glaciation cycles, 2. The 100,000-year cycle. Paleoceanography, 8, pp.699-735.

IPCC (1995): Climate Change 1995: The science of climate change, Houghton, J. T., Jenkins, G. J. and Ephraums, J. J. (ed.), Cambridge Univ. Press, 365p.
Japan Association for the Quaternary Research (ed.) (1987): Quaternary Maps of Japan, University of Tokyo press (in Japanese).
Kaizuka,S. (1962): Vegetation of the Wuerm glacial age and some climatic terraces in Japan, The Quat. Res., 2, pp.159-160 (in Japanese with English abstract).
Kaizuka, S., Chinzei, K., Koaze, T., Iozawa, T. Matsuda, T. and Huzita, K. (1995): Nature in Japan 2, -Japanese mountains-, Iwanami Shoten, 277p. (in Japanese).
Kadomura, H. (Chief scientist) (1995): Environmental changes in humid tropic during the past 20,000 years, A report for 1994-1995 grant-in-aid for Scientific Research : general study (B), 140p. (in Japanese).
Kasahara, K. and Sugimura, A. (ed.) (1978): Mobile Earth I: Recent and Quaternary, (Iwanami Chair: Earth Science 10), 296p. (in Japanese).
Kobayashi, K. and Sakaguchi, Y.(1977): Reexamination of Glacial epoch, Kagaku, 47, pp.578-591 (in Japanese).
Kondo, S., Nogawa, K., Migitani, Y. and Segawa, H. (1978): Permafrost in the Tokachi-mitsumata region, Monograph of the association for the geological collaboration in Japan, 22, pp. 335-341 (in Japanese).
MacAyeal, D.R. (1993a): A low order model of the Heinrich events cycle, Paleoceanography, 8, pp.767-775.
MacAyeal, D.R. (1993b): Binge/purge oscillations of the Laurentide Ice Sheet as a cause of the North Atlantic Heinrich events, Paleoceanography, 8, pp.775-784.
Maejima, I. (1980): Seasonal and regional aspects of Japan's weather and climate, In the associations of Japanese Geographers (ed.), Geography of Japan, Teikokushoin, pp.54-72.
Mann, M.E., Bradley, R.S. and Hughes, M.K.(1998): Global-scale temperature patterns and climate forcing over the past six centuries, Nature., 392, pp.779-787.
Masuda, F. (1996): Climate change of geologic time, In (Sumi, A. et al. ed.) Iwanami Chair 11, The subject on climatic change. pp.157-219 (in Japanese).
Masuda, K. and Abe, A.(1996): Quaternary climatic change, Climate changes, Iwanami shoten, pp.103-156 (in Japanese).
Mstsumoto, R., Okuda, Y. and Aoki, Y. (1994): Methane hydrates – Gigantic natural gas resources in 21 th Century, Scientific Japan, 253p. (in Japanese).
Matsusue, K., Fujiwara, O. and Sueyoshi, T. (1999): Climatic condition in the Last Glacial Maximum in Japan, JNC Technical Review, 6, pp.93-103 (in Japanese with English abstract).
Matsuno, T.(1989): Presumption for future climate change due to the increase of greenhouse effect gases, Science Jour. Kagaku, 59, pp.583-592 (in Japanese).
Miura, H. and Hirakawa, K. (1995): Origin of fossil periglacial wedges in northern and eastern Hokkaido, Japan. Jour. Geogr., 104, pp.189-224 (in Japanese with English abstract).
Nakada, M. and Lambeck, K (1988): The melting history of the late Pleistocene Antarctic ice sheet, Nature, 333, pp.36-40.
Nakada, M. and Lambeck, K(1989): Late Pleistocene and Holocene sea-level change in the Australian region and mantle rheology, Geophys. J., 96, pp.497-517.
Nakada, M., Yonekura, N. and Lamberck, K. (1991): Late Pleistocene and Holocene sea-level changes in Japan: implications for tectonic histories and mantle rheology, Palaeogeography, Palaeoclimatology, Palaeoecology, 85, pp.107-122.
Nakada, M., Maeda, Y., Nagaoka, S., Yokoyama, Y., Okuno, J., Matsumoto, E., Matsushima, Y., Sato, H., Matsuda, I. and Sanpei, Y. (1994): Glacio-hydro-isostacy and underwater

Jomon sites along the west coast of Kyushu, Japan. The Quat. Res., 33, pp.361-368.
Nakagawa, S., Gyomoto, S., Motoi, T. and Sugi, M. (1997): Presumption for future climate change. In Nisioka, S. and Harasawa, H. (ed.), Global warming and Japan, Presumption of its effect to man and nature, Kokonshoin, pp.1-35 (in Japanese).
Nakayama, T. (1995): Numerical estimation of the permafrost variation on the Daisetsu Mountains, Hokkaido, since the Last Glacial Maximum, Seppyo, 57, pp.125-132 (in Japanese with English abstract).
Nishi, H. and Sakai, H. (1997): Paleoceanographic changes of the Indian Ocean and corresponding tectonic events recorded in the Himalayan Range, Jour. Geol. Soc. Japan, 103, pp.313-327 (in Japanese with English abstract).
Oba, T., Kimura, A., Kato, M., Kitazato, H., Koizumi, I., Sakai, T., Takayama, T. and Kiyota, T. (1984): Paleoenvironmental history, Chikyu Monthly, 63, pp.571-575 (in Japanese).
Oeschger, H. and Langway, C.C.(eds.)(1989): The environmental record in glaciers and ice sheets, Wiley, 400p.
Ono, Y. (1990): The Northern Landbridge of Japan, The Quat. Res., 29, pp.183-192 (in Japanese with English abstract).
Ono, Y. (1993): Studies on Prehistoric Mongoloids: Last Glacial paleoenvironments of the eastern Asia, Japanese Scientific Monthly, 46, pp.61-65 (in Japanese).
Ono, Y and Naruse, T.(1997): Snowline Elevation and Eolian Dust Flux in the Japanese Islands During Isotope Stages 2 and 4, Quaternary International, 37, pp.45-54.
Rea, D.K. (1994): The paleoclimatic record provided by eolian deposition in the deep sea, The geologic history of wind, Rev. Geophys., 32, pp.159-195.
Ruddiman, W.F., and Kutzbach, J.E. (1989): Forcing of late Cenozoic northern hemisphere climate by plateau uplift in southern Asia and American west, J. Geophys. Res., 94, pp.18409-18427.
Saito, Y. (1997): Some problems of paleoenvironmental studies after the last Interglacial epoch in and around Japan-related to "continental shelves in the Quaternary (IGCP396)-, Chikyu Monthly, 19, pp.589-593 (in Japanese).
Shackleton, N. J. (1987): Oxygen isotope, Ice Volume and Sea Level, Quaternary Science Reviews, 6, pp.183-190.
SKI (Swedish Nuclear Power Inspectorate) (1995): The central scenario for Site-94: A climate change scenario, SKI Rep. 95, 42, 134p.
Sugai, T, (1992): River terrace development by concurrent fluvial processes and climatic changes, Geomorphology, 6, pp.243-252.
Tada, R. (1997): Paleoenvironmental changes in and around the Japan Sea since the Last Glacial Period, The Quat. Res., 36, pp.287-300 (in Japanese with English abstract).
Tada, R. (1998): Millennial-scale large and abrupt climatic changes -Global system dynamics in response to Dansgaard-Oeschger Cycles-, Jour. Geogr., 107, pp.218-233 (in Japanese with English abstract).
Takagi, T. and Fujiwara, O. (1997): Erosion rates of rocky coast in the Holocene, Substance of Japan Soc. Eng. Geol., Chubu branch, pp.17-20 (in Japanese).
The Association for the Geological Collaboration (ed.) (1996): Chgaku jiten, Heibonsha, 1443p. (in Japanese).
Tiedemann, R., Sarnthein, M. and Shackleton, N.J.(1994): Astronomic time scale for the Pliocene Atlantic $\delta^{18}O$ and dust flux records of Ocean Drilling Program site 659, Paleoceanography, 9, pp.619-638.
Winogarad, I.J., Coplen, T.B., Landwehr, J.M, Riggs, A.C., Ludwig, K.R., Szabo, B.J., Kolesar, P.T. and Revesz,K.M. (1992): Continuous 500000-year climate record from vein calcite in Devils Hole, Nevada, Science, 258, pp.255-260.
Yanagimachi, O. (1992): Periglacial and Transitional Zones in Japan, and Their Relations to

Permafrost Zone, Geographical Review of Japan, Ser. A, 65, 2, pp.143-157 (in Japanese with English abstract).

Yano,M. (1987): Paleovegetation of Hokkaido, In (Ito, K. ed.) Vegetation of Hokkaido, University of Hokkaido press, pp.283-331 (in Japanese).

Yasuda, Y. (1985): Climatic fluctuations in the last glacial period: Influences on the evolution of Japanese Paleolithic culture, Jour. Geogr., 94, pp.586-594 (in Japanese with English abstract).

Yasunari, T.(1987): Some problems about orogenic movement of Himalaya with a start of Monsoon climate, Chikyu Monthly, 9, pp.685-690 (in Japanese).

Chapter III

Characteristics of the Geological Environment of Japan

Chapter III Characteristics of the Geological Environment of Japan

The current policy for the R&D program on HLW disposal is, as mentioned in section 1.3, to consider the geological environment of a potential repository site in the broadest sense. This is achieved by investigating the general features of the geological environment of Japan, without specifying particular regions or rock types.

In H3, information accumulated in different fields of earth science was documented and presented to the Japanese Government for evaluation. The report contained information on geology, topography, rock types and groundwaters and provided a basis for understanding the characteristics of a wide range of geological environments in Japan. In addition, a survey of the published literature was conducted to obtain data on groundwater chemistry and the physical properties of rocks. The H3 report highlighted inadequacies in the data available at that time, which were due mainly to the fact that the data came largely from the existing literature and were not originally acquired with the specific purpose of evaluating the geological disposal of HLW. In particular, data on the flow and chemistry of deep groundwater and on solute transport in rock were fairly restricted. For these reasons, the Japanese Government indicated that more reliable data on rock formations and groundwaters should be obtained.

JNC therefore conducted detailed research programs in underground tunnels and boreholes in the Tono area of Gifu Prefecture and in the Kamaishi mine in Iwate Prefecture. The technologies and equipment needed to investigate deep geological environments with greater precision, and to acquire accurate data on the flow and chemistry of groundwater and the mechanical, mineralogical and chemical properties of rocks, were developed during investigations at these sites.

In the Tono mine, underground tunnels located in Neogene sedimentary rocks at a depth of approx. 130 m were utilized as well as boreholes drilled from the ground surface and in the tunnels. At the Kamaishi mine, underground tunnels in Cretaceous granite at two levels (at depths of approx. 300 m and 700 m) were utilized. In addition, a regional groundwater survey down to a depth of 1000 m is being conducted in the Cretaceous granite basement underlying the Neogene sedimentary rocks in the Tono area. Both the Neogene sediments and Cretaceous granite are rock types that are widely distributed in Japan.

This chapter mainly describes the investigations that have been carried out since the publication of H3 and the information obtained thereby. It focuses on the characteristics of the geological environment which are significant for the design and PA of a geological disposal system, assuming that a sufficiently stable geological environment is present, as discussed in the previous chapter (Figure 3.1-1). A discussion of the characteristics of a geological environment which are essential for disposal purposes is presented in section 3.1, in order to clarify the objectives of the R&D program. The following sections summarize the objectives, content and results of these studies.

3.1 Studies on the characteristics of the geological environment

3.1.1 Essential characteristics of a geological disposal environment

The most relevant characteristics of the geological disposal environment are those that potentially affect the construction, installation and performance of EBS and the role of the

geosphere as a natural barrier. For example, rock mechanical and thermal properties are important for the design and construction of the disposal facility and the engineered barriers, groundwater composition and flow influence overpack corrosion and the leaching and migration of radionuclides, and solute transport properties are particularly important aspects of the geosphere that determine its capacity to function as a natural barrier. In general, slow-moving reducing groundwater provides favorable conditions for limiting the degradation of the EBS and the dissolution and transport of radionuclides. Low temperature, high thermal conductivity, low in situ stress and low stress anisotropy, as well as adequate strength, are all desirable attributes of the host rock.

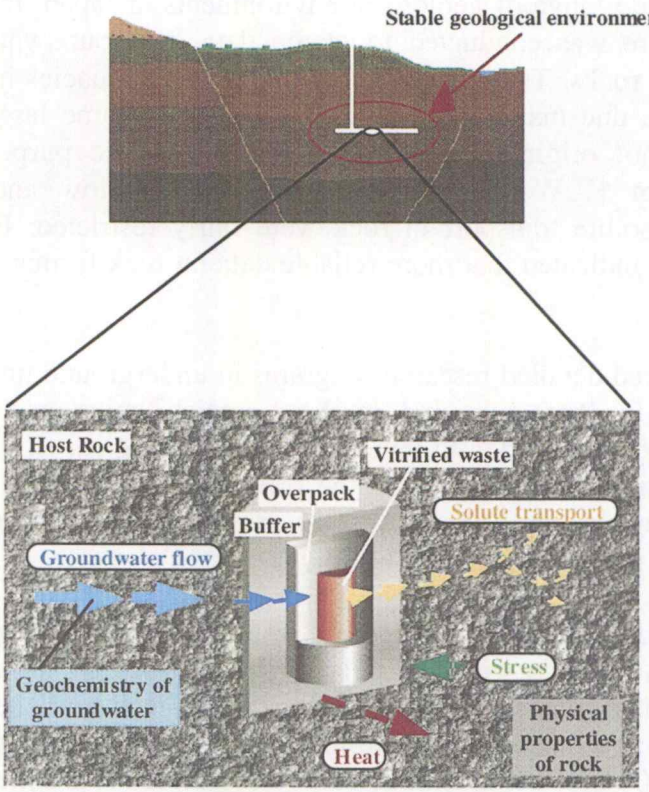


Figure 3.1-1 Characteristics of the geological environment of importance for a multibarrier system

The important characteristics of a geological disposal environment are thus considered to be:

i. groundwater flow characteristics;
ii. geochemical characteristics of the groundwater;
iii. thermal and mechanical properties of the rock mass;
iv. solute transport properties in the rock mass.

Information concerning geological structures is also fundamental to understanding the characteristics of the geological environment mentioned above. Each of these characteristics will now be discussed.

1) Geological structures

Geological structures control not only the properties of the rock mass itself but also the

geometry of groundwater flow and solute transport pathways and the chemical reactions between the rock and the groundwater. It is important to understand the physical and chemical characteristics of geological structures which form groundwater flow and solute transport pathways.

Active crustal movements, including faulting and volcanism, have resulted in the Japanese islands having a rather complicated geological structure. There has been extensive volcanic activity and effusive deposits are widely but heterogeneously distributed. Rock masses are commonly sub-divided by tectonic lines (major zones of deformation) and, in many cases, have been deformed and displaced by folds and faults. Basement rocks, consisting of older sedimentary rocks and crystalline rocks, are overlain by younger sedimentary formations or unconsolidated sediments. The thickness of the sedimentary cover varies greatly from place to place and, in some locations, the basement rocks are exposed. Volcanoes and volcanically derived deposits are superimposed locally on both the basement and the cover sequence.

2) Characteristics of groundwater flow

The rate of groundwater flow is an important factor to be considered when predicting the transport of radionuclides, both within the buffer material of the EBS and in the host rock. The flow rate also influences the corrosion rate of the overpack and the dissolution rate of the glass matrix. A high groundwater flow can also affect the physical stability of the buffer material.

To understand groundwater movement in the deep geological environment, it is important to determine the hydraulic gradient and rock permeability deep underground. In the areas considered here, groundwater flows mainly in zones of high permeability rock, from relatively high hydraulic heads near ridges towards lower hydraulic heads in valleys, and from inland towards the coast. Generally, the hydraulic gradient decreases with increasing depth because of the decreasing influence of local topography. In addition, where the effects of variable diagenesis and lithological characteristics can be ignored, there is a tendency for greater rock confining pressures at greater depth to generally decrease the permeability. Therefore, it may be expected that, within any particular rock formation, there will be a general decrease in the rate of groundwater flow with increasing depth.

For a given horizontal distance between recharge and discharge zones, deeper groundwater flowpaths will be longer than shallower flowpaths. Therefore, provided that head gradients and/or rock permeabilities do not increase with increasing depth, the residence times in the geosphere of deeper groundwaters will tend to be greater than those of shallower groundwaters.

Groundwater flow in the geosphere depends on the structure of the apertures (matrix pores and fractures) forming the groundwater flowpaths. The spatial distribution and properties of such structures reflect the lithology of the rock and the tectonic processes that it has undergone since it was formed. When flow occurs through matrix pores, it is controlled mainly by the average rock permeability and the anisotropy/heterogeneity of the rock mass. When flow is through fractures, it is controlled by their permeability and their spatial distribution.

The regional flow of groundwater also depends on the geographic conditions (e.g. topography, climate, etc.). The topographic relief and gradient, the distribution of river systems and climatic conditions related to precipitation and evaporation are important as they control the

recharge and discharge of groundwater. The topography of Japan is generally characterized by a transition from arcuate mountain ranges to hills then plains and, finally, to coastal areas. However, the mountains and hills are often in direct contact with the coast. The situation is made more complex in coastal areas due to the juxtaposition of fresh and saline (marine) groundwater. A freshwater-saline water interface or transition zone occurs in the subsurface, where freshwaters overlie more dense saline waters.

3) Geochemical characteristics of groundwater

The geochemical characteristics of groundwater will potentially affect the performance of all components of the EBS and the surrounding rock mass. Groundwater geochemistry will affect the rate of overpack corrosion and help to determine the rate of dissolution of the glass matrix and release of radionuclides. The redox conditions of the groundwater are a particularly important control on the extent of these reactions. Groundwater geochemistry may also control the chemical stability of the buffer material and the interactions between radionuclides, minerals and groundwater in both the buffer material and the host rock.

The geochemical characteristics of deep groundwater are attributable to the origin of the groundwater and its subsequent reaction with soil and rocks. In Japan, inland groundwater originates mainly as precipitation. In contrast, groundwaters from coastal areas originate as, or contain a proportion of, seawater. In volcanic areas inland, groundwaters may be affected by magmatism and/or contain a component of magmatic water. However, the influence of volcanically derived groundwater can be eliminated by avoiding volcanic areas (see section 2.4). Groundwaters that are unaffected by either seawater or magmatism generally have the lowest salinity.

The main reactions of groundwater with soils and rocks are expected to be mineral dissolution, mineral precipitation and ion exchange. Groundwater infiltrating into the deep subsurface environment will generally become more reducing due to the consumption of oxygen through reactions with organic matter, iron and sulfides contained in soils and rocks.

4) Thermal and mechanical properties of the rock mass

The thermal and mechanical properties of a rock mass are important factors relevant to the design and construction of an EBS and other components of the disposal facility. Thermal properties influence both the chemical reactions in the EBS and the working environment underground. Knowledge of rock mechanical properties is needed to predict the stability of underground cavities during the construction and operation of a repository and the mechanical stability of overpacks and buffer materials over long time periods.

The physical conditions of a rock mass depend on the characteristics of the site (e.g. geothermal setting and stress state) and the properties of the rock itself (e.g. thermal conductivity and strength). The latter also differ from place to place, depending on the type of rock. In Japan, civil engineers tend to classify rocks into "soft" and "hard" according to their strength. In this context, sedimentary rocks of the Neogene or younger are generally categorized as soft, while Pre-Neogene sedimentary rocks and crystalline rocks are hard.

When an underground tunnel is excavated, the mechanical, hydraulic and geochemical properties of the rock in a zone surrounding the tunnel will be disturbed. This zone is called the excavation disturbed zone (EDZ) and must be represented in quantitative assessments of the near-field.

5) Solute transport in the rock mass

Solute transport in the rock mass is an important factor determining the role of the host rock as a natural barrier to radionuclide migration. While a major determinant of the rate of solute transport is the rate of groundwater flow along hydraulic gradients, diffusion into the rock matrix along concentration gradients (known as matrix diffusion) may also play a role. Attention needs to be paid to this diffusion process and to sorption onto mineral surfaces. Micas and clay minerals generally display higher radionuclide sorption capacities than feldspars and quartz. A full understanding of solute transport requires studies of the physical structures and chemical properties of matrix pores and fractures that could act as groundwater transport pathways.

3.1.2 Data on characteristics of the geological environment

The characteristics of the rocks and groundwaters which are considered important for geological disposal depend to a large extent on the geological structure and the geographic conditions of the site. For instance, the spatial distribution (anisotropy, heterogeneity) of the physical properties of the rocks and the pore structures therein have a major influence on groundwater flow and on the thermal and mechanical properties of the rock. The mineralogical and chemical properties of rocks and their spatial variability control groundwater geochemistry and influence solute transport. Topographic and climatic conditions, which determine hydraulic gradients and groundwater recharge, are important controls on groundwater flow. The spatial distribution of temperature and in situ stresses, which are important in understanding thermal and mechanical conditions at depth, are closely related to the tectonic setting of the Japanese islands.

To understand the general trends in Japan with regard to parameters that are considered important for repository design and PA, it is important to integrate the information obtained from investigations in the Tono area and Kamaishi mine with the data obtained from literature surveys.

In Table 3.1-1, important properties relating to rock type, depth and topography are considered in order to take account of the variety of geological environments in Japan. Rock types have been classified into six categories; these have a range of geological characteristics that need to be considered in the analysis of potential repository designs and the PA of the disposal system:

- Acidic crystalline rocks (felsic igneous and metamorphic rocks such as granite)
- Basic crystalline rocks (mafic igneous and metamorphic rocks such as basalt)
- Pre-Neogene sedimentary rocks (arenaceous varieties)
- Pre-Neogene sedimentary rocks (muddy and tuffaceous varieties)
- Neogene sedimentary rocks (arenaceous varieties)
- Neogene sedimentary rocks (muddy and tuffaceous varieties)

Attention has been paid in particular to the following distinguishing properties of the different rock types:

- Pre-Neogene sedimentary rocks and Neogene or younger sedimentary rocks generally have different thermal and mechanical properties and different hydraulic properties. Pre-Neogene rocks are normally highly indurated and hence have a higher strength, lower porosity and are more fractured. Neogene rocks are generally poorly indurated and hence

have a lower strength, are more porous and less fractured.

- Different rocks have differing mineralogical and chemical compositions. These properties have an important influence on the geochemical evolution of groundwater and the sorption properties of the rocks. Crystalline rocks have been divided into acidic (felsic) and basic (mafic) types, whereas sedimentary rocks have been divided into muddy and tuffaceous varieties (rich in micas and clay minerals with relatively high sorption coefficients) and arenaceous varieties (rich in quartz, feldspar, and rock fragments) with lower sorption coefficients.

Table 3.1-1 Information on characteristics of the geological environment

	Rock type	Depth	Topography	Main sources
Characteristics of groundwater flow	Relationship between permeability and rock type[1),2)]	Relationship with hydraulic gradient and permeability[1),2)]	Relationship between hydraulic gradient and topography[3)]	1)literature data; 2)measurements in Tono & Kamaishi; 3)analysis based on literature data
Geochemical characteristics of groundwater	Geochemistry of crystalline and sedimentary rocks[1),2)]	Geochemical evolution of groundwater with depth[1),2)]	Meteoric origin[1),2)] and seawater origin[1)]	1)literature data; 2)measurements in Tono & Kamaishi;
Thermal and mechanical properties of rock mass	Relationship between physical properties and rock type[1),2)]	Relationship between rock pressure and depth[1),2)]; geothermal gradient[3)]	Nationwide distribution of geothermal gradient[3)]	1)literature data; 2)measurements in Tono & Kamaishi; 3)analysis based on literature data
Characteristics of solute transport in rock mass	Sorption by minerals[1)]; pore structures of rocks[1)]			1)observations and tests in Tono & Kamaishi

3.2 Geological structures

3.2.1 Characteristic features of geological structures in Japan

Japan is located in the Circum-Pacific orogenic belt, one of the most tectonically active areas in the world. The central part of the island of Honshu, the largest of the Japanese islands, has a number of mountains higher than 3,000 m; three-quarters of Japan is occupied by mountainous areas, including volcanoes. The general features of the geology, geological structures and distribution of rock types in Japan are summarized in H3 (PNC, 1992).

The boundaries of four tectonic plates lie close to Japan and the overall geological structure of the archipelago is closely related to the movement of these plates. For example, Pre-Neogene geological structures are characterized by significant tectonic lines, which can often form the boundaries between adjacent basement rock units. In particular, the Itoigawa-Shizuoka Tectonic Line separates the geology of northeast Japan from that of southwest Japan. The Median Tectonic Line divides the island of Honshu into an Inner Zone on the continental side and an Outer Zone on the Pacific Ocean side. The Pre-Neogene formations consist mainly of marine sediments, such as sandstones and mudstones, which are intercalated with limestone and chert, and granitic intrusions. Granitic rocks are widely distributed from Hokkaido to Kyushu and around 70 % of them are of Cretaceous to Palaeogene age (Ishihara and Sasaki, 1991).

The geological structures formed since the Neogene are closely related to the development of the present island-trench system, which is reflected in the stratigraphy of the geological formations (Otsuki, 1989; Amano and Sato, 1989). These formations can be divided into Green Tuff formations, which are distributed mainly in northeast Japan, and arenaceous to tuffaceous formations, which are widely developed in the Outer Zone of southwest Japan. The geological structures developed in these formations are characterized mainly by gentle folds and small-scale faults. The Pre-Neogene basement, consisting of sediments and granitic intrusions, is either exposed or overlain by Neogene and younger sediments (Figure 3.2-1).

It is vital to know the distribution of the different geological formations if the characteristics of geological environments; particularly the distribution of different hydrogeological and hydrochemical regimes are to be understood. For example, the existence of an unconsolidated sedimentary cover is considered to affect the rate of recharge and groundwater flow at depth. The chemistry of groundwater is believed to be closely related to the presence of organic matter in poorly consolidated surface deposits and to the mineralogical and chemical compositions of the rocks.

The importance of structures in the rock mass, their role as transport pathways or as barriers to transport and their influence on groundwater chemistry are summarized in the next section.

3.2.2 Geological structures and transport pathways

Geological structures have a major influence on solute transport and significantly affect the ability of subsurface rocks to behave as natural barriers (e.g. Chapman and McKinley, 1987).

The general geological structure of Japan is outlined in H3 and is considered further in Chapter II. In contrast, this section concentrates on the physical and chemical characteristics of structures that are important as transport pathways for both groundwater and solutes. When discussing solute transport by groundwater, it is important not only to consider groundwater

movement, but also phenomena such as the diffusion of solutes into the rock matrix and the sorption of solutes onto mineral surfaces. Natural analogue studies are helpful for understanding the long-term behavior of solute transport (see Section 3.7).

In non-volcanic areas, the geosphere is generally composed of basement rocks, consisting of Pre-Neogene sedimentary rocks and crystalline rocks, and overlying younger sedimentary rocks or unconsolidated sediments (Figure 3.2-1). However, the thickness of the sedimentary cover differs from place to place and the basement rocks directly crop out in some areas.

The main structural features of the rock mass that may act as transport pathways and need to be considered in performance assessment include (see also Figure 3.2-2):

i. fractures and faults;
ii. dikes and sills;
iii. bedding planes;
iv. unconformities;
v. matrix porosity.

Here, faults mean "inactive faults" where recent movement has not been detected within a time frame of 10^5 years and hence future movement is not expected. These faults can be distinguished from the "active faults" which should be avoided during siting, as described in Section 2.3. Fractures are structural discontinuities in the broadest sense and include faults, which are characterized by shear deformation along the fracture. In this report, however, fractures stand for joints in a narrower sense, which are extensional features, characterized by a pull-apart movement normal to the discontinuity where almost no shear deformation occurs.

Although insignificant for advective fluid transport, microstructures may be important controls on solute transport on the microscopic scale, because they influence the diffusion of solutes and water into the rock matrix. Connections between macroscopic fractures and microscopic fractures or matrix pores enable solutes to diffuse from the surface of the macroscopic fractures into the rock matrix. This phenomenon is termed matrix diffusion (e.g. Neretnieks, 1980) and is considered to be an important radionuclide retardation process in the geosphere (e.g. SKB, 1992). The nature of microscopic structures surrounding fractures is internationally recognized as a significant control on this diffusion process (e.g. Alexander et al., 1996).

In addition, in highly consolidated basement rocks, intrusive bodies such as dikes (Nagra, 1994) can also serve as transport pathways.

The structural features that provide transport pathways consist of primary structures formed at the same time as the rocks and secondary structures formed by subsequent processes, such as tectonic movements.

1) Matrix porosity, bedding planes, unconformities, dikes and sills
These transport pathways are mostly primary structural features, but they may also be formed or modified by processes occurring after the formation of a rock body.

In crystalline rocks, interconnected matrix porosity is generally low. In rocks such as granite, the porosity is generally less than a few percent (Sato et al., 1992; Yamaguchi et al., 1997). By comparison, in sedimentary rocks, such as the Neogene rocks that often overlie the crystalline basement, the porosity may exceed 30 - 40%. Pores in these sedimentary rocks can

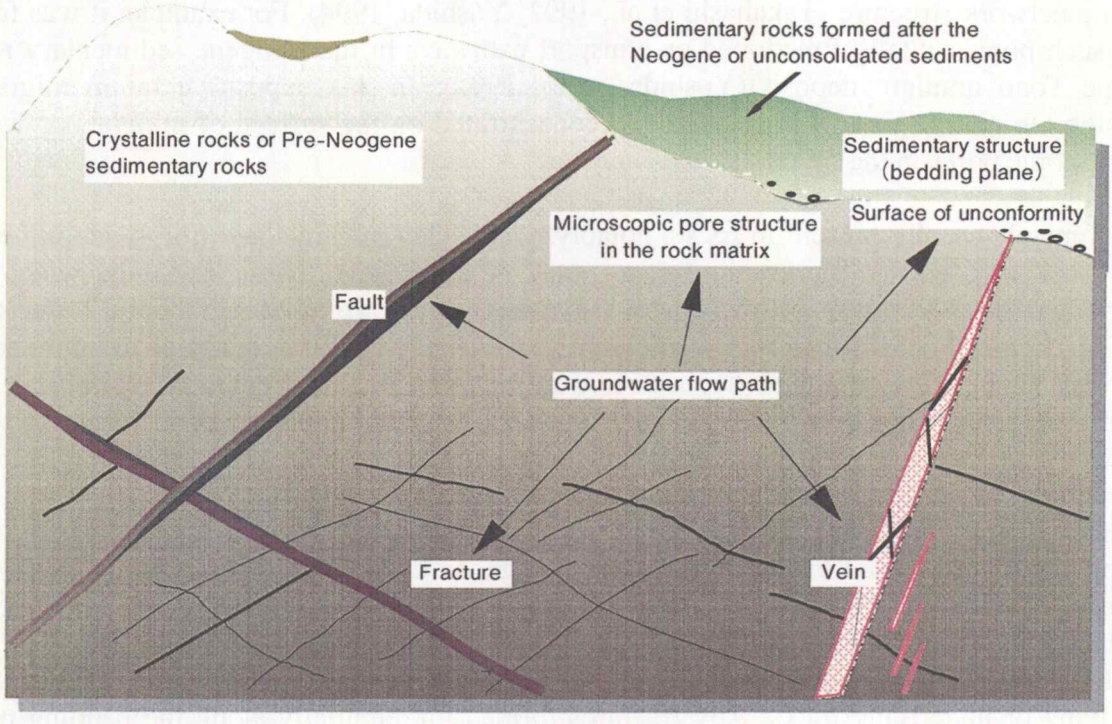


Figure 3.2-1 Geological structures of significance to waste disposal

The geosphere is generally composed of basement rocks, consisting of Pre-Neogene sedimentary rocks and crystalline rocks, and overlying younger sedimentary rocks or unconsolidated sediments. Various sizes of structures of importance as transport pathways exist in these rocks.

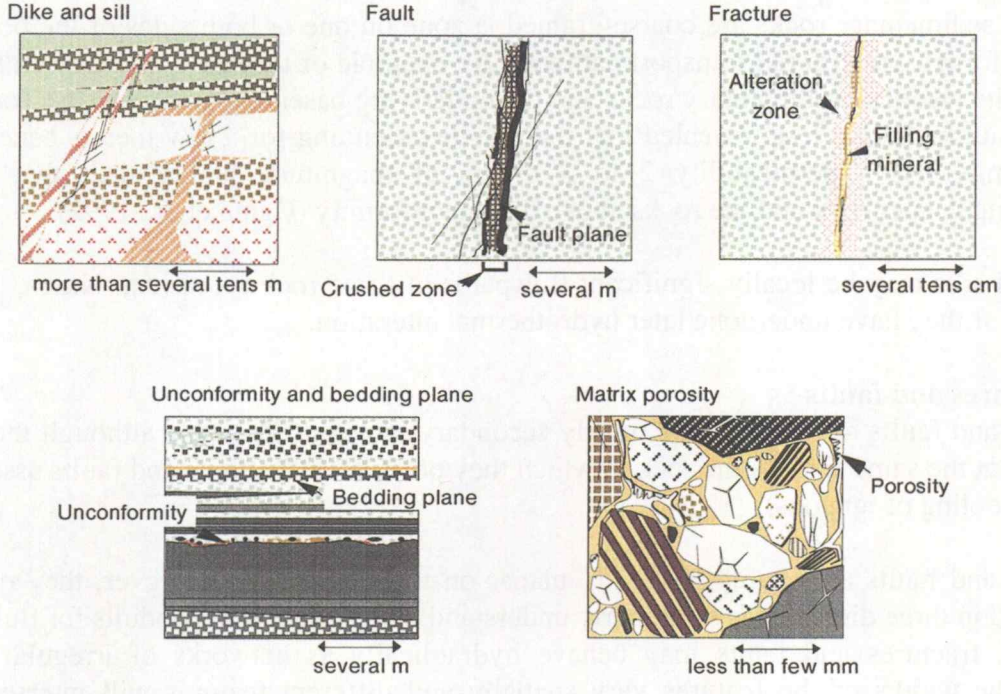


Figure 3.2-2 Structural elements relevant as transport pathways

Geological structures of various sizes form important transport pathways. To clarify the characteristics of groundwater and solute transport, it is important to understand the physical and geochemical properties of the transport pathways (the lengths shown in the figure are approximate).

form a network structure (Takahashi et al., 1992; Yoshida, 1994). For example, it was found that such pores actually functioned as transport pathways in the Neogene sedimentary rocks of the Tono uranium deposit (Yoshida et al., 1994). In this deposit, uranium migrating through the matrix pores was trapped and concentrated on the surface of minerals or within microscopic pores in the minerals.

The minerals usually present in rocks, notably micas, clay minerals and iron oxide minerals, are excellent sorbents for uranium (e.g. Yusa et al., 1993). These minerals, which are distributed along transport pathways, are also expected to sorb other radionuclides that have similar chemical behavior to that of uranium (e.g. Allard, 1982). A study of uranium series nuclides in the Tono uranium deposit showed that the uranium presently concentrated in microscopic pores has been retained there for at least several hundreds of thousand of years (Section 3.6). This is a good example of how microscopic pore spaces can function effectively to retain radionuclides for long periods of time (Yoshida et al., 1994).

A bedding plane is a sedimentation structure that generally occurs due to a change in the rate of sedimentation and/or a change in the size distribution or composition of the particles that are being deposited. If the constituents differ significantly between sedimentation layers, the bedding plane may be distinct and may show a different propensity to fracturing than overlying or underlying rocks. Any fractures formed preferentially along the bedding plane may act as transport pathways.

Unconformities exist at boundaries between rock formations and reflect significant past changes in the nature of sedimentation; for example, unconformities may occur between the basement and the overlying sedimentary rocks. Generally, rocks that are in contact at the unconformity have different physical properties and the boundary often functions as a transport pathway. In particular, where the surfaces of basement rocks are weathered, or overlying sedimentary rocks are coarse-grained, a zone on one or both sides of the boundary may also form a preferential transport pathway. An example of this phenomenon can be seen between the Neogene sedimentary rocks and the underlying basement granite in the Tono area. Here, in situ hydraulic tests revealed that the granite extending for a few meters beneath the unconformity has a permeability 2 to 3 orders of magnitude higher than that of the surrounding deeper rock and the rocks above the unconformity (Ogata et al., 1992).

Dikes and sills may be locally significant flowpaths in some rock types (e.g. Nagra, 1994a), especially if they have undergone later hydrothermal alteration.

2) Fractures and faults

Fractures and faults are likely to be mostly secondary structural features, although they may also form at the same time as the rock in which they occur (e.g. fractures and faults associated with the cooling of igneous).

Fractures and faults are characteristically planar on the field scale. However, they must be considered in three dimensions to properly understand their function as conduits for fluid flow. In reality, fractures and faults may behave hydraulically as networks of irregular tubes, because the widths of the features vary spatially and different features will intersect. For example, a particular fracture may be predominantly impermeable, but may be permeable where it intersects another fracture. In such a case, fluid flow will occur predominantly along the intersection. This feature may behave more like a one-dimensional feature than a two-dimensional planar feature. In addition, a fracture may be filled wholly or partly with crushed rock or filling minerals (Figure 3.2-3). Fluid flowing through the fracture will tend to follow a

convoluted pathway between the filling materials; these filling materials are also expected to play an important role in the sorption of radionuclides (e.g. McKinley and Hadermann, 1984).

Faults tend to have the greatest continuity of all the structures considered in this section and are usually associated with crushed zones that consist of breccia and fault clay (e.g. Kanaori et al., 1988). However, these faults do not always function as transport pathways for groundwaters and solutes. A good illustration of this is provided by the Tsukiyoshi fault in the Tono uranium deposit. Here, the fault functions as a barrier to water flow across it (e.g. Yamane et al., 1996). Furthermore, uranium and associated nuclides display very low mobility across the fault, due to the effects of fault clay. Such immobility is observed even in a part of the fault that displaces the uranium ore body (Shinjo et al., 1997).

Fractures in both crystalline and sedimentary rocks can be classified according to their morphological characteristics (Yoshida et al., 1989). Many fractures are filled partly or completely with minerals and may show wallrock alteration. Such alteration may be an important influence on the ability of a fracture to retard solutes through processes such as sorption and matrix diffusion. Water-conducting fractures may be linked to one another to form a fracture network system. It is important to understand these systems in order to predict radionuclide transport in the geosphere (e.g. NEA, 1991).

Many relevant features of fractured crystalline rocks can be illustrated by the results from investigations at the Kamaishi mine. Here, tectonic fractures in the granite post-date the rock, i.e. they are secondary features. Many of the fractures contain minerals formed subsequently and some have wallrock alteration (Figure 3.2-4). The hydraulic transmissivities of fractures measured at Kamaishi ranges mainly from 10^{-11} to 10^{-7} m^2 s^{-1}, with a mean value of 10^{-9} $m^2 s^{-1}$ (e.g. JNC, 1999). However the distribution, frequency and form of the fractures vary, depending upon their origin, rock type and hydrothermal alteration history. Such factors would affect the migration of radionuclides in the buffer material and the rock mass. Furthermore, if an interconnected fracture network were to allow relatively rapid groundwater flow in the environs of the repository, this might in turn influence the stability of the buffer material itself.

Matrix diffusion was also recognized in the granite at the Kamaishi mine. Here, the observed depth of matrix diffusion ranges from 0.01 m to 0.1 m (Ota et al., 1997; see Section 3.6).

There are wide variations in the frequencies of fractures developed in different lithologies (Figures 3.2-5, 6). These variations are partly a function of the different mechanical characteristics of different lithologies and partly a function of the differing tectonic settings within which they tend to occur. However, there is not necessarily a simple correlation between the abundance of fractures and their importance as fluid pathways. There are in fact considerable variations between different rock types in the relative importance of rock matrix porosity and fracture porosity as conduits for fluid flow. However, in general, in relatively uncompacted sedimentary rocks, pores in the rock matrix are more important fluid conduits than fractures. As a sedimentary rock becomes more indurated and/or cementation becomes more extensive, fractures become relatively more important fluid conduits than matrix pores.

3.2.3 Fracture parameters

1) Fracture orientation

Fracture orientations are usually unevenly distributed, even within the same site, due to local variations in the stress field. However, Watanabe et al. (1982) point out that certain trends

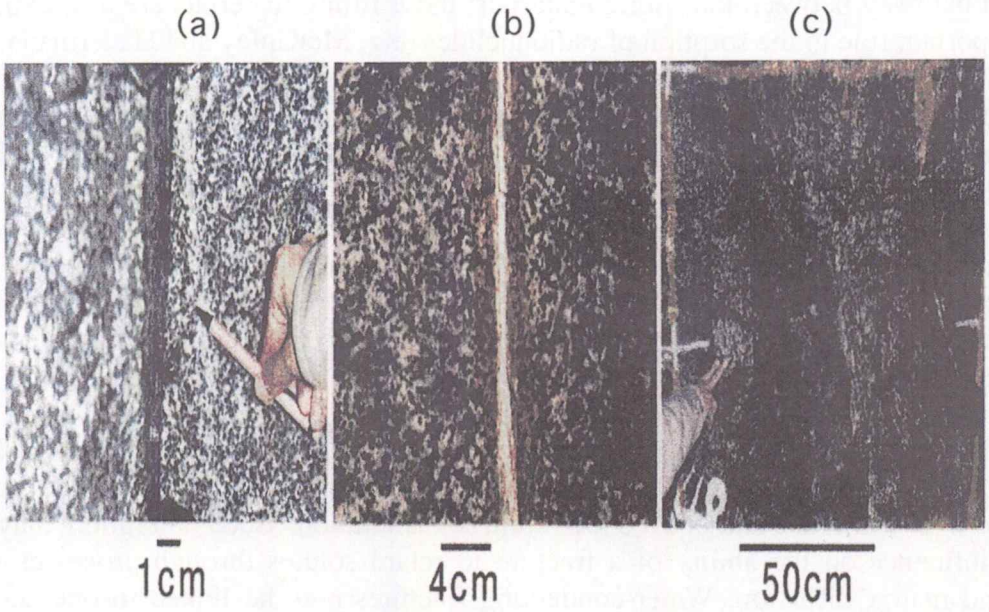


Figure 3.2-3 Fracture patterns observed at the Kamaishi mine

In the Kamaishi mine, fracture geometry changes from a single fracture to fracture zone in the granitic rock (see Figure 3.2-4).

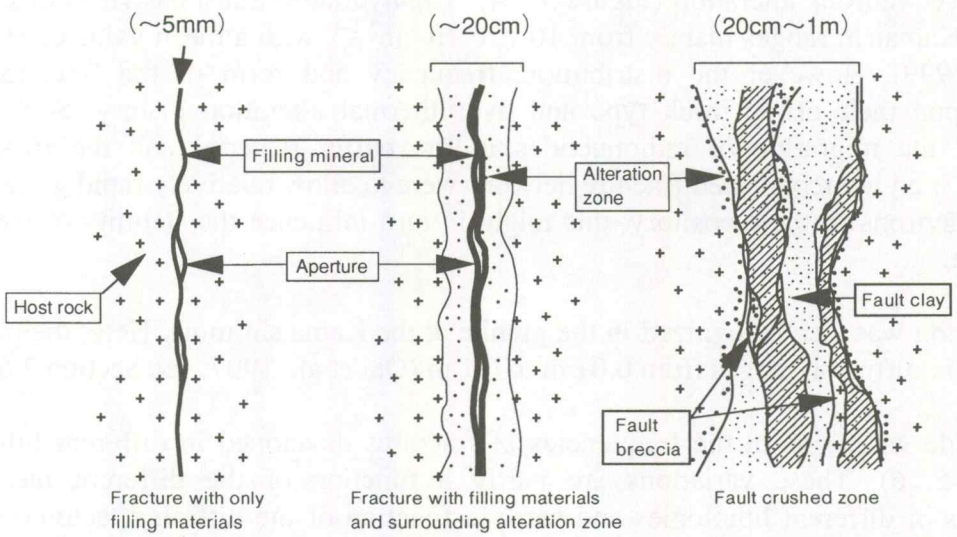


Figure 3.2-4 Major fracture structures identified at the Kamaishi mine
(reinterpretation of Osawa et al.,1995 by Yoshida et al.,2000)

These three types of fractures, which may act as transport pathways, have been observed at the Kamaishi mine.

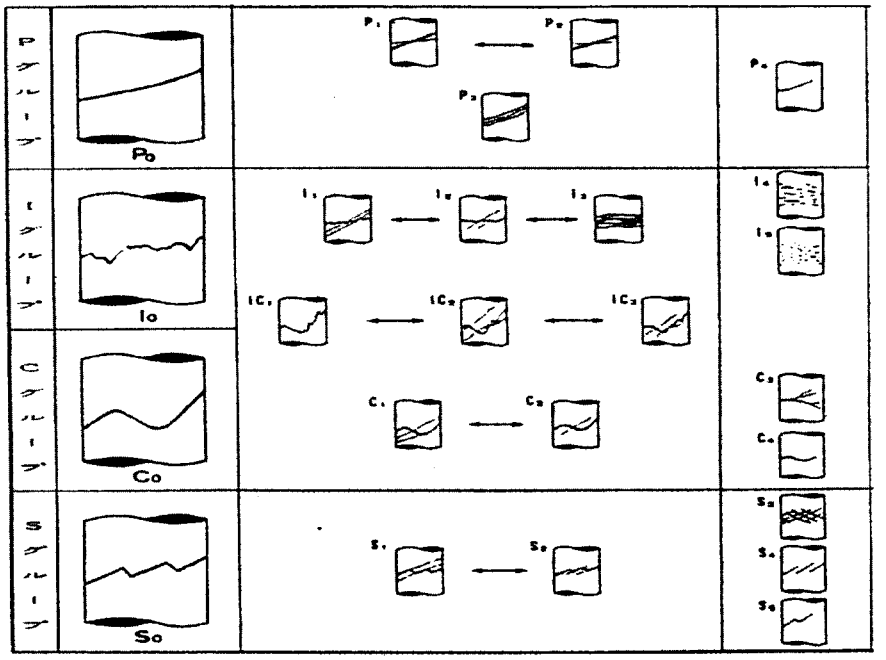


Figure 3.2-5 Fracture geometry observed on core samples in granite
(Yoshida et al., 1989)

Fracture patterns identified in the granite core specimens obtained in the Tono area.

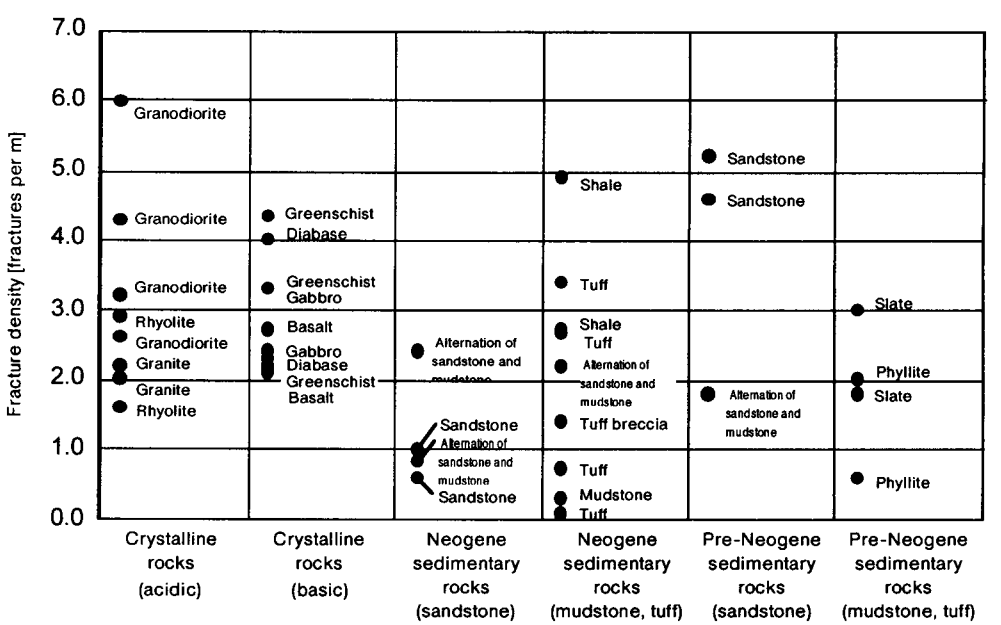


Figure 3.2-6 Fracture density in different rock types
(after Ijiri et al., 1999)

Investigations of fractures were conducted in mines and in surface outcrops throughout Japan (Fractures that intersect the horizontal line and are longer than 1m, were counted). Fracture density tends to be smaller in the Neogene sedimentary rocks than in other rock types .

can be observed on a macroscopic scale in many cases. Good correlations exist between the average fracture direction and the prevailing fault or lineament direction (e.g. Kojima et al., 1981). For example, a general directional trend of fractures has been observed in granite at the Kikuma underground oil storage facility (Shimo et al., 1992; Hatsuyama et al., 1993). Kimura (1981) has pointed out that fracture directions near the surface are fairly random, while more directional regularity is found deeper underground.

In general, fractures in granite have relatively high directional regularity (Ogata, 1978) and three orthogonal fracture sets are known to exist in many cases (e.g. Oda, 1985). Horizontal fracture sets are more common near the surface due to stress relief. Consequently, at depth, there are fewer horizontal fractures and two orthogonal groups of vertical fractures are more prevalent. This has been observed at the 250 m-level drift (about 700 m below the ground surface) of Kamaishi mine and in the Kikuma underground oil storage facility, which is about 50 m deep (Hatsuyama et al., 1993), as illustrated in Figure 3.2-7.

2) Shape defined by lateral limit of fracture surface

There are no in situ measurements of the shape of fractures in heterogeneous rock. However, shear fractures in homogeneous isotropic elastic media are known to be disc-shaped (Scholz, 1990). Dershowitz (1984) has pointed out the validity of using polygons to represent the shape of fracture planes by explaining that, as fractures are cut by each other, their geometry becomes polygonal.

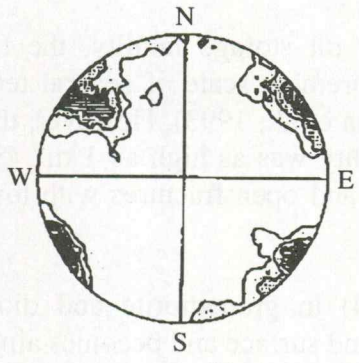
3) Distribution of fracture radius

Information on the size of fractures is obtained from studies of their trace length in drifts and outcrops. In the published literature, the distribution of trace lengths has been described by a log normal distribution (e.g. Barton, 1977) or a negative exponential distribution (e.g. Priest and Hudson, 1981; Kikuchi et al., 1987). Field studies at the Kikuma site have shown that the frequency of microcracks is relatively low and that a log normal distribution with a maximum at several meters is applicable in many cases (e.g. Oda, 1985; Ohnishi et al., 1992). One possible reason for this may be that microcracks are not fully sampled by the in situ measurements. However, Kojima et al. (1981) pointed out that another possible reason relates to the selection of a log normal distribution function. In general, the larger the difference between the observation and modeling scales, the lower the accuracy of the fracture distribution becomes (Oda and Kimura, 1990).

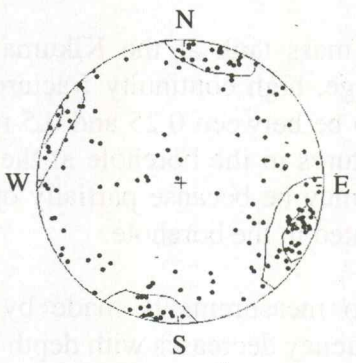
Ohno and Kojima (1993) have measured trace lengths over different scales and have shown that the trace length distribution follows a power distribution, which implies a fractal nature (Oda and Kimura, 1990). At the Kikuma underground oil storage facility, while the distribution of trace lengths measured in the rock mass tank (20.5 m wide and 30 m high) was between several meters and several tens of meters (Hatsuyama et al., 1993), a relatively large number of major faults was confirmed to be located across the rock mass tank at the site, as indicated in Figure 3.2-8 (Hayashi et al., 1993).

4) Distribution of fracture frequencies

Figure 3.2-9 shows fracture frequencies derived from the literature (Ikeda, 1979; Hatsuyama et al., 1993; Shimo et al., 1992) and from observations at the Kamaishi mine. The fracture frequency at the Kamaishi mine represents the average of fracture frequencies measured in the drifts and boreholes. In general, the fracture frequency is affected not only by location but also by the measurement method (e.g. borehole TV, scanning line method), size and nature of the measured fracture (e.g. aperture size and the presence of flowing water). For example, at the Kamaishi mine, the fracture frequency differs between the drift walls and boreholes and,



(a) Kikuma underground oil storage site
(Hatsuyama et al., 1993)



(b) Kamaishi mine 250m-level drift
(Open fracture; JNC, 1999a)

Figure 3.2-7 Stereographic projection of fracture orientations (Schmidt plot, under hemispheric projection)

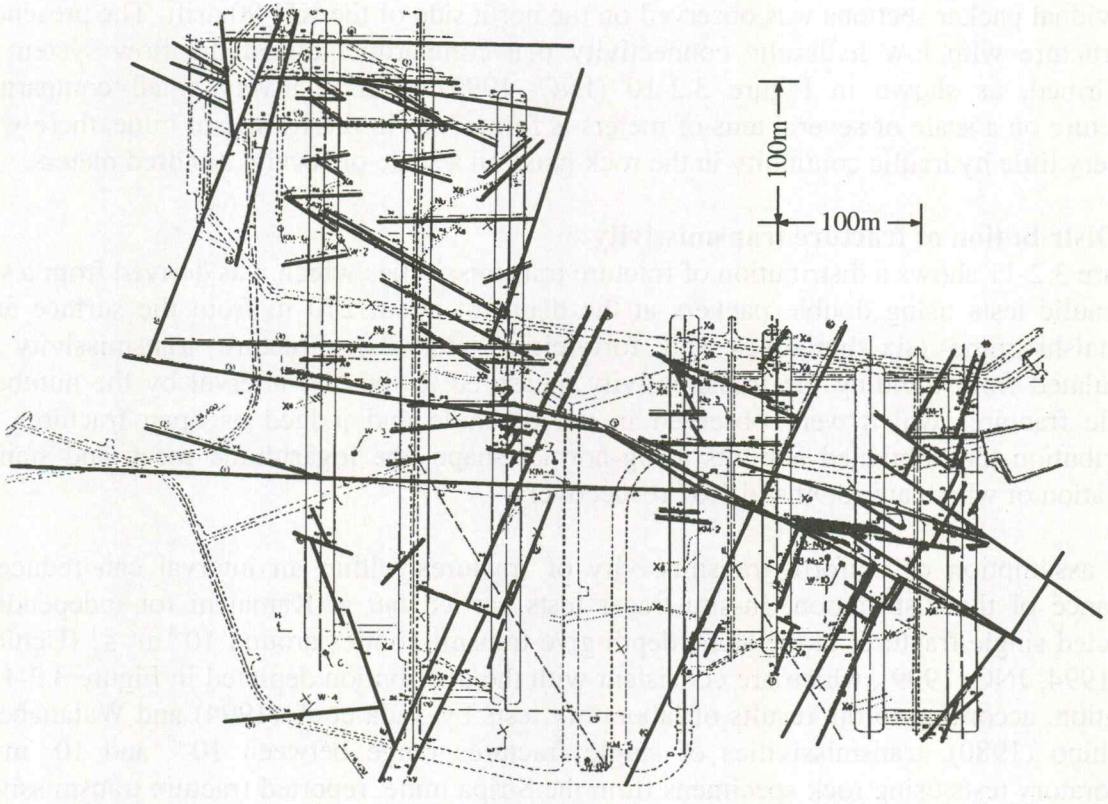


Figure 3.2-8 Fracture map for Kikuma underground oil storage site
(after Hayashi et al., 1993)

even on the same drift wall, the frequency depends on fracture size (fractures of 3 m or longer trace length for the NW drift and 0.5 m or longer for the KD-90 drift were counted). The presence of flowing water was also found to significantly affect the measured frequency.

In the rock mass tank at the Kikuma underground oil storage facility, the frequency of relatively large, high continuity fractures on a measurement scale of several tens of meters was found to be between 0.25 and 0.5 m^{-1} (Hatsuyama et al., 1993). However, the frequency of open fractures in the borehole at the Kikuma facility was as high as 1 m^{-1} (Shimo et al., 1992). This may be because partially open fractures and open fractures with low continuity are also counted in the borehole.

According to measurements made by Ogata (1984) in granodiorite and dioritic gneiss, fracture frequency decreases with depth from the ground surface and becomes almost constant at depths of 100 m or more. The dependence of fracture frequency on depth varies substantially with rock type and geological factors (Ogata, 1984).

5) Spatial distribution of fractures

Ohno and Kojima (1992) have demonstrated that the fractal dimension of fracture density on a two-dimensional plane at 14 sites is between 1.5 and 1.99, suggesting that fracture distribution is non-uniform. At the Kamaishi mine, fracture distributions were also demonstrated to be heterogeneous in the boreholes (Uchida et al., 1994). At the same time, disagreement between the hydraulic response in boreholes and the water pressure in individual packer sections was observed on the north side of the KD-90 drift. The presence of a structure with low hydraulic connectivity that compartmentalized the flow system was confirmed, as shown in Figure 3.2-10 (JNC, 1999). If a relatively small compartment structure on a scale of several tens of meters is formed, as in the Kamaishi mine, there would be very little hydraulic continuity in the rock mass on a scale of several hundred meters.

6) Distribution of fracture transmissivity

Figure 3.2-11 shows a distribution of fracture transmissivities which was derived from a set of hydraulic tests using double packers at the depth of about 270 m from the surface at the Kamaishi mine (six boreholes and forty-eight intervals). Fracture transmissivity was calculated from dividing the transmissivity measured in the test interval by the number of single fractures which were observed in the borehole and judged as open fractures. The distribution thus obtained exhibits a log-normal shape, the logarithmic mean and standard deviation of which are -8.99 and 1.07 respectively.

The assumption of uniform transmissivity of fractures within an interval can reduce the variance of the distribution. In-situ tracer tests carried out at Kamaishi for independently selected single fractures at the same depth give transmissivities around 10^{-8} m^2 s^{-1} (Uchida et al., 1994, JNC, 1999), which are consistent with the distribution depicted in Figure 3.2-11. In addition, according to the results of laboratory tests by Tada et al. (1994) and Watanabe and Hoshino (1980), transmissivities of single fractures range between 10^{-10} and 10^{-7} m^2 s^{-1}. Laboratory tests using rock specimens from the Stripa mine, reported fracture transmissivities between 10^{-10} and 10^{-6} m^2 s^{-1} (Gale et al., 1990; Makurat et al., 1990), and transmissivities estimated from the results of in-situ tracer tests were approximately $10^{-9}$$m^2$ s^{-1} (Abelin et al., 1982). These ranges are also included in the distribution depicted in Figure 3.2-11.

7) Distribution of fracture apertures

In general, there is a correlation between transmissivity and fracture aperture. For example, for a parallel plate fracture, the transmissivity is proportional to the cube of the aperture.

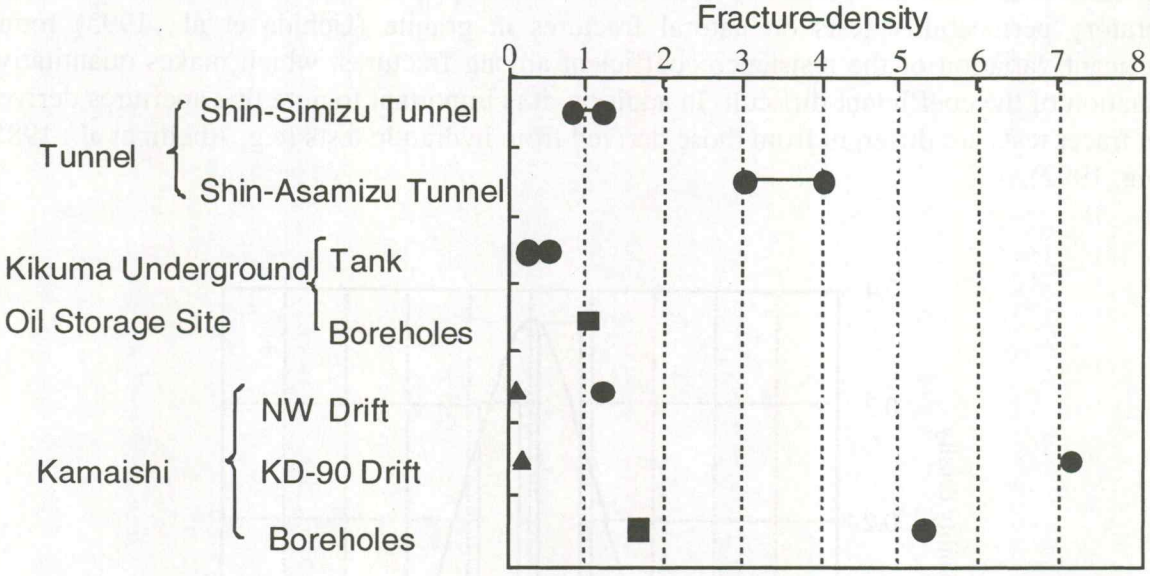


Figure 3.2-9 Fracture density distribution in granite

(Ikeda, 1979; Hatsuyama et al., 1993; Shimo et al., 1992)

●: all fractures observed ▲: fractures with water flow ■: open fractures

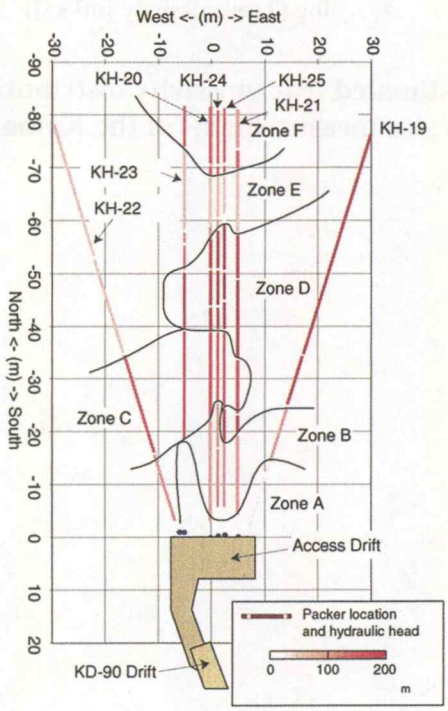


Figure 3.2-10 Flow compartments observed at the Kamaishi mine

Witherspoon et al. (1980) suggested that a modified cubic law, which includes a resistance coefficient to account for fracture roughness, should be applied to natural fractures. However, laboratory permeability tests on natural fractures in granite (Uchida et al., 1995) found significant variation of the resistance coefficient among fractures, which makes quantitative evaluation of the coefficient difficult. In addition, it is important to note that apertures derived from tracer tests are different from those derived from hydraulic tests (e.g. Abelin et al., 1985; Tsang, 1992).

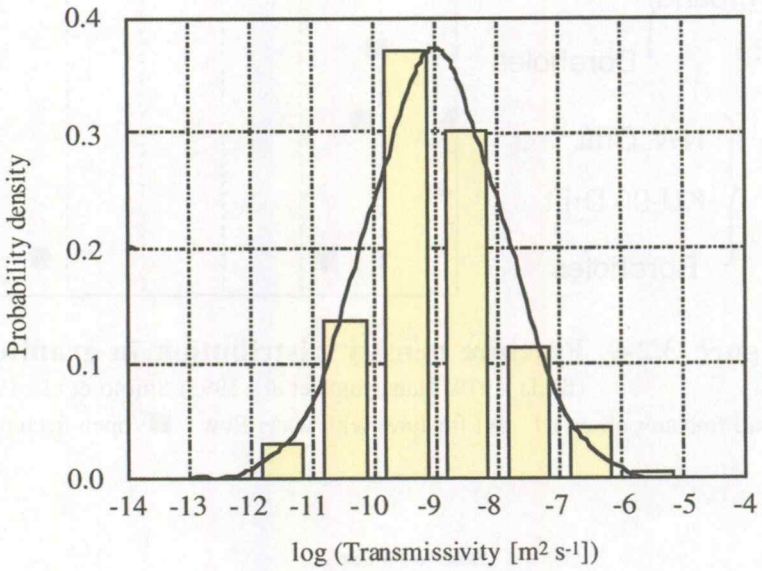


Figure 3.2-11 Estimated transmissivity distribution based on in situ measurements at the Kamaishi mine

3.3 Groundwater flow characteristics

3.3.1 Groundwater flow properties in the deep underground environment of Japan

In the geographical settings of interest, groundwater flow through a rock mass is generally driven by changes in elevation. Thus, water will tend to flow along hydraulic gradients from inland areas towards the coast and through the more permeable sections of the rock. It is important to understand the spatial variations in hydraulic gradients and distributions of permeability in order to understand groundwater movement at depth (Figure 3.3-1).

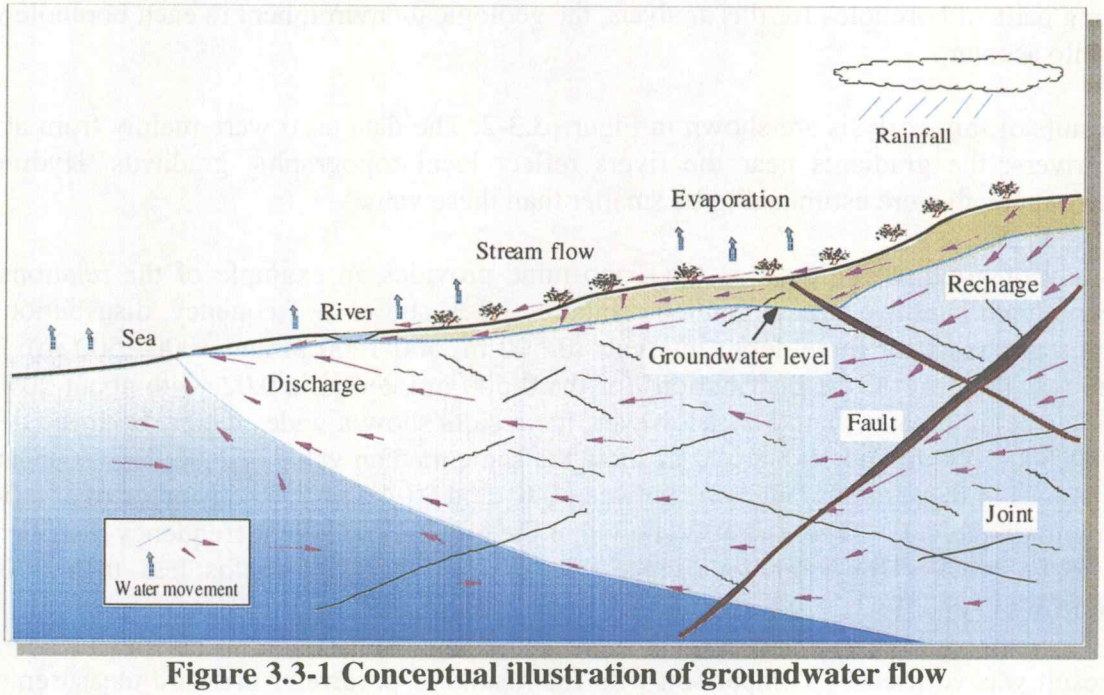


Figure 3.3-1 Conceptual illustration of groundwater flow

Regional groundwater movement generally depends on the hydraulic gradient and the permeability of the rock formation. As depth increases, hydraulic gradients generally decrease. Deep groundwater generally has a longer transport pathway from a recharge area to a discharge area as well as lower hydraulic gradients and thus longer residence times underground.

Over the depth range of relevance to HLW disposal, and in the absence of complicating diagenetic and tectonic effects, rock permeability will generally decrease with increasing depth. This is due to an increase in confining pressure with increasing depth, which results in the closure of pores and a reduction in fracture apertures. Groundwater movement often tends, therefore, to decrease with depth. However, it is important to understand how the flow of groundwater is controlled by factors such as the local presence of more transmissive features. In general, groundwater moving along deeper flowpaths will take longer to travel from the recharge area to the discharge area than groundwater following shallow flowpaths (Tanaka et al., 1997). The groundwater in the sedimentary rocks of the Tono area was estimated to be over ten thousand years old, based on measurements of the stable isotope ratios of oxygen and hydrogen and radioactive isotope concentrations of tritium and radioactive carbon (Mizutani et al., 1992).

1) Hydraulic gradients deep underground

Hydraulic gradient is normally determined by dividing the difference between the hydraulic

heads at upstream and downstream points by the distance between the two points. Information on hydraulic gradients at depth is important for the evaluation of the geological disposal of HLW. There are, however, very few in situ measurements of such gradients available for the Japanese geological environment.

General trends for hydraulic gradients were therefore calculated from hundreds of local government reports on groundwater supplies, by estimating groundwater level gradients.

It was considered reasonable to assume that the groundwater flow direction was parallel to the direction of maximum slope when analyzing the borehole data. The distance between these boreholes are generally in the range of a few kilometers (the average is 2.5 km). When selecting pairs of boreholes for this analysis, the geological environment in each borehole was taken into account.

The results of this analysis are shown in Figure 3.3-2. The data used were mainly from along major rivers; the gradients near the rivers reflect local topographic gradients. Hydraulic gradients at depth were estimated to be smaller than these values.

The study of groundwater flow at the Tono mine provides an example of the relationship between depth and hydraulic gradient. Figure 3.3-3 shows a frequency distribution of hydraulic gradients for three depth intervals (0-500 m, 500-1000 m and 1000-1500 m). The median (i.e. the peak of the distribution) for the 0-500 m interval is 0.02, with about 20% of the values being greater than 0.04. However, the results show a wide scatter. Both the depth intervals 500-1000 m and 1000-1500 m show the same median value of 0.02. However, most of the values in these depth ranges lie between 0.01 and 0.04, and the percentage over 0.04 is only approximately 1%. These results show that the hydraulic gradient frequency distribution tends to be smaller for intervals deeper than 500 m than for depths less than 500 m (Yanagizawa et al., 1992).

This result was verified by comparison with the results of porewater pressure measurements in a new 1000 m deep borehole at Tono. Figure 3.3-4 shows the hydraulic gradient between two 1000 m deep boreholes drilled into granite at Tono and separated by a distance of 1300 m. The data used for the comparison were taken from boreholes with a similar elevation above sea-level and with similar measurement intervals and horizontal separation. The height difference between the tops of the boreholes was about 70 m, giving a topographic gradient of 0.054. The two boreholes were aligned approximately in the direction of groundwater flow, estimated from the topography. The hydraulic gradient measured at shallow depths (gradient of the groundwater table) in the boreholes was almost similar to the value for the topographic gradient. In contrast, the measured gradient at depths of 500 m and deeper was around 0.026, i.e. much smaller than the value closer to the surface.

2) Hydraulic conductivity of the deep underground rock mass

The results of literature data, and measurements in the Tono area and the Kamaishi mine, have been analyzed to evaluate the permeability of rock masses in Japan. About 1,500 sets of data on permeability were collected from the published literature; more than 80% were obtained from civil engineering work for dam and tunnel construction (Umeda et al., 1995). In Lugeon tests, which are used routinely in civil engineering projects, rock with 1 - 3 Lugeon (1 Lugeon is equivalent to a hydraulic conductivity of 1.33×10^{-7} m s^{-1}) is generally considered to have low permeability. It is very rare for lower values to be reported. It is also noted that data published in the civil engineering literature mainly relate to sites where some problems were encountered (e.g. Matsumoto and Yamaguchi, 1986). Therefore, it is expected

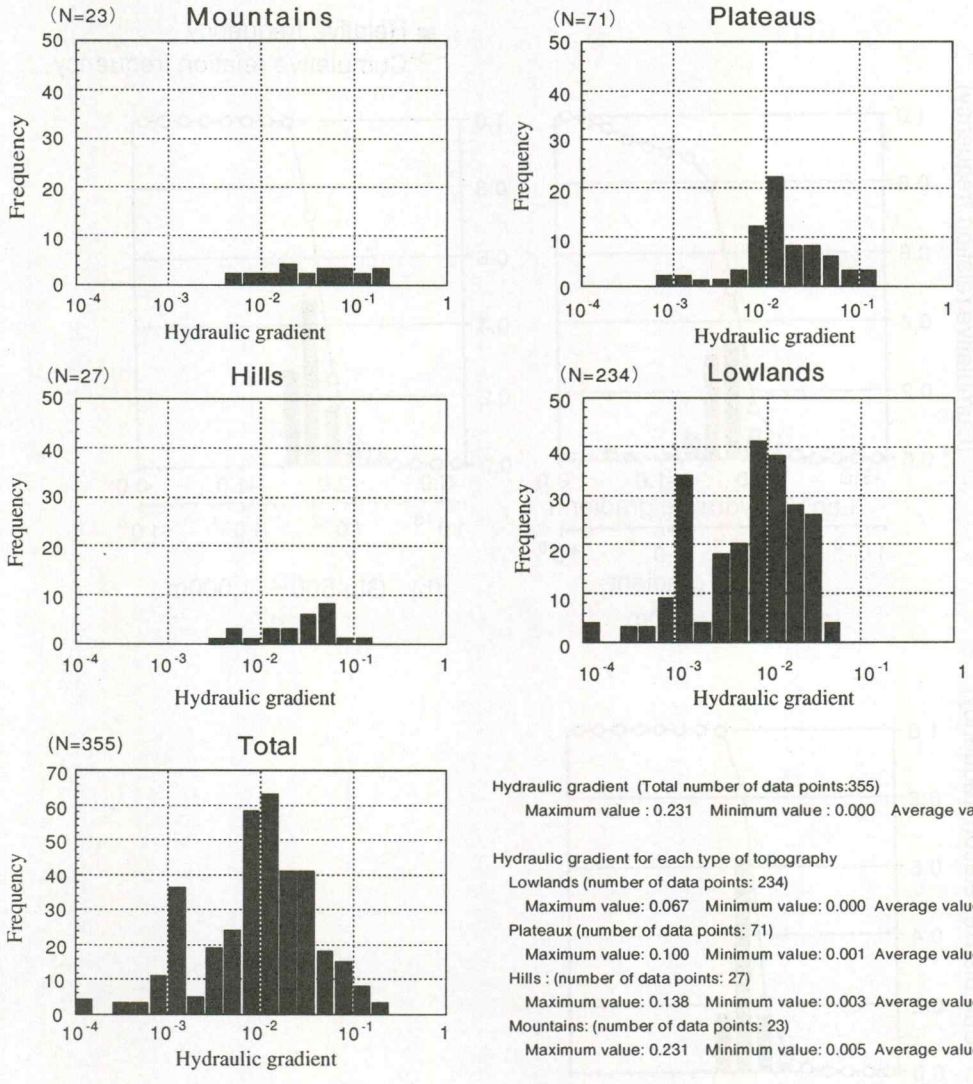


Figure 3.3-2 Histogram of near-surface hydraulic gradient for each topographic type

The hydraulic gradient in the near-surface zone was calculated using three different methods:

- Definite groundwater contour lines were selected from data on the groundwater table in the literature (Hibiya et al., 1999). The difference in the groundwater level between two points was divided by the horizontal distance to determine the hydraulic gradient.
- Observation wells that are located in the direction of the slope and have similar changes in the groundwater table over time are selected from Chronological Groundwater Tables (River Bureau, Ministry of Construction, 1994). The difference in the groundwater level between two points is then divided by the horizontal distance between them.
- From the report of Well Data Compiled from the Japanese Nation-wide Geothermal Surveys (Geological Survey of Japan, 1991), observation wells located in the direction of the slope and showing no notable changes in the geothermal gradient curve (obtained from temperature logging) were selected. The difference in the groundwater level between two points is then divided by the horizontal distance between them.

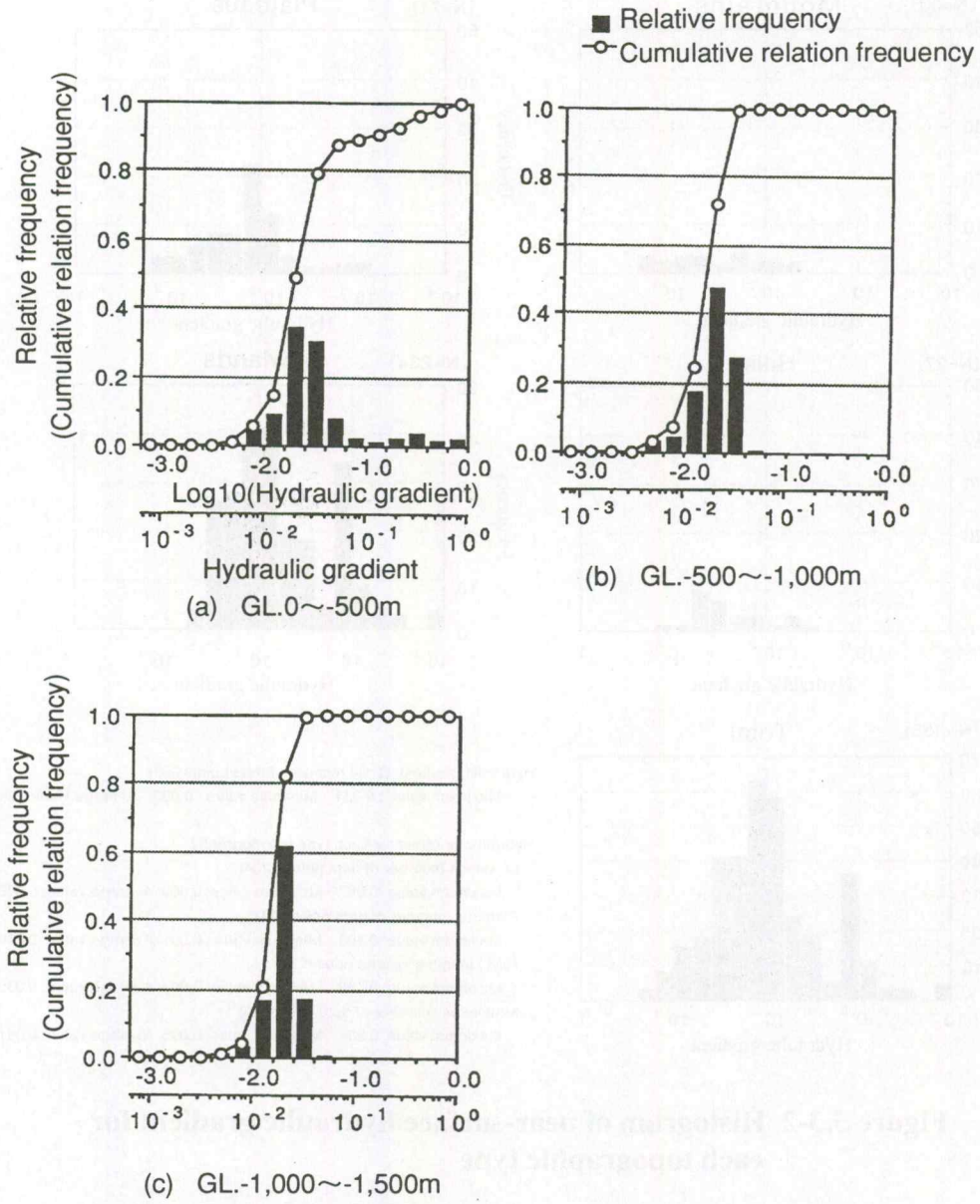


Figure 3.3-3 Histogram of hydraulic gradient calculated in the groundwater flow analyses in the Tono region (Yanagizawa et al.,1992)

It is clearly seen in the figure that the maximum for the 0~500 m interval is at 0.02 with about 20% over 0.04, and a wide scattered. On the other hand for both the depth intervals of 500~1,000 m and 1,000~1,500 m, the maximum value at 0.02 is the same as for the 0~500 m interval, but most values are between 0.01 and 0.04, and the percentage over 0.04 is markedly fewer at around 1%. Thus it is shown that the hydraulic gradient frequency distribution tended to be smaller in an interval deeper than 500 m than in those shallower than 500 m.

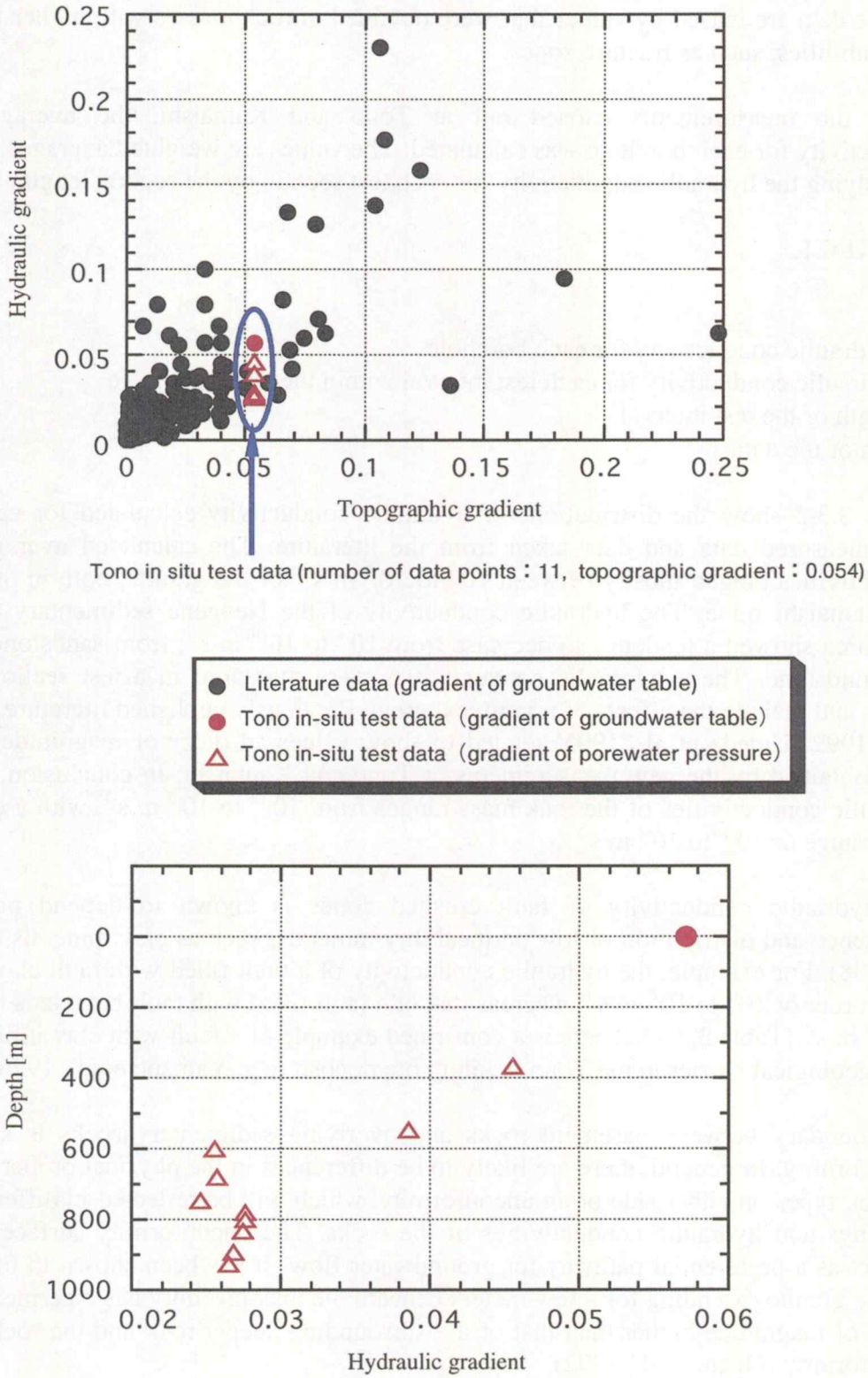


Figure 3.3-4 Relationship between topographic and hydraulic gradients

Literature data are the same as those shown in Figure 3.3-6 (Total number :355). In-situ test data for the Tono area suggest that the hydraulic gradient becomes smaller with increasing depth.

that the data are biased by values that were obtained in rock masses with higher than average permeabilities, such as fracture zones.

Using the measurements carried out at Tono and Kamaishi, the average hydraulic conductivity for each borehole was calculated. The values are weighted averages, obtained by multiplying the hydraulic conductivity for each test section by the section length, as follows:

$K' = \Sigma KL / \Sigma L$

where
K': hydraulic conductivity for each borehole
K: hydraulic conductivity for each test interval within the same borehole
L: length of the test interval
Σ: sum of the data

Figure 3.3-5 show the distributions of hydraulic conductivity calculated for each borehole from measured data and data taken from the literature. The calculated average hydraulic conductivities ranged mostly between 10^{-9} to 10^{-7} m s^{-1} for the granite, both in the Tono area and Kamaishi mine. The hydraulic conductivity of the Neogene sedimentary rocks in the Tono area showed a tendency to decrease from 10^{-8} to 10^{-10} m s^{-1}, from sandstone to tuff and then mudstone. These hydraulic conductivities were measured in a test section of several meters and include the effects of fractures therein. Previously published literature data (Shimo et al, 1992; Umeda et al., 1995) tended to show values an order of magnitude higher than those obtained by the new measurements at Tono and Kamaishi. In conclusion, the average hydraulic conductivities of the rock mass ranges from 10^{-12} to 10^{-6} m s^{-1}, with a central value in the range of 10^{-10} to 10^{-8} m s^{-1}.

The hydraulic conductivity of fault crushed zones is known to depend partly on the occurrence and distribution of low permeability minerals, such as clay minerals (Okamoto et al., 1988). For example, the hydraulic conductivity of a fault filled with fault clay is typically in the order of 10^{-8} to 10^{-5} m s^{-1}, whereas that of a fault filled with fault breccia is typically 10^{-6} to 10^{-3} m s^{-1} (Table 3.3-1). There is a confirmed example of a fault with clay infill acting as a hydrogeological barrier in the Tono uranium ore deposit (e.g. Yamane et al., 1996).

The boundary between basement rocks and overlying sedimentary rocks is known as an unconformity. In general, there are likely to be differences in the physical properties between the rock types on either side of an unconformity, which will be reflected in differences in the porosities and hydraulic conductivities of the rocks. The unconformity surface itself could also act as a preferential pathway for groundwater flow. It has been shown in the Tono area that the granite extending for a few meters beneath the unconformity has a permeability 2 to 3 orders of magnitude higher than that of the surrounding deeper rock and the rocks above the unconformity (Ogata et al., 1992).

All data currently available on granite in Japan are plotted in Figure 3.3-6 as a function of depth, which includes measurements in boreholes at Tono area and Kamaishi mine and those taken from the literature. Individual data in the figure represents a measured hydraulic conductivity for each test intervals, which are shown as an average of a borehole for granite in the Figure 3.3-5. The distribution of transmissivity of a fracture shown in Figure 3.2-11 in Section 3.2.3 is derived from the measurements at the depth of about 270 m from the surface at Kamaishi for which the number of fractures in the test interval were identified. Excluding data measured in the damaged zone around the Tsukiyoshi Fault at Tono and data in the

Table 3.3-1 Hydraulic conductivity of fault and fracture zones

(Tanaka and Inoue, 1995)

Rock type	Geological time	Filling width of fault and fracture zone		Cohesion (kgf cm^{-2})	linternal friction angle (°)	Hydraulic conductivity ($m\ s^{-1}$)
Sandstone, slate	Mesozoic	clay	10～15cm	0.25	35	1×10^{-5}～1×10^{-6}
Granodiorite	Mesozoic	clay	1～30cm	2～3	30～40	——
——	——	sandy	5-～6m	5～6	40～45	——
Varved clay	Palaeozoic	breccia	10～15m	——	——	1×10^{-3}～1×10^{-6}
——	——	clay	——	——	——	1×10^{-6}～1×10^{-8}
Granite	Mesozoic	clay	9m	0.5	20	1×10^{-6}～1×10^{-7}
Hornfels	Palaeozoic	breccia	——	——	——	1×10^{-5}
——	——	sandy	——	0.5	20	1×10^{-6}
——	——	clay	——	——	——	1×10^{-7}
Sandstone	Palaeozoic	breccia	——	——	——	1×10^{-5}
——	——	clay	——	——	——	1×10^{-5}～1×10^{-6}
Slate, chert	Palaeozoic	——	——	——	——	1×10^{-6}

The hydraulic conductivity of a fault filled with clay is in the order of 10^{-8} ~ 10^{-5}m s^{-1}, while that of a fault filled with breccia is 10^{-6} ~ 10^{-3}m s^{-1}.

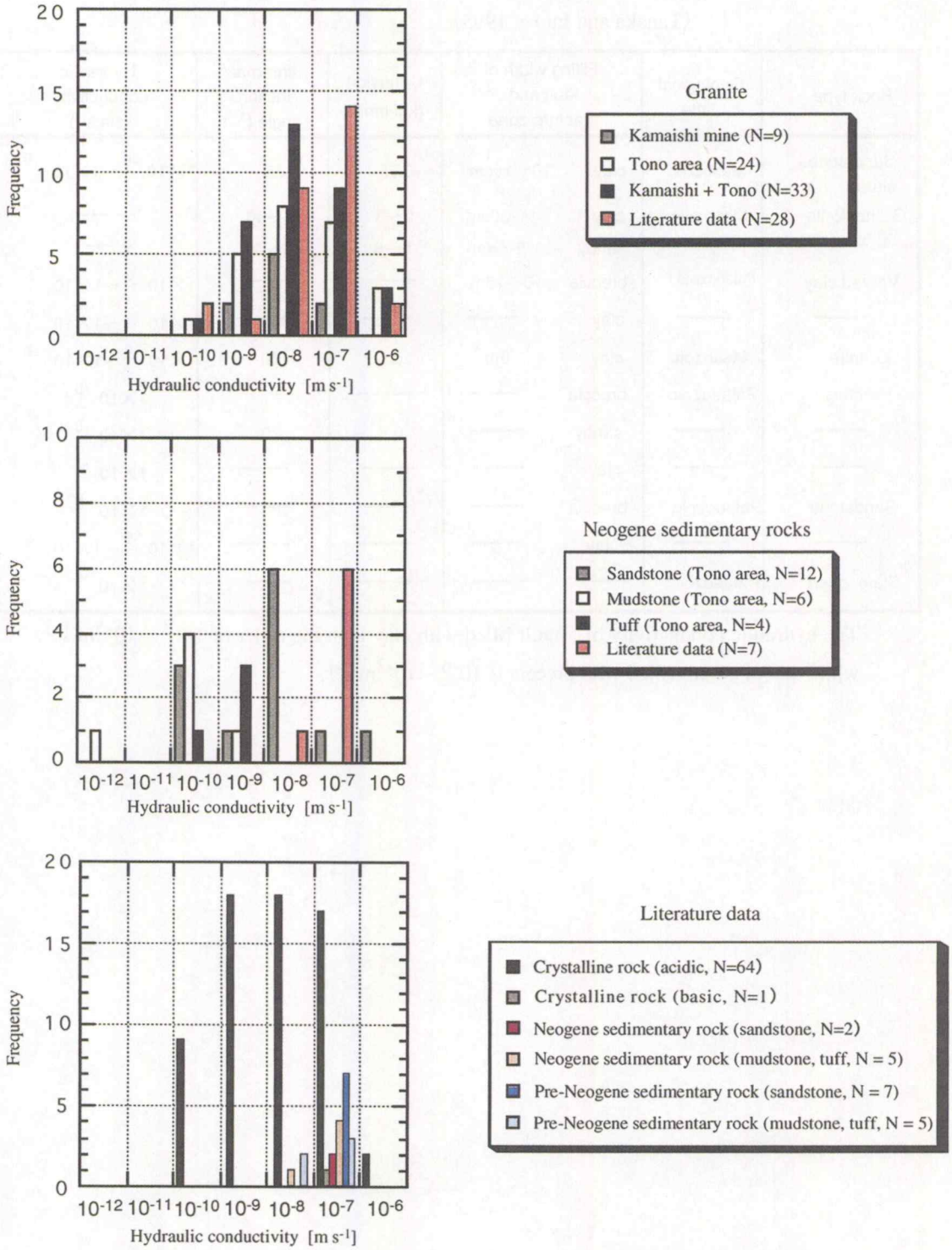


Figure 3.3-5 Histogram of hydraulic conductivity

Data from the Tono area and the Kamaishi mine show the average hydraulic conductivity value calculated for each borehole. Literature data show the measured value for each test section. The average hydraulic conductivity value of granite is distributed around 10^{-8}m s^{-1}. The average hydraulic conductivity value of the Neogene sedimentary rocks in the Tono area decreases from 10^{-8}m s^{-1} to 10^{-10}m s^{-1}, from sandstone to tuff and then mudstone.

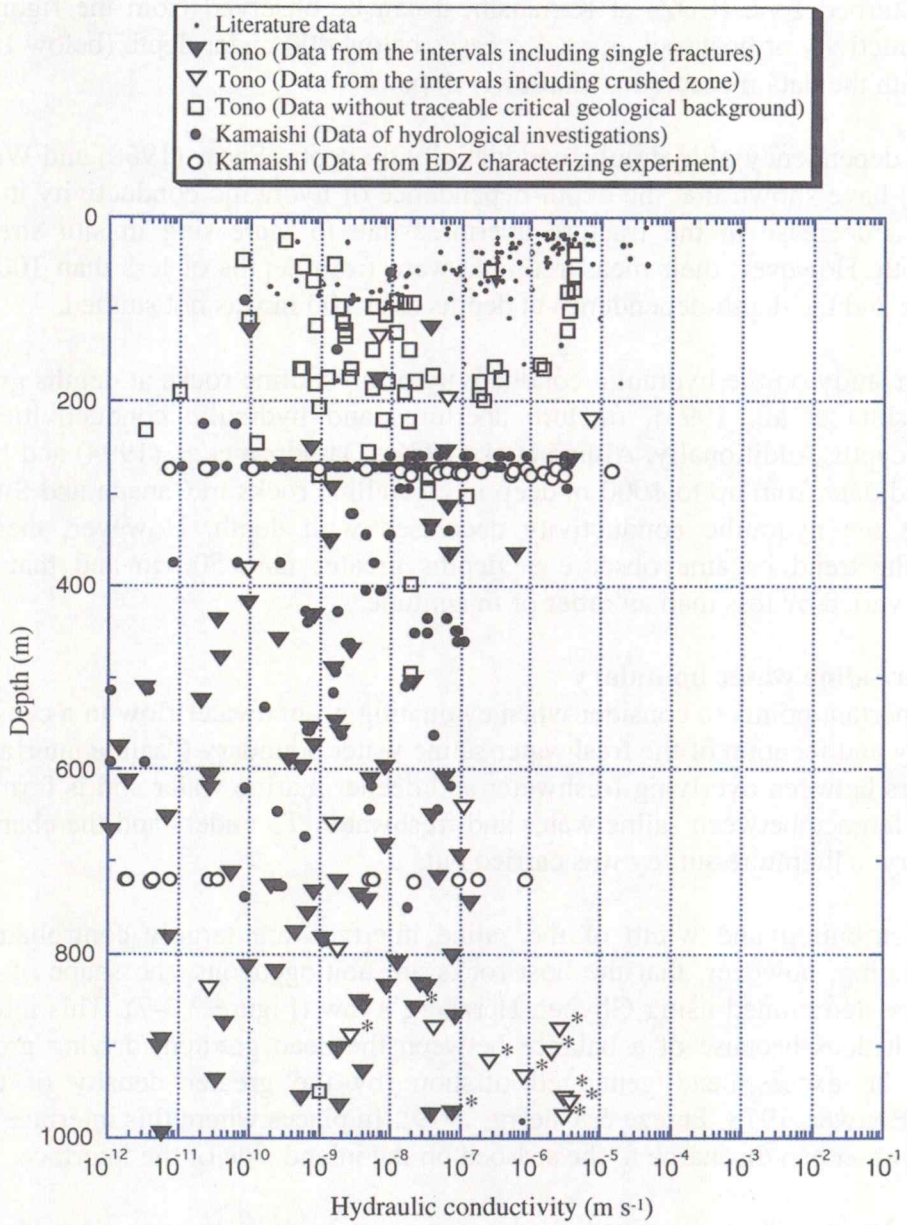


Figure 3.3-6 Relationship between depth and hydraulic conductivity in granite

Hydraulic conductivity data for granite obtained from a literature survey (Umeda et al., 1995) and in-situ measurements in the Tono area and Kamaishi mine are plotted. Among Tono data, those from the DH-series and MIU-series boreholes can be clearly traced with sufficient information of the geological settings for measurement intervals (JNC, 1998a, b, c, d, 1999a). The geological information was not clearly recorded for other data obtained at earlier stages of R&D program. All data obtained from the Tono area are classified according to the geological observation into 3 categories. Namely, 1) data from the intervals including a set of single fractures (the fractures observed in the packer interval are, in principle, independently identified as a single fracture without the development of network structures and crushed zones), 2) data from intervals including crushed zones (wall rocks are crushed due to minor or major faulting) and 3) data for which the geological setting cannot be traced precisely from the borehole loggings. The data marked with " * " show those from the damaged zone or the crushed zone that occurs around the Tsukiyoshi Fault at depths of about 800 – 1000 meters below the surface in two boreholes. The data from Kamaishi include those obtained for the hydrological characterization of the host rock and the EDZ. The measurements of the EDZ were performed very close to the gallery wall (e.g. 30 cm - 1 m) with smaller intervals (a few tens of centimeter at largest) focussing on the disturbed zone and/or features due to excavation.

excavation disturbed zone (EDZ) at Kamaishi, it can be observed from the figure that the hydraulic conductivity of host rock mass decreases below 400 meter depth (below 10^{-7} m/s) in comparison with the data measured at shallower depth.

Regarding the dependency of hydraulic conductivity on depth, Snow (1968) and Watanabe & Kojima (1980) have shown that the depth-dependence of hydraulic conductivity in granite is explained by a decrease in the fracture apertures due to increasing in situ stresses with increasing depth. However, their measured data were from depths of less than 100 m below ground surface and the depth-dependence at depths over 100 m was not studied.

According to a study on the hydraulic conductivity of crystalline rocks at depths greater than 100 m (Kinoshita et al., 1993), fracture apertures and hydraulic conductivities tend to decrease with depth. Additionally, Almén et al. (1986), Davidson et al. (1994) and Neretnieks (1993) reported data from up to 1000 m deep in crystalline rocks in Canada and Sweden that suggested that the hydraulic conductivity decreased with depth. However, these studies showed that the trend became obscure at depths greater than 500 m and that hydraulic conductivities varied by less than an order of magnitude.

3) Freshwater/saline water boundary

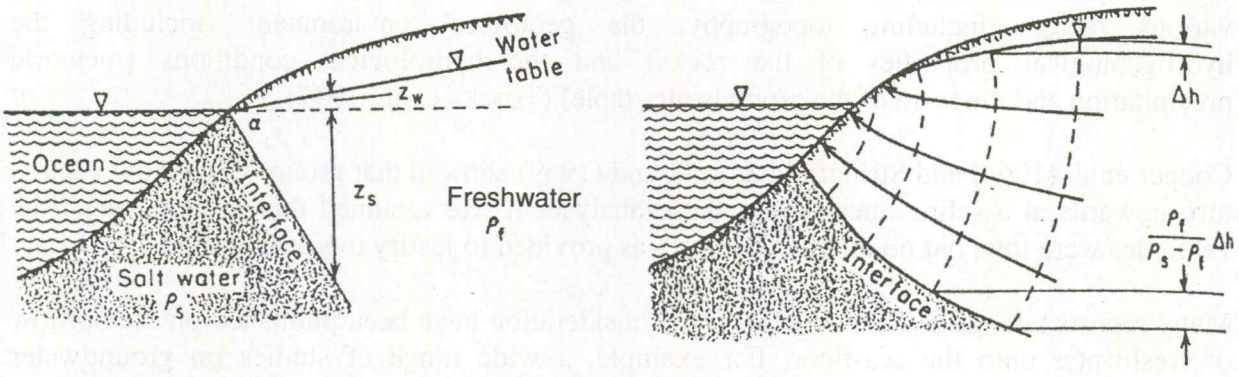
One of the important points to consider when evaluating groundwater flow in a coastal region is the geometry and location of the freshwater/saline water boundary ("saline interface"). This interface occurs between overlying freshwater and deeper marine water and is formed due to the density difference between saline water and freshwater. To understand the characteristics of this boundary, a literature survey was carried out.

The shape, distribution and width of the saline interface are largely controlled by local geology. Assuming, however, that the host rocks are homogeneous, the shape of the saline interface can be determined using Ghyben-Herzberg's law (Figure 3.3-7). This interface has the form that it does because of a balance between the head gradient driving groundwater offshore and the excess head generated offshore by the greater density of the saline groundwater (Bouwer, 1978; Freeze & Cherry, 1979). In places where this interface is located offshore, freshwater can discharge to the sea-bed on the inland side of the interface.

Reilly & Goodman (1985) described freshwater seepage onto the sea-floor due to high groundwater heads generated inland. They also noted that the saline interface was located further offshore when a layered sedimentary sequence dipped offshore. A study by Lusczynski & Swarzenski (1966) on Long Island (New York) showed that several saline groundwater wedges exhibited complex intercalations with fresh groundwater lenses. This finding reflects the variability in the hydraulic conductivities of near-horizontal sedimentary rocks in this area.

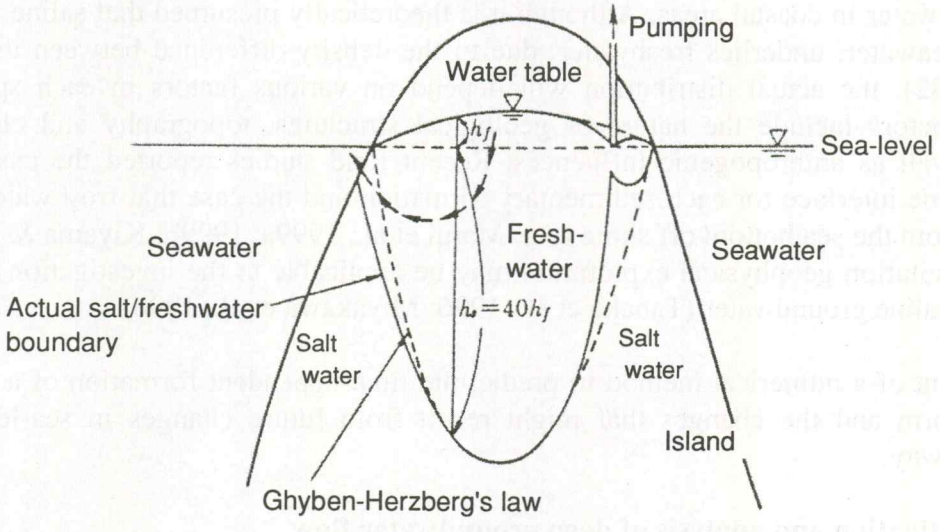
Reports on the saline interface in Japan are largely related to the excessive pumping of fresh groundwater and the resultant invasion of saline water in areas of the coastal plains. These saline water movements occur due to a reduction in the freshwater head and a resultant decrease in the hydraulic gradient from land to sea. Other examples include the destruction of a low permeability geological barrier by harbor construction work, resulting in an invasion by seawater.

The above examples show many variations in the position of the saline interface, resulting from geological differences (e.g. the distribution of permeable and less permeable beds), the hydraulic characteristics of permeable beds, the recharge elevations for the groundwater,



Ghyben-Herzberg's law

(Freeze, R. A. and Cherry, J. A., 1979)



hs = ρf／(ρs-ρf) hf

hs：depth of salt/freshwater interface below sea level

hf：height of water table above sea level

ρf：density (fresh water)

ρs：density (salt water)

（ρf=1.0, ρs=1.025：hs = 40 hf）

Figure 3.3-7 Ghyben-Herzberg's law between freshwater and seawater

General characteristics of the salt water/fresh water boundary are complex, reflecting various factors including land topography (e.g. mountains, valleys, river pattern and coastal topography), geology (sequence of rocks and their distributions and the physical nature of rock formation), hydrological conditions (precipitation and distribution pattern of water head) (Tosaka et al., 1997).

differences in the amount of pumping from wells and the positions of wells. It has been demonstrated that the general characteristics of the saline interface are complex, reflecting various factors including topography, the geological environment (including the hydrogeological properties of the rocks) and the hydrological conditions (meteoric precipitation and the form of the groundwater table) (Tosaka et al., 1997).

Cooper et al. (1964) and Stringfield & LeGrand (1969) showed that groundwater flow vectors turn upwards at a saline interface. In these analyses it was assumed that groundwater flow velocities were low, but no direct evidence was provided to justify this assumption.

Many reports taking the above factors into consideration have been published on the outflow of freshwater onto the sea-floor. For example, a wide range of studies on groundwater seepage onto the sea-floor have been reported based on data on salt content determinations (e.g. Brooks, 1961; Burdon, 1964; Vanek & Lee, 1991; SKB, 1987), isotopic determinations (e.g., Moore, 1996; Tsunogai et al., 1996) and remote sensing and infrared temperature measurements (e.g. Banks et al., 1996; Bogle & Loy, 1995; Roxburgh, 1985).

There remain many uncertainties concerning the distribution and patterns of underground saline and freshwater in coastal areas. Although it is theoretically presumed that saline water, derived from seawater, underlies freshwater, due to the density difference between the two (Murashita, 1982), the actual distribution will depend on various factors in each specific region. Such factors include the nature of geological structures, topography and climatic conditions as well as anthropogenic influences. Recent field studies reported the case that there was a saline interface for each sedimentary formation and the case that freshwater was springing out from the sea bottom off shore (e.g. Marui et al., 1999a, 1999b; Kiyama & Marui, 1999). High-resolution geophysical exploration may be applicable to the investigation of the distribution of saline groundwater (Tanaka et al., 1996; Miyakawa et al., 1998).

The development of a numerical method to predict the time-dependent formation of a saline interface, its form and the changes that might result from future changes in sea-level is currently underway.

3.3.2 Investigation and analysis of deep groundwater flow

In order to understand the characteristics of groundwater flow down to depths of 1000 m, it is necessary to carry out an analysis of the regional flow system. To do this, it is necessary to study both the geological and hydrogeological environments over sufficiently large areas. This has to include a study of any large-scale geological features, such as faults, which might influence groundwater flow, as well as a study of the water balance in the system and the identification of the locations of recharge and discharge. This is followed by drilling, which allows accurate information to be obtained on hydraulic heads and hydraulic conductivities at depth. The final stage of this process could be the construction of an underground research facility, which would allow detailed analyses to be carried out around underground openings and data to be obtained on a local scale. This type of progressive investigation program was carried out in Sweden and Canada at two sites where such underground facilities were constructed (e.g. SKB, 1993).

Studies have been carried out in Japan on regional groundwater flow and on the influence of shaft excavation on groundwater flow and chemistry in the Tono area (including the Tono mine); studies of groundwater flow have also been performed around tunnels in the Kamaishi mine.

Studies of regional groundwater flow and of the influence of shaft excavation were carried out to clarify groundwater flow patterns. These studies included the following components:

- obtaining characteristic hydrogeological data (to provide an understanding of the hydrogeological environment)
- constructing a conceptual model to represent the flow system
- analyzing groundwater flow using numerical methods
- validation of the model by comparison with the actual measured data.

A study of groundwater flow around a tunnel has been carried out in the Kamaishi mine. The main objectives of this study were to develop a model to describe the fractured rocks and to examine the applicability of the model.

1) Study of regional groundwater flow in the Tono area

(1) Establishment of a study area

The aim of the regional analysis of the groundwater flow system in the Tono area was to develop a standard method for investigation and analysis which can be used to obtain reliable hydrogeological data and to understand any regional flow system in a similar geological setting.

To understand the groundwater flow system in an area on the spatial scale of a repository, it is important to understand its relationship with the regional groundwater flow regime. In order to obtain an understanding of the regional groundwater flow system in the Tono area, a literature search was carried out to acquire information on the regional topography and faults. One of the conclusions of this survey was that the flow system in the Tono area is determined by flow within a region of approximately 30 km × 30 km, which is bounded by faults (Figure 3.3-8). This area is considered to be similar to the type of area in which a regional groundwater flow analysis might be carried out (Saegusa et al., 1997).

(2) Method for determining groundwater flow characteristics

To evaluate the characteristic features of groundwater flow in an area, it is necessary firstly to examine the geological structure. It is important to try to relate the directions of groundwater flow, groundwater flow rates and potential flowpaths to geological features. Information on permeability distributions and the influence of topography on recharge and discharge allow boundary conditions to be set.

The evaluation of the groundwater flow characteristics was carried out by:

- conducting a surface hydrologeogical survey
- undertaking a deep hydrogeological survey
- constructing a groundwater flow model and verifying it using head measurements in boreholes.

Firstly, surface and deep hydrogeological surveys were conducted to set the boundary conditions for the hydrogeological model and to determine the hydrological conditions in the area. Following this, a conceptual geological model was developed and then a groundwater flow model was constructed, based on data obtained from the hydrogeological surveys. This model was used to make predictions of transit times for groundwater from surface to depth.

The results of this groundwater flow simulation were evaluated for accuracy by comparison with suitable data obtained from independent measurements.

(3) Measurement of hydraulic and groundwater properties

Studies included:

- measurement of surface water flow volumes
- mapping of the surface geology
- investigation of surface hydrology, including the analysis of remote sensing data
- collection of hydrogeological test data from boreholes and tunnels
- chemical analysis of groundwater.

Firstly, the hydrogeological boundary conditions were set for the study area, based on the surface and groundwater surveys (e.g. Carlsson & Gidlund, 1983; TVO, 1992; Thore, 1986).

At Tono, a study was made of river flow at times of low flow, by making measurements of stream flow rate, electrical conductivity and water quality. It became clear that the unconsolidated sand/gravel beds at the surface have a high storage capacity and the major source of outflow from the ground to the river is from these unconsolidated beds. In addition, the study of river water quality revealed that the dissolved components in the river water depended on the surface geology.

Surface geological structures, hydrogeological characteristics (i.e. hydraulic conductivity) and water quality were studied using shallow boreholes (depth range 30-50 m) in areas with different surface geology in the Tono area.

As part of the analysis of deep groundwater flow, studies were carried out in boreholes to depths of about 1000 m. These included geophysical wireline logging, borehole TV and packer testing, in order to determine hydraulic heads, hydraulic conductivities, groundwater flowpaths and the hydraulic characteristics of a fault crushed zone.

In order to carry out hydraulic tests in the low permeability granite in the Tono area, new equipment had to be developed, since testing at these depths and in such low permeability environments is not routinely carried out in civil engineering. The equipment developed was similar to that which has been developed in other countries, for example the umbilical hose system developed in Sweden (SKB, 1991). This equipment had to be designed to withstand relatively high temperatures and pressures and yet maintain its accuracy. A new instrument which could be used to depths of 1000 m in low permeability rocks was subsequently developed (Yanagizawa et al., 1988).

This instrument measures the hydrogeological parameters of the rock mass using a sensor which is connected to a rod and is moved up and down the borehole wall. Borehole wall collapse is taken into account. With this instrument, the following three hydrotesting methods were possible: the JFT (Johnston's Formation Test) method for transient measurements, the pulse method developed for low permeability rocks and a steady-state pumping test. Using these methods, a wide range of hydraulic conductivity measurements covering the range from 10^{-6} m s^{-1} to 10^{-12} m s^{-1} were made.

In addition to the above, a method was developed to complement the original method for making in situ hydraulic conductivity measurements in sedimentary rocks. This new method provides an estimate of hydraulic conductivity based on the apparent distribution of specific resistance, which was measured using a basic geophysical logging method (Ogata et al., 1992). The new method made use of the good correlation between apparent specific resistance

and hydraulic conductivity. A new formula was developed to represent this relationship. At Tono, fractured rocks such as granite showed a reasonable correlation between the flow velocity measured from flow meter logging and fluxes calculated from measurements of hydraulic conductivity and head using a conventional packer system. A new method for estimating the hydraulic conductivities of such rocks, using a new formula, was also developed (Ogata et al., 1997).

If it were possible to find a correlation between the results of well logging and conventional packer testing using these methods, continuous estimation of hydrogeological characteristics of the rock mass, measured in boreholes, would be possible. In addition, a method for determining the spatial distribution of hydraulic conductivity in the rock mass was developed.

It has been demonstrated that the hydraulic conductivity distribution in many fractured rocks obeys the law of fractal scaling (Humm & Impey, 1994). To test this theory in the laboratory, an experiment was carried out in which a heterogeneous conductivity field was constructed using glass beads. The law was found to be reproducible on this scale by comparing computer simulations of the flow-field with the experimental results (Hatanaka et al., 1995). The same method was used in real fractured rocks to confirm its applicability. A test was performed in an area in the Tono mine containing four 100 m vertical boreholes. The distribution of hydraulic conductivity was estimated from an algorithm relating the hydraulic conductivity to the results of wireline logging. To test if the estimated hydraulic conductivity distribution was valid, a uranium tracer test using particle tracking was carried out. It was demonstrated that the location of the maximum density of particles coincided with the main zone of uranium mineralization, thereby demonstrating the applicability of this method (Clark et al., 1995). An extension of this method to three dimensions is under consideration (Takeuchi et al., 1997).

(4) Construction of a conceptual hydrogeological model

A conceptual hydrogeological model was constructed by including hydrogeological information in the geological structural model. The areal extent of the model and the boundary conditions were determined from hydrogeological testing and from preliminary groundwater flow simulations.

The applicability of this model was evaluated by comparing the results of groundwater flow simulations, based on this model, with actual hydrogeological test data, precipitation data, surface water data from river flows, long-term data on hydraulic heads and groundwater quality and age data.

A geological structural model, based on a survey of surface waters and hydrogeological testing, was constructed for the Tono mine area. The distribution of hydraulic conductivity values measured in boreholes in the granitic basement was upscaled to three dimensions, using a geostatistical method. The usefulness of the MKM (Multi-Kernel Modulation: Williams, 1988) estimation method over the kriging method was confirmed by applying the geostatistical method to the distribution of permeability of the sedimentary rocks in the Tono area. From the results of these analyses, a hydrogeological model of the study area was constructed.

Estimation of the hydraulic conductivity of the rock mass between measured data points (e.g. boreholes) can be made using geostatistics. This method is based on the distribution and correlation of spatial hydraulic conductivity data and is an effective method for allowing the heterogeneity of the rock mass to be taken into account.

(5) Modeling of groundwater flow and verification of results

To obtain a regional picture of the groundwater flow system in the Tono area, the flow of groundwater over a fault-bounded area of about 30 km^2 was modeled (Saegusa et al., 1997).

The results of this simulation showed that the area north of the Tono mine is a recharge zone and that the southern part (the Toki River) is an area of discharge (Figure 3.3-8). This means that the area around the Tono mine forms the main groundwater flow system relevant to understanding flow at the depth of the mine.

In order to model groundwater flow, the heterogeneous, low permeability rocks in the study area were assumed to be porous and the groundwater flow within the rock was treated as a three-dimensional saturated-unsaturated seepage flow. A finite element model which obeys Darcy's law was used. Groundwater flow modeling was carried out using the program TAGSAC (Three-Dimensional Analysis of Groundwater Flow, a SAitama University Code; Imai & Yanagizawa,1990).

2) Investigation of the effect of shaft excavation on groundwater flow in the Tono area

(1) Background

An analysis of the effect of shaft excavation on groundwater flow was carried out in order to investigate groundwater flow from the surface to the sub-surface in a small area of the rock mass. A shaft with a diameter of 6 m and a depth of 150 m, known as the No. 2 shaft, was excavated in the Tono mine for this purpose; an area of 1 km^2 around this shaft was monitored during its construction and the data used for analysis of groundwater flow (Figure 3.3-9). In addition to investigations on groundwater flow, measurements were carried out to try to verify the results of the groundwater flow modeling and to investigate the analytical methods that had been applied.

(2) Methodology for evaluation of groundwater flow characteristics

The objectives of this study were:

- to understand the effect of excavation of the shaft on the surrounding rock mass
- to verify if the three-dimensional, transient saturated-unsaturated seepage flow analysis based on Darcy's law was applicable, assuming that the rock mass which contained discontinuities and had a spatially variable conductivity could be treated as porous media
- to confirm that the above approach was applicable for analyzing the characteristics of groundwater flow.

The study consisted of:

- estimation of recharge based on measurements of the amounts of precipitation, river flow and evaporation
- measurements of in situ hydrogeological data, including hydraulic conductivity and hydraulic heads from boreholes
- construction of a hydrogeological model based on data from surface mapping, geophysical surveys and boreholes.

(3) Measurement of hydraulic properties

To understand surface and near-surface groundwater flow, a long-term monitoring system for determining surface water hydrological coefficients, consisting of meteorological observation instruments, river flow meters, soil moisture meters etc. (Okazaki et al., 1997), was employed and the surface water balance was measured (Figure 3.3-10). This system enabled the extent of surface recharge, as an upper boundary condition, to be measured. A value of 340 mm a^{-1} was obtained for the recharge area and 69 mm a^{-1} for the whole drainage area for this study.

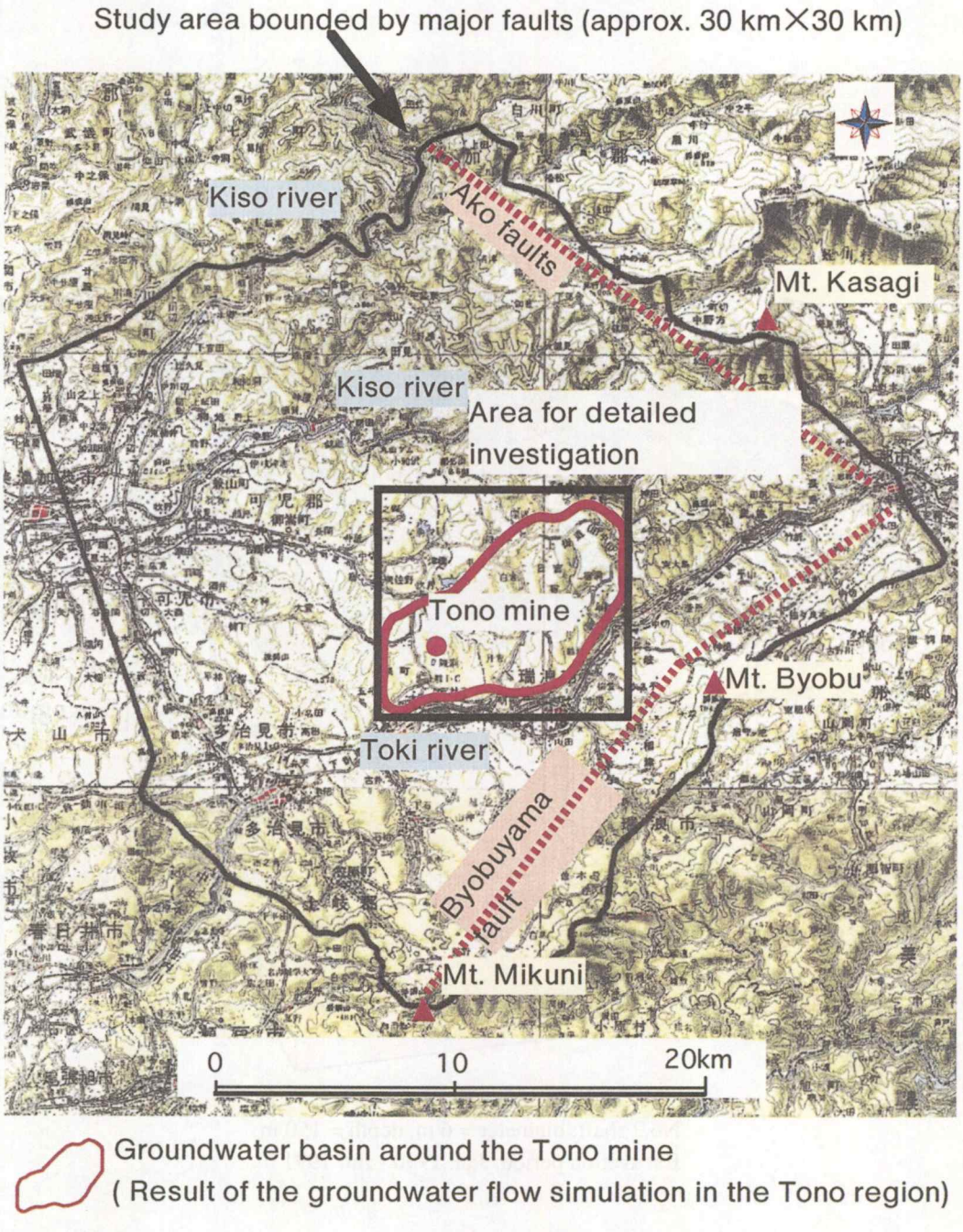
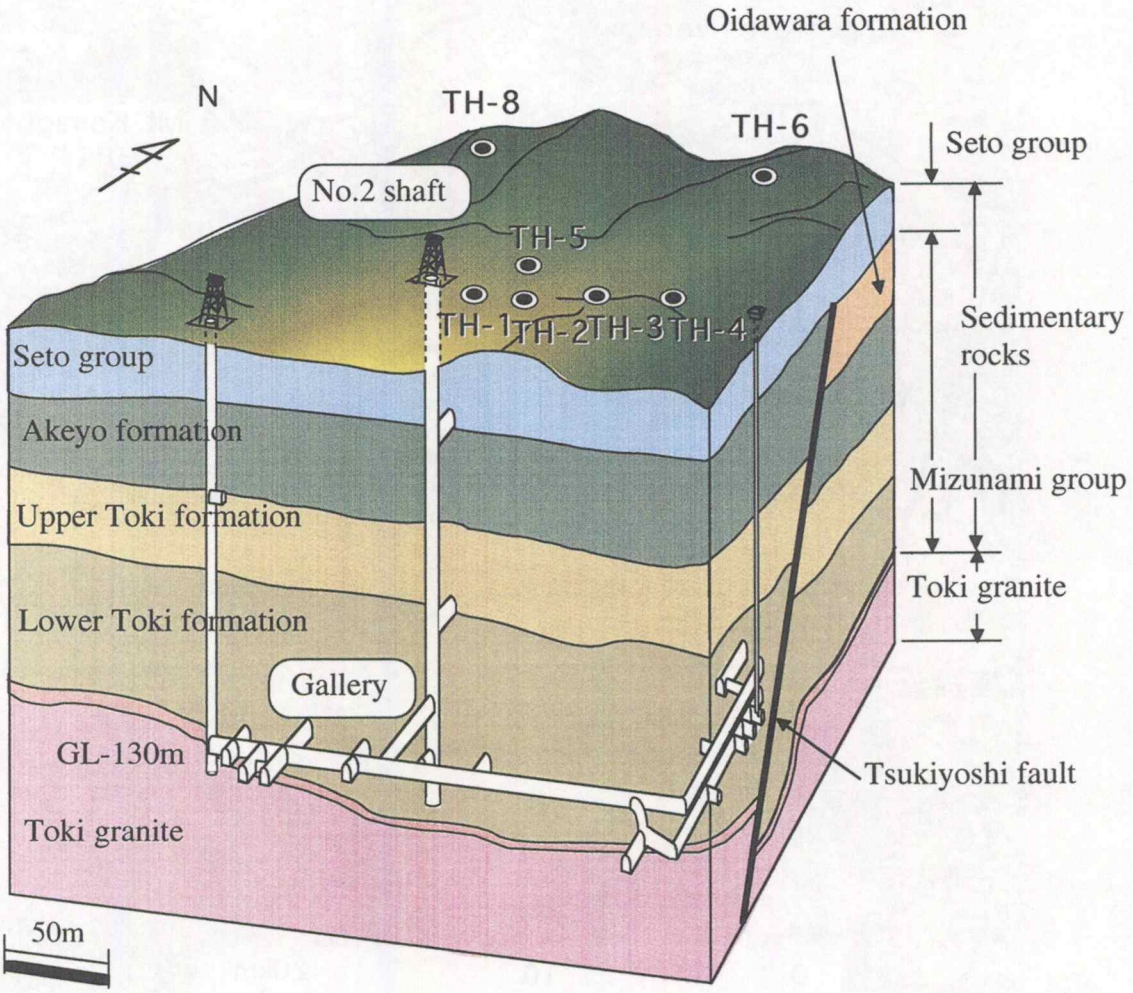


Figure 3.3-8 Example of the groundwater flow simulation in the Tono region

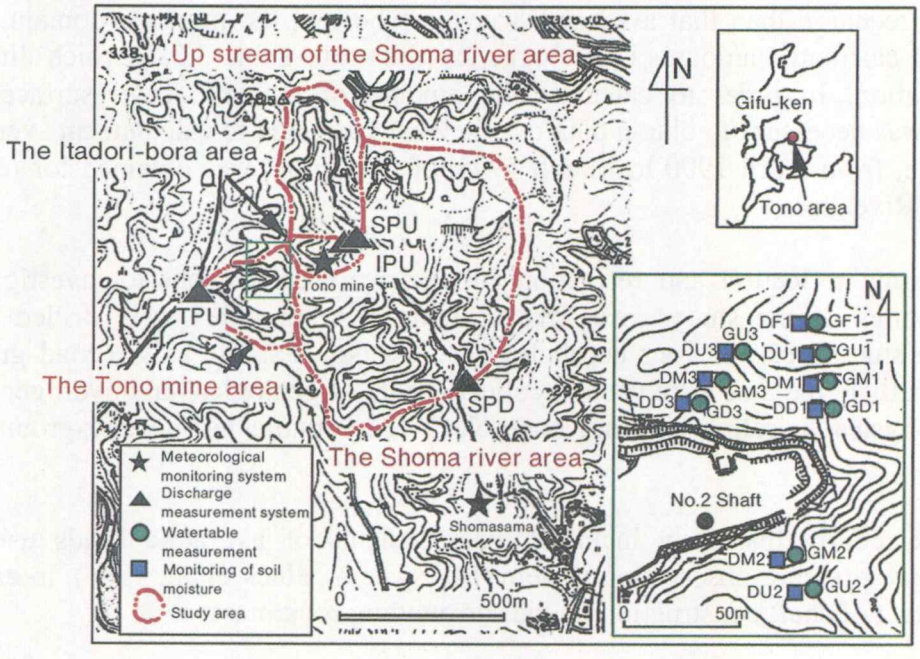
To understand the overall groundwater flow system in the Tono area, a literature survey on surrounding topography and faults was carried out. One of the conclusions of this survey was that a region of about 30 km×30 km bounded by major faults constricted the overall groundwater flow system of the Tono area. A simulation of groundwater flow showed that the northern part of the area around the Tono mine is the recharge area (from rain etc.) and the southern part (Toki River area) is the discharge area.



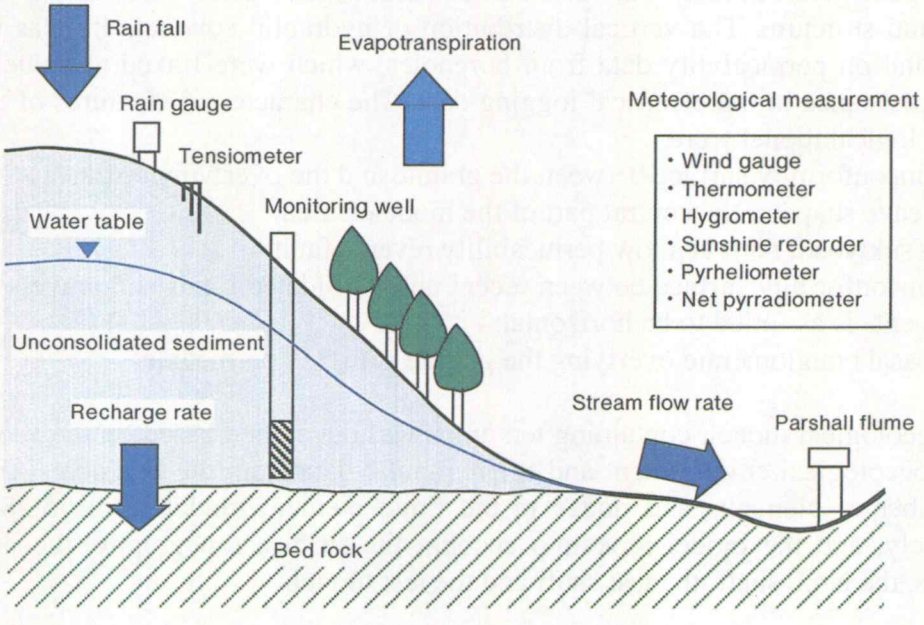
No.2 shaft: diameter = 6 m, depth = 150 m,
Excavation period: Jan. 1990 - Jul. 1991

Figure 3.3-9 Geological setting of the Tono mine

No.2 shaft, with a diameter of 6 m and depth of 150 m, was drilled in the Tono mine area to investigate the hydrological effect of shaft excavation in the surrounding rocks. The target area was 1 km x 1 km surrounding the No.2 shaft (depth was from ground surface to 0 m above sea level).



Location of study area



Subsurface hydrological monitoring system

Figure 3.3-10 Subsurface hydrological investigation system

These values were obtained from unconsolidated gravels overlying Neogene sedimentary rocks for the period between 1990 and 1994. The recharge area is therefore associated with five times more recharge than that averaged over the whole of the modeled domain. Water balance data and calculated amounts of recharge are shown in Table 3.3-2, which illustrates the annual variation. In order to calculate the amount of recharge from surface water observations, it was necessary to obtain data over several years and to calculate an average. A five-year average, from April 1990 to March 1995, of 69 mm a^{-1} was obtained for recharge from the Shoma River area.

In addition, seismic reflection and refraction surveys were carried out to investigate the geological structures of the study area. Five 200 m deep boreholes were drilled on the periphery of the study area and four boreholes near the No. 2 shaft. This second group of boreholes were fully cored and were used to collect a suite of geological and hydrogeological data using geophysical wireline logging, borehole TV, hydraulic testing and groundwater sampling.

Other data collected in this study included measurements of hydraulic heads using the multiple point pore pressure observation system (MP system, Black et al., 1986), to examine the long-term effect of shaft construction on the surrounding rock mass.

(4) Construction of a hydrogeological model

A hydrogeological model was constructed using geological information to define the background structure. The vertical distribution of hydraulic conductivity was based on core logging and on permeability data from boreholes, which were linked to values for apparent specific resistance in the electrical logging data. The characteristic features of the conceptual hydrogeological model were:

- The unconformity surface between the granite and the overlying sediments in this area has a concave shape in the central part of the modeled area.
- The Tsukiyoshi fault is a low permeability reverse fault.
- The unconformity surface between recent unconsolidated sands and gravels and Mesozoic sediments is assumed to be horizontal.
- The basal conglomerate overlying the granite is highly permeable.

A hydrogeological model, containing ten units, was developed based on the above features of the hydrogeological environment and the hydraulic data from the boreholes (Figure 3.3-11). The number of elements and nodes in the finite element model were 15,283 and 17,280 respectively, and the model took into account the surface topography, the position of the boreholes, the No.2 shaft, the test shaft and the test tunnel.

(5) Groundwater flow modeling and calibration of the model

The following factors were taken into consideration in the groundwater flow modeling:

- surface topography
- the tunnels of the Tono mine
- the Tsukiyoshi fault
- the boreholes.

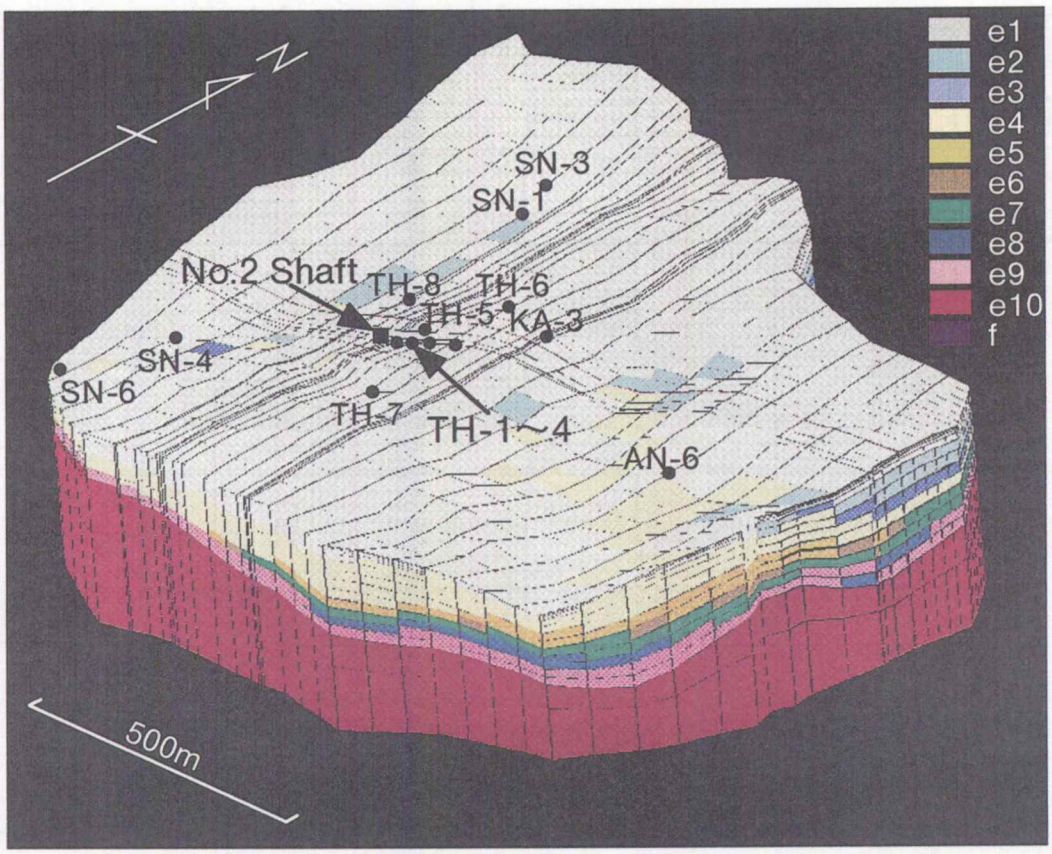
Other data used to develop the model included:

- geological survey data around the Tono mine
- in situ hydraulic test data
- data from the surface water hydrological observations.

Table 3.3-2 Water balance of the Shoma river area and the Tono mine area

year		1990	1991	1992	1993	1994	average
rain fall (mm a^{-1})		1,532	1,885	1,304	1,657	1,079	1,491
evapotranspiration (mm a^{-1})		525	463	495	414	492	478
rain fall / evapotranspiration		34%	25%	38%	25%	46%	32%
up stream of the Shoma river area	stream flow rate (mm a^{-1})	666	958	521	877	337	672
	stream flow rate / rain fall	43%	51%	40%	53%	31%	44%
	recharge rate (mm a^{-1})	341	464	288	366	250	341
	recharge rate / rain fall	22%	25%	22%	22%	23%	23%
the Shoma river area	stream flow rate (mm a^{-1})	970	1,348	790	1,180	434	944
	stream flow rate / rain fall	63%	72%	61%	71%	40%	61%
	recharge rate (mm a^{-1})	37	74	19	63	153	69
	recharge rate / rain fall	2%	4%	1%	4%	14%	5%
the Tono mine area	stream flow rate (mm a^{-1})	–	1,303	–	–	410	857
	stream flow rate / rain fall	–	69%	–	–	38%	54%
	recharge rate (mm a^{-1})	–	119	–	–	177	157
	recharge rate / rain fall	–	6%	–	–	16%	11%

The recharge rate in the Shoma River area was 0.19 mm per day (69 mm per year).
(a five year average from April 1990 to March 1995)



unit number	hydraulic conductivity (m s^{-1})	specific storage (m^{-1})	porosity	stratigraphy
f	1.0×10^{-10}	1.0×10^{-4}	0.3	Tsukiyoshi fault
e1	1.0×10^{-7}	1.0×10^{-4}	0.4	surface soil + Seto group
e2	5.0×10^{-10}	1.0×10^{-5}	0.3	Oidawara formation
e3	5.0×10^{-8}	1.0×10^{-5}	0.3	Oidawara formation
e4	1.0×10^{-8}	1.0×10^{-5}	0.3	Akeyo formation
e5	5.0×10^{-10}	1.0×10^{-5}	0.3	Akeyo formation
e6	1.0×10^{-9}	1.0×10^{-5}	0.3	Akeyo formation
e7	5.0×10^{-9}	1.0×10^{-5}	0.3	Toki formation
e8	1.0×10^{-8}	1.0×10^{-5}	0.3	Toki formation
e9	1.0×10^{-7}	1.0×10^{-5}	0.3	Basal conglomerate + weathered granite
e10	1.0×10^{-9}	1.0×10^{-7}	0.1	Granite

Figure 3.3-11 Hydrological-geological structural model for analysis of the Tono area

A grid was constructed (number of elements 15,283 and number of nodes 17,280) taking the following factors into account; topography, position of boreholes, No.2 shaft, test shaft, test galleries and hydrological-geological structure.

The aim of this analysis was to simulate the transient changes in groundwater heads accompanying shaft excavation and seepage to the No. 2 shaft. The results of the modeling were compared with the amount of seepage measured in the No. 2 shaft and the long-term observation of hydraulic heads in the boreholes in the vicinity of the shaft. The results showed a good match with the observed hydraulic heads (Figure 3.3-12). In addition, the predicted seepage into the No. 2 shaft showed a good agreement with the measured value and, at the end of the excavation phase, the seepage returned to a steady-state value (Figure 3.3-13). Figure 3.3-14 shows the relationship between the horizontal distance from the No. 2 shaft and the drawdown measured from the Tono mine tunnel, illustrating the decrease in hydraulic head due to excavation of the No. 2 shaft. The model predicted that the zone showing a decrease in head in excess of 10 m would be restricted to within 100 m of the shaft.

It was confirmed from the above analysis that:

- The assumption that heterogeneous, low permeability rocks with a hydraulically significant discontinuity, such as a fault, can be treated as a porous medium is essentially correct. In addition, groundwater flow within such rocks could be modeled assuming Darcy's law. Therefore, three-dimensional, transient unsaturated seepage flow analysis is applicable.
- It was found to be appropriate to adopt a systematic approach consisting of (1) hydrogeological data acquisition, (2) construction of a hydrogeological model, (3) making predictions regarding groundwater flow and (4) further developing the model, taking long-term observation data into account.

3) Investigation of groundwater flow around the tunnels in the Kamaishi mine

The flow of groundwater around the tunnels in the Kamaishi mine has been investigated. The groundwater flow characteristics were evaluated using a model in which a network of pathways was assumed to exist associated with fractures in the rocks. A systematic investigation was carried out of the spatial variability of the groundwater flow system, using hydraulic test data and information on the structure of the rock mass derived using geophysical techniques. In addition to the construction of this fracture network model for groundwater flow, a tracer test was used to examine the flow of water through a single fracture (JNC, 1999b).

The effect of tunnel excavation on the hydraulic conditions in the surrounding rocks was investigated by measuring the hydraulic conductivity and the hydraulic head in the excavation disturbed zones around tunnels at Tono and Kamaishi (Adachi & Sugihara, 1996). Equipment was also developed to allow high precision measurements to be made of the extent of evaporation from a tunnel wall and was subsequently applied at Tono and Kamaishi and also in the Stripa Project in Sweden (Watanabe et al., 1989; 1990).

(1) Hydraulic properties around tunnels in a fractured rock mass

It is reasonable to assume that fracture networks in hard rocks will control the flow of groundwater around underground tunnels. Within a single fracture, dispersion within the fracture and diffusive transport out of the fracture and into the surrounding rock mass are both possible. The complex geometry of fractures and the variable porosity of the adjacent rock mass will complicate these processes. In order to try and understand the hydrogeological characteristics of such fracture systems, a zone several tens of meters wide surrounding a tunnel was investigated. The fracture network, in particular those fractures that were considered to be most significant in controlling the flow of groundwater, was examined. In order to understand the transport of solutes, in situ tests on a single fracture and on a fracture zone were carried out.

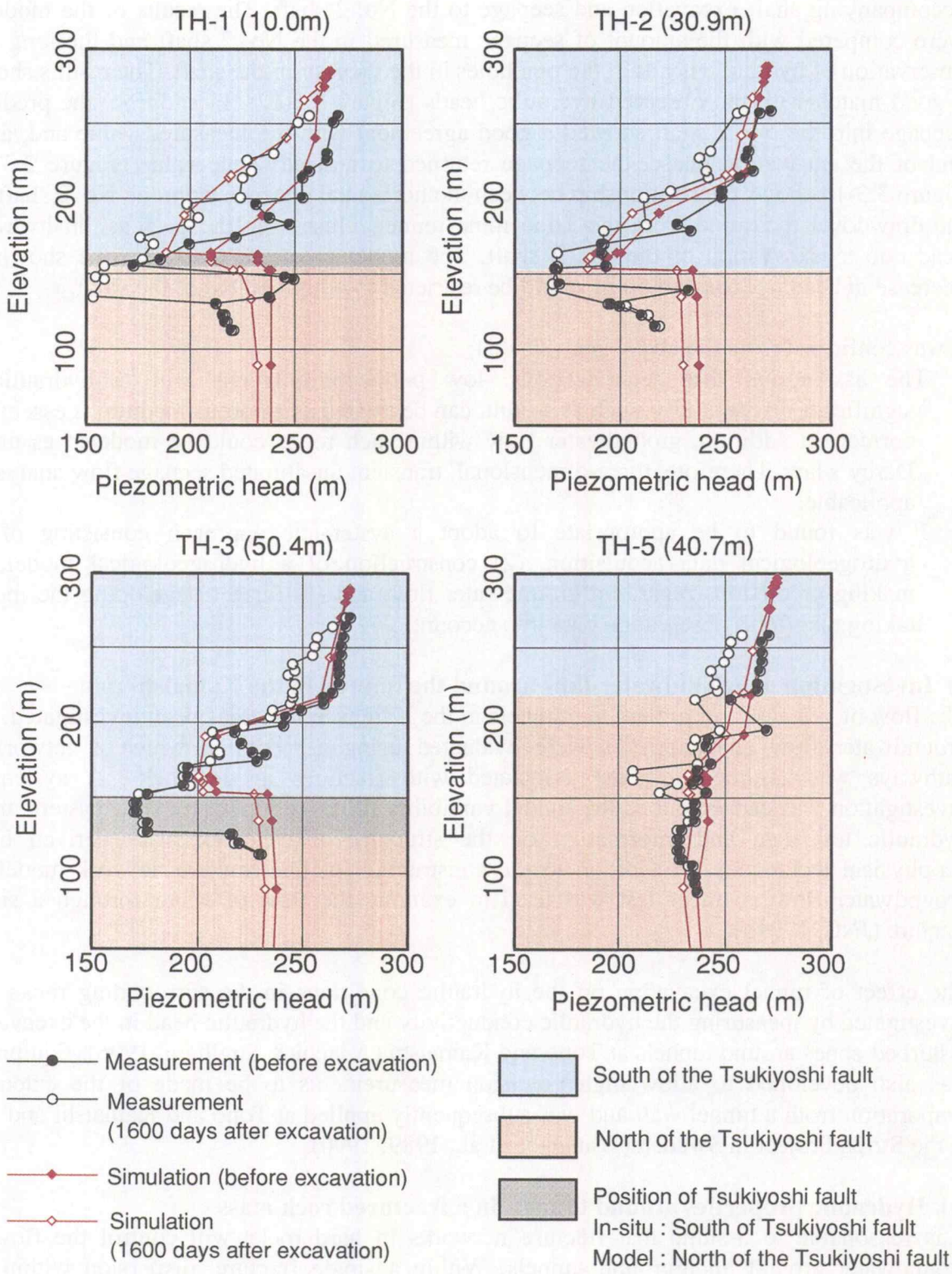


Figure 3.3-12 Piezometric head distribution along the boreholes measuring porewater pressure during sinking of the No.2 shaft

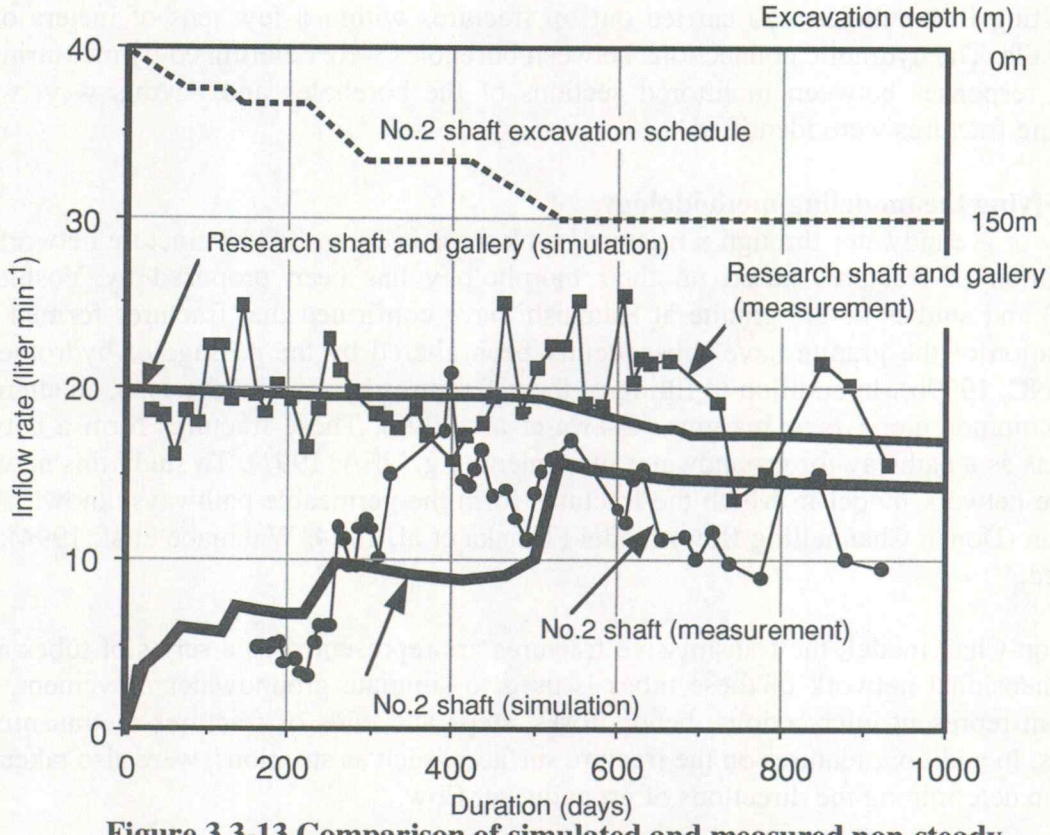


Figure 3.3-13 Comparison of simulated and measured non-steady transition of inflows

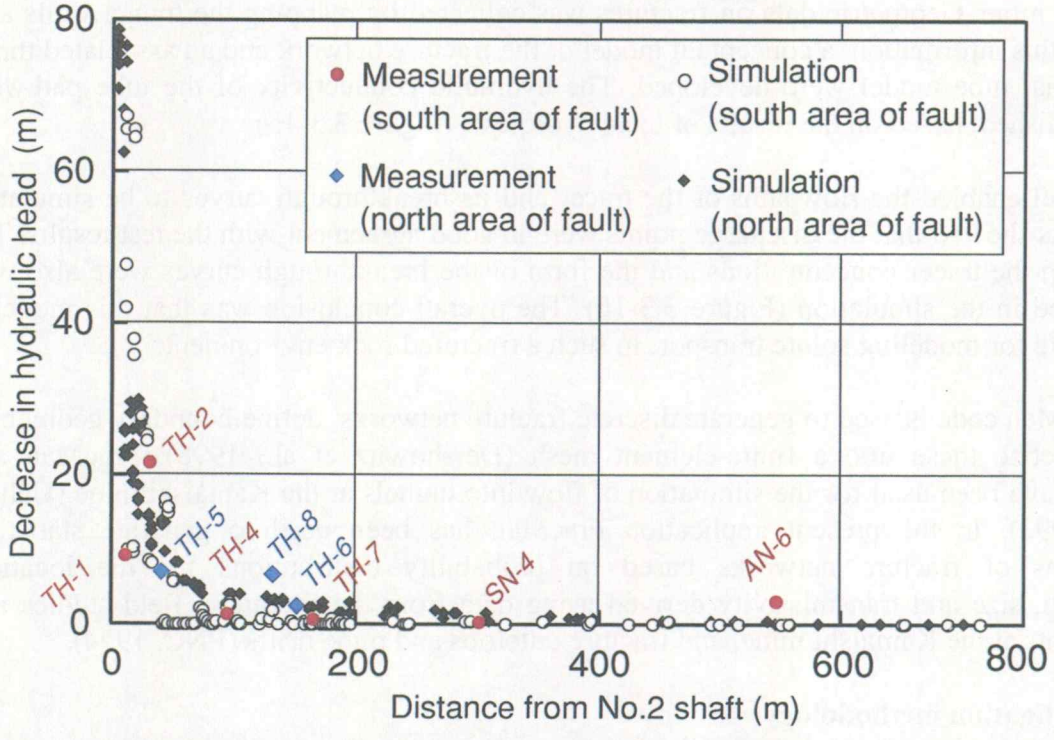


Figure 3.3-14 Relationship between distance from No.2 shaft and decrease in hydraulic head (160~162 m above sea level, 1600 days after No.2 shaft excavation)

This figure shows the relationship between horizontal distance from the No.2 shaft and the decrease in hydraulic head in the Tono mine gallery (160~162 m above sea-level). The decrease in hydraulic head caused by the excavation of No.2 shaft is shown. It was predicted that the area showing a decrease in hydraulic head of more than 10 m was restricted to within 100 m of the shaft.

Hydrotesting in boreholes was carried out on fractures within a few tens of meters of the tunnel walls. The hydraulic connections between boreholes were determined by measuring the pressure responses between monitored sections of the boreholes and, in this way, water-conducting fractures were identified.

(2) Verifying the modeling methodology

The flow of groundwater through a fractured rock mass is controlled by fracture networks. A classification of fractures based on their morphology has been proposed by Yoshida et al.(1989) and studies of the granite at Kamaishi have confirmed that fractures formed after solidification of the granite have subsequently been altered by the passage of hydrothermal fluids (JNC, 1999b). In addition to filling of these fractures by mineral deposits, an alteration zone is common along their margins (Osawa et al., 1995). These fractures form a network which acts as a pathway for groundwater movement (e.g. NEA, 1991). To study this network, a fracture network model in which the fractures form the permeable pathways, known as the Don-Chan (Donen Channelling flow) model (Tanaka et al, 1994; Watanabe et al, 1994), was developed.

In the Don-Chan model, the transmissive fractures are represented as a series of tubes and a three-dimensional network of these tubes is used to simulate groundwater movement. This model can represent intersections, bends, forks, steps and ends of fractures as transmissive pathways. In addition, features on the fracture surfaces, such as striations, were also taken into account in determining the directions of groundwater flow.

To evaluate the applicability of the Don-Chan model, a tracer test was carried out at the Kamaishi mine. Geometric data on fractures was collected by mapping the tunnel walls and, based on this information, a conceptual model of the fracture network and an associated three-dimensional tube model were developed. The hydraulic conductivity of the tube pathways was established, based on the results of local hydrotests (Figure 3.3-15).

This model enabled the flowpaths of the tracer and its breakthrough curves to be simulated. The results showed that the discharge points were in good agreement with the test results. The maxima in the tracer concentrations and the form of the breakthrough curves were also well represented in the simulation (Figure 3.3-16). The overall conclusion was that this model is appropriate for modeling solute transport in such a fractured rock environment.

The FracMan code is used to generate discrete fracture networks, define boundary geometries and discretize these into a finite-element mesh (Dershowitz et al., 1998). FracMan and MAFIC have been used for the simulation of flow into tunnels at the Kamaishi mine (Uchida et al., 1993). In the present application FracMan has been used to generate statistical realizations of fracture networks based on probability distributions for the location, orientation, size and transmissivity derived using data from the literature, field studies and experiments at the Kamaishi mine, and fracture outcrops and mine drifts (PNC, 1994).

(3) Investigation methodology

Two modeling approaches were used for the fractured rocks at Kamaishi - a spatially variable, continuous porous medium approach (using normal three-dimensional finite element codes) and a discontinuous approach (using the FracMan code and the Don-Chan model). The approach followed has to reflect the actual distribution and characteristics of the permeable fractures. The discontinuous modeling approach (FracMan, Don-Chan) represented the scale effects better and was therefore judged to be more suited to the analysis of granite (Shimo and Iihoshi, 1996; Shimo et al., 1997). However, all the methods used were shown to provide

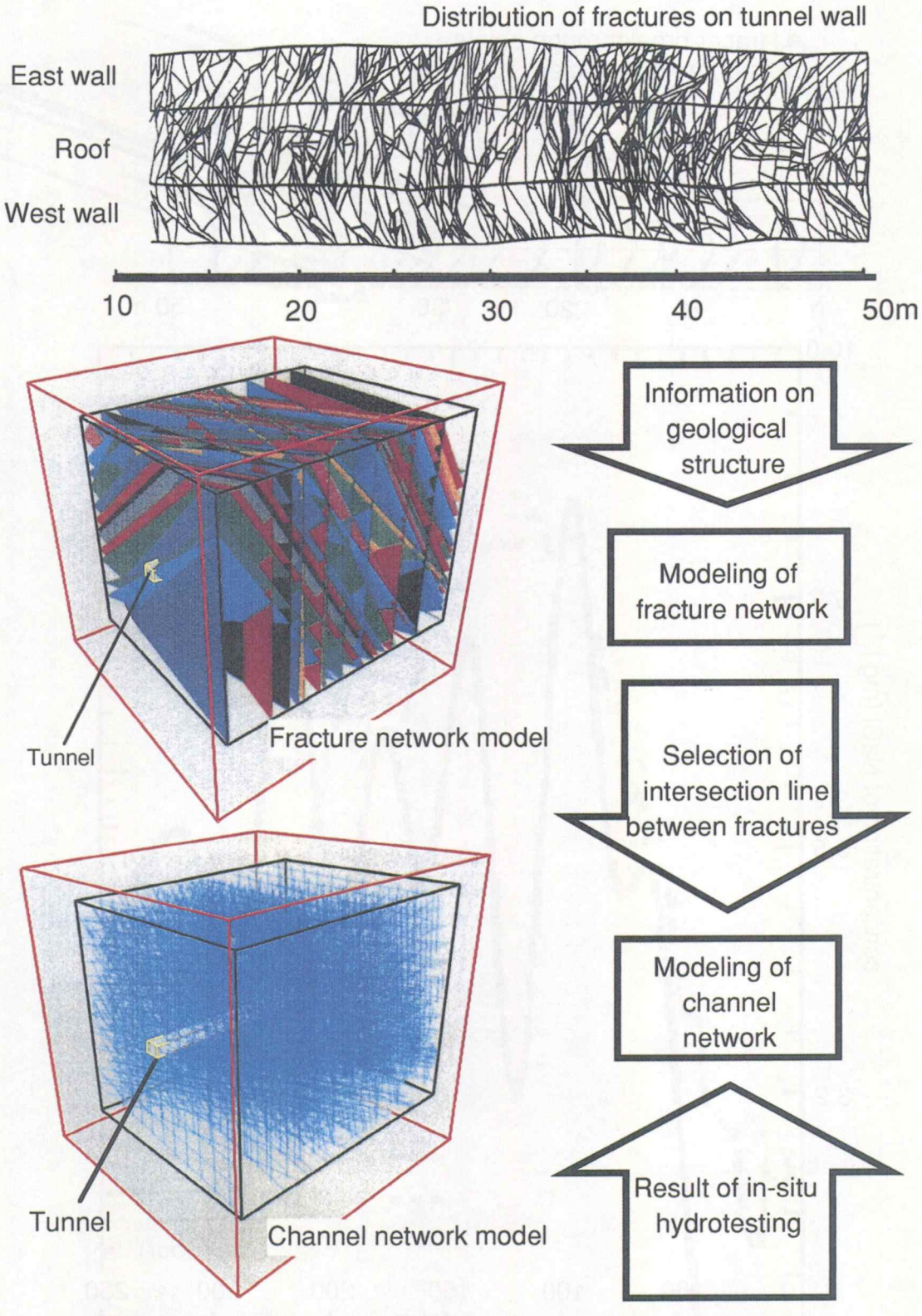


Figure 3.3-15 Modeling of a 3-dimensional channel network using the Don-Chan model

To evaluate the applicability of the Don-Chan model, a tracer test was carried out at the Kamaishi mine. To model the fractures, fracture shape and other geometric information was collected from the tunnel wall. Based on this information, a fracture model and three-dimensional tube network were formulated and the hydraulic conductivity of the tube pathways, based on the in situ test, was established.

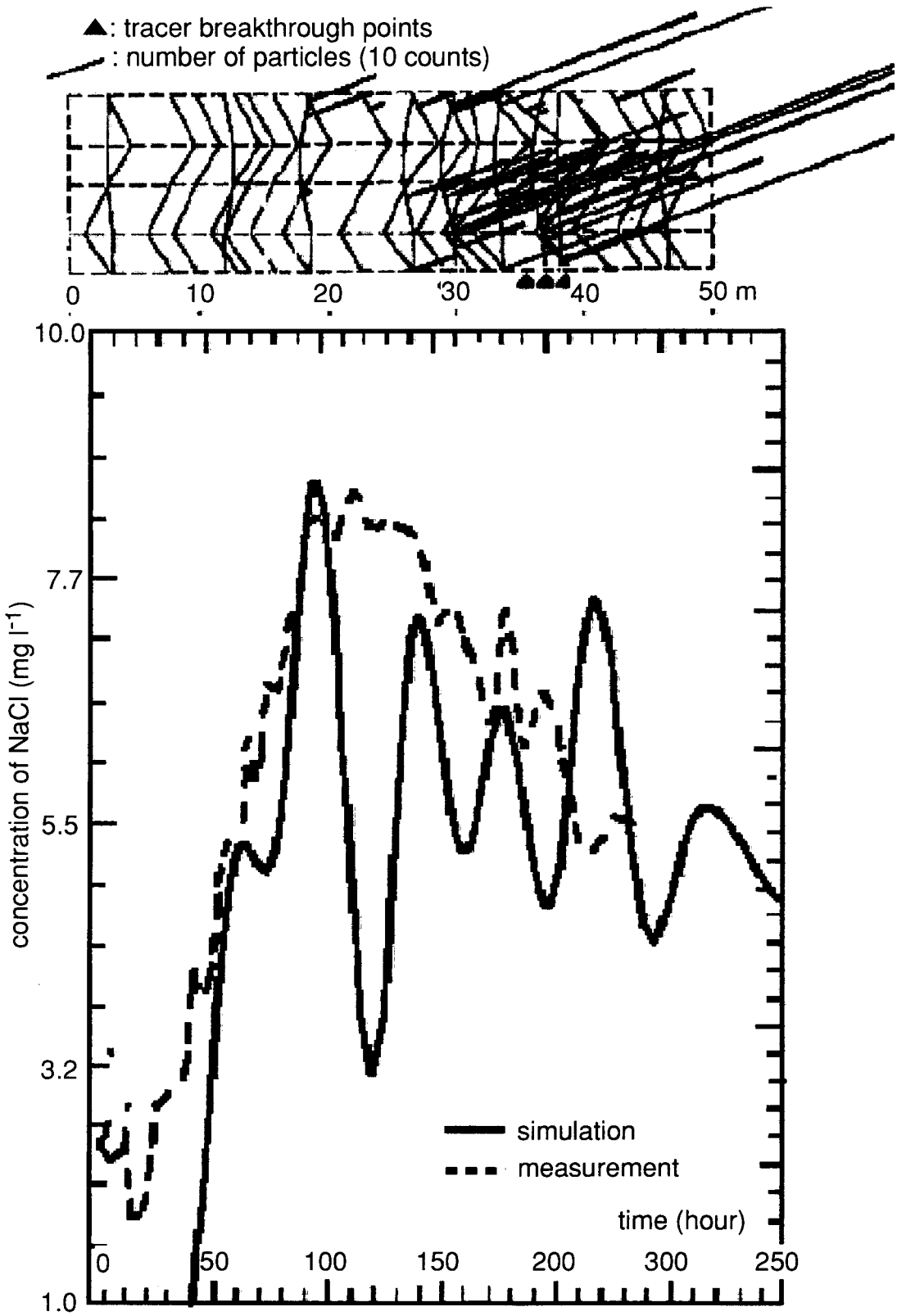


Figure 3.3-16 Concentration of recovered tracer versus time after tracer injection; a comparison of measured values and values simulated by the Don - Chan model

Using this model, the locations of tracer breakthrough and the shape of the breakthrough curves were simulated. The simulated locations of tracer breakthrough matched well with the test results. The observed peak positions and trend of the breakthrough curve were also well matched by the simulation. It was concluded that the method was appropriate.

reasonable estimates of the distribution of hydraulic heads and the variation in influx of groundwater into the tunnels.

Hydrotest results were combined with the results from specific resistance and electromagnetic methods to provide a better understanding of the three-dimensional nature of transmissive pathways. The methods included combining transient changes in hydraulic head with the three-dimensional permeation theory (Nishigaki et al., 1991; Nakaya et al., 1992), as well as matching changes in groundwater head with time and comparing these with theoretical curves (Hsieh & Neuman, 1985a, 1985b). Crosshole testing can be divided into the pulse method (Tosaka et al., 1990; Masumoto et al., 1992) and the sinusoidal method, which provided useful results when it was used during the Stripa Project in Sweden (Black & Ki, 1986; Black, 1986).

Crosshole testing equipment was applied at Kamaishi to confirm its performance and to examine the validity of the analysis method (Takeuchi et al., 1998). This equipment was specifically developed to obtain data such as the permeability of a single fracture, its specific storage coefficient, the heterogeneity of these hydrogeological attributes and the connectivity of the fracture network. The equipment can also be used for carrying out sinusoidal tests.

3.3.3 Summary

The following conclusions were reached on the characteristics of groundwater flow, based on a literature survey and on actual measurements performed at Tono and Kamaishi:

The stepwise approach that was applied in the Tono area for modeling groundwater flow was shown to be appropriate. Similarly, the modeling approaches that were used at Tono for examining the effects of shaft excavation, and at Kamaishi for modeling the excavation disturbed zone around a tunnel in fractured rock, were also shown to be appropriate.

Based on a theoretical analysis and measured data, it was confirmed that the hydraulic gradients at depth tend to be smaller than those closer to the surface. Data on the ranges of permeability for different rock types were collected and summarized. Although the permeability varies depending on the rock type and region, the average hydraulic conductivities of the rock mass mostly ranges from approximately 10^{-10} to 10^{-7} m s^{-1}, excluding fault crushed zones and damaged zones around faults.

To understand the characteristics of deep groundwater flow, various major geological structures, such as faults, which were expected to affect groundwater flow, were investigated. In addition, groundwater balance calculations were performed and surface hydrological characteristics were studied. Better information on hydraulic gradients and permeabilities at depth were obtained from these investigations.

3.4 Geochemical characteristics of groundwater

The geochemical characteristics of groundwater and the physico-chemical properties of the geosphere evolve with time due to rock-water interactions (e.g. Drever, 1988).

Various origins of groundwater can be considered, for example meteoric waters, seawater and hydrothermal solutions. Hydrothermal solutions are derived from interactions between water and magma or high-temperature rock bodies in geothermal areas. Meteoric waters are generally dilute, with characteristic isotopic compositions of hydrogen and oxygen. The geochemical evolution of these meteoric waters is typically characterized by increasing pH with depth, due to weathering reactions involving silicate minerals. Dissolved oxygen concentrations also typically decrease, due to progressive microbial decomposition of organic materials and dissolution of iron-bearing / sulfide minerals. Replacement of dissolved Ca by dissolved Na also occurs due to ion exchange reactions between clay minerals and groundwater (Ichikuni and Ogura, 1992; Stumm and Morgan, 1996). Groundwater chemistry in geothermal areas is controlled by interactions between rocks and groundwater at high temperatures and these groundwaters may have a relatively high total dissolved solids content. In coastal areas, groundwater may be derived from seawater incursion. Such water usually has a characteristic oxygen and hydrogen isotopic composition (both typically close to zero per mil) and Br/Cl ratios (usually around 3.4×10^{-3} on a mass basis).

The present section describes results obtained from a literature survey of the chemical composition of groundwaters in Japan and data acquired in the Tono area and at the Kamaishi mine.

3.4.1 Geochemical characteristics of groundwater in Japan

1) Geochemical characteristics of meteoric groundwater

Some 15,000 analyses of groundwater in Japan have been collected from the published literature (about 3,600 references). These data demonstrate that the pH ranges from 5 to 10, except for groundwaters from springs (Seo and Shimizu, 1992), bearing in mind the following constraints:

- Most of the data collected were for irrigation water, from hot springs or from oil wells.
- Many of the data were for groundwaters from Quaternary strata.
- Data for depths greater than 500 m are limited.
- Data concerning redox potential are more scarce than those for other parameters.

From the above survey, meteoric waters were identified and screened to select the most relevant compositions for evaluating potentially suitable areas to host a HLW repository. The screening was done using the following criteria:

- Groundwater samples from hot springs, geothermal wells and oil and gas wells were excluded.
- Taking account of the theoretical pH value when air is in equilibrium with water, and the fact that the upper pH limit increases due to water-rock reactions, only data with a pH value in the range 5.7 to 10 were used.
- Data suggesting an unusually high geothermal gradient (temperature > 30°C km^{-1} × depth, km + 20°C), indicative of possible effects of geothermal activity, were excluded.
- Data showing extraordinarily high concentrations of chlorine and sulfuric acid, that suggest possible effects of seawater or hydrothermal water, were excluded.

Groundwater of atmospheric origin in sedimentary and igneous rocks in Japan shows the following features:

- pH changes from neutral near the surface to slightly alkaline in the deep subsurface environment
- chemistry changes from Na-Ca-(Mg-)HCO_3 type to Na-HCO_3 type with increasing depth (Figure 3.4-1).

The groundwaters in the Tono area and the Kamaishi mine show a similar evolutionary trend with respect to depth (Tables 3.4-1 and 3.4-2). The published literature reports few reliable data concerning redox parameters and redox data are therefore restricted to those from the Tono area and the Kamaishi mine (Table 3.4-3). The mechanisms controlling the evolution of water chemistry and redox potential will be discussed in Section 3.4.2.

2) Geochemical characteristics of marine groundwater

Groundwaters of marine origin show a chemical composition rich in Cl, K, Na, Ca, Mg, HCO_3 and SO_4 (Seo and Shimizu, 1992). For example, detailed analyses of groundwater with a marine origin were undertaken in the Äspö area in Sweden (Bath et al., 1996; Witherspoon, 1996). In these groundwaters, reducing redox conditions at depth are created by ferrous ions leached from biotite and chlorite (Laaksoharju et al., 1993). In Japan there are similar examples in the Horonobe area (Ii et al., 1997).

Groundwater sampled from Neogene sedimentary strata at a depth of 1000 m near the coast in the Horonobe area shows Na and Cl enrichment. Although this groundwater has almost the same concentrations of Na, Cl and K as those of seawater, the concentrations of Mg and Ca are less than one tenth of those of seawater, while the concentrations of Si, P, I and Fe are several thousand times higher than those of seawater (Table 3.4-4; Ii et al., 1997). These relative changes compared to seawater are characteristic of fossil seawater (Motojima and Masuko, 1973). The redox potential of the groundwater is about -220mV (pH=8.4). As this value corresponds to the redox boundary of key chemical species of sulfur, reactions involving sulfur may dominate redox processes in these groundwaters.

From the above case studies, the following conclusions may be drawn concerning deep groundwater derived from seawater or fossil seawater:

- the chemical composition is rich in Na and Cl
- compared with surface water, these groundwaters tend to be more reducing due to microbial decomposition of organic materials and to reactions involving sulfur.

3.4.2 Case studies on the geochemical characteristics of deep groundwater

To obtain information on the geochemical characteristics of deep groundwater, it is necessary to sample groundwater, to estimate its origin and age from its chemical and isotopic compositions, to understand groundwater flow mechanisms and, finally, to measure in-situ physico-chemical parameters such as redox potential. It is also important to collect and chemically analyze samples to understand both the major inorganic and organic chemical processes. For these reasons, investigations should be carried out using the following techniques (Iwatsuki et al., 1998):

i. Construction of a geochemical dataset from the results of surface surveys, borehole sampling and sampling in underground drifts. Physico-chemical parameters (water

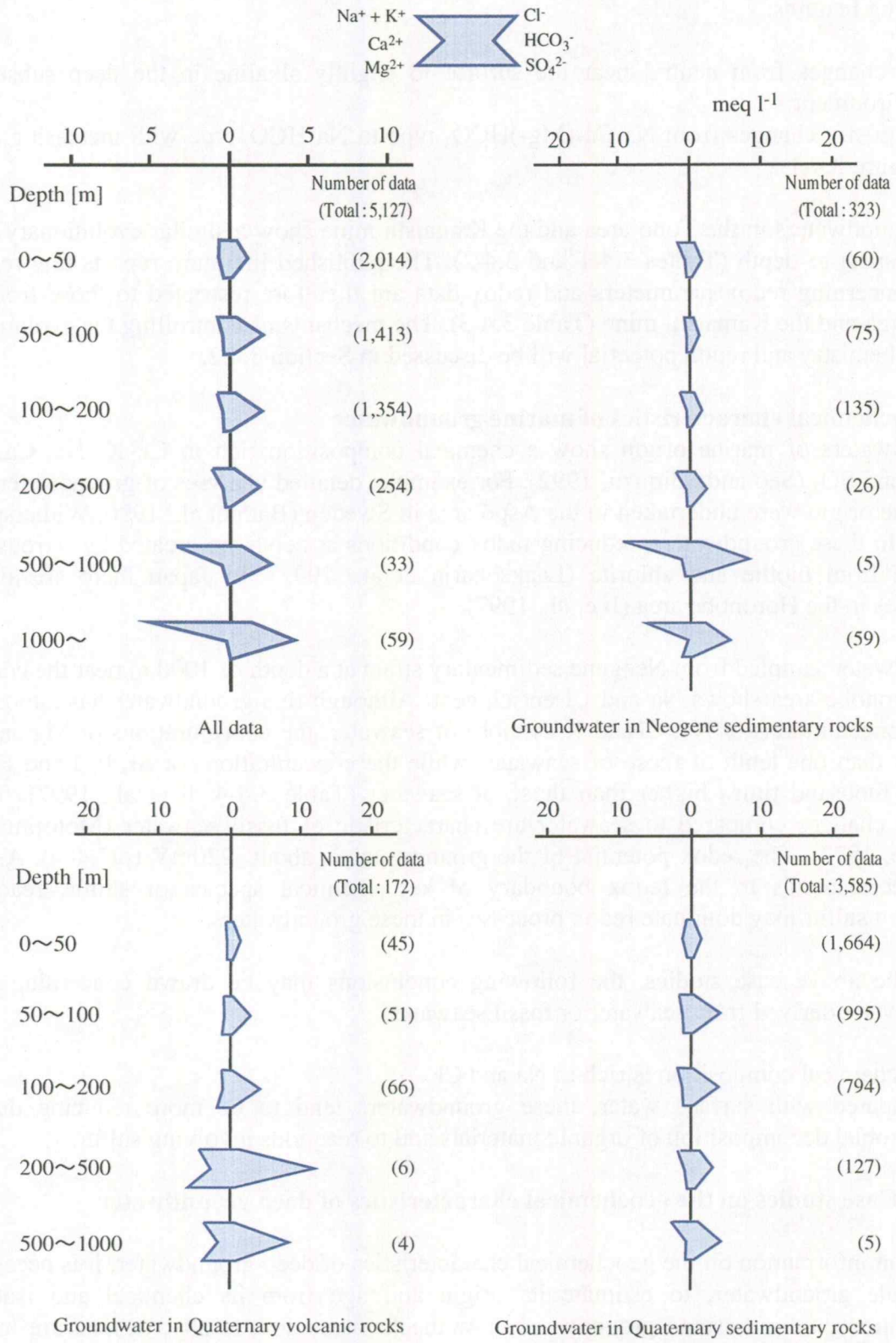


Figure 3.4-1 Hexadiagrams illustrating the variation in groundwater chemistry as a function of depth (Seo and Shimizu, 1992)

Na^+ and HCO_3^- tend to increase with increasing depth.

Table 3.4-1 Groundwater chemistry in the Tono area

Formation	Depth	Altitude	pH	EC	Si	Al	Fe^{2+}	Fe^{3+}	ΣFe	Mn	Mg^{2+}	Ca^{2+}	Sr^{2+}	Na^{+}	K^{+}	F^{-}	Cl^{-}	NO_2^{-}	NO_3^{-}	PO_4^{-}	Br^{-}	SO_4^{2-}	IC	TOC	CO_3^{2-}	HCO_3^{-}
	(G.L.-m)	(S.L.m)		(μS/cm)	(ppm)	(ppm)	(ppm)	(ppm)	(ppm)	(ppm)	(ppm)	(ppm)	(ppm)	(ppm)	(ppm)	(ppm)	(ppm)	(ppm)	(ppm)	(ppm)	(ppm)	(ppm)	(ppm)	(ppm)	(ppm)	(ppm)
Surface	0.0		5.8	246	9.6	<0.02	<0.02	<0.02	<0.02	<0.01	0.60	2.40	<0.01	3.0	0.6	0.0	1.4	<0.02	<0.02	<0.02	<0.02	12.0	2.2	n.m.	0.0	11.0
Oidawara F.	28.5	246.2	7.7	165	31.3	<0.02	<0.02	<0.02	<0.02	<0.01	0.46	7.40	0.05	30.5	2.0	1.0	1.0	<0.02	<0.02	0.12	<0.02	0.3	21.3	n.m.	0.3	107.7
	68.0	244.8	7.8	171	28.8	<0.02	<0.02	<0.02	0.09	<0.01	0.41	7.50	0.04	27.9	2.2	0.7	3.0	0.11	0.23	0.11	<0.02	12.2	16.7	n.m.	0.3	84.7
Akeyo F.	14.0	240.1	7.7	219	19.3	<0.02	<0.02	<0.02	<0.02	<0.01	0.23	4.57	0	29.7	0.8	0.2	0.9	0.1	0.09	0.4	<0.02	1.6	18.5	n.m.	0.3	93.7
	32.8	256.5	7.2	130	36.3	<0.02	<0.02	<0.02	0.58	0.25	1.28	12.10	<0.01	13.7	1.5	0.2	0.9	<0.02	<0.02	0.25	<0.02	4.9	13.8	n.m.	0.1	69.9
	33.8	252.6	7.6	147	36.0	<0.02	<0.02	<0.02	0.07	0.17	1.07	12.10	0.09	18.0	1.6	0.2	1.0	<0.02	<0.02	0.51	<0.02	4.2	16.5	n.m.	0.2	83.8
	46.5	251.1	7.5	143	36.3	<0.02	<0.02	<0.02	0.04	0.19	1.17	12.50	0.06	16.3	1.1	0.2	1.9	<0.02	<0.02	0.53	<0.02	5.8	17.3	n.m.	0.2	87.8
	61.0	248.5	7.6	180	32.3	<0.02	<0.02	<0.02	<0.02	0.03	0.48	6.60	0.02	32.3	1.3	0.3	2.8	<0.02	<0.02	0.19	<0.02	5.4	20.7	n.m.	0.3	104.8
	64.0	212.1	8.1	232	28.4	<0.02	<0.02	<0.02	<0.02	0.01	0.14	4.97	0.02	44.7	1.6	1.9	1.3	<0.02	<0.02	<0.02	<0.02	1.2	28.1	n.m.	1.1	141.9
	104.0	208.8	8.8	223	17.4	<0.02	0.03	0.04	0.06	<0.01	0.09	4.73	0.03	42.7	1.1	2.5	3.7	<0.02	<0.02	0.04	<0.02	35.0	16.0	n.m.	3.1	78.0
Toki lignite-bearing F.	70.8	215.6	8.0	257	26.7	<0.02	<0.02	<0.02	0.09	<0.01	0.21	4.30	0.02	50.5	1.8	2.9	3.3	<0.02	<0.02	0.45	<0.02	10.7	26.4	n.m.	0.8	133.2
	74.8	214.5	8.2	311	24.6	<0.02	<0.02	<0.02	<0.02	<0.01	0.23	5.23	0.02	65.0	1.4	2.8	1.1	<0.02	<0.02	0.78	<0.02	1.1	35.6	n.m.	1.8	179.2
	83.0	227.1	7.6	230	26.3	<0.02	<0.02	<0.02	<0.02	<0.01	0.19	3.57	0.01	46.7	1.4	1.5	3.7	<0.02	0.09	<0.02	<0.02	4.7	25.6	n.m.	0.3	129.7
	85.5	212.1	8.4	271	29.7	<0.02	<0.02	<0.02	<0.02	<0.01	0.17	4.13	0.01	62.0	1.3	4.8	1.5	<0.02	<0.02	<0.02	<0.02	1.3	31.3	n.m.	2.4	156.5
	91.0	185.1	7.6	213	4.9	<0.02	<0.02	<0.02	<0.02	<0.01	0.10	1.83	0.03	13.3	1.0	0.8	1.9	<0.02	<0.02	<0.02	<0.02	4.8	6.7	n.m.	0.1	33.9
	109.8	179.5	8.6	210	9.6	<0.02	<0.02	<0.02	<0.02	<0.01	0.04	1.87	<0.01	45.0	0.5	2.7	2.0	<0.02	<0.02	0.14	<0.02	9.7	20.9	n.m.	2.6	103.4
	121.0	155.1	7.9	145	6.7	<0.02	<0.02	<0.02	<0.02	<0.01	0.04	1.07	<0.01	21.3	0.3	0.9	0.9	<0.02	<0.02	1.29	<0.02	3.6	10.4	n.m.	0.3	52.8
	124.0	173.6	8.8	200	14.1	<0.02	<0.02	<0.02	<0.02	<0.01	0.03	1.54	<0.01	40.7	0.4	3.1	3.9	<0.02	<0.02	0.11	<0.02	17.1	15.5	n.m.	3.0	76.0
	132.0	180.8	8.7	370	15.0	<0.02	<0.02	<0.02	0.04	<0.01	0.10	6.20	0.03	73.0	1.6	2.8	8.4	<0.02	<0.02	<0.02	<0.02	51.0	26.4	n.m.	4.0	130.0
	138.3	148.1	9.5	181	12.9	<0.02	<0.02	<0.02	<0.02	<0.01	0.03	1.45	<0.01	38.7	0.3	3.0	1.9	<0.02	<0.02	0.04	<0.02	12.2	10.0	n.m.	8.3	42.5
	152.5	157.6	9.0	272	10.6	<0.02	<0.02	<0.02	<0.02	<0.01	0.03	2.89	<0.01	55.3	0.4	3.5	4.2	<0.02	<0.02	<0.02	<0.02	29.8	13.2	n.m.	3.9	63.0
	153.0	159.8	9.0	237	6.4	<0.02	<0.02	<0.02	<0.02	<0.01	0.02	2.09	0.04	45.0	0.4	4.2	4.3	<0.02	<0.02	<0.02	<0.02	41.0	11.8	n.m.	3.5	56.6
Toki granite	130.0	226.0	7.9	145	9.6	<0.02	<0.02	<0.02	<0.02	<0.01	0.31	7.00	0.02	36.3	0.9	1.6	2.5	<0.02	<0.02	0.16	<0.02	14.7	23.4	n.m.	0.6	118.4
	160.0	116.1	7.8	319	5.6	<0.02	<0.02	<0.02	<0.02	0.10	0.41	15.10	0.05	46.0	1.3	1.4	12.1	0.04	<0.02	<0.02	<0.02	82.0	14.8	n.m.	0.3	74.7
	166.3	120.1	7.7	202	8.1	<0.02	<0.02	<0.02	0.02	<0.01	0.26	10.70	0.1	15.7	0.8	2.1	1.0	<0.02	<0.02	<0.02	<0.02	2.5	14.0	n.m.	0.2	70.8
	177.5	135.3	6.2	n.m.	6.0	0.16	n.m.	n.m.	0.2	0.76	0.18	1.04	<0.01	12.3	10.1	0.2	1.4	<0.02	0.08	<0.02	<0.02	1.4	8.4	38.6	0.0	42.8
	185.5	81.1	7.8	131	7.8	<0.01	n.m.	n.m.	<0.02	0.09	0.87	14.90	0.1	6.9	3.2	1.4	1.9	<0.02	<0.02	0.06	<0.02	8.6	n.m.	n.m.	-	-
	208.0	148.0	9.6	131	8.2	<0.1	n.m.	n.m.	<0.02	<0.01	0.12	16.31	0.12	8.0	3.5	2.0	2.3	<0.02	<0.02	<0.02	<0.02	2.4	12.0	2.0	12.0	48.8
	327.0	-19.6	9.7	n.m.	2.5	<0.01	<0.05	<0.05	0.03	<0.01	0.03	9.60	0.1	19.5	1.6	3.5	4.2	<0.02	<0.02	0.08	<0.02	12.7	7.9	7.9	9.5	30.5
	330.0	26.0	8.9	125.2	13.8	<0.01	n.m.	n.m.	0.06	<0.01	0.12	12.16	0.12	11.6	0.9	4.1	3.7	<0.02	<0.02	0.04	<0.02	6.7	9.2	2.6	2.2	44.7
	564.0	-223.8	9.6	198	5.6	<0.01	n.m.	n.m.	0.02	<0.01	0.03	4.09	0.04	36.5	1.2	10.9	3.5	<0.02	<0.02	0.19	<0.02	9.1	n.m.	n.m.	-	-
	645.0	-375.2	9.0	188	4.1	<0.01	n.m.	n.m.	<0.02	<0.01	0.19	4.68	0.04	36.0	1.2	8.9	3.9	<0.02	0.06	0.11	<0.02	6.8	16.2	3.1	4.8	77.5
	645.6	-289.6	9.3	202	5.5	<0.01	n.m.	n.m.	<0.02	<0.01	0.05	3.72	0.03	39.5	0.8	9.7	3.1	<0.02	<0.02	<0.02	0.04	6.2	13.5	0.5	7.5	61.0
	697.0	-427.2	6.8	172	5.6	<0.02	9.34	<0.05	9.34	0.77	1.88	17.60	0.11	13.3	6.1	5.0	2.7	<0.02	0.02	<0.02	0.08	0.1	n.m.	n.m.	-	-
	700.0	-344.0	7.8	n.m.	19.6	<0.01	0.24	n.m.	0.41	0.32	0.82	19.00	0.15	10.3	3.0	2.5	1.4	<0.01	<0.01	0.1	0.0	7.8	14.5	1.7	0.3	73.4
	737.0	-417.7	8.9	n.m.	8.6	0.043	0.2	n.m.	0.22	0.01	0.06	3.20	<0.01	22.0	0.6	4.1	3.4	<0.01	<0.01	<0.02	<0.1	5.5	12.4	1.7	2.8	60.2
	749.0	-479.2	10.1	n.m.	1.9	0.19	8.5	n.m.	9.6	0.18	0.43	6.90	<0.01	28.3	2.9	2.1	4.4	0.005	0.01	0.086	<0.1	4.6	18.4	2.4	40.7	52.1
	790.0	-434.0	9.6	n.m.	8.5	1.2	6.9	n.m.	7.8	0.12	0.63	4.30	<0.01	36.5	11.2	10.0	3.1	0.1	0.05	0.039	<0.1	5.6	20.3	1.3	20.0	82.9
	837.0	-496.8	9.5	n.m.	14.7	4.3	8.8	n.m.	12	0.49	0.80	5.80	<0.01	48.8	25.0	8.6	5.1	0.09	0.03	0.328	<0.1	5.4	22.0	2.8	16.6	94.9
	840.0	-484.0	9.0	n.m.	13.6	0.68	0.03	n.m.	0.042	0.01	0.04	2.80	<0.01	23.4	5.2	3.2	3.8	0.005	<0.01	0.01	<0.1	n.d.	14.2	0.8	3.9	68.2
	872.0	-602.2	8.5	n.m.	17.0	0.052	0.17	n.m.	0.21	0.02	0.14	7.20	<0.01	24.3	0.5	3.6	3.8	0.087	0.005	<0.005	<0.1	4.2	17.2	0.9	1.6	85.8
	883.0	-542.8	8.4	n.m.	16.7	0.32	0.21	n.m.	0.24	0.01	0.10	1.20	<0.01	28.4	4.9	4.4	3.9	0.008	<0.01	0.001	<0.1	3.7	16.3	1.0	1.4	81.5
	978.0	-708.2	8.8	n.m.	12.8	0.98	0.08	n.m.	0.08	0.01	0.68	4.30	<0.01	39.6	11.1	11.2	19.2	<0.01	0.005	<0.005	<0.1	3.1	15.1	0.6	2.8	73.9

n.m. : not measured

CO_3^{2-}, HCO_3^{-}concentrations were calculated from IC conc. and pH

G.L.- : Ground level, S.L. : Sea level

Table 3.4-2 Chemistry of the Kamaishi groundwater

Formation	Location	Sea level	pH	EC	SiO_2	Si^{4+}	Al^{3+}	Fe^{2+}	T.Fe	Mg^{2+}	Ca^{2+}	Na^{+}	K^{+}	F^{-}	Cl^{-}	SO_4^{2-}	HCO_3^{-}	CO_3^{2-}	TOC	IC	TC	δD	$\delta^{18}O$	^3H
		(m)		(μS/cm)	(ppm)	(ppm)	(ppm)	(ppm)	(ppm)	(ppm)	(ppm)	(ppm)	(ppm)	(ppm)	(ppm)	(ppm)	(ppm)	(ppm)	(ppm)	(ppm)	(ppm)	(‰)	(‰)	(T.U.)
Surface	Kamaishi city	815	6.1	18.0	10.50	-	-	-	-	0.40	1.80	2.50	0.60	-	1.70	-	11.6	0.0	-	-	-	-63.2	-9.9	7.6±0.2
		650	5.8	20.5	9.40	-	-	-	-	0.30	2.70	2.70	0.50	-	2.60	1.9	10.4	0.0	-	-	-	-65.5	-9.5	7.5±0.2
		588	5.3	22.5	10.00	-	-	-	-	0.40	2.30	2.70	0.70	-	3.10	2.0	10.4	0.0	-	-	-	-59.6	-9.4	7.6±0.2
		800	6.3	25.1	12.90	-	-	-	-	0.70	3.30	2.80	0.70	-	2.50	1.7	15.2	0.0	-	-	-	-	-	-
		785	7.4	33.0	14.80	-	-	-	-	0.50	2.90	3.10	0.90	-	2.40	0.2	21.0	0.0	-	-	-	-61.9	-10.2	7.0±0.1
Kurihashi granodiorite	550 mL gallery	575	8.8	75.7	12.60	-	-	-	-	0.30	9.20	6.00	0.90	-	2.40	6.2	32.4	0.9	-	-	-	-64.9	-10.3	13.0±0.2
	KD-89	575	8.7	90.6	11.00	-	-	-	-	0.20	6.90	8.80	1.00	-	1.80	11.3	28.7	0.6	-	-	-	-60.8	-10.4	9.5±0.2
	2.01-101.17	524	-	-	10.70	-	<0.1	-	0.1	<0.02	4.40	11.90	0.60	0.10	2.20	8.0	-	-	0.5	4.3	-	-	-	-
	102.25-236.41	406	-	-	15.10	-	<0.1	-	0	<0.02	3.10	16.80	0.30	0.20	2.50	9.4	-	-	0.5	3.5	4.0	-	-	-
	237.49-337.14	288	-	-	14.80	-	<0.1	-	0	<0.02	2.70	16.60	0.40	0.20	2.40	9.7	-	-	0.5	3.7	4.2	-	-	-
	338.22-410.94	201	-	-	18.60	-	<0.1	-	0	<0.02	2.60	19.30	0.60	0.30	2.50	12.1	-	-	0.5	4.4	4.9	-	-	-
	412.02-500.00	119	-	-	25.40	-	<0.1	-	0	<0.02	3.90	21.30	0.50	0.40	2.20	21.4	-	-	0.5	3.3	3.8	-	-	-
	GL-222~GL-226	560	9.4	129.4	12.80	-	<0.1	<0.05	0.1	0.20	5.00	11.40	1.10	-	1.80	8.4	31.0	2.0	-	-	-	-61.1	-10.1	10.6±0.2
	GL-489~GL-495	293	10.0	81.0	16.30	7.60	0.3	<0.05	0	0.00	6.30	11.00	0.60	0.20	1.90	8.9	28.4	6.9	0.4	7.0	7.4	-73.0	-11.1	2.8±0.1
	GL-740~GL-747	41	9.3	106.0	9.70	4.50	0.2	<0.05	0	0.10	7.20	17.30	0.60	0.40	2.90	17.1	31.8	2.4	0.2	6.7	7.0	-73.1	-10.6	3.4±0.1
	GL-785~GL-791	-4	9.0	118.0	16.65	3.10	0.1	-	0	0.30	6.80	14.70	0.80	0.00	3.50	8.6	45.7	1.6	0.8	9.3	10.1	-67.5	-10.1	4.7±0.1
	250 mL gallery	258	9.6	78.2	15.10	7.10	<0.1	<0.05	<0.3	<0.02	8.20	5.30	0.20	<0.1	2.10	13.4	23.1	3.3	0.4	5.2	5.6	-70.1	-10.9	5.2±0.1

Table 3.4-3 Redox potential and pH of groundwater in Japan

Formation	Location	Depth from surface (m)	pH	Eh (mV)	Method	Reference
Quaternary volcanic rocks	Nagasaki	212	6.70	110		(1)
Quaternary volcanic rocks	Nagasaki	212	6.85	60		(1)
Quaternary volcanic rocks	Nagasaki	300	6.29	170		(1)
Quaternary volcanic rocks	Nagasaki	353	6.92	140		(1)
Quaternary volcanic rocks	Nagasaki	801	6.72	100		(1)
Quaternary sedimentary rocks	Nagasaki	250	7.30	-80		(1)
Quaternary sedimentary rocks	Nagasaki	300	6.70	25		(1)
Tertiary sedimentary rocks	Mobara	*1	7.74	-73～-34	Handy meter	(2)
Tertiary sedimentary rocks	Tono	160	9.60	-300±10	Continuous monitoring apparatus	(3)
Neogene sedimentary rocks	Horonobe	1178	8.39	-225±10	HGP-10	(4)
Palaeogene sedimentary rocks	Nagasaki	300	8.30	120		(5)
Palaeogene sedimentary rocks	Saga	316	8.62	-220		(5)
Cretaceous granite	Tono	180	8.20	0±10	Continuous monitoring apparatus	(6)
Cretaceous granite	Tono	327	7.76	-16±10	Downhole chemical probe	(7)
Cretaceous granite	Tono	564	10.1	-385±10	Downhole chemical probe	(7)
Cretaceous granite	Tono	645	8.98	-355±10	Downhole chemical probe	(7)
Cretaceous granite	Tono	697	8.46	-260±10	Downhole chemical probe	(7)
Cretaceous granite	Tono	737	8.80	-302±10	Downhole chemical probe	(7)
Cretaceous granite	Tono	749	8.24	-294±10	Downhole chemical probe	(7)
Cretaceous granite	Tono	837	9.57	-374±10	Downhole chemical probe	(7)
Cretaceous granite	Tono	872	8.78	-376±10	Downhole chemical probe	(7)
Cretaceous granite	Tono	883	9.50	-349±10	Downhole chemical probe	(7)
Cretaceous granite	Tono	978	8.79	-355±10	Downhole chemical probe	(7)
Cretaceous granodiorite	Kamaishi	*2	9.80	-320±10	Continuous monitoring apparatus	(8)

* 1 Spring water from a borehole with a depth of 1,000 m
* 2 Porewater in a borehole drilled from the tunnel at 700 m below the ground surface

(1) Ohta (1973) (2) Kamei (1997), Kamei et al. (2000) (3) Seo et al. (1989)
(4) Ii et al. (1997) (5) Ohta (1971) (6) Iwatsuki and Yoshida (1999b)
(7) Hama and Iwatsuki (1998) (8) Sasamoto et al. (1996)

Reliable data on the redox potential of deep groundwater in Japan are limited in number. In-situ measurements show that groundwaters become reducing at a depth between one hundred meters to two hundred meters in sedimentary rocks and at a depth more than about 500 m in granite. Measurements using a portable potential meter were carried out at the ground surface.

Table 3.4-4 Chemistry of the Horonobe groundwater (after Ii et al., 1997)

Strainer depth	1000 m	1000 m	1000 m	1000 m	1000 m	800 m
Water volume sampled	0.01m^3	0.524m^3	1.145m^3	1.736m^3	1.9m^3	
pH	8.51	8.39	8.36	8.48	8.39	–
Eh(mV)	-247	-131	-106	-215	-225	–
EC(25℃)	48700	48200	48000	48000	48200	–
Temperature(℃)	34.55	34.57	34.61	34.62	34.59	–
Si^{4+} (mg l^{-1})	14.2	18.0	20.6	17.2	16.4	30.7
Mg^{2+} (mg l^{-1})	74.2	80.9	99.1	102	100	3.08
Ca^{2+} (mg l^{-1})	21.2	33.7	40.7	40.4	35.9	3.65
Na^{+} (mg l^{-1})	10700	10700	11000	11200	10800	200
K^{+} (mg l^{-1})	421	409	409	383	390	19
Fe^{2+} (mg l^{-1})	1.2	0.31	0.13	0.03	0.17	0.68
Fe^{3+} (mg l^{-1})	0.7	0.15	0.17	0.31	0.13	n.d.(<0.2)
CO_3^{2-} (mg l^{-1})	246	168	348	348	396	120
HCO_3^{-} (mg l^{-1})	1030	1090	834	866	744	909
F^{-} (mg l^{-1})	0.76	n.d.(<0.3)	n.d.(<0.3)	n.d.(<0.3)	n.d.(<0.3)	n.d.(<0.3)
Cl^{-} (mg l^{-1})	16500	16100	16100	14600	14600	27.2
Br^{-} (mg l^{-1})	170	170	150	170	160	n.d.(>5.0)
I^{-} (mg l^{-1})	68	71	71	63	63	0.31
PO_4^{3-} (mg l^{-1})	9.2	9.3	8.1	8.1	7.6	4.8
δD(‰)	-22.1	-16.7	-11.2	-10.7	-13.9	-93.3
$\delta^{18}O$ (‰)	0.14	0.99	0.99	0.11	0.11	-12.66
^3H (T.U.)	0.99	–	0.8	–	0.58	n.d.(<0.27)
U(mg l^{-1})	n.d.(<0.1)	n.d.(<0.1)	1.35	1.35	1.05	n.d.(<0.1)

temperature, electrical conductivity, pH and redox potential, etc.), major and trace dissolved components, dissolved gases, isotopes (hydrogen, oxygen, carbon, and sulfur), colloid/organic materials, microbes, etc. should be measured.

ii. Evaluation of the mechanisms controlling water chemistry and particularly water-mineral interactions which determine redox potentials at depth. These evaluations involve interpretation of stable isotopic ratios, saturation indices and mass balances. Biochemical reactions deduced from the varieties, amounts and activities of microbes and varieties and amounts of organic materials, which may represent nutrition sources for microbes, will also be relevant.

iii. Construction of conceptual models that explain the evolution of the physico-chemical properties of groundwaters and rocks. Consideration of chemical reactions using chemical equilibrium theories or kinetics are relevant (Figure 3.4-2; Yui et al., 1992).

The data from the Tono area and the Kamaishi mine show water chemistries and depth-dependent variations virtually identical to those reported in the published literature for groundwater in Japan that originates as meteoric water. In order to investigate these geochemical groundwater characteristics, JNC developed a groundwater sampler and a downhole chemical probe that can be used to a depth of 1000 m and their applicability was verified in field tests (Iwatsuki et al., 1998).

1) The Tono area

(1) Geochemical characteristics of groundwaters in sedimentary rocks and their evolutionary processes

In the Tono area (Figure 3.4-3), Neogene sedimentary rocks (maximum thickness around 200 m) unconformably overlie basement granite of Cretaceous age. Major constituent minerals of the sedimentary rocks are quartz, feldspar, plagioclase, biotite, amphibole, clay minerals and calcite, etc. In the lower part of the sedimentary sequence, immediately above the unconformity, carbonate minerals and pyrite occur and a major uranium ore body is present. In contrast, in the upper part of the sedimentary sequence, gypsum is observed to replace pyrite and calcite (Yoshida et al., 1994; Shikazono and Utada, 1997). The groundwater in these sedimentary rocks (Mizunami Group) is estimated from O and H stable isotopes and ^{14}C data to be derived from meteoric water recharged during the Würm glacial period (Mizutani et al., 1992). The infiltration rate of this groundwater is consistent with the hydraulic data obtained in the subsurface environment. These groundwaters have the following features:

- Groundwater in the upper part of the sedimentary rocks (Oidawara Formation and Akeyo Formation) is dominated by Na, Ca and HCO_3, whereas the groundwater in the lower part (Toki Lignite-bearing Formation) is dominated by Na and HCO_3 (Figure 3.4-4).
- The pH increases from neutral at the surface, through the Oidawara and Akeyo Formations, and continues to alter slightly with depth.
- HS^- is detected at depths greater than 60 m.
- The redox potential of the groundwater at a depth of some 160 m is approximately –300 mV (Table 3.4-3; Seo et al., 1989).

A similar geochemical evolution of groundwaters has been described from the Äspö area of Sweden, where the water chemistry is controlled mainly by dissolution of calcite and ion exchange between Na-bearing minerals and groundwater (Laaksoharju et al., 1993).

In order to clarify the evolution mechanisms of groundwater chemistry in the Tono area,

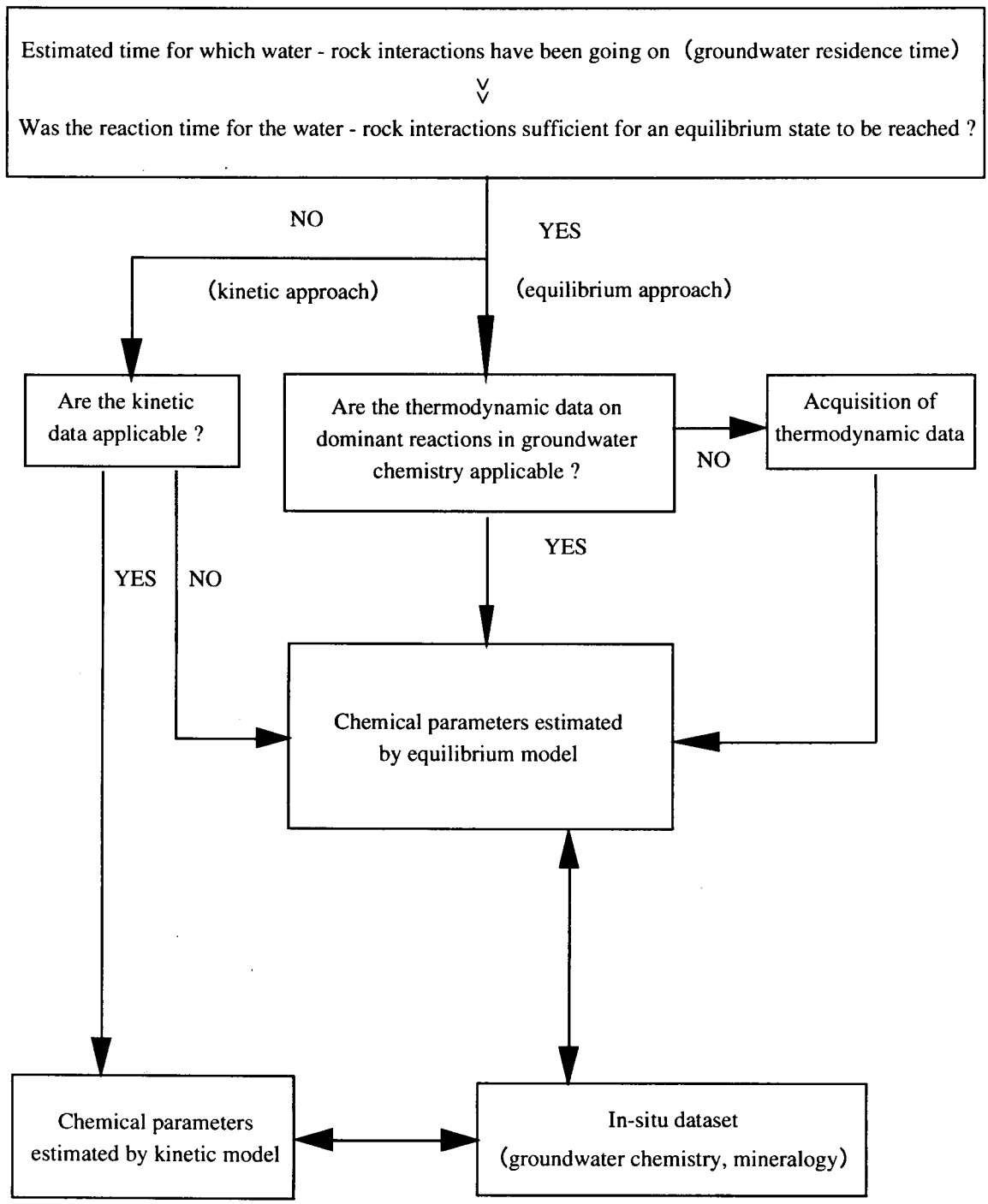


Figure 3.4-2 Basic approach for groundwater evolution model
(Yui et al.,1992)

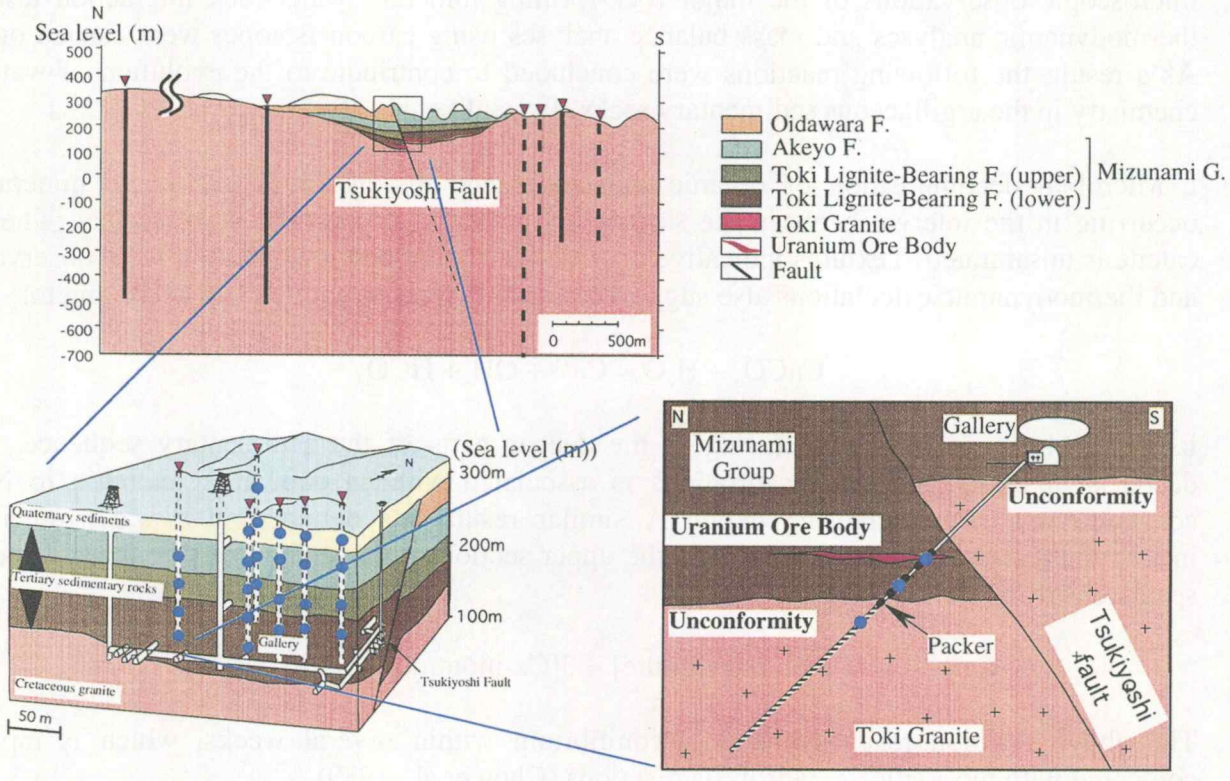
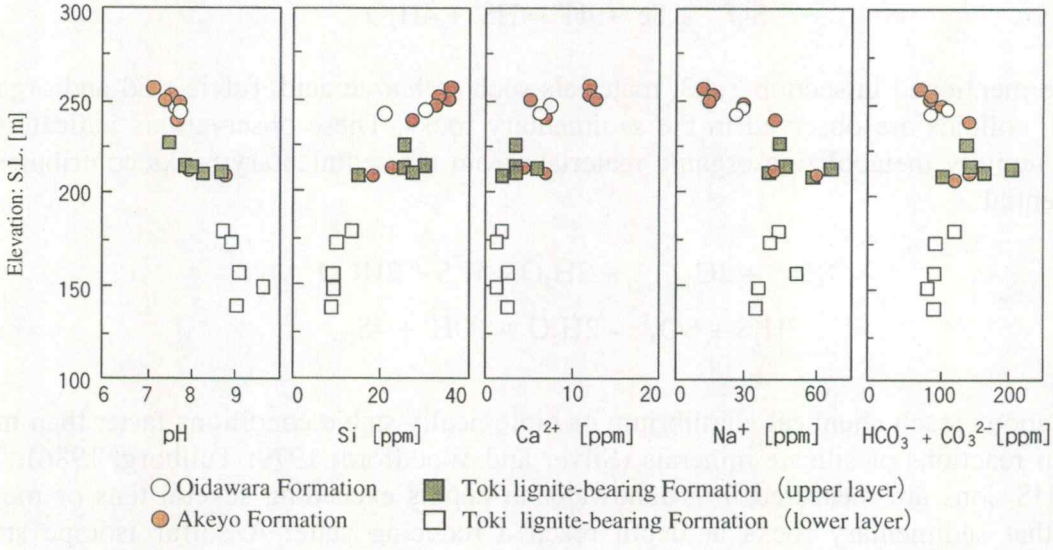


Figure 3.4-3 Schematic view of the Tono area

More than ten boreholes were drilled in sedimentary and granitic rocks for geochemical investigations



(Iwatsuki et al., 1995)

Figure 3.4-4 Changes in groundwater chemistry in sedimentary rocks in the Tono area as a function of depth (Iwatsuki et al., 1995)

As depth increases, groundwater changes from neutral to alkaline, there are decreases in concentration of Si,Ca^{2+} and increases in concentration of Na^{+} and HCO_3^{-}.

microscopic observations of the major rock-forming minerals, water-rock interaction tests, thermodynamic analyses and mass balance analyses using carbon isotopes were carried out. As a result, the following reactions were concluded to contribute to the evolution of water chemistry in the argillaceous sedimentary rocks (Iwatsuki et al., 1995):

i. Microbial decomposition of organic substances and dissolution of carbonate minerals occurring in the interval between the surface and a depth of several tens of meters, where calcite is unsaturated. Textures indicative of both dissolution and precipitation were observed and thermodynamic calculations also suggest that calcite reaches equilibrium according to:

$$CaCO_3 + H_2O = Ca^{2+} + OH^- + HCO_3^-$$

ii. Ion exchange reactions occurring in the deeper parts of the sedimentary sequence. A decrease in dissolved Ca concentrations is associated with an equivalent increase in Na concentrations with increasing depth. A similar result was obtained in a water-mineral interaction test using groundwater from the upper section of the sedimentary rocks and rock specimens from the lower part:

$$Ca^{2+} + 6[\text{Na-montmorillonite}] = 3[\text{Ca-montmorillonite}] + 2Na^+$$

The above reaction reaches chemical equilibrium within several weeks, which is rapid compared with most silicate hydrolysis reactions (Chou et al., 1989).

Redox reactions between HS^- and SO_4^{2-} are expected to contribute to controlling the redox potential. This is because HS^- is measured in groundwaters at a depth of 60 m or more and the measured values of redox potential are almost equal to values calculated on the assumption that HS^- is in redox equilibrium with SO_4^{2-} according to:

$$SO_4^{2-} + 8e^- + 9H^+ = HS^- + 4H_2O$$

As will be mentioned in section 3.4.3, materials such as humic acid, fulvic acid and organic sulfur-rich colloids are observed in the sedimentary rocks. These observations indicate that microbial activity metabolizing organic materials from the sedimentary rocks contributes to redox potential:

$$SO_4^{2-} + 2C_{(organic)} + 2H_2O = H_2S + 2HCO_3^-$$

$$3H_2S + SO_4^{2-} = 2H_2O + 2OH^- + 4S_{(S)}$$

These reactions reach chemical equilibrium or biologically stable conditions faster than most dissolution reactions of silicate minerals (Silver and Woodford, 1979; Tullborg, 1986). The fact that HS^- ions are measured in groundwater at depths exceeding several tens of meters suggests that sedimentary rocks at depth reach a reducing state. A sulfur isotope study (Shikazono and Utada, 1997) led to the conclusion that such reducing conditions have been maintained for a long period of time. In addition, long-term maintenance of the same hydrogeological environment has been identified as a reason why the reducing environment has also persisted for a long time (Yusa et al., 1993).

(2) Geochemical characteristics and evolutionary processes of groundwater in the granite

Fractures and fracture zones play a dominant role in the chemical evolution of groundwater in

the Toki Granite. The chemical properties of the groundwater are controlled by interactions with minerals generated within these fractures and fracture zones. Depending upon their widths, distribution frequencies and alteration states, these fractures and fracture zones are classified into fracture zones associated with so-called "green" alteration and those with "white" alteration (Iwatsuki and Yoshida, 1999a). The major rock-forming minerals of the Toki Granite are quartz, feldspar, K-feldspar and biotite, associated with accessory minerals such as pyrite, ilmenite and zircon. Chlorite and clay minerals are observed in the fracture zones. The major clay mineral is montmorillonite, associated with small amounts of kaolinite. The surfaces of fractures up to depths of 270 m are coated with iron hydroxide (limonite), which is considered to be a result of divalent iron leached from rocks being oxidized and precipitated (Ota et al. 1999). Furthermore, crystalline pyrite is observed in non-altered zones, whereas pyrite dissolution textures are observed in fracture zones that are considered to be groundwater flowpaths (Figure 3.4-5). The groundwater in the granite is assumed to originate from meteoric water on the basis of stable isotopic ratios of oxygen and hydrogen. Detection of significant amounts of tritium suggests direct penetration of surface water to a depth of 800 m in the specific fracture zones (Iwatsuki et al., 1999).

The pH and redox potential of the groundwater between depths of 180 m and 330 m correspond to the redox boundary between Fe^{2+} and Fe^{3+}. Therefore, redox reactions of aqueous iron species are inferred to contribute to the redox potential as shown below.

$$Fe^{2+} + 3H_2O = Fe(OH)_3 + 3\ H^+ + e^-$$

Furthermore, the pH and redox potential of the groundwater at depths between 500 m and 1000 m correspond to the redox boundary between HS^- and SO_4^{2-}, so that redox reactions of chemical species of sulfur are believed to be one of the major reactions which contribute to the redox potential as shown below (Figure 3.4-6).

$$SO_4^{2-} + 8\ e^- + 9\ H^+ = HS^- + 4\ H_2O$$
$$FeS_2 + 8\ H_2O = 2\ SO_4^{2-} + 16\ H^+ + 14\ e^- + Fe^{2+}$$

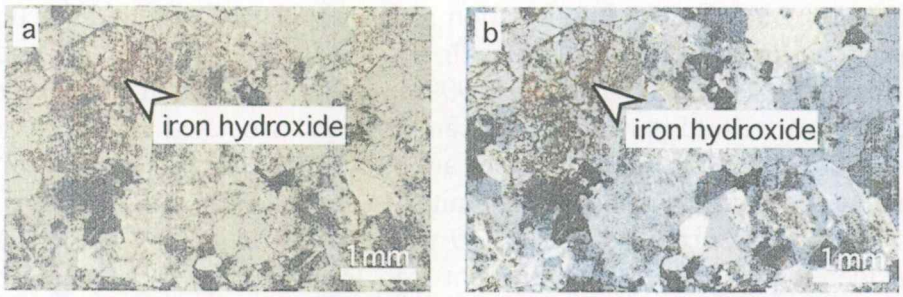
These redox reactions also reach a stable state rapidly compared with most silicate hydrolysis reactions. Therefore, it can be supposed that the oxidized water derived by direct penetration from the surface becomes reducing with depth over a relatively short period. Additionally, the groundwater compositions exhibit the following characteristics:

- They are neutral in the upper part of the granite (up to a depth of about 200 m), but change to weakly alkaline with increasing depth.
- Dominant dissolved ions are Na^+, Ca^{2+} and HCO_3^- up to a depth of about 500 m and Na^+ and HCO_3^- at a depth exceeding about 500 m (Figure 3.4-7).

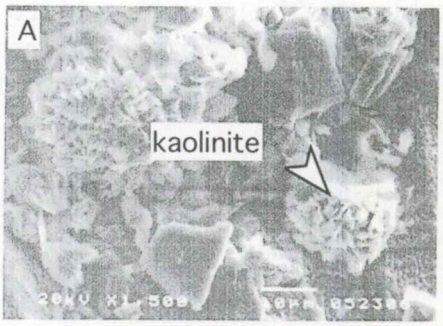
Dissolution of feldspar and calcite are considered to be the dominant mechanisms controlling groundwater chemistry in the upper part of the granite, as shown below. Ion exchange reactions between groundwater and clay minerals are considered to contribute to the variation of water chemistry with depth, because the decrease in Ca is almost equal to the increase of Na (on an equivalent basis). Additionally, clay minerals such as montmorillonite are found ubiquitously in the fractures (Iwatsuki and Yoshida, 1999a, b).

The most important water/rock interactions are concluded to be:

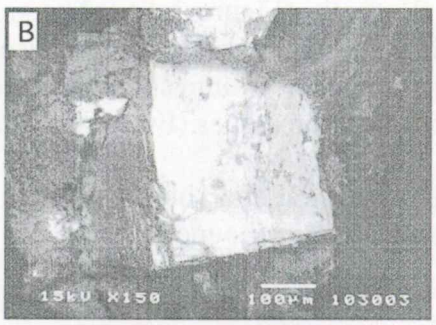
i. Feldspar alteration to montmorillonite:



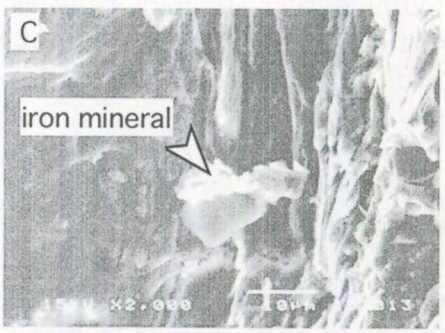
Iron hydroxide precipitation observed at depths shallower than 300 m
(a : open Nicol, b : cross Nicol)



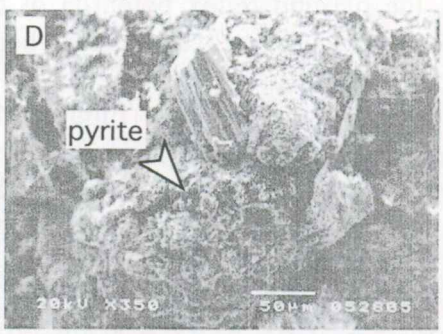
Plagioclase surface and kaolinite
(intact zone; 840m)



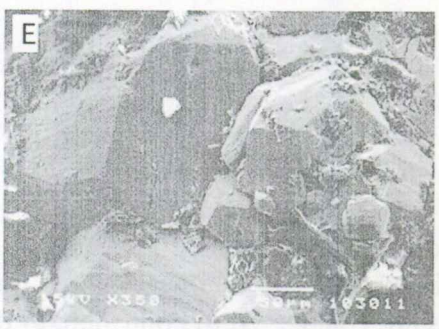
Euhedral pyrite suggesting no intense interaction with groundwater
(intact zone; 136m)



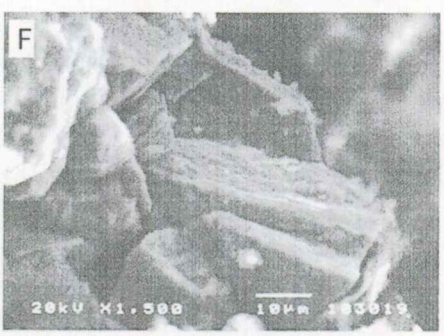
Biotite and iron mineral
(intact zone; 840m)



Dissolution textures shown by pyrite
(moderately fractured zone; 186m)



Dissolution textures shown by pyrite
(moderately fractured zone; 644m)



Dissolution textures shown by pyrite
(moderately fractured zone; 790m)

Figure 3.4-5 Microscopic and SEM observation of granite
(Iwatsuki and Yoshida, 1999 b)

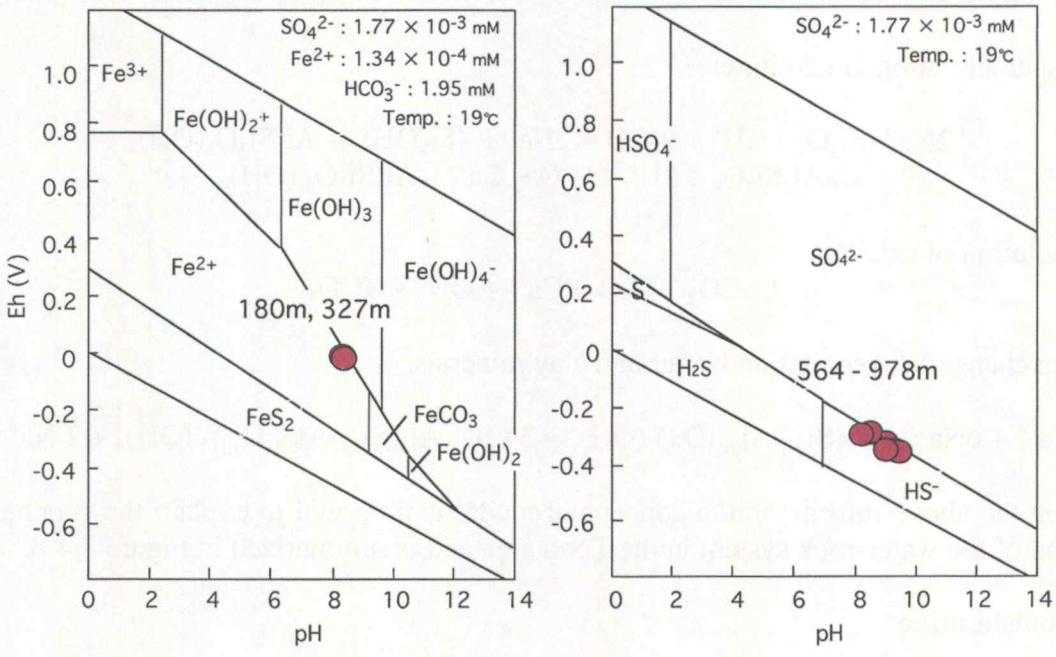


Figure 3.4-6 Eh-pH diagrams of iron and sulfur species
(modified from Iwatsuki and Yoshida, 1999 b)

In-situ Eh values of groundwaters in the shallow zone of the granite plot on a boundary between field of predominance of different iron species while its in deep zone lies on a border line of sulfur species.

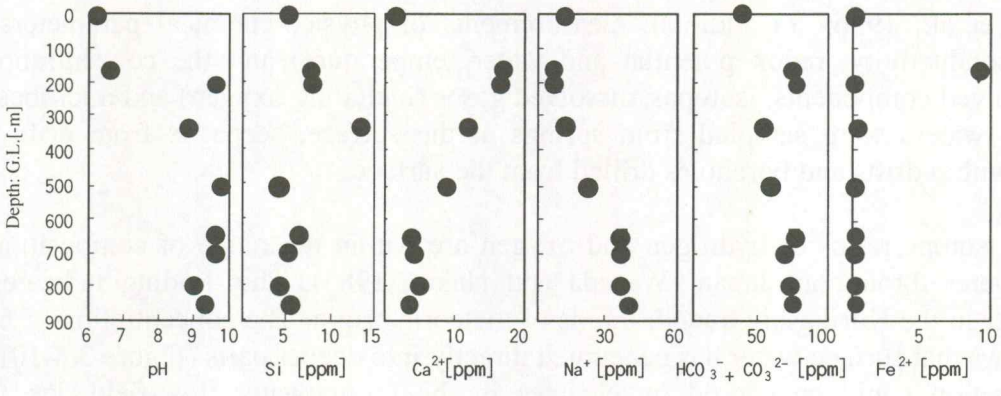


Figure 3.4-7 Changes in groundwater chemistry in granite in the Tono area as a function of depth (Iwatsuki and Yoshida, 1999 b)

As depth increases, groundwater changes from neutral to alkaline pH, concentrations of Ca^{2+} decrease and concentrations of Na^+, HCO_3^- increase.

$$7NaAlSi_3O_8 + 6H^+ + 20\ H_2O = 6Na^+ + 10Si(OH)_4 + 3Na_{0.33}Al_2\ (Si_{3.67}Al_{0.33}O_{10})\ (OH)_2$$
$$7CaAl_2Si_2O_8 + 12H^+ + 8Si(OH)_4 = 6Ca^{2+} + 16H_2O + 3Ca_{0.33}Al_4(Si_{3.67}Al_{0.33}O_{10})_2\ (OH)_4$$

ii. Feldspar alteration to kaolinite:

$$2NaAlSi_3O_8 + 2H^+ + 9H_2O = 2Na^+ + 4Si(OH)_4 + Al_2Si_2O_5(OH)_4$$
$$CaAl_2Si_2O_8 + 2H^+ + H_2O = Ca^{2+} + Al_2Si_2O_5\ (OH)_4$$

iii. Dissolution of calcite:

$$CaCO_3 + H_2O = Ca^{2+} + OH^- + HCO_3^-$$

iv. Ion exchange between groundwater and clay minerals:

$$Ca^{2+} + 6Na_{0.33}Al_2\ (Si_{3.67}Al_{0.33}O_{10})\ (OH)_2 = 3\ Ca_{0.33}Al_4(Si_{3.67}Al_{0.33}O_{10})_2\ (OH)_4 + 2\ Na^+$$

Based on the above information, a conceptual model is proposed to explain the geochemical evolution of the water-rock system in the Tono area and is summarized in Figure 3.4-8.

2) Kamaishi mine

(1) Geochemical characteristics of the groundwater in the granite

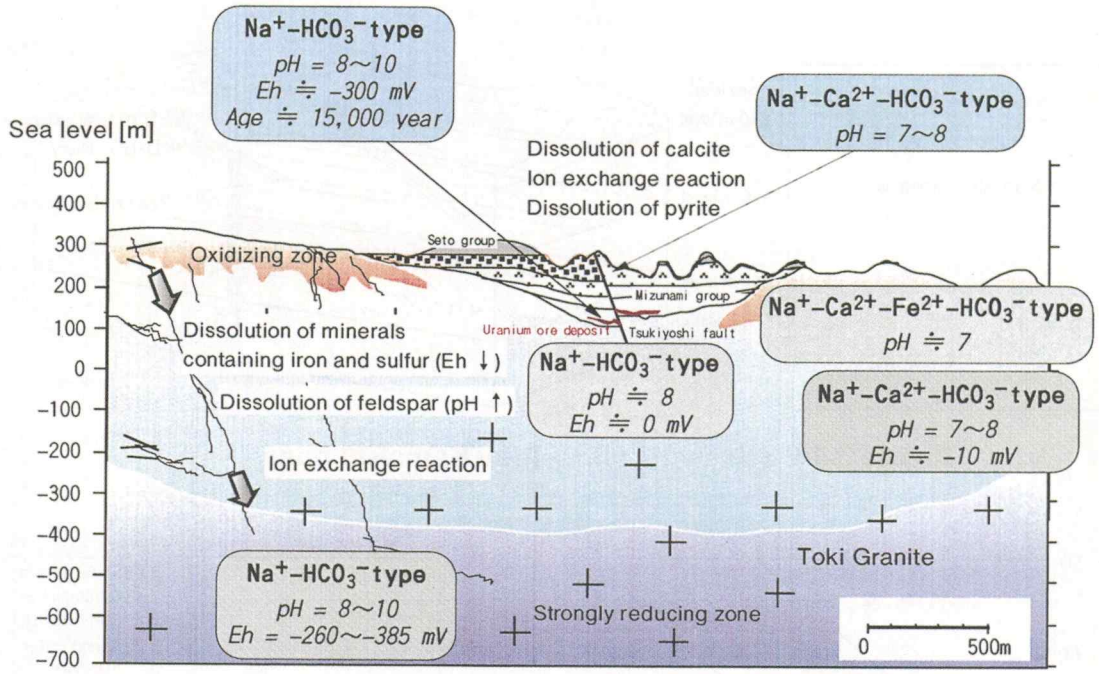
At the Kamaishi mine, a variety of investigations, including studies of the geochemical effects of drifts on the groundwater in the Kurihashi Granodiorite, have been carried out (Figure 3.4-9). To compare the geological features and the distribution of the whole rock geochemistry, both of which are considered to control the genesis of water chemistry, surveys of fracture distribution in the rock body and mineralogical investigations were conducted. The Kurihashi Granodiorite consists mainly of quartz, plagioclase, K-feldspar, biotite and amphibole. In contrast, calcite, zeolite, prehnite, epidote and clay minerals are observed to fill fracture zones (Sasamoto et al., 1996). In addition, measurements of physico-chemical parameters (pH, electrical conductivity, redox potential and water temperature) and the concentrations of major dissolved components, isotopes, dissolved gases (including oxygen) and microbes were made. The waters were sampled from springs at the surface, seepages from drift walls, boreholes within drifts and boreholes drilled from the surface.

The stable isotope ratios of hydrogen and oxygen are within the range of compositions for meteoric water throughout Japan (Waseda and Nakai, 1983). This finding indicates that groundwater in the Kurihashi Granodiorite is of meteoric origin. The concentration of tritium clearly shows that surface water has penetrated directly into deeper parts (Figure 3.4-10). This deep infiltration could be caused by changes in the groundwater flow-field due to the excavation of drifts (Morita et al., 1991; Shimada, 1989; JNC, 1999).

Groundwater changes with depth from a composition dominated by Na, Ca and HCO_3 to one dominated by Na and HCO_3 (Figure 3.4-11), similarly to groundwaters in the granite in the Tono area. Although Na concentrations of groundwaters sampled from drift wall seepages are scattered in this Figure, there is trend towards increasing Na concentration with depth.

(2) Processes associated with chemical evolution of groundwater

The changes in concentrations of Na, Ca, HCO_3, SiO_2 and carbonic acid ($HCO_3 + CO_3$) with increasing depth can be explained by the following reactions. Firstly, water with a relatively high partial pressure of carbon dioxide gas near the surface alters albite to kaolinite and causes cations such as Na, K, Ca, Mg and Si to be leached from silicates. As the partial



Geochemical reactions in sedimentary rocks

Dissolution and precipitaion of calcite	$CaCO_3 + H_2O = Ca^{2+} + OH^- + HCO_3^-$
Ion exchange reaction	$Ca^{2+} + 2(\text{Na-Montmorillonite}) = \text{Ca-Montmorillonite} + 2Na^+$
Redox reaction of sulfur minerals	$FeS_2 + 8H_2O = 2SO_4^{2-} + Fe^{2+} + 16H^+ + 14e^-$ $SO_4^{2-} + 8e^- + 9H^+ = HS^- + 4H_2O$
Microbial activity	$SO_4^{2-} + 2C(\text{organic}) + 2H_2O = H_2S + 2HCO_3^-$ $3H_2S + SO_4^{2-} = 2H_2O + 2OH^- + 4S$

Geochemical reactions in granite

Dissolution and precipitation of calcite	$CaCO_3 + H_2O = Ca^{2+} + OH^- + HCO_3^-$
Redox reaction of iron minerals	$Fe^{2+} + 3H_2O = Fe(OH)_3 + 3H^+ + e^-$
Dissolution of feldspar	$\text{Albite} + 2H^+ + 9H_2O = 2Na^+ + 4Si(OH)_4 + \text{Kaolinite}$ $\text{Anorthite} + 2H^+ + H_2O = Ca^{2+} + \text{Kaolinite}$ $\text{Albite} + 6H^+ + 20H_2O = 6Na^+ + 10Si(OH)_4 + \text{Montmorillonite}$ $\text{Anorthite} + 12H^+ + 8Si(OH)_4 = 6Ca^{2+} + 16H_2O + \text{Montmorillonite}$
Ion exchange reaction	$Ca^{2+} + 2(\text{Na-Montmorillonite}) = \text{Ca-Montmorillonite} + 2Na^+$
Redox reaction of sulfur minerals	$FeS_2 + 8H_2O = 2SO_4^{2-} + Fe^{2+} + 16H^+ + 14e^-$ $SO_4^{2-} + 8e^- + 9H^+ = HS^- + 4H_2O$

Figure 3.4-8 Geochemical evolution of deep groundwater
(after Iwatsuki and Yoshida, 1999)

In the Tono area, the groundwater chemistry changes from Na-Ca-HCO_3 type to Na-HCO_3 type with depth.

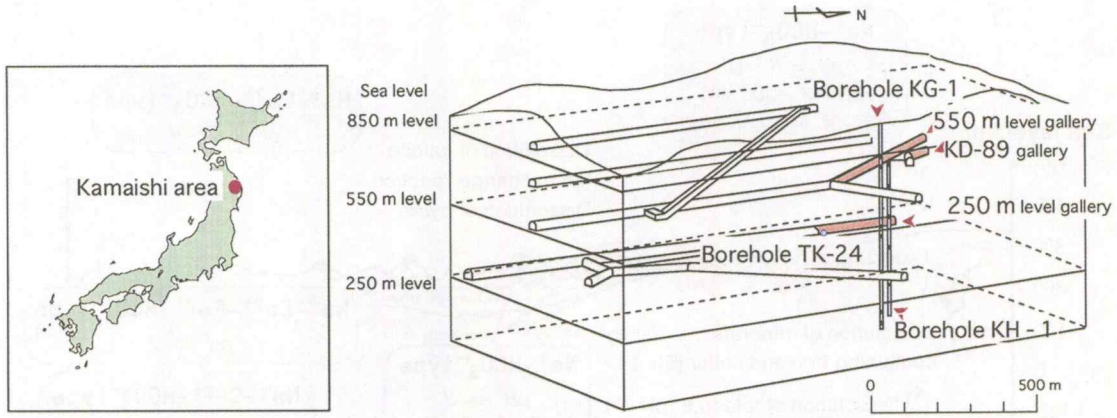


Figure 3.4-9 Schematic view of the Kamaishi mine

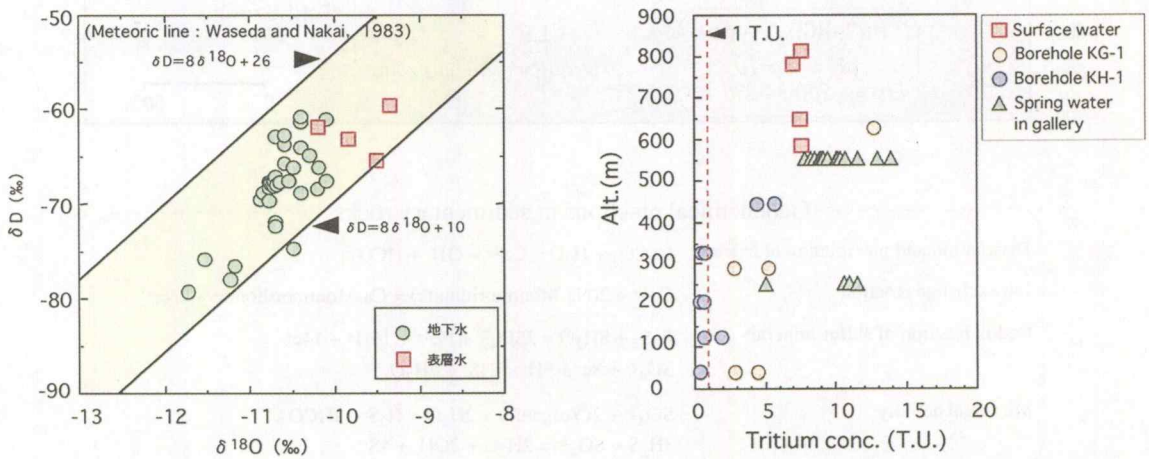


Figure 3.4-10 Isotopic composition of the Kamaishi groundwater

(Sasamoto et al, 1996)

Isotopic compositions show that groundwater is of meteoric origin and that surface water penetrates to several hundred meters depth.

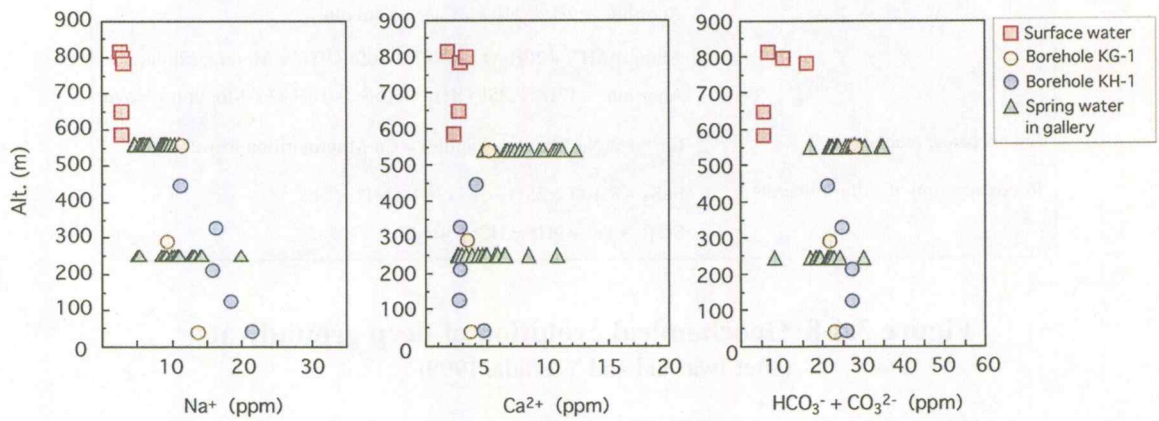


Figure 3.4-11 Groundwater variations in the Kamaishi mine

(Sasamoto et al., 1996)

pressure of carbon dioxide gas decreases and pH, HCO_3 and cation concentrations increase with depth, kaolinite reacts with dissolved SiO_2, HCO_3 and Ca to form montmorillonite and calcite. At the Kamaishi mine, montmorillonite is found at a depth ranging from 100 m to 200 m (Morita et al., 1991). In contrast, fractures at depth contain no kaolinite as an alteration mineral of albite. This suggests that ion exchange reactions involving montmorillonite result in an increase in sodium concentration in the groundwater. In the groundwater of the Kamaishi mine, however, a decrease in calcium concentration with depth is not observed (cf. Tono). Consequently, it is concluded that the abundance of clay minerals, including montmorillonite, is low at Kamaishi. Here, the ion exchange capacity is assumed to be too low to condition the chemistry of recharge waters. Alternatively, most of the montmorillonite has already been converted to Ca-montmorillonite. Therefore ion exchange reactions are less important controls on water chemistry than dissolution reactions involving sodium-bearing minerals such as albite. It is probable that these reactions are responsible for increasing sodium concentrations with depth.

Calculations of saturation indices using the speciation-solubility code EQ3/6 (Wolery, 1983) demonstrate that the following equilibria involve albite and calcite in groundwaters with pH greater than 9 (Figure 3.4-12):

$$\underset{\text{albite}}{7\ NaAlSi_3O_8} + 6\ H^+ + 20\ H_2O = 6\ Na^+ + 10\ Si(OH)_4 + 3\ \underset{\text{montmorillonite}}{Na_{0.33}Al_2(Si_{3.67}Al_{0.33}O_{10})(OH)}$$

$$\underset{\text{calcite}}{CaCO_3} + H_2O = Ca^{2+} + OH^- + HCO_3^-$$

$$\underset{\text{quartz}}{SiO_2(s)} + 2\ H_2O = Si(OH)_4(aq)$$

The above reactions provide a reasonable explanation for the increase in pH, Na, Ca, SiO_2 and carbonic acid (HCO_3 + CO_3) with depth. Equilibration of calcite may be relatively rapid in natural systems, but silicates and alumino-silicates may require timescales of a million years or more to equilibrate (Holdren and Berner, 1979; Brantley, 1992).

The redox potential of the groundwater from a borehole (TK-24) in the 250 m-level drift of the Kamaishi mine was measured to be –320 mV at pH = 9.8 (Sasamoto et al., 1996). This value corresponds to the redox boundary between dissolved sulfate and disulfide:

$$SO_4^{2-} + 8\ e^- + 9\ H^+ = HS^- + 4\ H_2O$$

$$\text{or} \quad FeS_2 + 8\ H_2O = 2\ SO_4^{2-} + Fe^{2+} + 16\ H^+ + 14\ e^-$$

Based on the results obtained from the above investigations, geochemical conditions at depth in the Kamaishi mine are summarized as follows:

i. Groundwater chemistry changes from neutral to weakly alkaline and concentrations of Na and HCO_3 increase with increasing depth.
ii. Dissolution reactions of feldspars and calcite are involved in the evolution of the groundwater chemistry.
iii. While some of the groundwaters sampled from drifts contain tritium, the groundwater from newly drilled boreholes contains no tritium and retains a partially reducing state.

These findings imply that the general geochemical environment of the Kamaishi mine is

selectively oxidizing in old drifts and geological structures controlled by large fracture zones, whereas remaining rock volumes away from excavations maintain a reducing state.

3.4.3 Case studies on colloids, organic materials and microbes in deep groundwater

Colloids are defined as particles smaller than one micron across. They include inorganic particles, for example silica, ferrous hydroxide and aluminum hydroxide and organic particles derived, for example, from humic acid. The impact of these colloidal particles on the geochemical characteristics of the groundwater is not clear. It is possible that organic colloids and sulfur-bearing colloids contribute to the metabolism of microbes associated with oxidation and reduction processes; therefore, colloids may indirectly affect the redox potential of the groundwater. Since radionuclides may be sorbed by colloidal particles mobile in groundwater, colloids are concluded to affect the migration behavior of radionuclides in the geological environment. Organic materials in groundwater are thought to influence not only the redox potential of the groundwater by methane fermentation due to microbial activity (Stumm and Morgan, 1996), but also the migration behavior of trace elements due to sorption (Thurman, 1985; Nelson et al., 1985; Buffle, 1988). It has been demonstrated in laboratory experiments that only the concentrations of trivalent actinides are affected by organic materials in groundwaters in granites and sedimentary rocks where groundwaters have a high concentration of carbonate or organic material (Moulin, 1995). It has also been ascertained that fulvic acid does not affects sorption of elements such as Sr, Tc, Cs, and U in an oxidizing environment and under chemical conditions similar to those in granitic groundwaters (Ticknor et al., 1996). In addition, it has been pointed out that a unique microbiological ecosystem exists in the deep geosphere (Naganuma, 1997). Microbial activity is considered to influence the geochemical environment deep underground through association with redox processes and the formation of organic complexes in the generation and metabolic processes of carbon dioxide and sulfide (Bath et al., 1987; Milodowski et al., 1990; Chapman et al., 1991; West, 1996). In order to understand the geochemical characteristics of groundwater, it is therefore important to assess the influence of organo-chemical characteristics of colloidal/organic materials and microbes.

So far, few data concerning colloids, organic materials and microbes have been collected in Japan. This is because such studies require survey points to guarantee a constant supply of groundwater, anaerobic conditions for water sampling and a clean environment for sample preparation.

1) Colloids

Characteristics of colloidal particles differ depending on rock type and the chemical properties of the groundwater (Avogadro and de Marsily, 1984; Grindrod, 1991). In Japan, colloids in deep groundwater have been investigated only in sedimentary rocks at depths of about 160 m in the Tono area.

As a result, the following information has been acquired on colloids in the groundwaters in the sedimentary rocks at Tono:

- Colloidal particles in the groundwater consist mainly of sulfur-rich particles, silicate minerals and carbonate minerals. The sulfur-rich colloidal particles are thought to be organic colloids generated by microbial activity. Microbes are therefore assumed to contribute to the redox reactions of chemical species of sulfur.
- The concentration of colloidal particles in the groundwater ranges from 1 to 1.5 mg l^{-1} (Figure 3.4-13).

- As concentrations of U, Th and rare-earth elements are not correlated with the size of colloidal particles, no effect of colloidal particles on the concentrations of these elements in groundwater is recognized (Seo and Moulin, 1995).

Since information on colloids available in Japan is restricted to this locality, it is considered that the data are insufficient to allow a general understanding of colloid characteristics in the natural groundwater systems of Japan. Future research is required to investigate colloids in groundwaters in crystalline rocks and other deep environments.

2) Organic materials

The concentration of dissolved organic materials (mainly humic matter) is measured as the concentration of the total organic carbon (TOC). TOC concentrations range widely, from 0.3 to 500 mg l^{-1} in groundwater at a depth of 100 m or less, and fluctuate greatly from location to location. In contrast, TOC in groundwater at a depth of more than 100 m ranges from 1 to 10 mg l^{-1} (Nagao, 1995). Humic materials are classified into hydrophilic acid, humic acid (which precipitates at a pH of less than 1) and fulvic acid (which does not precipitate at a pH of less than 1). The concentrations of these materials range from several ppm to tens of ppm, depending on the rock type.

The investigation of organic materials in sedimentary rocks and granite in the Tono area has highlighted the following features.

i. The concentration of organic carbon in the groundwater ranges from 0.1 to 8 mg C l^{-1} (Iwatsuki and Moulin, 1998; Iwatsuki and Yoshida, 1999b).
ii. Trace elements such as I, Cs, Th, Cr and rare-earth elements in the groundwater are barely detectable in humic and fulvic acids. Other trace elements (Cu, Mn, etc.) confirmed to be sorbed on organic materials range from 10^{-2} to 10^{-7} times the amount dissolved in the groundwater (Table 3.4-5).
iii. Atomic composition ratios of humic and fulvic acids indicate that these acids in deep groundwater are not generated from soil. Instead, humic and fulvic acids are generated from organic materials (lignite, etc.) in the sedimentary rocks and organic materials (organic colloids rich in sulfur and other components) in the deep groundwater are assumed to be generated by microbial decomposition of these materials in the sedimentary rocks.

Information available in Japan is mostly restricted to data on organic materials in shallow groundwater and those in weakly alkaline and chemically reducing deep groundwater. Therefore, future investigations are needed on the characteristics of organic materials in other types of groundwater.

3) Microbes

It is believed that the amount of microbes ranges from 10^5 cells l^{-1} in groundwater poor in nutrients to some 10^{11} cells l^{-1} in soils (Rosevear, 1991). From a reconnaissance survey on organic materials in sedimentary rocks and granites in the Tono area and in granites at the Kamaishi mine, the following results have been acquired:

In groundwater in the sedimentary rocks and granites of the Tono area :

i. The total number of bacteria ranges from 10^{10} cells l^{-1} (sedimentary rocks) to 10^9 cells l^{-1} (granites) and is generally ten times higher in the sedimentary rocks than in the granites. The number of living bacteria ranges from 10^6 to 10^9 CFU (Colony Forming Unit) l^{-1}

Table 3.4-5 Trace element concentrations and the organic components in the Tono groundwater

	Granite (KNA-6G ; G.L.-180m)					Sedimentary rocks (KNA-6U ; G.L.-160m)				
	Groundwater	Organics (Wt %)		Trace elements migrating with organics		Groundwater	Organics (Wt %)		Trace elements migrating with organics	
		Fulvic acid	Humic acid	Fulvic acid	Humic acid		Fulvic acid	Humic acid	Fulvic acid	Humic acid
DOC	84 (μgC·l⁻¹)				(ppb)	111 (μgC·l⁻¹)				(ppb)
C		50.07	46.66				47.76	46.43		
H		5.62	6.87				5.55	6.98		
N		0.52	8.36				0.60	8.65		
Al	<0.1 (ppm)	0.026	0.047	7.68E-04	5.22E-04	<0.01 (ppm)	0.011	0.026	1.64E-03	1.27E-03
Br	<0.02 (ppm)	<0.001	<0.001	-	-	<0.02 (ppm)	<0.001	<0.001	-	-
Ca	1.23E+01 (ppm)	<0.005	0.09	-	1.00E-03	2.34E+00 (ppm)	0.053	0.05	7.92E-03	2.45E-03
Cl	1.06E+00 (ppm)	0.08	<0.01	2.36E-03	-	8.70E-01 (ppm)	0.02	0.01	2.99E-03	4.89E-04
K	4.30E-01 (ppm)	0.043	<0.005	1.27E-03	-	2.50E-01 (ppm)	0.01	0.041	1.49E-03	2.01E-03
Mg	1.80E-01 (ppm)	0.0013	0.015	3.84E-05	1.67E-04	2.00E-02 (ppm)	0.0075	0.01	1.12E-03	4.89E-04
Na	2.93E+01 (ppm)	0.48	0.11	1.42E-02	1.22E-03	4.25E+01 (ppm)	0.16	0.13	2.39E-02	6.36E-03
Si	1.04E+01 (ppm)	<0.05	<0.05	-	-	7.51E+00 (ppm)	<0.05	<0.05	-	-
Fe	<0.02 (ppm)	0.14	1.15	4.13E-03	1.28E-02	<0.02 (ppm)	0.007	0.038	1.05E-03	1.86E-03
Ti	1.50E-02 (ppb)	0.001	0.002	2.95E-05	2.22E-05	1.50E-02 (ppb)	0.001	0.006	1.49E-04	2.94E-04
Mn	1.30E+01 (ppb)	0.0015	0.0015	4.43E-05	1.67E-05	5.50E-01 (ppb)	0.0003	0.00029	4.48E-05	1.42E-05
Ni	7.30E-02 (ppb)	0.0005	0.016	1.48E-05	1.78E-04	1.40E-02 (ppb)	0.0002	0.0008	2.99E-05	3.92E-05
Cu	2.80E-02 (ppb)	0.0039	0.002	1.15E-04	2.22E-05	5.00E-02 (ppb)	0.0036	0.0016	5.38E-04	7.83E-05
Sr	1.90E+01 (ppb)	0.00013	0.00055	3.84E-06	6.11E-06	1.20E+00 (ppb)	0.00055	0.00025	8.22E-05	1.22E-05
Sb	2.20E-03 (ppb)	0.0005	0.0001	1.48E-05	1.11E-06	8.00E-04 (ppb)	<0.0001	0.0002	-	9.79E-06
T.I	2.30E-02 (ppb)	<0.001	<0.001	-	-	2.00E-02 (ppb)	<0.001	<0.001	-	-
Cs	2.24E-01 (ppb)	<0.0001	<0.0001	-	-	5.90E-02 (ppb)	<0.0001	<0.0001	-	-
Pb	1.70E-02 (ppb)	0.00053	0.00024	1.57E-05	2.67E-06	2.20E-02 (ppb)	0.00013	0.00024	1.94E-05	1.17E-05
Th	6.00E-02 (ppb)	<0.0001	<0.0001	-	-	7.60E-02 (ppb)	<0.0001	<0.0001	-	-
W	8.40E+00 (ppb)	0.029	0.018	8.56E-04	2.00E-04	1.50E+01 (ppb)	0.023	0.025	3.44E-03	1.22E-03
U	2.30E-02 (ppb)	<0.0001	0.0042	-	4.67E-05	1.90E-03 (ppb)	<0.0001	0.00069	-	3.38E-05
Cr	1.10E-02 (ppb)	<0.001	<0.001	-	-	1.70E-02 (ppb)	<0.001	<0.001	-	-
Co	1.30E-02 (ppb)	0.00034	0.0004	1.00E-05	4.44E-06	3.40E-03 (ppb)	0.00042	0.00021	6.28E-05	1.03E-05
Zn	7.90E-02 (ppb)	0.0032	0.0027	9.45E-05	3.00E-05	2.10E-02 (ppb)	0.0017	0.0017	2.54E-04	8.32E-05
Mo	2.30E-01 (ppb)	0.0017	0.001	5.02E-05	1.11E-05	1.80E-01 (ppb)	0.0011	0.001	1.64E-04	4.89E-05
As	<0.2 (ppb)	<0.001	<0.001	-	-	<0.2 (ppb)	<0.001	<0.001	-	-
V	1.30E-02 (ppb)	<0.0001	0.00024	-	2.67E-06	2.30E-03 (ppb)	<0.0001	<0.0001	-	-
Ag	2.30E-02 (ppb)	<0.0001	0.0088	-	9.78E-05	8.70E-03 (ppb)	<0.0001	<0.0001	-	-
Lu	n.m. (ppb)	<0.0001	<0.0001	-	-	n.m. (ppb)	<0.0001	<0.0001	-	-
Tb	n.m. (ppb)	<0.0001	<0.0001	-	-	n.m. (ppb)	<0.0001	<0.0001	-	-
Yb	n.m. (ppb)	<0.0001	<0.0001	-	-	n.m. (ppb)	<0.0001	<0.0001	-	-
Ho	n.m. (ppb)	<0.0001	<0.0001	-	-	n.m. (ppb)	<0.0001	<0.0001	-	-
Eu	n.m. (ppb)	<0.0001	<0.0001	-	-	n.m. (ppb)	<0.0001	<0.0001	-	-
Sm	n.m. (ppb)	<0.0001	<0.0001	-	-	n.m. (ppb)	<0.0001	<0.0001	-	-
Pr	n.m. (ppb)	<0.0001	<0.0001	-	-	n.m. (ppb)	<0.0001	<0.0001	-	-
Er	n.m. (ppb)	<0.0001	<0.0001	-	-	n.m. (ppb)	<0.0001	<0.0001	-	-
Ce	n.m. (ppb)	0.0001	0.0001	2.95E-06	1.11E-06	n.m.. (ppb)	<0.0001	0.0002	-	9.79E-06
Au	n.m. (ppb)	0.0002	0.0002	5.91E-06	2.22E-06	n.m. (ppb)	<0.0001	<0.0001	-	-

n.m. : not measured

(See Table 3.4-6). These numbers represent bacteria that could be viable under aerobic culture conditions but, given that the underground environment is generally anaerobic, most of them may actually be anaerobic bacteria. Moreover, of all living bacteria present in the in situ environment, only several percent may be culturable, while the remaining are classified as "viable but non-culturable" (VBNC). Accordingly, considering VBNC anaerobic bacteria, the number of microbes cultured in the underground environment is expected to be large (Murakami et al., 1999).

ii. In the granites, the number of morphological varieties of microbes changes with increasing depth.

iii. At a depth of some 200 to 300 m in the granite, a peak in the number of iron-related viable bacteria is observed. This depth corresponds to a redox boundary ($Fe^{2+}/Fe(OH)_3$; pH=7.8 - 8.2, Eh = 0 - 16 mV). Energy associated with the conversion of ferric to ferrous iron may be used by bacteria. Therefore, at such depths, iron-related bacteria are expected to increase. Through this process, the redox potential and pH of the groundwater could change, possibly forming the redox boundary.

iv. At a depth of 450 m in the granite, the existence of sulfate-reducing bacteria has been determined. At this depth, the concentration of sulfate ions is relatively high, while the redox potential ranges from -100 to -200 mV. Under these conditions, sulfate-reducing bacteria could increase in abundance.

v. Methane-generating bacteria, nitrous acid bacteria, nitric acid bacteria and denitrifying bacteria were not detected.

In the groundwater in granites in the Kamaishi mine:

i. The total number of bacteria is as high as 8.6×10^5 to 1.2×10^9 cells l^{-1} (Aoki et al., 1997).

ii. None of the living forms of iron-oxidizing bacteria, methane-generating bacteria, nitrous acid bacteria, nitric acid bacteria and denitrifying bacteria has been detected

iii. Sulfate-reducing bacteria number 5.0×10^2 to 1.3×10^6 l^{-1} (as Most Probably Numbers)

iv. General bacterial abundance is estimated at 5.3×10^5 to 3.9×10^7 CFU l^{-1}.

Considerable numbers of bacteria are found in deep groundwater both in the Tono area and the Kamaishi mine. It is expected not only that the existence and activity of microbes in deep geological environments are closely related to underground geochemical processes, but also that sulfate-reducing bacteria influence the redox environment at depth (Figure 3.4-14). In future, it will be necessary to define the extent of this influence, as well as the range of microbial activity in the deep subsurface environment.

3.4.4 Summary

Through analyses of data acquired from the published literature, foreign case studies and investigations in the Tono area and the Kamaishi mine, the following information has been obtained on the geochemical characteristics of deep groundwater of meteoric origin in sedimentary rocks and granites in Japan:

i. Groundwater chemistry at depth is weakly alkaline and dominated by Na and HCO_3.

ii. Dissolution of feldspars and calcite and ion exchange reactions between clay minerals and groundwater are cited as the major reactions controlling the chemical evolution of the groundwater.

iii. Redox reactions involving chemical species of sulfur and iron and microbial dissolution of organic materials influence the redox potential of groundwater in sedimentary rocks.

Table 3.4-6 Characterization of microbial activities in the groundwater at the Tono area (after Murakami et al.,1999)

Borehole	Formation	Depth	Total bacteria	Aerobic bacteria		Sulfur oxidizing Bacteria	Total aerobic Bacteria	Iron relating Bacteria	Sulfate reducing Bacteria	Denitrification Bacteria	Nitrifying Bacteria
		(G.L.- m)	(cells ml^{-1})	(CFU ml^{-1}) 1/2LB・G	×10(1/2LB・G)	(CFU ml^{-1})	(CFU ml^{-1})	(CFU ml^{-1})	(CFU ml^{-1})	(CFU ml^{-1})	(CFU ml^{-1})
TH-6	Akeyo F.	-104	1.6791E+06	—	—	—	5.00E+06	1.00E+05	4.20E+03	m.a.	n.d.
TH-6	Toki lignite-bearing F.	-132	1.4850E+06	—	—	—	5.00E+06	1.00E+05	2.00E+02	b.l.	n.d.
TH-6	Toki lignite-bearing F.	-153	2.2488E+06	—	—	—	5.00E+06	1.00E+05	n.a.	b.l.	n.d.
KNA-6	Toki lignite-bearing F.	-160	3.66E+05	—	—	—	2.01E+05	n.a.	n.a.	n.d.	n.d.
TH-6	Toki granite	-177.5	1.9334E+06	—	—	—	5.00E+06	7.51E+03	2.40E+02	b.l.	n.d.
KNA-6	Toki granite	-180	2.42E+05	—	—	—	n.a.	8.01E+03	2.78E+03	b.l.	n.d.
DH-3	Toki granite	-19	3.1429E+05	9.07E+03	2.21E+04	8.83E+03	5.00E+05	7.51E+03	n.a.	n.d.	n.d.
DH-3	Toki granite	-130	6.7757E+05	3.60E+03	1.48E+04	5.43E+03	3.33E+06	1.00E+05	n.a.	b.l.	n.d.
DH-3	Toki granite	-209	1.1036E+06	2.00E+02	3.60E+03	0.00E+00	3.33E+06	4.50E+04	n.a.	b.l.	n.d.
DH-3	Toki granite	-330	1.6021E+06	7.40E+03	1.13E+04	7.23E+03	1.00E+03	1.00E+05	n.a.	n.d.	n.d.
DH-3	Toki granite	-458	2.2426E+06	9.10E+03	1.62E+04	8.97E+03	5.00E+06	1.76E+04	1.70E+04	no data	n.d.
DH-3	Toki granite	-485	1.1404E+06	2.23E+03	6.17E+03	1.97E+03	1.00E+03	1.76E+04	3.30E+01	b.l.	n.d.
DH-3	Toki granite	-600	1.0302E+06	3.07E+03	7.60E+03	3.30E+03	5.00E+05	1.00E+05	n.a.	b.l.	n.d.
DH-3	Toki granite	-645	6.6131E+05	3.37E+03	5.87E+03	1.20E+03	5.00E+05	1.00E+05	n.a.	b.l.	n.d.
DH-3	Toki granite	-767	1.2522E+06	1.33E+03	6.73E+03	2.03E+03	1.00E+03	4.50E+04	n.a.	b.l.	n.d.
DH-3	Toki granite	-790	9.0854E+05	9.03E+03	1.24E+04	7.43E+03	5.00E+05	9.19E+03	n.a.	n.d.	n.d.
DH-3	Toki granite	-840	8.9319E+05	3.70E+03	5.73E+03	2.33E+03	1.67E+05	1.76E+04	n.a.	n.d.	n.d.
DH-5	Toki granite	-330	8.5526E+05	2.11E+04	4.45E+04	2.29E+04	5.00E+05	1.76E+04	6.67E+02	n.d.	n.d.

n.d. = not detected CFU = Colony Forming Unit n.a. = not aggressive, m.a. = moderately aggressive, b.l. = background level

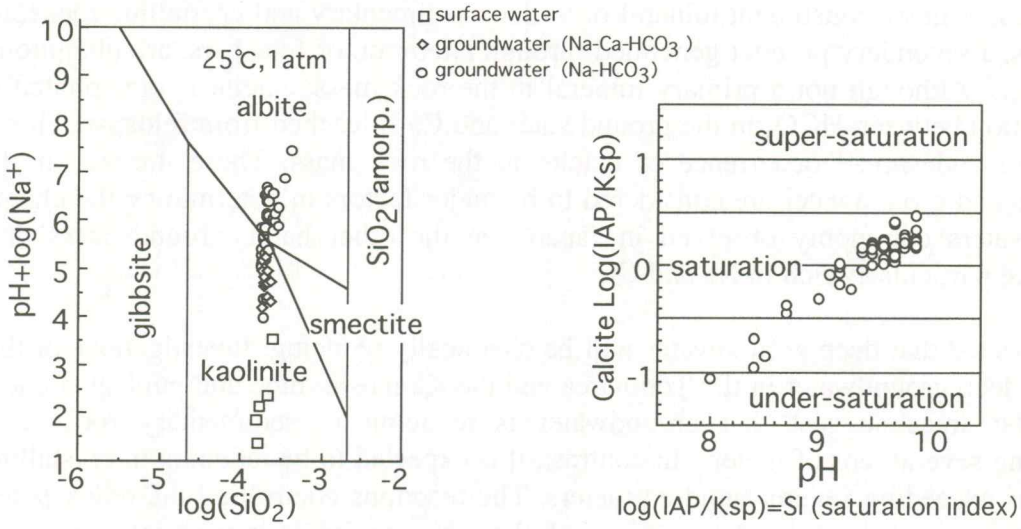
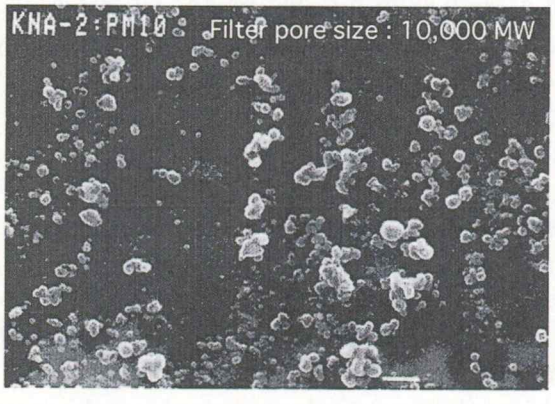


Figure 3.4-12 Phase diagram and saturation index of the Kamaishi groundwater

The phase diagram is consistent with kaolinite and albite being stable in the Ca^{2+} - HCO_3^- type groundwater of the shallow zone and in the Na^+ - HCO_3^- type groundwater of the deep zone, respectively. The saturation index of calcite implies that calcite is in equilibrium with the deep groundwater.

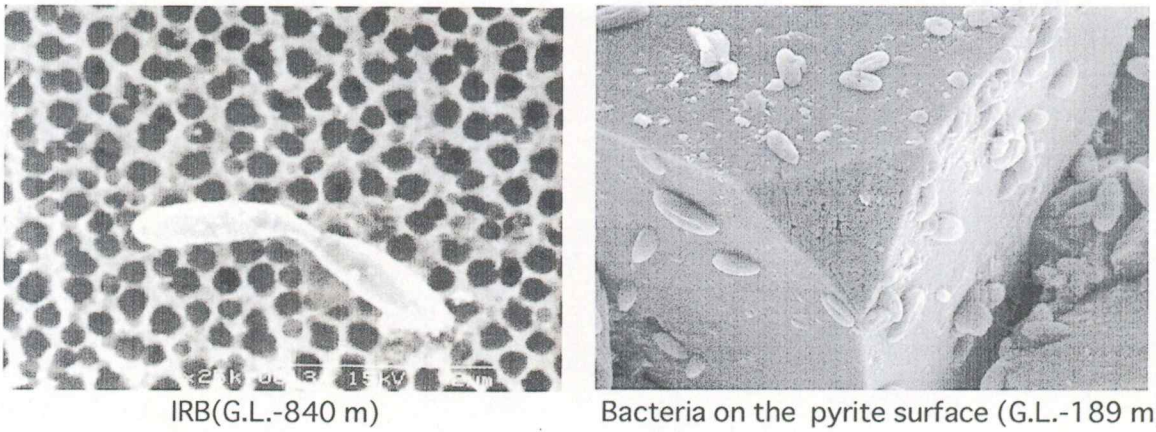


Colloids wt % (cut off 0.02 μm)
: 1.3±0.2 mg l^{-1}

Chemical composition : S, Si, Ca, clay

Figure 3.4-13 Colloid particles sampled from groundwater in the sedimentary rocks at the Tono area

The origin of colloids rich in S is probably the bacterial decomposition of organic sulfate and sulfide.



IRB(G.L.-840 m)

Bacteria on the pyrite surface (G.L.-189 m)

Figure 3.4-14 Bacteria observed in the granite of the Tono area

There is a possibility that microbial activity influences the geochemical condition of the groundwater.

Feldspars, a major constituent mineral of various sedimentary and crystalline rocks, and clay minerals, a secondary product generated through alteration of feldspars, are ubiquitous in the rock mass. Although not a primary mineral in the rock mass, calcite is precipitated through the reaction between HCO_3 in the groundwater and Ca is leached from feldspar. This process results in widespread occurrence of calcite in the rock mass. These interactions between minerals and groundwater are considered to be major factors in determining the chemistry of groundwaters commonly observed in Japan. On the other hand, groundwaters of marine origin are particularly rich in Na and Cl.

It is expected that deep groundwater will be chemically reducing. Investigations of the redox state of deep groundwater in the Tono area and the Kamaishi mine and published data for the Horonobe areas suggest that groundwater is reducing in sedimentary rocks at depths exceeding several tens of meters. In contrast, it is expected to be reducing in crystalline rocks at depths exceeding several hundred meters. The reactions controlling the redox potential of groundwater are believed to be reactions of chemical species of iron or sulfur and microbial decomposition of organic materials. These reactions are considered to occur widely deep underground based on the following:

i. Groundwater contains various organic materials used for microbial metabolism (Nagao, 1995)
ii. Large numbers of reducing bacteria, such as iron-reducing and sulfate-reducing bacteria, are found under reducing conditions in various rock facies at depths (Lovley and Chapelle, 1995).
iii. Reduced iron-bearing minerals (biotite, iron hydroxide etc.) and sulfur-bearing minerals (gypsum, pyrite etc.) occur widely in sedimentary and igneous rocks.

Reactions such as ion exchange, dissolution of carbonates and redox reactions involving chemical species of iron and sulfur reach a chemical equilibrium or a biologically stable state more easily than the dissolution of silicate minerals (Wikberg, 1987; Chou et al., 1989; Brantley, 1992). They are therefore considered to be applicable to geochemical modeling where chemical equilibrium is assumed. As shown in the case study in the Tono area, a suitable geochemical environment can contribute to a reducing state over long periods of time. It has also been concluded that the redox state of groundwater can be estimated from data on the mineralogical compositions of the rocks and fracture infills.

3.5 Thermal and mechanical properties of the rock mass

The thermal and mechanical properties of rocks are important factors in determining the layout of a repository and in specifying the components of the EBS. The temperatures and thermal properties of the rock mass affect the rate of the chemical reactions that take place in the EBS. The mechanical properties and initial stress state of the rock mass are important for optimizing the design and construction of a repository, for estimating the stability of cavities during construction and operation and for designing the stability of the overpacks and buffer materials. In addition, the properties of the rock mass adjacent to underground openings could be altered by excavation and information on the effects of such excavation on the surrounding rock mass is also required.

In order to understand the general thermal and mechanical properties of rock masses at depth, data were compiled from the published literature in Japan and collected from investigations carried out at Kamaishi and Tono. This work allowed an examination to be conducted of the distribution of these properties with reference to the various rock types of interest, as well as of the relationships between these properties. Experimental studies were carried out as part of the drift excavation programs in Neogene sedimentary rocks at Tono mine and crystalline rocks at Kamaishi mine. These were included not only to determine the characteristics and extent of the excavation disturbed zone (EDZ) and to understand the mechanisms of excavation disturbance, but also to confirm the applicability of existing investigation and analysis methods.

3.5.1 Thermal characteristics of the rock mass at depth

1) Thermal properties

Studies of the thermal properties of deep rock masses have been carried out mainly through reviewing the published literature. Literature surveys (Sato et al., 1992a) carried out for the H3 report succeeded in collecting data on the thermal conductivity of some rock types, but few data were available on specific heat and linear expansion coefficients. For H12, data on thermal conductivity and these two thermal coefficients were collected and categorized into those applicable to the following rock types (see Section 3.1.2):

- Acidic (felsic) crystalline rocks
- Basic (mafic) crystalline rocks
- Pre-Neogene sandstones
- Pre-Neogene mudstones and tuff
- Neogene sandstones
- Neogene mudstones and tuff

Thermal properties acquired through experimental studies in the Tono area and during in situ tests at the Kamaishi mine were also included in this comparative study. These new data are considered for the groups Neogene mudstones/tuff and acidic crystalline rocks. Although sediments in the Tono area include both sandstones and mudstones/tuff of Neogene age, there is little difference in either their thermal properties or in the other physical properties discussed below.

The thermal properties of rocks, as well as most of other physical properties, are sensitive to moisture content and measurement conditions. Published data were excluded from compilations if they came from specimens which were weathered and/or categorized as "poor rock". Published data giving indications of moisture content and test conditions are so scarce

that effects on published physical properties could not be examined. Therefore, the ranges listed for the various rock types include the unquantifiable effects of different moisture contents and test conditions. Table 3.5-1 shows the average and the standard deviation of the thermal and mechanical properties for rock types of interest.

(1) Thermal conductivity

Crystalline rocks showed a distribution of thermal conductivities with a frequency maximum around 2 - 3 W $m^{-1} K^{-1}$. In contrast, Neogene sedimentary rocks showed an equivalent maximum around 1 W $m^{-1} K^{-1}$ (Figures 3.5-1, 2, 3). Few data have been collected for Pre-Neogene sedimentary rocks. Data obtained at the Kamaishi mine show a similar distribution to that of the published data for acidic crystalline rocks. The data for the Tono area show a frequency distribution almost identical to that for Neogene sedimentary rocks (mudstones/tuff).

(2) Specific heat

Crystalline rocks have specific heat values in the range 0.7 - 1.1 kJ $kg^{-1} K^{-1}$. Few data have been collected for the other rock types (Figures 3.5-4, 5, 6).

(3) Thermal expansion coefficient

Thermal expansion coefficients for crystalline rocks are concentrated in the range 1x 10^{-5} to 1.5x$10^{-5} K^{-1}$. Few data are available for other rock types (Figures 3.5-7, 8, 9). Some data have negative values, which are presumably caused by contraction of the test sample due to the dehydration of interlayer water in clay minerals due to heating.

(4) Dependence of thermal properties on depth

Some physical rock properties vary with depth. In particular, many sedimentary rocks become more indurated with depth due to diagenetic processes over geological timescales, resulting in an increase in density and a decrease in effective porosity. The relationship between depth and thermal conductivity is shown in Figure 3.5-10, which shows a large scatter of thermal conductivities at all depths for all rock types. In addition to these data, the Geological Survey of Japan (1991) collected data from 321 geothermal boreholes greater than 100 m deep. Figures derived from this analysis show relationships between density, effective porosity and thermal conductivity with respect to depth. A good correlation is seen between these parameters for many sedimentary rocks such as tuff, sandstones and mudstones.

2) Geothermal gradients

Temperature data from 1979 boreholes, which cover the majority of the country, have been compiled (Yano et al., 1999). Ideally, geothermal gradients should be calculated from temperature measurements made along a borehole. However, few suitable linear gradients were available, with the result that the majority of the geothermal gradients were calculated from temperatures measured at the tops and bottoms of boreholes. Mean temperatures for respective areas were used as the temperature at the tops of boreholes, while measured values were used as temperatures at the bottoms of boreholes. According to the histogram of geothermal gradients, 7% of the total distribution has values less than 2°C per 100m, 40% of the distribution lies in the range 2 - 5°C per 100m, 30% in the range 5 - 10°C per 100m and 23% of the values are more than 10°C per 100m. The most common geothermal gradient is 2 - 3°C per 100m (Figure 3.5-11). This distribution is in agreement with the general understanding that thermal gradients throughout the country, outside geothermal areas, average 3°C per 100 m (Okubo et al., 1993; Yano et al., 1994).

The regional distribution of geothermal gradients is characterized by an approximate

Table 3.5-1 Statistical table of physical properties of rocks in Japan

Based on the literature data from Sato et al. (1992) and subsequent publications (Sato et al., 1999) .

Rock type	Physical properties	Thermal properties			Porosity			Seismic velocity					Density			Strength					
		Thermal conductivity	Specific heat	Linear expansion coefficient	Absorption coefficient	Moisture content	Effective porosity	Ultrasonic wave Velocity		Active Poisson's ratio	Elastic coefficient	Seismic velocity on the ground	Saturation density	Natural density	Dry density	Unconfined compressive strength	Young's modulus	Poisson's ratio	Tensile strength	Triaxial compressive test	
								P wave	S wave											Cohesion	Internal friction angle
		[$Wm^{-1}K^{-1}$]	[$kJ\ kg^{-1}K^{-1}$]	[$10^{5}K^{-1}$]	[%]	[%]	[%]	[km s^{-1}]	[km s^{-1}]		[GPa]	[km s^{-1}]	[g cm^{-3}]	[g cm^{-3}]	[g cm^{-3}]	[MPa]	[GPa]		[MPa]	[MPa]	[deg]
Crystalline rocks (acidic rocks)	Number	102	71	70	402	105	315	748	160	210	193	73	250	643	307	493	495	171	259	216	119
	Maximum	5.38	1.08	1.29	27.9	38.7	58.2	9.30	4.03	0.50	88.7	6.00	3.12	3.60	3.11	405.7	136.2	0.56	94.1	52.2	62.0
	Minimum	1.10	0.73	0.04	0.1	<0.1	0.0	1.04	<0.1	0.02	<0.1	0.33	1.76	1.05	1.48	0.4	<0.1	0.04	0.1	0.0	4.6
	Average	2.86	0.99	1.05	1.0	2.0	4.0	5.03	2.38	0.28	40.8	3.61	2.67	2.63	2.64	115.8	35.0	0.25	8.2	14.7	38.5
	Median	2.76	1.03	1.18	0.5	0.4	1.3	5.05	2.37	0.28	41.7	4.30	2.67	2.65	2.66	107.8	28.1	0.23	7.1	13.2	40.0
	Standard dev.	0.62	0.01	0.46	2.1	6.3	7.7	1.15	0.56	0.10	20.9	1.82	0.18	0.22	0.20	70.5	27.3	0.10	9.4	9.9	11.8
Crystalline rocks (basic rocks)	Number	183	55	50	433	37	248	662	190	183	310	149	125	529	230	529	448	68	238	191	60
	Maximum	4.23	1.28	1.29	12.3	11.5	25.2	8.08	4.13	0.42	123.4	5.20	3.09	3.37	3.06	437.5	160.7	0.50	23.1	53.6	55.3
	Minimum	0.68	0.72	0.03	0.1	0.1	0.1	1.50	0.67	0.10	<0.1	0.14	2.15	1.56	1.84	3.9	<0.1	0.07	0.5	1.0	5.5
	Average	2.36	0.96	0.82	1.9	4.2	7.0	4.79	2.38	0.26	24.7	1.51	2.66	2.63	2.60	134.0	26.5	0.25	9.9	22.8	36.3
	Median	2.39	1.06	0.81	1.2	4.1	5.4	4.86	2.32	0.26	18.4	1.11	2.66	2.65	2.63	127.4	20.7	0.23	9.6	20.9	39.0
	Standard dev.	0.77	0.17	0.22	2.1	3.4	5.7	1.19	0.61	0.06	25.7	1.11	0.24	0.24	0.25	72.1	27.8	0.09	4.7	9.9	10.0
Pre-Neogene sedimentary rocks (sandstones)	Number	75	1	1	16	22	110	220	31	1	8	409	87	277	108	78	70	23	15	30	31
	Maximum	4.74	0.77	0.70	24.4	53.6	55.1	6.85	2.99	0.25	68.6	6.13	2.64	2.98	2.78	205.8	82.2	0.45	31.4	30.0	62.1
	Minimum	0.47	0.77	0.70	0.2	1.1	0.1	0.70	0.25	0.25	<0.1	0.41	1.74	1.28	1.09	0.2	<0.1	0.11	0.1	0.1	22.0
	Average	1.56	0.77	0.70	7.3	21.2	17.9	2.83	1.49	0.25	30.7	3.75	2.27	2.20	2.01	31.2	11.0	0.32	7.9	5.2	35.8
	Median	1.30	0.77	0.70	4.1	18.8	16.1	2.70	1.25	0.25	23.6	3.74	2.29	2.25	1.98	17.2	3.2	0.33	6.7	3.5	32.0
	Standard dev.	0.78	-	-	7.8	14.4	13.7	1.20	0.99	-	30.3	0.76	0.25	0.36	0.39	36.8	19.6	0.12	7.6	6.3	10.8
Pre-Neogene sedimentary rocks (mudstones, tuff)	Number	90	6	6	91	106	203	412	57	5	21	61	155	537	183	380	364	61	93	132	149
	Maximum	3.63	0.93	2.44	125.0	60.0	55.4	6.40	3.51	0.31	20.3	5.30	2.62	2.99	2.66	377.6	58.8	0.50	54.8	98.0	60.0
	Minimum	0.35	0.77	0.83	0.7	0.6	0.2	0.70	0.30	0.21	1.9	0.64	1.40	1.05	0.68	<0.1	<0.1	0.07	0.1	<0.1	7.0
	Average	1.62	0.85	1.42	14.9	21.7	20.0	2.58	1.38	0.28	15.0	2.52	2.23	2.02	1.99	25.8	6.7	0.27	3.7	5.1	25.8
	Median	1.37	0.85	1.36	10.3	19.9	20.0	2.32	1.30	0.30	17.5	2.38	2.29	1.98	2.01	9.1	4.1	0.28	1.8	1.1	26.0
	Standard dev.	0.87	0.07	0.56	19.5	11.6	12.8	1.07	0.59	0.04	5.4	0.81	0.28	0.35	0.41	38.0	9.4	0.11	6.4	11.7	10.8
Neogene sedimentary rocks (sandstones)	Number	16	4	4	215	9	124	420	102	47	82	35	48	333	95	355	493	25	72	92	124
	Maximum	4.48	1.08	1.08	3.4	4.7	40.0	7.00	4.22	0.45	87.5	5.40	2.79	2.98	2.80	414.5	150.9	0.32	22.1	78.0	61.6
	Minimum	2.38	1.05	0.65	0.1	0.0	0.0	1.08	1.39	0.17	<0.1	0.50	1.23	1.60	2.45	0.3	<0.1	0.10	0.5	<0.1	14.0
	Average	3.19	1.06	0.93	0.7	1.3	6.5	4.57	3.05	0.28	35.1	2.15	2.58	2.52	2.61	134.4	18.6	0.20	8.7	16.9	38.4
	Median	2.97	1.06	1.00	0.5	1.1	3.1	4.61	3.21	0.26	43.0	1.90	2.63	2.58	2.56	127.4	13.7	0.20	7.6	15.8	39.0
	Standard dev.	0.59	0.01	0.19	0.6	1.4	9.0	1.24	0.75	0.07	26.0	1.38	0.28	0.26	0.08	83.6	19.7	0.07	5.4	15.5	8.3
Neogene sedimentary rocks (mudstones, tuff)	Number	14	6	5	58	3	53	201	26	19	68	16	18	214	35	178	321	16	40	85	78
	Maximum	3.65	1.04	1.09	2.6	0.9	46.0	7.80	3.96	0.39	97.7	5.50	3.05	3.05	3.04	344.0	105.8	0.39	24.7	98.0	45.0
	Minimum	1.88	1.09	0.80	0.1	0.6	0.4	1.07	1.46	0.20	1.8	0.90	1.90	1.41	2.08	1.5	0.2	0.06	0.1	0.4	7.0
	Average	2.68	1.06	0.96	0.6	0.8	7.7	4.59	2.69	0.30	42.9	2.82	2.69	2.48	2.72	104.9	17.8	0.26	7.6	15.9	25.5
	Median	2.68	1.06	0.94	0.4	0.8	1.8	4.95	2.53	0.29	45.6	2.26	2.70	2.66	2.74	89.7	8.2	0.30	5.4	1.8	25.5
	Standard dev.	0.48	0.02	0.11	0.5	0.2	11.4	1.64	0.60	0.05	24.3	1.60	0.25	0.38	0.19	76.4	19.9	0.09	6.6	20.8	10.9

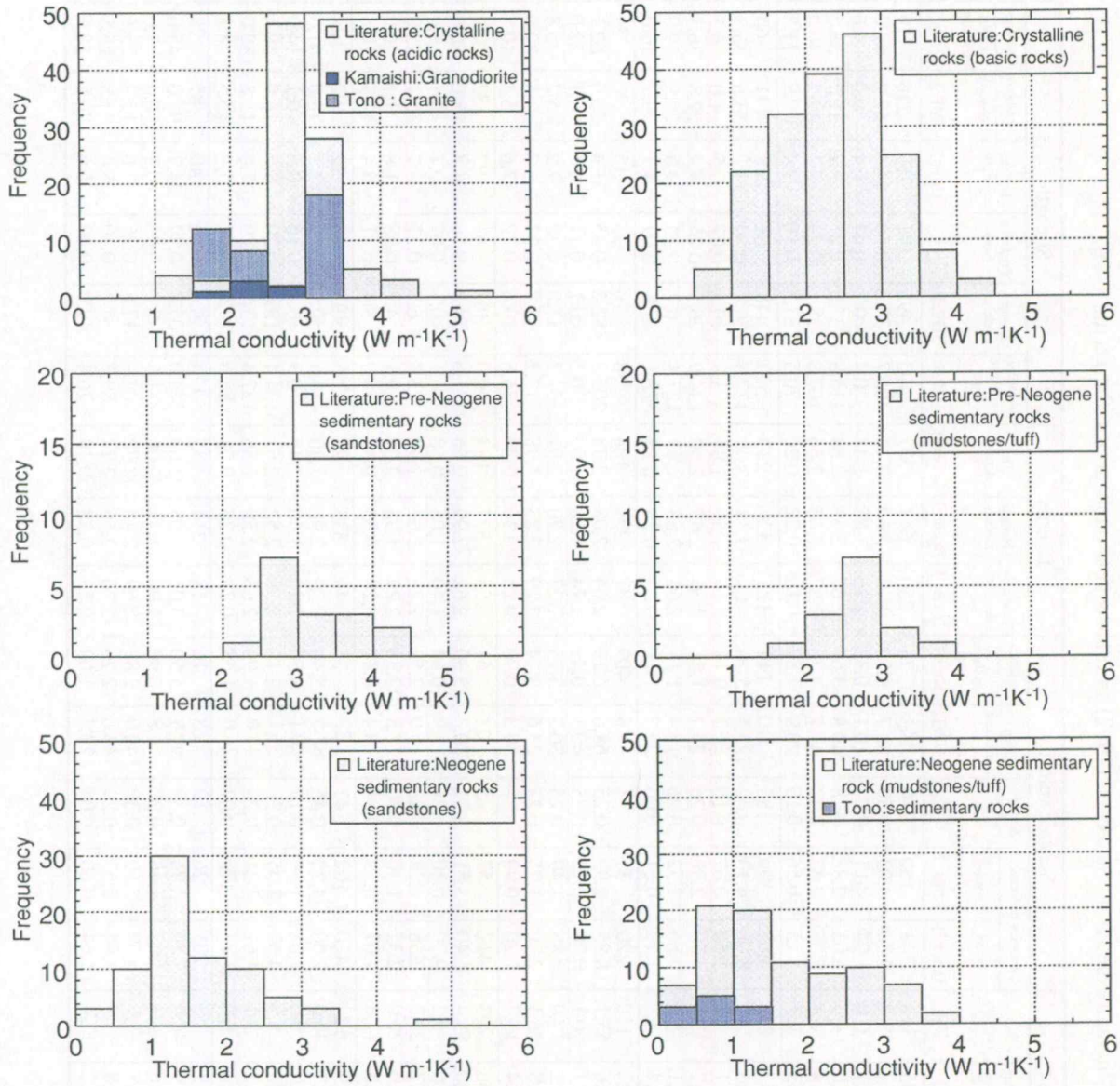


Figure 3.5-1 Histograms showing thermal conductivity

Literature data are mainly based on Sato et al. (1999).

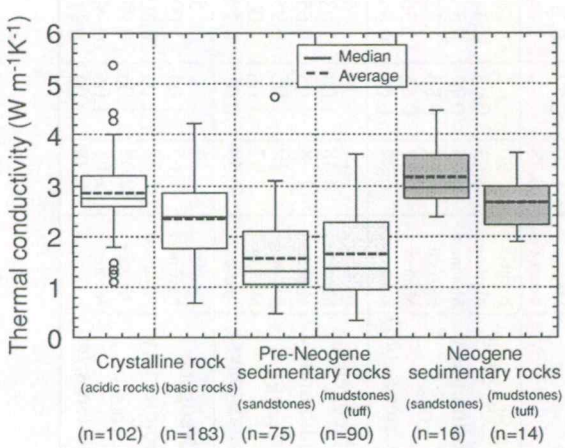


Figure 3.5-2 Distribution of thermal conductivity

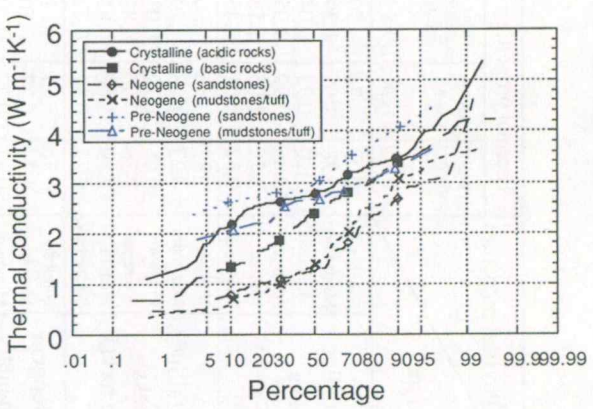


Figure 3.5-3 Probability curve of thermal conductivity

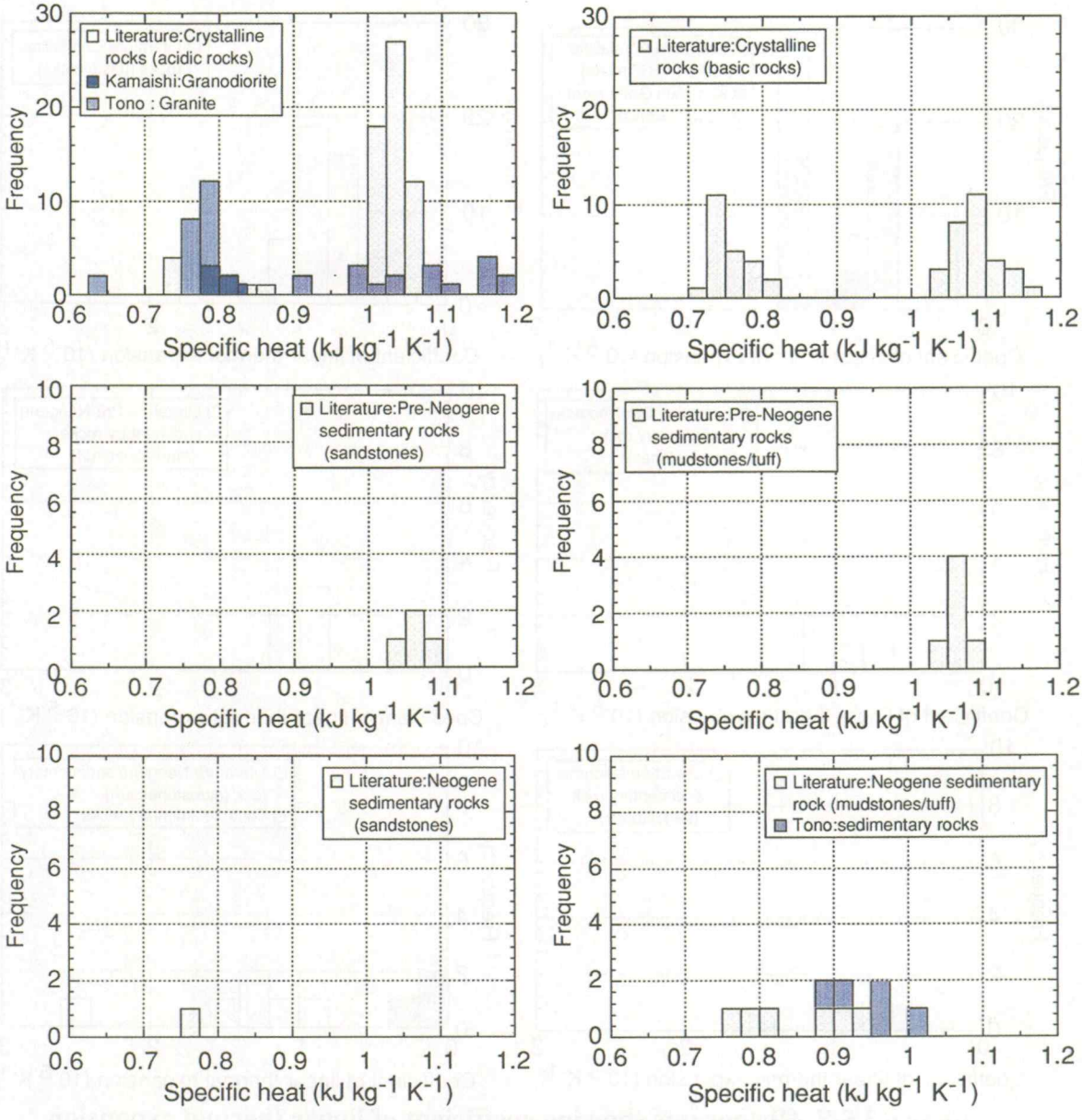


Figure 3.5-4 Histograms showing specific heat

Literature data are mainly based on Sato et al. (1999).

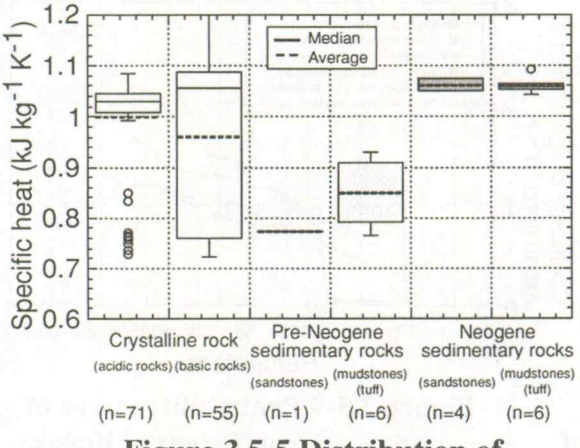


Figure 3.5-5 Distribution of specific heat

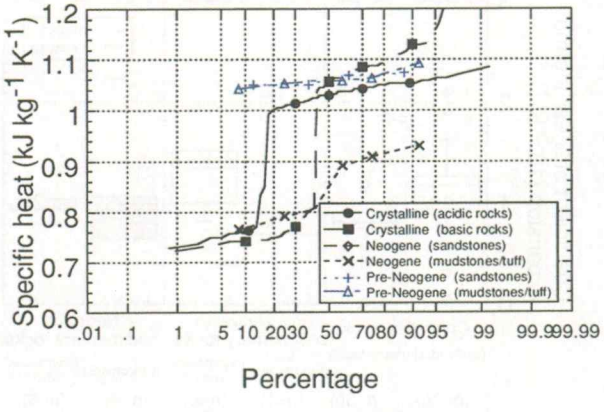


Figure 3.5-6 Probability curve of specific heat

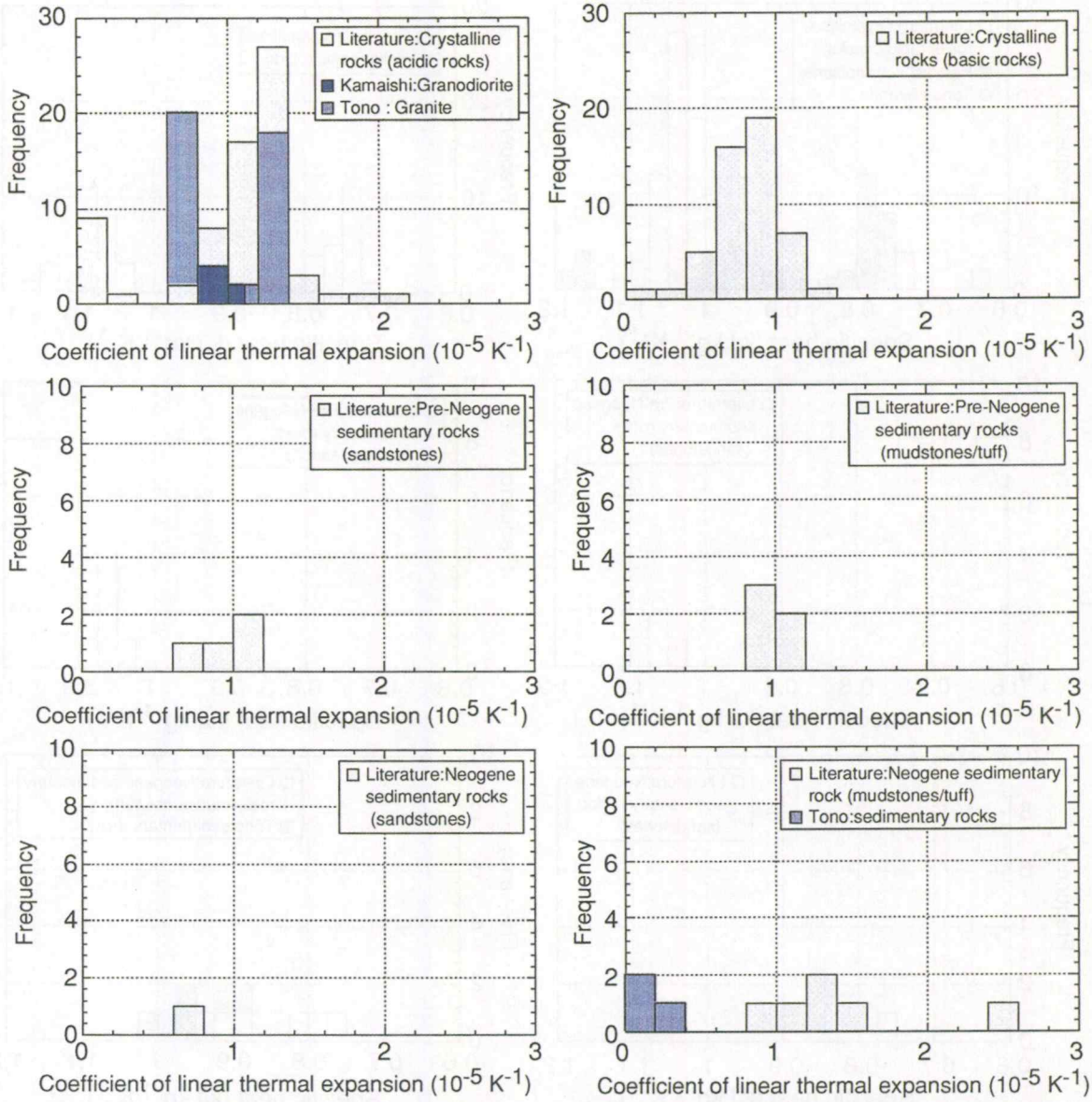


Figure 3.5-7 Histograms showing coefficient of linear thermal expansion

Literature data are mainly based on Sato et al. (1999).

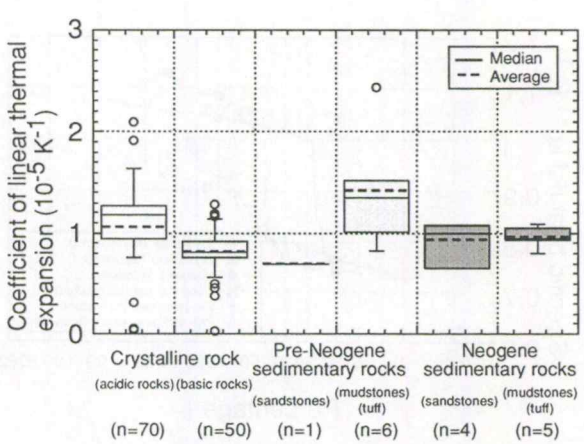


Figure 3.5-8 Distribution of coefficient of linear thermal expansion

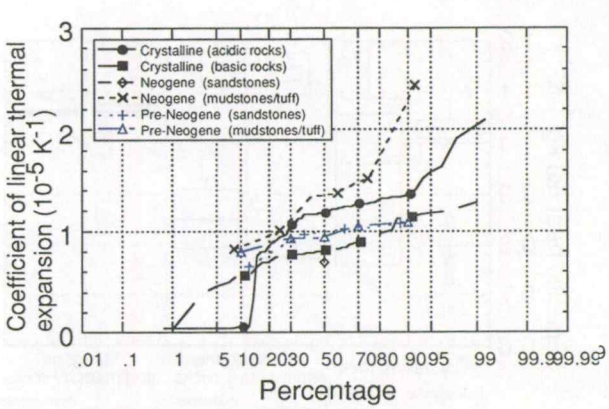


Figure 3.5-9 Probability curve of coefficient of linear thermal expansion

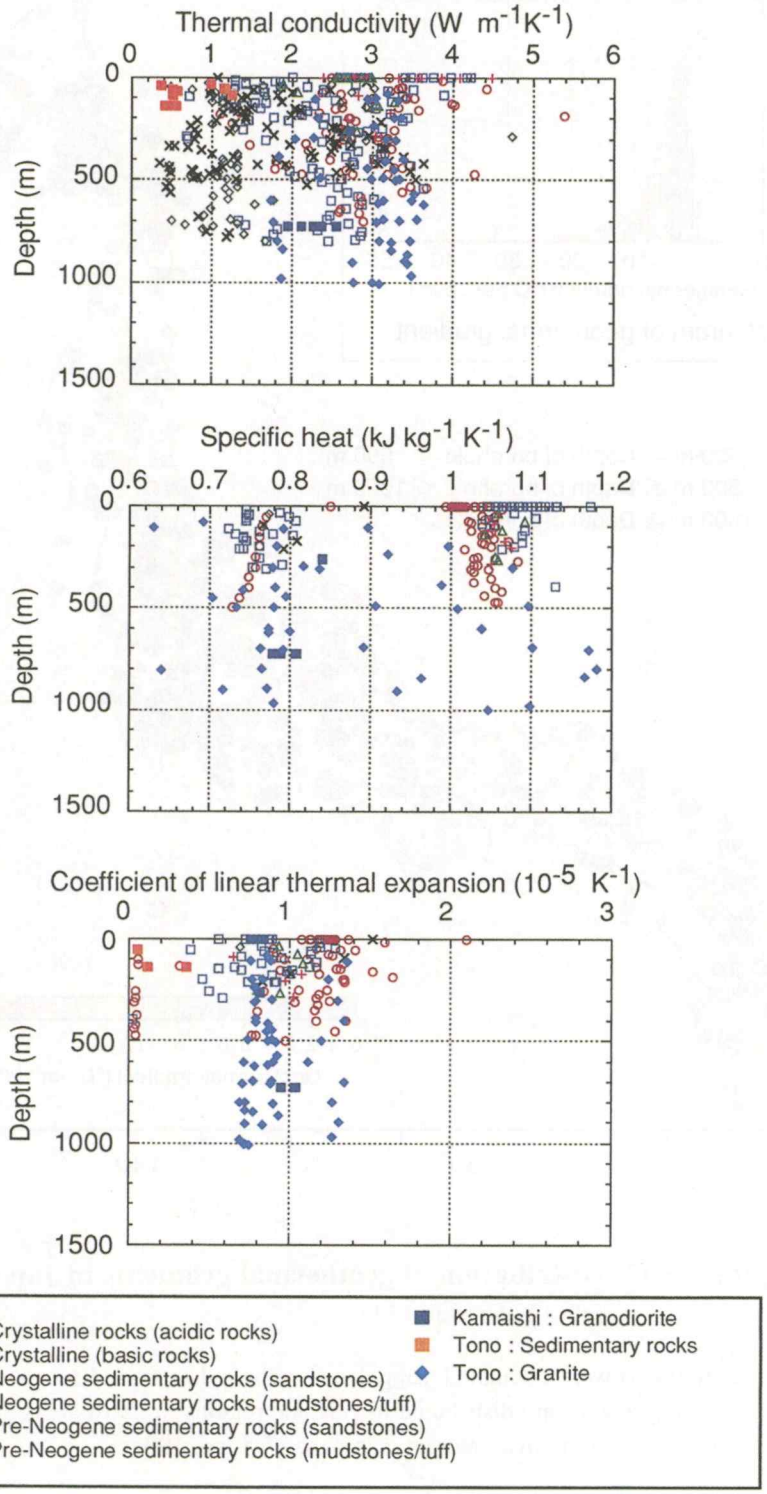


Figure 3.5-10 Correlation between depth and thermal properties

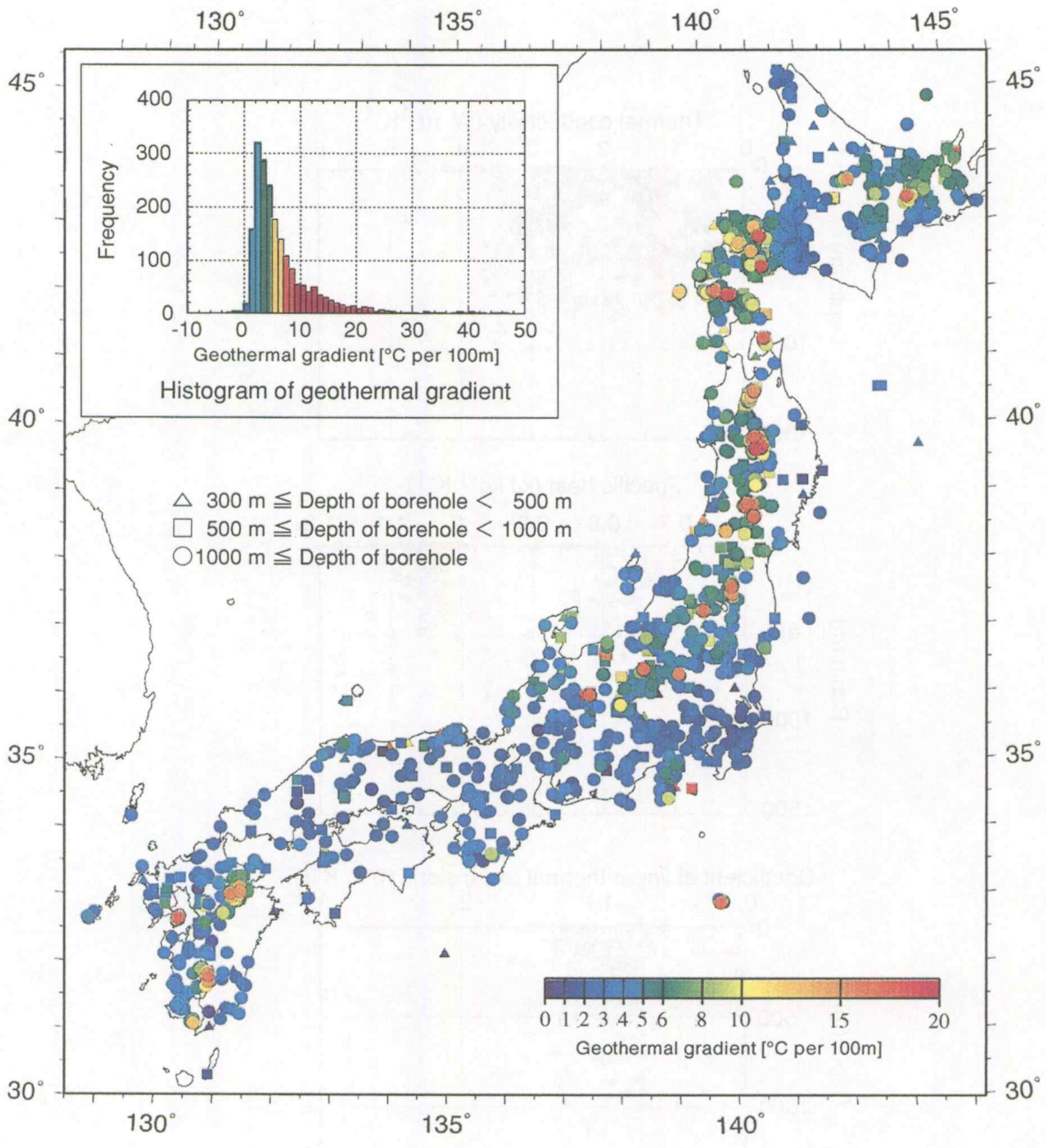


Figure 3.5-11 Distribution of geothermal gradients in Japan

(after Yano et al.,1999)

Geothermal gradients were calculated using deep borehole data from throughout Japan. High geothermal gradients are distributed in volcanic regions. In most areas excluding volcanic regions, the geothermal gradient is less than 5°C per 100m.

coincidence of high gradient areas (> 10°C per 100m) with areas of Quaternary volcanism (see Section 2.4). Many of the high gradient areas are distributed along the volcanic front, whereas none are found in the vicinity of large Quaternary volcanoes on the back-arc side of Japan (Japan Sea side). Intermediate gradient areas (> 5°C per 100m) are widely distributed in northeast Japan, but are limited to a few areas in southwest Japan. Relatively high geothermal gradients in the Kii peninsula, Dogo hot springs, Joban coalfield, Arima hot springs and Nagashima hot springs are located distant from the Quaternary volcanic areas (Figure 3.5-11).

3.5.2 Mechanical properties of the rock mass at depth

In literature surveys (Sato et al., 1992a) for the H3 report, ranges of mechanical properties, such as unconfined compressive strengths and static elastic coefficients, were examined for several rock types. In addition, data obtained from subsequent literature surveys and experimental studies at Kamaishi and Tono have been included for H12. The statistics of mechanical properties have been determined for six rock types, namely crystalline rocks (acidic and basic), Neogene sedimentary rocks (sandstones and mudstones/tuff) and Pre-Neogene sedimentary rocks (sandstones and mudstones/tuff) (Table 3.5-1). The data from Kamaishi and Tono are sub-divided into those for crystalline rocks (acidic rock) and for Neogene sedimentary rocks (mudstones/tuff), respectively (Figures 3.5-12 - 32). Differences in the measured data for sandstones and mudstones in the Tono area are so small that they can be compared directly with the far more numerous published data for the Neogene sedimentary rocks (mudstones/tuff).

1) Statistical examination of physical properties

The ranges, means and medians of physical properties for individual rock types, obtained from published data, were examined by plotting histograms, box-range diagrams and probability density distributions.

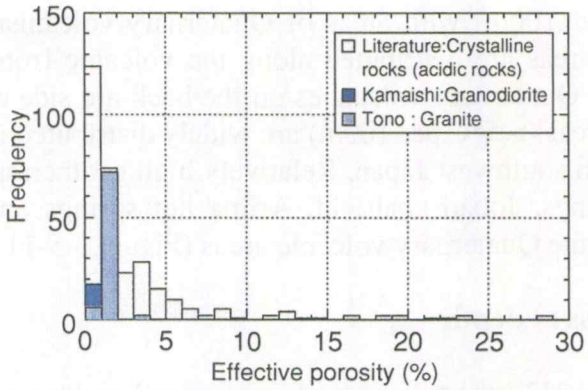
(1) Distribution of physical properties

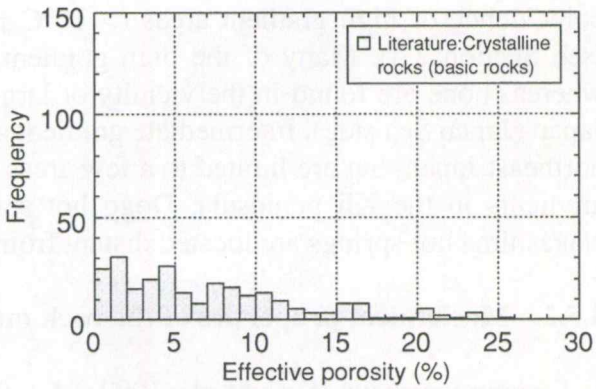
Effective porosity

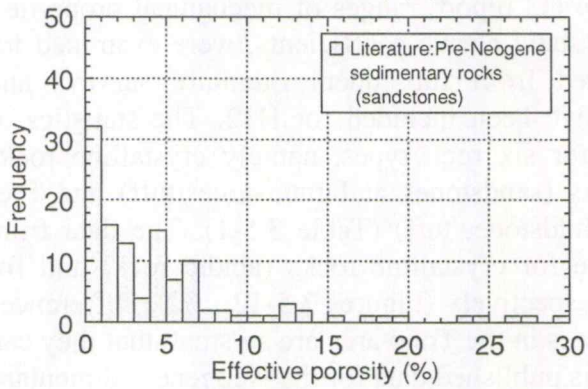
Effective porosity is closely related to thermal and mechanical properties and is one of the most important features of the rock mass. Effective porosities of crystalline rocks and Pre-Neogene sedimentary rocks are generally less than 10% and have a frequency maximum at 2% or less. In contrast, Neogene sedimentary rocks tend to show a wide range of porosities up to 60%. Porosities for the crystalline rocks at Kamaishi are less than 2%, which is identical to the frequency maximum of the published data for acidic crystalline rock. The measured porosities of the sediments at Tono range from 30 - 60%, which lie in the higher part of the porosity distribution of the published data for Neogene sedimentary rocks (mudstones/tuff) (Figures 3.5-12, 13, 14).

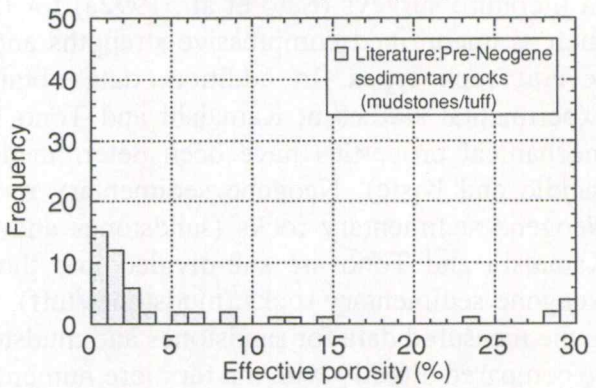
Unconfined compressive strength

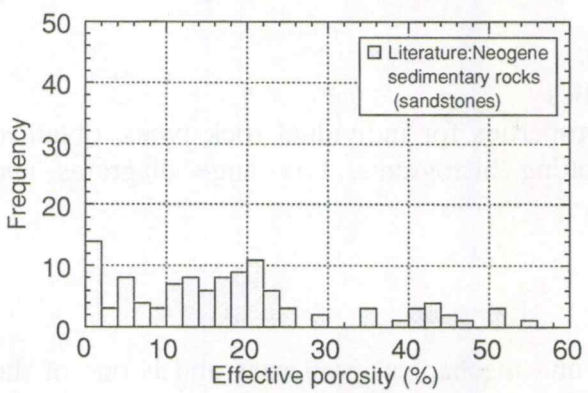
In Japan, rocks are classified into "soft" and "hard" according to their unconfined compressive strength. Rocks are classified as soft if their unconfined compressive strength is 10-20 MPa or lower and as hard if their unconfined compressive strength is higher. Crystalline rocks and Pre-Neogene sedimentary rocks are classified as hard; while a number of Neogene sedimentary rocks can be categorized as soft, their strengths range widely from soft to hard, without any distinct division between the two. The data for acidic crystalline rocks at Kamaishi have a frequency maximum that exhibits a slightly larger strength value than that of the published data, averaging some 150 MPa. Neogene sedimentary rocks at Tono are so poorly indurated that their strength values are less than 10 MPa and average 7 MPa (Figures 3.5-15, 16, 17).

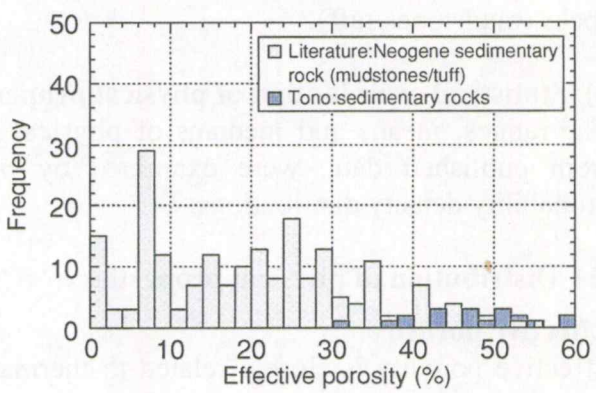












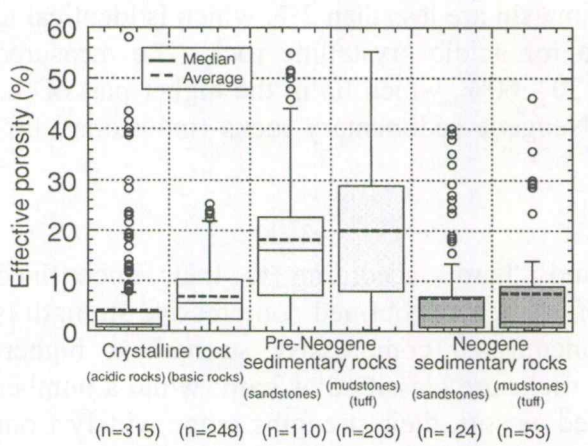


Figure 3.5-13 Distribution of effective porosity

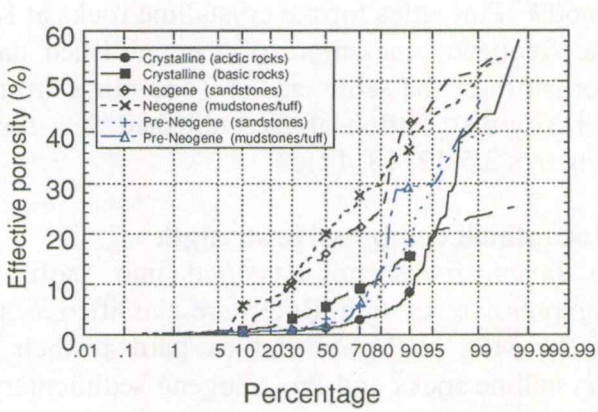


Figure 3.5-14 Probability curve of effective porosity

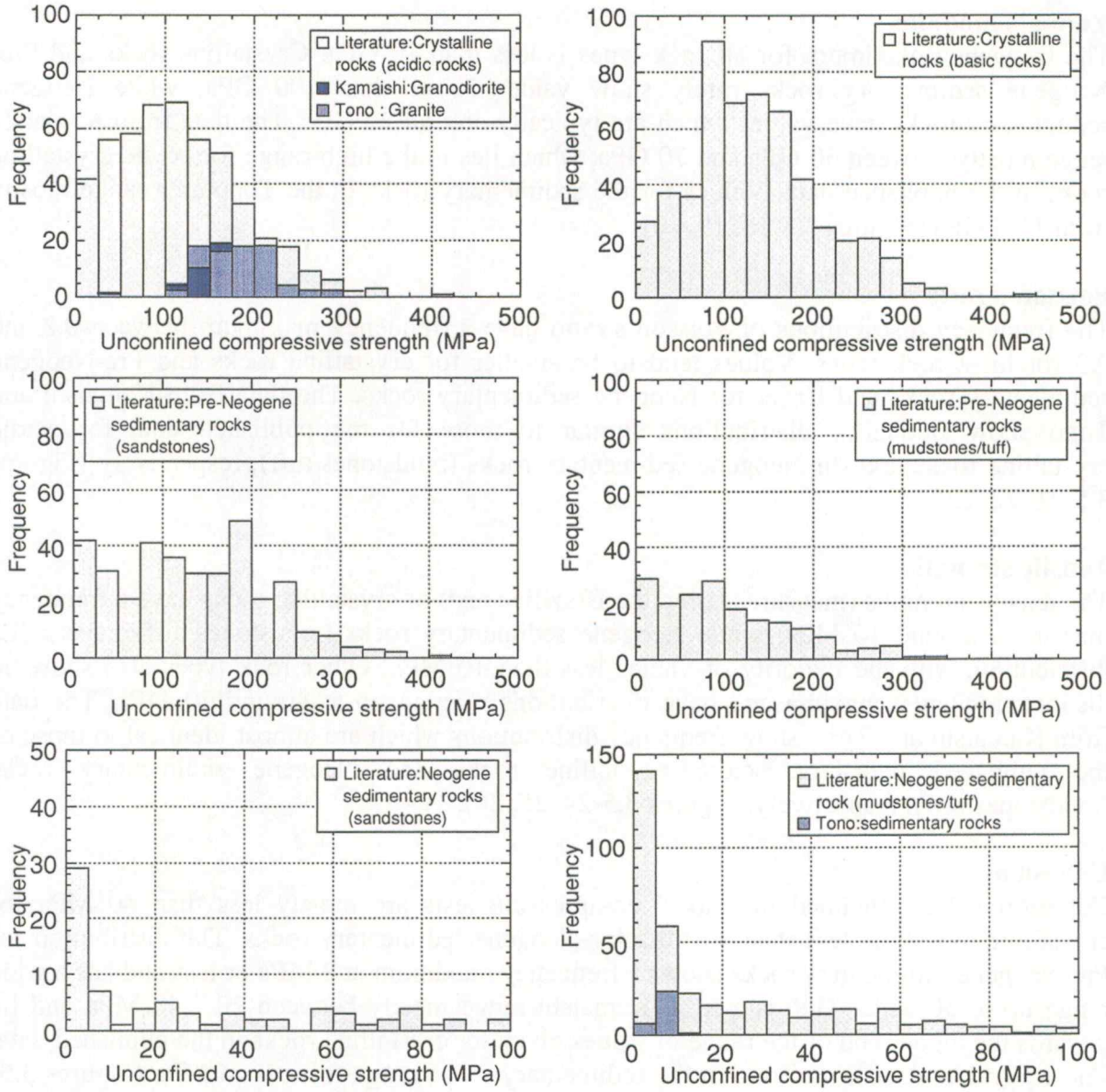


Figure 3.5-15 Histograms showing unconfined compressive strength

Literature data are mainly based on Sato et al. (1999).

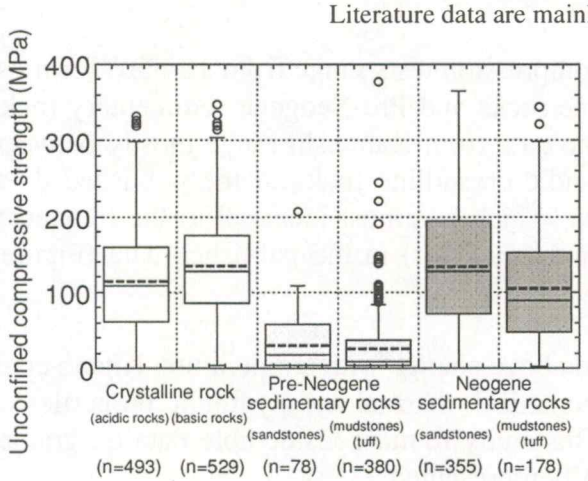


Figure 3.5-16 Distribution of unconfined compressive strength

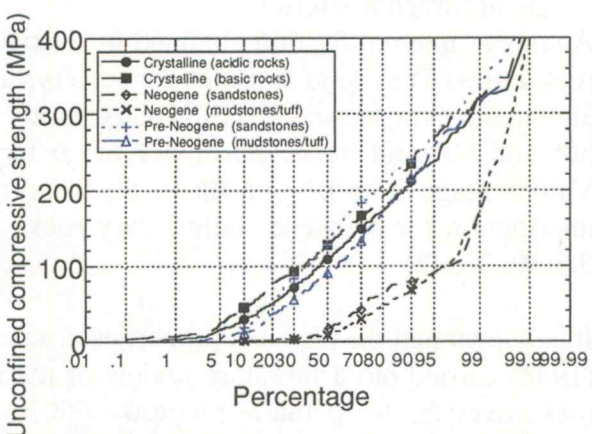


Figure 3.5-17 Probability curve of unconfined compressive strength

Young's modulus
The frequency maximum for all rock types is less than 10 GPa. Crystalline rocks and Pre-Neogene sedimentary rocks rarely show values larger than 100 GPa, while Neogene sedimentary rocks have values which are typically around 20 GPa. The data from Kamaishi range mostly between 50 GPa and 70 GPa, which lies in the high range for acidic crystalline rocks in the published data. Values for the sedimentary rocks in the Tono area range mostly from 1 - 4 GPa (Figures 3.5-18, 19, 20).

Poisson's ratio
The frequency distributions of Poisson's ratio have a frequency maximum between 0.2 and 0.3 for most rock types. Values tend to be smaller for crystalline rocks and Pre-Neogene sedimentary rocks and larger for Neogene sedimentary rocks. The data from Kamaishi and Tono show frequency distributions similar to those for the published data for acidic crystalline rocks and for Neogene sedimentary rocks (mudstones/tuff), respectively (Figures 3.5-21, 22, 23).

Tensile strength
The tensile strengths (measured using the Brazilian test) of crystalline rocks have a frequency maximum around 10 MPa, while Neogene sedimentary rocks (mudstones/tuff) have a flat distribution, with the majority of values less than 10 MPa. Other rock types also show no distinct frequency maxima and have distributions ranging up to around 20 MPa. The data from Kamaishi and Tono show frequency distributions which are almost identical to those of the published data for acidic crystalline rocks and Neogene sedimentary rocks (mudstones/tuff), respectively (Figures 3.5-24, 25, 26).

Cohesion
Cohesion values obtained in triaxial compression tests are mostly less than 40 MPa for crystalline rocks and less than 10 MPa for Neogene sedimentary rocks. The distribution for Pre-Neogene sedimentary rocks shows a frequency maximum at 2 MPa or less and has a wide range up to 50 MPa. The data from Kamaishi range mostly between 20 - 40 MPa and lie towards the higher end of the range of values given for crystalline rocks in the published data. The equivalent data from Tono in the sedimentary rocks range from 1 - 4 MPa (Figures 3.5-27, 28, 29).

Angle of internal friction
Angles of internal friction obtained in triaxial compression tests range from 10 - 50° for most rock types. They tend to be larger for crystalline rocks and Pre-Neogene sedimentary rocks and smaller for Neogene sedimentary rocks. The data from Kamaishi range mostly between 50° and 60° and lie in the higher range for acidic crystalline rocks in the published data. Values range from 0° and 30° in the Tono area, which is almost identical to the frequency distribution for Neogene sedimentary rocks (mudstones/tuff) in the published data (Figures 3.5-30, 31, 32).

It is known that the physical properties discussed above change with temperature. Kitano et al. (1988) carried out a literature review of the mechanical, thermal and hydraulic properties of rocks over the temperature range 0 - 600°C. This study found considerable data on granite and andesite, whereas other rock types were poorly represented.

The temperature in the rock mass adjacent to the EBS is estimated to be less than 100°C. At 100°C and atmospheric pressure, it is thought that rock properties are likely to be between 10% and 20% different from those at ambient temperature. However, there were insufficient

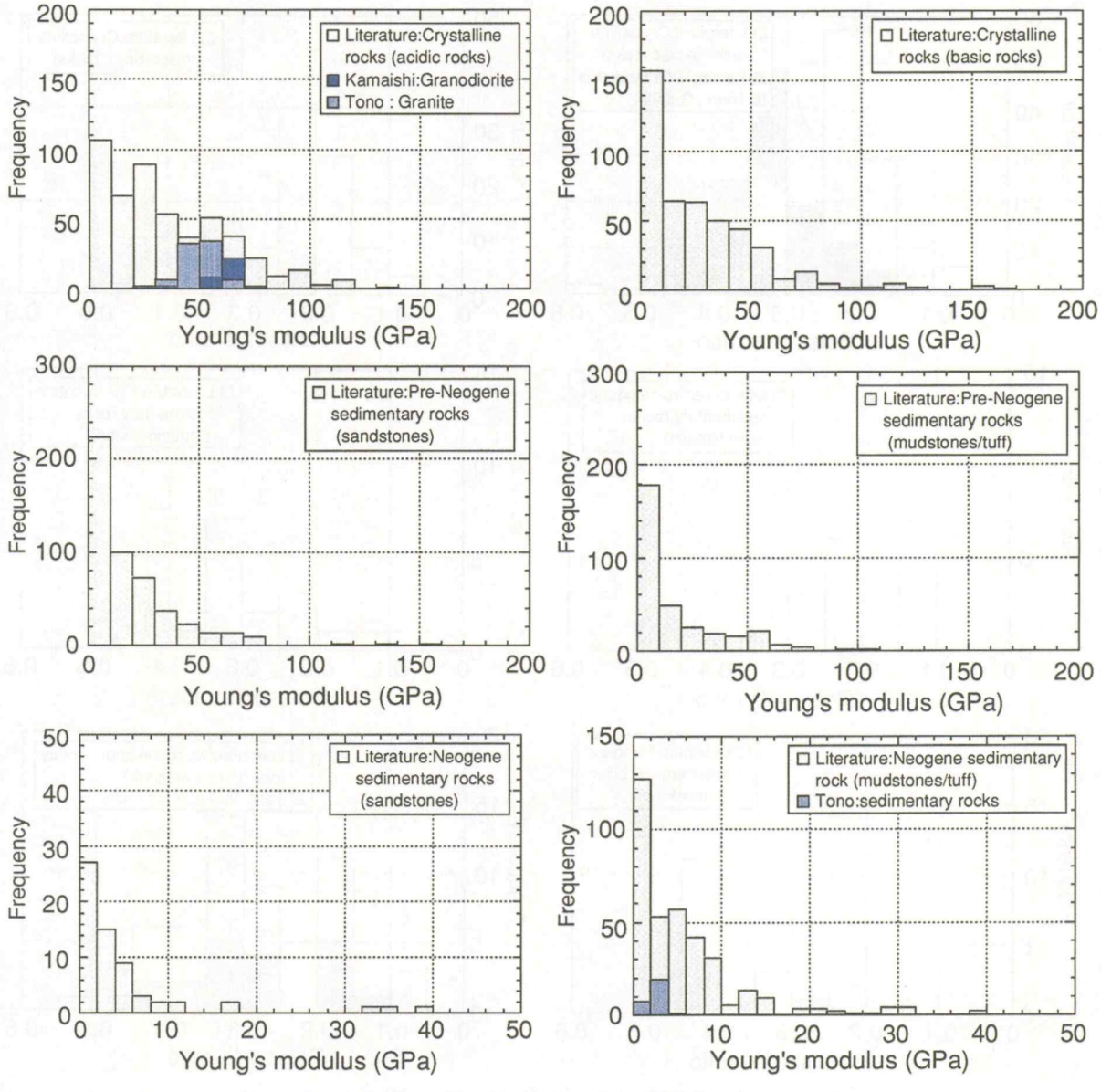


Figure 3.5-18 Histograms showing Young's modulus

Literature data are mainly based on Sato et al. (1999).

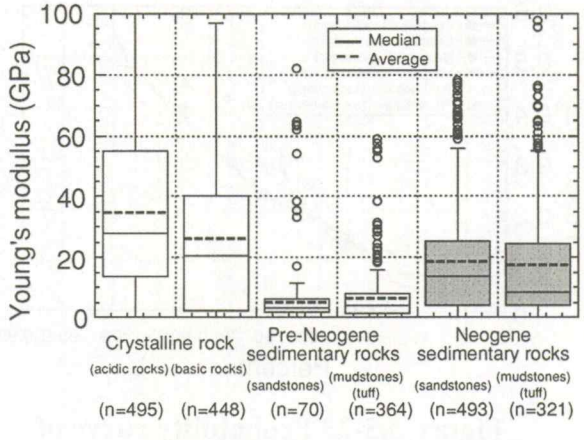


Figure 3.5-19 Distribution of Young's modulus

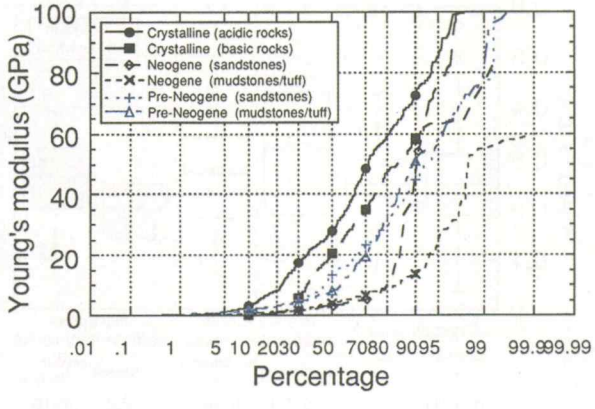


Figure 3.5-20 Probability curve of Young's modulus

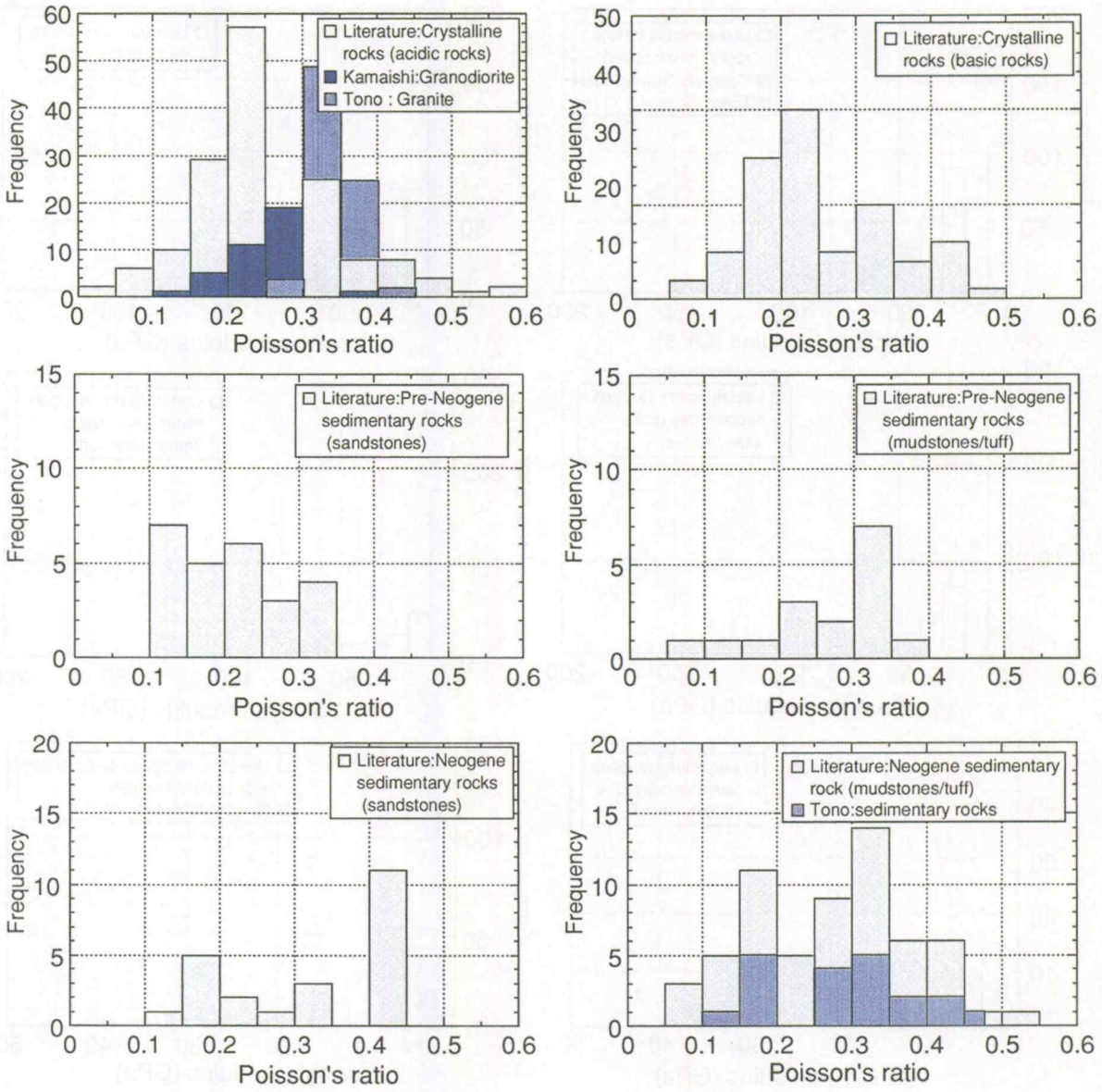


Figure 3.5-21 Histograms showing Poisson's ratio

Literature data are mainly based on Sato et al. (1999).

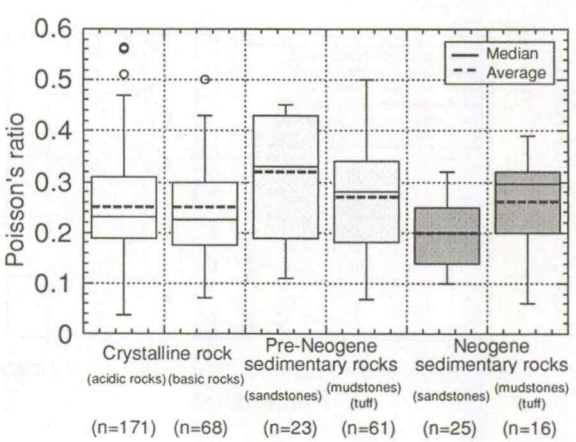


Figure 3.5-22 Distribution of Poisson's ratio

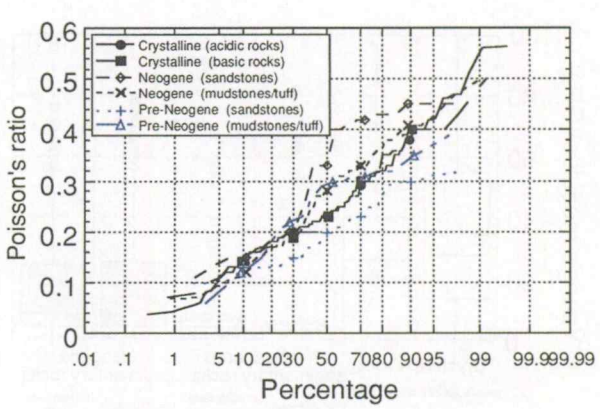


Figure 3.5-23 Probability curve of Poisson's ratio

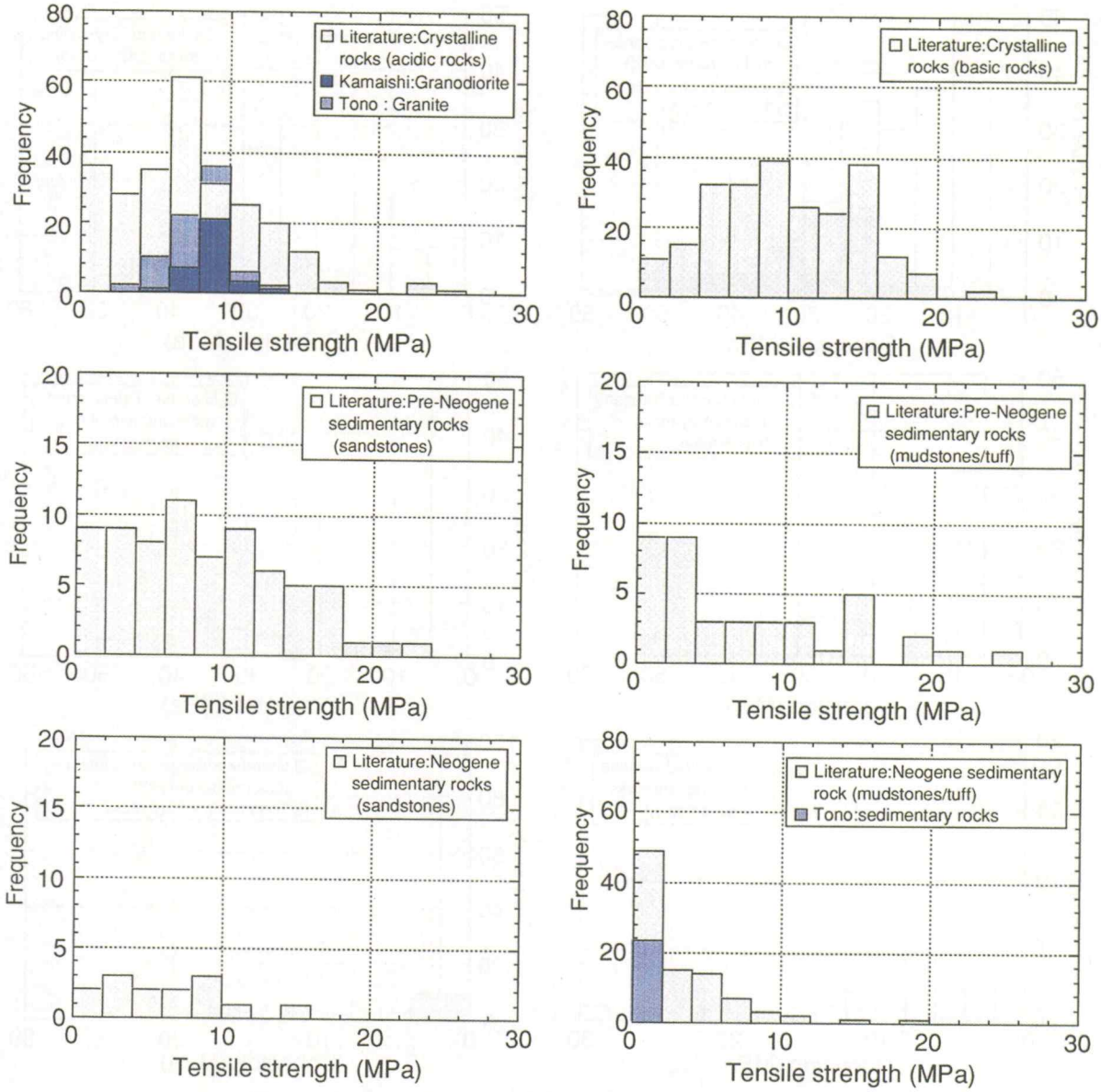


Figure 3.5-24 Histograms showing tensile strength

Literature data are mainly based on Sato et al. (1999).

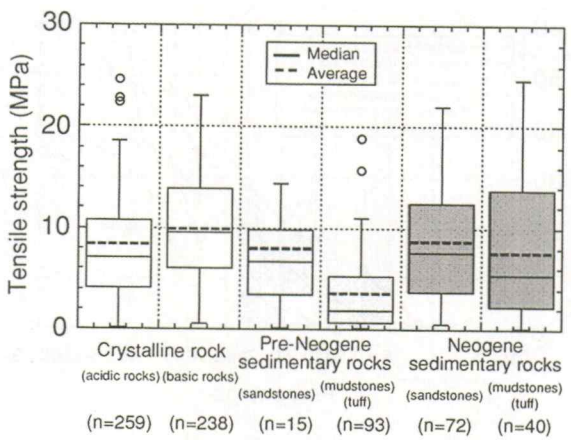


Figure 3.5-25 Distribution of tensile strength

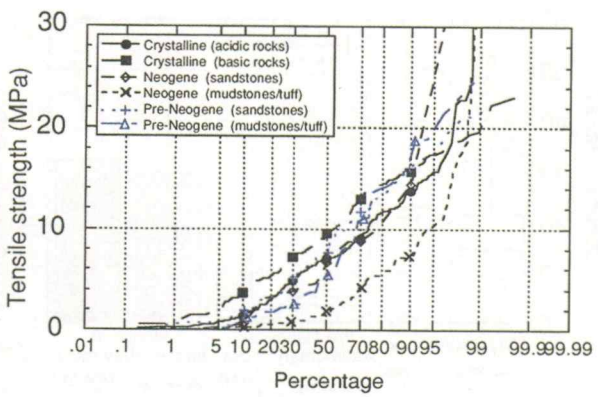


Figure 3.5-26 Probability curve of tensile strength

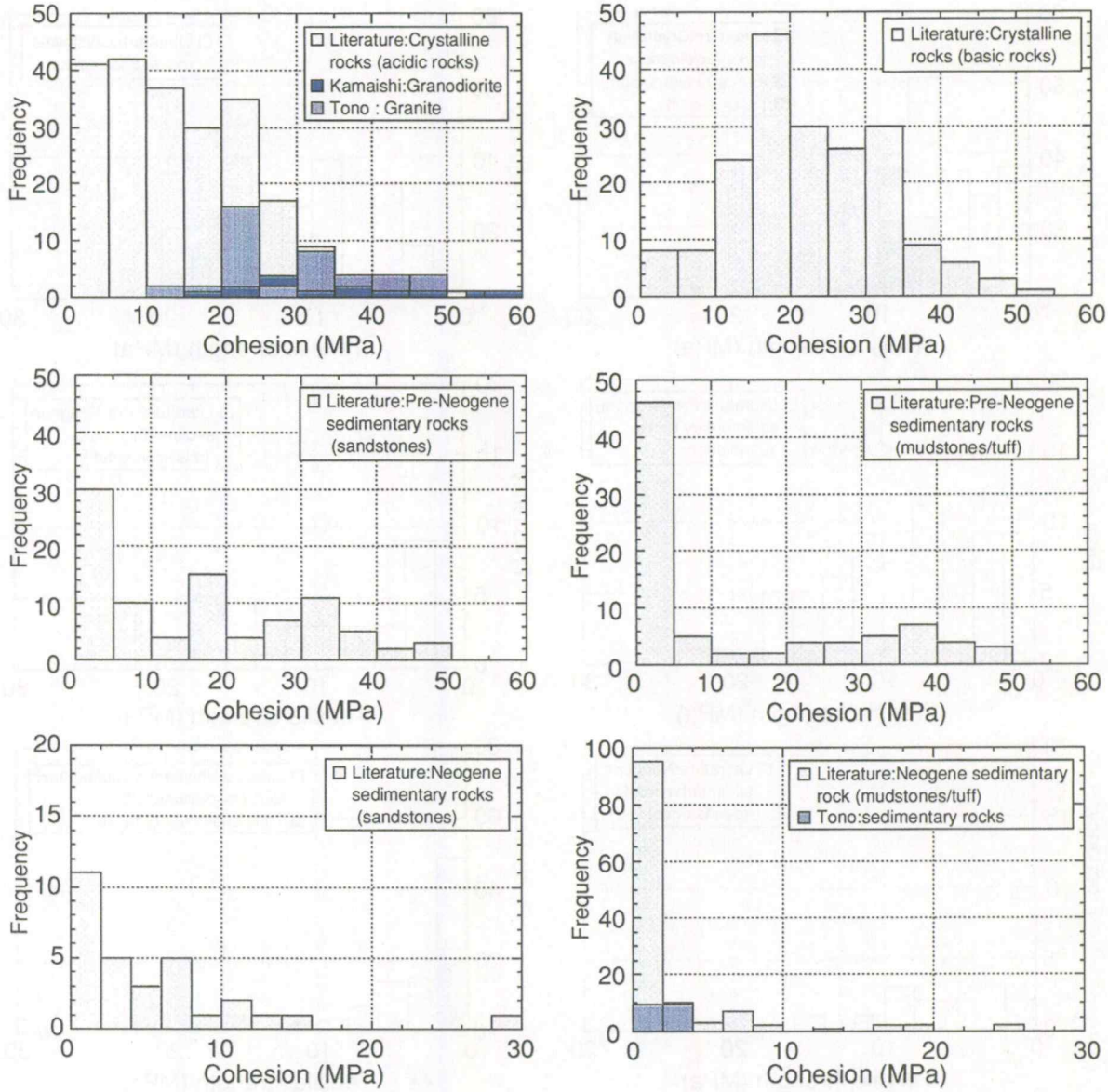


Figure 3.5-27 Histograms showing cohesion

Literature data are mainly based on Sato et al. (1999).

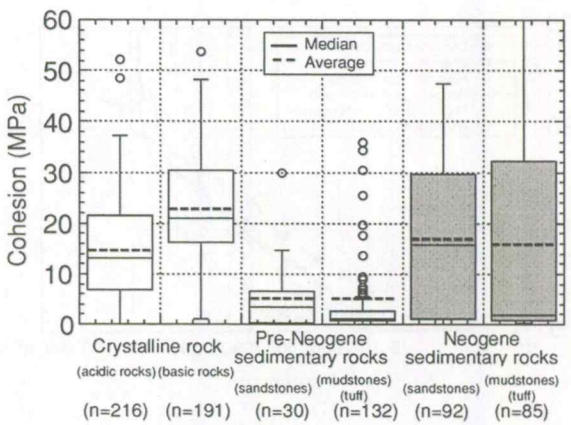


Figure 3.5-28 Distribution of cohesion

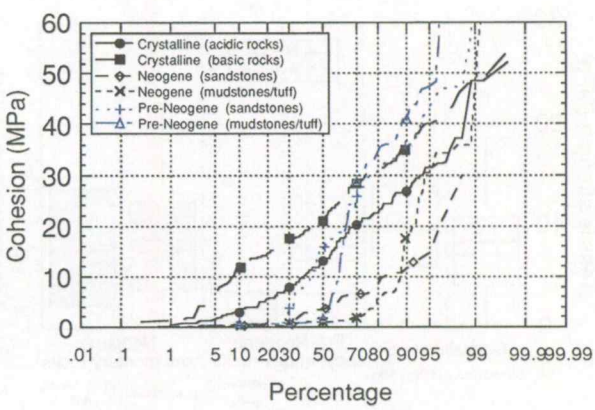


Figure 3.5-29 Probability curve of cohesion

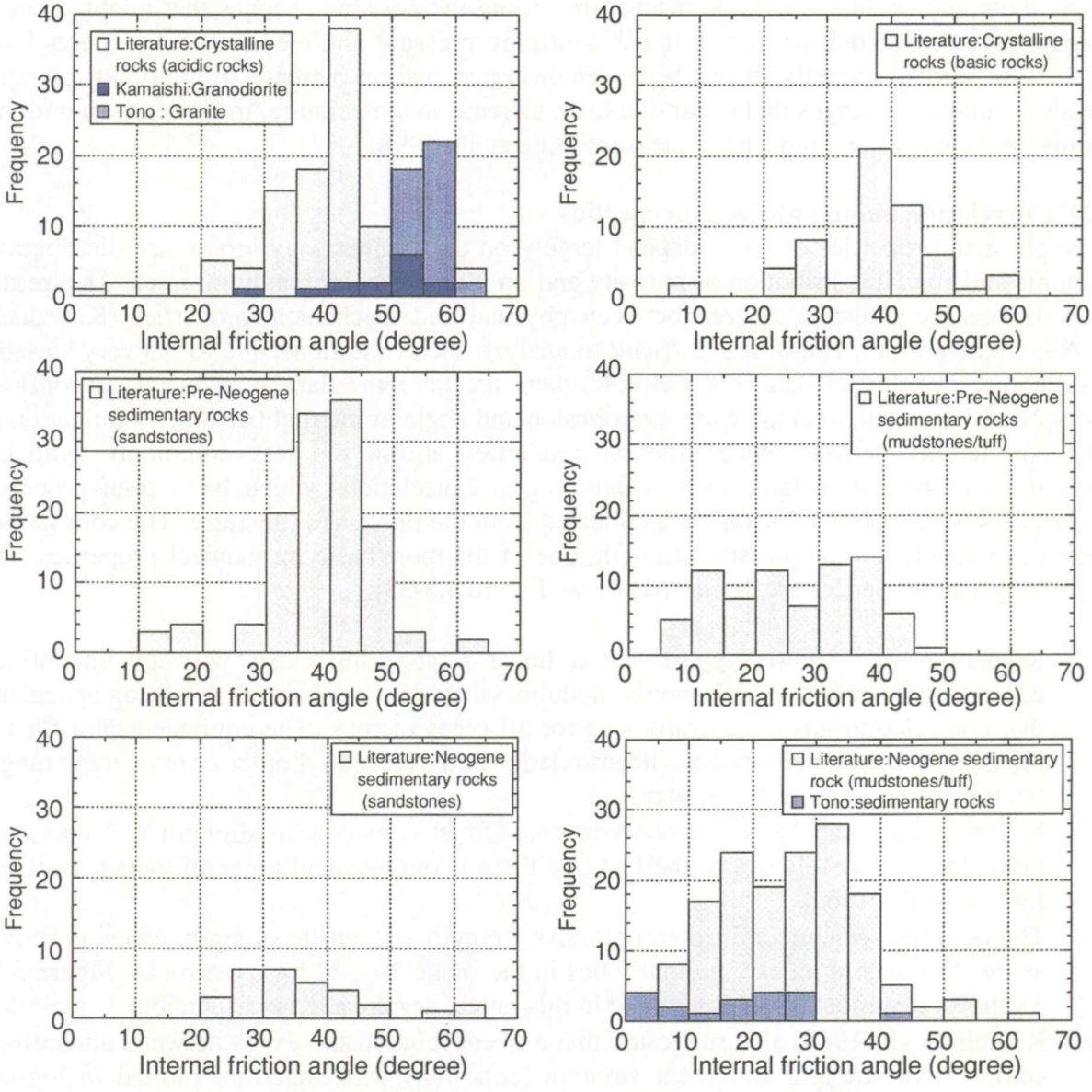


Figure 3.5-30 Histograms showing internal friction angle

Literature data are mainly based on Sato et al. (1999).

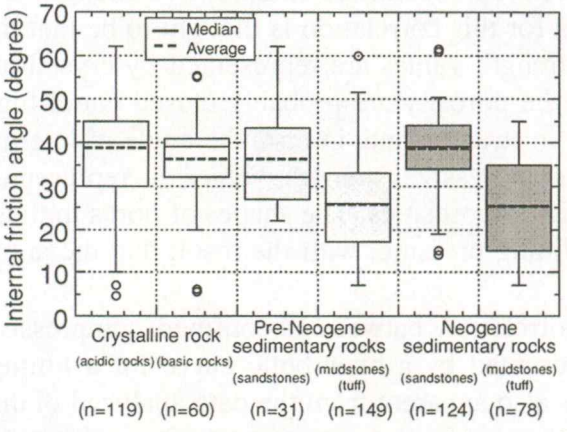


Figure 3.5-31 Distribution of internal friction angle

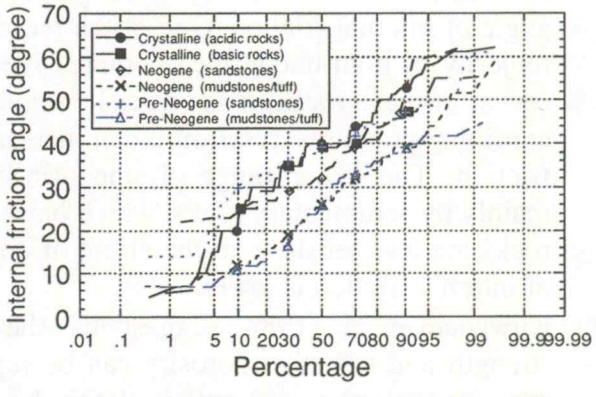


Figure 3.5-32 Probability curve of internal friction angle

data allow any conclusions to be reached regarding the possible changes that might occur at higher pressures. Rock properties under confining pressure and elevated temperatures have also been studied recently. It has been demonstrated that an increase in confining pressure tends to limit the changes that occur due to an increase in temperature, in comparison with the equivalent changes at atmospheric pressure (Kita et al., 1998)

(2) Correlation among physical properties

The physical properties of rocks depend largely on their mineralogy, grain size distribution, volume and spatial distribution of porosity and on interparticular bonding forces. As a result, correlations are often recognized between physical and mechanical properties (Kuwahara, 1984; Kikuchi et al., 1984). It is difficult to analyze such conditions, due to the very variable availability of relevant data. For example, there are far more data available on unconfined compressive strength than there are for cohesion and angle of internal friction. Examination of the correlations between such physical properties allows the less commonly available properties to be extrapolated over wider ranges. Correlations which have been proposed previously were examined using data collected from the published literature. The correlations between unconfined compressive strength, one of the most basic mechanical properties, and other physical properties are discussed below (Figure 3.5-33):

i. Kikuchi et al. (1984) suggest that a linear relationship exists between unconfined compressive strength and Young's modulus when data are plotted in log-log space and that this relationship is generally true for all types of rock. The equivalent plot for the rocks investigated here shows a linear relationship over a 3 - 4 order of magnitude range, but with a large associated scatter.
ii. No correlation can be found between unconfined compressive strength and Poisson's ratio. This is possibly due to the fact that there is only a small range of values available for Poisson's ratio.
iii. The ratio between unconfined compressive strength and tensile strength, which is known as the "brittleness index", normally lies in the range 10 - 20 for most rocks. Figure 3.5-33 shows that most of the data do lie in this range, despite a large dispersion.
iv. Kikuchi et al. (1984) also suggested that a linear relationship exists between unconfined compressive strength and shear strength (cohesion) when data are plotted in log-log space and that this relationship is generally valid for all rock types in dry conditions. The equivalent plot for the rocks investigated here shows a linear relationship over a 3 - 4 order of magnitude range, but with a large associated scatter.
v. A weak positive correlation is recognized between unconfined compressive strength and angle of internal friction. One of the reasons for this correlation is thought to be that the majority of high unconfined compressive strength values are represented by crystalline rocks. In these rocks, microcracks forming the porosity are probably closed under high confining pressures, resulting in an increase in strength and, in turn, the angle of internal friction. The lower range of unconfined compressive strength values is represented mainly by sedimentary rocks, which have higher porosities. The shapes of pores in these rocks are less sensitive to the effect of confining pressure, with the result that the angle of internal friction is lower.
vi. Kuwahara et al. (1984) suggest that the correlation between unconfined compressive strength and effective porosity can be represented by a hyperbolic curve for a limited range of rock types. A similar relationship is also apparent from the data analyzed in this study.

(3) Dependence of physical properties on depth

If values for mechanical properties for the complete range of rock types are plotted against

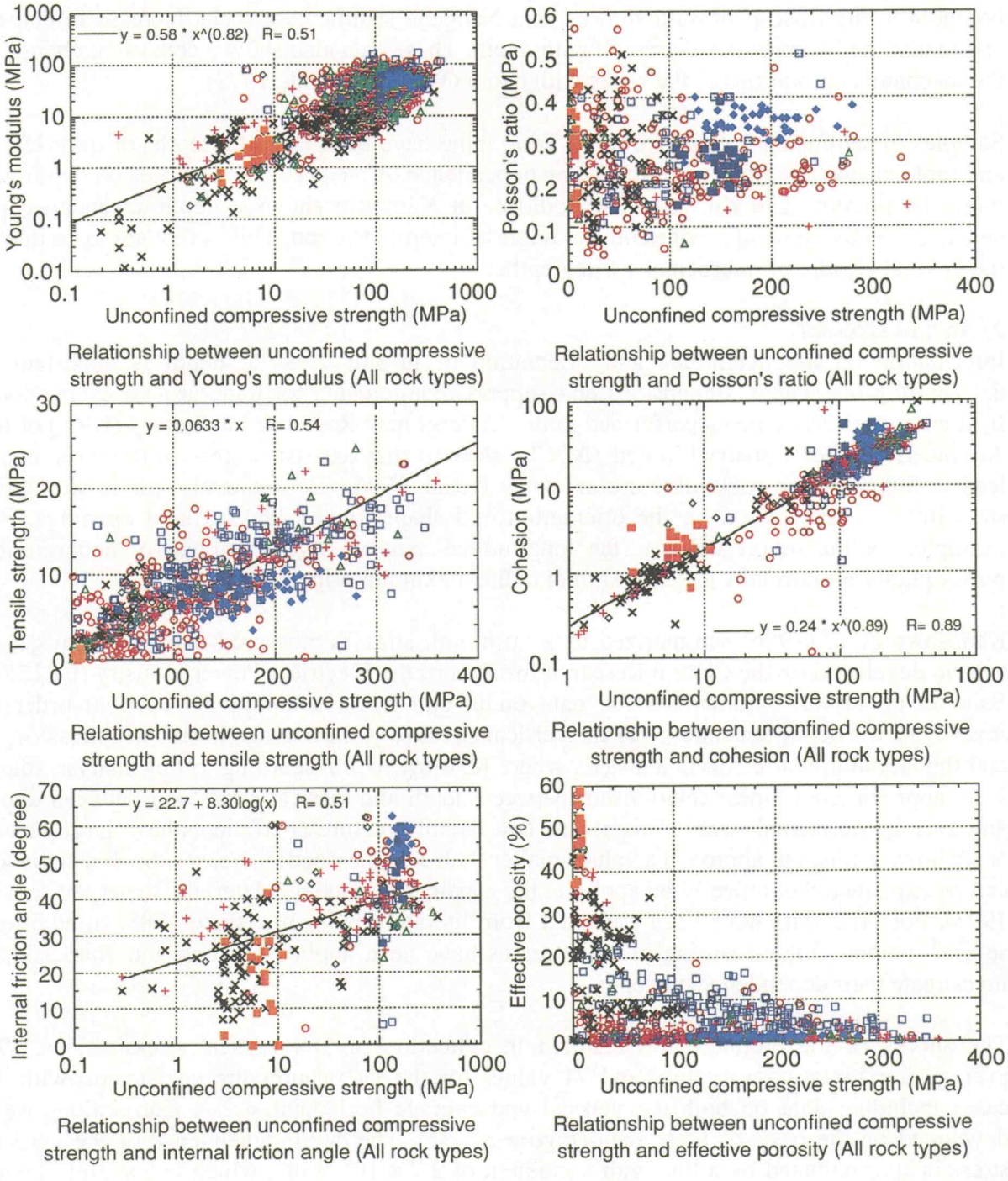


Figure 3.5-33 Relationship between unconfined compressive strength and other properties

depth (Figure 3.5-34), there is a considerable scatter and it is difficult to find any depth-dependent relationship. Laboratory testing of cores from depths of 300 to 1200 m in a borehole in the Boso peninsula showed that Neogene sedimentary rocks increase in density and unconfined compressive strength with depth. These data also show a consistent change in the mechanical properties of the rocks with depth (Watanabe et al., 1992).

Samples of sedimentary rocks from the Tono mine have been taken to depths of only 150 m and rapid changes in lithofacies mask any dependence of mechanical properties on depth that might be present. The Kurihashi Granodiorite at Kamaishi shows a depth-dependence for density, effective porosity, cohesion and angle of internal friction. This is thought to be due to the gradual closure of microcracks with depth.

2) In situ stresses

Information on the magnitude and orientation of in situ stress at depth is important in determining the shapes, dimensions and support requirements for underground excavations. In situ stress measurements performed in the Underground Research Laboratory (URL) of the Atomic Energy of Canada Limited (AECL) showed that excessive stress differences could lead to failure of the rock mass around drifts (Read, 1996). Consequently, the in situ stress state imposes restrictions on the orientation and shape of any underground openings. For example, for maximum stability, the longitudinal axis of large openings for underground power plants are normally aligned parallel to the maximum principal stress.

Kanagawa et al. (1986) summarized data on in situ stresses measured using a strain gauge system developed by the Central Research Institute of the Electrical Power Industry (CRIEPI). Saito et al. (1988) summarized the data on in situ stress acquired in Japan in order to investigate the depth-dependence of the vertical stress (σ_v), the average horizontal stress (σ_{hAv}) and the lateral pressure coefficients (K_o where $K_o = \sigma_{hAv}/\sigma_v$). According to this analysis, there is an approximately linear relationship between depth and vertical stress and between depth and average horizontal stress. This means that lateral pressure coefficients have large values at shallow depths, but approach a value smaller than 1 as the depth increases. Such a tendency can be explained theoretically by applying the elastic shell model (Materials Society of Japan, 1993). For H12, data have been collected from literature published since 1988. In addition, several methods for measuring in situ stresses have been applied at Tono and Kamaishi to investigate their dependence on depth.

The survey of the literature has resulted in collection of 108 vertical stress values, 178 average horizontal stress values and 71 values for the lateral pressure coefficient, with 49 cases including data on both the vertical and average horizontal stress. Correlations were developed on the basis of these data (Figure 3.5-35). The depth-dependence of the vertical stress is approximated by a line with a gradient of 2.7×10^4 N m^{-3}, which is a slightly larger than that obtained by Saito et al. (1988); a similar situation also exists for the relationship between depth and average horizontal stress. Lateral pressure coefficients are calculated from the relationship between the vertical stress and the average horizontal stress and, as a result, they decrease with depth to approach a value of less than 1 as indicated by Saito et al. (1988). The results from Tono and Kamaishi are also included in these figures and indicate tendencies similar to those of the published data.

Several techniques were used to measure in situ stresses in the No. 2 shaft and the NATM (New Austrian Tunneling Method) drift and in the vertical boreholes drilled from ground surface in the Tono area, as well as in the various levels at the Kamaishi mine (Maeda et al., 1999; Matsui et al., 1997; Sato et al., 1998a). The different rock types at Tono and Kamaishi

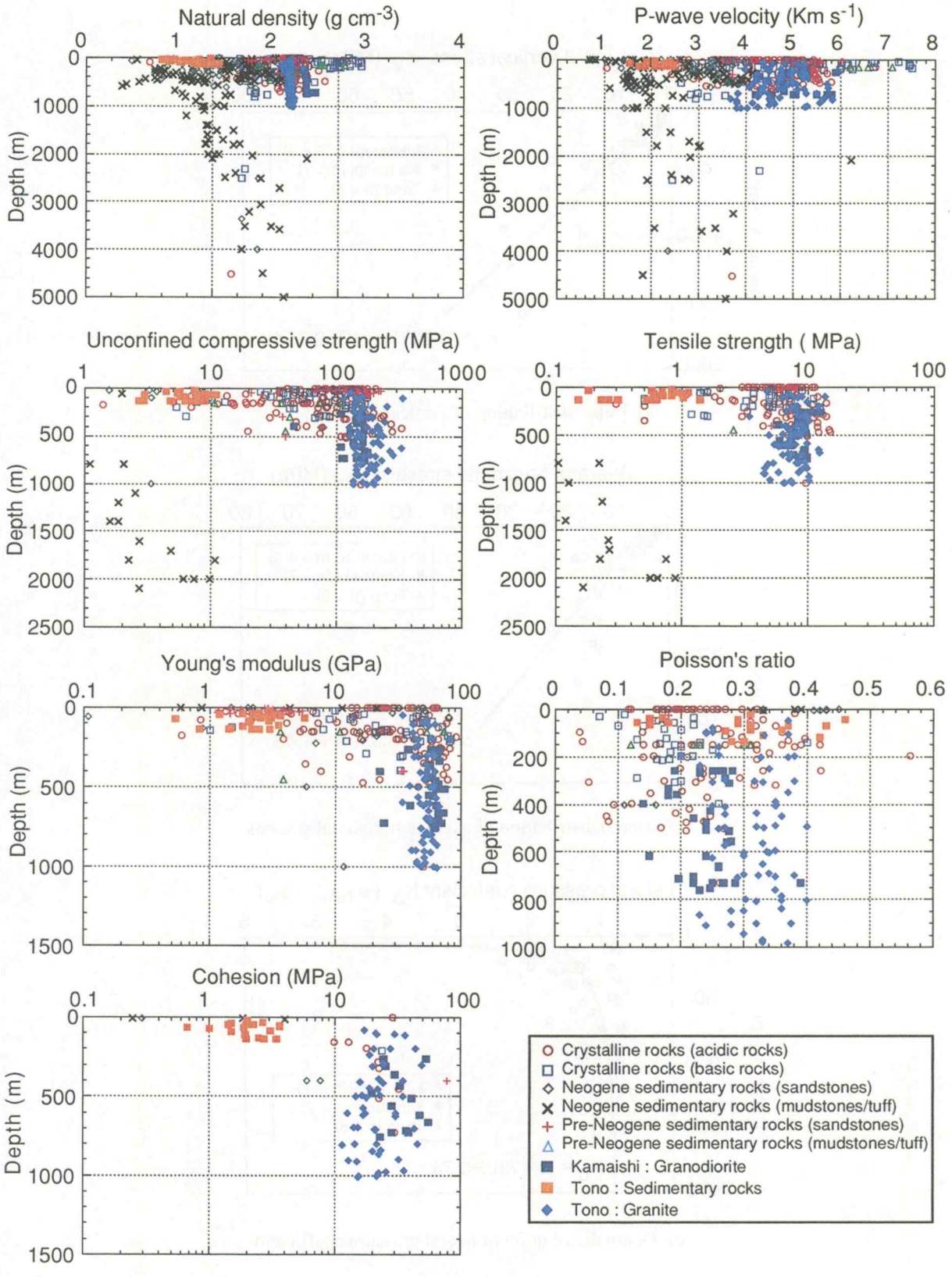
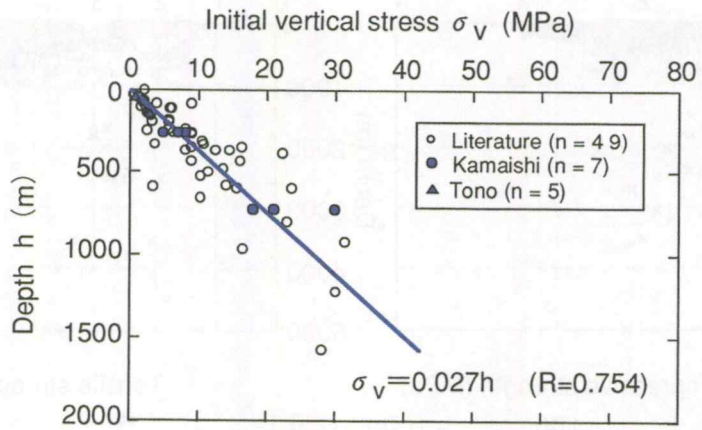
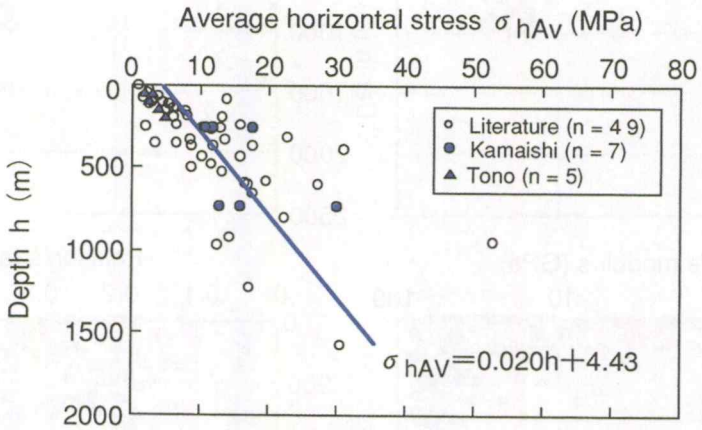


Figure 3.5-34 Correlation between depth and rock physical properties

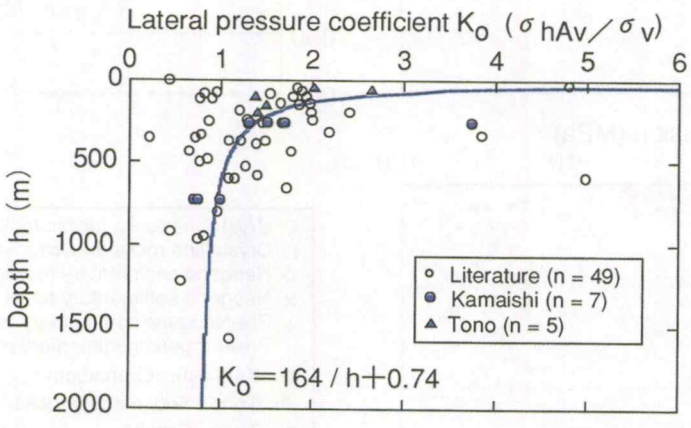
Natural density and unconfined compressive strength of Neogene sedimentary rocks have a tendency to increase with depth.



a) Depth distribution of vertical stresses



b) Depth distribution of average horizontal stresses



c) Depth distribution of lateral pressure coefficient

Figure 3.5-35 Distribution of initial stress as a function of depth

Literature data are mainly based on Saito et al. (1988). Only the data which included both vertical and horizontal stresses are plotted.

meant that different techniques had to be used at these sites. The overcoring method (using the CRIEPI 8 element strain gauge system), the hydraulic fracturing method, the double fracturing method and the AE (Acoustic Emission) method were applied in the Tono area. Investigations at Kamaishi used the hemispherical-ended borehole technique, the hydraulic fracturing method, the AE (Acoustic Emission) method, the DRA (Deformation Rate Analysis) method and the DSCA (Differential Strain Curve Analysis) method. The results of these measurements for two locations at Tono and Kamaishi are shown in Figures 3.5-36 and 3.5-37.

The results for Tono show that the minimum principal stress is equal to or less than the overburden pressure and the maximum principal stress is less than twice the minimum principal stress. The orientation of the maximum principal stress does not coincide with the WNW-ESE direction of compression estimated from plate movement, the distribution of active faults and the results of land surveying and shallow earthquake solutions. Instead, the orientation of the maximum principal stress is determined rather by the orientation and location of local faults and by the topography.

At the Kamaishi mine, the intermediate and minimum principal stresses are approximately equal to the overburden stress and the maximum principal stress is approximately twice as large. The maximum principal stress is oriented N-S and normal to the E-W compression due to plate movement. This difference is assumed to be due to the distribution of fractures around the measurement point.

The magnitudes and orientations of the principal stresses obtained using different methods are not the same at either Kamaishi or at Tono. The reasons for this are assumed to be that:

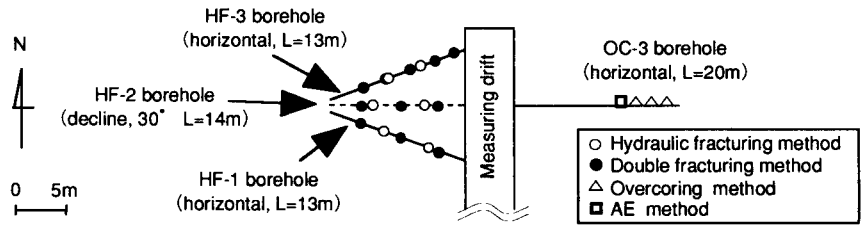
- there are differences in the stress state and the distribution of fractures across the volume of rock for which stress measurements have been made (e.g. Figures 3.5-36 and 3.5-37);
- there are differences in the assumptions used to calculate the in situ stresses using these various techniques;
- the various measurement methods determine the stress state over different volumes of the rock mass.

A detailed comparison of these methods should be carried out to allow the most appropriate stress values to be quoted.

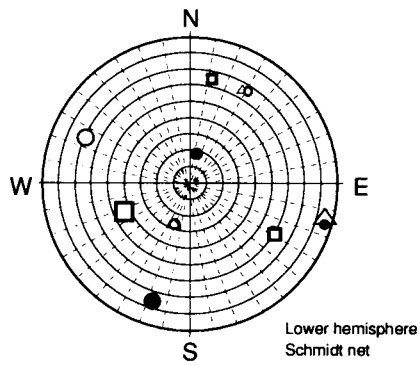
3) Time-dependent behavior of the rock mass

In common with a number of other materials, rocks undergo creep, so that, under a constantly applied stress, strain will increase with time (Cristescu and Hunsche, 1998). In a situation where the strain stays constant, the applied stress is seen to decrease with time, a process that is known as stress relaxation. The evaluation of the long-term stability of underground openings requires an understanding of such time-dependent rock behavior. Creep of the rock mass is expected to occur depending on the depth, the shape of the underground openings and the mechanical properties of the rock mass. In some cases, it might be necessary to take account of rock creep in the design of the overpack and buffer materials to be used in a HLW repository.

Laboratory tests on rock creep have been carried out over the past few decades. These tests have shown primary creep to take place, the rate of which is given by a logarithmic creep law. While a considerable amount of information on secondary creep (or steady-state creep) has been accumulated, reports on what is known as tertiary creep are limited. Yamashita et al.



a) Layout and measuring point (Plane section)

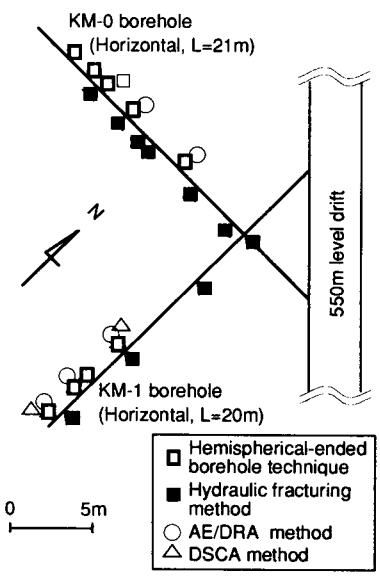


b) Direction of principal stresses

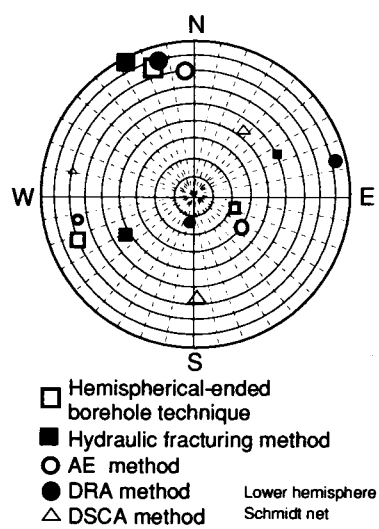
Method		Stress (MPa)
Hydraulic fracturing method △	σ_1	1.84±0.41
	σ_2	1.49±0.33
	σ_3	0.91±0.34
Double fracturing method ●	σ_1	1.40±0.01
	σ_2	1.05±0.01
	σ_3	0.78±0.01
Over-coring method ○	σ_1	0.96
	σ_2	0.85
	σ_3	0.76
AE method □	σ_1	0.48
	σ_2	0.37
	σ_3	0.29

c) Principal stresses

Figure 3.5-36 Layout and result of initial stress measurements at the Tono mine



a) Layout (Plane section)



b) Direction of principal stresses

Method		Stresses (MPa)
Hemispherical-ended borehole technique	σ_1	29.9
	σ_2	7.8
	σ_3	3.0
	σ_v	4.8
Hydraulic fracturing method	σ_1	17.4
	σ_2	8.7
	σ_3	4.5
	σ_v	7.0
AE method	σ_1	15.6
	σ_2	7.6
	σ_3	5.6
	σ_v	7.0
DRA method	σ_1	15.5
	σ_2	7.7
	σ_3	6.3
	σ_v	8.1

c) Principal stresses

Figure 3.5-37 Layout and result of initial stress measurements at the Kamaishi mine

(1997) and Yamauchi et al. (1998) reported studies on failure mechanisms in rocks, including the tertiary creep of soft rock. They investigated the microscopic changes that occur in the rock during the creep process and the relationship between the failure due to creep and the failure mechanism for unconfined compression. In addition to such laboratory tests, mechanical models have also been developed to describe such processes. An initial model that has been developed represents the rock by a combination of elastic elements (springs), viscous elements (dashpots) and yielding elements (sliders). These allow a qualitative explanation of the time-dependent behavior of the rock to be modeled. A few equations have been proposed recently, based on the non-linear visco-elastic theory, by which quantitative interpretations of time-dependent rock behavior can be made (Okubo, 1991).

Numerous case studies have been reported concerning the temporal evolution of the in situ behavior of rocks in tunnels, underground power plants and mining drifts. Further studies on the time-dependent behavior of rock masses around underground structures are thought to be necessary, due to the complex nature of the Japanese geological environment.

Experimental studies at Tono have included not only unconfined creep tests on core samples, but also long-term in situ post-excavation tests, such as measurements of rock mass displacement and convergence. Both of these tests have been set up to study the excavation disturbance in horizontal tunnels and in a vertical shaft. The unconfined creep tests confirmed that the time-dependent axial strain followed a logarithmic creep law. The measured in situ displacements all lay below the resolution level of the equipment.

Experimental studies at the Kamaishi mine have included laboratory tests, such as unconfined creep tests and fatigue tests on core samples, and in situ AE measurements and rock mass displacement measurements one year after drift excavation. The unconfined creep tests indicated that the axial strain under constant stress follows a logarithmic creep law, while the fatigue tests showed deformation behavior of the samples that was identical to that observed in creep tests. The in situ AE monitoring has shown that events are very few, the energy is much smaller than that during excavation and that the rock mass did not undergo progressive failure. The in situ rock mass displacement measurements detected no deformation following that associated with the immediate post-construction response.

It is not a simple task to elucidate the long-term time-dependent behavior of a rock mass and a multi-faceted approach to the problem is needed as outlined below:

i. Data collection: this will continue and will be combined with a continuous analysis of past data.
ii. Modeling and experiments: new modeling methods will be proposed, as required, and experiments will be planned and carried out with the intention of validating the models developed.
iii. Microscopic approach: an analysis will be carried out of the basic mechanisms of time-dependent behavior, by implementing a long-term program of observation of microstructures, such as the development of microcracks, and by making use of the newest techniques and theories (e.g. molecular dynamics) to make the analysis more reliable.
iv. In situ observations: the time-dependent behavior of rock masses will be studied by investigating old underground openings in order to assist in the validation of the proposed time-dependent model. In addition, measurements of micro-strain velocity might also be necessary for acquiring information on the structure of the surrounding rock mass.

3.5.3 Excavation disturbance

The excavation of underground openings results in the development of fractures (in sufficiently brittle rock) and in changes in the stress state and the distribution of porewater pressure in the rock mass close to the opening. Such changes alter the mechanical properties of the surrounding rock mass, such as its strength and deformability, and hydraulic properties and also influence geochemical conditions such as the redox potential of groundwater. The region in which these properties are changed due to the excavation is referred to as the excavation disturbed zone (EDZ). Information on the extent and properties of the EDZ is important for optimizing the design and construction of a deep repository. The evaluation of the EDZ is considered to be of particular importance, since its presence may result in changes to the transport characteristics of the rock mass adjacent to underground openings, which may persist for considerable periods after closure of the repository.

A Special Committee on the Zone of Relaxation (the equivalent term for the EDZ used in geotechnical studies) was organized by the Japan Tunneling Association. This Committee classified the measurement methods and concepts required in excavation disturbed zones, collected and compiled data which had been reported for such zones and compared the effects produced by different excavation methods used in the construction of waterway tunnels in hard rocks (Japan Tunneling Association, 1982). Sakurai (1983) summarized the data to illustrate the width of disturbed zones produced in 5 m and 10 m wide tunnels excavated using conventional tunneling methods such as the New Austrian Tunneling Method (NATM) and the Tunnel Boring Machine (TBM) for different types of rock. For example, a 5 m wide tunnel excavated in a rock mass with Young's modulus of 6 GPa susing the NATM is reported to produce a 1 m-wide disturbed zone. Tests on the effects of excavation have also been carried out in Sweden, Switzerland, Canada and Belgium (OECD/NEA Workshop, 1989; Excavation Disturbed Zone Workshop, 1996). These countries are promoting research programs with a view to optimizing repository design, construction and operation and the collection of information relevant for the PA of the disposal system. Programs concerning the EDZ include work in the following areas:

- determining the properties and extent of the EDZ and understanding the mechanisms of its formation
- understanding the effect of excavation methods on the rock mass and the extent of the EDZ
- determining the hydrogeological properties of the EDZ
- developing instruments and methodologies which can be used to investigate the EDZ.

Studies with similar objectives have also been carried out at Tono and Kamaishi (Sato et al., 1995; Sugihara et al., 1999).

1) Studies on excavation disturbance at Tono

Experimental studies have been carried out at Tono to investigate the effects of excavation disturbance in soft sedimentary rocks (Figure 3.5-38). Laboratory tests and initial stress measurements have also been carried out to assess the results of the experimental studies.

(1) Excavation disturbance experiment in the shaft

A study of the excavation disturbance undergone by soft Tertiary sediments was conducted by excavating a 150 m deep shaft (No. 2 shaft of Tono mine) with an internal diameter of 6 m and a 40 cm-thick concrete lining (Figure 3.5-39). The shaft was excavated using a drilling and blasting method to investigate the deformation behavior of the surrounding rock mass and

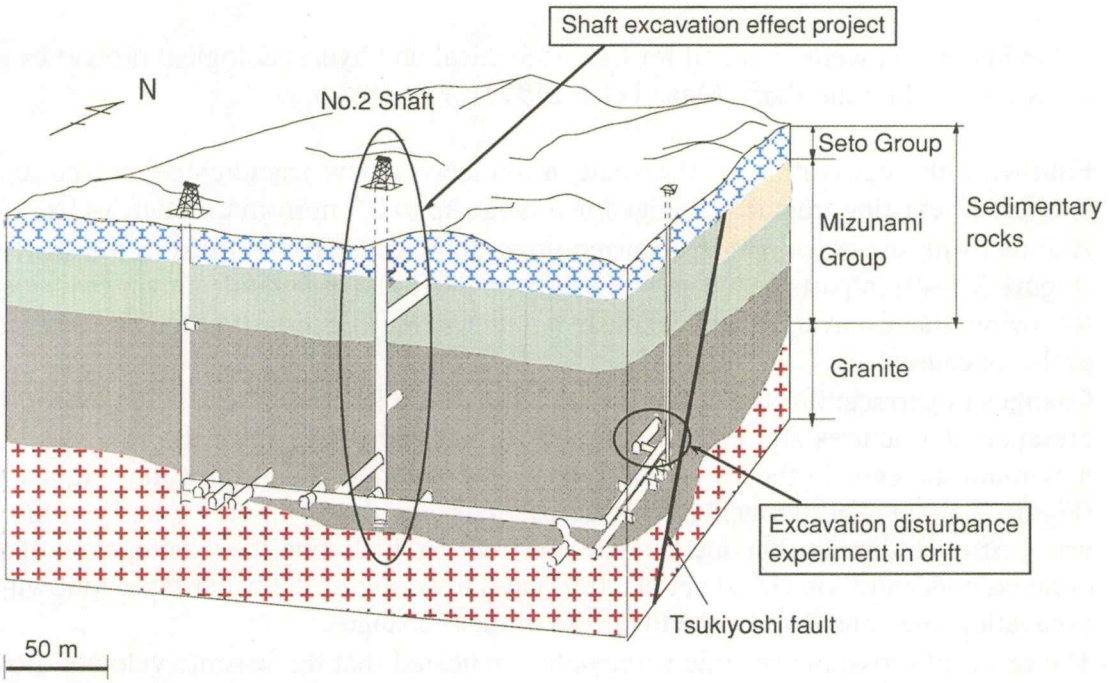


Figure 3.5-38 Geology and in-situ experimental area at the Tono mine

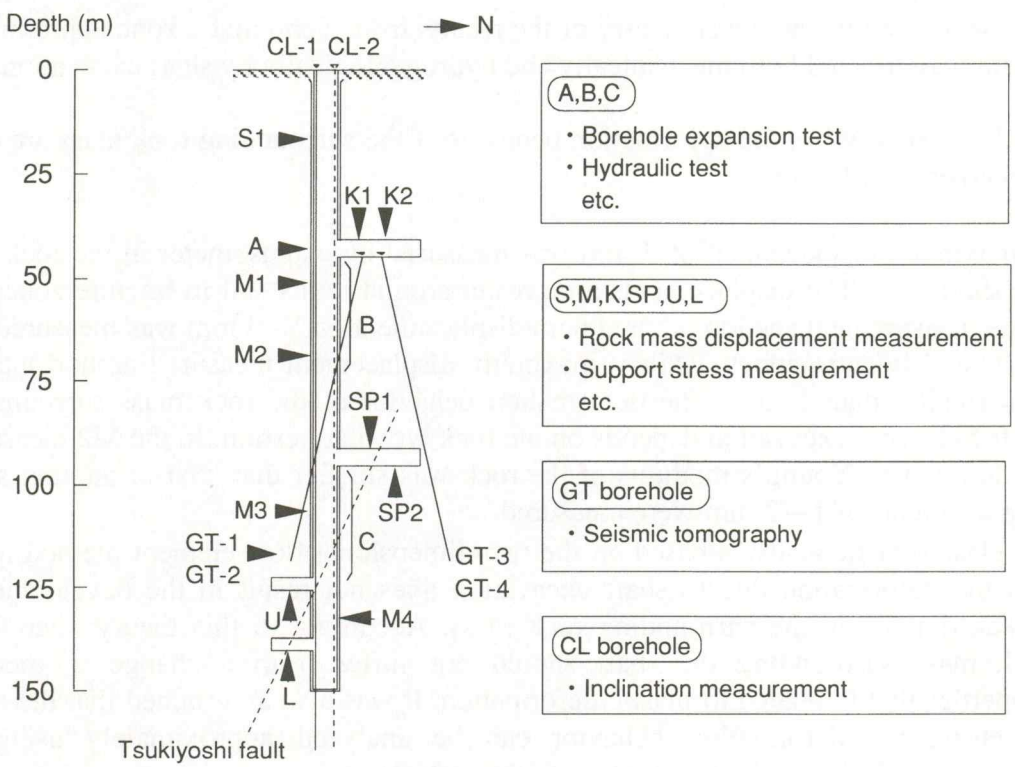


Figure 3.5-39 Section view of No.2 shaft

A shaft with a diameter of 6 m and depth of 150 m was excavated by a short step method in soft sedimentary rock at the Tono mine. The effect of shaft excavation on the surrounding rock mass was investigated (Sugihara et al., 1993).

the variations in mechanical and hydrogeological properties due to the excavation (Sugihara et al., 1993).

The following results were obtained for the mechanical and hydrogeological properties of the rock mass surrounding the shaft (Matsui et al., 1992):

i. Following the excavation of the shaft, a number of new fractures developed and the aperture of existing fractures changed in a range up to 0.9 m from the shaft walls.
ii. A zone of plastic deformation occurred up to approximately 0.4 m from the shaft walls (Figure 3.5-40) in parts of the shaft away from the Tsukiyoshi fault. Stress redistribution following the excavation and explosive damage during construction are considered probable causes.
iii. Changes in permeability associated with the shaft are influenced to a great extent by the presence of fractures and extend between 0.4 m and 0.9 m from the shaft walls. The maximum increase in the permeability is in the order of 3 - 4 times the original value (Figure 3.5-41). The permeability is occasionally increased up to 1.1 m from the shaft walls. Stress redistribution due to shaft construction, including the development of zones of stress concentration (Ishida et al., 1991) and lowering of the water table following the excavation, are considered to be the cause of these changes.
iv. The result of crosshole seismic surveys has indicated that the seismic velocity drops by 30 - 50% up to 1 m from the shaft walls. The main reason for this is thought to be the decrease in water saturation adjacent to the shaft walls which, itself, is probably connected with the development of new fractures.

It can be seen from the above summary of the results from Tono that a zone approximately 1 m in width was affected both mechanically and hydrogeologically by shaft excavation.

The results of surveys on the deformation behavior of the surrounding rock mass are outlined below (Sato et al., 1992b):

i. A maximum displacement of 3 mm was measured by extensometer in the rock mass at the shaft wall. The displacements are greater around faults and in fracture zones. In the same measurement section, a maximum displacement of 2 - 3 mm was measured around faults and fracture zones, while a maximum displacement measured around intact rock was smaller than 1 mm. The deformation behavior of the rock mass surrounding the shaft following excavation depends on the rock type in question. In the M2 measurement section, where Young's modulus of the rock was smaller than that of another sections, displacements of 1 – 3 mm were measured.
ii. An elasto-plastic analysis based on the two-dimensional flow element method indicated that the deformation due to shaft excavation does not result in the development of a plastic domain in the surrounding rock mass. According to this theory, therefore, the rock mass surrounding the shaft should not suffer from a change in mechanical properties that is related to plastic deformation. It was also ascertained that the effect of faults on the deformation behavior can be analyzed approximately using three-dimensional FEM (Finite Element Method) analysis.
iii. The results of continuous strain measurements allowed an evaluation of the stress redistribution (change in strain) in the rock mass to be made (Yoshioka et al., 1992). It was shown from this evaluation that radial strains change to negative (tensile) and tangential strains change to positive (compressive) well in advance of the shaft face. However, it was also shown that, where the distance from the shaft face is equal to or

greater than the shaft diameter (i.e. 6 m), the values for the radial and tangential strains are unaffected by the presence of the shaft. A two-dimensional, axially symmetric FEM analysis showed that the stress redistribution accompanying the shaft excavation can be simulated approximately by a continuous model, in which the input parameters are changed according to the fracture frequencies (Figure 3.5-42).

(2) Excavation disturbance experiment in horizontal drifts

A drift of 3 m wide and 3 m high was excavated using the NATM in the sedimentary rocks at Tono, to investigate the rock mass behavior during the excavation and the changes in physical properties before and after the excavation (Figure 3.5-43). To analyze and evaluate the rock mass behavior, Sugihara et al. (1998) conducted an initial FEM analysis of the drift excavation. The analysis used the results of laboratory tests as input parameters. After the excavation, a follow-up analysis was carried out, taking into account the various in situ measurements that had been made. A similar approach was also applied to the mechanically excavated portion of the drift (see below), to investigate the dependence of EDZ development on excavation methods (Figure 3.5-44).

The results obtained from tests on the effects of excavation due to drilling and blasting in the horizontal drift were as follows:

i. The final displacement of the rock mass at a distance of 1 m from the drift wall was 1.5 mm. The displacement decreases with distance from the drift, becoming nearly zero at a distance of 6 m.
ii. A low velocity zone, 0.8 m in thickness, was observed around the drift by measuring the velocity of seismic waves (refraction and tomography methods) (Figure 3.5-45).
iii. A hydraulic test carried out following excavation of the drift indicated that a more permeable zone had been formed at a distance of between 0.5 and 1.0 m from the drift wall. It is thought that this is probably due to fractures generated by blasting. No changes were detected before and after the excavation at distances of 1.4 m or more from the drift wall and the thickness of the EDZ was thus estimated to be 1.4 m or less.

Part of the drift was constructed using a mechanical technique (i.e. without blasting), in order to investigate the differences between the effects of mechanical excavation and the effect of conventional blasting method (Figure 3.5-44) (Sato et al., 1999). The mechanical technique was believed to cause the least possible damage to the surrounding rock mass. A Boom-header (mini-loadheader) was used for the mechanical excavation. The results of this experiment were :

i. The final displacement in the rock mass at a distance of 0.5 m from the drift wall was 1 mm. The value decreased with distance from the drift wall, being 0.2 mm or less at a distance of 6 m (Yamamoto et al., 1998). According to the convergence measurements, the displacement was 2 - 4 mm at the roof and approximately 1.5 mm in a horizontal direction along the drift. Both of the displacements converge to zero at a distance of 1 - 2 D (where D = drift diameter, which is 2.5 m at present) from the drift face.
ii. A low velocity zone measuring some 0.3 m in thickness was detected around the drift using the seismic refraction method. No low velocity zone was detected using seismic tomography and no change in resistivity was detected using resistivity tomography.
iii. No significant change in hydraulic conductivity was detectable within 0.3 m of the drift wall using a constant pressure injection test with a test section of 0.1 m (Kikuchi et al., 1997) (Figure 3.5-46).

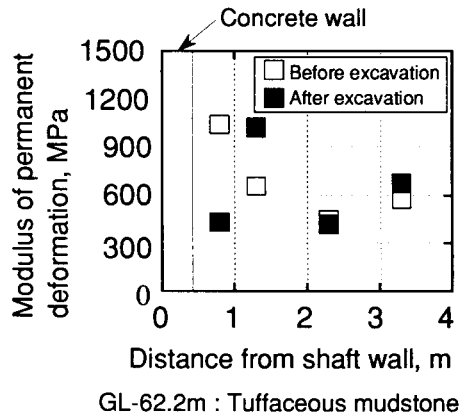


Figure 3.5-40 Result of borehole expansion test in section B of No.2 shaft

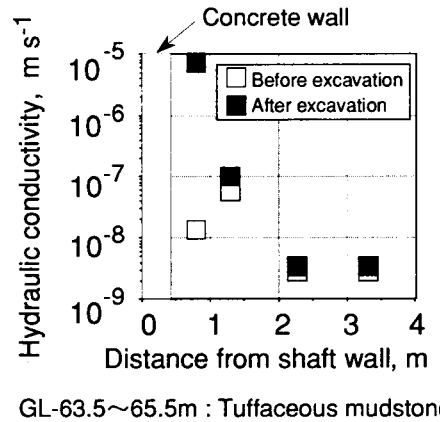


Figure 3.5-41 Result of hydraulic test in section B of No.2 shaft

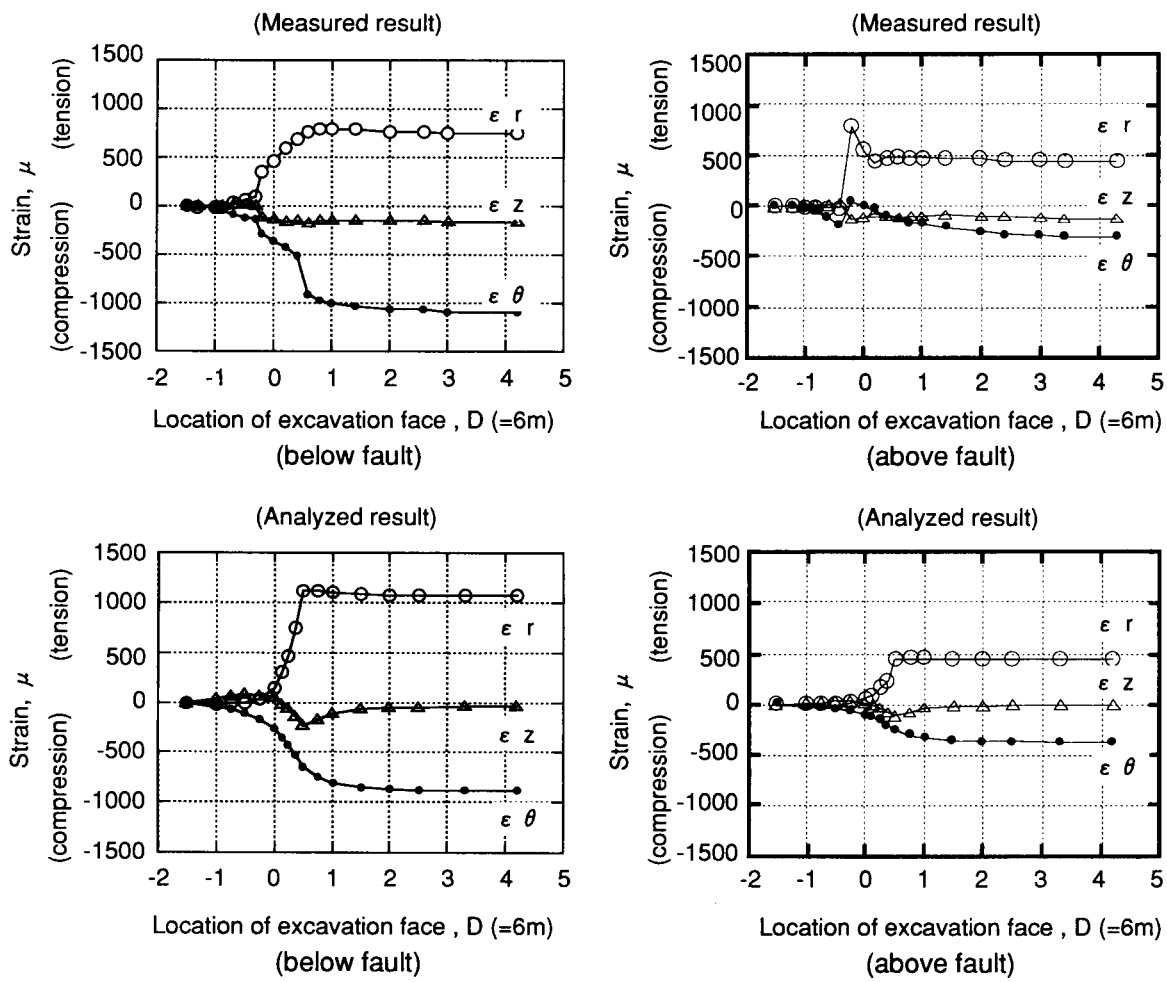


Figure 3.5-42 Measured and analyzed strain variation due to shaft excavation

The radial and tangential strain started to vary when the shaft face reached 1 D (D : shaft diameter) above the gauge level, and became stable when the shaft face passed the gauge level by 1 to 2 D. FEM (Finite Element Analysis) analysis using a continuous model can simulate these strain patterns .

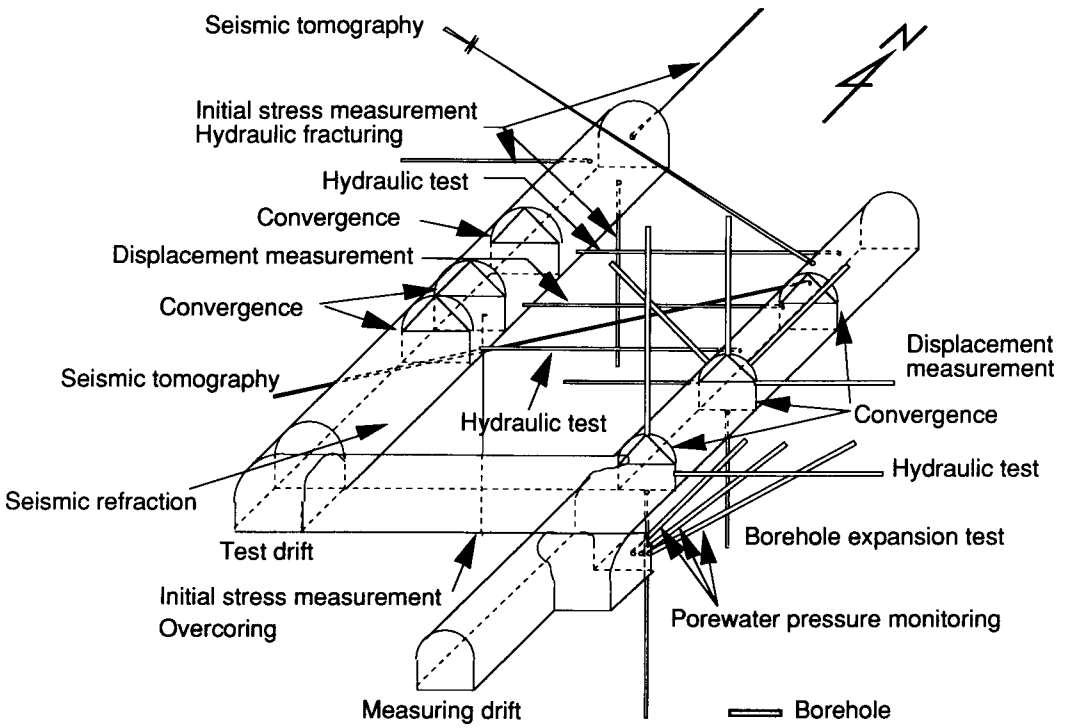


Figure 3.5-43 Layout of the excavation disturbance experiment by blasting in the NATM drift at the Tono mine

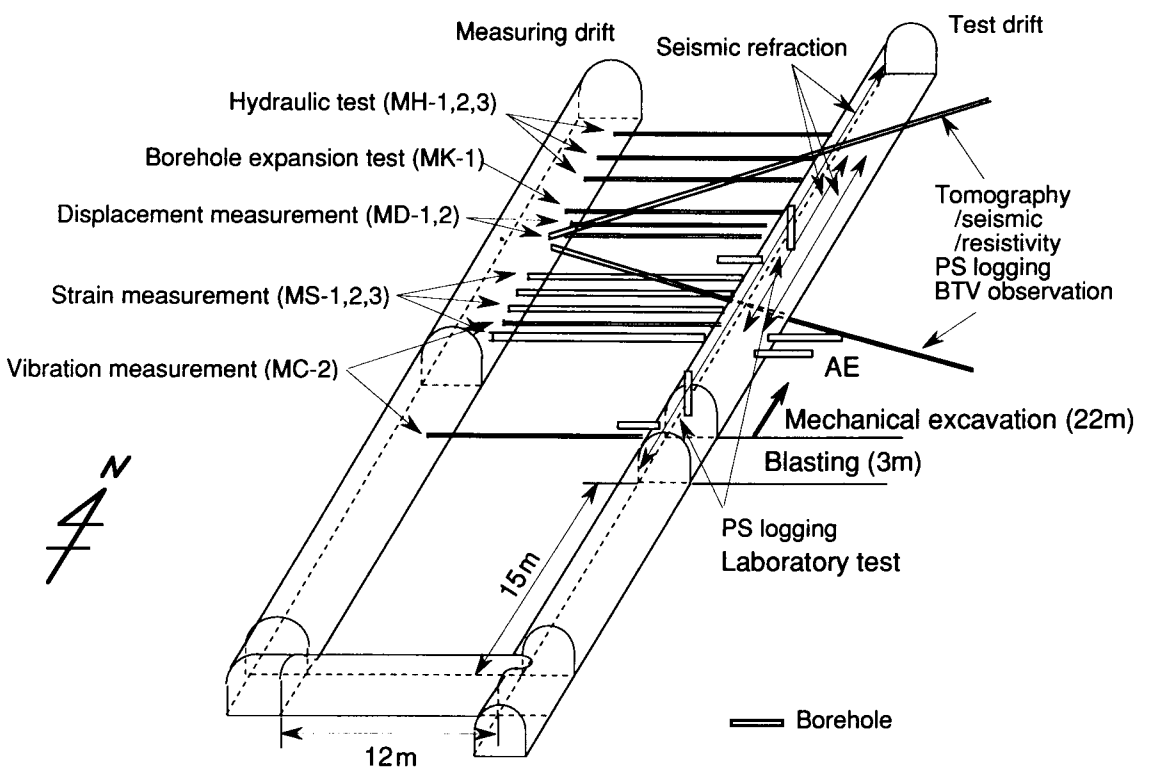


Figure 3.5-44 Layout of the excavation disturbance experiment by mechanical excavation in the NATM drift at the Tono mine

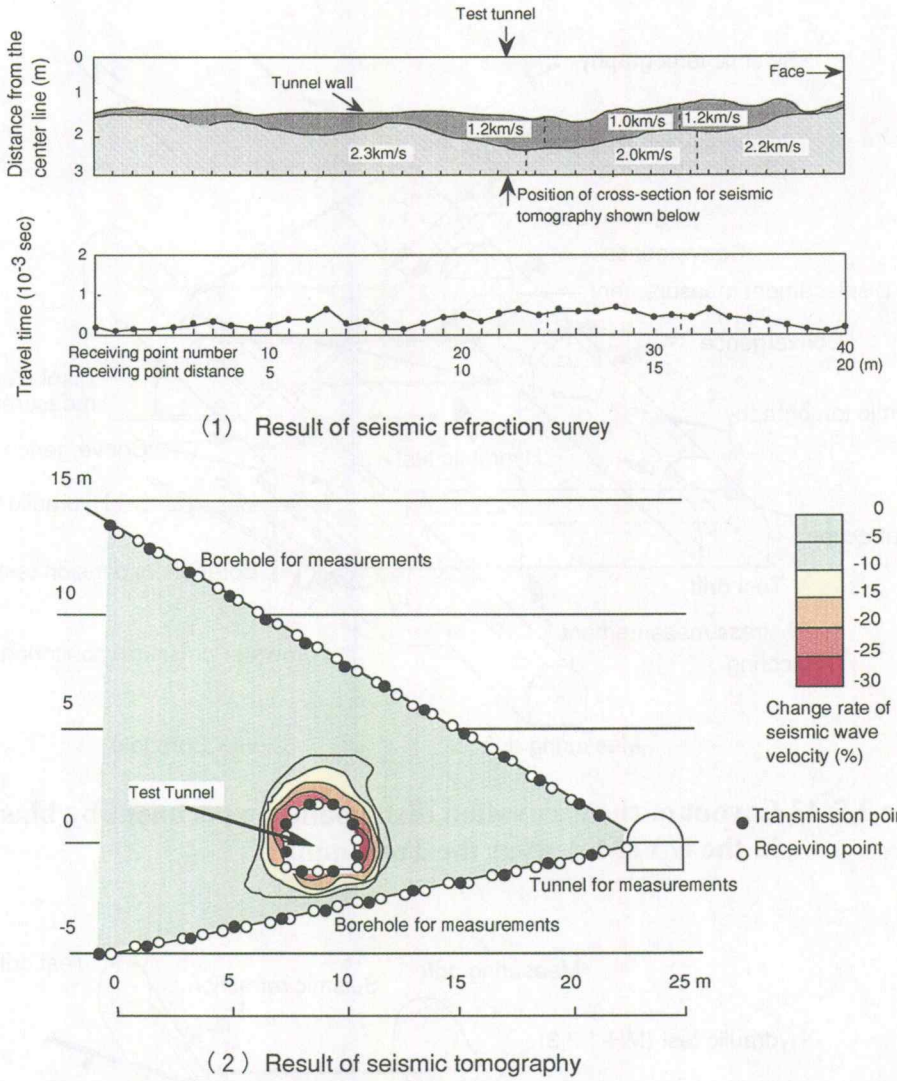


Figure 3.5-45 Results of a geophysical survey of the EDZ in the Tono mine

(Sugihara et al., 1998)

Investigations using seismic waves detected a low velocity zone extending approximately 80 cm from the tunnel wall.

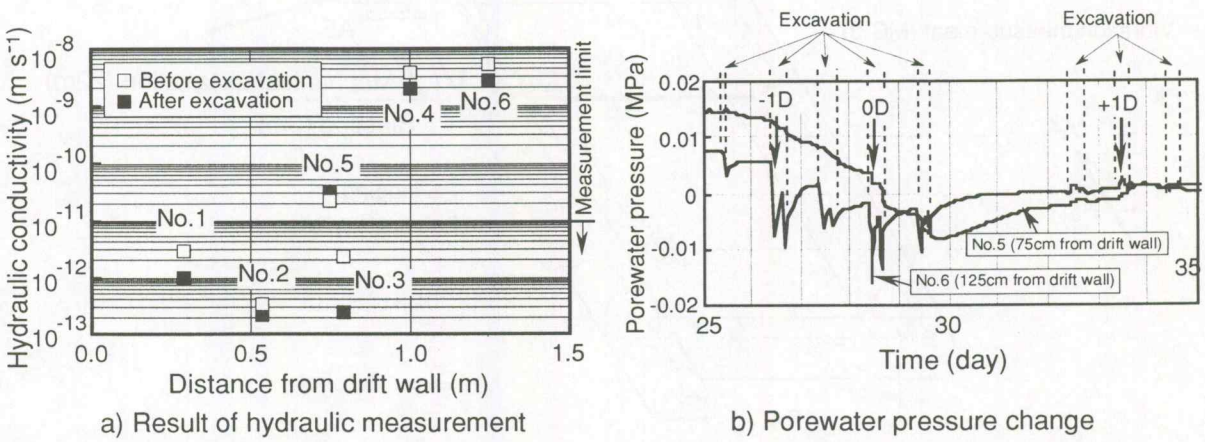


Figure 3.5-46 Porewater pressure and hydraulic conductivity changes due to mechanical excavation in the Tono mine

The predicted displacement of the face of the drift, which was made using a two-dimensional elasto-plastic finite element code with measured in-situ stresses and rock mass properties, was shown to be approximately consistent with the measured in situ values. This suggested the possibility of a method for estimating the response in advance of construction. The input data for the follow-up simulation included those from the disturbed zones (0.8 m in the NATM blasted section, 0.3 m in the machine excavated section) estimated from the results of seismic surveys. The input also included measured values for in situ stress and the results of laboratory tests on drillcores (Figure 3.5-47). The calculated values for the displacement were more or less consistent with the measured values (Figure 3.5-48). For the NATM blasted section, the consistency between the estimated and measured values in the region where there was an abrupt increase in displacement towards the drift wall was improved by taking account of the disturbed zones. In the mechanically excavated section, the estimated and measured values are consistent regardless of whether or not the disturbed zones were taken into consideration.

The results of seismic refraction surveys have demonstrated that the process of mechanical excavation produces a smaller disturbed zone than that produced by blasting, the average thickness of these two zones being 0.3 and 0.8 m, respectively. An empirical formula for estimating the effects of vibration on the concrete linings of tunnels (Industrial Explosives Society, 1976) was applied to the evaluation of the disturbed zones. This approach calculated widths of damaged zones that are more or less consistent with the widths of low velocity zones detected by the seismic refraction survey for both the mechanical and blasted excavations (Sato et al., 1998b). The deformation behavior of the surrounding rock mass associated with the excavation can be calculated using an elasto-plastic FEM approach (Sato et al., 1999).

2) Study of excavation disturbance at Kamaishi

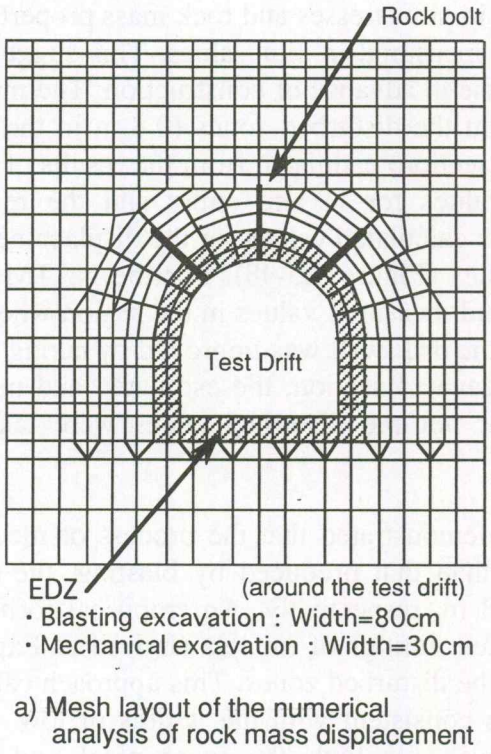
The excavation disturbance in the underground openings at Kamaishi was assessed using the same techniques as were used at Tono (Sato et al., 1995; JNC, 1999). This experimental study was carried out in the 550 m level drift (260 m below the surface) and in the 250 m level drift (730 m below the surface) to examine the change in excavation disturbance with depth.

(1) Excavation disturbance experiment at 550 m level drift

The effects of excavation damage were examined in the drifts KD-88 and KD-89 at a depth of 260 m below the surface (Fukuda, 1990). KD-88 has a horseshoe-shaped cross-section, 3.0 m wide and 2.5 m high, and was excavated perpendicular to the dominant fracture direction using a conventional blasting method. KD-89 has a rectangular cross-section, 5.2 m wide and 3.2 m high, and was excavated parallel to the dominant fracture direction using the smooth blasting method. The experimental layout is shown in Figure 3.5-49.

Excavation disturbance experiment in the KD-88 drift

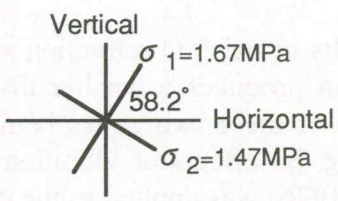
Prior to drift excavation, an axially symmetric elasto-plastic FEM simulation was carried out and the change in stress due to excavation was estimated. Overburden pressure was used as a boundary condition, because there were no in situ stress measurement data. This analysis predicted that the rock should behave elastically and that there should be no plastic response, which was consistent with the general trend of the measured results. According to a low-pressure Lugeon test in borehole KE-3, conducted before and after excavation, the permeability measured within 2 m from the drift wall was reduced by an order of magnitude after the excavation. It is thought that this was due to the partial closure of fractures due to the stress concentrations developed around the drift. A borehole expansion test using a borehole jack (KKT), conducted before and after excavation, showed no distinct change in the



a) Mesh layout of the numerical analysis of rock mass displacement

b) Input parameter values for the numerical analysis of rock mass displacement

Input parameter	Intact rock	EDZ
Young's modulus	1.5 GPa	0.4 GPa
Poisson's ratio	0.3	0.3
Cohesion	1.3 MPa	0.39 MPa
Angle of internal friction	25°	25°



c) Initial stress condition

Figure 3.5-47 Mesh layout and input data for numerical analysis of rock mass displacement

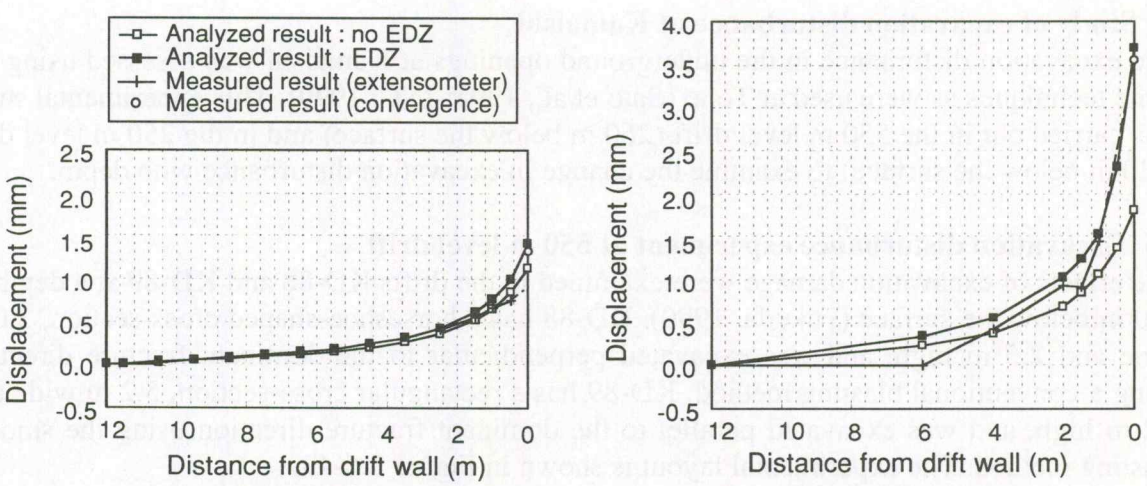


Figure 3.5-48 Rock mass displacements measured by extensometers compared to the numerical analysis using FEM

In the case of mechanical excavation, the displacements obtained from numerical analysis (assuming the EDZ / without the EDZ) and measurement were almost same. In the case of blasting excavation, the results of numerical analysis assuming the EDZ were different to those without the EDZ within about 1 m of the drift wall. The EDZ was narrower for the mechanical excavation than for blasting excavation. The rock mass around the test drift behaved elastically in the case of the machine excavation. The EDZ has to be considered in numerical analysis when there is blasting excavation.

deformation modulus.

Excavation disturbance experiment in the KD-89 drift

A plane strain two-dimensional elasto-plastic FEM simulation of a rectangular section (drift shape) was carried out in advance of construction. Values for the in situ stress obtained using the overcoring method were used as the initial input conditions. It was predicted from this simulation that a plastic region would form only in restricted sections of the near-drift environment, while the rock mass would behave elastically as a whole. The vertical stress component would reach a maximum value at a distance of approximately 1 m from the drift wall and would then decrease to the initial stress value at greater distances into the rock. The stress values measured following the excavation were tensile near the drift wall and compressive at some distance from it, consistent with the general trend of the simulation results. According to low-pressure Lugeon tests in boreholes KE-6 and KE-7 (Figure 3.5-50), the permeability of most of the tested sections decreased following excavation; however, it increased in one section in borehole KE-6 that was parallel to, and 1 m from, the drift wall. A borehole expansion test using a jack (KKT), carried out in the same borehole, showed a slight decrease in the deformation modulus, in the same part of the borehole in which the permeability had shown an increase. It is presumed that both these effects were caused by the dilation of fractures.

(2) Excavation disturbance experiment at 250 m level drift

The objective of this experiment was to determine the properties and extent of the EDZ at a greater depth and also to understand the mechanisms of excavation disturbance. Prior to planning this experiment, a preliminary field survey was carried out to establish the detailed experimental plan (Sugihara et al., 1996). The preliminary survey indicated that the EDZ was too small to detect, so a test drift was set up normal to the maximum principal stress, but also parallel to the strike of the dominant set of fractures. This approach ensured that the EDZ would be as broad as possible. The opportunity was also taken for examining the applicability of measurement techniques that had not been used in previous experiments at Kamaishi.

The experimental set-up used for examining the effects of excavation in this drift is shown in Figure 3.5-51. The test drift has a horseshoe-shaped cross-section, measuring 3.5 m by 3.5 m. In order to investigate the dependence of the EDZ on excavation methods, the drift was excavated using both the conventional blasting method and the smooth blasting method. Both vibration and AE were measured in these two sections of the drift. In addition, a section for investigating the stress redistribution and the associated change in physical properties was established in the smooth blasted section. This enabled strains and displacements of the rock mass to be measured and a permeability test to be conducted. An elasto-plastic FEM simulation and a simulation using the crack-tensor theory and the DEM (distinct element method) were also carried out. The results of the surveys and simulations are as follows :

i. According to the rock mass displacement measurement, the total displacement caused by the excavation was about 1 mm. After the passage of the drift face, the roof sank by 0.7 mm and the floor rose by 0.4 mm. The strain measurement of the rock mass indicated a negative value of 860 x 10^{-6} (tensile) in a radial direction and a vertical negative value (tensile) of 670 x 10^{-6} in the vicinity of the drift wall. Given that the strain distribution is heterogeneous, it is possible for the rock mass to behave as a block as excavation progresses. The result of the joint displacement measurements indicates a change in width of fracture apertures, suggesting that the rock mass did indeed behave as a block.
ii. The results of the vibration measurements (Kinoshita et al., 1998) indicate that the relationship between the distance and the vibration velocity is linear on a log-log plot.

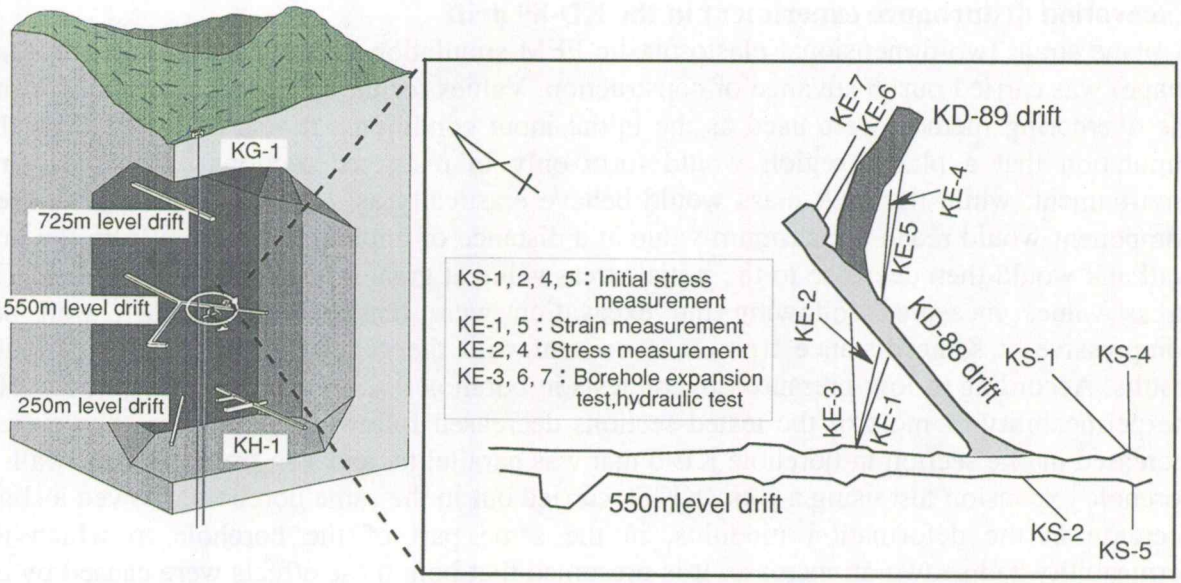
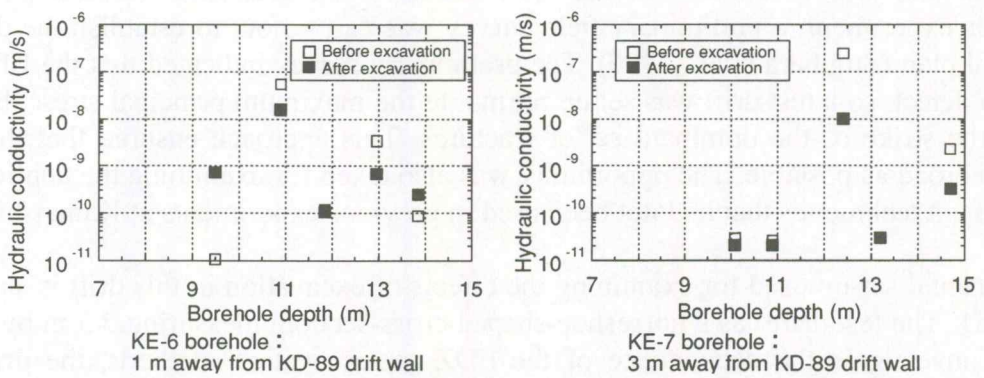
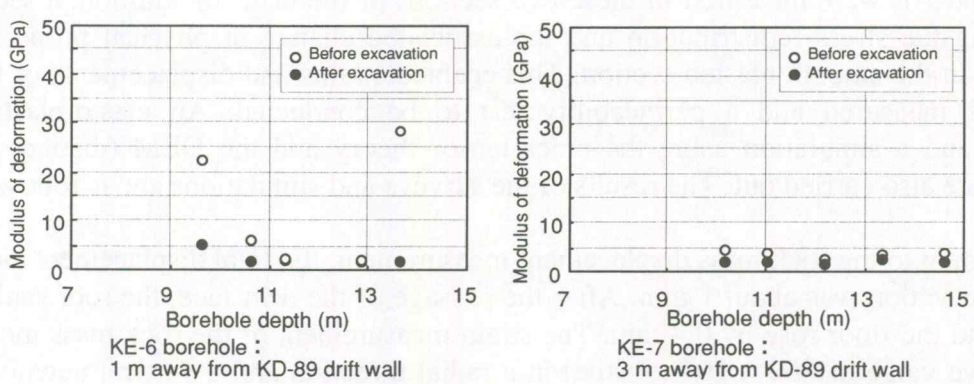


Figure 3.5-49 Layout of the excavation disturbance experiment in the 550 m level drift in the Kamaishi mine



a) Result of hydraulic test



b) Result of borehole expansion test

Figure 3.5-50 Hydraulic conductivity and modulus of deformation changes due to KD-89 drift excavation at the Kamaishi mine

This relationship possibly occurs even in the immediate vicinity of the blasting point. A large difference between the two blasting techniques was seen in the vibration velocities in the monitoring boreholes, thus confirming the effectiveness of smooth blasting, at least in this respect. The AE measurement showed a concentration of AE within 2 m of the excavation surface (Kinashi et al., 1998) and also at the base of the drift walls where the greatest shear stresses are concentrated according to the FEM simulation. The amplitude and energy of AE are smaller for the smooth blasting method, which affects the rock mass to a lesser extent.

iii. According to the seismic refraction surveys, the regions of the rock mass that exhibit a decrease in seismic velocity (in comparison with the pre-excavation values) are from 0.3 - 0.5 m thick around the drift for the both excavation methods. The magnitude of the decrease in seismic velocity is, however, greater for the conventional blasting than for the smooth blasting method (Figure 3.5-52) (Sasamoto et al., 1999).

iv. According to measurements made using the low-pressure Lugeon test, the range of permeability values changed from 10^{-8} - 10^{-10} m s^{-1} before the excavation to 10^{-8} - 10^{-11} m s^{-1} after the excavation. The maximum decrease for any one measurement point was an order of magnitude. Permeability increased in sections closest to the drift wall by a factor of less than 2. Measurements were also made with the Pac-ex (Packer-extensometer) developed by AECL (Canada). This instrument measured the porewater pressure and the fracture displacement associated with the progress of drift excavation and demonstrated the possibility of measuring the stress redistribution and the change in porewater pressure simultaneously (Figure 3.5-53).

v. According to the results of redox monitoring, the concentration of dissolved oxygen ranged from 6.5 - 9.5 ppm in the water seeping from the drift wall and decreased to 0.3 ppm at a distance of 2 m from the drift and 0 ppm at distances of 20 m and 300 m from the drift.

vi. Simulations were conducted using the DEM and three-dimensional FEM. Geometric information on fractures was collected by fracture surveys on the drift wall (scan line survey) and from fracture observations on drilling cores and in boreholes and was used as input for the simulations. The physical properties of fractures were obtained by compression tests and shear tests on fracture planes. The results of the post-excavation analysis, which had access to more information on fracture distribution and in situ stresses than the pre-execution simulation, demonstrated that the results of the modeling were, in both cases, similar to the measured values. A requirement for improving future modeling methodology was identified, so that local displacements and variations in strain can be incorporated into any future numerical analysis (Figure 3.5-54).

The results of the excavation disturbance experiments conducted at the 550 m and 250 m levels, where drifts have been constructed by smooth blasting parallel to the dominant fracture trend, show consistent results that are in general agreement with the predictions of the numerical simulations. In both cases, a local increase in permeability of approximately an order of magnitude, due to the dilation of fractures, is recognized within 1 m from the drift wall. Damage to the rock mass due to high stress concentrations was observed in the 250 m level drift, but this effect was not observed in the 550 m level drift. This suggests that depth might be a significant factor in determining the extent of the excavation disturbed zone.

3.5.4 Summary

Data on the thermal properties of rock masses were collected through literature surveys. These data led to development of frequency distributions of thermal conductivities for the various rock types and also distributions of the specific heat and linear expansion coefficients

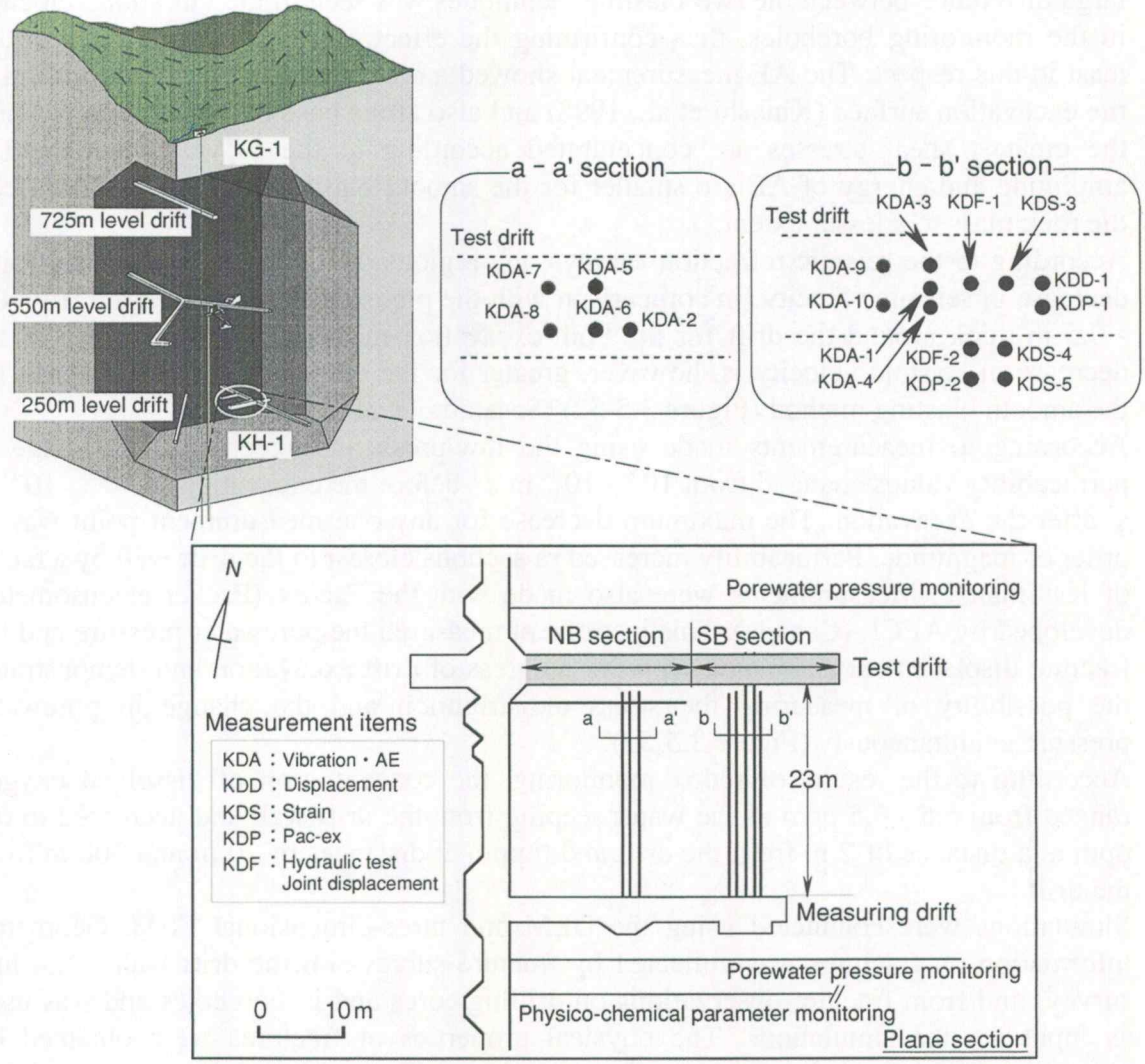


Figure 3.5-51 Layout of the excavation disturbance experiment in the 250 m level drift of the Kamaishi mine

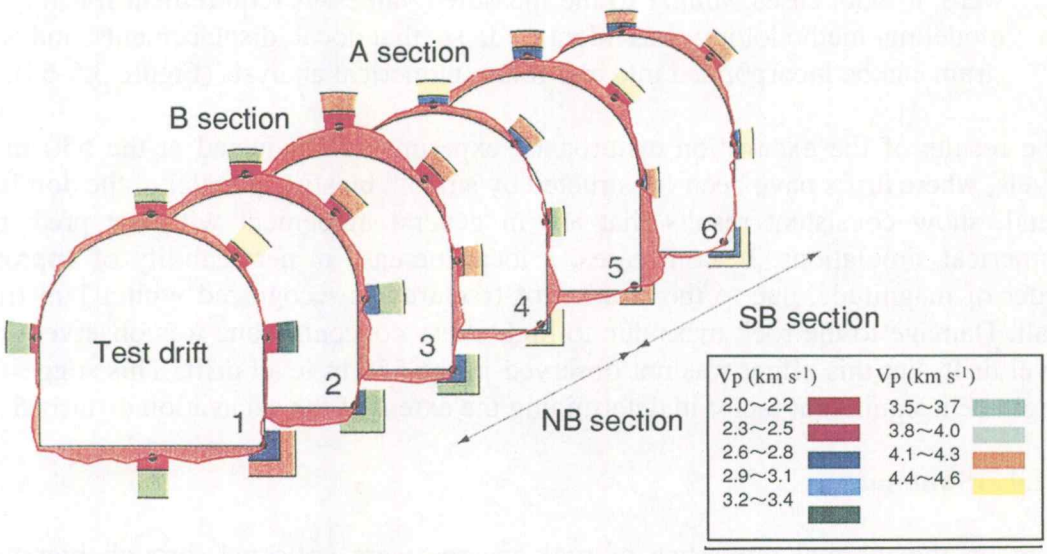


Figure3.5-52 Result of seismic refraction survey (250 m level drift of the Kamaishi mine)

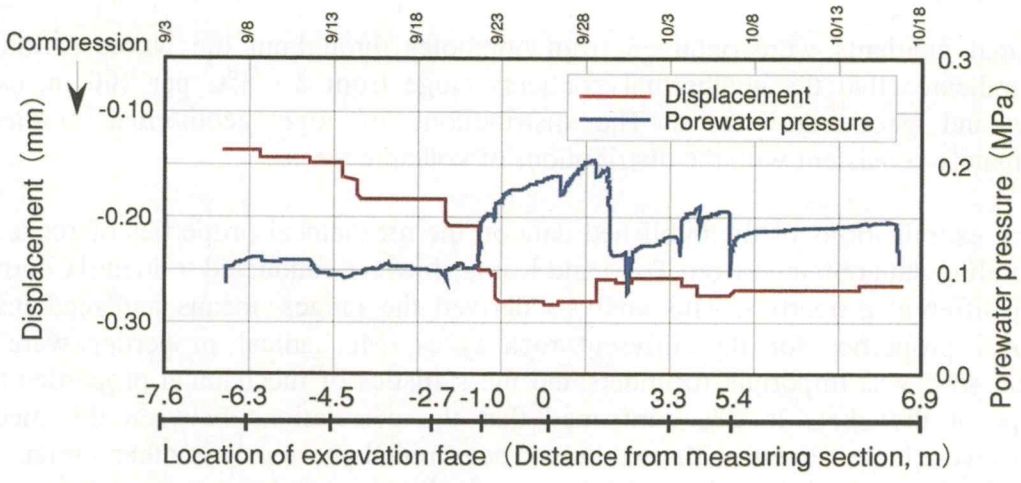
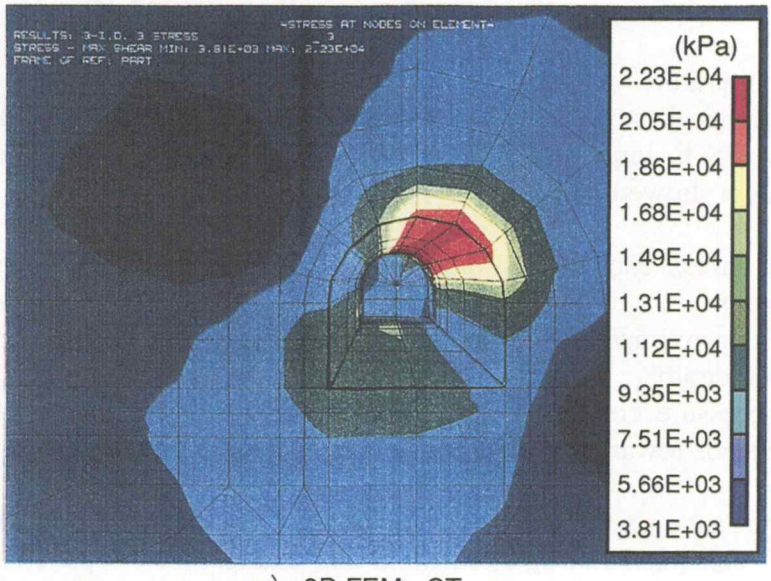
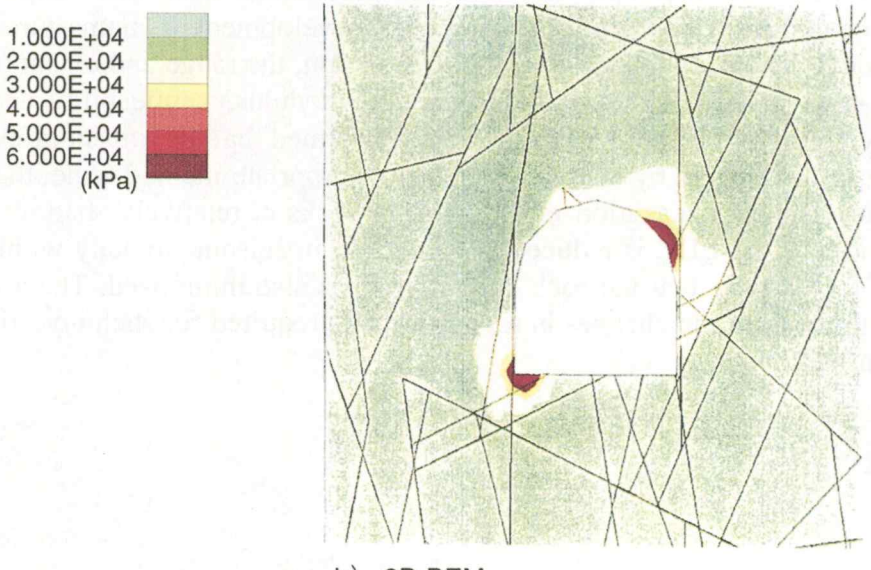


Figure 3.5-53 Result of measurement using Pac-ex at the Kamaishi mine



a) 3D FEM - CT



b) 2D DEM

Figure 3.5-54 Result of numerical analysis of rock mass stress (250 m level drift of the Kamaishi mine)

for crystalline rocks.

Geothermal gradients were obtained from boreholes throughout the whole country. This review indicated that the geothermal gradients range from 2 - 5°C per 100 m, except in volcanic and geothermal areas. The distributions of high geothermal gradients are approximately consistent with the distributions of volcanic areas.

Statistical examinations of the published data on the mechanical properties of rocks and the corresponding data obtained from Tono and Kamaishi were conducted to identify correlations between different properties. This analysis derived the ranges, means and medians of the mechanical properties for the different rock types. Mechanical properties were widely dispersed, so it was important to understand the statistics of mechanical properties for each rock type at the sites. It was confirmed that the correlations between the mechanical properties were in agreement with correlations determined previously in other similar surveys. Data on the mechanical properties were generally too widely dispersed to note any dependence on depth. However, the unconfined compressive strength of Neogene sedimentary rocks showed a tendency to increase with increasing depth ($\geq$ 500 m).

The results of literature surveys were compiled into databases and were examined to determine the vertical stresses, the average horizontal stress and the lateral pressure coefficients of rocks in Japan. In addition, an examination of the measured data obtained at Tono and Kamaishi showed that:

i. the vertical stress can be approximated by the extent of gravitational loading at a particular point
ii. there is an approximately linear relationship between the average stress in a horizontal plane and the depth
iii. the lateral pressure coefficient tends to have a high value and large range at shallow depths, but tends towards a value less than 1 with increasing depth.

Excavation disturbance experiments were conducted at Tono and Kamaishi to observe the behavior of the rock mass during excavation and changes in the physical properties of the rock mass before and after excavation. It was ascertained from these experiments that the EDZ was due to the development of fractures, the development of an unsaturated zone and the redistribution of stress around the opening. In addition, the range and extent of the associated changes in rock properties, such as deformation modulus, permeability and seismic wave velocity, were clarified (Figure 3.5-55). It was confirmed that the impact of excavation on the rock mass can be reduced by adopting the most appropriate method (smooth blasting in hard rocks and mechanical excavation in sedimentary rocks at relatively shallow depths). In this way, the width of the EDZ is reduced and the drop in seismic velocity within it (which is a measure of the damage that the rock has suffered) is also minimized. The ability of existing techniques to measure the changes in rock properties required for such investigations has also been demonstrated.

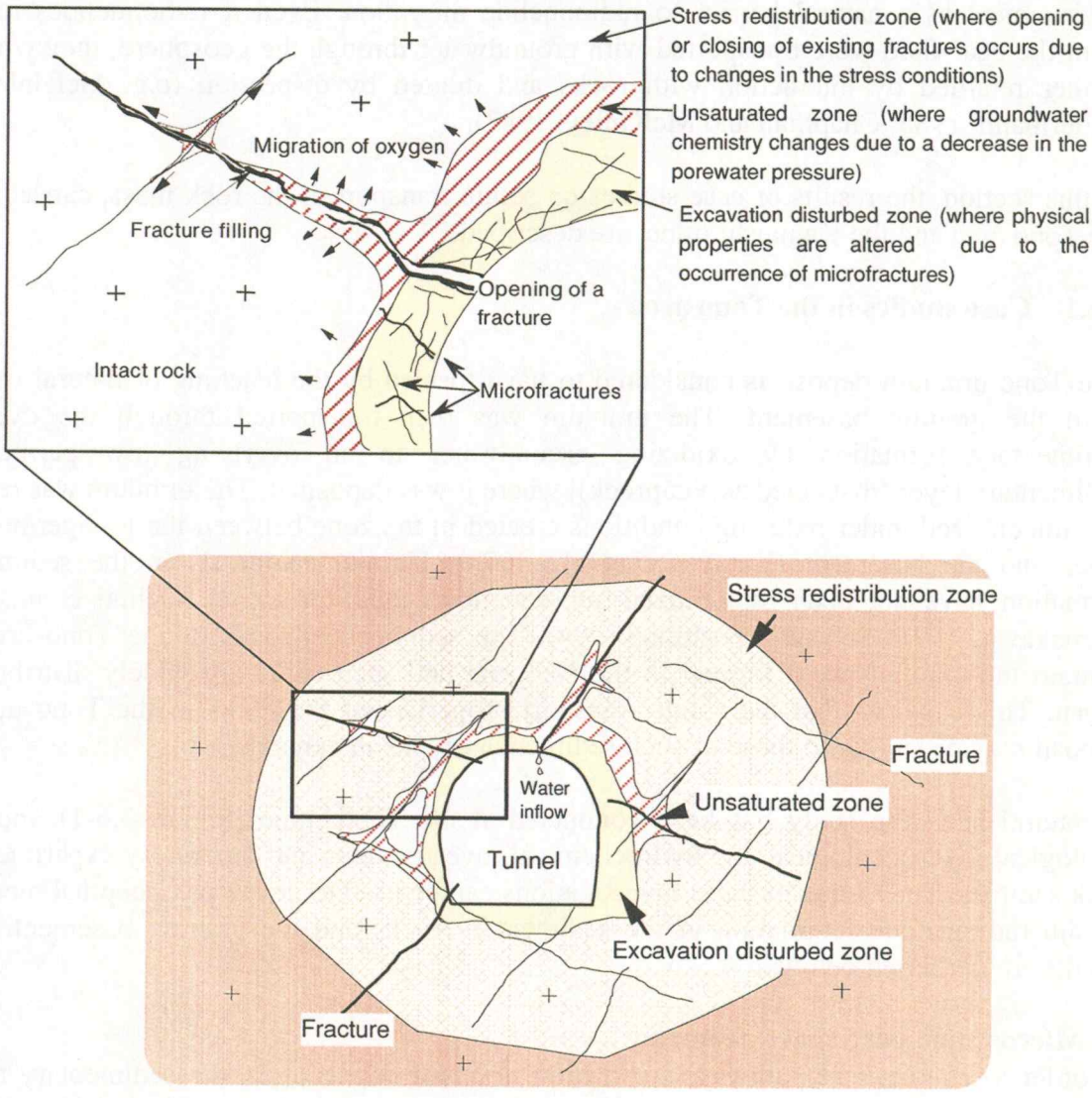


Figure 3.5-55 Conceptual illustration of the geological environment surrounding a tunnel

Excavation of underground cavities may cause the occurrence of microfractures and induce changes in stress conditions and porewater pressures. These changes may in turn cause changes in the mechanical and hydraulic properties of the surrounding rocks. Geochemical properties, such as the redox potential of the groundwater, may vary if air penetrates into this zone.

3.6 Solute transport in the rock mass

Solute transport in the rock mass is directly related to the performance of the geological environment as a natural barrier to radionuclide migration. Even if radionuclides released from the near-field were transported with groundwater through the geosphere, they would be further retarded by interaction with rocks and diluted by dispersion (e.g. McKinley and Hadermann, 1985; Chapman and McKinley, 1987).

In this section, the results of case studies on solute transport in the rock mass, carried out in the Tono area and the Kamaishi mine, are described.

3.6.1 Case studies in the Tono area

The Tono uranium deposit is considered to have formed by the leaching of natural uranium from the granitic basement. The uranium was then transported through the overlying sedimentary formation by oxidizing groundwater to an overlying low permeability sedimentary layer (that acted as a caprock), where it was deposited. The uranium was retarded and mineralized under reducing conditions created in the zone between the low permeability layer and the basement (Katayama et al., 1974). Uranium minerals in the sedimentary formation have not been remobilized subsequent to their formation (Ochiai et al., 1989; Yamakawa, 1991; Seo and Yoshida, 1994). The sedimentary rocks of the Tono area that contain the uranium were formed in the Neogene and such rocks are widely distributed in Japan. This suggests that the solute transport properties of the rocks in the Tono uranium deposit may be similar to those of such sedimentary rocks in general.

A natural analogue study has been conducted at the Tono mine (Figure 3.6-1), including geological, hydrogeological and hydrochemical investigations and laboratory experiments on rock samples. The results of these investigations can be used to develop conceptual models of in situ radionuclide retardation in the sedimentary rocks and the granitic basement. These results are discussed below:

1) Microscopic pore space geometry

In order to characterize pathways for natural uranium migration in the sedimentary rock, a rock specimen containing uranium was collected from the Tono mine (Figure 3.6-2). Following resin impregnation of the rock specimen, detailed investigations were carried out by the combined use of alpha-autoradiography, SEM (Scanning Electron Microscope) and EPMA (Electron Probe Micro-Analyzer) techniques. In addition, observations using cathodoluminescence were made to confirm whether minerals were contributing to natural uranium migration.

The detailed microscopic examination revealed that a three-dimensionally interconnected network made up of three types of pore space is present in the sedimentary rocks:

i. microfractures in detrital grains (Figure 3.6-3a)
ii. cleavages of sheet silicates (Figure 3.6-3b)
iii. micropores in the matrix filled with clay minerals (Figure 3.6-3c).

These types of pore space have diameters which range in size from 0.1 to 10 μm (Yoshida, 1994; Yoshida et al., 1994a). Petrographic studies indicated that idiomorphic calcite has been crystallized in the microfractures within quartz and feldspar grains, as well as in the matrix

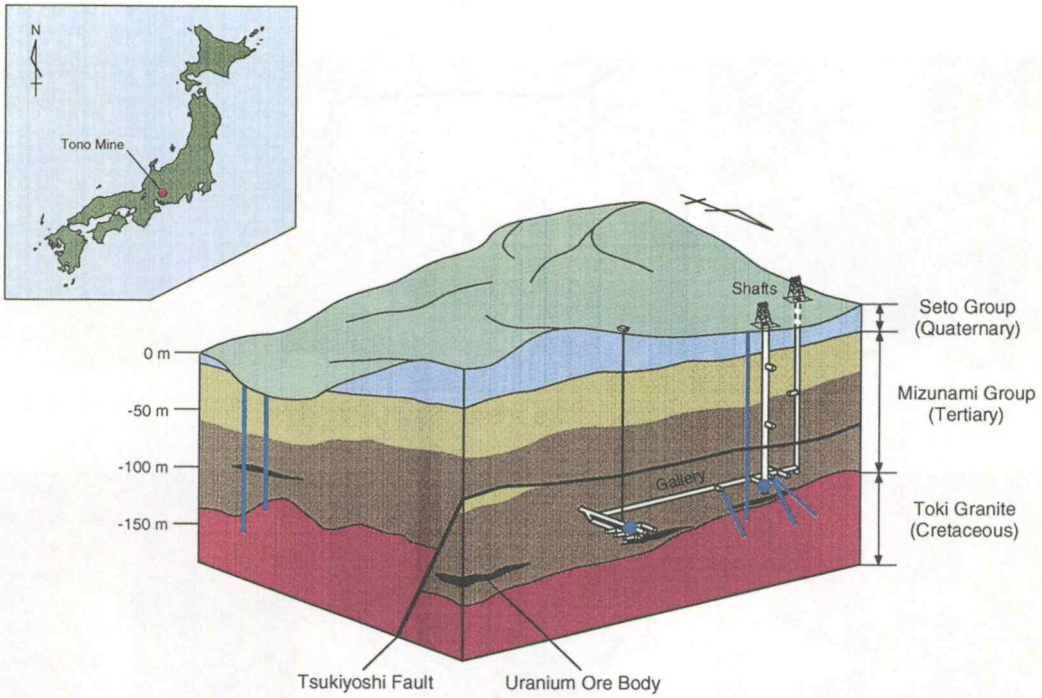


Figure 3.6-1 Geological overview of the Tono mine and location of investigated sections

The solute transport study was carried out using rock and groundwater samples collected from boreholes (blue lines) drilled from the surface and directly from the galleries (blue points) in the Tono mine.

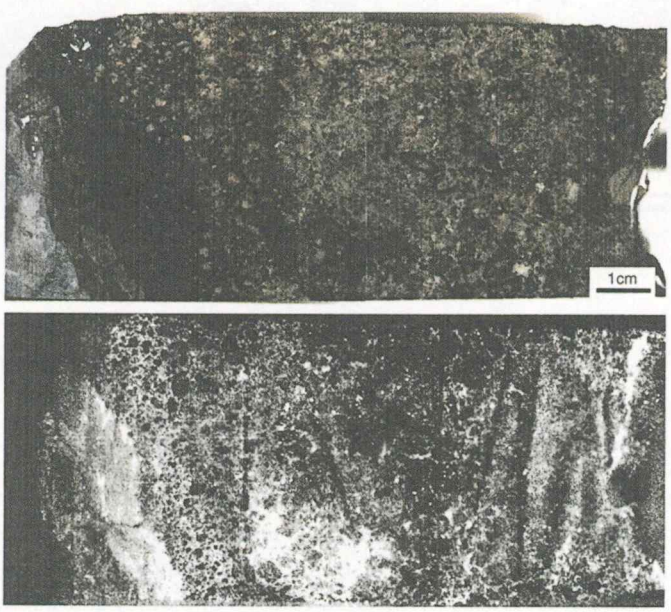
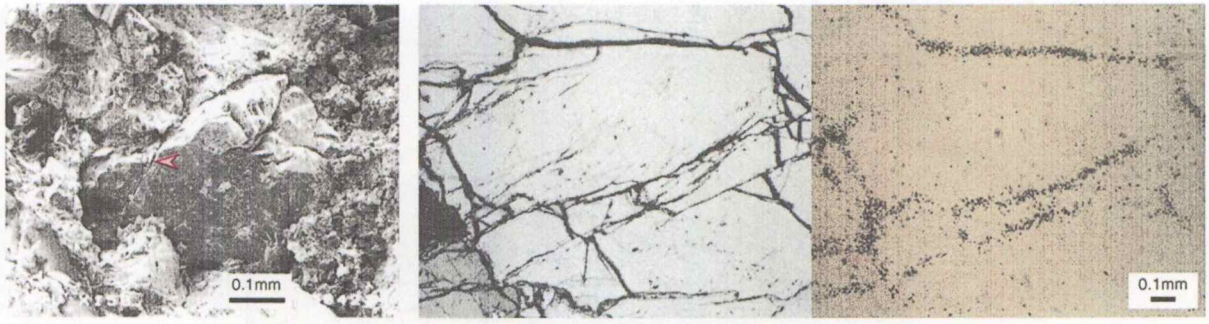
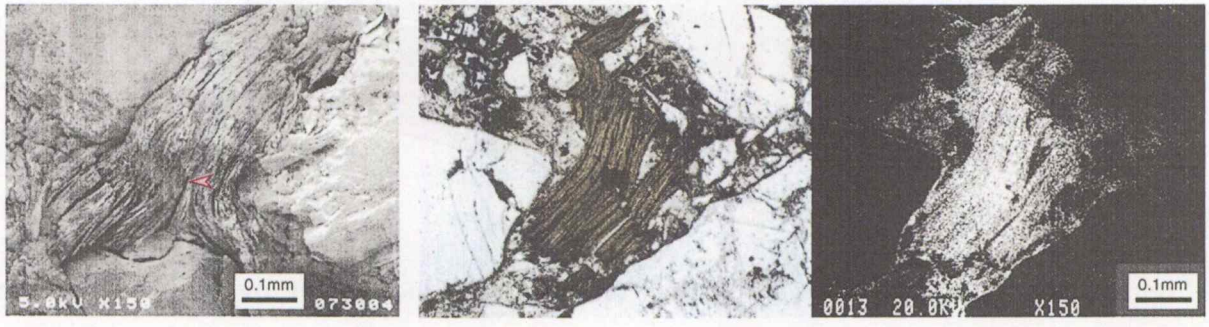


Figure 3.6-2 Natural uranium concentration in a sedimentary rock from the Tono mine

Top: Photograph of a section of sedimentary rock
Bottom: Autoradiograph of the same rock section
The white areas in the autoradiograph indicate natural uranium concentration which is heterogeneously distributed in the sedimentary rock and is controlled by the fabric of the rock.



a: Microfracture within detrital grains



b: Cleavage of sheet silicates



c: Micropores within clayey matrix

Figure 3.6-3 Pathways for nuclide migration in sedimentary rocks

Left: SEM images of porespaces
Middle: Photomicrographs (plane-polarized light)
Right: (a, c) α-track images and (b) U-Mα characteristic X-ray photograph
Natural uranium (black spots in the α-track images and white spots in the U-Mα characteristic X-ray photograph) is distributed along microfractures within detrital grains (e.g. quartz), cleavages of sheet silicates (e.g. biotite) and micropores in the matrix. Microscopic observations indicate that these porespaces have acted as pathways for natural uranium migration.

pores between grains. In addition, pore spaces were also impregnated with the resin. Pore-spaces of the above types i to iii are thought to have functioned as pathways for solute transport. Natural uranium is distributed along the pathways mentioned above (Figure 3.6-3a-c). In addition, a zone showing luminescence under UV light was developed along the microfractures within quartz grains and at the margins of the grains surrounded by the uranium-concentrated matrix. This indicates that the above three types of pore spaces were accessible to natural uranium migration (Yoshida, 1994; Yoshida et al., 1994b).

Hydraulic tests in boreholes were carried out in conjunction with the mineralogical and chemical characterization of the rock samples, to understand the relationship between the flow of groundwater and the accumulation of natural uranium. The hydraulic conductivity of the zone with high uranium contents is 2 to 3 orders of magnitude higher than that of the low uranium-concentration zone, which suggests that natural uranium has concentrated preferentially in permeable zones with multiple fluid pathways (Yoshida et al., 1994a).

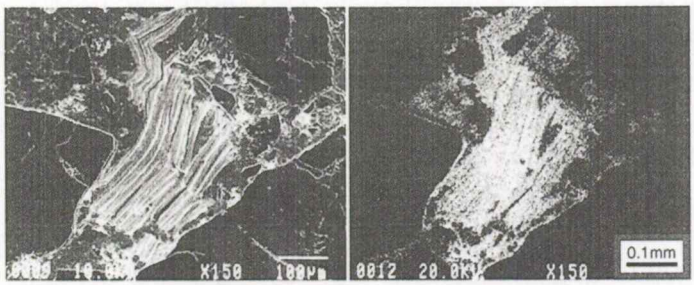
To summarize, radionuclides can migrate through, or be trapped by, the interconnected pore spaces in sedimentary rocks. The existence, geometry and degree of connectivity of the pathways, as well as the chemical retardation of radionuclides caused through water-rock interactions, will control solute transport in sedimentary rocks.

2) Chemical retardation (sorption / mineralization)

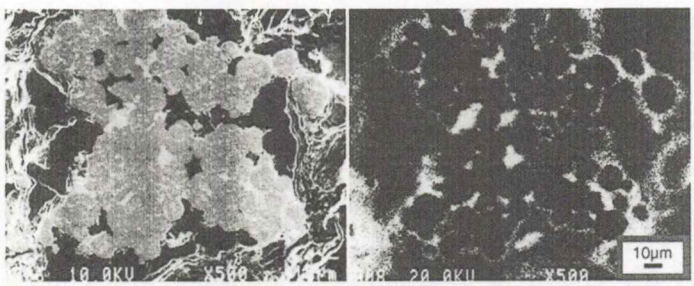
In the uranium-bearing sedimentary rocks of the Tono deposit, groundwater flow is so slow that solute transport occurs principally by diffusion (Yoshida et al., 1994b; Ota and Yoshida, 1995). In such formations, chemical interactions between radionuclides and the host rock are the most important processes that retard their migration relative to that of groundwater. Sorption and mineralization are particularly important as retardation mechanisms (e.g. McKinley and Hadermann, 1985). In order to assess chemical retardation processes, batch sorption experiments with uranium solutions were undertaken. Also, detailed petrological and radiochemical investigations using SEM, alpha-autoradiography and EPMA techniques were applied to rock specimens and to minerals separated from them. Moreover, to clarify the extent of the natural uranium migration and retardation to date in the sedimentary rocks, studies of ^{238}U decay series (^{238}U, ^{234}U, and ^{230}Th) disequilibrium were carried out.

Batch sorption experiments using ^{233}U as a tracer show that the uranium sorbing ability of rocks with low uranium concentrations is 2 orders of magnitude greater than that of rocks rich in uranium (Yoshida et al., 1994a). This is contradictory to the evidence from natural uranium distributions. A possible explanation is that there may be a large number of uranium sorption sites remaining in rocks with low uranium concentrations. In contrast, rocks with high uranium concentrations may no longer have the ability to sorb uranium due to the saturation of their uranium sorption sites.

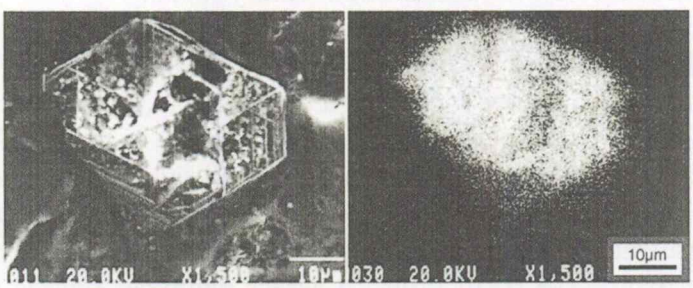
In the sedimentary rocks of the Tono area, natural uranium has concentrated along the cleavages of biotite (Figure 3.6-4a), around framboidal pyrite (Figure 3.6-4b), inside altered ilmenite (Figure 3.6-4c), in sericitized plagioclase and on the surface of lignite (Yamana and Nohara, 1990; Yamakawa, 1991; Yoshida et al., 1994a, c). Laboratory experiments (Ota et al., 1994) (Figure 3.6-5) have shown that iron-containing minerals, clay minerals and lignite have a higher ability to take up uranium under reducing conditions. Uranium sorption is higher for more argillaceous or tuffaceous siltstones than for sandstones (Figure 3.6-5), which clearly indicates that the content of micas and clay minerals will control the ability of the rock to sorb uranium. In previous studies, it has already been ascertained that uranium Kd values for clay



a: Cleavage of biotite



b: Framboidal pyrite



c: Altered ilmenite

Figure 3.6-4 Natural uranium retardation associated with iron-containing minerals in sedimentary rocks from the Tono mine

Left: BSE images, *Right*: U-Mα characteristic X-ray photographs
Natural uranium has been retarded in iron-containing minerals such as biotite, pyrite and altered ilmenite (white spots in the U-Mα characteristic X-ray photographs).

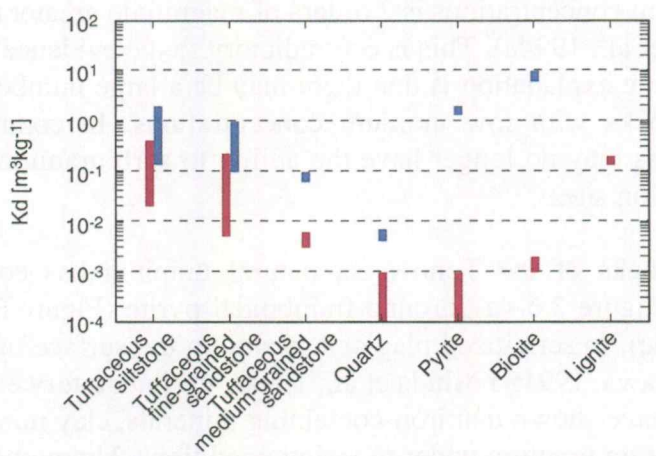


Figure 3.6-5 Batch Kd values for various sedimentary rocks from the Tono mine and their constituents

Red lines: Kd under reducing conditions, Blue lines: Kd under oxidizing conditions
Biotite, pyrite and lignite, all of which are common constituents in sedimentary rocks in the Tono uranium deposit, and highly argillaceous rocks have higher uranium Kd values.

minerals (smectite, illite and kaolinite), muscovite, chlorite, zeolite, hematite and goethite (or iron oxyhydroxides) are generally high, whereas those for quartz, feldspar, calcite, epidote and gypsum are low (Ames et al., 1983a, b; Berry et al., 1991, 1994; Ticknor, 1993, 1994). This may result from the differences in the specific surface area of minerals, in addition to their surface chemical properties.

Uranium series disequilibrium studies show that the individual constituent minerals in sedimentary rocks with high uranium concentrations are in a significant disequilibrium state. However, the whole rock is in chemical equilibrium (Figure 3.6-6). Although preferential ^{234}U leaching from clay minerals and preferential ^{234}U accumulation in lignite must have occurred on a microscopic scale, the whole rock has not suffered geochemical disturbance. This indicates that, in the sedimentary rocks, reducing conditions have been maintained for at least the past several hundred thousand years (Yoshida et al., 1994a, b).

The occurrence of primary uranium minerals in sedimentary rocks with a high uranium content indicates that natural uranium was retarded by mineralization. Trace amounts of coffinite and pitchblende, with a size of 0.1 to 1 μm, were identified as primary uranium minerals on the surface of biotite cleavage and of lignite and around pyrite (Katayama et al., 1974; Komuro et al., 1990; Yoshida, 1994).

In summary, in the Tono uranium deposit very slow groundwater movement and reducing conditions have encouraged chemical retardation (sorption and mineralization) of natural uranium for the past ten million years (Yusa et al., 1993; Seo and Yoshida, 1994, Yoshida, 1994). This uranium deposit has been well preserved for a long time period in spite of tectonic disturbances such as faulting and uplift. This suggests that, as long as the ambient hydrogeological and geochemical environments are maintained, it is likely that rock formations could retain redox-sensitive radionuclides for long periods of time (Yamakawa, 1991; Yusa et al., 1993).

3) Chemical retardation (coprecipitation)

Iron oxides or oxyhydroxides occur in an altered zone over a distance of several cm from the surface of certain water-conducting fractures in the granite basement at Tono. It should be noted that, in these zones, the redox-buffering capacity of the rock is important for reducing the solubility and mobility of the radionuclides. Additionally, in these zones the groundwater at the redox front may form colloids (Alexander et al., 1990a). Such solute transport and retardation phenomena could thus represent a natural analogue of radionuclide migration in an environment where a redox front forms. Changes in chemical composition, geometry of pathways and the form of uranium mineralization extending from the surface of water-conducting fractures into the granite matrix were studied in detail. Various techniques were used, such as chemical analysis, pore space examination and ^{238}U decay series analyses of rock core specimens.

In the brown-colored altered zone near fractures, Fe^{3+} was precipitated and concentrated as iron oxides and oxyhydroxides (Figure 3.6-7), along with concentration (coprecipitation) of natural uranium. The porosity of the altered zone is lower than that of the unaltered host rock. This could be interpreted as the result of water/rock interactions, specifically the formation of iron oxides or the precipitation of iron oxyhydroxides, within the groundwater pathways. The formation of iron oxides could have resulted in a reduced permeability in the altered zones near water-conducting fractures, preventing the zones from being geochemically disturbed for the past several hundred thousand years (Hanamuro and Yoshida, 1997).

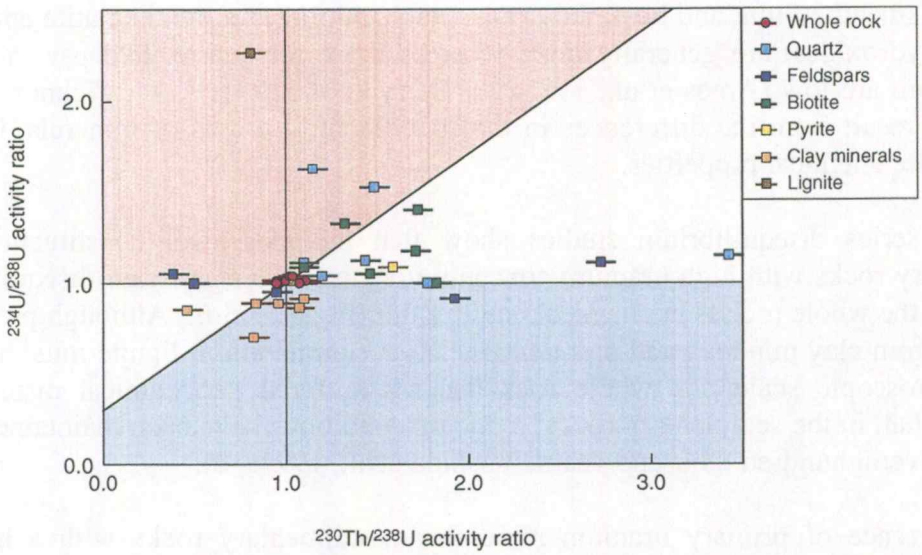


Figure 3.6-6 Geochemical processes of ^{238}U-decay series in sedimentary rocks from the Tono mine

In the Tono uranium deposit, although preferential uranium accumulation (pink area) and leaching (light blue area) have been occurring within the past several hundred thousand years, the whole rock has apparently maintained chemically stable conditions.

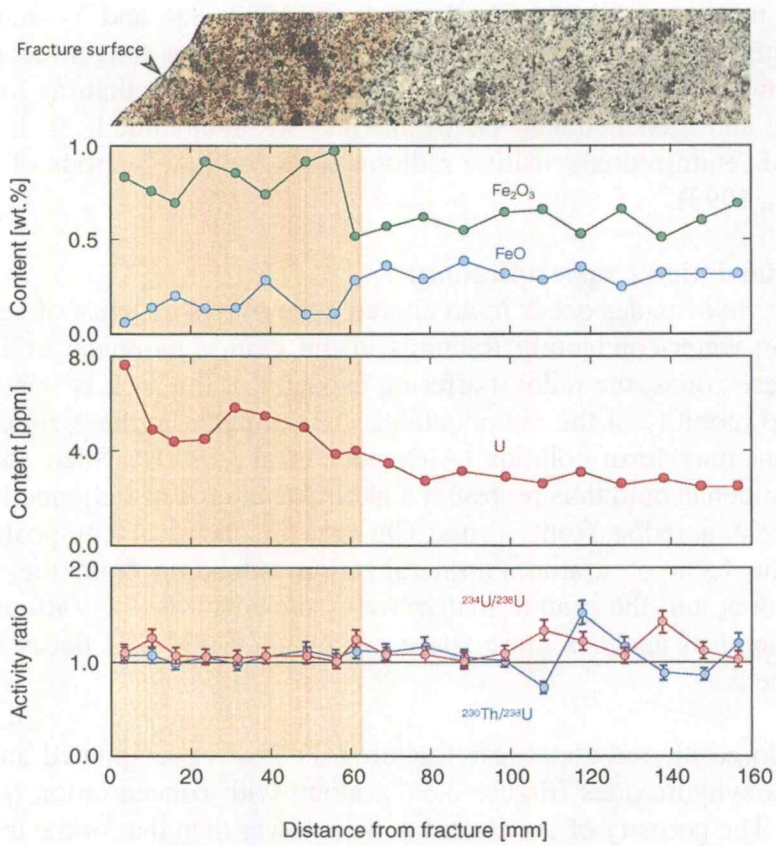


Figure 3.6-7 Iron and ^{238}U-decay series profiles from a water-conducting fracture into the Toki granite matrix

Top: Photograph of a section of investigated core sample

^{238}U-decay series have been retained for more than several hundred thousand years, without suffering geochemical disturbances, in Fe^{3+} concentrated altered zone (brown area) behind the water-conducting fracture.

This research suggests that altered and oxidized zones adjacent to water-conducting fractures function not only as chemical retardation sites but also physically control solute transport by the formation of secondary minerals. Therefore, these zones can retain radionuclides for long periods of time.

4) Colloid-facilitated solute transport

Groundwater colloids may be significant in facilitating solute transport, due to their large specific surface area and electrical charge and the availability of sorption sites (Ryan and Gschwend, 1990). To understand the effects of groundwater colloids on ^{238}U decay series migration, colloid properties were characterized in groundwater samples from Tono. Groundwater samples containing colloids were concentrated by ultrafiltration under anaerobic conditions and filtered groundwater samples were also collected to determine the concentrations of uranium, thorium and rare-earth elements (REEs).

The concentration of groundwater colloids is quite low in the Tono mine, with 1 to 1.5 mg l^{-1} (size range 1 μm to 20 nm). Colloids consist mainly of sulfur-rich particles and silicate and carbonate minerals (see Section 3.4). None of the colloids are associated with uranium, thorium and REEs. In the Tono mine, the concentration of groundwater colloids is too low to sorb significant amounts of radionuclides and thus to aggregate (Miller et al., 1994; Degueldre, 1994). Colloid-facilitated solute transport can, therefore, be ignored for groundwater in the Tono area (Seo and Moulin, 1995).

3.6.2 Case studies at the Kamaishi mine

A natural analogue study and in situ experiments supported by laboratory and modeling work were carried out in the Cretaceous granodiorite of the Kamaishi mine, to develop an understanding of solute transport phenomena in fractured crystalline rocks (JNC, 1999). The granodiorite is considered to be typical of the Cretaceous granitoids that are widely distributed throughout Japan. It is assumed that solute transport phenomena in the Kamaishi mine may thus be representative of such phenomena in fractured crystalline rocks in Japan.

1) Microscopic pore space geometry

In fractured (crystalline) rocks, radionuclides are significantly retarded relative to the velocity of groundwater flow by the process of matrix diffusion. In this process, radionuclides dissolved in the aqueous phase diffuse into stagnant porewater in the dead-end pore space (e.g. Neretnieks, 1980; Nagra, 1994). To investigate this process, the rock matrix behind fractures was impregnated in situ with a very low viscosity resin (Alexander et al., 1996; Frieg et al., 1998). The entire impregnated volume was then recovered by large diameter (150 to 200 mm) overcoring. These techniques proved to be the most suitable for minimizing the physical and chemical disturbances to the fracture and the adjacent rock matrix. A three-dimensional physical description of the matrix was carried out for core sub-samples recovered from the site.

In situ experiments revealed that, within fracture-filling layers, a stilbite and chlorite layer 1 to 2 mm thick occurred on either side of the boundaries between the altered wall rock and the fracture fillings. This layer functioned as a flow channel (Figure 3.6-8). In the matrix behind the fracture, an interconnected network consisting of the following four types of microporosity (10 nm to 0.1 mm in size) exists:

i. microfractures (Figure 3.6-9a);

ii. grain boundary porosity (Figure 3.6-9a);
iii. cleavage (Figure 3.6-9b);
iv. a zone with sheet silicate porosity (Figure 3.6-9c).

This network is accessible to migrating radionuclides (Ota et al., 1997). A slickensided plane occurs along the stilbite/chlorite layer where the fracture has reactivated. This plane is generally porous and includes open microfractures with lengths of 5 to 10 mm and widths of 0.1 to 1 mm.

The frequency and mean aperture of the microporosity features decreases with increasing distance from the main fracture and dramatically changes at the boundary (10 to 100 mm away from the fracture surface) between the hydrothermally altered matrix and the unaltered granodiorite matrix (Figure 3.6-10). Grain boundary porosity and microfractures with apertures smaller than 10 μm dominate the in situ connected porosity within the unaltered matrix. However, in the altered matrix, microfractures predominantly orientated sub-parallel to the larger fractures increase in frequency and size towards the main fracture. Adjacent to larger fractures, connected porosity is also found along cleavages of chlorite and altered hornblende, as well as in clay-rich layers. A three-dimensional reconstruction of the in situ connected porosity reveals that the connectivity, as well as the porosity, of the matrix microporosity decreases with distance from the main fracture (Ota et al., 1999).

The microscopic pore space geometry recognized in the rocks of the Kamaishi mine is considered to be the result of past hydrothermal alteration and consequent reactivation of the fracture. This process might have resulted in a significant decrease in the rock volume available for solute transport away from the water-conducting fracture into the unaltered matrix. This suggests that radionuclide mobility due to physical processes decreases away from the fracture. Other case studies on fractured crystalline rocks (Alexander et al., 1990b; Heath et al., 1992) also reported that the extent and degree of microstructural alteration would control solute transport taking place in the vicinity of the water-conducting fracture.

In summary, on a scale of several decimeters, the principal elements of water-conducting fractures which will control solute transport are:

- the structure of fracture-filling minerals
- the structure of flow channels within the fracture
- the altered matrix surrounded by the unaltered host rock.

A conceptual model of the geometry of solute transport pathways in fractured rock is shown in Figure 3.6-11. The pathways are represented by a rectangular mesh of flow channels within a mineralized zone and an altered zone, both of which have a constant thickness. This conceptual model takes into account the principal factors at Kamaishi, especially the width, length and aperture of flow channels and the extent of connected porosity. Thus, conceptual modeling of water-conducting fractures was possible on a small-scale (Ota et al., 1999).

2) Physical retardation (matrix diffusion)
In order to examine matrix diffusion phenomena around water-conducting fractures, ^{238}U decay series (^{238}U, ^{234}U, ^{230}Th) profiles from fractures into the host granodiorite were obtained.

Work carried out on ^{238}U decay series disequilibrium shows that natural thorium concentrations are relatively invariable but there are distinct changes in the distribution of

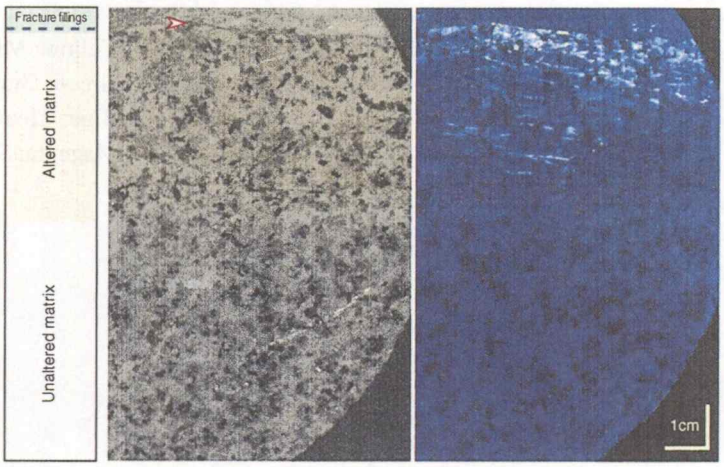


Figure 3.6-8 *In situ* connected porosity behind a water-conducting fracture in a crystalline rock from the Kamaishi mine

Left: Photograph of a section of resin-impregnated rock, *Right*: UV fluorescence image of the same section The white areas in the fluorescence image represent *in situ* connected porosity, which extends from a stilbite+chlorite layer (red arrow) as a flow channel into the Kurihashi granodiorite matrix.

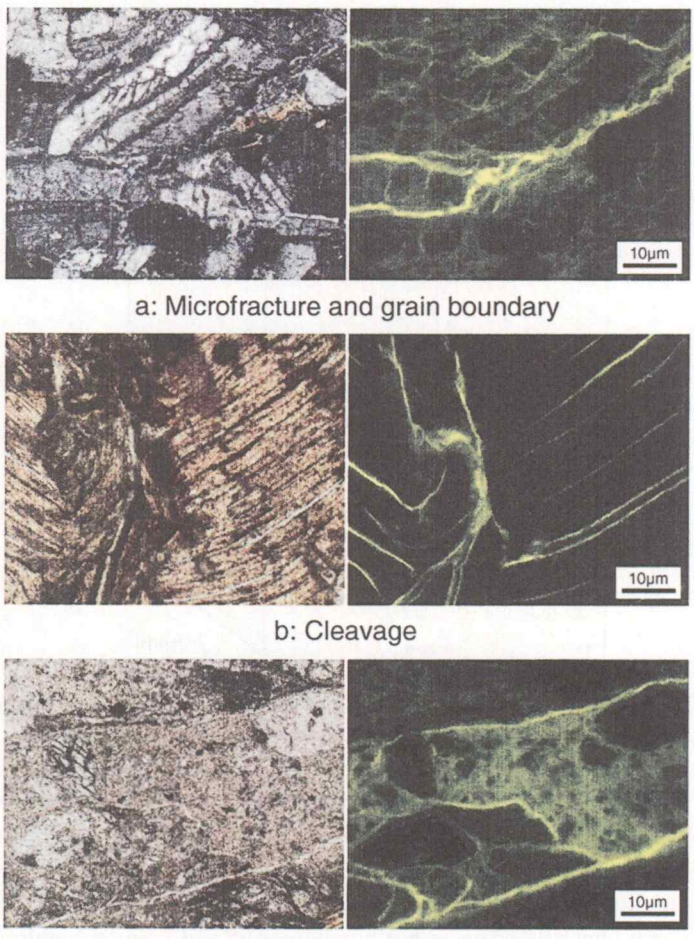


Figure 3.6-9 Pathways for nuclide migration in fractured crystalline rocks

Left: Photomicrographs in transmitted light

Right: Photomicrographs of the same field under UV ilumination

Microfractures and grain boundaries, cleavages and sheet silicate porosity in a porous zone have acted as pathways for nuclide migration (yellow areas in UV fluorescence photomicrographs).

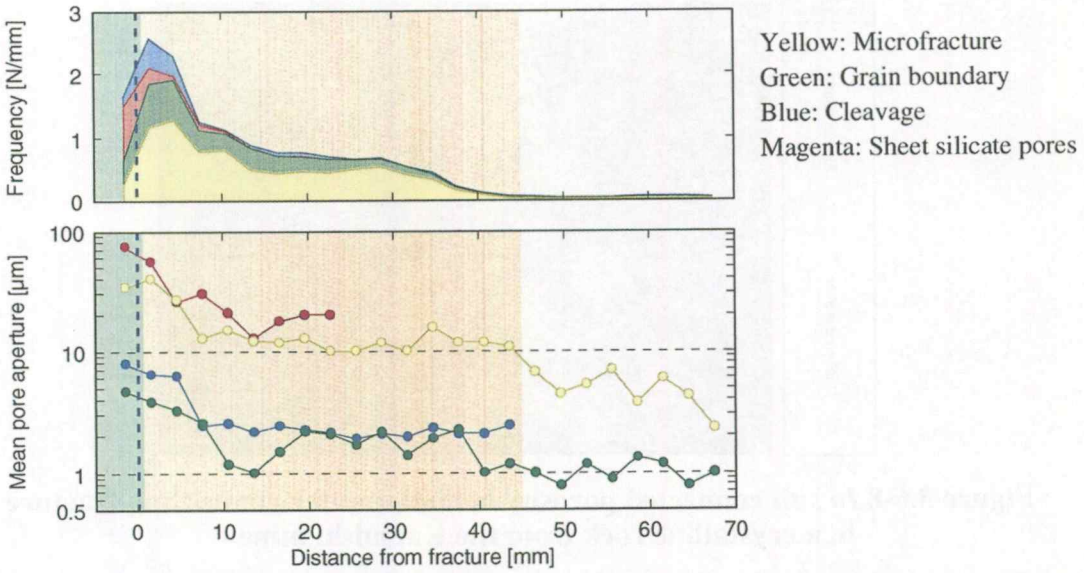


Figure 3.6-10 Distribution of *in situ* connected porosity behind a water-conducting fracture in Kurihashi granodiorite at the Kamaishi mine

Microfractures and sheet silicate pores dominate *in situ* connected porosity in the fracture fillings (light green areas) and the altered matrix (orange areas) , whereas grain boundaries dominate in the unaltered matrix (white areas). The frequency and mean aperture of the porosity decrease with increasing depth from the fracture (blue dashed lines).

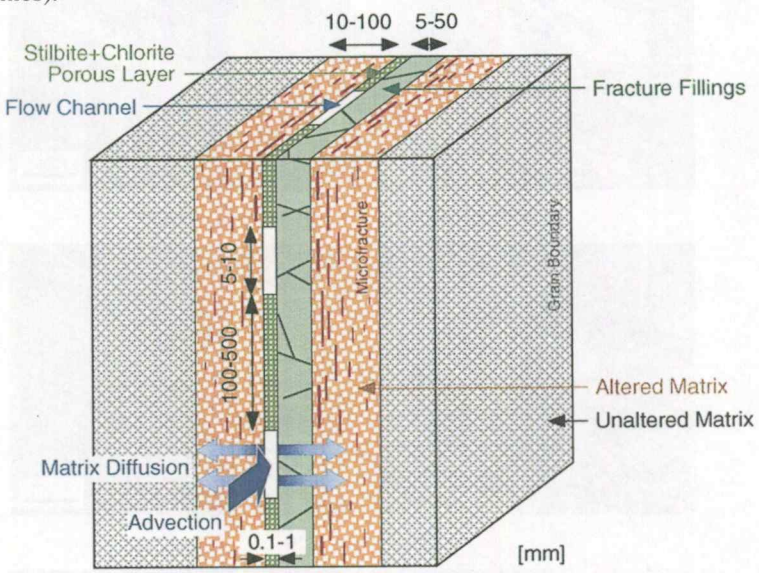


Figure 3.6-11 Small-scale conceptual model of a water-conducting fracture in Kurihashi granodiorite at the Kamaishi mine

The geometry of a water-conducting fracture in the Kurihashi granodiorite can be represented schematically by planar fracture fillings containing a mesh of flow channels and by a uniform altered matrix, both of which have defined thickness. Solute transport can be described as advective flow coupled with matrix diffusion. This figure is a considerable simplification of reality. In particular, resin impregnation experiments suggest that the stilbite/chlorite layer in which channels occur is not homogeneous and may be highly porous (and potentially water-conductive) around the channels. 40 - 50 % of the interface between this layer (including the channels) and the adjacent rock is accessed by resin injected in impregnation experiments, whereas a lower proportion (about 2 %~ 20 %) would be expected on the basis of the observed widths and separations of the channels (JNC, 1999). The results of resin injection experiments, rather than the observed widths and separations of the channels, are used in PA as a basis for the transport parameter F (Figure 5.3.2-1 of Supporting Report 3), although it is acknowledged that this may be non-conservative.

natural uranium. The $^{234}U/^{238}U$ activity ratios of the fracture-fillings are higher than unity, corresponding to high $^{234}U/^{238}U$ activity ratios in flowing groundwater. In contrast, $^{230}Th/^{234}U$ activity ratios are lower than unity (Figure 3.6-12). These profiles indicate that, in locations where immobility of thorium was assumed, fracture-filling minerals have taken up uranium from the groundwater within the past several hundred thousand years. Mineralogical and chemical (especially iron content) profiles indicate that redox fronts have not formed in the rock. This suggests that uranium diffusion has been occurring outwards into the unaltered matrix over long timescales, such that ^{238}U-^{234}U-^{230}Th equilibrium has been re-established (Ota et al., 1997, 1999). Moreover, in the altered matrix behind the fracture, uranium sorption would have occurred onto chlorite, sericitized plagioclase and clay minerals (Ticknor, 1993; 1994).

In summary, the ^{238}U decay series disequilibrium studies showed that the matrix diffusion depth of natural uranium is at least 10 to 100 mm in the Cretaceous granodiorite in the Kamaishi mine. This depth is controlled by the geometric properties of in situ connected porosity, such as the distribution and connectivity of pore spaces, and by the sorption properties of constituent minerals accessible to solute transport. Similar studies have been carried out in fractured crystalline rocks in many other countries. These studies have reported that depths of matrix diffusion are at least several cm from water-conducting fractures (e.g. Alexander et al., 1990b; Smellie et al., 1986; Ménager et al., 1994; Suksi et al., 1992). Hence, the results from the Kamaishi in situ experiments are consistent with those from other similar studies.

3) Chemical retardation (sorption)

Advective solute transport, coupled with matrix diffusion in water-conducting fractures, was assessed by in situ pulse injection of a range of inactive tracers. These included non-sorbing uranine, chlorine and weakly to moderately sorbing strontium and cesium; injection was into narrow dipole (d = 0.25 m) flow-fields.

Even over the short flow distance of the dipole configuration, sorbing strontium and cesium show a slight retardation of the breakthrough peak, compared with non-sorbing uranine and chlorine (Figure 3.6-13a). Depressed peak concentrations of the sorbing tracers are also notable; these are 3 to 4 orders of magnitude lower than those of the non-sorbing tracers. Also, concentrations of calcium and sodium ions recovered following the breakthrough are almost equivalent to those of the injected sorbing tracers (Figure 3.6-13b), which indicates that considerable retention of strontium and cesium occurred in the fracture-fillings. The dominant mechanism for the retention of the sorbing tracers in the fracture-fillings (or around the flow channels) is considered to be rapid cation exchange between the cation pairs strontium/calcium and cesium/sodium (Ota et al., 1999).

Laboratory work shows that fracture-filling minerals have a higher ability to sorb uranium, strontium, cesium and selenium than the altered and unaltered rock matrix (Sato et al., 1997). Fracture-fillings composed mainly of micas and clay minerals generally have a high ability to sorb radionuclides.

In summary, even in water-conducting fractures where advective solute transport may predominantly take place, the complex effects of chemical retardation (i.e. sorption) can be expected as well as those of physical retardation, which play a significant role in far-field retardation of solutes.

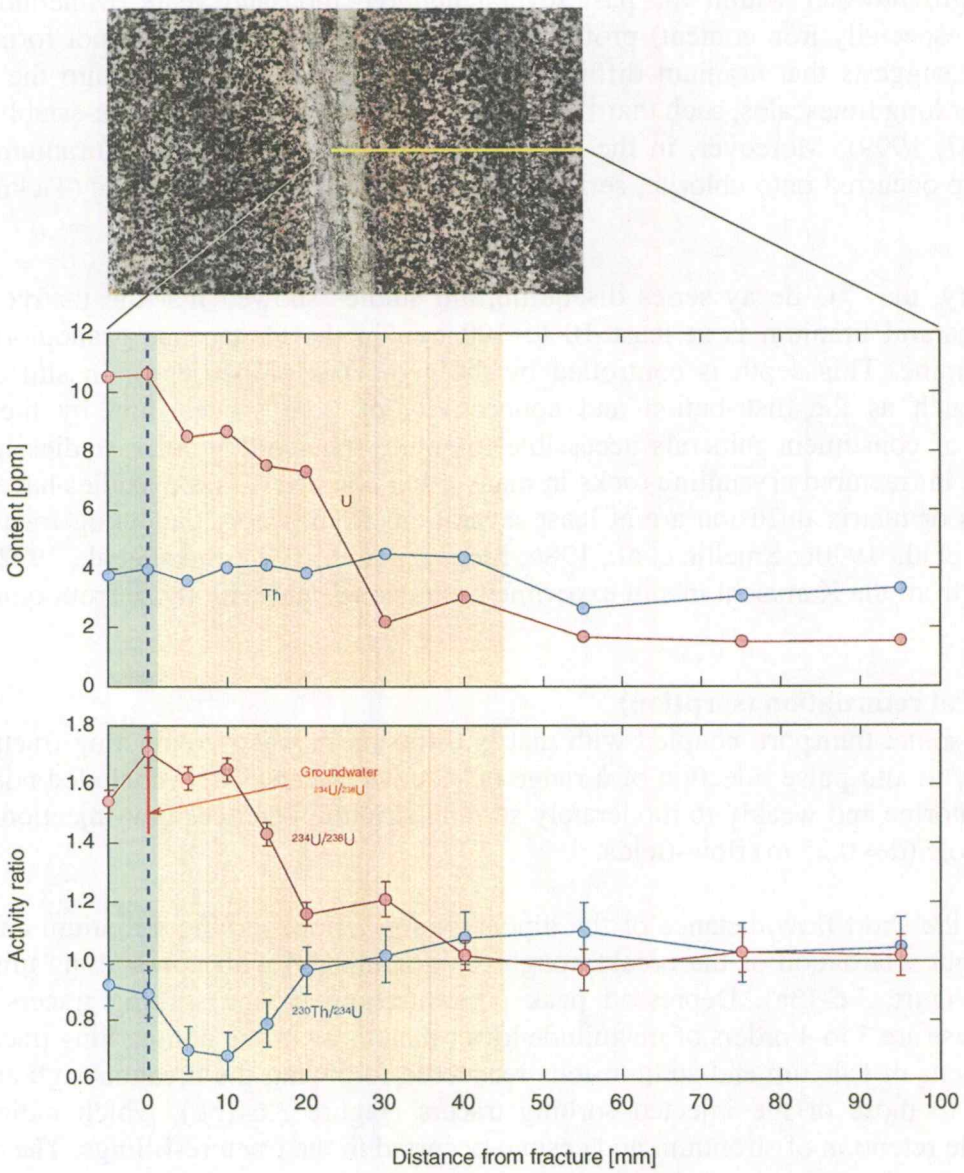


Figure 3.6-12 ^{238}U-decay series profiles from a water-conducting fracture into Kurihashi granodiorite matrix at the Kamaishi mine

Top: Photograph of the investigated water-conducting fracture in the Kamaishi mine Recent uranium uptake from groundwater on the fracture fillings (light green areas) has occurred, followed by uranium diffusion outwards into the unaltered matrix. Natural uranium diffusion reaches around the boundary between the altered matrix (orange areas) and the unaltered matrix (white areas).

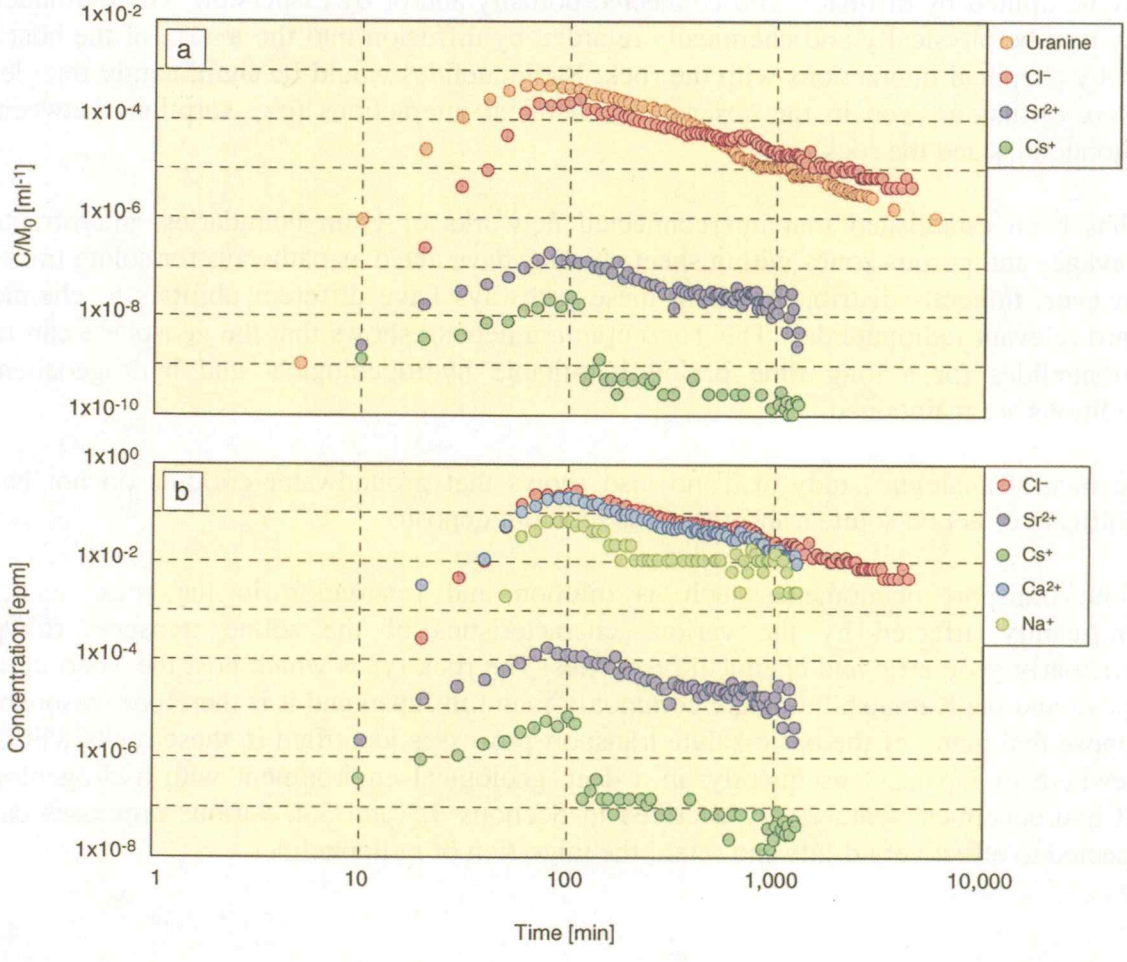


Figure 3.6-13 Retardation of different inactive tracers in a water-conducting fracture in Kurihashi granodiorite at the Kamaishi mine

a: Breakthrough profiles (C: tracer outflow concentration, M_0: mass of injected tracer),
b: Recovery profiles following the breakthrough

Injected Sr^{2+} and Cs^{+} were retained in the fracture fillings by cation exchange between cation pairs Sr^{2+}/ Ca^{2+} and Cs^{+}/ Na^{+}. The profiles of sorbing Sr^{2+} and Cs^{+} also show a small retardation of the breakthrough peak as compared with non-sorbing uranine and Cl^{-}.

3.6.3 Summary

Natural analogue studies and in situ experiments performed in the Tono uranium deposit and the Kamaishi mine clearly demonstrate that radionuclides transported in flowing groundwater may be diluted by diffusion into connected porosity and/or by dispersion. The radionuclides may also be physically and chemically retarded by diffusion into the matrix of the host rock and by chemical interactions with the rock. Radionuclides would be significantly retarded by matrix diffusion, even in the absence of chemical interactions (e.g. sorption) between the radionuclides and the rock.

It has been established that interconnected networks of grain boundaries, microfractures, cleavages and porous zones within sheet silicates have acted as pathways for solute transport. However, minerals distributed along these pathways have different abilities to chemically retard relevant radionuclides. The Tono uranium deposit shows that the geosphere can retain radionuclides for a long time period if suitable hydrogeological and hydrogeochemical conditions are maintained.

The natural analogue study at Tono also shows that groundwater colloids do not have a significant effect on solute transport in the uranium deposit.

Solute transport phenomena, such as dilution and retardation in the rock mass, are significantly affected by the various characteristics of the solute transport flowpath, particularly geometric and chemical properties. The rock types which host the Tono uranium deposit and the Kamaishi mine are commonly found in Japan and it is therefore reasonable to suppose that many of the basic solute transport processes identified in these rocks will occur elsewhere in Japan. Consequently, in a deep geological environment with hydrogeological and hydrochemical features as described in Sections 3.3 and 3.4, various processes can be expected to effectively dilute and retard the migration of radionuclides.

3.7 Natural analogue studies

The basic aims of natural analogue studies relevant to the geological disposal of radioactive waste are:

- to obtain an understanding of processes expected to occur over geological timescales within the disposal system by studying natural phenomena that are analogous to processes occurring within a repository (e.g. the migration and retardation of radionuclides);
- to improve the reliability of extrapolations of short-term laboratory data used for evaluating the safety of the disposal system (e.g. Côme and Chapman, 1986).

In natural analogue studies relevant to radionuclide migration and retardation in a geological disposal system, it is important to define the system to which the analogue is being applied, the processes concerned and the relationship between these processes and conceptual models.

A number of natural analogue studies have been based on uranium ore deposits, both in Japan and abroad. These studies have focused on chemical analogues of a repository system. One advantage of such studies is that they help to demonstrate the ability of geological environments (geochemical environments in particular) to retain radioactive materials. A good example is the natural fission reactor in the Oklo ore deposit in Gabon, Africa (IAEA, 1975, 1978). This high-grade uranium ore deposit underwent nuclear fission chain reactions in its natural setting soon after its formation about 2 billion years ago. As a result, fission products and transuranic elements were generated in the rock formations (e.g. Brookins, 1990). Researchers from France and other countries have studied the Oklo ore deposit and have confirmed that many radioactive elements generated there have been mostly contained within the geological environment over the past 2 billion years. This suggests that possible long-term immobilization of transuranic elements in the geosphere can be expected (e.g. Curtis et al., 1989).

Other natural analogue studies based on uranium ore deposits include the Koongarra project in Australia (e.g. Duerden et al., 1987), the Cigar Lake study in Canada (e.g. Goodwin et al., 1989) and the Osamu Utsumi project in Brazil (e.g. Chapman et al., 1990). It was found in all these cases that uranium, thorium and other radioactive elements had remained in the geological environment for a long period of time.

In Japan, studies have been carried out in the Tono uranium ore deposit in Gifu Prefecture (e.g. Yamakawa, 1991; Yusa et al., 1993; Yoshida, 1994). The Tono deposit has been preserved since its formation around 10 million years ago, although it has been exposed to various natural phenomena such as fault activity. Paleohydrological studies have also been carried out in the Tono region, with the aim of estimating the long-term, gradual changes that take place in the geological environment.

Studies of matrix diffusion carried out in underground tunnels of the Kamaishi mine are also described in this section. This process is very important in the retardation of radionuclide migration.

3.7.1 Examples of natural analogue studies

Natural analogue studies of the Tono, Oklo and Koongarra uranium ore deposits are summarized in the following sections. Particular attention is given to the retention of

radionuclides in the geological environments at these sites over geological timescales.

1) Migration and retardation of natural uranium series nuclides

(1) Tono uranium ore deposit

The Tono uranium ore deposit, the largest in Japan, is thought to have formed about 10 million years ago (Ochiai et al., 1989). The basement rock of the Tono region consists of granite that formed about 70 million years ago (Ishihara and Suzuki, 1969; Suzuki and Adachi, 1998). It is overlain by sandy and tuffaceous sedimentary layers of the Mizunami Group, which were deposited between 20 and 15 million years ago, when this region was covered by either an inland lake or a shallow marine sea (Itoigawa, 1974a). The same type of rock is widely distributed in a zone reaching from the Tono area to the Seto Inland Sea region (Itoigawa, 1980).

The uranium ore deposit, which is disseminated in the lowermost part of the Mizunami Group, is believed to have been formed when uranium in the granite was dissolved in migrating pore fluids and then deposited under reducing conditions (Katayama et al., 1974). It can be inferred that the uranium ore deposit has been preserved because a deep, chemically reducing geological environment has been maintained for a long period of time (Shikazono and Utada, 1997).

In the time period between 15 and 5 million years ago, the Tono region was uplifted and the Mizunami Group was subjected to denudation (Itoigawa, 1980). Because of the movement of the Tsukiyoshi fault, which is thought to have formed after the mineralization, the Mizunami Group was locally displaced vertically by as much as 30 m. Although the uranium ore body was cut by this fault, it has been preserved without migration of uranium across the fault (Figure 3.7-1) (Shinjo et al., 1997). Denudation continued until about 5 million years ago, when the region began to subside and the Mizunami Group was overlain by fluvial and lacustrine sand and clay deposits of the Seto Group (Itoigawa, 1974b). The deposition of the Seto Group continued until about 700,000 years ago, after which the region was again subjected to denudation.

Consequently, the Tono uranium ore deposit has been preserved, since its formation about 10 million years ago, despite fault movement, uplift, subsidence, denudation, deposition and climatic and sea-level changes. This means that in the deep geological environment in this area these processes did not significantly perturb the key geochemical parameters relevant for controlling uranium mobility, notably pH and Eh.

The above conclusion is also supported by the groundwater geochemistry. For example, studies of groundwater geochemistry indicate that the groundwater in the Mizunami Group, which contains the ore deposit, is reducing and originated from rain fall around at least 15,000 years ago (Mizutani et al., 1992). The geochemical conditions also imply that water/rock interactions cause major rock-forming minerals to approach saturation and produce the quite strong reducing environment (in the sulfide stability field; Iwatsuki et al., 1995) within timescales that are less than or equal to the residence time of the water in the formation.

Uranium series nuclides (^{238}U, ^{234}U and ^{230}Th) in rock samples collected from different locations in the deposit were found to be almost in radioactive equilibrium (e.g. Yusa and Yoshida, 1993; see also Figure 3.6-6). This indicates that these nuclides have been maintained in a closed system over a long period of time. Based on the time required for achieving radioactive equilibrium from the half-life of the parent nuclide, it is considered that uranium

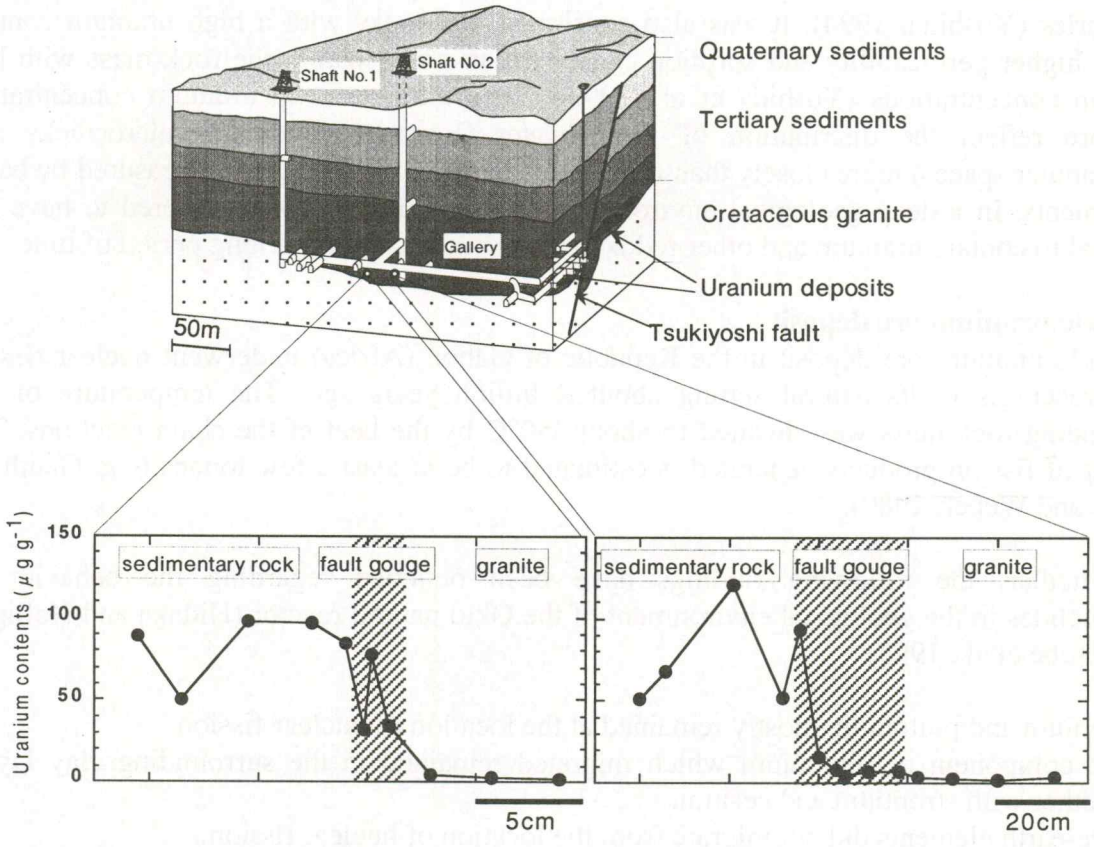


Figure 3.7-1 Concentration profile of uranium in the Tsukiyoshi fault, Tono uranium deposit (Shinjo et al., 1997)

The Tono uranium deposit is distributed in Tertiary sedimentary rocks, in the Tono area, central Japan. The uranium ore body is cut by the Tsukiyoshi fault. However, the migration of uranium has not been observed within Tsukiyoshi fault gouge.

and thorium have moved no further than a few centimeters during at least several tens of thousands of years (Yoshida et al., 1994a).

Observations using electron microscopy (e.g. SEM) indicate that uranium is concentrated in biotite and other rock-forming minerals, in fractures in quartz grains and on mineral grain boundaries (Yoshida, 1994). It was also confirmed that rocks with a high uranium content have a higher permeability and sorption capacity than zones within the rock mass with low uranium concentrations (Yoshida et al., 1994b). The differences in uranium concentration therefore reflect the distribution of groundwater flowpaths (such as microcracks and intergranular spaces) more closely than differences in the sorption capacity measured by batch experiments. In a deep geological environment, this type of rock is considered to have the potential to contain uranium and other redox-sensitive nuclides over a long period of time.

(2) Oklo uranium ore deposit

The Oklo uranium ore deposit in the Republic of Gabon (Africa) underwent nuclear fission chain reactions in its natural setting about 2 billion years ago. The temperature of the surrounding rock mass was elevated to about 350°C by the heat of the chain reactions. The amount of fission products generated is estimated to be at least a few tonnes (e.g. Gauthier-Lafaye and Weber, 1989).

In particular, the following findings have been obtained regarding the behavior of radionuclides in the geological environment of the Oklo natural reactor (Hidaka and Holliger, 1998; Isobe et al., 1995):

- Uranium and plutonium mostly remained at the location of nuclear fission.
- The component of plutonium which migrated remained in the surrounding clay layers together with strontium and cesium.
- Rare-earth elements did not migrate from the location of nuclear fission.
- Even in the near-surface oxidizing environment, only some of the elements present, including strontium and cesium, migrated from the location of nuclear fission.

The above findings indicate that radionuclide-containing phases may remain stable over a long period of time in deep geological environments, and that clay layers behaving like the clay-rich buffer materials of an EBS in the geological disposal system can play an effective role in retarding radionuclides.

(3) Koongarra uranium ore deposit

The Koongarra uranium ore deposit in Australia was formed about 1.7 billion years ago. The deposit consists of a primary zone, which reflects the original deposit, and a secondary zone, which was probably formed by the dissolution of uranium in oxygen-rich groundwater, followed by uranium reconcentration.

While uranium coexisted in a stable state with uranium minerals in the primary zone, it was dissolved from areas in the secondary zone that came into contact with oxygen-containing groundwater. The results of geochemical analyses and electron microscopy indicate that ferrous minerals played an important role in reconcentrating the dissolved uranium (e.g. Ohnuki et al., 1995; Yanase et al., 1991).

The above finding suggests that the carbon steel overpack now under consideration for use in the EBS will effectively sorb radionuclides even if they are dissolved in oxygen-containing

groundwater.

2) Natural analogue studies relevant to matrix diffusion

Matrix diffusion is an important process that retards the transport of nuclides in a rock mass in which fractures represent the main transport pathways. In order to evaluate this effect in deep geological environments, a study was conducted in existing tunnels of the Kamaishi mine.

The distribution and radioactive equilibrium/disequilibrium of natural uranium series nuclides (^{238}U, ^{234}U and ^{230}Th) were investigated. The variation in abundance of the nuclides was determined in profiles from a fracture surface to the rock matrix using rock samples collected from boreholes drilled into the tunnel walls.

While the profile of the natural uranium content in the rock is almost uniform, the $^{234}U/^{238}U$ activity ratio (>1) of fracture fillings is the same as that of groundwater and the $^{230}Th/^{234}U$ activity ratio is less than unity. This indicates that natural uranium in the groundwater is being supplied to the fracture fillings. Since geochemical changes in the rock matrix appear to be minimal, only the natural uranium series nuclides contained in the fracture fillings can diffuse into the rock matrix by taking a sufficient time to achieve radioactive equilibrium (see Figure 3.6-12) (Ota et al.,1999). Chlorite, sericite (within altered plagioclase) and other minerals that have a high uranium sorption potential (Ticknor, 1993, 1994) are abundant in the altered zone of rock surrounding fractures and the diffusion of natural uranium is considered to be affected by chemical interactions with these rock-forming minerals.

The overall results of the study of the distribution of natural uranium series nuclides indicate that the depth of matrix diffusion in the Cretaceous granodiorite of the Kamaishi mine ranges from 10 to 100 mm. The depth of matrix diffusion is considered to be controlled by the network structure of the porosity (distribution, connectivity and pore shapes) and by the sorption potential of minerals along transport pathways. A number of similar studies have also been carried out in other countries and have demonstrated that the depth of matrix diffusion from permeable fractures of crystalline rocks was in the order of a few centimeters (e.g. Alexander et al., 1990; Smellie et al., 1986; Menager et al., 1994; Suksi et al., 1992).

Natural analogue studies of matrix diffusion do not necessarily require a concentration of specific elements, such as uranium ore deposits, but can be applied to geological environments in general.

3.7.2 Summary

Natural analogue studies are considered to be useful for demonstrating the long-term stability of geological environments and disposal systems (e.g. Chapman et al., 1984). They can be used to evaluate the suitability of particular rock formations as natural barriers and as suitable environments for engineered barrier performance (Miller et al., 1994).

Uranium ore deposits, such as the Tono uranium ore deposit in Japan, have been used frequently for natural analogue studies. In most of these studies, the migration and retardation of natural radionuclides are investigated to assess the validity of computer codes used for PA and to obtain information on the long-term isolation properties of natural barriers.

At Tono, the geological environment of the uranium-rich ore body is reducing; under these

conditions, uranium series nuclides have been preserved for a long period of time. The deposit itself has been preserved since its formation around 10 million years ago, even though the ore body has been subjected to various geological events such as fault movement and uplift. Geochemically stable conditions were thus maintained over a long period of time, meaning that uranium was not significantly mobilized.

The approach used for studying the Tono uranium ore deposit can also be applied to other geological environments. For instance, a study of matrix diffusion, focusing on the altered zone of rock around fractures, has been carried out for various geological environments.

Future evolution of the geological environment may also be predicted using the paleohydrogeological approach that focuses on changes in topographic, geological and hydrological conditions on a geological timescale. The term "paleohydrogeology" has conventionally been used in the fields of petroleum and uranium exploration (e.g. Sanford, 1982, 1990). Chapman and McEwen (1993) considered this approach to be appropriate for validating methods for comprehensive evaluation of the performance of specific geological environments. Yusa et al. (1993) also emphasized the advantages of paleohydrogeological studies in the Tono uranium ore deposit, suggesting that they would be an appropriate way of providing integrated validation methods, not only for geology, geochemistry and hydrogeology, but also for solute migration and retardation.

Paleohydrogeological studies are still at a relatively early stage of development and there are still problems to be dealt with, e.g. recovery of old geographic information. These studies should, however, be developed as natural analogue studies (in the wide sense) with a view to providing integrated validation methods.

References

(3.2 Geological structures)

Abelin, H., Gidlund, J. and Neretnieks, I. (1982): Migration in a single fracture, Scientific Basis for Radionuclide Waste Management-V, W. Lutze (ed), Elsevier Sci. Pub. Co., pp.529-538.

Abelin, H., Neretnieks, I., Tunbrant, S. and Moreno, L. (1985): Migration in a single fracture: Experimental results and evaluation, Final report, Stripa Project Technical Report 85-03,

Alexander, W.R., Frieg, B., Ota, K. and Bossart, P. (1996): The RRP Project: Investigating radionuclide retardation in the host rock. Nagra Bulletin No.27, 43-55, Nagra, Wettingen, Switzerland.

Allard, B. (1982): Sorption of Actinides in Granitic Rock, SKBF/KBS Teck. Rep. KBS TR82-21, SKBF/KBS, Stockholm.

Amano, K. and Sato, H. (1989) : Neogene Tectonics of the Central Part of Northeast Honshu Arc, Chishituron (Geological Report), Vol.32, pp.81-96 (in Japanese).

Barton, N. (1977): A review of the shear strength of filled discontinuities in rock, Saertrykk, Fjellspreng, p.19.

Chapman, N.A. and McKinley, I.G. (1987): The Geological Disposal of Nuclear Waste, John Wiley & Sons, Chichester, UK.

Dershowitz, W.S. (1984): Rock joint systems, Ph.D. Dissertation, Massachusetts Institute of Technology, Cambridge, MA.

Gale, J., MacLeod, R. and LeMessurier, P. (1990): Site characterization and validation – Measurement of flowrate, solute velocities and aperture variation in natural fractures as a function of normal and shear stress, Stage 3, Stripa Project Report 90-11.

Hatsuyama, Y., Otsu, H., Oya, T. and Okamoto, J. (1993): A Study on Estimation of Permeability of in situ Rock Masses by Crack Tensor Theory, Proceedings of the 25th Symposium of Rock Mechanics, pp.313-317.

Hayashi, N., Tanaka, K., Kitamura, M. and Kamiyama, K. (1993): Technology Development on Construction of Large Scale Underground Cavity – Example : Underground Oil Storage Base -, -Denryoku-doboku-, No.244, pp.344-440 (in Japanese).

Ijiri, Y., Sawada, A., Akahori, K., Sugiyama, K., Ikeda, N., Saito, S., Morooka, K. and Uchida, M. (1999): Hydrological properties of fracture in rock, JNC Tech. Rep. (in press) (in Japanese).

Ikeda, K. (1979): The Property and Strength of Fissured Rock Masses, Journal of the Japan Society of Engineering Geology, Vol.20, No.9, pp.20-32 (in Japanese).

Ishihara, S. and Sasaki, A. (1991): Ore Deposits Related to Granitic Magmatism in Japan: A Magmatic Viewpoint, Episodes, Vol.14, pp.286-292.

JNC (1999): Final Report of Kamaishi In situ Experiment, JNC Technical Report, JNC TN7410 99-001 (in Japanese with English abstract).

Kanaori, Y., Yairi, K. and Miyakoshi, K. (1988): Deformation microstructures and their genetic rocks in the northeastern region of the Atotsugawa fault, central Japan, Jour. Geol. Soc. Japan, Vol.94, pp.887-901 (in Japanese with English abstract).

Kikuchi, K., Kuroda, and Mito, Y. (1987): Stochastic estimation and modelling of jointed rock masses based on statistical sampling, 6th Int. Congress ISRM, Montreal, Canada, pp.425-428.

Kimura, T. (1981): Investigation Approaches for Faults, especially for Faults with fracture zone, Journal of the Japan Society of Engineering Geology, Vol.22, No.1, pp.4-16 (in Japanese).

Kojima, K., Ohtsuka, Y. and Yamada, T. (1981): Distribution of Fault Density and -Fault

Dimension- in Rockmass and Some Trials to Estimate Them, Journal of the Japan Society of Engineering Geology, Vol.22, No.2, pp.88-103 (in Japanese).
McKinley, I.G. and Hadermann, J. (1984): Radionuclide Sorption Database for Swiss Safety Assessments, Nagra Tech. Rep. NTB 84-40, Nagra, Baden, Switzerland.
Nagra (1994): Kristallin-1: Conclusions from the Regional Iinvestigation Programme for Siting a HLW Repository in the Crystalline Basement of Northern Swizterland, Nagra Tech. Rep. NTB 93-09E, Nagra, Wettingen, Switzerland.
NEA (1991): Proceedings of an NEA/CEC Workshop on Heterogeneities in Hydrogeological Systems, Paris, October 1990, OECD, Paris.
Neretnieks, I. (1980): Diffusion in the rock matrix: An important factor in radionuclide retardation? J. Geophys. Res., Vol.85, pp.4379-4397.
Oda, M. (1985): Permeability tensor for discontinuous rock masses, Geotechnique, Vol.35, pp.483-495.
Oda, M. and Kimura, K. (1990): Size Distribution of Cracks in Rock Masses - On the Basis of Fractal Geometry -, Proceedings of the 8th Japan Symposium on Rock Mechanics, pp.55-60 (in Japanese).
Ogata, N., Ohsawa, H., Nakano, K., Yanagizawa, K. and Nishigaki, M. (1992): Relationships among Lithology, Permeability and Resistivity and their Application to Modelling of Hydrogeology, Journal of the Japan Society of Engineering Geology, Vol.32-6, pp.51-62.
Ogata, S. (1978): Quantitative Characterization of Distribution Parameters of Joints in Rock Masses, Journal of the Japan Society of Engineering Geology, Vol.19, No.1, pp.12-20 (in Japanese).
Ogata, S. (1984): Discontinuities in Rock Mass as a Factor of Rock Classification, Journal of the Japan Society of Engineering Geology, Special Issue, pp.17-24 (in Japanese).
Ohnishi, Y., Tanaka, M., Nakagawa, S., Matsuda, Y. and Torii, S. (1992): Estimation of Properties of Unexcavated Rock Mass in Tunnel from Investigation of Side Pilot Tunnel, The 27th Japan National Conference on Soil Mechanics and Foundation Engineering, pp.1315-1318 (in Japanese).
Ohno, H. and Kojima, K. (1992): Fractal on the Spatial Distribution of Fractures in Rock Mass Part 1: Fractal Distribution, Journal of the Japan Society of Engineering Geology, Vol.33, No.3, pp.11-24 (in Japanese).
Ohno, H. and Kojima, K. (1993): Fractal on the Spatial Distribution of Fractures in Rock Mass Part 2: Fractal Characteristics and Variability of Fractal Distribution, Journal of the Japan Society of Engineering Geology, Vol.34, No.2, pp. 12-26 (in Japanese).
Otsuki, K. (1989): Reconstruction of Neogene Tectonic Stress Fields of Northeast Honshu Arc from Metalliferous Veins, Chishituron (Geological Report), Vol.32, pp.281-304 (in Japanese).
Osawa, H., Sasamoto, H., Nohara, T., Ota, K. and Yoshida, H. (1995): Development of a Conceptual Flow-path Model of Nuclide Migration in Crystalline Rock: A Case Study at the Kamaishi In situ Test Site, Japan, Sci. Basis Nucl. Waste Manag. XVIII, pp.1267-1273.
Ota, K., Amano, K., Sato, H., Shibutani, T. and Tachi, Y. (1997): In situ Matrix Diffusion in Fractured Crystalline Rock, Kamaishi In situ Test Site, North-east Japan. In: 6th International Conference on the Chemistry and Migration Behavior of Actinides and Fission Products in the Geosphere, Abst. Migration'97, Sendai, Japan, 26-31 Oct. 1997, pp.98-99.
PNC (1992): Research and Development on Geological Disposal of High-Level Radioactive Waste, First Progress Report, PNC TN1410 93-059.
Priest, S.D. and Hudson, J.A. (1981): Estimation of discontinuity spacing and trace length

using scanline surveys, Int. Journal of Rock Mech. Sci. & Geomech. Abstr., Vol. 13, pp.135-148.

Sato, T., Ishimaru, T., Sugihara, K. and Shimizu, K. (1992): Data Collection by Literature Survey on Rock Physical Properties in Japan, PNC TN7410 92-018 (in Japanese with English abstract).

Scholz, C.H. (1990): The Mechanics of Earthquakes and Faulting, Cambridge University Press.

Shimo, M., Ijiri, Y., Iihoshi, S., Hashimoto, N. and Nagata, K (1992): Detection of Groundwater Flow Paths in a Rock using Geotomography and Cross-hole Injection Test, Proceedings of the 24th Symposium of Rock Mechanics, pp.31-35.

Shinjo, N. Yoshida, H. and Ota, K. (1997): An Analogue Study on Nuclide Migration in Tsukiyoshi Fault, Tono Uranium Deposit. In: 6th International Conference on the Chemistry and Migration Behavior of Actinides and Fission Products in the Geosphere, Abst. Migration'97, Sendai, Japan, 26-31 Oct. 1997, pp.94-95.

SKB (1992): SKI-91, Final Disposal of Spent Nuclear Fuel. Importance of the Bedrock for Safety, SKB Tech. Rep. 92-29. Swedish Nuclear Fuel and Waste Management Company, Stockholm, Sweden.

Takahashi, M., Xue, Z., Oowada, A. and Ishijima, Y. (1992): On the study of interconnected pore network using a blue dyed epoxy impregnated thin section, Jour. Japan Society of Engineering Geology,Vol.33, pp.50-62 (in Japanese with English abstract).

Tsang, Y.W. (1992): Usage of equivalent apertures for rock fractures as derived from hydraulic and tracer tests, Water Resources Research, Vol.28, No.5, pp.1451-1455.

Uchida, M., Doe, T., Dershowitz, W., Thomas, A., Wallmann, P. and Sawada, A. (1994): Discrete-fracture modelling of the Äspö LPT-2, large-scale pumping and tracer test, SKB International Cooperation Report 94-09.

Uchida, M., Noda, K., Maruyama, M. and Sudo, K. (1995): Laboratory Experiment on Flow and Mass Transport Properties of Single Fracture Rock Block, Proceedings of the 26th Symposium of Rock Mechanics, pp.156-160.

Watanabe, K., Obara, K. and Shinjo E. (1982): Investigation on Distribution of Fracture Properties and Anisotoropy of Permeability in Rock, Japan Society of Engineering Geology, Proceedings of Showa-57 Symposium, pp.57-60 (in Japanese).

Witherspoon, P.A., Wang, J.S.Y., Iwai, K. and Gale, J.E. (1980): Validity of cubic law for fluid flow in a deformable rock fracture, Water Resources Research, Vol.16, No.6, pp.1016-1024.

Yamaguchi, T., Isobe, H. and Nakayama, S. (1997): Analysis of microporous structure in granite, Radioactive Waste Research, Vol.3, pp.99-107 (in Japanese with English abstract).

Yamane, M., Nakano, K. and Sugihara, K. (1996): Long-term Observation of Ground Water Pore Pressure Change due to Shaft Excavation, Tsuchi-to-kiso, The Japanese Geotechnical Society, Vol.44, pp.24-26 (in Japanese with English abstract).

Yoshida, H. (1994): Relation between U-series nuclide migration and microstructural properties of sedimentary rocks, Appl. Geochem., Vol.9, pp.479-490.

Yoshida, H., Ohsawa, H., Yanagizawa, K. and Yamakawa, M. (1989): Analysis of fracture system in granitic rock, - Case study for the granitic rock, Gifu Prefecture, Japan - , Jour. Japan Society of Eng. Geol., Vol.30, pp.11-22.

Yoshida, H., Yui, M. and Shibutani, T. (1994): Flow-path structure in relation to nuclide migration in sedimentary rocks: An approach with field investigations and experiments for uranium migration at Tono uranium deposit, central Japan, J. Nucl. Sci. Technol., Vol.31, pp.803-812.

Yoshida, H., Aoki, K., Semba, T., Ota, K., Hama, K., Kawamura, M. and Tsubota, K. (2000):

Overview of the stability and barrier functions of the granitic geosphere at the Kamaishi Mine: relevance to radioactive waste disposal in Japan, J. Eng. Geol. Vol.56, pp.151-162.
Yusa, Y., Ishimaru, K., Ota, K. and Umeda, K. (1993): Geological and Geochemical Indicators of Paleohydrogeology in Tono Uranium Deposits, Japan, Proc. NEA Workshop, Paleohydrogeological Methods and thier Applications, OECD/NEA, pp.117-146.

(3.3 Groundwater flow characteristics)

Adachi, T. and Sugihara, K. (1996): Measurement of hydraulic conductivity in the excavation disturbed zone of sedimentary soft rock, Proceedings of the 51st annual conference of the Japan Society of Civil Engineers, 3-B, pp.362-363 (in Japanese).
Almen, K.E., Andersson, O., Fridh, B., Gustafsson, E., Nilsson, G. and Axelsen, K. (1986): Site investigation equipment for geological, geophysical, hydrogeological and hydrochemical characterization, SKB Tech. Rep. 86-16, SKB, Stockholm.
Banks, W.S.L., Paylor, R.L. and Hughes, W.B. (1996): Using Thermal-Infrared Imagery to Delineate Ground-Water Discharge, Ground Water, Vol.34, pp.434-443.
Black, J.H. (1986) : Crosshole investigations: The method, theory and analysis of crosshole sinusoidal pressure tests in fissured rock, Stripa Project IR 86-03, SKB, Stockholm.
Black, J.H. and Ki, K.L. (1986): Determination of hydrogeological parameter using sinusoidal pressure tests: A theoretical araisal, Water Resources Res., Vol.17, pp.686-692.
Black, W.H., Smith, H.R. and Patton, F.D. (1986): Multiple level groundwater monitoring with the MP System, In: Proc. NWWA-AGU Conf. on Surface and Borehole Geophysical Methods and Groundwater Instrumentation, pp.41-61.
Bogle, F.R. and Loy, K. (1995) : The Application of Thermal Infrared Thermography in the Identification of Submerged Springs in Chickamauga Reservoir, Hamilton County, Tennessee, Karst Geohazards, 1995, pp. 415-424.
Bouwer, H. (1978): Groundwater Hydrology, McGrawhill, New York.
Brooks, J. (1961): The submarine spring off Crescent Beach, Frolida. Fla. Acad. Sci. Q. J., Vol.24, pp.122-134.
Burdon, H. (1964): Karst groundwater investigation in Greece, Food and Agriculture Organization, Rome, p.99.
Carlsson, L. and Gidlund, G. (1983): Evaluation of the hydrogeological conditions at Finnsjon, KBS/SKBF Tech. Rep. 83-56, KBS/SKBF, Stockholm.
Clark, K.J., Takase, H., Impey, M.D., Humm, J.P., Maekawa, K., Ogata, N. and Yanagizawa, K. (1995): Natural Analogue Study of Uranium Migration in the Tono Mine, Sci. Basis Nucl. Waste Manag., XIX, pp.767-773.
Committee on Rock Mechanics J.S.C.E. (1986): Geological survey of a dam-site, Japan Society of Civil Engineers, pp.20-30 (in Japanese).
Cooper, H.H., Kohout, F.A., Henry, H.R. and Glover, R.E. (1964): Sea Water in Coastal Aquifers, USGS, Water-Suly Pap. 1913-C, p.84.
Davidson, C.C., Brown, R.A., Everitt, R.A., Gascoyne, M., Lodha, G.S., Martin, C.D., Soonawala, N.M., Stevenson, D.R., Thorne, G.A. and Whitaker, S.H. (1994): The disposal of Canada's Nuclear Fuel Waste, Site Screening and Site Evaluation Technology, AECL-10713, COG-93-3, p.154.
Dershowitz, W., Lee, G., Geier, J., Foxford, T., LaPointe, P. and Thomas, A. (1998): FracMan Interactive Discrete Feature Data Analysis, Geometric Modeling, and Exploration Simulation, User documentation, Version 2.6, Golder Associates Inc., Seattle, USA.
Freeze, R.A. and Cherry, J.A. (1979): Groundwater, Prentice Hall, Englewood Cliff.
Geological Survey of Japan (1991): Well Data Compiled from Japanese Nation-wide Geothermal Surveys, Part 2 Logging Data and Geologic Columns Data, Geological

Survey of Japan Report No.273 (in Japanese with English abstract).
Hatanaka, K., Watari, S., Uchida, M., Takase, H. and Impey, M.D. (1995): Experimental Study on Groundwater Flow and Mass Transport in a Heterogeneous Porous Medium, Sci. Basis Nucl. Waste Manag., XIX, pp.739-746.
Hibiya, K., Inaba, T., Shiogama, Y., Yamamoto, T., Masumoto, K. and Furuichi, M. (1999): A Study of Groundwater Flow in Japan, JNC TN7400 99-004 (in Japanese with English abstract).
Hsieh, P.A. and Neuman, S.P. (1985a): Field Determination of the Three-Dimensional Hydraulic Conductivity Tensor of Anisotopic Media, 1. Theory, Water Resources Res., Vol.21, pp.1655-1665.
Hsieh, P.A. and Neuman, S.P. (1985b): Field Determination of the Three-Dimensional Hydraulic Conductivity Tensor of Anisotopic Media, 2. Methodology and Application to Fractured Rocks, Water Resources Res., Vol.21, pp.1667-1676.
Humm, J. and Impey, M. (1994): Fractal fitting of the Tono mine data, Intera Report, version 1, QuantiSci, UK.
Imai, H. and Yanagizawa, K. (1990): Overviews of groundwater flow analysis code: TAGSAC, PNC TN7410 90-026 (in Japanese with English abstract).
JNC (1998a) Drilling Survey (MIU-1) of Mizunami Underground Research Laboratory Project in Shomasama-bora site, JNC TJ7440 98-001.
JNC (1998b) Investigation of Regional Flow of Groundwater (DH-6), JNC TJ7440 99-025, Vol.1.
JNC (1998c) Investigation of Regional Flow of Groundwater (DH-7), JNC TJ7440 99-025, Vol.2.
JNC (1998d) Investigation of Regional Flow of Groundwater (DH-8), JNC TJ7440 99-025, Vol-3.
JNC (1999a) Investigation Program in Borehole MIU-2 for the Mizunami Underground Research Laboratory Project in the Shomasama site, JNC TJ7420 99-016.
JNC (1999b): Final Report of Kamaishi In-situ Experiment, JNC Technical Report, JNC TN7410 99-001 (in Japanese with English abstract).
Kinoshita, T., Abe, T., Takemura, T. and Yokomoto, S. (1993): Investigation of Hydraulic Properties in Rock Mass around Tunnels Using Injection Test, Proceedings of the 25th Symposium on Rock Mechanics, pp.481-485 (in Japanese with English abstract).
Kiyama, T. and Marui, A. (1999): Study on Groundwater Flow and Fresh-water Interface in Hasunuma Parkland, Chiba -Part 2; Observation of the Depth of Sea-water and Fresh-water Interface by Using Core Sample of Well #1-, Chishitsu News, July, pp.55-59 (in Japanese).
Lusczynski, N.J. and Swarzenski, W.V. (1966): Salt-Water Encroachment in Southern Nassau and Southeastern Queens Counties Long Island, NY. USGS, Water-Suly Pap. 1616-F, p.76.
Marui, A., Ishii, T., Uchida, Y. and Hayashi, T. (1999a): Study on Groundwater Flow and Fresh-water Interface in Hasunuma Parkland, Chiba -Part 1; Study Plan and Situation of Drilling about Well #1-, Chishitsu News, July, pp.47-54 (in Japanese).
Marui,A., Hayashi,T. and UUchida,Y. (1999b): Study on Groundwater Flow and Fresh-water Interface in Hasunuma Parkland, Chiba -Part 3; Research of Submarine Groundwater Discharge-, Chishitsu News, August, pp.45-48 (in Japanese).
Masumoto, K., Tosaka, H. and Ito, K. (1992): A Study of Improving Numerical Technique for the Inversions of Spatial Rock Permeability Distribution utilizing Interference Well Testing, Proceedings of the 24th Symposium on Rock Mechanics, pp.56-60 (in Japanese with English abstract).
Matsumoto, N. and Yamaguchi, Y. (1986): Deformation of Foundation and Charge of

Permeability Due to Fill Placement in Embankment Dams, Journal of Geotechnical Engineering, Vol.370, pp.281-290 (in Japanese with English abstract).
Miyakawa, K., Tanaka, K., Mahara, Y., Suzuki, K., Kono, A., Chiba, A. and Mizuochi, Y. (1998): Hydrogeological Survey in Fractured Rock with Saline and Fresh Groundwater, Proceedings of annual conference of the Japan Society of Engineering Geology, pp.37-40 (in Japanese).
Mizutani, Y., Seo, T., Ota, K., Nakamura, N. and Murai, Y. (1992): Carbon -14 ages of deep groundwater from the Tono uranium mine, Gifu Pref., Japan, In: Proc. of Symposium on Accelerator Mass Spectrometry and Interdisciplinary Application of Carbon Isotopes, Dating and Mat. Res. Center, Nagoya Univ., pp.159-168.
Moore, H. (1996): Large groundwater inputs to castal waters revealed by ^{226}Ra enrichments, Nature, Vol.380, pp.612-614.
Murashita, T. (1982): Salt-water intrusion into aquifers in Japan, Bull. Geol. Surv. Japan, Vol.33, No.10, pp.479-530 (in Japanese with English abstract).
Nakaya, S., Nishigaki, M. and Kono, I. (1992): A new field measurement method to determine the three dimensional hydraulic parameters of a rock mass by means of cross-hole testing with information on fissure orientation, Journal of Groundwater Hydrology, Vol.34-2, pp.81-98 (in Japanese with English abstract).
NEA (1991) : Proceedings of an NEA/CEC Workshop on Heterogeneities in Hydrogeological Systems, Paris, October, 1990, OECD, Paris.
Neretnieks, I. (1993): Solute transport in fractured rock- Applications to radionuclide waste repositories, Inflow and contaminant transport in fractured rock, Chapter 2, pp.39-128, Academic Press Inc.
Nishigaki, M., Nakaya, S. and Kono, I. (1991): A New Method for the Field Measurement of Three Dimensional Anisotropic Hydraulic Conductivities in Jointed Rock Mass Using a Single-hole, Japanese Society of Soil Mechanics and Foundation Engineering, Vol.31, No.3, pp.185-199 (in Japanese).
Ogata, N., Ohsawa, H., Nakano, K., Yanagizawa, K. and Nishigaki, M. (1992): Relationships among Lithology, Permeability and Resistivity and their Application to Modelling of Hydrogeology, Journal of the Japan Society of Engineering Geology, Vol.32-6, pp.51-62 (in Japanese with English abstract).
Ogata, N., Koide, K., Takeichi, A. and Matsuoka, K. (1997): Investigated conductive fracture in the granitic rocks by flow-meter logging, Proceedings of annual conference of the Japan Society of Engineering Geology, pp.249-252 (in Japanese).
Okamoto, R., Ogata, M. and Kojima, K. (1988): A new framework for civil engineering, Japan Society of Civil Engineers, Vol.14, pp.65-71 (in Japanese).
Okazaki, H., Nakashima, M., Mikake, S., Ogata, N., Koide, K. and Nishigaki, M. (1997): Effect of measuring soil suction by means of antifreeze liquid, Proceedings of the fall conference of Groundwater Hydrology, pp.24-29 (in Japanese).
Osawa, H., Sasamoto, H., Nohara, T., Ota, K. and Yoshida, H. (1995): Development of a Conceptual Flow-path Model of Nuclide Migration in Crystalline Rock : A Case Study at the Kamaishi In situ Test Site, Japan, Sci. Basis Nucl. Waste Manag. XVIII, pp.1267-1273 (in Japanese with English abstract).
PNC (1994): Current status of research and development on giological disposal (FY1993), PNC Technical Report, PNC TN1410 94-094, pp.138-141 (in Japanese).
Public Works Research Institute, Ministry of Construction (1986): A guide for the description of geologic columns, pp.11-14 (in Japanese).
Reilly, T.E. and Goodman, A.S. (1985): Quantitative Analysis of Saltwater-Freshwater Relationships in Groundwater Systems, A Historical Perspective, J. Hydrol., Vol.80, pp.125-160.

River Bureau, Ministry of Construction (1994): Chronological Groundwater Tables (The year of 1994) (in Japanese).

Roxburgh, I.S. (1985): Thermal Infrared Detection of Submarine Springs Associated with the Plymouth Limestone, Hydrol. Sci., Vol.30, pp.185-196.

Saegusa, H., Inaba, H., Koide, K. and Ogata, N. (1997): Simulation of regional scale groundwater flow in Tono area, Proceedings of the annual meeting of the Chubu branch of the Japan Society of Engineering Geology, pp.1-4 (in Japanese).

Shimo, M., Ijiri, Y., Iihoshi, S., Hashimoto, N. and Nagata, K. (1992): Detection of Groundwater Flow Paths in a Rock using Geotomography and Cross-hole Injection Test, Proceedings of the 24th Symposium on Rock Mechanics, pp.31-35 (in Japanese with English abstract).

Shimo, M. and Iihoshi, S. (1996): An Equivalent Heterogeneous Continuum Model for the Analysis of Groundwater Flow through Fractured Rocks, Proceedings of the 51st annual conference of the Japan Society of Civil Engineers, pp.618-619. (in Japanese)

Shimo, M., Yamamoto, H., Matsui, H. and Senba, T. (1997): Groundwater Flow Simulation around the Kamaishi in-situ Test Site using an Equivalent Heterogeneous Continuum Model, Proceedings of the 28th Symposium on Rock Mechanics, pp.278-282 (in Japanese with English abstract).

SKB (1987): Regional Well Water Chemistry, PR 25-87-08, pp.27-64, SKB, Stockholm.

SKB (1991): Results of hydraulic testing and groundwater sampling in borehole AN-1 at the Shomasama field in Japan, Report 6.053/15401, SKB, Stockholm.

SKB (1993): Stripa Project Overview Reports, Vol.1-3. SKB, Stockholm.

Snow, D.T. (1968): Rock fracture spacings, openings and porosities, In: Proc. of ASCE 96, pp.73-91.

Stringfield, V.T. and LeGrand, H.E. (1969): Relation of Sea Water to Fresh Water in Carbonate Rocks in Coastal Areas, with Special Reference to Florida, USA and Cephalonia (Kephallinia), Greece. J. Hydrol., Vol.9, pp.387-404.

Takeuchi, S., Inaba, H., Ogata, N. and Koide, K. (1997): Estimation of 3D Heterogeneous Hydraulic Conductivity Field Using Fractal Theory, Proceedings of the fall conference of Groundwater Hydrology, pp.50-55 (in Japanese).

Takeuchi, R., Senba, T., Amano, K., Shimo, M., Aoki, T. and Yamamoto, H. (1998): Development of Cross-hole Sinusoidal Test Instrument and its Application to Field Test, Proceedings of the 10th Japan Symposium on Rock Mechanics, pp.725-730 (in Japanese with English abstract).

Tanaka, K. and Inoue, D. (1995): Fault -definition and usage-, Tsuchi-to-kiso, The Japanese Society of Soil Mechanics and Foundation Engineering, Vol.43-3, pp.11-14 (in Japanese).

Tanaka, K., Tanaka, Y., Miyakawa, K., Mahara, Y., Yasuike, S. and Honsho, S. (1996): Proposal of Surveying System to Investigate Hydrogeological Structure of Fracture Developing Rock Mass and its Application, Journal of the Japan Society of Engineering Geology, Vol. 36-6, pp.18-30 (in Japanese with English abstract).

Tanaka, K., Miyakawa, K., Chigira, M., Suzuki, K., Komada, H., Kawanishi, M., Mahara, Y., Igarashi, T., Tanaka, Y. and Yasuike, S. (1997): Characterization of geological and hydrological conditions in deep underground -Systematization of surveying and evaluation methods for crystalline rock-, CRIEPI, Abiko Research Laboratory Report, No.U32 (in Japanese with English abstract).

Tanaka, T., Watanabe, K., Maekawa, K. and Nakamura, N. (1994): Fracture Network Analysis Based on the Geologic Model of Channels, Part 1: Ideas and Computer code, Journal of the Japan Society of Engineering Geology, Vol.35-3, pp.22-33 (in Japanese with English abstract).

Thore, G.A. (1986): Surface hydrology of two Underground Research Laboratory (URL) sub-basins and the Dead Creek watershed 1982-1983, preliminary report, TR-349, AECL, Pinawa, Manitoba, Canada.

Tosaka, H., Masumoto, K., Ito, K. and Otsuka, Y. (1990): A Study of Improving Three Dimensional Numerical Technique for the Inversions of Spatial Rock Permeability Distribution utilizing Interference Well Testing, Proceedings of the 8th Japan Symposium on Rock Mechanics, pp.399-404 (in Japanese).

Tosaka, H., Kojima, K., Tokunaga, T., Okada, M., Nitta, K., Inaba, H., Hama, K. and Koide, K. (1997): A Study on the Long-Term Behavior of Transition Zone between Landwater and Seawater, Proceedings of annual conference of the Japan Society of Engineering Geology, pp.229-232 (in Japanese).

Tsunogai, U., Ishibashi, J., Wakita, H., Gamo, T., Masuzawa, T., Nakatsuka, T., Nojiri, Y. and Nakamura, T. (1996): Fresh Water Seepage and Pore Water Recycling on the Seafloor, Sagami Trough Subducion Zone, Japan, Earth Planet. Sci. Lett., Vol.138, pp.157-168.

TVO (1992): Final disposal of spent nuclear fuel in the Finnish bedrock - Preliminary site investigations, Report YJT-92-32, TVO, Helsinki.

Uchida, M., Doe, T.W., Dershowitz, W. and Wallmann, P.(1993): Simulation of Fracture Flow to the Kamaishi Validation Drift, Proc. of the forth Annual International Conference of High Level Radioactive Waste Management, pp.437-442.

Umeda, K., Yanagizawa, K. and Yoneda, S. (1995): Data-base of Permeability of Rock Mass in Japan, Journal of Groundwater Hydrology, Vol.37-1, pp.69-77 (in Japanese with English abstract).

Vanek, V. and Lee, D.R. (1991): Maing Submarine Groundwater Discharge Areas, An Example From Laholm Bay, Southwest Sweden, Limnol. Oceanogr., Vol.36, pp.1250-1262.

Watanabe, K. and Kojima, K. (1980): Measurement and evaluation of geological properties concerning groundwater flow in the fault and fracture rock, Proceedings of the Symposium on the Japan Society of Engineering Geology, pp.2-16 (in Japanese).

Watanabe, K., Aizawa, T., Ono, M., Yanagizawa, K., Sakuma, H., Yamamoto, H. and Kanda, N. (1989): Evaporation Measurement to Map the Groundwater Discharge on a Tunnel Wall of the Low Permeable Rock Mass -Part 1 : Basic Theory and Laboratory Tests-, Journal of the Japan Society of Engineering Geology, Vol.30-4, pp.11-18 (in Japanese with English abstract).

Watanabe, K., Yanagizawa, K., Push, R., Sakuma, H., Aizawa, T., Yamamoto, H. and Kanda, N. (1990): Evaporation Measurement to Map the Groundwater Discharge on a Tunnel Wall of the Low Permeable Rock Mass -Part 2 : Field Measurement-, Journal of the Japan Society of Engineering Geology, Vol.31-1, pp.1-11. (in Japanese with English abstract)

Watanabe, K., Tanaka, T., Uchida, M. and Iwasaki, H. (1994): Fracture Network Analysis Based on the Geologic Model of Channels, Part 2 :Analysis of the Tracer Migration test carried out in the Kamaishi Mine, Japan, Journal of the Japan Society of Engineering Geology, Vol.35-4, pp.2-12 (in Japanese with English abstract).

Williams, R.L. (1988): A technique for the geometric modeling of underground surfaces, SANDIA REPORT SAND84-0303, SANDIA, New Mexico, USA.

Yamane, M., Nakano, K. and Sugihara, K. (1996): Long-term Observation of Ground Water Pore Pressure Change due to Shaft Excavation, Tsuchi-to-kiso, The Japanese Geotechnical Society, Vol.44. No.11, pp.24-26 (in Japanese with English abstract).

Yanagizawa, K., Nishigaki, M. and Hirata, Y. (1988): Theory of New PNC Aquifer Test

Method and its Application, Journal of Groundwater Hydrology, Vol.30-3, pp.127-137 (in Japanese with English abstract).
Yanagizawa, K., Imai, H., Furuya, K., Wakamatu, N. and Umeda, K. (1992): Groundwater flow analyses in Japan -Part 1 : Groundwater flow analyses in central Japan-, PNC TN7410 92-019 (in Japanese with English abstract).
Yoshida, H., Ohsawa, H., Yanagizawa, K. and Yamakawa, M. (1989): Analysis of Fracture System in Granitic Rock -Case Study for the Granitic Rock, Gifu Prefecture, Japan-, Journal of the Japan Society of Engineering Geology, Vol.30-3, pp.11-22 (in Japanese with English abstract).

(3.4 Geochemical characteristics of groundwater)

Avogadro, A. and Marsily, D.E. (1984): The role of colloids in nuclear disposal, Scientific Basis for Nuclear Waste Management VII, pp.495 - 505.
Aoki, K., Sasamoto, H., Semba, T., Amano, K., Takahara, H., Ohbuchi, S. and Matsushima, E. (1997): Microbial Analyses of Deep Groundwater in Fractured Granodiorite at the Kamaishi Mine, Japan, Proc. 7th Symp. Geo-Environments and Geo-technics, Dec., 1997, Tokyo, Japan, pp.81-86.
Bath, A.H., Christofi, N., Neal, C., Philip, J.C. Cave, M.R. and McKinley, I.G., (1987): Trace elements and microbiological studies of alkaline groundwater in Oman, Arabian Gulf ; a natural analogue for cement pore waters, NERC British Geological Survey Report FLPU 87-2, London, UK, 65p.
Bath, A.H., McCartney, R.A., Richards, H.G., Metcalfe, R. and Crawford, H.B. (1996): Groundwater chemistry on the Sellafield area: a preliminary interpretation, Journal of Engineering Geology, 29, pp.39 - 57.
Brantley, S.L. (1992): Kinetics of dissolution and precipitation - Experimental and field results, Proc. of the 7th international Symposium on Water-Rock Interaction, 7, UTAH, USA, 13-18, July 1992, pp.3-6.
Buffle, J. (1988): Complexiation reaction in aquatic systems, Wiley, New York.
Chapman, N.A., Mckinley, I.G., Shea, M.E., Smellie, J.A.T. (1991): The Poços de Caldas Project : Summary and implications for radioactive waste management, Report of an international project managed by SKB, SKB-TR-90-24, Stockholm, Sweden.
Chou, L., Garrels, R.M. and Wollast, R. (1989): Comparative study of the kinetics and mechanisms of dissolution of carbonate minerals, Chemical Geology, 78, pp.269-282.
Drever, J.I. (1988): The geochemistry of natural waters, Prentice Hall, Inc., 437p.
Grindrod, P. (1991): Radionuclide migration with in fractured rock : The impact of colloids upon geoshere calculations, SKI Technical Report 91, SKI Stockholm, Sweden.
Hama, K. and Iwatsuki, T. (1998): Regional hydrological study at Tono area - Characterization of groundwater geochemistry, Abstract of 1998 annual meeting of the Japan Society of Engineering Geology, pp.17-20 (in Japanese).
Holdren, G.R. and Berner, R.A. (1979): Mechanism of feldspar weathering - I. Experimental studies. Geochimica et Cosmochimica Acta, 43, pp.1161-1171.
Ii, H., Horie, Y., Ishii, T. and Shimada, J. (1997): Development of an apparatus to measure groundwater qualities in situ and to sample groundwater using boreholes, Environmental Geology, 32, pp.17-22.
Ichikuni, M. and Ogura, N. (1992): Chemistry of Terrestrial Water, KIKAN KAGAKU SOSETSU, No. 14. Nihonkagakukai (in Japanese with English abstract).
Iwatsuki, T., Sato, K., Seo, T. and Hama, K. (1995): Hydrogeochemical investigation of groundwater in the Tono area, Japan, Proc. Mat. Res. Soc. Symp., 23-27 Oct 1994, Kyoto, Japan, 353, pp.1251-1257.
Iwatsuki, T. and Moulin, V. (1998): Geological investigation of colloids/organics in the

groundwater at the Tono area, Japan, Abstracts 1998 Japan Earth and Planetary Science Joint meeting, p.230 (in Japanese).
Iwatsuki, T. Teshima, K. and Yoshida, H. (1998): Investigation technology and approaches for the deep groundwater geochemistry, Journal of Nuclear Fuel Cycle and Environment, 4, pp.73-81 (in Japanese with English abstract).
Iwatsuki, T. and Yoshida, H. (1999a): Characterizing the chemical containment properties of the deep geosphere: water-rock interaction analysis in relation to fracture systems in deep crystalline rock at the Tono area, Japan, Chemical Containment of Waste in the Geosphere, edited by R.Metcalfe and C.A.Rochelle, Geological Society Special Publication No.157, Geological Society of London, London, UK, pp.71-84.
Iwatsuki, T. and Yoshida, H. (1999b): Water chemistry and mineralogy of fracture systems in the basement granite in the Tono uranium mine area, Gifu Prefecture, central Japan, Geochemical Journal, 33, pp.19-32.
Iwatsuki, T. Xu, S. and Itoh, S (1999): Application of Tandem Accelerator Mass Spectrometer (TAMS) in estimation of groundwater age, Proc. International workshop on Frontiers in Accelerator Mass Spectrometry, 1-8 Jan. 1999, Tsukuba, Japan, pp.98-103.
JNC (1999): Final Report of Kamaishi In-situ Experiment, JNC Technical Report, JNC TN7410 99-001 (in Japanese with English abstract).
Kamei, K. (1997): Natural analogue study of a state of glass in bentnite (translate), Power Reactor and Nuclear Fuel Development cooperation, Technical Report, PNC TN 8410 97-035 (in Japanese).
Kamei, G., Yusa, Y. and Arai, T (2000): A natural analogue of nuclear waste glass in compacted bentnite, Applied Geochemistry, 15, pp.153-167.
Laaksoharju, M., Smellie, J., Ruotsalainen. P. and Snellman, M. (1993): An approach to quality classification of deep groundwaters in Sweden and Finland, SKB Technical Report 93-27, SKB Stockholm, Sweden.
Lovley, D.R. and Chapelle, F.H. (1995): Deep subsurface microbial processes, Reviews of Geophysics, 33, pp.365-381.
Milodowski, A.E., West, J.M., Pearce, J.M., Hyslop, E.K., Basham, I.R. and Hooker, P.J. (1990): Uranium mineralized microorganisms associated with uraniferous hydrocarbons in southwest Scotland, Nature 347, pp.465-467.
Mizutani, Y., Seo, T., Ota, K., Nakamura, N. and Murai, Y. (1992): Carbon -14 ages of deep groundwater from the Tono uranium mine, Gifu Pref., Japan, In: Proc. of Symposium on Accelerator Mass Spectrometry and Interdisciplinary Application of Carbon Isotopes, Dating and Mat. Res. Center, Nagoya Univ., pp.159-168 (in Japanese with English abstract).
Moulin, V.(1995): Fate of actinides in the presence of humic substances under conditions relevant to nuclear waste disposal, Applied Geochemistry, 10, pp.573-580.
Morita, S. Shimada, J. and Cho, H. (1991): Chemical characteristics and flow regime of groundwater in deep cristalline bedrock, part 1 : Chemical characteristics of groundwater and its classification at Ohmine area in Kamaishi mine, Iwate Prefecture, Japan, Journal of Japan Society of Engineering Geology, 32, pp.11-22 (in Japanese with English abstract).
Motojima, K. and Masuko, Y. (1973): The analysis of groundwater and hot spring, Kodansha Scientific Books (in Japanese).
Murakami, Y., Naganuma, T. and Iwatsuki, T. (1999): Deep subsurface microbial communities in the Tono area, central Japan, Journal of Nuclear Fuel Cycle and Environment, 5, pp.59-66 (in Japanese with English abstract).
Naganuma, T. (1997): A study of microbiological environment in deep underground

(translate), Chikyu Monthly, No.19, pp.199-203 (in Japanese).
Nagao, S. (1995): Characteristics of humic substances and TRU-humate complexes in groundwater, Journal of Nuclear Fuel Cycle and Environment, 1, pp.231-242 (in Japanese with English abstract).
Nelson, D.M., Penrose, W.R., Karttunen, J.O. and Mahlhaff, P. (1985): Effects of dissolved organic carbon on the adsorption properties of plutonium in natural waters, Environ. Sci. Technol., 19, pp.127-131.
Ohta, K. (1971): A study of hot springs on the Shimabara peninsula, Report of Shimabara hot spring, Kyushu University, No.8, pp.1-33 (in Japanese with English abstract).
Ohta, K. (1973): The groundwater in the Isahaya coal field, commemorative thesis of prof. Mathuhisa Hisamichi, Kyushu University, pp.391-406 (in Japanese with English abstract).
Ota, K., Amano. K., Suyama, Y. and Saegusa, H (1999): 3D Geological modelling in regional hydrogeological study in the Tono area, JNC Technical Review No. 4, JNC TN1340 99-003, pp. 101-110.
Rosevear, A. (1991): Review of natural research programmes on the microbiology of radioactive waste disposal, NSS/R263 Report UK Nirex Ltd.
Sasamoto, H., Seo, T., Yui, M. and Sasaki, Y. (1996): Geochemical investigation of groundwater in the Kamaishi in situ test site, Japan (part 1), PNC Technical Report, PNC TN 8410 96-203 (in Japanese with English abstract).
Seo, T., Ochiai. Y., Takeda. S. and Nakashima, N. (1989): A natural analogue study on Tono sand-stone uranium deposit in Japan, Proc. Joint Int. Waste Management Conf., 2, pp.353-358.
Seo, T. and Moulin, V. (1995): Study of colloids in groundwater at the Tono uranium deposit, Japan, In: 5th International Conference on the Chemistry and Migration Behavior of Actinides and Fission Products in the Geosphere, Abst. Migration'95, Saint-Malo, France, 10-15 Oct. 1995, p.45.
Seo, T. and Shimizu, K. (1992): Literature survey and analysis of groundwater geochemistry in Japan, PNC Technical Report, PNC TN7410 92-017 (in Japanese with English abstract).
Shikazono, N. and Utada, M. (1997): Stable isotope geochemistry and diagenetic mineralization associated with the Tono sandstone-type uranium deposit in Japan, Mineralium Deposita, 32, pp.596-606.
Silver, R. and Woodford, N. (1979): Dissolution kinetics and weathering of mafic minerals, Geochim. Cosmochim. Acta, 43, pp.717-724.
Shimada, J. (1989): Use of environmental stable isotope as 3-dimentional groundwater flow tracer, Environment Research Center, Univ. of Tsukuba, pp.63-70 (in Japanese).
Stumm, W. and Morgan, J.J. (1996): Aquatic chemistry, John Wiley and Sons, Inc. 1022p.
Thourman, E.M. (1985): Organic geochemistry of natural waters, Nijihoff and Junk Publishers, Dordrecht.
Ticknor, K.V., Vilks, P. and Vandergraaf, T.T. (1996): The effect of fulvic acid on the sorption of actinides and fission products on granite and selected minerals, Applied Geochemistry, 11, pp.555-565.
Tullborg, E-L. (1986): Fissure fillings from Klieras study site, SKB Technical Report 86-10, SKB Stockholm, Sweden.
Waseda, A. and Nakai, S. (1983): Isotopic compositions of meteoric and surface waters in Central and Northwest Japan, Chikyukagaku, 17, pp.83-91 (in Japanese with English abstract).
West, J.M. (1996): A review of progress in the geomicrobiology of radioactive waste disposal, Harwood academic publishers, 20, RWMREG 20 (2-3) pp.73-212.

Wikberg, P. (1987): The chemistry of deep groundwaters in crystalline rocks, Ph. D. Thesis, Development of Inorganic Chemistry, The Royal Institute of Technology, Stockholm, Sweden.
Witherspoon, P.A. (1996): Geological problems in radioactive waste isolation - Second Worldwide Review, Lawrence Berkeley National Laboratory University of California, LBNL - 38915, UC-814, USA, 270p.
Wolery, T.J. (1983): EQ3NR a computer program for geochemical aqueous speciation-solubility calculations, user's guide and documentation, Lawrence Livermore Laboratory, UCRL-MA-110662PT-I, USA, 191p.
Yoshida, H., Yui, M. and Shibutani, T. (1994): Flow-path structure in relation to nuclide migration in sedimentary rocks: An approach with field investigations and experiments for uranium migration at Tono uranium deposit, central Japan, J. Nucl. Sci. Technol., 31, pp.803-812.
Yui, M., Takeda, S., Komuro, K., Makino, H., Shibutani, A., Umeki, H., Ishiguro, K., Takase, H. and Neyama, A. (1992): Modelling of groundwater geochemistry for isolation systems of high level radioactive wastes, PNC Technical Report, PNC TN 8410 92-166 (in Japanese).
Yusa, Y., Ishimaru, K., Ota, K. and Umeda, K. (1993): Geological and geochemical indicators of paleohydrogeology in Tono uranium deposits, Japan, In: Paleohydrogeological Methods and their Allocations, Proc. NEA Workshop, Paris, 9-10 Nov. 1992, pp.117-146, OECD, Paris.

(3.5 Thermal and mechanical properties of the rock mass)

Cristescu, N.D. and Hunsche, U. (1998): Time Effects in Rock Mechanics, John Wiley & Sons, Chichester, UK.
Excavation Disturbed Zone Workshop (1996): Designing the Excavation Disturbed Zone for a Nuclear Repository in Hard Rock, International Conference on Deep Geological Disposal of Radioactive Waste, Winnipeg, Manitoba Canada.
Fukuda, K. (1990): Mechanical Behavior and Property Changes of Rock induced by Tunnel Excavation in Granite, Proceedings of the 8th Japan Symposium on Rock Mechanics, pp.231-236 (in Japanese with English abstract).
Geological Survey of Japan (1991): Well data compiled from Japanese nation - wide geothermal surveys, Part 1 core sample data - physical properties, geology, age, chemical composition -, Report Geological Survey of Japan, No.271 (in Japanese with English abstract).
Hirahara, N., Ishihara, T., Maeda, N., Sugihara, K. and Sato, T. (1999): In-Situ Experiment of Effect of Excavation Method on Excavation Disturbed Zone at the Tono Mine in Japan, The 7th International Conference Proceedings on Radioactive Waste Management and Environmental Remediation (ICEM '99), CD-ROM.
Industrial Explosives Society (1976): Blasters' Handbook (in Japanese).
Ishida, T., Kanagawa, T., Yada, A. and Tanaka, M. (1991): Proposing of a New Method to Detect Loosened Regions Around a Rock Chamber, Taking Note of Stress Redistribution due to Excavation, Proceedings of the 23rd Symposium on Rock Mechanics, pp.227-231 (in Japanese with English abstract).
Japan Tunnelling Association (1982): Investigation of loosened zone induced by tunnel excavation (in Japanese).
JNC (1999): Final Report of Kamaishi In-situ Experiment, JNC Technical Report, JNC TN7410 99-001 (in Japanese with English abstract).
Kanagawa, T., Hibino, S., Ishida, T., Hayashi, M. and Kitahara, Y. (1986): *In Situ* Stress Measurements in the Japanese Islands : Over-coring Results from a Multi-element

Gauge Used at 23 Sites, Int. J. Rock Mech. Min. Sci. & Geomech. Abstr. Vol. 23, No.1, pp.29-39.

Kikuchi, K., Fujieda, M., Oka, N. and Kobayashi, T. (1984): Geotechnically Integrated Evaluation on the Stability of Dam Foundation Rocks, Journal of the Japan Society of Engineering Geology, pp.103-118 (in Japanese with English abstract).

Kikuchi, T., Sato, T., Sugihara, K. and Nishigaki, M. (1997): Change of porewater pressure due to drift excavation, Proceedings of the Symposium of the Mining and Materials Processing '97, Sapporo, (D), p.250 (in Japanese).

Kinashi, H., Hata, K., Matsui, H. and Sugihara, K. (1998): Estimation of drift excavation damage with acoustic emission technique, Proceedings of the 10th Japan Symposium on Rock Mechanics, pp.611-616 (in Japanese with English abstract).

Kinoshita, N., Matsui, H., Kikuchi, T. and Horita, M. (1998): Characterization of blast vibration in rock adjacent to drift, Proceedings of the 10th Japan Symposium on Rock Mechanics, pp.755-760 (in Japanese with English abstract).

Kita, H., Kiyama, T., Sato, T. and Ishijima, Y. (1998): Effect of temperature on mechanical property of Inada granite and Shirahama sandstone, Japanese Geotechnical Society Symposium, pp.143-150 (in Japanese).

Kitano, K., Shin, K., Kinoshita, N. and Okuno, T. (1988): Mechanical, Thermal Properties and Permeability of Rock under High Temperature, Journal of the Japan Society of Engineering Geology, 29-3, pp.36-47 (in Japanese with English abstract).

Kuwahara, K. (1984): Rock classification by Uniaxial Compressive Strength and Shear Strength, Journal of the Japan Society of Engineering Geology, pp.25-33 (in Japanese with English abstract).

Maeda,N., Sato,T., Matsui,H. and Sugihara,K (1999): Estimation of Applicability of Stress Measurement Methods and Three Dimensional Stress State in Soft Sedimentary Rock, Proc. of the '99 Japan-Korea Joint Symposium on Rock Engineering, Fukuoka Japan, pp.277-284.

Material Society of Japan (1993): Rock Mechanics, Maruzen, pp.357-361 (in Japanese).

Matsui, H., Sato, T., Sugihara, K. and Nakamura, N. (1997): Comparizon of the results of stress measurements determined by various methods at the Kamaishi mine, Proceedings of the International Symposium on Rock Stress, pp.95-100.

Matsui, H., Sugihara, K., Sato, T. and Yoshioka, H. (1992): Mechanical and Hydraulic variation of Rock Mass around a shaft excavated in Neogene Sedimentary Rocks, PNC TN7410 92-046 (in Japanese with English abstract).

OECD/NEA (1989): Excavation Response in Deep Radioactive Waste Repositories ; Implications for Engineering Design and Safety Performance, Winnipeg, OECD Workshop, Paris.

Okubo, S. (1991): Creep of Rocks, Journal of the Mining and Materials Processing Institute of Japan, Vol.107, No.5, pp.245-252 (in Japanese).

Okubo, Y. (1993): Temperature Gradient Map of the Japanese Islands, Journal of the Geothermal Research Society of Japan, Vol.15, No.1, pp.1-21 (in Japanese with English abstract).

Read, R.S. (1996): Characterizing Excavation Damage in Highly-Stressed Granite at AECL's Underground Research Laboratory, Proc. of the Excavation Disturbed Zone Workshop, Int. Conference on Deep Geological Disposal of Radioactive Waste, Winnipeg, Canada, pp.35-46.

Saito, T., Ishida, T., Takeda, M. and Tanaka, Y. (1988): The General Tendency of Initial Stress State in Japan with the Data of in-situ Measurements, Proceedings of the Japan Society of Civil Engineering, Vol.394, III-9, pp.71-78 (in Japanese with English abstract).

Sakurai, S. (1983): Study on Loosening Zone in Connection with Tunnel Excavation, Journal of the Tunnels and Underground, Vol.14, No.1, pp.35-41 (in Japanese).
Sasamoto, H., Yui, M. and Hama, K. (1999): Redox Conditions in Host Rocks Surrounding a Drift in the Kamaishi *In-Situ* Tests Site, Japan, JNC Technical Report JNC TN8400 99-013 (in Japanese with English abstract).
Sato, T., Ishimaru, T., Sugihara, K. and Shimizu, K. (1992a): Data Collection by Literature Survey on Rock Physical Properties in Japan, PNC TN7410 92-018 (in Japanese with English abstract).
Sato, T., Kikuchi, T. and Sugihara, K. (2000): In-situ Experiments on an Excavation Disturbed Zone Induced by Mechanical Excavation in Neogene Sedimentary Rock at Tono Mine, Central Japan, Engineering Geology Vol.56, Nos.1-2, pp.97-108.
Sato, T., Matsui, H. and Sugihara, K. (1998a): Present Status of Mechanical Investigation in Deep Rock Mass -Initial Stress Measurements with Various Methods-, Journal of Nuclear Fuel Cycle and Environment, Vol.4, No.2, pp.83-90 (in Japanese with English abstract).
Sato, T., Matsui, H., Kikuchi, T., Sugihara, K. and Okubo, S. (1998b): Seismic Velocity Structure of EDZ around the Drifts at the Kamaishi and Tono Mines in Japan, Sci. Basis for Nucl. Waste Manag., XXI, MRS '97 Symposium Proc. Vol. 506, pp.813-820.
Sato, T., Matsui, H., Sugihara, K. and Yoshioka, H. (1992b): Shaft Excavation Effect Project -Excavation Effect Evaluation by Extensometer Measurements-, PNC TN7410 92-051 (in Japanese with English abstract).
Sato, T., Sugihara, K. and Matsui, H. (1995): Geoscientific Study at the Tono Mine and the Kamaishi Mine in Japan, Proc. of 8th ISRM Congress, pp.47-51.
Sato, T. Taniguchi, W., Fujita, A. and Hasegawa, H. (1999): Data Collection by Literature Survey on Rock Physical Properties in Japan (II), JNC Technical Report JNC TN7410 99-011 (in Japanese with English abstract).
Sugihara, K., Kamemura, K. and Ninomiya, Y. (1998): Estimation by *in-situ* measurement of excavation disturbance by blasting in sedimentary soft rock, Proceedings of the Japan Society of Civil Engineering, Vol.589, III-42, pp.239-251 (in Japanese with English abstract).
Sugihara, K., Matsui, H., Ishijima, F. and Sato, T. (1996): Study on Excavation Disturbance in the Kamaishi Mine, Japan, Proc. of the Excavation Disturbed Zone Workshop, Int. Conference on Deep Geological Disposal of Radioactive Waste, Winnipeg, Canada, pp.15-24.
Sugihara, K., Matsui, H. and Sato ,T. (1999): *In-situ* Experiments on Rock Stress Condition and Excavation Disturbance in JNC's Geoscientific Research Program in Japan - A Rock Mechanical Basis of Underground Research Laboratory Project -, Proceedings of the International Workshop on the Rock Mechanics of Nuclear Waste Repositories, Edited by: Saeid Saeb and Christopher Francke, pp.159-183.
Sugihara, K., Yoshioka, H., Matsui, H. and Sato, T. (1993): Preliminary Results of a Study on the Responses of Sedimentary Rocks to Shaft Excavation, Engineering Geology, 35, pp.223-228.
Watanabe, K., Hoshino, K., Miyamoto, T. and Kamai, T. (1992): Mechanical Properties of the Deep Underground Layers in the Boso Peninsula, The 27th Japan National Conference on Soil Mechanics and Foundation Engineering, pp.1223-1224 (in Japanese).
Yamamoto, T., Kikuchi, T., Sato, T. and Sugihara, K. (1998): Field measurements of the effect of excavation method on the excavation disturbance, Proceedings of the 10th Japan Symposium on Rock Mechanics, pp.791-796 (in Japanese with English abstract).
Yamashita, S., Sugimoto, F., Yamauchi, M., Mori, S. and Namsrai ,D. (1997): Changes of Micro-Structures of a Soft Rock on the Creep Loading Process -Studies on the creep

mechanism under compressive load of rocks (Part -1)-, Journal of the Mining and Materials Processing Institute of Japan, No.113, pp.817-824 (in Japanese with English abstract).

Yamauchi, M., Yamazaki, T., Yamashita, S. and Sugimoto, F. (1998): Relationship between Failure Process of Creep Test and Conventional Compression Test on Soft Rocks - Studies on the creep mechanism under compressive load of rocks (Part -2)-, Journal of the Mining and Materials Processing Institute of Japan, No.114, pp.163-168 (in Japanese with English abstract).

Yano, Y., Okubo, Y. and Shibuya, A. (1994): Temperature Gradient Map of the Japanese Islands Based on Borehole Logging Data, Proceedings of the 91st SEGJ Conference, pp.153-156 (in Japanese).

Yano, Y., Tanaka, A., Takahashi, M., Okubo, Y., Sasada, M., Umeda, K. and Nakatsuka, N. (1999): Geothermal gradient map of Japan (in Japanese).

Yoshioka, H., Sugihara, K., Kinashi, H., Hata, K. and Inoue, A. (1992): A Study on Stress Redistribution in Rock Formation by Shaft Excavation, Proceedings of the 24th Symposium on Rock Mechanics, pp.356-360 (in Japanese with English abstract).

(3.6 Solute transport in the rock mass)

Alexander, W.R., Frieg, B., Ota, K. and Bossart, P. (1996): The RRP Project: Investigating radionuclide retardation in the host rock, Nagra Bulletin No.27, Nagra, Wettingen, Switzerland, pp.43-55.

Alexander, W.R., MacKenzie, A.B., Scott, R.D. and McKinley, I.G. (1990a): Natural analogue studies in crystalline rock: The influence of water-bearing fractures on radionuclide immobilisation in a granitic repository, Nagra Tech. Rep. NTB 87-08, Nagra, Baden, Switzerland.

Alexander, W.R., McKinley, I.G., MacKenzie, A.B. and Scott, R.D. (1990b): Verfication of matrix diffusion by means of natural decay series disequilibria in a profile across a water conducting fracture in granitic rock, Sci. Basis Nucl. Waste Manag. XIII, pp.567-576.

Ames, L.L., McGarrah, J.E. and Walker, B.A. (1983a): Sorption of trace constituents from the aqueous solutions onto secondary minerals, I, Uranium, Clays Clay Miner. Vol.31, pp.321-334.

Ames, L.L., McGarrah, J.E. and Walker, B.A. (1983b): Sorption of uranium and radium by biotite, muscovite, and phlogopite, Clays Clay Miner. Vol.31, pp.343-351.

Berry, J.A., Bishop, H.E., Cowper, M.M., Fozard, P.R., McMillan, J.W. and Mountfort, S.A. (1994): The use of microanalytical techniques to measure the distribution of uranium and plutonium sorbed on rocks and minerals, Radiochim. Acta, Vol.66/67, pp.243-250.

Berry, J.A., Cowper, M.M., Green, A., Jefferies, N.L. and Linklater, C.M. (1991): Sorption of radionuclides on mineral surfaces, In: Proc. 3rd International Conference on Nuclear Fuel Reprocessing and Waste Management, Vol.2, pp.988-993.

Chapman, N.A. and McKinley, I.G. (1987): The Geological Disposal of Nuclear Waste, John Wiley & Sons, Chichester, UK.

Degueldre, C. (1994): Colloid properties in groundwaters from crystalline formations, Nagra Tech. Rep. NTB 92-05, Nagra, Wettingen, Switzerland.

Frieg, B., Alexander, W.R., Dollinger, H., Bühler, C., Haag, P., Möri, A. and Ota, K. (1998): In situ resin impregnation for investigating radionuclide retardation in fractured repository host rocks, J. Contam. Hydrol., Vol.35, pp.115-130.

Hanamuro, T. and Yoshida, H. (1997): An analogue of the oxidation process along a fracture in Toki granite, central Japan, In: 6th International Conference on the Chemistry and Migration Behavior of Actinides and Fission Products in the Geosphere, Abst. Migration'97, Sendai, Japan, 26-31 Oct. 1997, p.96.

Heath, M.J., Montoto, M., Rodriguez Rey, A., Ruiz de Argandoña, V.G. and Menendez, B. (1992): Rock matrix diffusion as a mechanism of radionuclide retardation: A natural analogue study of El Berrocal granite, Spain, Radiochim. Acta, Vol.58/59, pp.379-384.

JNC (1999): Final Report of Kamaishi In-situ Experiment, JNC Technical Report, JNC TN7410 99-001 (in Japanese with English abstract).

Katayama, N., Kubo, K. and Hirono, S. (1974): Genesis of uranium deposits of the Tono mine, Japan, In: Proc. IAEA-SH-183/11, pp.437-452, IAEA, Vienna.

Komuro, K., Yamamoto, M., Suzuki, S., Nohara, T. and Takeda, S. (1990): Uranium occurrences in the Tsukiyoshi ore deposit, Tono district, Abst. The 40th Annual Meeting of the Society of Mining Geologists of Japan, Tokyo, 31 Jan.-2 Feb. 1990, p.44.

McKinley, I.G. and Hadermann, J. (1985): Radionuclide sorption database for Swiss safety assessment, Nagra Tech. Rep. NTB84-40, Nagra, Baden, Switzerland.

Mènager, M.T., Heath, M.J., Ivanovich, M., Montjotin, C., Barillon, R., Camp, J. and Hasler,S.E. (1994): Uranium migration/retention processes in core profiles from El Berrocal (Spain): implications for matrix diffusion in fractured granite, Radiochim. Acta, Vol.66/67, pp.475-483.

Miller, W., Alexander, W.R., Chapman, N.A., McKinley, I.G. and Smellie, J.A.T. (1994): Natural analogue studies in the geological disposal of radioactive wastes, Studies in Environmental Science 57, Elsevier, Amsterdam.

Nagra (1994): Kristallin-1 Safety Assessment Report, Nagra Tech. Rep. NTB 93-22, Nagra, Wettingen, Switzerland.

Neretnieks, I. (1980): Diffusion in the rock matrix: An important factor in radionuclide retardation? J. Geophys. Res., Vol.85, pp.4379-4397.

Ochiai, Y., Yamakawa, M., Takeda, S. and Harashima, F. (1989): Natural analogue study on Tono uranium deposit in Japan, In: Côme,B. and Chapman,N.A. (editors) CEC natural analogue working group; Third meeting, Snowbird, near Salt Lake City, USA, 15-17 June 1988, CEC Nuclear Science and Technology Series, EUR 11725, CEC, Luxembourg, pp.126–138.

Ota, K., Amano, K., Sato, H., Shibutani, T. and Tachi, Y. (1997): In situ matrix diffusion in fractured crystalline rock, Kamaishi in situ Test Site, north-east Japan, Abst. The 6th International Conference on the Chemistry and Migration Behavior of Actinides and Fission Products in the Geosphere (Migration '97), Sendai, Japan, 26-31 Oct. 1997, pp.98-99.

Ota, K., Amano, K. and Ando, T. (1999): Brief overview of in situ contaminant retardation in fractured crystalline rock at the Kamaishi In situ Test Site, In: Proceedings of an International Workshop for the Kamaishi In situ Experiments, Kamaishi, Japan, 24-25 Aug. 1998, JNC Tech. Rep., JNC TN7400 99-007, pp.67-76.

Ota, K., Kodama, K. and Yoshida, H. (1994): A study of uranium sorption onto sedimentary rocks, Abst. 1994 Annual Meeting of the Atomic Energy Society of Japan, Tsukuba, Japan, 29-31 March 1994, p.92 (in Japanese).

Ota, K. and Yoshida, H. (1995): Influence of microscopic heterogeneity on diffusion for sedimentary rocks, In: Geoval'94, Validation Through Model Testing. Proc. NEA/SKI Symposium, Paris, 11-14 Oct. 1994, OECD, Paris, pp.237-243.

Ryan, J.N. and Gschwend, P.M. (1990): Colloid mobilization in two Atlantic Coastal Plain aquifers: Field studies, Water Resour. Res., Vol.26, pp.307-322.

Sato, H., Shibutani, T., Tachi, Y., Ota, K., Amano, K. and Yui, M. (1997): Diffusion behaviour of nuclides considering pathways in fractured crystalline rocks, PNC Tech. Rep. PNC TN8410 97-127, PNC, Tokai, Japan.

Seo, T. and Moulin, V. (1995): Study of colloids in groundwater at the Tono uranium deposit, Japan, Abst. The 5th International Conference on the Chemistry and Migration Behavior

of Actinides and Fission Products in the Geosphere (Migration'95), Saint-Malo, France, 10-15 Oct. 1995, p.45.

Seo, T. and Yoshida, H. (1994): Natural analogue studies of the Tono uranium deposit in Japan, In: von Maravic,H. and Smellie,J. (editors), Fifth CEC natural analogue working group meeting and Alligator Rivers analogue project (ARAP) final workshop - Proceedings of an international workshop held in Toledo, Spain, 5-9 Oct. 1992. CEC Nuclear Science and Technology Series, EUR 15176, CEC, Luxembourg, pp.179-184.

Smellie, J.A.T., MacKenzie, A.B. and Scott, R.D. (1986): An analogue validation study of natural radionuclide migration in crystalline rocks using uranium-series disequilibrium studies, Chem. Geol., Vol.55, pp.233-254.

Suksi, J., Ruskeeniemi, T. and Rasilainen, K. (1992): Matrix diffusion - Evidences from natural analogue studies at Palmottu in SW Finland, Radiochim. Acta, Vol.58/59, pp.385-393.

Ticknor, K.V. (1993): Actinide sorption by fracture-infilling minerals, Radiochim. Acta, Vol.60, pp.33-42.

Ticknor, K.V. (1994): Uranium sorption on geological materials, Radiochim. Acta, Vol.64, pp.229-236.

Yamakawa, M. (1991): Geochemical behaviour of natural uranium-series nuclides in the geological formation, In: Global Environment and Nuclear Energy, Proc. The 3rd International Symposium on Advanced Nuclear Energy Research, Mito, Japan, 13-15 March 1991, JAERI, Japan, pp.150-158.

Yamana, S. and Nohara, T. (1990): Mineralogical analysis on fixable environment of uranium nuclide at Tsukiyoshi uranium deposit, Abst. 1990 Fall Meeting of the Atomic Energy Society of Japan, Sendai, Japan, 2-5 Oct. 1990, p.719 (in Japanese).

Yoshida, H. (1994): Relation between U-series nuclide migration and microstructural properties of sedimentary rocks, Appl. Geochem., Vol.9, pp.479-490.

Yoshida, H., Yui, M. and Shibutani, T. (1994a): Flow-path structure in relation to nuclide migration in sedimentary rocks: An approach with field investigations and experiments for uranium migration at Tono uranium deposit, central Japan, J. Nucl. Sci. Technol., Vol.31, pp.803-812.

Yoshida, H., Kodama, K. and Ota, K. (1994b): Role of microscopic flow-paths on nuclide migration in sedimentary rocks - A case study from the Tono uranium deposit, central Japan, Radiochim. Acta, Vol.66/67, pp.505-511.

Yoshida, H., Seo, T., Nohara, T., Ota, K., Hama, K., Kodama, K. and Iwatsuki, T. (1994c): Data compilation of geoscientific studies of Tono uranium deposits, central Japan, PNC Tech. Rep. PNC TN7410 94-015, PNC, Toki, Japan.

Yusa, Y., Ishimaru, K., Ota, K. and Umeda, K. (1993): Geological and geochemical indicators of paleohydrogeology in Tono uranium deposits, Japan, In: Paleohydrogeological Methods and their Applications, Proc. NEA Workshop, Paris, 9-10 Nov. 1992, OECD, Paris, pp.117-146.

(3.7 Natural Analogue studies)

Alexander, W.R., McKinley, I.G., MacKenzie, A.B. and Scott, R.D. (1990): Verfication of matrix diffusion by means of natural decay series disequilibria in a profile across a water conducting fracture in granitic rock, Sci. Basis Nucl. Waste Manag. XIII, pp.567-576.

Brookins, D.G. (1990): Radionuclide Behaviour at the Oklo Nuclear Reactor, Gabon, Waste Management, Vol.10, pp.285-296.

Chapman, N.A. and McEwen, T.J. (1993): The Application of Palaeohydrogeological Information to Repository Performance Assessment, Proc. Paleohydrogeological Methods and their Applications, NEA Workshop, Paris, 9-10 Nov., OECD, pp.23-38.

Chapman, N.A., McKinley, I.G. Shea, M.E. and Smellie, J.A. (1990): The Pocos de Caldas Project: Summary and Implications for Radioactive Waste Management, SKB Technical Report, TR 84-16, SKB, Stockholm.

Chapman, N.A., McKinley, I.G. and Smellie, J.A. (1984): The Potential of Natural Analogues in Assessing Systems for Deep Disposal of High-Level Radioactive Waste, Nagra Tech. Rep.84-41, Nagra Baden, Switzerland.

Côme, B. and Chapman, N.A.(ed.) (1986): CEC Nuclear Science Technical Report, EUR 13024.

Curtis, D.B., Benjamin, T.M., Gancarz, A.J., Loss, R., Rosman, J.K.R., De Laeter, J.R., Delmore, J.E. and Maeck, W.J. (1989): Fission Product Retention in the Oklo Natural Fission Reactors, Jour. Applied Geochemistry, Vol.4, pp.49-62.

Duerden, P., Golian, C., Hardy, C.J., Nightingale, T. and Payne, T. (1987): Alligator Rivers Analogue Project: Review of Research and its Implications for Model Validation, CEC Radioactive Waste Management Series, EUR 11037, pp.82-91.

Gauthier-Lafeye, F.and Weber. F. (1989): The Francevillian (Lower Proterozoic) Uranium Ore Deposit of Gabon, Ecol. Geol., Vol.84, pp.2267-2285.

Goodwin, B.W., Cramer, J.J. and McConnell, D.B. (1989): The Cigar Lake Uranium Deposit: An Analogue for Nuclear Fuel Waste Disposal, In: Natural Analogues in Performance Assessments for the Disposal of Radioactive Waste. IAEA Technical Report 304.

Hidaka, H. and Holliger, P. (1998): Geochemical and Neutronic Characteristics of the Natural Fossil Fission Reactors at Oklo and Bangombe, Gabon, Geochim. Cosmochim. Acta, Vol.62, pp.89-108.

IAEA (1975): Proceedings of a Symposium on the Oklo Phenomena, IAEA Technical Report, STI/PUB/405.

IAEA (1978): Proceedings of the Technical Committee Meeting on Natural Fission Reactors, IAEA Technical Report, STI/PUB/475.

Ishihara, S. and Suzuki, Y. (1969): Basement Granites of the Toki Uranium Deposits in Tono Region, Bulletin of Geological Survey of Japan, Vol.232, pp.113-127 (in Japanese with English abstract).

Isobe, H., Ohnuki, T., Murakami, T. and Gauthier-Lafeye, F. (1995): Migration Behaviour of Uranium under Oxidizing Condition in the Oklo Natural Reactor Zone 2, Gabon, Sci. Bas. Nucl. Was. Manag. XVIII, pp.1211-1218.

Itoigawa, J. (1974a): Geology of Mizunami Group, Monograph of the Mizunami Fossil Museum, No.1, pp.9-42 (in Japanese).

Itoigawa, J. (1974b): Seto Group, Monograph of the Mizunami Fossil Museum, No.1, pp.373-384 (in Japanese).

Itoigawa, J. (1980): Geology of the Mizunami district, central Japan, Monograph of the Mizunami Fossil Museum, No.1, pp.1-50 (in Japanese).

Iwatsuki, T. Sato, K. Hama, K. and Seo, T. (1995): Hydrogeochemical Investigation of Groundwater In the Tono Area, Japan, Proc. Mat. Res. Sci., Vol.353, pp.1251-1257 (in Japanese).

Katayama, N., Kubo, K., Hirono, S. (1974): Genesis of Uranium deposits of the Tono Mine, Japan, Proc. IAEA-SH-183/11, pp.437-452.

Miller, W., Alexander, R., McKinley, I. and Chapman, N. (1994): Natural Analogue Studies in the Geological Disposal of Radioactive Wastes, Studies in Environmental Science, Vol.57, pp.395, Elsevier.

Mizutani, Y., Seo, T., Ota, K., Nakamura, N. and Murai, Y. (1992): Accelerator Mass Spectrometry and Interdisciplinary Application of Carbon Isotopes, Proc. Symposium on pp.159-168.

Mènager, M.T., Heath, M.J., Ivanovich, M., Montjotin, C., Barillon, R., Camp, J. and Hasler,

S.E. (1994): Uranium migration/retention processes in core profiles from El Berrocal (Spain): implications for matrix diffusion in fractured granite, Radiochim. Acta, Vol. 66/67, pp.475-483.

Ochiai, Y., Yamakawa, M., Takeda, S. and Harashima, F. (1989): A Natural Analogue Study on Tono Uranium Deposit in Japan, CEC Natural Analogue Working Group 3rd Meeting, Snowbird near Salt Lake City, pp.126-138.

Ohnuki, T., Murakami, T., Isobe, H., Sato, T. and Yanase, N. (1995): Modelling Study on Uranium Migration in the Rock under Weathering Condition, Sci. Bas. Nucl. Was. Manag., XVIII, pp.1227-1234.

Ota, K., Amano, K. and Ando, T. (1999): Brief overview of in situ containment retardation in fractured crystalline rock at the Kamaishi In Situ Test Site, In: Proceedings of an International Workshop for the Kamaishi In Situ Experiments, Kamaishi, Japan, 24-25 August 1998, JNC Tech. Rep., JNC TN7400 99-007, JNC, Japan.

Sanford, A.F. (1982): Preliminary model of regional Mesozoic groundwater flow and uranium deposition in the Colorado Plateau, Geology, pp.348-352.

Sanford, A,F. (1990): Fluid-Mineral Interactions (Spencer et al. ed.), Special Publication No.2, Geochem. Soc., pp.285-311.

Shikazono, N. and Utada, M. (1997): Stable Isotope Geochemistry and Diagenetic Mineralization Associated with the Tono Sandstone-type Uranium Deposit in Japan, Mineralium Deposita, Vol.32, pp.596-606.

Shinjo, N. Yoshida, H. and Ota, K. (1997): An Analogue Study on Nuclide Migration in Tsukiyoshi Fault, Tono Uranium Deposit, Proc. Migration 97, pp.94-95.

Smellie, J.A.T., MacKenzie, A.B. and Scott, R.D. (1986): An analogue validation study of natural radionuclide migration in crystalline rocks using uranium-series disequilibrium studies, Chem. Geol., Vol.55, pp.233-254.

Suksi, J., Ruskeeniemi, T. and Rasilainen, K. (1992): Matrix diffusion - evidences from natural analogue studies at Palmottu in SW Finland, Radiochim. Acta, Vol.58/59, pp.385-393.

Suzuki, K. and Adachi, M. (1998): Denudation History of the High T/P Ryoke Metamorphic Belt, Southwest Japan: Constraints from CHIME Monazite Ages ao Gneisses and Granitoids, Jour. Metamorphic Geol., 16, pp.23-37.

Ticknor, K.V. (1993): Actinide sorption by fracture-infilling minerals, Radiochim. Acta, Vol.60, pp.33-42.

Ticknor, K.V. (1994): Uranium sorption on geological materials, Radiochim. Acta, Vol.64, pp.229-236.

Yamakawa, M. (1991): Geochemical Behaviour of Natural Radionuclides in the Geological Formation, Proc. The 3rd International Symposium on Advanced Nuclear Energy Research; Global Environment and Nuclear Energy, pp.150-158.

Yanase, N., Nightingale, T., Payne, T. and Duerden, P. (1991): Uranium Distribution in Mineral Phases of Rock by Sequential Extraction Procedure, Radiochim. Acta, Vol.52/53, pp.373-380.

Yoshida, H. (1994): Relation between U-series Nuclide Migration and Microstructural properties of Sedimentary Rocks, Vol.9, pp.479-490.

Yoshida, H., Kodama, K. and Ota, K. (1994a): Role of Microscopic Flow-paths on Nuclide Migration in Sedimentary rocks, A Case Study form the Tono Uranium Deposit, Central Japan, Radiochim. Acta, Vol.66/67, pp.505-511.

Yoshida, H., Yui, M. and Shibutani, T. (1994b): Flow-path Structure in Relation to Nuclide Migration in Sedimentary Rocks, An Approach with field Investigations and experiments for Uranium Deposit, Central Japan, Jour. Nucl. Sci. Tech., Vol.31, pp.803-812.

Yusa, Y. and Yoshida, H. (1993): Migration behaviour of natural radionuclides in geological formation, - A case study of the Tono uranium deposits, Japan -, Radioisotope, Vol.20, pp.29-39 (in Japanese with English abstract).

Yusa, Y., Ishimaru, K., Ota, K. and Umeda, K. (1993): Geological and Geochemical Indicators of Paleohydrogeology in Tono Uranium deposits, Japan, Proc. NEA Workshop, Paleohydrogeological Methods and their Applications, OECD/NEA, pp.117-146.

Appendix

Techniques for Investigating the Geological Environment

Appendix Techniques for Investigating the Geological Environment

Investigations of the geological environment as part of site selection differ from those for traditional civil engineering as follows:

i. investigations related to high level radioactive waste disposal typically consider much greater depths and much longer time intervals (for example, the features to be investigated in the present case are rock formations and groundwater at depths up to approximately 1,000 meters below the ground surface while traditional civil engineering usually considers depths up to around 50 m);
ii. sufficiently accurate data are required for extreme conditions (e.g. extremely low permeabilities) in order to facilitate long-term assessment;

In order to assess groundwater flow and nuclide migration over a long period of time, it is required to investigate accurately the permeability of rock formations and the distributions of faults and fractures which could represent major transport pathways. In addition, it is essential to study the geochemical characteristics of groundwater in-situ, in order to assess the long-term corrosion rate of the overpack and the dissolution rate of nuclides. Therefore, the following investigation techniques in particular are required:

i. permeability testing techniques for impermeable rock formations deep underground;
ii. accurate investigation techniques for geological structures;
iii. water sampling techniques which is capable of maintaining in-situ conditions;
iv. in-situ measuring techniques for redox potential.

On the other hand, not all these data are peculiar to geological disposal. Most of them have also been investigated for traditional industrial and academic research. A variety of techniques which have been used for civil engineering research and resource exploration can also be used to investigate the characteristics of rock formations and groundwater from the ground surface by borehole drilling, shaft sinking or using underground tunnels. These techniques have been improved as earth science and the utilization of the underground environment has progressed. At the same time, commonly used techniques can be developed into specialist techniques which are effective for investigations of the geological environment considered here.

In JNC, emphasis has been placed on the development of equipment for acquiring data on the flow characteristics and geochemistry of deep groundwater and the development of geophysical exploration technologies to investigate detailed geological structures near tunnels as well as the influence of excavation. JNC has also utilized new technology along with existing technology for conducting investigations in the Tono area (Neogene sedimentary rock and granitic rock) and the Kamaishi mine (granitic rock). These technologies have been verified and their applicability and effectiveness have been compared. As a result, JNC has successfully developed basic technology for investigating the geological environment.

R&D of hydraulic investigation tool

Equipment to measure the permeability of rock formations in deep boreholes to a depth of up to 1000 m, has been developed. Additionally, equipment has been produced for groundwater sampling as well as measurring in-situ pH and Eh in deep boreholes to a depth of up to 1000 m. Techniques have also been developed for long-term monitoring of in-situ hydrological and geochemical conditions. These techniques will provide basic information which can be used to estimate the long-term evaluation of hydrology and solute transport and also to calculate

the rate of overpack corrosion and solubility of radionuclides. In particular, JNC has developed the following equipment (see Figures 1~7).

Development of geophysical investigation methods

Geophysical methods for investigating geological structures, which are important for site characterization have been developed. Particularly, the applicability of high resolution geophysical investigation methods (e.g. tomography), has been tested at the Kamaishi and Tono mines. Methods which can be used for site characterization during aerial investigations, ground surface investigations as well as borehole studies have also been checked through the study of regional hydrology in the Tono area. Geophysical investigation methods used in site characterization are as follows:

a) Aerial reconnaissance surveys
- Remote sensing (satellite images, aerial photographs) : lineament information
- Airborne electromagnetic survey : regional geological structure shown by apparent resistivity map
- Airborne magnetic survey : regional geological structure shown by magnetic map
- Airborne radiometric survey : information in related to regional radiometric map

b) Ground reconnaissance survey
- Gravity survey : gravity map related to geological structure
- Seismic reflection survey : seismic wave velocity profile generated by differences in geology and geological structure
- Marine seismic reflection survey : geological information on coast and seabed
- Ground electromagnetic survey : resistivity profile related to geological structure
- DC (Direct Current) resistivity survey : resistivity profile related to geological structure
- Seismic refraction survey : seismic wave velocity profile generated by differences in geology and geological structure

c) Borehole survey
- Borehole logging : various geophysical logs (e.g. electrical resistivity logs, density logs and neutron logs) mainly for understanding one-dimensional geological features
- Borehole radar survey : three-dimensional distribution of water-bearing fractures and fracture zones (see Figure 8)
- Hydrophone VSP survey : information related to the distribution of water-bearing fractures and fracture zones (see Figure 9)

d) Surveys using underground facilities
- Geotomography survey : two or three dimensional information on an investigation area using several boreholes to characterize the detailed geological structure

The usefulness of existing techniques for borehole drilling and rock mechanical investigations have also been tested. Methods for investigating the excavation disturbed zone around a gallery (see Section 3.5.3) and in-situ tracer experiments have been developed as site characterization techniques (see Section 3.6.1).

During actual site investigations, it will be necessary to optimize the basic techniques and improve the equipment mentioned above, taking into consideration the particular conditions

of the site. In the future, improvements in technical reliability, practicality and cost efficiency (such as weight reduction and simplification) will become important requirements. JNC intends to develop systematic techniques for surveys and analyses and to improve their practicality in a planned deep underground research laboratory in Mizunami City, Gifu Prefecture and other projects. The accumulation of relevant technologies and know-how will be promoted, aiming at reflecting them in site characterization.

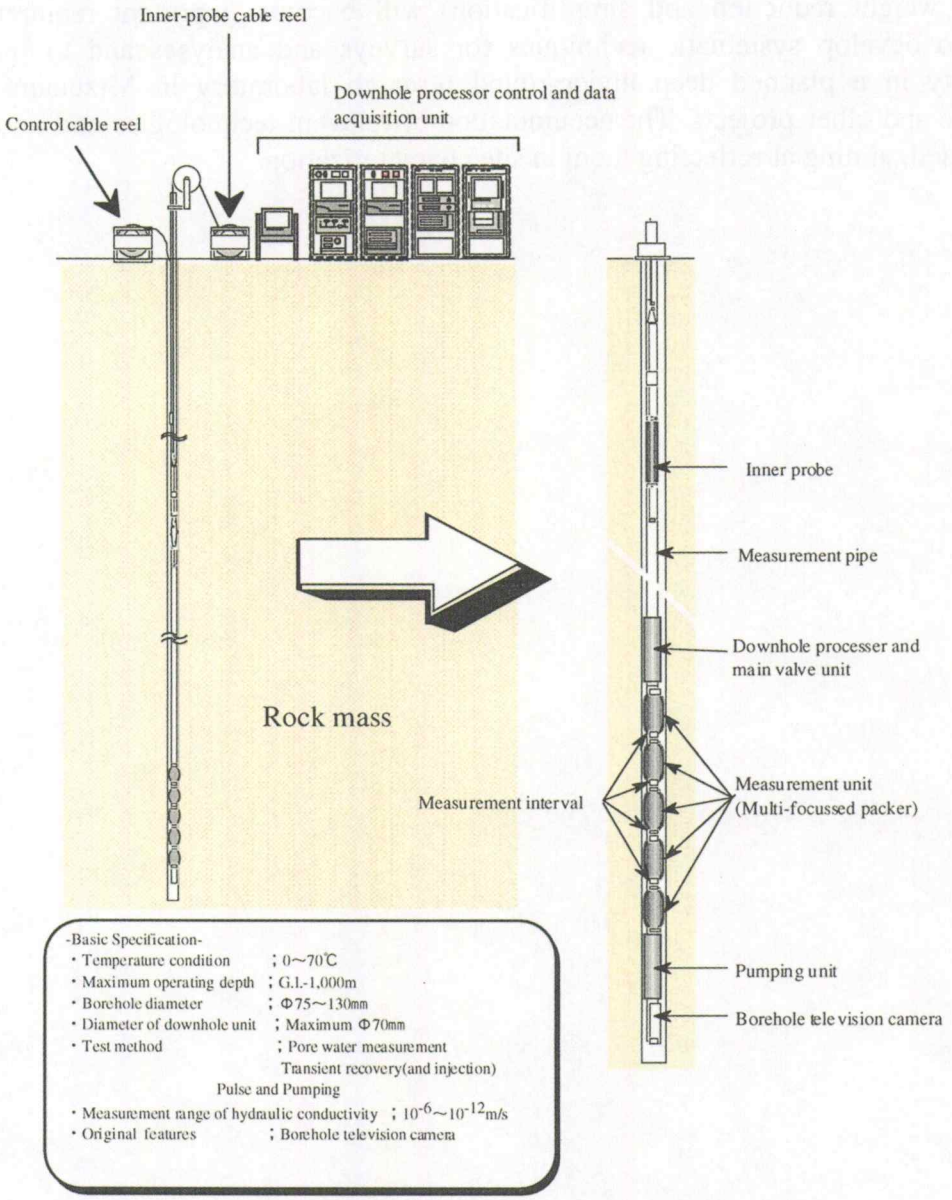


Figure 1 Hydraulic test equipment for depths of up to 1,000 m

A hydraulic test instrument has been developed for measuring the hydraulic conductivities of low permeablity geological media (hydraulic conductivity $<10^{-8}$m s^{-1}) in boreholes at depths up to 1,000 m. A combination of several tools for hydraulic testing is able to measure hydraulic conductivities in the range from 10^{-6}m s^{-1} to 10-12m s^{-1}. The measurement interval in the borehole is 2 to 12 meters. This instrument can also carry a borehole TV at the foot of the experimental probe. Thus, real time observations of the physical conditions in the borehole can support decisions concerning precise locations for hydraulic measurements. This tool can operate at up to 70℃ and 15 MPa.

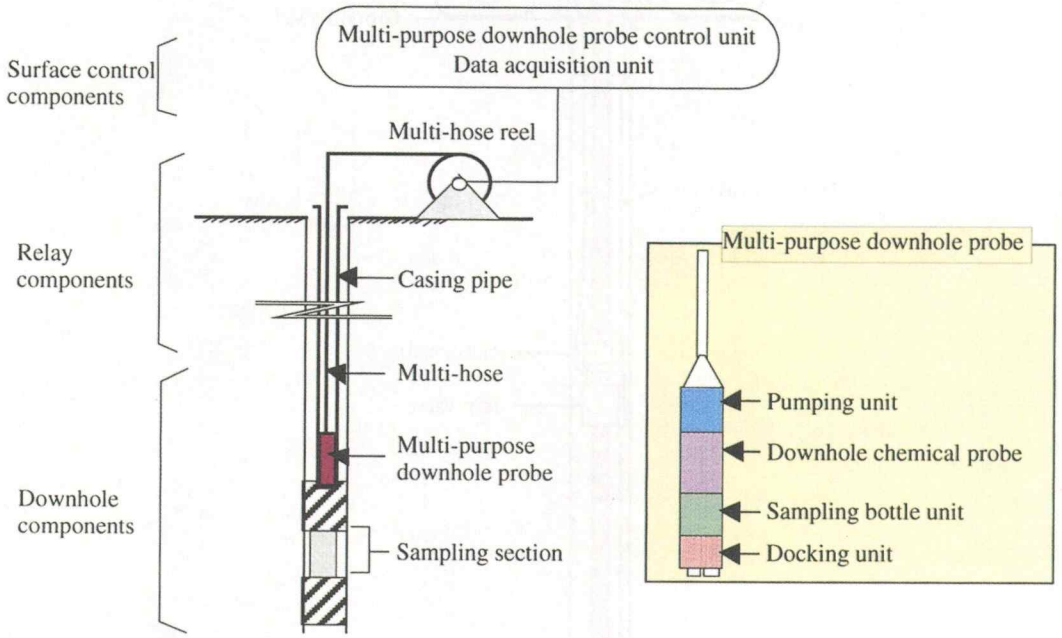


Figure 2 Downhole chemical probe for depths up to 1,000 m

Equipment has been developed to sample in-situ groundwater from packed off intervals in boreholes without perturbing the redox state of the water. The method involves collecting the in-situ groundwater after displacing the drilling fluid from the sampling interval. An additional chemical probe can be attached to the system to measure physico-chemical conditions (e.g. pH, redox potential, electric conductivity and temperature) of in-situ groundwater. This system can also be used under in-situ conditions of up to 70℃ and 15 MPa.

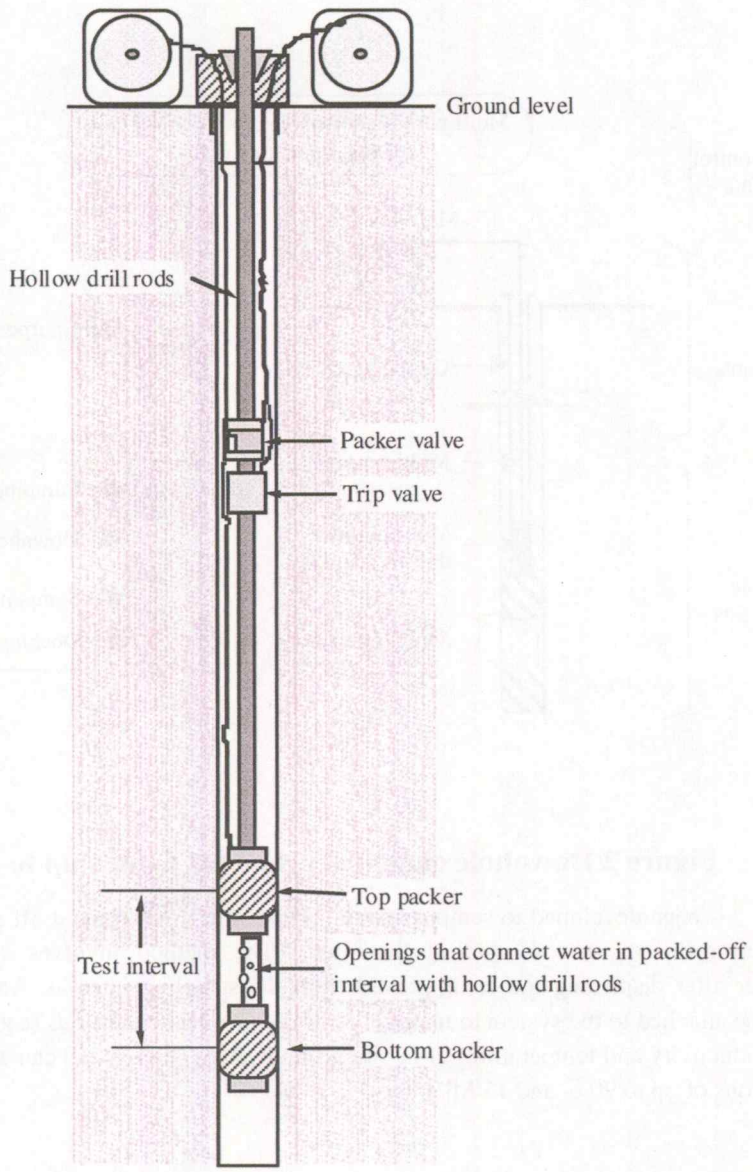


Figure 3 Pumping test equipment for depths up to 1,000 m

Three dimensional hydrological conditions will be characterized by pumping tests using this instrument in boreholes up to 1,000 m deep. This system can also be used under in-situ conditions of up to 70℃ and 15 MPa, like the other hydrological instruments.

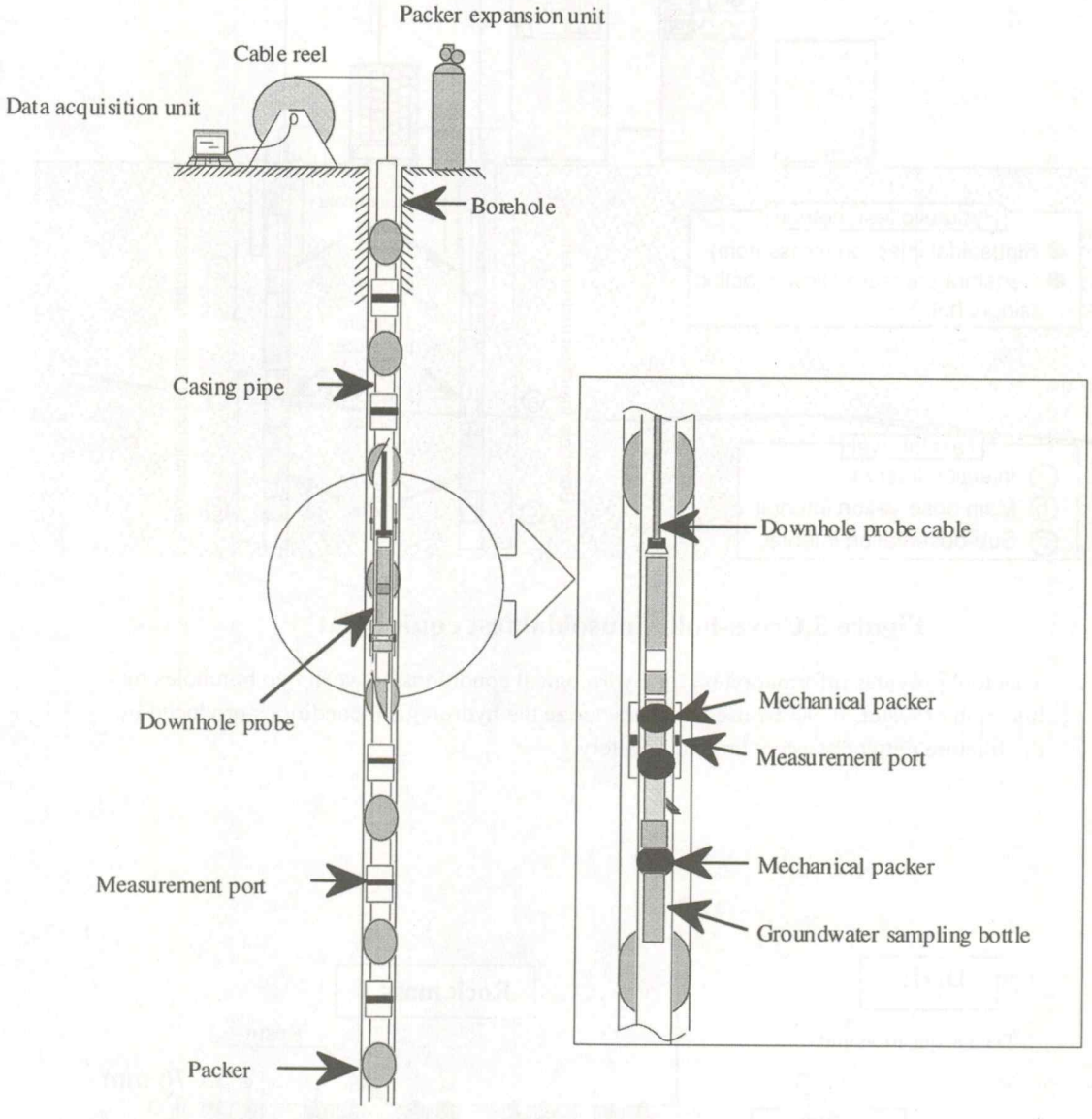


Figure 4 Long-term porewater pressure monitoring system for depths of up to 1,000 m

This system was developed for measurement of in-situ porewater pressure and sampling of groundwater using a multi-packer system for depths up to 1,000 m in a borehole. In particular, the system can be used for monitoring porewater pressure changes of up to 3 MPa due to excavation.

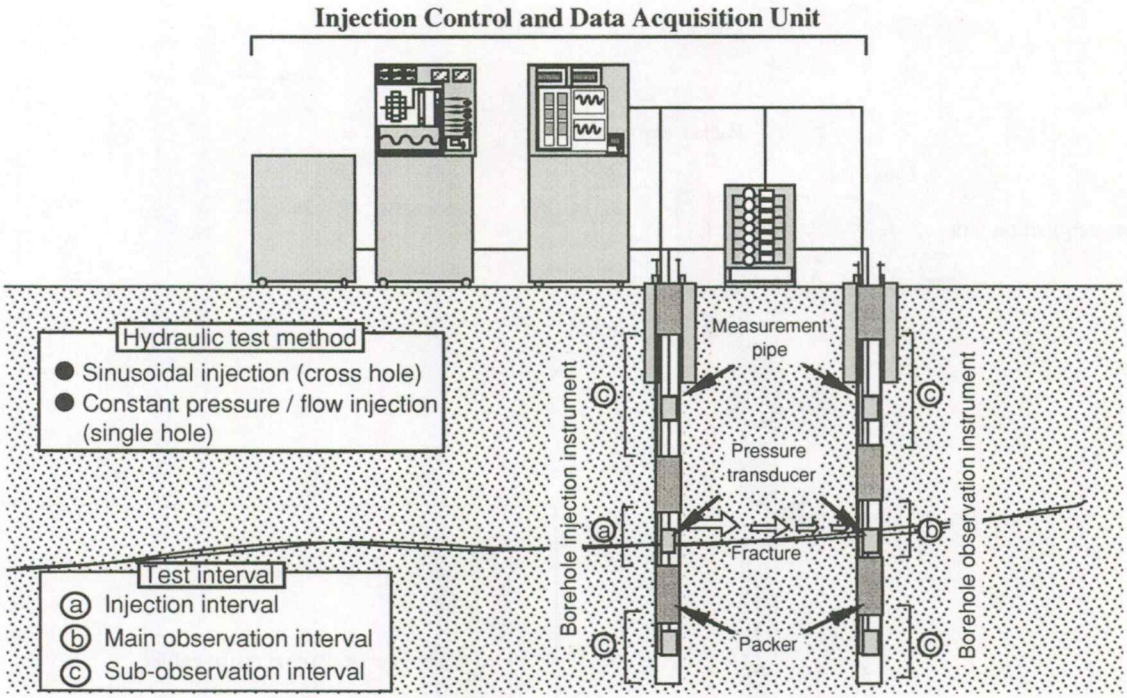


Figure 5 Cross-hole sinusoidal test equipment

This tool provides information on the hydrological conditions between two boreholes by injection of water. It can be used to characterize the hydrological conditions produced by the fracture network system around a gallery.

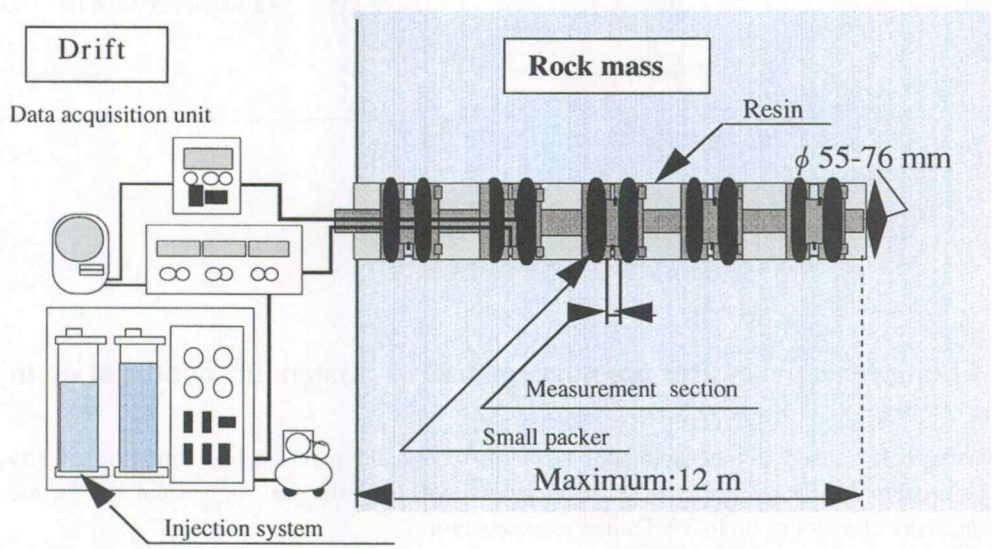


Figure 6 Hydraulic test equipment for disturbed zone

This instrument was developed for obtaining information on the hydrological conditions around a gallery where excavation disturbances cause unsaturated conditions. Measurements of hydraulic conductivity and porewater pressures in the disturbed zone have usually been carried out by re-saturation of water.

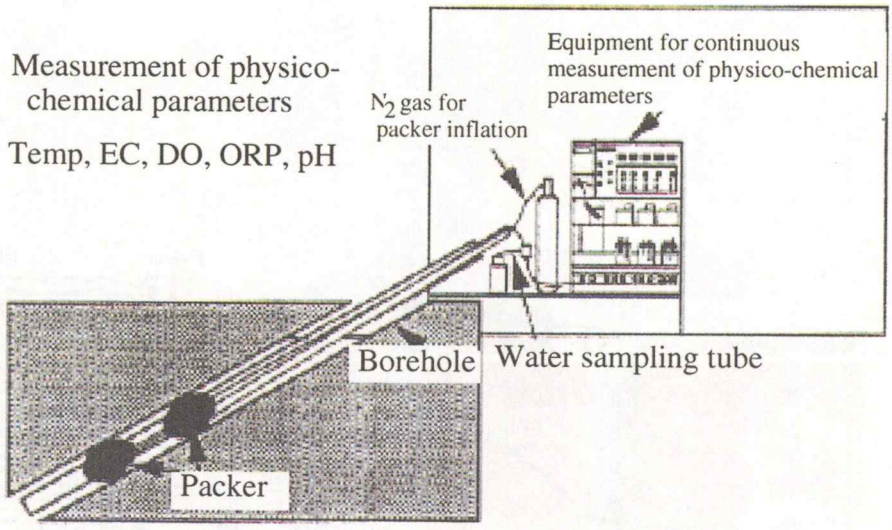
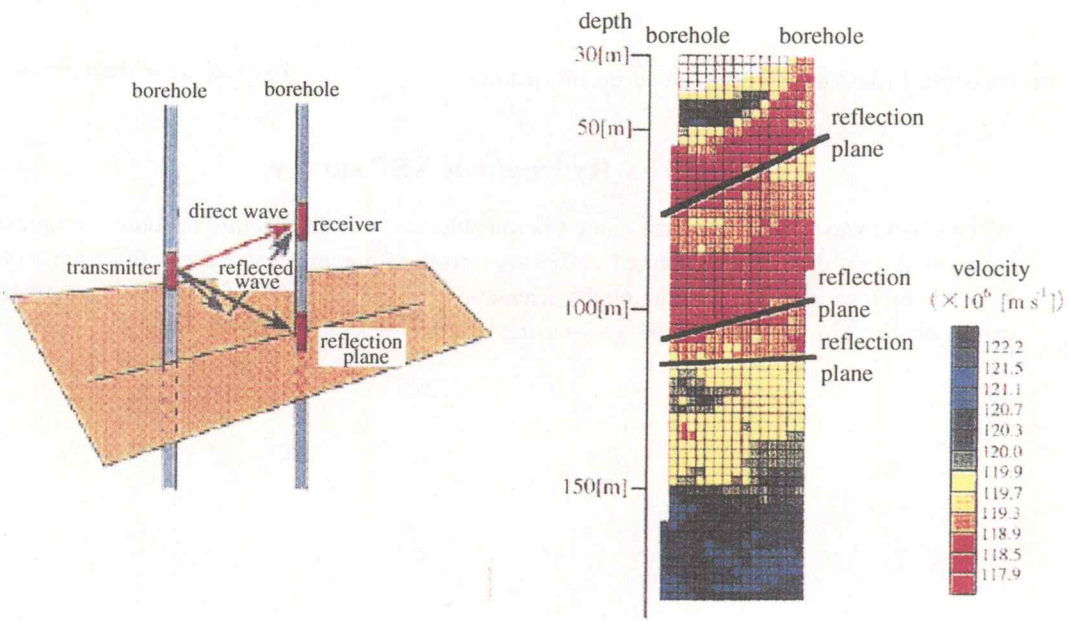


Figure 7 Geochemical parameter monitoring system

This system has been developed for continuous monitoring of in-situ groundwater chemistry (e.g. pH, redox potential, electric conductivity, dissolved oxygen and temperature) without any contact with air using a well-sealed packer system in a borehole.

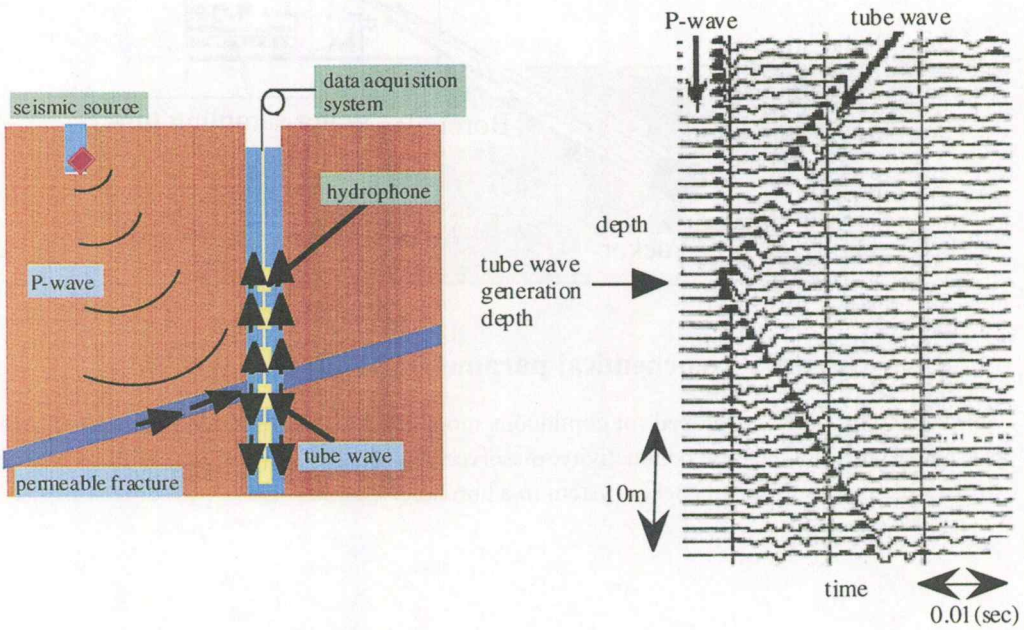


(a) schematic illustration of the measurement approach

(b) example of a tomography image

Figure 8 Borehole radar survey

In borehole radar surveys, radar probes are lowered into boreholes and short-wavelength electromagnetic pulses are generated to investigate the velocity and attenuation pattern of the electromagnetic waves, which are affected by the rock water content. As a result, the three-dimensional distribution of fractures and fracture zones, which are closely related to the hydrogeological properties of rock formations, can be determined non-destructively. In the single-hole method, a transmitter probe and a receiver probe are connected and lowered together into one borehole to measure electromagnetic waves reflected in the rock mass. In the cross-hole method, transmitter and receiver probes are lowered into different boreholes to measure electromagnetic waves propagated through the rock.



(a) conceptual illustration of the measurement method

(b) example of data produced

Figure 9 Hydrophone VSP survey

When elastic waves from a source enter a permeable fracture, the fracture becomes compressed, some of the groundwater is ejected and waves propagating in the borehole fluid are excited (forming tube waves). Information on the orientation of such fractures and also their permeability can be obtained by measuring tube waves using hydrophones placed in the borehole.

Postscript

In this Supporting Report, the results of research on the geological environment have been compiled. The objective of H12 is to demonstrate the technical feasibility of geological disposal in Japan and the R&D results presented in H12 will be used as a scientific and technical basis for identifying criteria for the selection of candidate disposal sites and for establishing a regulatory infrastructure for geological disposal of HLW. The progress made in this area is documented in the H12 Project Overview Report by integrating the results of R&D in three fields, namely studies of the geological environment, disposal technologies and PA of the disposal system. In this report, emphasis has been placed on studies on the geological environment, to supplement the description of the geological environment of Japan presented in the Overview Report.

Following government policy, the R&D program on geological disposal has been carried out by examining a variety of geological environments, without specifying particular rock types or locations. For practical reasons, however, studies of the geological environment have been carried out at only a limited number of sites, but not with the intention of demonstrating that these sites are potential candidates for a repository. Such investigations will only take place when potentially suitable sites have been selected following a site selection program. The geological information in this report is presented in such a way as to provide an explanation of the general geological conditions in Japan. A short description of the information provided in each chapter of the report is presented below.

To identify the challenges involved in studies of the geological environment in H12, background information, such as the role of the geological environment in deep disposal and government guidelines issued on this subject, were summarized in Chapter I. Although the progress made varies for the different issues identified in this chapter, the general goal of achieving a broad understanding of the geological environment in Japan has more or less been achieved.

Chapter II discussed the impact on the geological environment of natural phenomena that may perturb its long-term stability and are considered significant for the deep disposal of HLW. Although the volume and quality of data in this area are dependent on the type of natural phenomena being considered and the region of Japan in question, the spatial distributions of such phenomena and their effects can be traced back several hundred thousand years or more. The results of these studies will allow areas which have not been subjected to unacceptable activity levels of these phenomena to be identified; the possible future effects of such phenomena can be taken into account in the design of a repository and in the associated PA. For instance, the effects of local events, such as volcanic activity and fault movement, can be reduced or even eliminated altogether by maintaining a sufficient distance from areas subject to such activities. Phenomena which have cumulative effects, such as uplift, denudation and climatic and sea-level changes, can be overcome by, for example, placing a repository at a sufficient depth and in an area not expected to be subjected to high levels of uplift and denudation.

Because of local variations in the magnitude and occurrence of natural phenomena in Japan, local characteristics need to be fully taken into account when discussing the effects of such phenomena at specific sites. The data and information presented in Chapter II are considered sufficient, in principle, for discussing generic characteristics of these geological environments

in Japan. Although up-to-date data have to be taken into account as the general understanding of the geological environment progresses, it is not efficient to acquire new data constantly for the whole of Japan simply for the purpose of studying geological disposal. In future, the effects and consequences of natural phenomena will therefore be evaluated by focusing on specific areas of the country.

Data on rocks and groundwaters in Japan are summarized in Chapter III, from the viewpoint of the importance attached to the characteristics of the geological environment in controlling the design and functioning of the engineered barriers and the role of the natural barrier. The data are derived mainly from published reports in the fields of earth science and civil engineering and also from studies in the Tono area and at the Kamaishi mine. The published data, which cover a wide range of rock types and areas, are voluminous, but may not be sufficient in terms of reliability and precision. The data from Tono and Kamaishi are associated with particular levels of reliability and precision, but were obtained for very restricted areas of the country. The distribution of physical rock properties, the spatial distribution of geothermal gradients and depth profiles of in situ rock stresses were obtained from the published literature in the fields of civil engineering and geothermal exploration, which are well advanced in Japan. The broad distribution of hydraulic gradients and groundwater compositions was presented by compiling data from published literature, although many of these data were possibly of insufficient quality. General trends in the geological environment at depth, such as the permeability of rock mass and the redox state of groundwater, were evaluated by making comparisons with the measured data from Tono and Kamaishi.

The information presently available on the characteristics of rocks and groundwaters in Japan is not exhaustive; similarly it does not necessarily allow standard or average values to be defined for the whole of Japan. Nevertheless, it can be understood from the data compiled here that deep groundwater in Japan generally flows slowly and its chemistry is reducing. The data also suggest that deep rock masses where the ground temperature is acceptably low and the rock pressure is almost homogeneous are widely distributed throughout Japan. The data presented in this report are being used to develop parameter distributions for each of the properties of the geological environment, for the purposes of repository design and PA of the disposal system. In these studies, efforts have been made to adopt realistic or typical parameter values with the aid of statistical analysis, model-based simulations and using engineering assumptions. However, the parameter values selected often have to rely on limited or indirect data. In either case, it has to be remembered that these values are for reference purposes only and are not meant to be definitive, nor are they meant to be site-specific. What is important is to realize that there may be many areas in Japan in which more favorable values can be found; in other words, the reference values have been set conservatively to make many areas potentially suitable for disposal. As the deep disposal program proceeds, more site-specific data will be obtained, which will allow a more realistic assessment of the geological environment to be made.

Natural analogue studies of the geological environment are summarized at the end of Chapter III. Here, in addition to studies on the behavior of natural radionuclides in uranium ore deposits over long periods of time, methods of analyzing the effects of matrix diffusion were described. In addition to the results of PA, the effectiveness of geological disposal is supported by the fact that uranium ore deposits and many other metal and non-metal deposits have been preserved at depth for long periods of time. However, this does not mean that all ore deposits formed in the past have been preserved; it has to be understood that only ore

deposits that have been preserved can be recognized at present. What is important is not only the fact that they have been preserved, but the reasons and mechanisms for their preservation. For instance, the Tono uranium ore deposit has been preserved because groundwater in a reducing environment has only a limited ability to dissolve materials and the rate of groundwater movement and solute transport at depth is very slow. In fact, no indication of uranium migration can be found, even along faults that cut the ore body.

The Tono uranium ore deposit will continue to be preserved in the future, as long as the reducing environment and the slow solute transport, which are characteristic of many deep geological environments, are maintained. In fact, there are many uranium ore deposits in the world which have been preserved for over two billion years. However, it seems unlikely that the Tono deposit will be preserved for a further million years. Because the deposit is at a depth of 150 m, it is likely that it will either be removed by denudation or it will move up into the zone of oxidizing groundwater and will be leached away. For example, if a denudation rate of 0.1 - 1.0 mm per year is assumed, the ore body would be completely removed over the period from 150,000 to 1.5 million years from now. For a uranium ore deposit to be preserved for even longer times into the future, it needs to remain below a certain depth. Even if it remains at depth, it could still be affected by other geological events, such as the intrusion of magma, and it could be disturbed, possibly only temporarily, by fault movements. In other words, a uranium ore deposit will be preserved as long as its deep geological environment is not disturbed to too great an extent by denudation, volcanism and large-scale faulting.

The techniques and equipment used for investigating the geological environment were summarized in an Appendix. Not all the techniques and equipment are readily applicable in site investigations; some were designed for scientific research and are not suitable for practical use and some require further development for use under certain geological conditions. However, these techniques have been used in a range of investigations at Tono and Kamaishi in order to acquire key data on the characteristics of the geological environment. These surveys and tests have allowed techniques to become reasonably well established. Further work is planned in this area of technique and equipment development using deep underground research laboratories; investigation techniques specific to particular geological conditions also need to be developed.

In H12, the R&D program on geological disposal has been restricted by the requirement to consider a wide range of geological environments throughout Japan. This restriction was aimed at demonstrating the technical feasibility of geological disposal in Japan, before specifying areas and rock types for disposal purposes. What is important in this generic approach is not to present detailed discussions of localized data related to specific areas, but to develop a broad understanding of the geological environment (in particular, the processes occurring in the geological environment of Japan), based on the distributions and correlations of relevant data. As has been demonstrated in this report, a geological environment which is sufficiently stable over long periods of time, and in which the EBS can operate as planned, can be found by following a proper site selection program. Definite criteria for judging the adequacy of a geological environment for disposal purposes need to be developed, based on the time frame for PA and the dose limits to be defined. Such criteria also need to take into consideration the relationships between the geological environment at a specific site and the appropriate specifications for the engineered barriers.

Challenges to be addressed in the future R&D program will be discussed in the government review of H12. The AEC Guidelines suggested that research and development on the

geological environment after H12 should be directed towards:

- the development of a systematic investigation technology;
- enhancing the understanding of the deep geological environment;
- the assessment of future natural phenomena in specific areas.

The development of a systematic investigation technology and understanding of the deep geological environment will be the main objectives of the studies to be conducted in the deep underground research laboratories at Mizunami (Gifu Prefecture) for crystalline rocks (1996~), and at Horonobe (Hokkaido) for sedimentary rocks (proposed to the local governments in 1998). To develop and acquire techniques and data which are useful for the evaluation of natural phenomena at specific sites, studies of local geological characteristics will be carried out, applying and improving the techniques used in H12, namely case studies aimed at understanding the generic characteristics of Japan.

Acknowledgements

The H12 production team would like to thank the many experts from JNC, other Japanese R&D organizations, private companies and universities who contributed to the work reported in this Project or were involved in the review of the Project documentation. Thanks also go to the members of the international community who provided review comments - in particular the NEA review panel who provided input to the content of this Supporting Report via their review of the Project Overview Report, and Nagra review teams. Thanks also go to colleagues from research institutes in the USA and Canada who participated in the H12 North American Workshop and to JNC's International Fellows working at the Tono Geoscience Center.

JNC TN1410 2000-002

Second Progress Report on Research and Development for the Geological Disposal of HLW in Japan

H12 : Project to Establish the Scientific and Technical Basis for HLW Disposal in Japan

Supporting Report 1
Geological Environment in Japan

April 2000

JNC
Japan Nuclear Cycle Development Institute